New Records of the Great Dying in South China

Wei-Hong He · G.R. Shi
Ke-Xin Zhang · Ting-Lu Yang
Shu-Zhong Shen
Yang Zhang *Editors*

Brachiopods around the Permian-Triassic Boundary of South China

Springer

New Records of the Great Dying in South China

Series Editors
Wei-Hong He, State Key Laboratory of Biogeology and Environmental Geology, School of Earth Sciences, China University of Geosciences, Wuhan, China
Jian-Xin Yu, State Key Laboratory of Biogeology and Environmental Geology, School of Earth Sciences, China University of Geosciences, Wuhan, China
Hai-Shui Jiang, China University of Geosciences, Wuhan, China

New Records of the Great Dying in South China series systematically documents the recently discovered Permian–Triassic biota, including fossil plants, brachiopods, bivalves, radiolarians, conodonts, foraminifers, ostracods, and stratigraphy across the PTB interval. The series focuses the taxonomy, phylogeny, biodiversity, biostratigraphy, evolution of biota, palaeoecology and palaeogeography. The series summarizes the processes of mass extinction and environmental crisis.

More information about this series at http://www.springer.com/series/15421

Wei-Hong He • G. R. Shi • Ke-Xin Zhang
Ting-Lu Yang • Shu-Zhong Shen
Yang Zhang
Editors

Brachiopods around the Permian-Triassic Boundary of South China

Springer

Editors
Wei-Hong He
State Key Laboratory of Biogeology and Environmental Geology, School of Earth Sciences
China University of Geosciences
Wuhan, China

Ke-Xin Zhang
State Key Laboratory of Biogeology and Environmental Geology, School of Earth Sciences
China University of Geosciences
Wuhan, China

Shu-Zhong Shen
State Key Laboratory of Palaeobiology and Stratigraphy, Nanjing Institute of Geology and Palaeontology and Center for Excellence in Life and Palaeoenvironment
Chinese Academy of Sciences
Nanjing, Jiangsu, China

G. R. Shi
School of Life and Environmental Sciences
Burwood, Victoria, Australia

Deakin University
Geelong, Victoria, Australia

Ting-Lu Yang
Faculty of Geosciences
East China University of Technology
Nanchang, China

Yang Zhang
School of Earth Sciences and Resources
China University of Geosciences
Beijing, China

ISSN 2524-4574 ISSN 2524-4582 (electronic)
New Records of the Great Dying in South China
ISBN 978-981-13-1040-9 ISBN 978-981-13-1041-6 (eBook)
https://doi.org/10.1007/978-981-13-1041-6

Library of Congress Control Number: 2018950227

This Springer imprint is published by the registered company Springer Nature Singapore Pte Ltd.
The registered company address is: 152 Beach Road, #21-01/04 Gateway East, Singapore 189721, Singapore

Preface for the Series

The Permian–Triassic transition witnessed the greatest mass extinction during the Phanerozoic. Generations of palaeontologists have been inspired to interrogate this great dying with ever-growing interests. Collections and researches for fossils of this interval in South China already began in the 1970s or even earlier. Since the establishment of GSSP of the Permian–Triassic boundary (PTB) in 2001, palaeontologists have conducted vigorous researches of the great PTB mass extinction in South China during the past 15 years. During this period, the Changhsingian (Late Permian)–Induan (Early Triassic) biota of South China have been intensively collected and described from scores of sections with continuous Permian–Triassic sedimentary successions, and a great number of fossils are newly discovered. Marvelously, more than ten palaeontologists and dozens of students, covering major invertebrate and plant fossil categories, have been attracted to work simultaneously on so many continuous PTB sections that outcrop nowhere else than in South China. Thanks to their rigorous researches for more than one decade, a large quantity of newly discovered Permian–Triassic biota and stratigraphy has been systematically documented, and the taxonomy or classification of many fossils has been further evaluated and reexamined.

The editorial committee proposes to publish a series of monographs on marine biota and terrestrial plants of PTB in South China, based on their solid fossil collections identified to species level and timed at conodont/ammonoid zone level. It is a rare chance to have such a group of experts to work simultaneously on major fossil taxa of one geologically critical interval covering a whole region. The series will contain brachiopods, plants, ostracods, bivalves, radiolarians, conodonts, foraminifers, and stratigraphy that ranged from (but not limited to) the Changhsingian to Induan, especially the PTB interval.

The series will systematically describe the above mentioned fossil groups at species level, based on the classification of recently published treatise, and review some disputable species or even genera (especially the synonymum or homonimum). The series will also summarize the extinction, and partly recovery, patterns of different categories across varied palaeogeographic settings and analyze the causes/dynamics for changes of lives during the Permian–Triassic crisis. Stratigraphy, the last book of the series, will provide the basic and important information for the study of fossil occurrences and biodiversity evolution, e.g., lithologic feature and biostratigraphic correlation among the key sections.

Our world is undergoing another critical period resembling the PTB interval in many ways, and the "sixth mass extinction" is now a theme of debate. This series will not only greatly contribute to the knowledge of the greatest mass extinction, which is extremely important for us to know the life history of the past, but will also enlighten us to predict the future through comparison with the past and inspire the next generation to become interested about the evolution of life on the Earth.

Wuhan, China
19 April 2018

Hong-Fu Yin

Preface for the Book (Brachiopod Part)

Both my master and doctoral theses were on the Lopingian (Late Permian) brachiopods of South China. It has long been my dream to publish a series of monographs on the Permian-Triassic brachiopods. Regrettably, so far only one was published (Shen and Shi 2007). This book, led by Wei-Hong He, has helped to realize a part of my dream. It systematically describes 66 species in 34 genera, representing the most abundant brachiopod fauna from the Permian-Triassic boundary interval in the world. Correct taxonomic work is essential to understand the brachiopod faunal composition and evolutionary pattern. The authors not only studied the interspecific and intraspecific morphological variations among some similar genera or species, but also corrected many synonymous names based on over 10,000 well-preserved specimens from 15 Changhsingian to lowest Triassic sections in South China, thus provided high-quality data of brachiopods across the Permian-Triassic critical transition.

Brachiopods are one of the most diverse and abundant benthic fossil groups during the Paleozoic. Although they suffered great losses and changeovers during the end-Ordovician and Late Devonian mass extinctions, this fossil group did not change substantially in the remaining part of the Paleozoic in general diversity. On the contrary, they reached their highest level in diversity during the Lopingian, and many specialized brachiopods (e.g., *Leptodus*, *Richthofenia, Permianella*) occurred during this time. The most severe catastrophe at the end-Permian killed over 90% of the brachiopod species and changed the brachiopod world dramatically. After the end-Permian mass extinction, brachiopods never recovered to the Paleozoic level in diversity and no longer played an important role in the marine benthic ecosystem. They basically gave way to bivalves and ammonoids in the Mesozoic.

Researches on the Permian brachiopods of China began as early as 1883 by Kayser. Since then, numerous papers/monographs have been published and about 2500 brachiopod species have been described from China, of which many were only briefly described in Chinese during 1960s–1980s. Although the Permian brachiopod genera with the type species from China have been re-described, updated and illustrated by the Permian brachiopod group recently (Shen et al. 2017), a detailed monographic study at the species level with a high-resolution biostratigraphic framework in the Permian-Triassic boundary interval is still lacking. This book provides such kind of data in a timely fashion.

Permian brachiopods underwent an extremely complex process during the largest extinction. Therefore, studies on the temporal and spatial patterns of brachiopods in varied palaeogeographic settings are particularly important for scientists to understand the extinction and associated environmental changes. Most of the brachiopods documented in the previous publications in China were mainly collected from shallow-water carbonate facies. Brachiopods are relatively rare in deep-water facies. Consequently, systematic knowledge of the Lopingian deep-water brachiopods is very limited in the world. The brachiopods described in this book are mostly from the deep-water facies, therefore provided important supplementary materials for the brachiopod world living on the deep sea floor. In addition, did body size of brachiopods change across the Permian-Triassic boundary interval? What caused the extinction of most brachiopods? Which types of brachiopods survived the extinction? All these questions and more have been discussed in detail in this book.

Nanjing, China
20 November 2018

Shu-Zhong Shen

Acknowledgments

We are grateful to the senior adviser of the editorial committee, Professor Hong-Fu Yin for his organization, push, and encouragement during the preparation of this book. One of the authors, Wei-Hong He, especially wishes to express her sincere thanks to Qing-Lai Feng for his supervision in the junior stage of her research career. We also wish to thank Professor Shun-Bao Wu for his great contribution to the research on ammonite and bivalve biostratigraphy in this book and help in supervising the students.

We are also grateful to Bruce Waterhouse, Zhong-Qiang Chen, Zhi-Fei Zhang, and E. A. Weldon for their helpful discussions on some of the genera described in this book. We thank Dao-Jun Yuan from the Paleontology Museum of Nanjing Institute of Geology and Palaeontology, Chinese Academy of Sciences for providing an opportunity for us to check and photograph the type specimens of published species. We also thank Yi-Chun Zhang and Cun-Ying Chu from the library of Nanjing Institute of Geology and Palaeontology for providing old and rare references.

We express our sincere thanks to E. A. Weldon, Zhi-Jun Niu, Song-Zhu Gu, Ming-Liang Yue, Bin Chen, Fei Teng, and Zong-Yan Zhang, for their help in the fieldwork and collection of brachiopod fossils.

This work has been supported by NSFC (Grant Nos. 41772016, 41472004, 41730320, 41602017, 41772107, 41372030, 40872008, 40502001, 40921062, 40839903), the Foundation of the Geological Survey of China (1212011220529, 121201102000150012), the Ministry of Education of China (B08030 of 111 Project, NCET-10-0712), an Australian Research Council (ARC) research grant to GRS (DP0772161) and the Key Research Program of Frontier Sciences (QYZDY-SSW-DQC023), Strategic Priority Research Program (B) (XDB26000000, XDB18000000) of the Chinese Academy of Sciences to SSZ.

We sincerely thank several publishers for their kind permissions for reprinting some published fossil images, including Cambridge University Press, Elsevier, and Taylor & Francis Ltd, www.tandfonline.com (more details are given in the notes of Appendix 1).

Contents

Introduction

1

Wei-Hong He, G. R. Shi, and Shu-Zhong Shen

The Permian–Triassic transition witnessed the greatest mass extinction and ecosystem turnover of the Phanerozoic (Alroy et al. 2008; Chen and Benton 2012). The event has inspired (and would inspire) generations of palaeontologists to interrogate this great dying, with no sign of abating. South China, as an isolated block, was located in the eastern Palaeotethyan gape during the Late Permian–earliest Triassic (Blakey 2008) and contains some of the most complete Permian–Triassic marine-facies sequences (Erwin 1993; Yin 1996). Tens of sections with continuous Permian–Triassic depositional successions have been recognized in South China (Zhao et al. 1981; Sheng et al. 1984; Yang et al. 1987; Li et al. 1989; Yang et al. 1991; Shen et al. 1995; Yin et al. 2001). These sections have attracted many geologists to conduct detailed research on the stratigraphy, palaeontology and palaeoenvironment centred around the Permian–Triassic mass extinction (e.g., Jin et al. 2000; Xie et al. 2005; Shen et al. 2001; Joachimski et al. 2012; Algeo et al. 2013; Song et al. 2013; He et al. 2015). Based on the research, an episodic mass-extinction pattern (e.g., single- or two-episode) has been proposed (Yang et al. 1991; Jin et al. 2000; Song et al. 2013).

However, this pattern is mainly based on statistical analysis using fossil occurrences pooled from multiple compounded sections in the predominantly shallow-water carbonate facies. As such, the extinction pattern recognized may not be representative of all depositional facies, thus making it difficult to depict and elucidate the process of environmental change and associated biotic responses across the Permian–Triassic trasntion. For example, in which depositional environment did the Permian–Triassic mass extinction first begin in South China? And how did it propagate thereafter?

Brachiopods were among the most diverse and abundant marine invertebrate faunas in the

W.-H. He (✉)
State Key Laboratory of Biogeology and Environmental Geology, School of Earth Sciences, China University of Geosciences, Wuhan, China
e-mail: whzhang@cug.edu.cn

G. R. Shi
School of Life and Environmental Sciences, Burwood, Victoria, Australia

Deakin University, Geelong, Victoria, Australia
e-mail: grshi@deakin.edu.au

S.-Z. Shen
State Key Laboratory of Palaeobiology and Stratigraphy, Nanjing Institute of Geology and Palaeontology and Center for Excellence in Life and Palaeoenvironment, Chinese Academy of Sciences, Nanjing, Jiangsu, China
e-mail: szshen@nigpas.ac.cn

W.-H. He et al. (eds.), *Brachiopods around the Permian-Triassic Boundary of South China*, New Records of the Great Dying in South China, https://doi.org/10.1007/978-981-13-1041-6_1

Permian seas of South China. It is therefore no surprising that they have attracted many detailed monographic studies (Chao 1927, 1928; Huang 1932, 1933; Zhan in Hou et al. 1979; Liao 1980, 1987; Liao in Zhao et al. 1981; Xu in Yang et al. 1987; Zhan in Li et al. 1989; Zhu 1990; Xu and Grant 1994; Zeng et al. 1995; Shen and Shi 2007). However, almost all these monographs were based on collections from shallow-water carbonate facies, because brachiopods are usually more abundant and better preserved in limestones. By comparison, far less attention has been paid to the Late Permian deep-water brachiopods, despite a handful of papers published over the past 50 years (Liao 1979, 1984; He et al. 2005, 2007, 2014; Chen et al. 2006, 2009; Zhang and He 2009). Another challenge facing the Late Permian deep-water brachiopod faunas of South China is that many genera and species referred to in previous publications lacked taxonomically important internal structures discernable only in well-preserved materials, and therefore their taxonomic status requires a timely review in the wake of new and adequately preserved collections.

In this book, we systematically describe over 66 species (including 17 indeterminate species) in 34 genera, based on detailed examination of over 10,000 specimens from the Changhsingian to lowermost Triassic rocks of 15 sections in South China. Most of these specimens were collected from deep-water facies (the definition of deep-water facies is given below). Thanks to the excellent preservation of the materials at hand, we have been able to clarify the morphological differences between similar genera or species, correct species names with synonymum or homonimum problems, and summarize the spatio–temporal differences of brachiopod body sizes and diversity evolution patterns between deep-water and shallow-water facies. Additionally, we also review the morphological features and possible causes as to why some brachiopod species survived the end-Permian mass extinction in South China.

References

Algeo TJ, Henderson CM, Tong JN, Feng QL, Yin HF, Tyson RV. 2013. Plankton and productivity during the Permian–Triassic boundary crisis: an analysis of organic carbon fluxes. Global Planetary Change, 105: 52–67.

Alroy J, Aberhan M, Bottjer DJ, Foote M, Fursich F, Harries PJ, Hendy AJW, Holland SM, Ivany LC, Kiessling W, Kosnik MA, Marshall CR, McGowan AJ, Miller AI, Olszewski T, Patzkowsky DME, Peters SE, Villier L, Wagner PJ, Bonuso N, Borkow PS, Brenneis B, Clapham ME, Fall LM, Ferguson CA, Hanson VL, Krug AZ, Layou KM, Leckey EH, Nurnberg S, Powers CM, Sessa JA, Simpson C, Tomasovych A, Visaggi CC. 2008. Phanerozoic trends in the global diversity of marine invertebrates. Science, 321: 97–100.

Blakey RC. 2008. Gondwana paleogeography from assembly to breakup–A 500 m.y. odyssey. Geological Society of America Special Papers, 441: 1–28.

Chao YT. 1927. Productidae of China, Part 1. Palaeontologia Sinica, Series B, 5: 1–244.

Chao YT. 1928. Productidae of China. Palaeontologia Sinica, Series B, 5: 1–85.

Chen ZQ, Benton MJ. 2012. The timing and pattern of biotic recovery following the end-Permian mass extinction. Nature Geoscience, 5: 375–383.

Chen ZQ, Shi GR, Yang FQ, Gao YQ, Tong JN, Peng YQ. 2006. An ecologically mixed brachiopod fauna from Changhsingian deep-water basin of South China: consequence of end-Permian global warming. Lethaia, 39: 79–90.

Chen ZQ, Shi GR, Gao YQ, Tong JN, Yang FQ, Peng YQ. 2009. A late Changhsingian (latest Permian) deep-water brachiopod fauna from Guizhou, South China. Alcheringa, 33: 163–183.

Erwin DH. 1993. The Great Paleozoic Crisis: Life and Death in the Permian. Columbia University Press, New York, 327 pp.

He WH, Shen SZ, Feng QL, Gu SZ. 2005. A late Changxingian (Late Permian) deep-water brachiopod fauna from the Talung Formation at the Dongpan Section, Southern Guangxi, in South China. Journal of Paleontology, 79: 927–938.

He WH, Shi GR., Feng QL., Peng YQ. 2007. Discovery of late Changhsingian (latest Permian) brachiopod *Attenuatella* species from South China. Alcheringa, 31: 271–284.

He WH, Shi GR, Zhang Y, Yang TL, Zhang KX, Wu SB, Niu ZJ, Zhang ZY. 2014. Changhsingian (latest Permian) deep-water brachiopod fauna from South China. Journal of Systematic Palaeontology, 12: 907–960.

He WH, Shi GR, Twitchett RJ, Zhang Y, Zhang KX, Song HJ, Yue ML, Wu SB, Wu HT, Yang TL, Xiao YF. 2015. Late Permian marine ecosystem collapse began in deeper waters: evidence from brachiopod diversity and body size changes. Geobiology, 13: 123–138.

Hou HF, Zhan LP, Chen BW, Others. 1979. The coal-bearing strata and fossils of the Late Permian from Guangdong. Geological Publishing House, Beijing, 166 pp. [in Chinese].

Huang TK. 1932. Late Permian brachiopoda of southwestern China, Part 1. Palaeontologia Sinica, Series B, 9: 1–138.

Huang TK. 1933. Late Permian brachiopoda of southwestern China, Part 2. Palaeontologia Sinica, Series B, 9: 1–172.

Jin YG, Wang Y, Wang W, Shang QH, Cao CQ, Erwin DH. 2000. Pattern of marine mass extinction near the Permian–Triassic boundary in South China. Science, 289: 432–436.

Joachimski MM, Lai XL, Shen SZ, Jiang HS, Luo GM, Chen B, Chen J, Sun YD. 2012. Climate warming in the latest Permian and the Permian–Triassic mass extinction. Geology, 40: 195–198.

Li ZS, Zhan LP, Zhu XF, Zhang JH, Huang HQ, Xu DY, Yan Z, Li HM. 1989. Study on the Permian–Triassic biostratigraphy and event stratigraphy of northern Sichuan and southern Shaanxi. Geological Publishing House), Beijing, 435 pp. [in Chinese].

Liao ZT. 1979. Brachiopod Assemblage Zone of Changhsing Stage and brachiopods from Permo–Triassic Boundary Beds in China. Acta Stratigraphica Sinica, 3: 200–208. [in Chinese].

Liao ZT. 1980. Upper Permian Brachiopods from western Guizhou, p. 241–277. In: Nanjing Institute of Geology and Paleontology (Ed.), Stratigraphy and Palaeontology of Upper Permian Coal-Bearing Formations in western Guizhou and eastern Yunnan, China. Science Press, Beijing. [in Chinese].

Liao ZT. 1984. New genus and species of Late Permian and earliest Triassic brachiopods from Jiangsu, Zhejiang and Anhui Provinces. Acta of Palaeontologica Sinica, 23: 276–285. [in Chinese with English abstract].

Liao ZT. 1987. Paleoecological characters and stratigraphic significance of silified brachiopods of the Upper Permian from Heshan, Laibin, Guangxi, p. 81–125. In: Nanjing Institute of Geology and Paleontology (Ed.), Stratigraphy and Palaeontology of Systemic Boundares in China Perman and Triassic Boundary (1). Nanjing University Press, Nanjing. [in Chinese].

Shen SZ, Shi GR. 2007. Lopingian (Late Permian) brachiopods from South China, Part 1, Orthotetida, Orthida and Rhynchonellida. Bulletin of the Tohoku University Museum, 6: 1–102.

Shen SZ, He XL, Shi GR. 1995. Biostratigraphy and correlation of several Permian–Triassic boundary sections in southwestern China. Journal of Southeast Asian Earth Science, 12: 19–30.

Shen SZ, Archbold NW, Shi GR. 2001. A Lopingian (Late Permian) brachiopod fauna from the Qubuerga Formation at Shengmi in the Mount Qomolangma Region of southern Xizang (Tibet), China. Journal of Paleontology, 75: 274–283.

Sheng JZ, Chen CZ, Wang YG, Rui L, Liao ZT, Bando Y, Ishii K, Nakazawa K, Nakamura K. 1984. Permian–Triassic boundary in middle and eastern Tethys. Journal of the Faculty of Science, Hokkaido University, Series 4, Geology and Mineralogy, 21: 133–181.

Song HJ, Wignall PB, Tong JN, Yin HF. 2013. Two pulses of extinction during the Permian–Triassic crisis. Nature Geoscience, 6: 52–56.

Xie SC, Pancost RD, Yin HF, Wang HM, Evershed RP. 2005. Two episodes of microbial change coupled with Permo/Triassic faunal mass extinction. Nature, 434: 494–497.

Xu GR, Grant RE. 1994. Brachiopods near the Permian–Triassic boundary in south China. Smithsonian Contributions to paleobiology, 76: 1–68.

Yang ZY, Yin HF, Wu SB, Yang FQ, Ding MH, Xu GR. 1987. Permian–Triassic boundary stratigraphy and fauna of South China. Geological Publishing House, Beijing, 378 pp. [in Chinese with English abstract].

Yang ZY, Wu SB, Yin HF, Xu GR, Zhang KX. 1991. Permo–Triassic Events of South China. Geological Publishing House, Beijing, 183 pp. [in Chinese with English abstract].

Yin HF. 1996. The Palaeozoic–Mesozoic Boundary Candidates of Global Stratotype Section and Point of the Permian–Triassic Boundary. China University of Geosciences Press, Wuhan. 137 pp.

Yin HF, Zhang KX, Tong JN, Yang ZY, Wu SB. 2001. The Global Stratotype Section and Point (GSSP) of the Permian–Triassic boundary. Episodes, 24: 102–114.

Zeng Y, He XL, Zhu ML. 1995. Brachiopod communities and their succession and replacement in the Permian of Huayingshan Area. China University of Mining and Technology Press, Xuzhou, 187 pp. [in Chinese with English summary].

Zhang Y, He WH. 2009. Brachiopod fauna of Duanshan Section in Guizhou Province, and its geological significance. Geological Science and Technology Information, 28: 15–37. [in Chinese with English abstract].

Zhao JK, Sheng JZ, Yao ZQ, Liang XL, Chen CZ, Rui L, Liao ZT. 1981. The Changhsingian and the Permian–Triassic Boundary in South China. Nanjing Institute of Geology and Palaeontology, Bulletin, 2: 1–112. [in Chinese with English abstract].

Zhu T. 1990. The Permian coal-bearing strata and palaeobiocoenosis of Fujian. Geological Publishing House, Beijing, 127 pp. [in Chinese].

2 Geographical Location and Palaeogeographic Setting of Studied Sections

Wei-Hong He, Ke-Xin Zhang, and G. R. Shi

The specimens in this book were mainly collected from 15 sections from Zhejiang, Jiangsu, Anhui, Hubei, Hunan, Guizhou Provinces and Guangxi Zhuang Autonomous Region in South China (Fig. 2.1) and some of them have already been published (see Appendix 1). The studied sections mainly include Hushan (HS), Majiashan (MJS), Rencunping (RCP), Xinmin (XM), Duanshan (DS), Shaiwa (SW), Xiejiaping (XJP), Dengcaoba (DCB), Shangname (SNM), Dongpan (DP), Paibi (PB), Liuqiao (LQ), Zhongzhai (ZZ), Huangzhishan (HZS) and Daoduishan (DDS) (Fig. 2.1). Additionally, there two specimens were respectively collected from the Xichang (XC, see Appendix 1) and Dushan (DSH, see Appendix 1) sections.

W.-H. He (✉) · K.-X. Zhang
State Key Laboratory of Biogeology and Environmental Geology, School of Earth Sciences, China University of Geosciences, Wuhan, China
e-mail: whzhang@cug.edu.cn; kx_zhang@cug.edu.cn

G. R. Shi
School of Life and Environmental Sciences, Burwood, Victoria, Australia

Deakin University, Geelong, Victoria, Australia
e-mail: grshi@deakin.edu.au

Geographically, the Hushan section is located *ca* 20 km east of Nanjing City, Jiangsu Province (Fig. 2.2) and can be reached by bus in a half hour from Nanjing City. The Majiashan section is located about 5 km northwest of Chaohu City, Anhui Province (Fig. 2.2) and can be reached by bus in more than 10 min from Chaohu City (117°49′12″E, 31°37′33″N). The Huangzhishan and Daoduishan sections are respectively located in the Huangzhishan Village, Huzhou City and nearby Meishan Town, Changxing County, Zhejiang Province (Fig. 2.2). The Rencunping section is situated in the Rencunping Village, Sangzhi County, northwest Hunan Province (110°06′02″E, 29°34′49″N) (see Fig. 2.2). The Xinmin section is located in the Xinmin Village, Puding County (105°55′05″E, 26°22′35″N), Duanshan section in the Dapo Village, *ca* 5 km northwest to the Duanshan Town, Huishui County and Shaiwa section in 2 km southwest of the Shaiwa Village of the Sidazhai Town, Ziyun County, southern Guizhou Province (106°08′45″E, 25°35′56″N) (see Fig. 2.3). The Zhongzhai section is situated about 1 km northeast of Zhongzhai Village, Liuzhi County, southwestern Guizhou Province (Fig. 2.3). The Xiejiaping and Dengcaoba sections are respectively situated in the Xiejiaping Village (110°35′53″ E, 30°20′12″N), and Dengcaoba Village (110°29′40″ E, 30°21′09″N), Wufeng County, Hubei Province (Fig. 2.3). The

W.-H. He et al. (eds.), *Brachiopods around the Permian-Triassic Boundary of South China*, New Records of the Great Dying in South China, https://doi.org/10.1007/978-981-13-1041-6_2

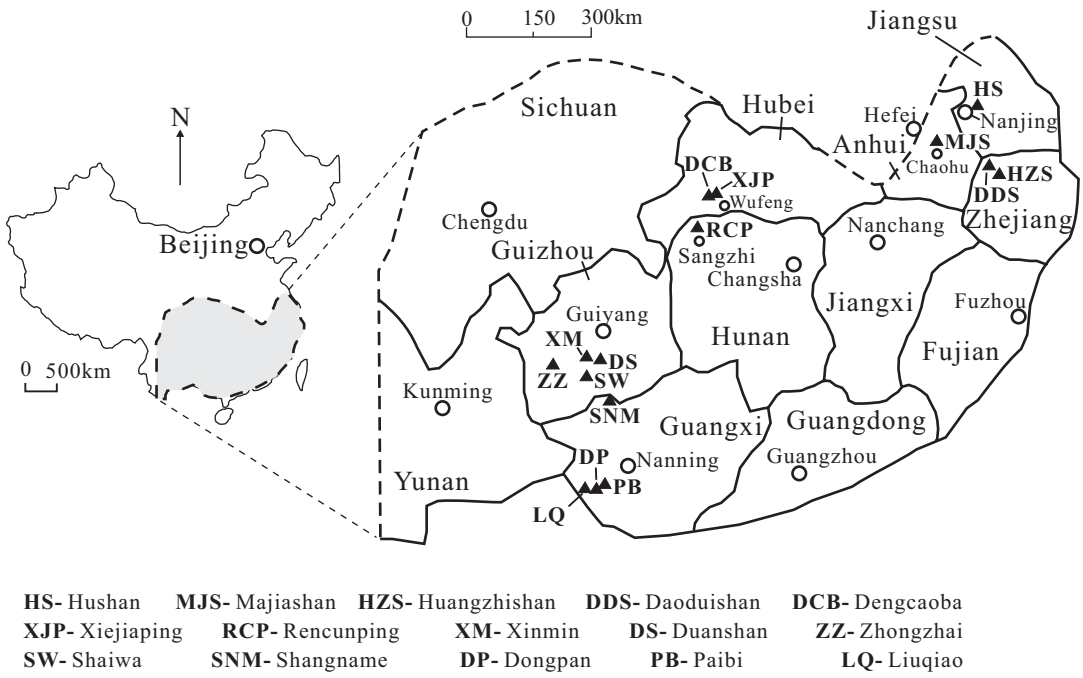

HS- Hushan **MJS-** Majiashan **HZS-** Huangzhishan **DDS-** Daoduishan **DCB-** Dengcaoba
XJP- Xiejiaping **RCP-** Rencunping **XM-** Xinmin **DS-** Duanshan **ZZ-** Zhongzhai
SW- Shaiwa **SNM-** Shangname **DP-** Dongpan **PB-** Paibi **LQ-** Liuqiao

Fig. 2.1 Distribution of studied sections in South China. Solid triangle indicates the approximate location

Shangname section is situated in the Shangname Village, Tiane County, Guangxi Zhuang Autonomous Region (Fig. 2.4). The Dongpan (107°41′47″E, 22°16′07″N), Paibi (107°43′10″E, 22°16′56″N), Liuqiao, Dushan and Xichang sections are located nearby the Liuqiao Town, Fusui County, Guangxi Zhuang Autonomous Region and outcropped along the 322 National Highway (Fig. 2.4).

Palaeogeographically, South China, in the Late Permian (Lopingian), was occupied by two major types of depositional environments: one characterized by deposition of deep-water facies, and the other by deposition of shallow-water facies (Fig. 2.5; also see Yang et al. 1991; He et al. 2007). Most studied sections in this book were located in deep-water facies, two sections in the shallow-water facies (Zhongzhai and Huangzhishan) (Fig. 2.5), and three sections between deep-water and shallow-water facies of South China (Dengcaoba, Xiejiaping and Daoduishan, see below). The deep-water facies is referred to the depositional sequence which is dominated by siliceous mudstones, cherts and siliceous limestones, intercalated with calcareous or manganese mudstones, yielding abundant ammonoids, radiolarians, associated with varied conodonts in the number of specimens and a few small brachiopods, bivalves, foraminifers and ostracods, with horizontal bedding in mudstones or Bouma sequences in siliceous limestones. The deep-water facies was distributed in a deep-water basin. The shallow-water facies is referred to the depositional sequence dominated by bioclastic limestones, calcareous mudstones or siltstones, intercalated with marls or sandstones, yielding abundant, diverse brachiopods (usually forming shell beds) and foraminfers, and a few larger bivalves, or yielding abundant bioclasts, and lacking ammonoids and radiolarians (or sparse for both of them). The shallow-water facies was distributed in a sandy- to silty-basin or on a carbonate platform. The sections including Xinmin, Hushan, Majiashan, Rencunping, Duanshan, Shaiwa, Shangname, Dongpan, Paibi and Liuqiao, were all located in the deep-water basin

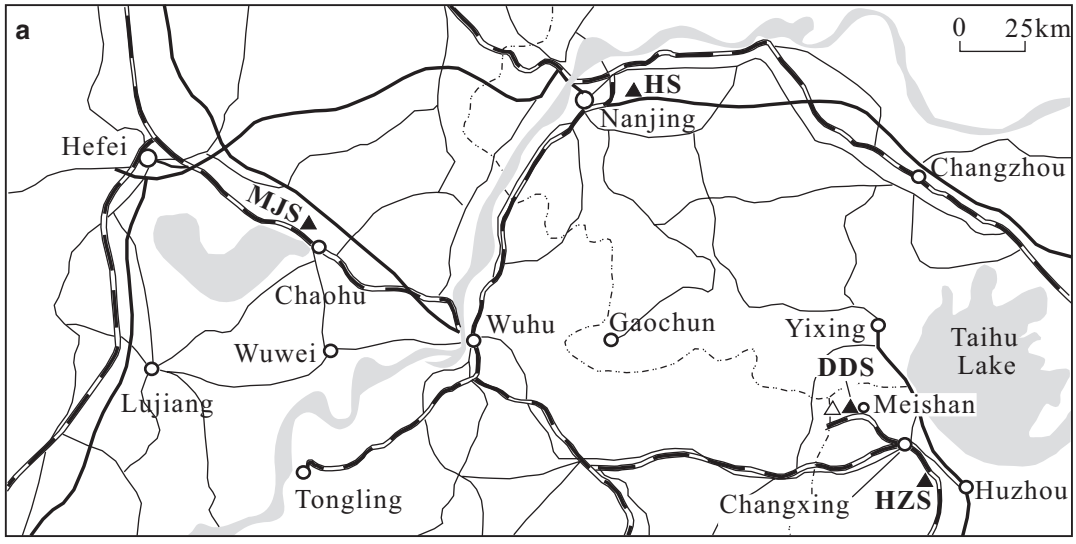

△ Meishan Section D, the GSSP of PTB

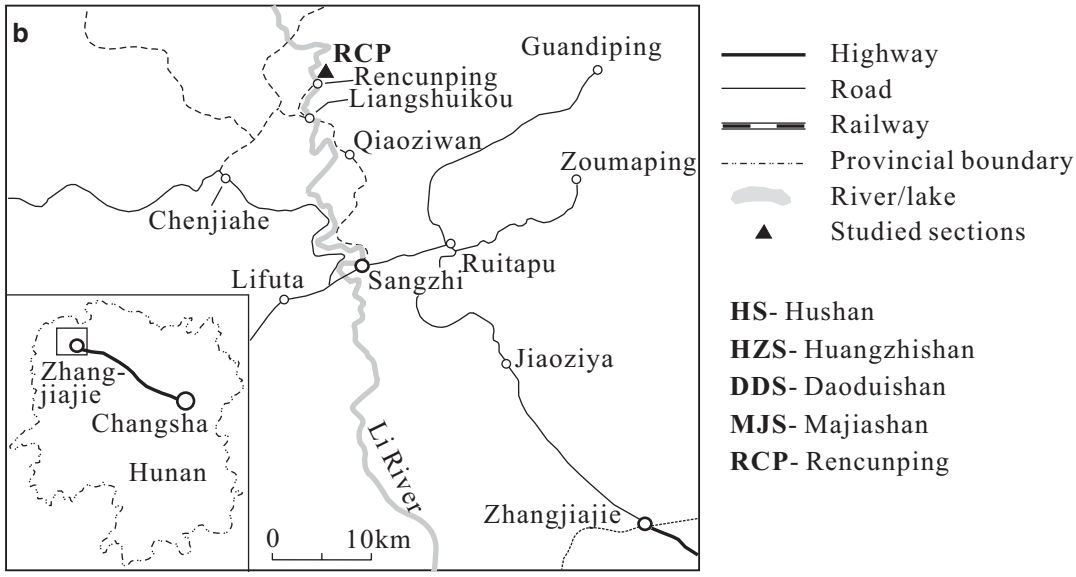

Fig. 2.2 Geographic location of Hushan, Huangzhishan, Daoduishan, Majiashan and Rencunping sections

(Fig. 2.5; also see He et al. 2014, 2015a, 2016). The Xiejiaping and Dengcaoba sections were located in a basin (possibly in an interplatform basin) (He et al. 2014). The Zhongzhai section was located in a silty basin, the Huangzhishan section on a carbonate platform (Fig. 2.5; also see Zhang et al. 2014; He et al. 2015b), and the Daoduishan section along the ramp of a carbonate platform (see He et al. 2017).

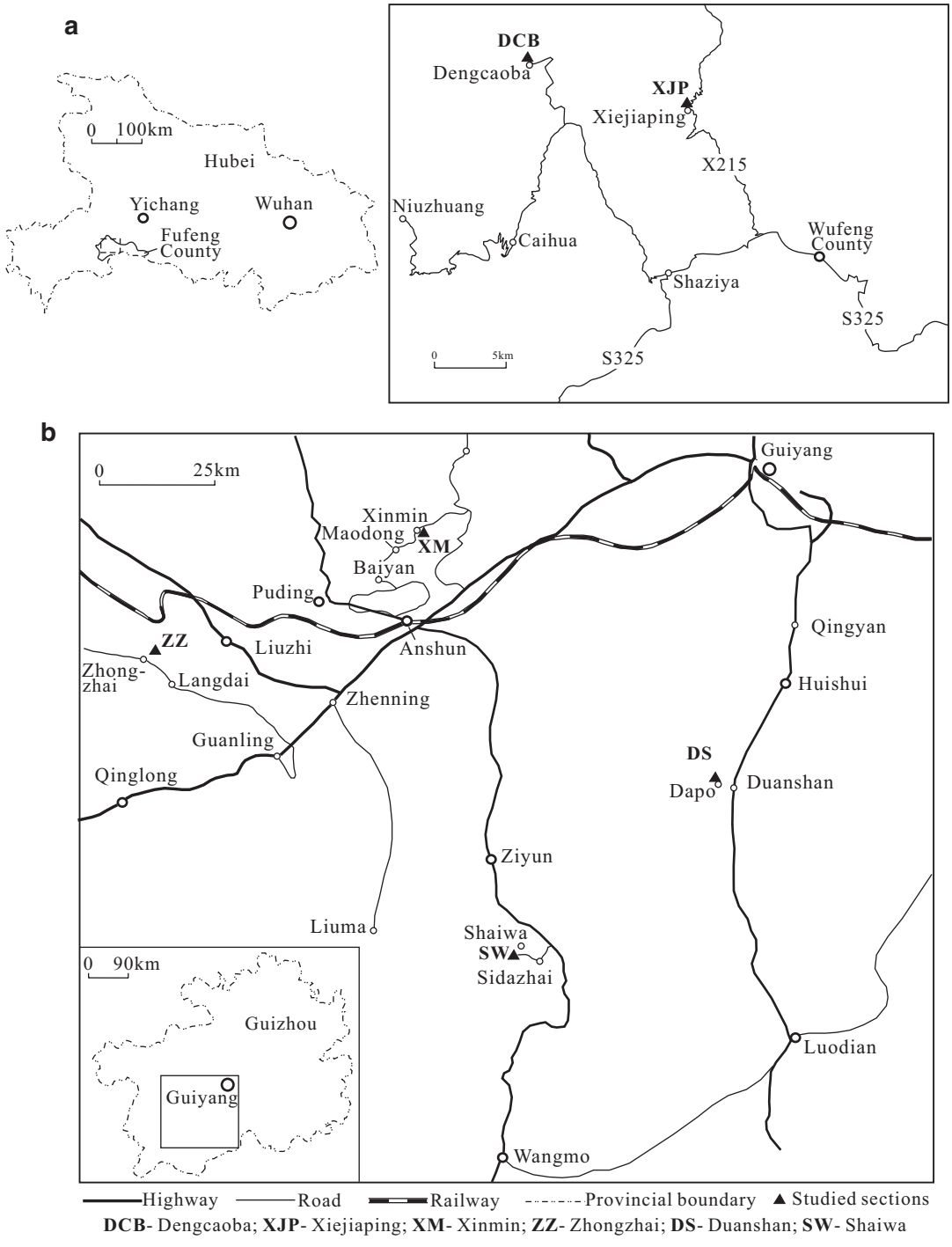

Fig. 2.3 Geographic location of Dengcaoba, Xiejiaping, Xinmin, Zhongzhai, Duanshan and Shaiwa sections

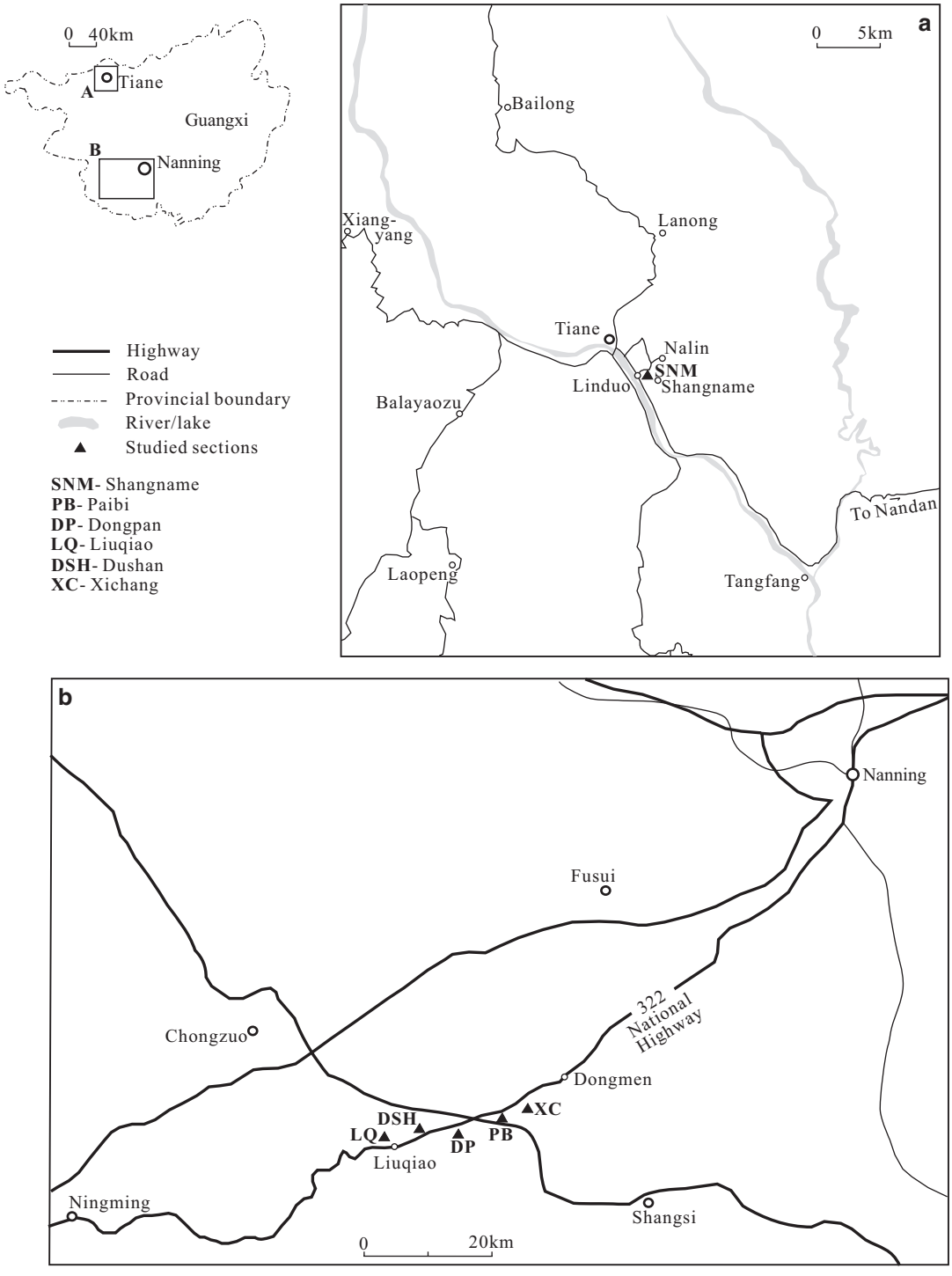

Fig. 2.4 Geographic location of Shangname, Paibi, Dongpan, Dushan, Xichang and Liuqiao sections

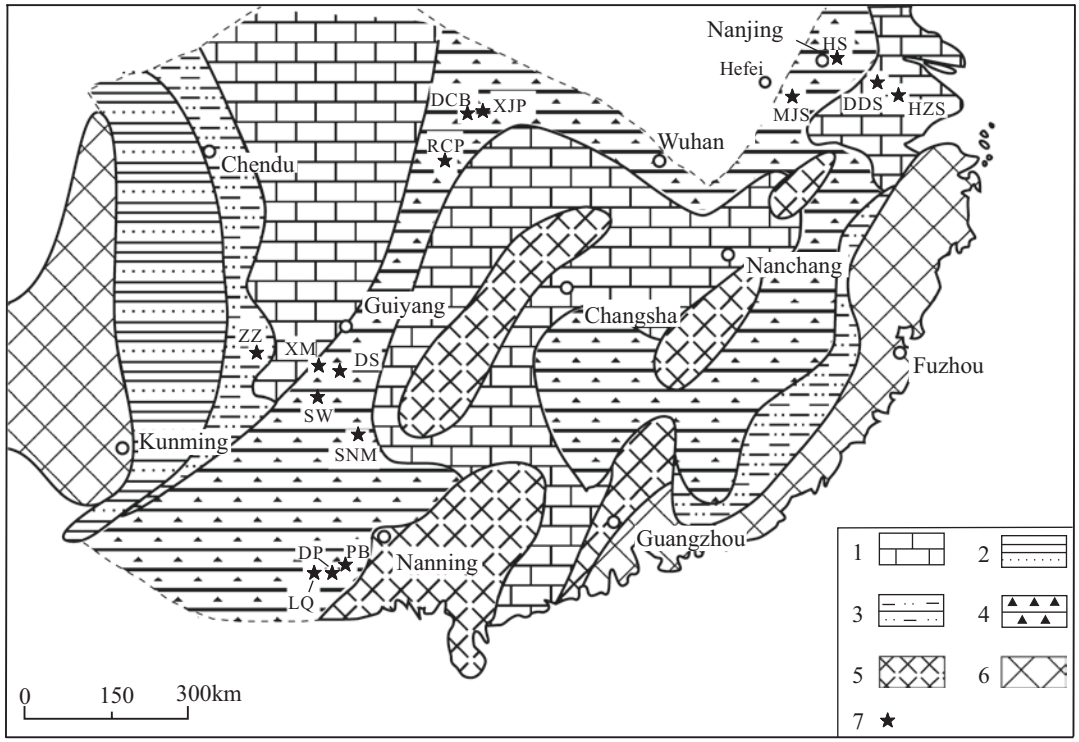

Fig. 2.5 Changhsingian palaeogeography of studied sections (revised after Feng and Gu 2002). 1- Shallow-water carbonate platform; 2- Terrestrial facies; 3- Shallow-water clastic shelf; 4- Deep-water siliceous basin; 5- Rise under sea surface; 6- Ancient land; 7- studied section. HS- Hushan, MJS- Majiashan, HZS- Huangzhishan, DDS- Daoduishan, XJP- Xiejiaping, DCB- Dengcaoba, RCP- Rencunping, ZZ- Zhongzhai, XM- Xinmin, DS- Duanshan, SW- Shaiwa, SNM- Shangname, DP- Dongpan, PB- Paibi, LQ- Liuqiao

References

Feng QL, Gu SZ. 2002. Uppermost Changhsingian (Permian) radiolarian fauna from southern Guizhou, southwestern China. Journal of Paleontology, 76: 797–809.

He WH, Shi GR, Feng QL, Campi MJ, Gu SZ, Bu JJ, Peng YQ, Meng YY. 2007. Brachiopod miniaturization and its possible causes during the Permian–Triassic crisis in deep water environments, South China. Palaeogeography, Palaeoclimatology, Palaeoecology, 252: 145–163.

He WH, Shi GR, Zhang Y, Yang TL, Zhang KX, Wu SB, Niu ZJ, Zhang ZY. 2014. Changhsingian (latest Permian) deep-water brachiopod fauna from South China. Journal of Systematic Palaeontology, 12: 907–960.

He WH, Zhang KX, Wu SB, Feng QL, Yang TL, Yue ML, Xiao YF, Wu HT, Zhang Y, Wang GD, Chen B. 2015a. End-Permian faunas from Yangtze basin and its marginal region: implications for palaeogeographical and tectonic environments. Earth Science-Journal of China University of Geosciences, 40: 275–289.

He WH, Shi GR, Twitchett RJ, Zhang Y, Zhang KX, Song HJ, Yue ML, Wu SB, Wu HT, Yang TL, Xiao YF. 2015b. Late Permian marine ecosystem collapse began in deeper waters: evidence from brachiopod diversity and body size changes. Geobiology, 13: 123–138.

He WH, Shi GR, Yang TL, Zhang KX, Yue ML, Xiao YF, Wu HT, Chen B, Wu SB. 2016. Patterns of brachiopod faunal and body-size changes across the Permian–Triassic boundary: evidence from the Daoduishan section in Meishan area, South China. Palaeogeography, Palaeoclimatology, Palaeoecology, 448: 72–84.

He WH, Shi GR, Xiao YF, Zhang KX, Yang TL, Wu HT, Zhang Y, Chen B, Yue ML, Shen J, Wang YB, Yang H, Wu SB. 2017. Body-size changes of latest Permian brachiopods in varied palaeogeographic settings in South China and implications for controls on animal miniaturization in a highly stressed marine ecosystem. Palaeogeography, Palaeoclimatology, Palaeoecolog, 486: 33–45.

Yang ZY, Wu SB, Yin HF, Xu GR, Zhang KX. 1991. Permo–Triassic Events of South China. Geological Publishing House, Beijing, 183 pp. [in Chinese with English abstract].

Zhang Y, Zhang KX, Shi GR, He WH, Yuan DX, Yue ML, Yang TL. 2014. Restudy of conodont biostratigraphy of the Permian–Triassic boundary section in Zhongzhai, southwestern Guizhou Province, South China. Journal of Asian Earth Sciences, 80: 75–83.

3 Depositional Sequences, Biotic Assemblages and Review on Changhsingian (or Late Changhsingian) Palaeo-Water Depths of Studied Sections

Wei-Hong He, Ke-Xin Zhang, G. R. Shi, Yi-Fan Xiao, and Jian-Jun Bu

3.1 Depositional Sequences and Biotic Assemblages

The Permian–Triassic depositional sequences at Hushan include the upper Talung Formation and Lower Chinglung Formation (Fig. 3.1; see He et al. 2011). The upper Talung Formation is dominated by dark grey thin-bedded cherts and siliceous mudstones, intercalated with medium-bedded grey argillaceous limestones, thin-bedded calcareous mudstones and volcanic ash. The siliceous mudstones abundantly yield horizontal beddings. The upper Talung Formation contains abundant radiolarians, ammonoids, conodonts, small brachiopods, bivalves, and a small number of ostracods and foraminifers. The lower Talung Formation at Hushan is covered by Quaternary sediments. The basal part of the Lower Chinglung Formation mainly comprises yellowish calcareous mudstones, thin- to medium-bedded argillaceous limestones, interbedded with volcanic ash, and contains ammonoids and bivalves.

The Permian–Triassic interval at Majiashan includes the upper Talung Formation and the basal part of the Yinkeng Formation (Fig. 3.1; see He et al. 2008a). The upper Talung Formation is characterized mainly by grey to greyish-black, thin-bedded, carbonaceous mudstones, siliceous mudstones and cherts. The upper Talung Formation yields a few small foraminifers, bivalves and brachiopods, microgastropods, ostracods, and abundant ammonoids, radiolarians. The basal part of the Yinkeng Formation is characterized by greyish green thin-bedded calcareous mudstones interbedded with argillaceous limestone, with ammonoids and bivalves.

W.-H. He (✉) · K.-X. Zhang
State Key Laboratory of Biogeology and Environmental Geology, School of Earth Sciences, China University of Geosciences, Wuhan, China
e-mail: whzhang@cug.edu.cn; kx_zhang@cug.edu.cn

G. R. Shi
School of Life and Environmental Sciences, Burwood, Victoria, Australia

Deakin University, Geelong, Victoria, Australia
e-mail: grshi@deakin.edu.au

Y.-F. Xiao
State Key Laboratory of Biogeology and Environmental Geology, Wuhan, China
e-mail: yifanxiao@hotmail.com

J.-J. Bu
Wuhan Centre for China Geological Survey, Wuhan, China
e-mail: jianjunbu@cug.edu.cn

W.-H. He et al. (eds.), *Brachiopods around the Permian-Triassic Boundary of South China*, New Records of the Great Dying in South China, https://doi.org/10.1007/978-981-13-1041-6_3

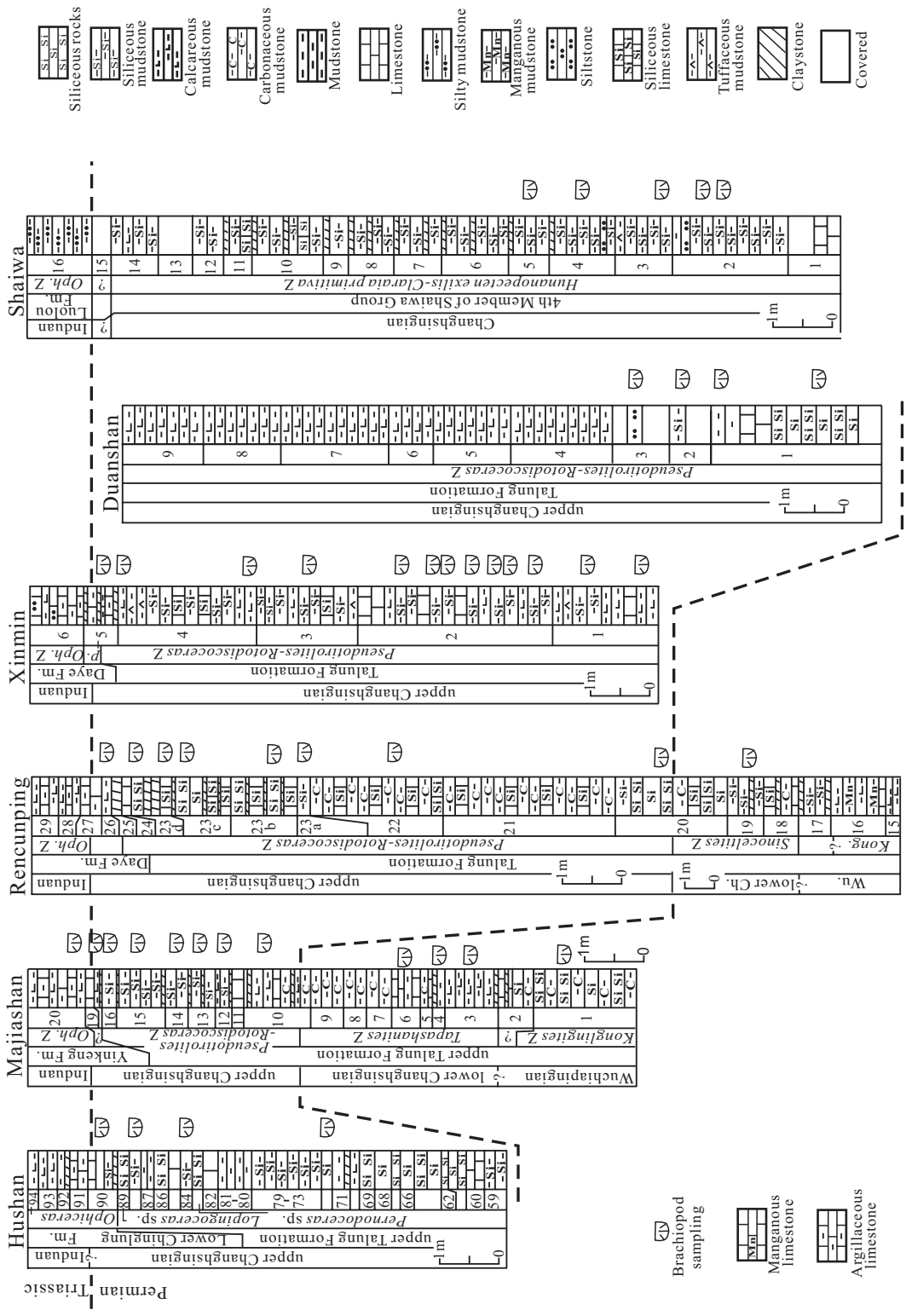

Fig. 3.1 Stratigraphic columns of Hushan, Majiashan, Rencunping, Xinmin, Duanshan and Shaiwa sections. Fm.- Formation, Wu.- Wuchiapingian, Ch.- Changhsingian, *Oph.- Ophiceras, Kong.- Konglingites* Zone, *p.- Hindeodus parvus* Zone, Z- Zone

The Permian–Triassic interval at Rencunping includes the Talung Formation and basal part of Daye Formation (Fig. 3.1; see Xiao et al. 2017). The Talung Formation is dominated by greyish-black thin-bedded cherts, siliceous mudstones, siliceous limestones and carbonaceous mudstones, intercalated with volcanic ash. The Talung Formation abundantly yields ammonoids, radiolarians, small brachiopods and a few small bivalves. The basal part of the Daye Formation is characterized by greyish green thin-bedded calcareous mudstones interbedded with argillaceous limestone, with abundant ammonoids and bivalves.

The Permian–Triassic transition at Xinmin spans the Changhsing, Talung and Daye Formations (Wu et al. 2018). This study focuses on the Talung Formation (Fig. 3.1). The Talung Formation mainly comprises dark grey siliceous mudstones, siliceous limestones and calcareous mudstones, intercalated with volcanic ash (Wu et al. 2018). It has abundantly yielded ammonoids and small brachiopods, and a few bivalves, foraminifers, spongy spicules and spherical radiolarians (Xiang et al. 2013), as well as transported plant fragments (Song et al. 2015). Bouma Sequence is commonly observed in siliceous and argillaceous limestone beds. The Daye Formation is composed of thin-bedded calcareous mudstones, argillaceous limestones (namely marls in the basal part) and silty limestones (overlying marls) (Fig. 3.1), with graded bedding and hummocky cross bedding in silty limestones.

The uppermost part of the Permian at Duanshan comprises the Talung Formation (Fig. 3.1; see Wu et al. 2018) and the Permian–Triassic boundary sequence is covered by the Quaternary sediments. The Talung Formation at Duanshan is dominated by light grey calcareous mudstones, with cherts in the lower part of the formation, and intercalated with limestones, siliceous mudstones and siltstones. Ammonoids have been found throughout the formation and a mixed brachiopod fauna (dominated by warm-water elements, but associated with cool-water elements, e.g., *Attenuatella* and *Costatumulus*) found in the lower part of the formation (Zhang and He 2009; He et al. 2014).

The Permian–Triassic transition at Shaiwa includes the Changhsingian Shaiwa Group and the Lower Triassic Luolou Formation. The Fourth Member of the Shaiwa Group is focused in this study (Fig. 3.1). It comprises greyish black thin-bedded siliceous mudstones, intercalated with greyish green thin-bedded siliceous limestones and pale volcanic ash. It yields abundant ammonoids, radiolarians and a few brachiopods, bivalves and foraminifers (Chen et al. 2006). The top part of Shaiwa Group and the Permian–Triassic boundary have been covered by the Quarternary sediments. The basal part of the Luolou Formation is composed of greyish yellow thin-bedded silty mudstones. It yields ammonoids and bivalves.

The Permian–Triassic intervals at Xiejiaping and Dengcaoba include the Talung Formation and basal part of the Daye Formation (Fig. 3.2). The Talung Formation at Xiejiaping is dominated by greyish black thin-bedded carbonaceous mudstones, siliceous mudstones and limestones, intercalated with cherts, calcareous mudstones and volcanic ash. It yields abundant ammonoids and a few brachiopods and conodonts. The basal Daye Formation comprises thin-bedded limestones and calcareous mudstones, with volcanic ash intercalations. It yields ammonids, conodonts and bivalves. The Talung Formation at Dengcaoba is dominated by greyish black thin-bedded cherts, carbonaceous mudstones and calcareous mudstones, with ammonoids in the lower part and small brachiopods, ammonoids and bivalves in the upper part. The basal Daye Formation comprises thin-bedded argillaceous limestones and calcareous mudstones, with ammonoids and brachiopods.

The Permian–Triassic interval at Shangname includes the Talung Formation and basal part of Luolou Formation (Fig. 3.2). The Talung Formation comprises greyish green thin-bedded tuffceous mudstones, with ammonoids and abundant (monospecific) brachiopods. The Lower Triassic Luolou Formation overlies the Upper Permian Talung Formation by a fault. The Luolou Formation comprises yellowish green thin-bedded calcareous mudstones, with a few ammonoids.

The Permian–Triassic transitional sequence at Dongpan is continuous and includes the Talung Formation and basal part of the Luolou Formation,

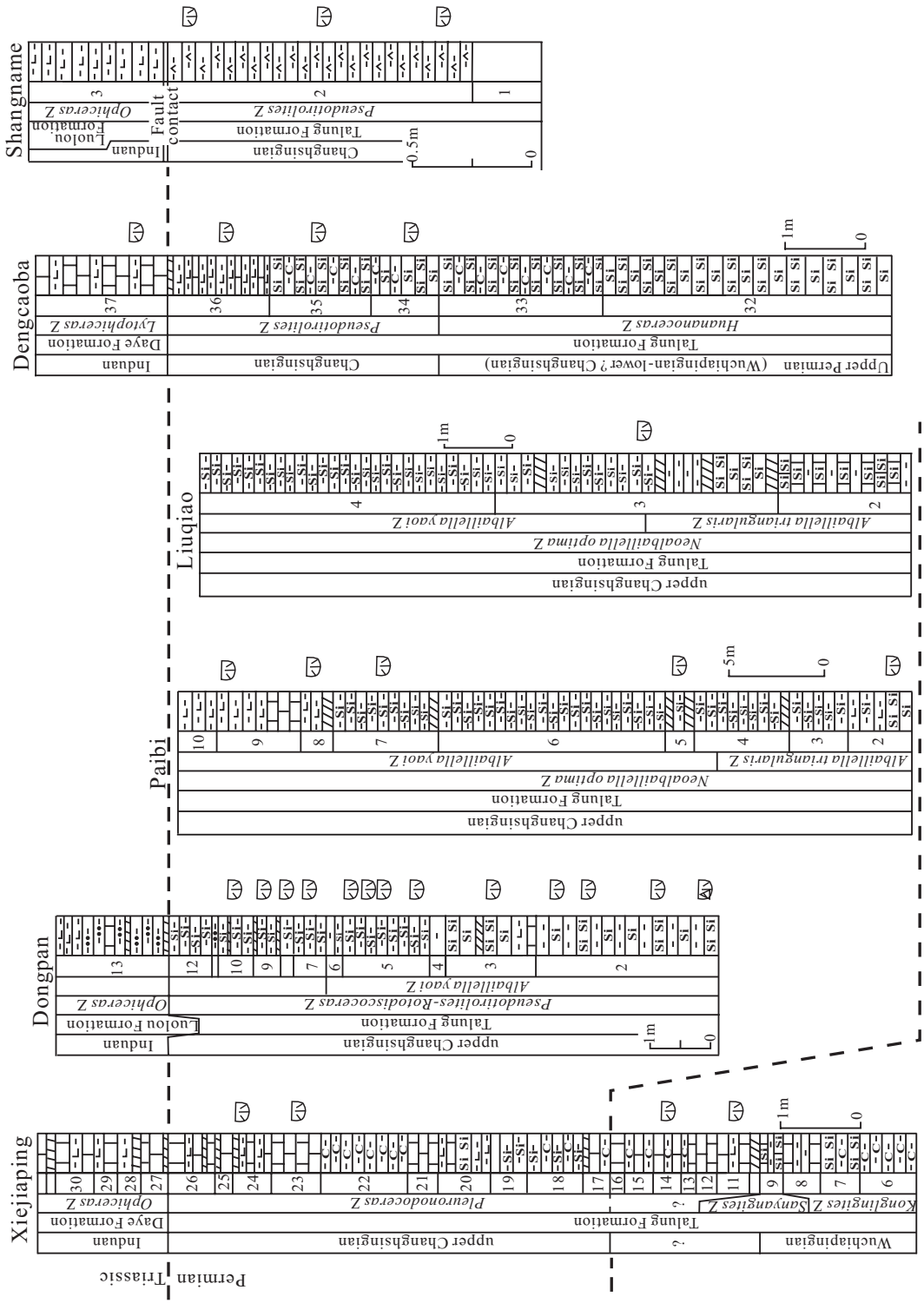

Fig. 3.2 Stratigraphic columns of Xiejiaping, Dongpan, Paibi, Liuqiao, Dengcaoba and Shangname sections. *Z*- Zone. Legends are same to Fig. 3.1

but the top part of Permian and the Lower Triassic at Paibi and Liuqiao are covered by the Quaternary sediments (Fig. 3.2). The Talung Formation is dominated by greyish green thin-bedded siliceous mudstones and cherts, intercalated with yellowish green thin-bedded mudstones, calcareous mudstones and manganous limestones at Dongpan, Paibi and Liuqiao. It yields abundant ammonoids, pelagic radiolarians and cool-water brachiopods, and a few bivalves, foraminifers and palaeopsychrospheric ostracods (He et al. 2005, 2007a; Bu et al. 2006; Feng et al. 2007; Gu et al. 2007; Yuan et al. 2007; Yang et al. 2015). The basal Luolou Formation comprises yellowish brown silty mudstones and calcareous mudstones, intercalated with light gray thin-bedded limestones. It yields abundant ammonoids and bivalves.

The Permian–Triassic interval at Zhongzhai includes the Lungtan Formation and basal part of Yelang Formation (Fig. 3.3). The Lungtan Formation is dominated by fine sandstones, muddy siltstones and calcareous mudstones, intercalated with limestones or lens-shaped limestones, with fine laminations in calcareous mudstones (Zhang et al. 2014). It yields abundant brachiopods (forming shell beds) and a few conodonts, bivalves, gastropods, foraminfers and ostracods. The basal Yelang Formation comprises light gray thin-bedded argillaceous limestones, yellowish green calcareous mudstones and silty mudstones, intercalated with pale volcanic ash, with conodonts, bivalves, gastropods and brachiopods (Peng et al. 2007; He et al. 2008b; Gao et al. 2009; Zhang et al. 2013).

The Permian–Triassic interval at Huangzhishan includes the top part of the Changhsing Formation and lower part of the Yinkeng Formation (Fig. 3.3). The top part of the Changhsing Formation comprises light gray medium- to thin-bedded bioclasitic limestones, with abundant corals, brachiopods, crinoids, sponges, gastropods, bryozoans, ostracods, foraminifers, algae and a few conodonts (Chen et al. 2008, 2009). The Yinkeng Formation comprises greyish green thin-bedded argillaceous mudstones and calcareous mudstones (He et al. 2015), with abundant brachiopods (forming shell beds) and a few bivalves, conodonts and foraminfers (Chen et al. 2008, 2009; He et al. 2015, 2017).

The Permian–Triassic interval at Daoduishan includes the Changhsing Formation and basal part of the Yinkeng Formation (Fig. 3.3). The Changhsing Formation comprises gray to light gray thin- to medium-bedded bioclastic limestones, occasionally intercalated with gray thick-bedded bioclastic limestones and black cherty nodules, with hummocky cross-stratification, parallel stratification, or wavy cross-bedding (He et al. 2016). It yields conodonts, brachiopods, foraminifers, algae, ostracods, fusulinids, sponges and crinoids. The basal Yinkeng Formation is composed of dark gray thin-bedded calcareous mudstones and dark gray thin- to medium-bedded argillaceous limestones, intercalated with pale volcanic ash, with fine laminations in calcareous mudstones (He et al. 2016). It yields conodonts, bivalves and a few foraminifers and brachiopods.

3.2 Palaeo-Water Depths of Studied Sections During the Changhsingian (or Late Changhsingian)

Lithological and biotic features are key and basic aspects for the analysis of sedimentary environments. Generally, carbonate deposits accumulate above the lysocline, siliceous carbonate accumulates between the lysocline and the carbonate compensation depth (CCD), and opal or siliceous sediments form below the CCD (Weber and Pisias 1999; Weber and von Stackelberg 2000; Dittert and Henrich 2000; Edmond and Huh 2003). As the position of the CCD is deeper than the lysocline (Weber and Pisias 1999), siliceous (opaline) mudstone will accumulate in deeper water than limestone and siliceous limestone. Additionally, the fine-grained sediments (e.g., siliceous mudstone) with weak bioturbation could have accumulated in a setting from outer shelf to basin, with >120 m water depths (Immenhauser 2009) and therefore indicates a deeper water setting.

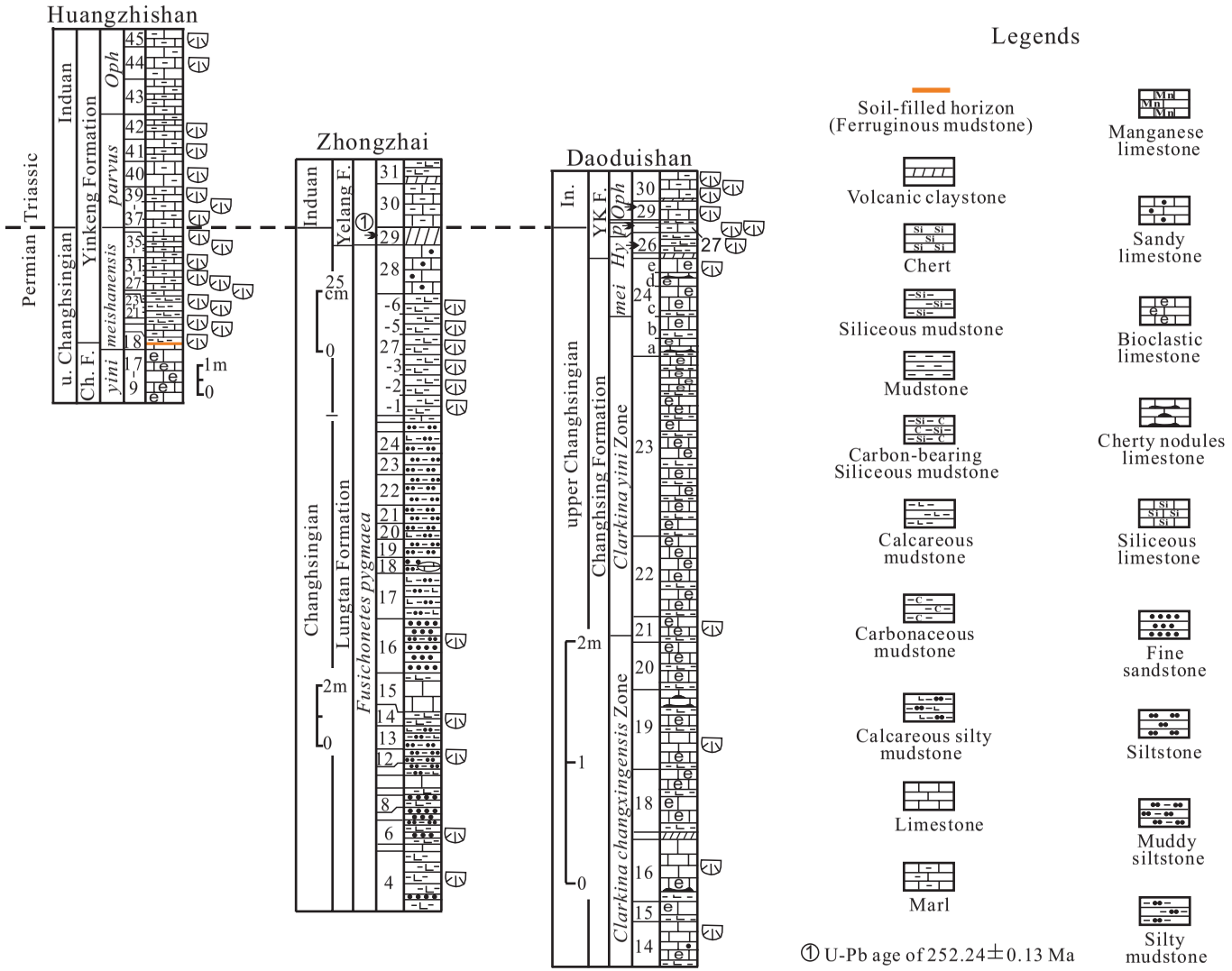

Fig. 3.3 Stratigraphic columns of Huangzhishan, Zhongzhai and Daoduishan sections. u.- upper, Ch.- Changhsing, F.- Formation, *yini- Clarkina yini* Zone, *meishanensis/mei- Clarkina meishanensis* Zone, *parvus/p- Hindeodus parvus* Zone, *Oph- Ophiceras* Zone, *Hy- Hypophiceras* Zone, In.- Inudan, YK- Yinkeng

The research on radiolarian palaeo-water depths revealed that the presence of spherical radiolarians (Entactinaria or Spumellaria forms), lack of Latentifistularia (excluding *Ishigaum obesum* and *Quadricaulis inflata*) and lack of Albaillellaria forms together are generally taken to indicate water depths <200 m (outer shelf), the presence of Latentifistularia or Albaillellaria forms generally indicates water depths of approximately 200 m or deeper. If Latentifistularia and Albaillellaria forms dominated a radiolarian fauna (especially the abundant presence of *Neoalbaillella* forms), it would mean that water depths were more than 500 m (Kozur 1993; He et al. 2008a, 2011; Xiao et al. 2017).

At Hushan, the upper Talung Formation is overwhelmingly dominated by cherts and siliceous mudstones, with abundant presence of radiolarian Albaillellarians and Latentifistularians in a few horizons and abundant presence of ammonoids and conodonts in most beds (He et al. 2011). Therefore, the water depths would have reached about 200 m or deeper when the maximum transgression took place during the late Changhsingian at Hushan (Fig. 3.4).

At Majiashan, the upper Talung Formation is dominated by carbonaceous mudstones, siliceous mudstones and cherts, with the presence of radiolarian Latentifistularians (*Ishigaum obesum*, *Quadricaulis inflata* and *Foremanhelena robusta*) in a few horizons (He et al. 2008a; Gui et al. 2009), abundant presence of ammonoids and a few presences of small benthonic invertebrates. Therefore, the water depth was 100–200 m when the maximum transgression took place during the late Changhsingian (Fig. 3.4; He et al. 2008a; Xiao et al. 2017).

At Rencunping, the Talung Formation is dominated by cherts, siliceous mudstones, siliceous limestones and carbonaceous mudstones, with abundant presences of Entactinaria, Spumellaria and Latentifistularia elements (e.g., *Ishigaum trifustis*, *Foremanhelena robusta*, *Nazarovella scalae*, *Latentifistula similicutis*) and a few presences of Albaillellaria elements (*Albaillella triangularis*, *Albaillella yaoi yaoi*, *Albaillella yaoi longa*, *Albaillella protolevis*, *Albaillella angusta* and *Albaillella excelsa*) in some intervals (Xiao et al. 2017) and small benthonic invertebrates. Therefore, the water depths would have reached deeper than 200 m (or deep to 300 m) during the Changhsingian at Rencunping (Fig. 3.4; see Xiao et al. 2017).

At Xinmin, the Talung Formation is dominated by siliceous limestones and siliceous mudstones. The biotic association in this formation is mainly composed of planktonic cephalopods, associated with spherical radiolarians (Xiang et al. 2013) and small benthonic invertebrates, indicating the water depths would have been <200 m in an outer shelf (Fig. 3.4; see Xiao et al. 2017).

At Duanshan, the Talung Formation is dominated by siliceous limestones and siliceous mudstones. The biotic association in this formation is mainly composed of planktonic cephalopods,

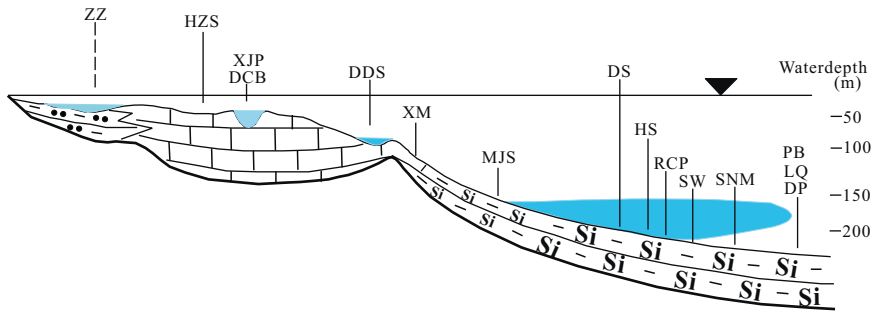

Fig. 3.4 Sketch diagram showing the palaeogeographic setting and palaeo-bathymetry of studied section (revised after He et al. 2017). Blue represents anoxic and light blue represents dysoxic. ZZ- Zhongzhai, HZS- Huangzhishan, XJP- Xiejiaping, DCB- Dengcaoba, DDS- Daoduishan, XM- Xinmin, MJS- Majiashan, DS- Duanshan, HS- Hushan, RCP- Rencunping, SW- Shaiwa, SNM- Shangname, PB- Paibi, LQ- Liuqiao, DP- Dongpan

associated with mixed brachiopods (warm- and cool-water elements). Radiolarian Latentifistularia and Albaillellaria elements have been found in a few horizons of the Talung Formation from the other section nearby Duanshan. Therefore, the water depths would have reached about 200 m when the maximum transgression took place during the Changhsingian at Duanshan (Fig. 3.4).

At Shaiwa, the Fourth Member of Shaiwa Group is dominated by siliceous mudstones, with pelagic radiolarians, bathyal trace fossil *Nereites*, small invertebrates and deep-water sedimentary structures (e.g., Bouma Sequence) (Chen et al. 2006). All these features indicate a bathyal setting (deeper than 200 m; see Chen et al. 2006) during the Changhsingian at Shaiwa (Fig. 3.4).

At Xiejiaping and Dengcaoba, the Talung Formation is dominated by carbonaceous mudstones, siliceous mudstones and limestones, with planktonic cephalopods and small benthonic invertebrates and lack of radiolarians, indicating a setting of interplatform basin (water depths slightly deeper than a carbonate platform) (Fig. 3.4).

At Shangname, the Talung Formation is uniquely composed of tuffceous mudstones, with abundant and monospecific brachiopiod *Martinia liuqiaoiensis* which commonly occurred in the Talung Formation of the deep-water Dongpan section (see below). Outlines of Radiolarian shells have been observed in the rocks and most of shells have not been preserved because of weathering. These features probably indicate a deep-water setting (probably similar to the Dongpan section) during the Changhsingian at Shangname (Fig. 3.4).

At Dongpan, Paibi and Liuqiao, the Talung Formation is overwhelmingly dominated by cherts and siliceous mudstones, with quite abundant presence of deep-water radiolarian Albaillellarians (e.g., *Neoalbaillella grypa*, *Albaillella levis*, *Albaillella triangularis*) in most beds and presences of ammonoids, small bivalves and foraminifers, mixed brachiopods (warm-water and cool-water elements), siliceous sponges and cold-water ostracods (He et al. 2005, 2007a, b; Feng et al. 2007; Gu et al. 2007; Yuan et al. 2007; Liu et al. 2013; Yang et al. 2015). The research on radiolarians and palaeo-bathymetry at Dongpan revealed that the water depths were commonly deeper than 200 m and even deeper than 500 m through some intervals of the Talung Formation (Fig. 3.4; He et al. 2007c; Xiao et al. 2017).

At Zhongzhai, the upper part (Beds 4–26) of the Lungtan Formation is dominated by fine-grained sandstones and muddy siltstones, representing a littoral setting (Zhang et al. 2014). The top part (Bed 27) of the Lungtan Formation is dominated by calcareous mudstones, with fine laminations (see Zhang et al. 2014). The fauna from Bed 27 at Zhongzhai mainly comprises densely-populated, well-preserved brachiopods (forming shell beds) and lacks radiolarians. These features suggest that this interval represents a low-energy back-barrier shallow-marine setting above the fair-weather wave-base (generally shallower than 50 m deep, see Immenhauser 2009; Shen et al. 2011) (Fig. 3.4; He et al. 2017).

At Huangzhishan, the basal part (Beds 19–36) of the Yinkeng Formation is dominated by calcareous mudstones and marls, abnormally with abundant brachiopods and lacks radiolarians. The microfacies and palaeontological features suggest these intervals were mainly deposited in a shallow, low-energy setting just below the fair-weather wave-base (slightly deeper than 50 m deep; see Chen et al. 2009; Immenhauser 2009) (Fig. 3.4; He et al. 2017).

At Daoduishan, the upper part (Beds 14–24) of the Changhsing Formation is dominated by bioclastic limestones, with tempestite-related structures (He et al. 2016), and with abundant conodonts and benthonic invertebrates, together with a few spherical radiolarians. The presence of tempestite-related structures suggests that the palaeo-water depth was near the storm wave base (50–250 m deep, see Immenhauser 2009), while the presence of spherical radiolarians indicates a water depth deeper than Huangzhishan or Zhongzhai but <100 m. Therefore, the water depths would have been 50–100 m during the late Changhsingian at Daoduishan (Fig. 3.4; He et al. 2017).

In summary, the depth-related palaeoenvironments in South China are further classified into three types in this chapter, based on the above bathymetric analysis, in order to discuss on the relationship between body-size changes and palaeobathmetry. Type 1 is of shallow-water settings (i.e., *ca* 0–50 m deep, including Zhongzhai, Huangzhishan, Xiejiaping, Dengcaoba) (Fig. 3.4). Type 2 is of moderately deep-water setting (i.e., 50–100 m, including Daoduishan). Type 3 is of deep-water settings (i.e., *ca* 100–500 m or even deeper than 500 m, represented by Xinmin, Majiashan, Duanshan, Hushan, Rencunping, Shaiwa, Shangname, Dongpan, Paibi, Liuqiao) (Fig. 3.4).

References

Bu JJ, Wu SB, Zhang HL, Meng YY, Zhang F, Zhang LY. 2006. Permian–Triassic Cephalopods from Dongpan Section, Guangxi, and its geological significance. Geological Science and Technology Information, 25: 47–51. [in Chinese with English abstract].

Chen J, Henderson CM, Shen SZ. 2008. Conodont succession around the Permian–Triassic Boundary at the Huangzhishan section, Zhejiang and its stratigraphic correlation. Acta Palaeontologica Sinica, 47: 91–114.

Chen ZQ, Shi GR, Yang FQ, Gao YQ, Tong JN, Peng YQ. 2006. An ecologically mixed brachiopod fauna from Changhsingian deep-water basin of South China: consequence of end-Permian global warming. Lethaia, 39: 79–90.

Chen ZQ, Tong JN, Zhang KX, Yang H, Liao ZT, Song HJ, Chen J. 2009. Environmental and biotic turnover across the Permian–Triassic boundary on a shallow carbonate platform in western Zhejiang, South China. Australian Journal of Earth Sciences, 56: 775–797.

Dittert N, Henrich R. 2000. Carbonate dissolution in the South Atlantic Ocean: evidence from ultrastructure breakdown in Globigerina bulloides. Deep-Sea Research I, 47: 603–620.

Edmond JM, Huh Y. 2003. Non-steady state carbonate recycling and implications for the evolution of atmospheric Pco_2. Earth and Planetary Science Letters, 216: 125–139.

Feng QL, He WH, Gu SZ, Meng YY, Jin YX, Zhang F. 2007. Radiolarian evolution during the latest Permian in South China. Global and Planetary Change, 55: 177–192.

Gao Y, Shi GR, Peng YQ. 2009. A new bivalve fauna from the Permian–Triassic boundary section of southwestern China. Alcheringa, 33: 33–47.

Gu SZ, Feng QL, He WH. 2007. The latest Permian deep-water fauna: Latest Changhsingian small foraminifers from southwestern Guangxi, South China. Micropaleontology, 53: 311–330.

Gui BW, Feng QL, Yuan AH. 2009. Late Changhsingian (Latest Permian) Radiolarians from Chaohu, Anhui. Journal of Earth Sciences, 20: 797–810.

He WH, Shen SZ, Feng QL, Gu SZ. 2005. A late Changxingian (Late Permian) deep-water brachiopod fauna from the Talung Formation at the Dongpan Section, Southern Guangxi, in South China. Journal of Paleontology, 79: 927–938.

He WH, Shi GR., Feng QL., Peng YQ. 2007a. Discovery of late Changhsingian (latest Permian) brachiopod *Attenuatella* species from South China. Alcheringa, 31: 271–284.

He WH, Feng QL, Elizabeth AW, Gu SZ, Meng YY, Zhang F, Wu SB. 2007b. A Late Permian to Early Triassic bivalve fauna from the Dongpan section, southern guangxi, South China. Journal of Paleontology, 81: 1009–1019.

He WH, Shi GR, Feng QL, Campi MJ, Gu SZ, Bu JJ, Peng YQ, Meng YY. 2007c. Brachiopod miniaturization and its possible causes during the Permian–Triassic crisis in deep water environments, South China. Palaeogeography, Palaeoclimatology, Palaeoecology, 252: 145–163.

He WH, Zhang Y, Zheng YE, Zhang KX, Gui BW, Feng QL. 2008a. A late Changhsingian (latest Permian) radiolarian fauna from Chaohu, Anhui and a comparison with its contemporary faunas of South China. Alcheringa, 32: 199–222.

He WH, Shi GR, Gao YQ, Peng YQ, Zhang Y. 2008b. A new Early Triassic microgastropod fauna from the Zhongzhai section, southwestern China. Proceedings of Royal Society of Victoria, 120: 157–166.

He WH, Zhang Y, Zhang Q, Zhang KX, Yuan AH, Feng QL. 2011. A latest Permian radiolarian fauna from Hushan, South China and its geological implications. Alcheringa, 35: 471–496.

He WH, Shi GR, Zhang Y, Yang TL, Zhang KX, Wu SB, Niu ZJ, Zhang ZY. 2014. Changhsingian (latest Permian) deep-water brachiopod fauna from South China. Journal of Systematic Palaeontology, 12: 907–960.

He WH, Shi GR, Twitchett RJ, Zhang Y, Zhang KX, Song HJ, Yue ML, Wu SB, Wu HT, Yang TL, Xiao YF. 2015. Late Permian marine ecosystem collapse began in deeper waters: evidence from brachiopod diversity and body size changes. Geobiology, 13: 123–138.

He WH, Shi GR, Yang TL, Zhang KX, Yue ML, Xiao YF, Wu HT, Chen B, Wu SB. 2016. Patterns of brachiopod faunal and body-size changes across the Permian–Triassic boundary: evidence from the Daoduishan section in Meishan area, South China. Palaeogeography, Palaeoclimatology, Palaeoecology, 448: 72–84.

He WH, Shi GR, Xiao YF, Zhang KX, Yang TL, Wu HT, Zhang Y, Chen B, Yue ML, Shen J, Wang YB, Yang H, Wu SB. 2017. Body-size changes of latest Permian brachiopods in varied palaeogeographic settings in South China and implications for controls on animal miniaturization in a highly stressed marine ecosystem.

Palaeogeography, Palaeoclimatology, Palaeoecolog, 486: 33–45.

Immenhauser A. 2009. Estimating palaeo-water depth from the physical rock record. Earth Science Reviews, 96: 107–139.

Kozur H. 1993. Upper Permian radiolarians from the Sosio Valley Area, Western Sicily (Italy) and from the uppermost Lamar Limestone of West Texas. Jahrbuch der Geologischen Bundesanstalt Wien, 136: 99–123.

Liu GC, Feng QL, Shen J, Yu JX, He WH, Algeo T. 2013. Decline of siliceous sponges and spicule miniaturization induced by marine productivity collapse and expanding anoxia during the Permian–Triassic crisis in South China. Palaios, 28: 664–679.

Peng YQ, Shi GR, Gao YQ, He WH, Shen SZ. 2007. How and why did the Lingulidae (Brachiopoda) not only survive the end-Permian mass extinction but also thrive in its aftermath? Palaeogeography, Palaeoclimatology, Palaeoecology, 252: 118–131.

Shen SZ, Crowley JL, Wang Y, Bowring SA, Erwin DH, Sadler PM, Cao CQ, Rothman DH, Henderson CM, Ramezani J, Zhang H, Shen YA, Wang XD, WangW, Mu L, Li WZ, Tang YG, Liu XL, Liu LJ, Zeng Y, Jiang YF, Jin YG. 2011. Calibrating the End-Permian Mass Extinction. Science, 334: 1367–1372.

Song QQ, Yu JX, Feng JP, Huang QS. 2015. Palaeobotany of the Upper Permian Dalong Formation (Marine Facies) in South Guizhou. Geological Science and Technology Information, 34: 63–66. [in Chinese with English abstract].

Weber ME, Pisias NG. 1999. Spatial and temporal distribution of biogenic carbonate and opal in deep-sea sediments from the eastern equatorial Pacific: implications for ocean history since 1.3 Ma. Earth and Planetary Science Letters, 174: 59–73.

Weber ME, von Stackelberg U. 2000. Variability of surface sediments in the Peru Basin: dependence on water depth, productivity, bottom water flow, and seafloor topography. Marine Geology, 163: 169–184.

Wu HT, He WH, Shi GR, Zhang KX, Yang TL, Zhang Y, Xiao YF, Chen B, Wu SB. A new Permian–Triassic boundary brachiopod fauna from Xinmin section, southwestern Guizhou, South China and its extinction patterns. 2018, 42: 339–372.

Xiang Y, Feng QL, Shen J, Zhang N. 2013. Changhsingian radiolarian fauna from Anshun, Guizhou, and its relationship to TOC and paleoproductivity. Science China: Earth Sciences, 43: 1047–1056. [in Chinese with English Abstract].

Xiao YF, Suzuki N, He WH. 2017. Water depths of the latest Permian (Changhsingian) radiolarians estimated from correspondence analysis. Earth-Science Reviews, 173: 141–158.

Yang TL, He WH, Zhang KX, Wu SB, Zhang Y, Yue ML, Wu HT, Xiao YF. 2015. Palaeoecological insights into the Changhsingian–Induan (latest Permian–earliest Triassic) bivalve fauna at Dongpan, southern Guangxi, South China. Alcheringa, 40: 98–117.

Yuan AH, Crasquin-Soleau S, Feng QL, Gu SZ. 2007. Latest Permian deep-water ostracods from southwestern Guangxi, South China. Journal of Micropalaeontology, 26: 169–191.

Zhang Y, He WH. 2009. Brachiopod fauna of Duanshan Section in Guizhou Province, and its geological significance. Geological Science and Technology Information, 28: 15–37. [in Chinese with English abstract].

Zhang Y, He WH, Shi GR, Zhang KX. 2013. A new Changhsingian (Late Permian) Rugosochonetidae (Brachiopoda) fauna from the Zhongzhai section, southwestern Guizhou Province, South China. Alcheringa, 37: 223–247.

Zhang Y, Shi GR, He WH, Zhang KX, Wu HT. 2014. A new Changhsingian (Late Permian) brachiopod fauna from the Zhongzhai section (South China), Part 2: Lingulida, Orthida, Orthotetida and Spiriferida. Alcheringa, 38: 480–503.

4 Age Analysis and Biostratigraphic Correlation

Wei-Hong He, G. R. Shi, Ke-Xin Zhang, and Shun-Bao Wu

In order to decipher brachiopod diversity and body-size changes in relation to varied palaeobathymetry and time, the stratigraphic divisions in each section and age correlation among sections are essential for the study. Details of each section are thus given below.

At Hushan, the cephalopod *Lopingoceras* sp. was found in Bed 89 of the section, ammonoids *Pernodoceras* sp. and *Pleuronodoceras* sp. were found in Bed 83 in the upper part of the Talung Formation, and the bivalve *Hunanopecten exilis* was found in Beds 73 and 88 (He et al. 2011). The ammonoid *Ophiceras* sp. was found in Bed 94 of the basal part of the Lower Chinglung Formation at Hushan (Fig. 3.1; He et al. 2011). According to the study of the Permian–Triassic biostratigraphy, *Lopingoceras* sp. is common within the Upper Permian of South China (Zhao et al. 1978). Both *Pernodoceras* sp. and *Pleuronodoceras* sp. from the upper Talung Formation are regarded as index fossils of the *Pseudotirolites–Pleuronodoceras* Zone of late Changhsingian age (Zhao et al. 1978; Yang et al. 1987). *Hunanopecten exilis* is typical for the Late Permian (Yin 1985). The genus *Ophiceras* is typical for the Induan (earliest Triassic) (Guo 1982). Therefore, the upper Talung Formation is assigned approximately to the late Changhsingian (latest Permian) while the basal part of the Lower Chinglung Formation can be considered to belong to the Induan (earliest Triassic) (Fig. 3.1; He et al. 2011).

At Majiashan, the ammonoid *Konglingites* sp. was found from Bed 1, *Tapashanites* sp. from Bed 3 to the basal part (20 cm) of Bed 10, *Pseudotirolites* spp. and *Rododiscoceras* spp. from the lower part of Bed 10 to Bed 16 and *Ophiceras* sp. from Bed 20 (Fig. 3.1; see He et al. 2008). *Konglingites* is the index fossil of the *Konglingites* Zone and typical of the Wuchiapingian (Zhao et al. 1978; Yang et al. 1987). *Tapashanites* is the index fossil of the *Tapashanites* Zone and typical for the early Changhsingian (Zhao et al. 1978; Yang et al.

W.-H. He (✉) · K.-X. Zhang
State Key Laboratory of Biogeology and Environmental Geology, School of Earth Sciences, China University of Geosciences, Wuhan, China
e-mail: whzhang@cug.edu.cn; kx_zhang@cug.edu.cn

G. R. Shi
School of Life and Environmental Sciences, Burwood, Victoria, Australia

Deakin University, Geelong, Victoria, Australia
e-mail: grshi@deakin.edu.au

S.-B. Wu
School of Earth Sciences, China University of Geosciences, Wuhan, China
e-mail: sbwu@cug.edu.cn

W.-H. He et al. (eds.), *Brachiopods around the Permian-Triassic Boundary of South China*, New Records of the Great Dying in South China, https://doi.org/10.1007/978-981-13-1041-6_4

1987). *Pseudotirolites* and *Rododiscoceras* are both index fossils of the *Pseudotirolites–Rododiscoceras* Zone and typical for the late Changhsingian (Zhao et al. 1978; Yang et al. 1987). As mentioned above, *Ophiceras* is typical for the earliest Triassic. Beds 3–16, therefore, are assigned to the Changhsingian, and Bed 20 to the earliest Triassic (Fig. 3.1; He et al. 2015). Although no index fossils characteristic of the PTB has been found from Beds 17–19, we place the PTB in the middle of Bed 19, based on its similarity and equivalence to the Permian–Triassic Boundary Stratigraphic Set (PTBS) (see Peng et al. 2001 for description and correlation of PTBS), which has been precisely matched with the same set at Meishan (Fig. 3.1). It is because this correlation, Bed 17 at Majiashan, a 4-cm interval of pale volcanic claystones, can be matched to the 'White clay' of Bed 25 of the Meishan section. Likewise, Bed 18 at Majiashan, comprised of dark green calcareous mudstones, can be correlated to the 'Black clay' of Bed 26 of Meishan, and Bed 19 (gray limestones) correlated to the limestones of Bed 27 at Meishan.

At Rencunping, the *Clarkina yini* Zone has been found from Bed 22 to the middle part of Bed 23d (He et al. 2015). Conodont *Clarkina meishanensis* first appears in the upper part of Bed 23d (He et al. 2015). These suggest that Bed 22 to the middle part of Bed 23d are equivalent to the top part of Bed 22 to Bed 24d at Meishan (as constrained by the *C. yini* Zone), and the upper part of Bed 23d is equivalent to the base of Bed 24e at Meishan (He et al. 2015). Additionally, ammonoids of the *Sinoceltites* Zone (equivalent to the *Tapashanites* Zone) and of the *Pseudotirolites–Rotodiscoceras* Zone have been found, respectively, from Bed 18 to the lower part of Bed 20 and from the upper part of Bed 20 to Bed 24 at Rencunping (Fig. 3.1; see Zhang et al. 2009). Ammonoids of the *Sinoceltites* and *Pseudotirolites–Rotodiscoceras* Zones, respectively, suggest ages of early and late Changhsingian (Yang et al. 1987). Ammonoids of the *Ophiceras* Zone, typical for the Induan (Yin et al. 2001), have been found in the upper part of Bed 27 at Rencunping (Fig. 3.1; see Zhang et al. 2009). Beds 18–24 at Rencunping, therefore, can be reliably assigned to the Changhsingian, and the upper part of Bed 27 to Bed 29 to the earliest Triassic, with the PTB placed in the middle of Bed 27, as defined by the first appearance of *Ophiceras* sp. (Fig. 3.1).

At Xinmin, ammonoids *Pseudotirolites* spp., *Rotodiscoceras* sp., and *Pleuronodoceras* sp. (index fossils of *Pseudotirolites–Rotodiscoceras* Zone) were commonly found from Bed 1 to the lower part of Bed 5, suggesting that the Talung Formation is of late Changhsingian in age. The ammonoid *Ophiceras* sp. was found in Bed 6 and thus indicates that the basal part of the Daye Formation should be assigned to the Induan (earliest Triassic). Conodont *Hindeodus parvus* was found in the middle part of Bed 5, signaling the base of the Triassic at this level (Fig. 3.1; see Zhang et al. 2014).

At Duanshan, ammonoids *Pseudotirolites* spp., *Huananoceras* sp. and *Xenodiscus* sp. were commonly found from the Talung Formation. At Kejiao (close to Duanshan), ammonoids *Rotodiscoceras* spp. and *Pleuronodoceras* spp. occur abundantly in the Talung Formation. These elements suggest the presence of the *Pseudotirolites–Rotodiscoceras* Zone in the Talung Formation, indicating a late Changhsingian age (Fig. 3.1; see Zhang and He 2009).

At Shaiwa, bivalves *Hunanopecten exilis* and *Claraia primitiva* were found from the Fourth Member of the Shaiwa Group (Yang et al. 2001) and suggest the presence of the *Hunanopecten exilis–Claraia primitiva* Zone (Fig. 3.1). This bivalve zone is equivalent to the bivalve *Hunanopecten exilis* Assemblage of Yin (1985), the latter being typical for the Changhsingian (Yin 1985). Therefore, the Fourth Member of the Shaiwa Group is approximately of Changhsingian (Fig. 3.1; see He et al. 2014).

At Xiejiaping, the ammonoid *Pleuronodoceras* sp. was found in the upper part of the Talung Formation and *Ophiceras* sp. was found in the basal part (Bed 27) of the Daye Formation. Additionally, the Late Permian ammonoid *Huananoceras* sp. and brachiopod *Fusichonetes pygmaea* were found in the upper Talung Formation. These lines of evidence suggest that the upper Talung Formation (Beds 17–26) at Xiejiaping approximately should be assigned to

the late Changhsingian (Fig. 3.2; see He et al. 2014). The ammonoid *Sanyangites* sp. and *Konglingites* sp., both typical for the Wuchiapingian (Zhao et al. 1978; Yang et al. 1987), were found in the lower part of the Talung Formation (Beds 6–9), suggesting a Wuchiapingian age for these beds (Fig. 3.2).

At Dengcaoba, the ammonoid *Pseudotirolites* sp. and brachiopod *Paracrurithyris pygmaea* were found in the upper Talung Formation (Beds 34–36) and both elements are typical for the Changhsingian (Zhao et al. 1978; Yang et al. 1987; Xu and Grant 1994). The Late Permian ammonoid *Huananoceras* sp. was commonly found in the lower Talung Formation. Therefore, the upper Talung Formaton (Beds 34–36) is assigned to the Changhsingian and the lower Talung Formation (Beds 32–33) approximately to the Late Permian (or Wuchiapingian to early? Changhsingian) (Fig. 3.2; see He et al. 2014). The ammonoid *Lytophiceras* sp. was found in Bed 37 of the basal Daye Formation, indicating Bed 37 should be assigned to the Induan (Fig. 3.2).

At Shangname, ammonoids *Pseudotirolites* sp. and *Ophiceras* sp. were respectively found in Bed 2 (Talung Formation) and basal part of Bed 3 (Luolou Formation), suggesting a Changhsingian age for the former and Induan for the latter although these two beds are in fault contact (Fig. 3.2; see He et al. 2014).

At Dongpan, ammonoids *Pseudotirolites* sp., *Rotodiscoceras* sp., *Pernodoceras* sp. and *Dushanoceras* sp., which have been regarded as index fossils of the *Pseudotirolites*–*Rotodiscoceras* Zone, were commonly found in the Talung Formation (Bu et al. 2006). Radiolarian *Albaillella yaoi*, typical for the late Changhsingian (Wu et al. 2010; Zhang et al. 2017), was found in Beds 2–6 in the Talung Formation. The ammonoid *Ophiceras* sp. and bivalve *Claraia wangi* were commonly recorded in the basal part of the Luolou Formation (Bu et al. 2006; He et al. 2007; Yang et al. 2015). Therefore, the Talung Formation should be assigned to the late Changhsingian while the basal Luolou Formation to the Induan (Fig. 3.2).

At Paibi and Liuqiao, radiolarians *Albaillella triangularis* and *A. yaoi* Zones, both of which are equivalent to the *Neoalbaillella optima* Zone and typical for the late Changhsingian (Wu et al. 2010; Zhang et al. 2017), were found in the Talung Formation, suggesting a late Changhsingian age for this formation at Paibi and Liuqiao (Fig. 3.2).

At Huangzhishan, conodonts *Clarkina yini* and *C. meishanensis* Zones were respectively found in the top part of the Changhsing Formation (Beds 9–17) and the basal part of the Yinkeng Formation (Beds 18–36). *Hindeodus parvus* Zone (in Beds 37–42), together with *Ophiceras* sp. (in Bed 43 and upwards), was found in the lower Yinkeng Formation (Fig. 3.3; Chen et al. 2008; He et al. 2015). Therefore, the PTB has been defined at the horizon between Beds 36 and 37 (Fig. 3.3).

At Zhongzhai, the abundant presence of brachiopod *Fusichonetes pygmaea* in Beds 4–27 of the section, typical for the Changhsingian in South China (Shen and Archbold 2002; Zhang et al. 2013), suggests these intervals should have been assigned to the Changhsingian. The U–Pb age in Bed 29 of the section is of 252.24 ± 0.13 Ma and basically equivalent to the calibrated PTB age of 252.17 ± 0.06 Ma in Bed 27c at the GSSP section of Meishan (Shen et al. 2011; Zhang et al. 2014), thus indicating that the PTB is between Beds 29 and 30 (Fig. 3.3).

At Daoduishan, conodonts *Clarkina changxingensis*, *C. yini* and *C. meishanensis* Zones were respectively found in Bed 14 to base of Bed 21, upper part of Bed 21 to Bed 24b and Beds 24c to 26 of the Changhsing Formation (Fig. 3.3; see He et al. 2017). *Hindeodus parvus* was found in the middle of Bed 27 and *Ophiceras* sp. was found in Bed 29 (Fig. 3.3; see He et al. 2017). Therefore, the PTB has been placed in the middle of Bed 27 at Daoduishan (Fig. 3.3).

References

Bu JJ, Wu SB, Zhang HL, Meng YY, Zhang F, Zhang LY. 2006. Permian–Triassic Cephalopods from Dongpan Section, Guangxi, and its geological significance. Geological Science and Technology Information, 25: 47–51. [in Chinese with English abstract].

Chen J, Henderson CM, Shen SZ. 2008. Conodont succession around the Permian–Triassic boundary at the Huangzhishan section, Zhejiang and its stratigraphic correlation. Acta Palaeontologica Sinica, 47: 91–114.

Guo PX. 1982. The stratigraphy and ammonites of Qinglong Group, Anhui. Bulletin of Nanjing Institute of Geology and Mineral Resources, Chinese Academy of Geological Sciences, 3: 92–110. [in Chinese with English abstract].

He WH, Feng QL, Elizabeth AW, Gu SZ, Meng YY, Zhang F, Wu SB. 2007. A Late Permian to Early Triassic bivalve fauna from the Dongpan section, southern guangxi, South China. Journal of Paleontology, 81: 1009–1019.

He WH, Zhang Y, Zheng YE, Zhang KX, Gui BW, Feng QL. 2008. A late Changhsingian (latest Permian) radiolarian fauna from Chaohu, Anhui and a comparison with its contemporary faunas of South China. Alcheringa, 32: 199–222.

He WH, Zhang Y, Zhang Q, Zhang KX, Yuan AH, Feng QL. 2011. A latest Permian radiolarian fauna from Hushan, South China and its geological implications. Alcheringa, 35: 471–496.

He WH, Shi GR, Zhang Y, Yang TL, Zhang KX, Wu SB, Niu ZJ, Zhang ZY. 2014. Changhsingian (latest Permian) deep-water brachiopod fauna from South China. Journal of Systematic Palaeontology, 12: 907–960.

He WH, Shi GR, Twitchett RJ, Zhang Y, Zhang KX, Song HJ, Yue ML, Wu SB, Wu HT, Yang TL, Xiao YF. 2015. Late Permian marine ecosystem collapse began in deeper waters: evidence from brachiopod diversity and body size changes. Geobiology, 13: 123–138.

He WH, Shi GR, Xiao YF, Zhang KX, Yang TL, Wu HT, Zhang Y, Chen B, Yue ML, Shen J, Wang YB, Yang H, Wu SB. 2017. Body-size changes of latest Permian brachiopods in varied palaeogeographic settings in South China and implications for controls on animal miniaturization in a highly stressed marine ecosystem. Palaeogeography, Palaeoclimatology, Palaeoecolog, 486: 33–45.

Peng YQ, Tong JN, Shi GR, Hansen HJ. 2001. The Permian–Triassic boundary set: characteristicsand correlation. Newsletters on Stratigraphy, 39: 55–71.

Shen SZ, Archbold NW. 2002. Chonetoidea (Brachiopoda) from the Lopingian (Late Permian) of South China. Alcheringa, 25: 327–349.

Shen SZ, Crowley JL, Wang Y, Bowring SA, Erwin DH, Sadler PM, Cao CQ, Rothman DH, Henderson CM, Ramezani J, Zhang H, Shen YA, Wang XD, WangW, Mu L, Li WZ, Tang YG, Liu XL, Liu LJ, Zeng Y, Jiang YF, Jin YG. 2011. Calibrating the End-Permian Mass Extinction. Science, 334: 1367–1372.

Wu J, Feng QL, Gui BW, Liu GC. 2010. Some new radiolarian species and genus from Upper Permian in Guangxi Province, South China. Journal of Paleontology, 84: 879–894.

Xu GR, Grant RE. 1994. Brachiopods near the Permian–Triassic boundary in south China. Smithsonian Contributions to paleobiology, 76: 1–68.

Yang FQ, Peng YQ, Gao YQ. 2001. Study on the Late Permian *Claraia* in South China. Science in China (Series D)-Earth Sciences, 44: 797–807.

Yang TL, He WH, Zhang KX, Wu SB, Zhang Y, Yue ML, Wu HT, Xiao YF. 2015. Palaeoecological insights into the Changhsingian–Induan (latest Permian–earliest Triassic) bivalve fauna at Dongpan, southern Guangxi, South China. Alcheringa, 40: 98–117

Yang ZY, Yin HF, Wu SB, Yang FQ, Ding MH, Xu GR. 1987. Permian–Triassic boundary stratigraphy and fauna of South China. Geological Publishing House, Beijing, 378 pp. [in Chinese with English abstract].

Yin HF. 1985. Bivalves near the Permian–Triassic boundary in South China. Journal of Paleontology 59: 572–600.

Yin HF, Zhang KX, Tong JN, Yang ZY, Wu SB. 2001. The Global Stratotype Section and Point (GSSP) of the Permian–Triassic boundary. Episodes, 24: 102–114.

Zhang Y, He WH. 2009. Brachiopod fauna of Duanshan Section in Guizhou Province, and its geological significance. Geological Science and Technology Information, 28: 15–37. [in Chinese with English abstract].

Zhang Y, He WH, Shi GR, Zhang KX. 2013. A new Changhsingian (Late Permian) Rugosochonetidae (Brachiopoda) fauna from the Zhongzhai section, southwestern Guizhou Province, South China. Alcheringa, 37: 223–247.

Zhang Y, Shi GR, He WH, Zhang KX, Wu HT. 2014. A new Changhsingian (Late Permian) brachiopod fauna from the Zhongzhai section (South China), Part 2: Lingulida, Orthida, Orthotetida and Spiriferida. Alcheringa, 38: 480–503.

Zhang Y, Shi GR, Wu HT, Yang TL, He WH, Yuan AH, Lei Y. 2017. Community replacement, ecological shift and early warning signals prior to the end-Permian mass extinction: A case study from a nearshore clastic-shelf section in South China. Palaeogeography, Palaeoclimatology, Palaeoecology, 487: 118–135.

Zhang N, Jiang HS, Zhong WL. 2014. Conodont Biostratigraphy across the Permian–Triassic Boundary at the Xinmin Section, Guizhou, South China. Journal of Earth Science, 25: 779–786.

Zhang ZY, He WH, Zhang Y, Yang TL, Wu SB. 2009. Late Permian–earliest Triassic ammonoid sequences from the Rencunping section, Sangzhi County, Hunan Province, South China and their regional correlation. Geological Science and Technology Information, 28: 23–30. [in Chinese with English abstract].

Zhao JK, Liang XL, Zheng ZG. 1978. Late Permian cephalopods of South China. Palaeontologia Sinica, Series B, 12: 1–194. [in Chinese with English abstract].

Materials and Methods

5

Wei-Hong He, G. R. Shi, Ting-Lu Yang, and Yong-Biao Wang

5.1 Taphonomic Features of Brachiopods

Brachiopods collected from siliceous mudstone facies, including Hushan, Majiashan, Rencunping, Xinmin, Duanshan, Shaiwa, Xiejiaping, Dengcaoba, Dongpan, Paibi and Liuqiao sections, are devoid of abrasional signs. In these sections, they occur sparsely on bedding surfaces and occasionally have articulated valves. These taphonomic features indicate that the brachiopods have been preserved mostly *in situ*, with little postmortem transportation and reworking.

Brachiopods collected from Huangzhishan, Zhongzhai and Shangname sections also lack abrasional signs, are randomly arranged on bedding surfaces without particular orientation, and many contain articulated valves, all taphonomic features indicating very limited or no postmortem transportation. Brachiopods collected from the Daoduishan section have both complete and incomplete valves, but these valves are randomly arranged on bedding surfaces, suggesting limited transportation. Those incomplete valves possibly have suffered from stirring of storm, an inference also corroborated by the presence of hummocky cross stratification observed in some beds within the Changhsing Formation at Daoduishan (He et al. 2016).

5.2 Methods of Brachiopod Sampling and Selection of Studied Faunas

The fossil collection began in the summer of 2002 and continued to 2016. As mentioned in the part of Introduction, more than 10,000 brachiopod specimens have been collected from 15 sections in South China. Brachiopods were collected from the Changhsingian or the upper part of Changhsingian and the basal Induan of the studied sections. All brachiopods found during

W.-H. He (✉)
State Key Laboratory of Biogeology and Environmental Geology, School of Earth Sciences, China University of Geosciences, Wuhan, China
e-mail: whzhang@cug.edu.cn

G. R. Shi
School of Life and Environmental Sciences, Burwood, Victoria, Australia

Deakin University, Geelong, Victoria, Australia
e-mail: grshi@deakin.edu.au

T.-L. Yang
Faculty of Geosciences, East China University of Technology, Nanchang, China
e-mail: yang@geology.hk

Y.-B. Wang
School of Earth Sciences, China University of Geosciences, Wuhan, China
e-mail: wangybcug@163.com

W.-H. He et al. (eds.), *Brachiopods around the Permian-Triassic Boundary of South China*, New Records of the Great Dying in South China, https://doi.org/10.1007/978-981-13-1041-6_5

excavating beds included both complete individuals and fragments. To facilitate quantitative and statistical analyses of brachiopod diversity and body-size changes, we counted brachiopod individuals for each species (including indeterminate species) in each bed. During counting, if both a body fossil and its mold are preserved together, or both the ventral and dorsal valves of the same fossil are preserved, then all of these are counted as one individual. Isolated molds and ventral or dorsal valves found without counterparts, are treated as independent individuals.

In order to investigate the evolution of brachiopod diversity through time, the brachiopod faunas from Huangzhishan, Meishan, Rencunping and Majiashan sections have been chosen for the study. The first two sections represent a shallow-water setting, in contrast to the last two sections which were deposited in relatively deep-water settings. As already outlined in Chap. 4, the ages and correlations of these four sections are well constrained, therefore enabling a detailed temporal analysis of the brachiopod diversity changes. Moreover, the taxonomy of the brachiopods has been studied in detail at the four sections, thus bringing taxonomic consistency and integrity to the diversity analysis.

Alongside the species diversity analysis through time, body-size changes of the brachiopods in varied palaeogeographic settings have also been investigated, using two most commonly found Changhsingian chonetid brachiopod species, *Fusichonetes pygmaea* and *Fusichonetes quadrata*, from five sections (Zhongzhai, Huangzhishan, Daoduishan, Majiashan, Rencunping). These sections have been selected because together they constituted an approximately-defined basinwide bathymetric gradient spanning the shallow-water clastic shelf, shallow-water carbonate platform and ramp, and deep-water siliceous basinal settings. Parallel to this analysis, we also performed a temporal analysis of brachiopod body-size changes to test whether or not, and how, the brachiopod body sizes responded to the end-Permian mass extinction. This analysis was carried out by using two most commonly found species from three different sections: *Paracrurithyris pygmaea* at Rencunping and Majiashan and *Fusichonetes pygmaea* at Daoduishan. Additionally, the two species were chosen because they both survived the end-Permian mass extinction.

5.3 Definition and Measurement of Body Sizes of Brachiopods

The width of each brachiopod individual refers to the shell width and the length of each individual refers to the shell length (Fig. 5.1). The width and length of all individuals were measured with an electronic calliper to the nearest 0.1 mm. The body size (g) of a brachiopod individual refers to the geometric mean of the length and width, following Jablonski (1996).

The mean size (X) for each species in each bed of the section is determined by the following equation:

$$X = 1 / N^{*} \sum_{i=1}^{N} gi$$

where X equals the mean size, N equals the total number of individuals in a bed of the section, and g is the geometric mean of length and width of each individual in each bed of the section.

The X_{mean} is the average value of geometric means (g) for all individuals of a species through the section. As such, the X_{mean} was used to represent the average size of a fauna in a section.

The X_{median} was also used to represent the average size of a fauna from a section. It refers to the median value of geometric means (g) for all individuals of a species through the section. The X_{median} values from the studied sections were plotted using the software PAST (see Hammer et al. 2001). Usually, the X_{median} is close to the value of X_{mean} and the statistically significant differences of X_{median} from the studied sections can be tested by the Mann–Whitney test (see below). So both X_{median} and X_{median} are adopted to study the difference of body sizes among different sections (different palaeogeographic settings).

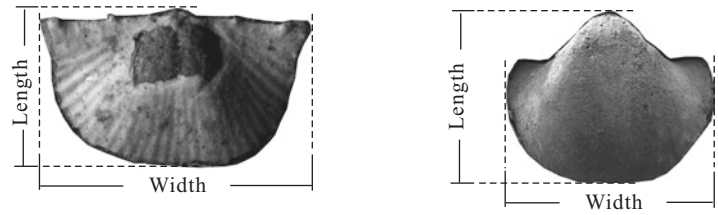

Fig. 5.1 Biometric measurements of varied shell morphology of brachiopods used for this book

5.4 Notes on Other Statistic Techniques

To determine the sampling efficiency to see how well each bed was sampled, a rarefaction analysis was conducted at Huangzhishan, Rencunping and Majiashan (These three sections were sampled for brachiopod collection, proper for the rarefaction analysis; but the Meishan section is a referred section and was not sampled for brachiopod collection in this book, not proper for the rarefaction analysis.) This is an interpolation technique that allows an estimation of how many species would have been found had the sample been larger than it actually was (for the technique see Raup 1975). A curve that is approaching an asymptote indicates that the sample is relatively complete, and any further collection is unlikely to add new taxa, while a curve that is still relatively steep indicates incomplete sampling, as unrecorded species are still likely to be found. The results of rarefaction analysis revealed that most intervals have been well sampled, while the intervals above the mass extinction horizon (or horizons) are less complete, because of the natural scarcity of fossils in these layers (see Fig. 5.2).

To test the numbers of pulses in a mass extinction event before estimating the position of the extinction boundary, the method of Wang and Everson (2007) was used (see Chap. 6). And to estimate the position of a mass extinction boundary for brachiopods near the PTB at the Huangzhishan, Meishan, Rencunping and Majiashan sections and to compare the initial timing of disappearances/extinctions among varied palaeogeographic settings, the improved confidence interval technique of Wang and Marshall (2004) was deployed (see Chap. 6).

5.5 Statistical Tests of the Significance of Body-Size Changes

To investigate the changes of body size at varied palaeogeographic settings and to test whether the body-size changes are statistically significant among the studied sections (Zhongzhai, Huangzhishan, Daoduishan, Majiashan, Rencunping), first, the Shapiro–Wilk test and Histogram (using Software PAST), were adopted to determine whether or not the size frequency distribution in each of the sections followed the normal distribution (Fig. 5.3). For the Shapiro–Wilk test, if the given p is <0.05, normal distribution can be rejected ($N > 3$ and <5000, see Hammer and Harper 2006 or http://folk.uio.no/ohammer/past) and if $N < 30$, the power of Shapiro–Wilk test is still low (Razari and Wah 2011). Thus, Fig. 5.3a–c and e are not normal distributions ($p < 0.05$). Additionally, both Fig. 5.3h and i are perhaps not normal distributions based on the histograms. Therefore, the results show that most size frequency distributions from the studied sections are not normal distributions (Fig. 5.3). Consequently, the non-parametric Mann–Whitney test (using Software PAST) was used to determine the significant differences in the median sizes (X_{median}) of the brachiopods among the studied sections. The results show that the difference in median sizes between the two groups of sections (i.e., the Huangzhishan and Zhongzhai as one group representing shallow-water settings while the Daoduishan, Majiashan, and Rencunping together representing the other group of moderately deep- to deep-water settings) is statistically significant ($P < 0.05$, see

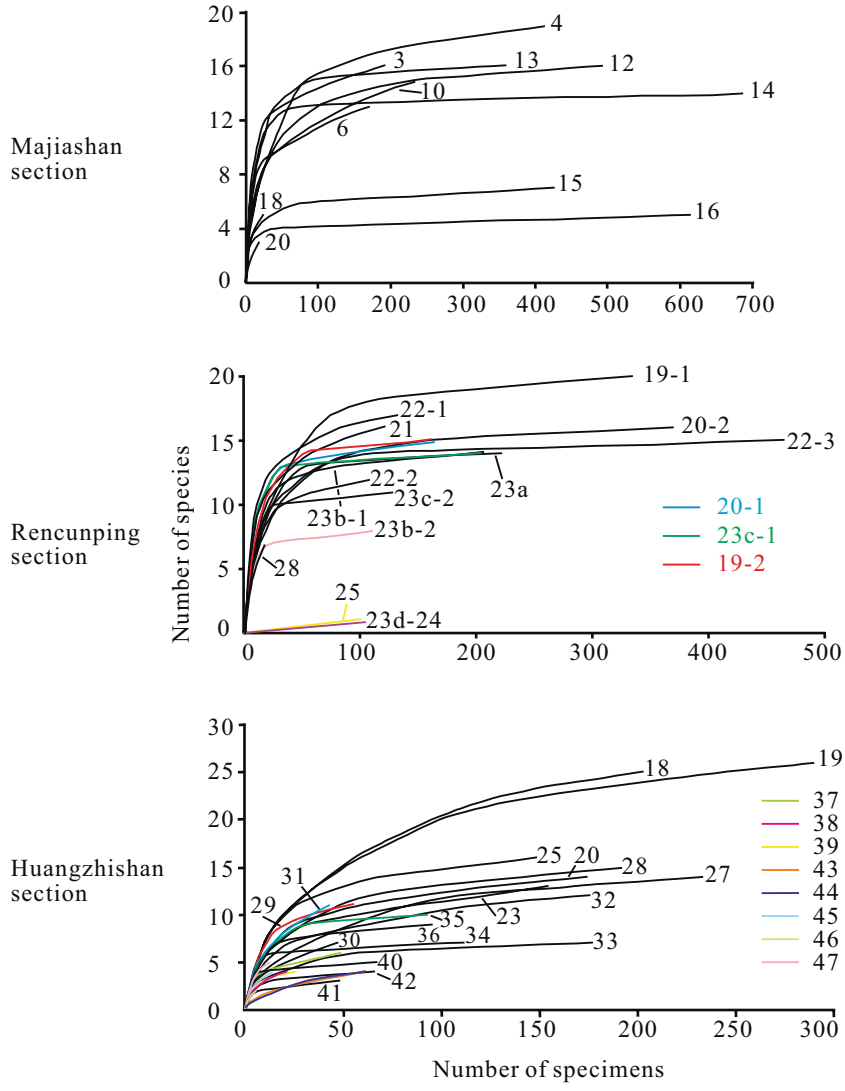

Fig. 5.2 Rarefaction curves (specimens vs. species) for each bed at the studied sections used for comparing the diversity evolution among varied palaeogeographic settings (Revised after He et al. 2015a)

Table 5.1), although the difference of medians for *F. quadrata* is not significant between Zhongzhai and Majiashan (P = 0.3622, see Table 5.1).

To investigate whether the brachiopod body sizes before and after the end-Permian mass extinction were statistically different, and to determine whether successively recorded changes in mean body size were statistically significant, we performed the following analyses in steps. First, the mean sizes (the definition sees 5.3 in this chapter) of *Paracrurithyris pygmaea* from Rencunping and Majiashan and *Fusichonetes pygmaea* from Daoduishan were calculated (details see He et al. 2015a, 2016). Then, the means were subjected to the confidence interval test (He et al. 2015a, 2016). The test has generated the following results: the body sizes of *Paracrurithyris pygmaea* significantly decreased from Beds 22-3 to 23a and then significantly increased from Beds 23b to 23d–24 at Rencunping; the body sizes of *Paracrurithyris pygmaea* significantly decreased from Beds 10 to 12, followed by a significant

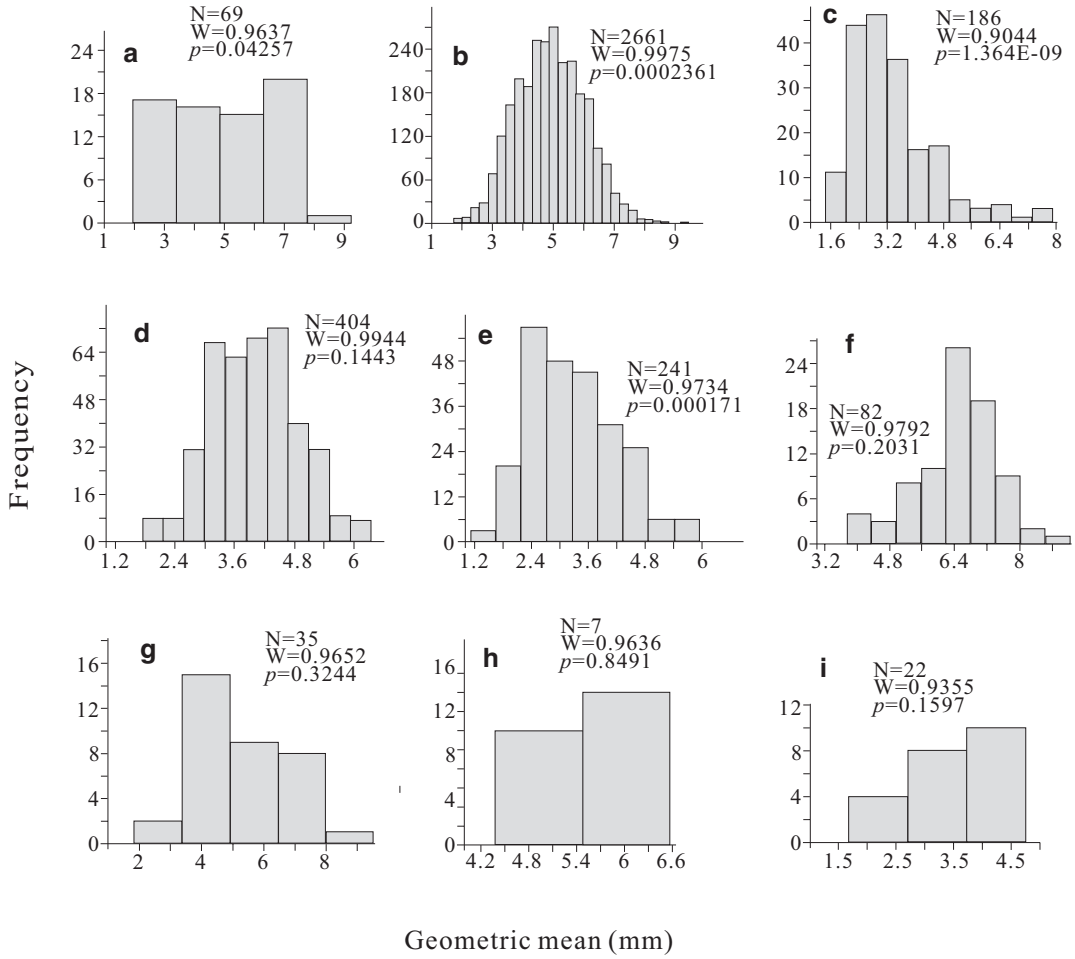

Fig. 5.3 Histograms of size-frequency distribution and results of Shapiro–Wilk test (revised after He et al. 2017). (**a**–**e**), for specimens of *Fusichonetes pygmaea*; (**f**–**i**), for specimens of *Fusichonetes quadrata*. a, f- Huangzhishan; b, g- Zhongzhai; c- Daoduishan; d, h- Majiashan; e, i- Rencunping. N- number of specimens. W- Shapiro–Wilk test statistic; if the given *p* is less than 0.05 for Shapiro–Wilk test, normal distribution can be rejected (N > 3 and <5000, see Palaeontological Statistics, version 3.0 or http://folk.uio.no/ohammer/past) and if N < 30, the power of Shapiro–Wilk test is still low, see Razali and Wah 2011), so Fig. 5**a**–**c** and **e** are not normal distributions, and both 5**h** and **i** are perhaps not normal distributions based on histograms

increase from Beds 14 to 15 at Majiashan; the body sizes of *Fusichonetes pygmaea* at Daoduishan significantly decreased from Beds 19 to 21 and again from Beds 24e to 26 (Fig. 5.4). These results are strongly corroborated by the outcomes of another two independent tests (Kolmogorov–Smirnov Test and "Jablonski plots") (see He et al. 2015a, 2016), suggesting the robustness of these derived body-size change patterns.

5.6 Phylogenetic Analysis

The genus *Parapygmochonetes* has some features suggesting affinities with both Subfamily Caenanopliinae Archbold, 1980 and Subfamily Linoproductinae Stehli, 1954. To determine which subfamily the genus should be assigned to, a parsimony analysis was conducted using the software PAUP version 4.0a (Swofford 2002). Parsimony analysis was chosen because among

Table 5.1 *P* values of Mann—Whitney test

F. pygmaea					
P values	Huangzhishan	Zhongzhai	Daoduishan	Rencunping	Majiashan
Huangzhishan		0.9531	**8.962E-11**	**3.92E-12**	**4.085E-05**
Zhongzhai			**9.48E-55**	**1.448E-78**	**2.381E-53**
Daoduishan				0.7623	**2.078E-16**
Rencunping					**3.776E-20**
Majiashan					
F. quadrata					
P values	Huangzhishan	Zhongzhai	Rencunping		Majiashan
Huangzhishan		**1.895E-05**	**5.32E-12**		**0.008953**
Zhongzhai			**1.251E-05**		0.3622
Rencunping					**0.0001465**
Majiashan					

After He et al. (2017)

Note: *P* values marked by bold show that the paired populations from two different sections are statistically significantly different with respect to median size at the 95% confidence level ($P < 0.05$)

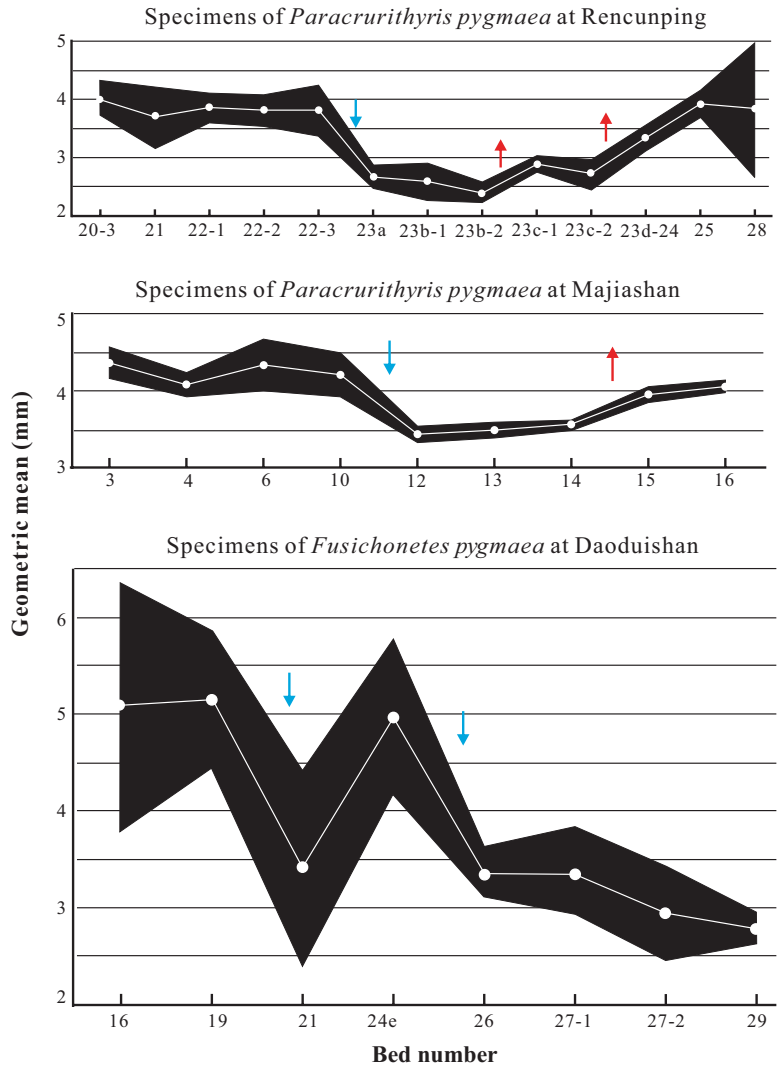

Fig. 5.4 Variation of means (X) of geometric means of the species at Rencunping, Majiashan and Daoduishan (Rencunping and Majiahsan after He et al. 2015a; Daoduishan after He et al. 2016). Note: The black area represents the 95% confidence interval of mean; the central line linking the white dots represents the mean at the 95% confidence interval; blue (down) arrows indicate significantly reduced means at the 95% confidence interval; red (up) arrows indicate significantly increased means at the 95% confidence interval

Table 5.2 Character descriptions of the genera of subfamilies Caenanopliinae and Linoproductinae

NC	Character	Character states (coding)
1	Shell width of type species for each genus	≧1 cm (1),<1 cm (0)
2	Outline	semicircle/sub-quadrate (0); sub-triangular (1)
3	Longitudinal profile	strongly- to moderately-arched (0); weakly-arched (1)
4	Lateral profile	concavoconvex (0); planoconvex (1)
5	Greatest width	at hinge (0); not at hinge (1)
6	Flanks	steeply sloping (1); gently sloping (0)
7	Interarea	Developed (1); not developed or line-shaped (0)
8	Pseudodeltidium	Developed (1); not developed (0)
9	Ears	Large (1); small to medium (0)
10	Ears radially- or concentrically-ornamented	Smooth or radially-ornamented (0); concentrically-ornamented (1)
11	Ears spinosely-ornamented or not	Spinose (1); no spine (0)
12	Costellae bifurcated or not	Bifurcated (1); no bifurcation (0)
13	Costellae strong or weak	Coarse/strong (1); thin/weak/smooth (0)
14	Costellae wavy or straight	Wavy (0); straight (1)
15	Ventral spines	Present (1); absent (0)
16	Dorsal spines/dimples	Present (1); absent (0)
17	Endospines/papillae	Present (1); absent (0)
18	Tail	Present (1); absent (0)
19	Marginal ridges	Present (1); absent (0)
20	Ventral median septum	Present (1); absent (0)
21	Dorsal median septum	Present (1); absent (0)
22	Dorsal accessory septa	Present (1); absent (0)
23	Interspace between costellae	Wide or weak (0); narrow but prominent(1)

NC- number code for characters

all approaches of phylogenetic analysis, it is probably the most intuitive (Jaynes 2003; He et al. 2015b) and requires the smallest number of character changes to suggest the most likely correct phylogenetic inference (Sober 1983; Jaynes 2003). The detailed analytical procedure follows Jaynes (2003).

Most of the 24 genera known in the subfamilies of Caenanopliinae Archbold, 1980 and Linoproductinae Stehli 1954 have been selected for the parsimony analysis.?*Mistproductus* Yang (1991), *Bandoproductus* Jing and Sun (1981), *Corbicularia* Ljaschenko (1973), *Costachonetes* Waterhouse (1975) and *Costachonetina* Waterhouse (1981) were excluded because of their uncertain generic indentity or poor knowledge of interior features. A total of 23 characters were coded for the studied genera (Table 5.2). All characters were equally weighted in the quantitative analysis (Table 5.2). All of these 23 characters occurring in each genus were carefully checked and verified based on the features (details of values see Table 5.2), and then tabulated in the data matrix (Table 5.3). Except for the ingroup taxa that were targeted for the parsimony analysis, two outgroup taxa (*Chlupacina* Havlíček and Racheboeuf 1979 and *Leptochonetes* Havlíček and Racheboeuf 1979) from phylogenetically different groups were included in this analysis (Table 5.3). The result of the phylogenetic trees is given in Chap. 9.

Table 5.3 Characters dataset of ingroup genera within the subfamilies Caenanopliinae of Racheboeuf in Williams et al. (2000) and Linoproductinae of Brunton et al. in Williams et al. (2000) (including the study genus *Parapygmochonetes*) and both outgroup genera *Chlupacina* and *Leptochonetes*

	Characters																						
List of genera	1	2	3	4	5	6	7	8	9	10	11	12	13	14	15	16	17	18	19	20	21	22	23
Caenanoplia	0	1	0	0	0	0	1	1	0	0	0	1	0	1	0	0	1	1	0	1	0	0	0
Arcuaminetes	0	0	1	0	1	0	1	1	0	0	0	1	0	1	1	0	1	0	0	?	1	1	0
Caplinoplia	0	0	1	0	0	0	1	1	0	0	0	1	1	1	1	0	1	0	0	1	1	1	0
Celtanoplia	0	1	0	0	0	1	1	1	0	0	0	1	1	1	1	0	0	1	0	1	1	1	0
Devonaria	1	0	0	0	1	0	1	1	0	0	0	1	1	1	0	0	0	1	0	?	1	1	0
Globosochonetes	0	1	0	0	0	1	1	1	1	0	1	1	1	1	1	0	1	1	0	0	1	1	0
Klocinetes	0	1	1	0	0	0	1	1	1	0	0	1	0	1	1	0	1	0	0	0	1	1	0
Permochonetes	1	0	1	0	0	0	1	1	1	0	0	?	0	1	1	0	1	0	1	0	0	0	0
Plicanoplia	0	1	0	0	0	1	1	1	1	0	0	0	1	1	0	0	0	1	0	0	1	1	0
Semicaplinoplia	0	0	1	0	0	0	1	1	0	0	0	1	1	1	0	0	0	0	0	0	1	1	0
Songzichonetes	0	0	1	0	0	1	0	0	1	0	0	1	0	1	1	0	1	0	1	1	0	1	0
Subglobosochonetes	0	0	1	0	0	0	1	1	1	0	0	1	0	1	1	0	1	0	0	0	0	0	0
Pygmochonetes	0	1	0	0	0	1	0	0	1	0	0	1	0	1	1	0	1	0	0	1	0	1	0
Parapygmochonetes	1	0	0	0	0	1	1	1	1	1	1	1	1	0	1	0	1	1	0	1	0	0	1
Linoproductus	1	0	0	0	0	1	0	0	0	1	1	0	0	0	1	0	0	1	0	?	1	0	1
Balakhonia	1	0	1	0	0	0	0	0	1	1	?	0	0	0	1	0	0	1	0	?	1	0	1
Coolkilella	1	0	0	1	0	1	0	0	1	1	1	0	0	0	1	1	1	1	0	?	1	0	1
Fluctuaria	1	0	0	1	1	1	0	0	0	1	1	1	0	0	0	0	0	1	1	?	?	?	1
Kasetia	1	0	0	1	0	1	0	0	1	1	1	0	0	0	1	1	1	1	1	?	?	0	1
Marginovatia	0	0	0	0	0	1	0	0	1	1	1	0	0	0	1	0	1	1	1	?	1	0	1
Chlupacina	0	0	0	1	0	0	1	1	0	0	0	1	0	1	1	0	1	0	0	0	0	1	0
Leptochonetes	0	0	0	0	0	0	1	1	1	0	0	1	0	1	0	0	1	0	0	0	0	1	0

"?" = unknown; Number 1, 2, …, 23 in the second line equal to the NC (the number for each character) in Table 5.2; the feature or its measurement for each character of *Parapygmochonetes*, based on the specimens of this book and those of other genera, based on the figures of Treatise (Williams et al. 2000)

References

Archbold NW. 1980. Studies on western Australian Permian brachiopods. 1. The family Anopliidae (Chonetidina). Proceedings of the Royal Society of Victoria, 91: 181–192.

Hammer Ø, Harper DAT. 2006. Paleontological data analysis. Blackwell Publishing, Malden, Oxford, Carlton, 351 pp.

Hammer Ø, Harper DAT, Ryan PD. 2001. PAST: paleontological statistics software package for education and data analysis. Palaeontologia Electronica, 4: 1–9.

Havlíček V, Racheboeuf PR. 1979. Chonetacea (Brachiopodes) du Silurian et du Dévonien de Bohême (Tchécoslovaquie). Annales de Paléontologie (Invertébrés), 65: 69–138.

He WH, Shi GR, Twitchett RJ, Zhang Y, Zhang KX, Song HJ, Yue ML, Wu SB, Wu HT, Yang TL, Xiao YF. 2015a. Late Permian marine ecosystem collapse began in deeper waters: evidence from brachiopod diversity and body size changes. Geobiology, 13: 123–138.

He WH, Zhang KX, Chen ZQ, Yan JX, Yang TL, Zhang Y, Gu SZ, Wu SB. 2015b. A new genus *Liaous* of early Anisian Stage (Middle Triassic) brachiopods from southwestern China: systematics, reassessment of classification of the Spiriferinioidea, community paleoecology, and paleoenvironmental implications. Journal of Paleontology, 89: 966–979.

He WH, Shi GR, Yang TL, Zhang KX, Yue ML, Xiao YF, Wu HT, Chen B, Wu SB. 2016. Patterns of brachiopod faunal and body-size changes across the Permian–Triassic boundary: evidence from the Daoduishan section in Meishan area, South China. Palaeogeography, Palaeoclimatology, Palaeoecology, 448: 72–84.

He WH, Shi GR, Xiao YF, Zhang KX, Yang TL, Wu HT, Zhang Y, Chen B, Yue ML, Shen J, Wang YB, Yang H, Wu SB. 2017. Body-size changes of latest Permian brachiopods in varied palaeogeographic settings in South China and implications for controls on animal miniaturization in a highly stressed marine ecosystem. Palaeogeography, Palaeoclimatology, Palaeoecolog, 486: 33–45.

Jablonski D. 1996. Body size and macroevolution, p. 256–289. In: Jablonski D, Erwin DH, Lipps JH. (Eds), Evolutionary Paleobiology. University of Chicago Press, Chicago and London.

Jaynes ET. 2003, Probability Theory: the Logic of Science, Cambridge, Cambridge University Press, 753 pp.

Jin YG, Sun DL. 1981. Palaeozoic brachiopods from Xizang, p. 127–176, pls. 1–12. In: Nanjing Institute of Geology and Palaeontology (Ed.), Palaeontology of Xizang, Book 3 (The series of the Scientific Expedition to the Qinghai–Xizang Plateau). Science Press, Beijing. [In Chinese with English abstract].

Ljaschenko AI. 1973. Brakhiopody i Stratigrafiia Nizhnefranskikh Otlozhenii Iuzhnogo Timana i Volgo-Ural'skoi Neftegazonosnoi Provintsii. Vsesoiuznyi Nauchno-Issledovatel'skii Geologo-Razvedochnyi Neftianoi Institut (VNIGNI), Trudy, 134: 1–279.

Raup DM. 1975. Taxonomic diversity estimation using rarefaction. Paleobiology, 1: 333–342.

Razali NM, Wah YB. 2011. Power comparisons of Shapiro–Wilk, Kolmogorov–Smirnov, Lilliefors and Anderson–Darling tests. Journal of Statistical Modeling and Analytics, 2: 21–33.

Sober E. 1983. Parsimony in Systematics: Philosophical Issues: Annual Review of Ecology and Systematics, 14: 335–357.

Stehli FG. 1954. Lower Leonardian brachiopoda of the Sierra Diablo. Bulletin of the American Museum of National History, 105: 257–358.

Swofford L. 2002, PAUP: phylogenetic analysis using parsimony (and other methods), 4.0 beta 10, programme and documentation, Sunderland, Massachusetts, Sinauer Associates, 140 pp.

Wang SC, Marshall CR. 2004. Improved confidence intervals for estimating the position of a mass extinction boundary. Paleobiology, 30: 5–8.

Wang SC, Everson PJ. 2007. Confidence Intervals for pulsed mass extinction events. Paleobiology, 33: 324–336.

Waterhouse JB. 1975. New Permian and Triassic brachiopod taxa. Paper of Department of Geology of University of Queensland, 7: 1–23.

Waterhouse JB. 1981. Early Permian brachiopods from Ko Yao Noi and near Krabi, southern Thailand, p. 47–213. In: Waterhouse JB, Pitakpaivan K, Mantajit N (Eds), The Permian Stratigraphy and Palaeontology of southern Thailand. Geological Survey Division Department of Mineral Resources, Bangkok.

Williams A, Carlson SJ, Brunton CHC, Holmer LE, Popov LE, Mergl M, Laurie JR, Bassett MG, Cocks LRM, Rong JY, Lazarev SS, Grant RE, Racheboeuf PR, Jin YG, Wardlaw BR, Harper DAT, Wright AD, Rubel M. 2000. Linguliformea, Craniiforemea, and Rhynchonelliformea (part), p. 371, 374, 385–388, 527–530. In: Williams A et al. (Eds), Treatise on Invertebrate Paleontology, Part H, Brachiopoda (revised) 2, 3, Linguliformea, Craniiforemea, and Rhynchonelliformea (part). The Geological Society of America, and the University of Kansas, Lawrence.

Yang DL. 1991. The brachiopod fauna of Early Permian early Qixia Stage, Yishan area, Guangxi and its significance. Bulletin of the Yichang Institute of Geology and Mineral Resources. 17: 81–92. [in Chinese].

6 Evolution of Brachiopod Species Diversity Across the PTB in Varied Palaeogeographic Settings

Wei-Hong He and G. R. Shi

6.1 Research Background

The study on biodiversity evolution and occurrences of organisms is of importance for the study of mass-extinction patterns and causes. Numerous works have documented and discussed the patterns and processes of the Permian–Triassic extinction, resulting in the proposition of a variety of scenarios concerning the nature of these extinction, including one-episode, two-episode and multiple-episode models (or even more complex processes) (Yang et al. 1991; Shen and Shi 1996, 2002; Jin et al. 2000; Feng et al. 2007; Shen et al. 2011; Song et al. 2013; Wang et al. 2014; He et al. 2015; Grasby et al. 2015).

As for the processes of the mass extinction across varied palaeogeographic settings, Foster and Twitchett (2014) studied the global occurrences of all known benthic marine invertebrate genera and demonstrated that the ecological impact of the extinction varied between benthic ecosystems in different depositional settings from the proximal shelf through to basin and slope. Although deeper water settings are more poorly sampled than those from shallower waters, the differential responses across the PTB were considered robust even following corrections for sampling bias (Foster and Twitchett 2014). Concerning and correcting for the possible impact of sampling bias caused by stratigraphic incompleteness and facies control, Wang et al. (2014) applied the constrained optimization (CONOP) technique to a data set of 1450 species from 18 fossiliferous marine PTB sections in different palaeoenvironmental settings of South China and northern peri-Gondwanan region in search of spatial and temporal variability during the Late Permian extinction event. They found that the onset of the extinction in the Qian–Gui Basin (western part of South China, mainly representing deeper water environments) occurred at 252.47 Ma (slightly earlier than the onset of the main extinction in shallow-water PTB sections, compared to 252.39 Ma where the main mass extinction took place at Meishan). Thus, although their data suggest that the extinction occurred in deeper marine settings some 80 kyrs earlier than in shallow-water settings, Wang et al. (2014) attributed this result to possible differences in data quality and/or lack of high-precision and high-resolution temporal control. Despite this interpre-

W.-H. He (✉)
State Key Laboratory of Biogeology and Environmental Geology, School of Earth Sciences, China University of Geosciences, Wuhan, China
e-mail: whzhang@cug.edu.cn

G. R. Shi
School of Life and Environmental Sciences, Burwood, Victoria, Australia

Deakin University, Geelong, Victoria, Australia
e-mail: grshi@deakin.edu.au

W.-H. He et al. (eds.), *Brachiopods around the Permian-Triassic Boundary of South China*, New Records of the Great Dying in South China, https://doi.org/10.1007/978-981-13-1041-6_6

tation, it appears clear that the timing, magnitude and processes of the end-Permian mass extinction were complex and varied with respect to different palaeolatitudes and depositional settings.

Regarding the causes of the mass extinction, numerous scenarios have been proposed, including impact (Retallack et al. 1998; Basu et al. 2003), volcanism (e.g., Heydari et al. 2008; Burgess et al. 2017), regression (Yin et al. 2014; Tavakoli et al. 2017), productivity abnormality (Algeo et al. 2013), anoxia (e.g., Clarkson et al. 2016; Shen et al. 2016; Huang et al. 2017), warming (e.g., Joachimski et al. 2012; Chen et al. 2013; Cui and Kump 2015) and acidification (Payne et al. 2010; Clarkson et al. 2015). Among these causes, the anoxia scenario has been given more attention, but is still disputed in terms of its detailed working mechanisms including the possible spatio–temporal variability (When and how did the anoxia begin?) (Clarkson et al. 2016; Li et al. 2016; Shen et al. 2016; Xiang et al. 2016; Huang et al. 2017; Richards and Sengör 2017). Isozaki (2009) first proposed a 'superanoxia' model suggesting that deep anoxic waters first accummlated in deepsea settings and then migrated upward when the chemocline ascended in a stratified ocean (see also Takahashi et al. 2013). This scenario is mainly based on lithological and radiolarian records from open ocean (Panthalassan) settings (Isozaki 2009).

Marine invertebrates from the Permian–Triassic interval have been subjected to extensive studies in attempts to better understand the temporal and spatial modes of their diversity change, but most of these previous studies have been based on palaeontological data either from a single section or several sections from a single palaeogeographic setting/facies (mainly shallow-water carbonate facies) (e.g. Jin et al. 2000; Shen et al. 2011; Song et al. 2013). To date, few studies are available that compare the temporal patterns of marine species diversity changes across the Permian–Triassic boundary (PTB) from different marine palaeogeographic settings.

To provide insights into the temporal dynamics of diversity change across the PTB mass extinction in benthic marine ecosystems at different water depths and thereby decipher the cause(s) of this mass extinction, we have studied both shallow- and deep-water macrofossils from several temporarly well-resolved PTB sections in South China (He et al. 2015). In this chapter, we present a summary of the temporal diversity-change and extinction patterns of Changhsingian brachiopods from deep-water facies (Majiashan and Rencunping selected as the studied sections) and a comparison with those from shallow-water facies (Meishan as the section for comparison and Huangzhishan selected as the studied section) (Why these sections were selected see Chap. 5).

6.2 Brachiopod Extinctions in Varied Palaeogeographic Settings

The methods of brachiopod collection, sampling efficiency, and details of confidence-interval analysis for testing extinction pulses in a mass extinction and for estimating the position of the main extinction boundary are already given in Chap. 5. The age correlation among studied sections is presented in Fig. 6.1 (details see Chap. 4). The palaeogeographic setting (water depths) of studied PTB sections and the facies-related distribution pattern of brachiopod species diversity are summarized in Fig. 6.2 (details of water depths see Chap. 3).

The confidence-interval analysis (50% confidence intervals) revealed that there were two pulses of disappearance and/or extinction at Rencunping and Majiashan (indicated by the distribution of last occurrences of brachiopod species) (Fig. 6.3). The first disappearance/extinction pulse at Rencunping spans the middle part of Bed 23c to Bed 23d (Fig. 6.3) and at Majiashan it spans the middle part of Bed 15 (Fig. 6.3). According to the age correlation, the middle part

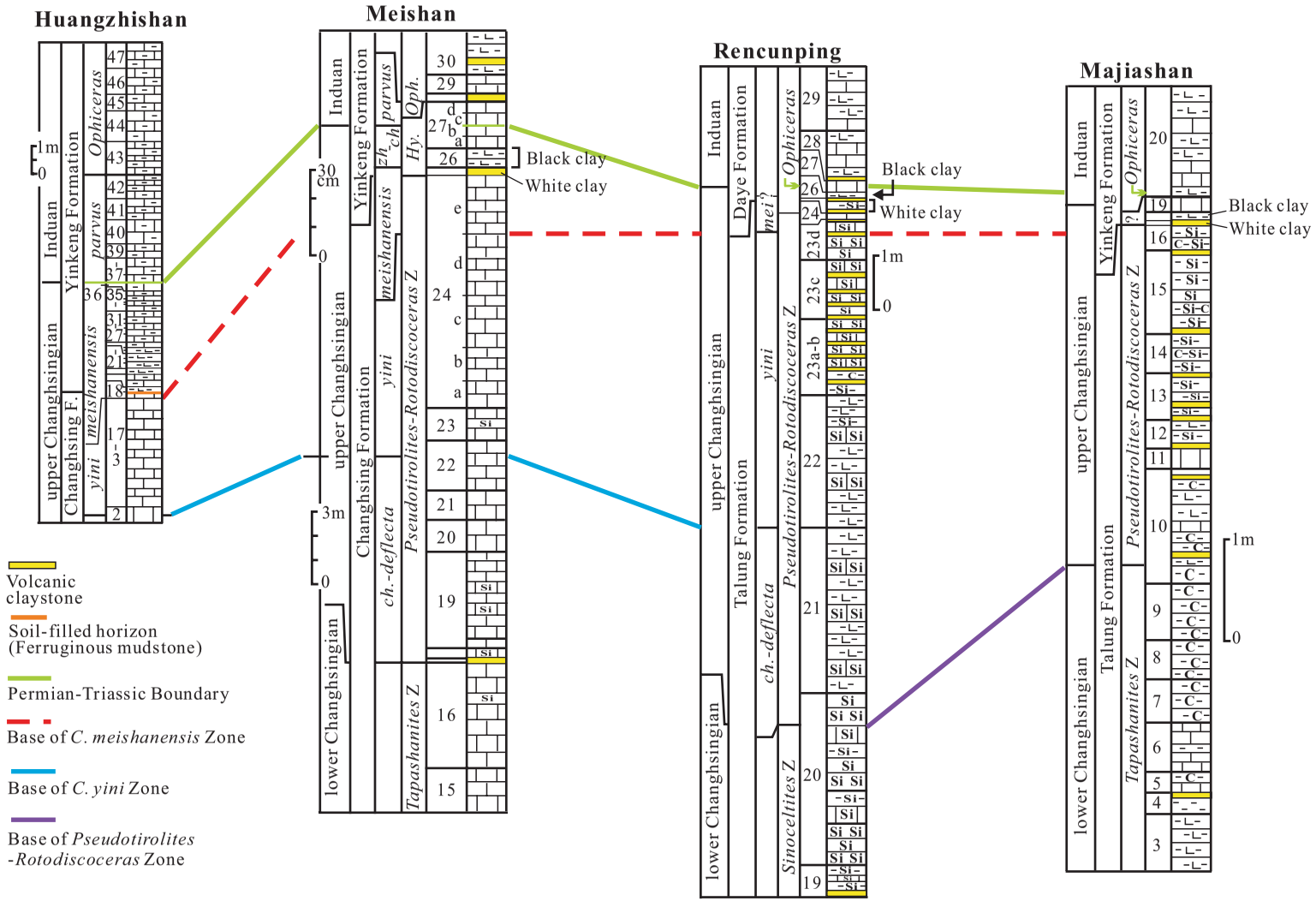

Fig. 6.1 Stratigraphic correlation of the four studied sections (revised after He et al. 2015). Data of conodonts and ammonites of Huangzhishan respectively after Chen et al. (2008) (revised) and Chen et al. (2009), conodont zones of Meishan after Yin et al. (2001) and Yuan et al. (2014), ammonite zones of Meishan after Yang et al. (1987), conodont zones of Rencunping after He et al. (2015), ammonite zones of Rencunping after Zhang et al. (2009), and data of ammonite zones of Majiashan from He et al. (2010); F.- Formation, *yini- Clarkina yini* Zone, *meishanensis/mei- Clarkina meishanensis* Zone, *parvus- Hindeodus parvus* Zone, *Ophiceras*/*Oph.- Ophiceras* Zone, Z- Zone, *changxingensis* (or abbrev *ch.*)*–deflecta- Clarkina changxingensis–C. deflecta* Zone, *zh–ch- Clarkina zhejiangensis–Hindeodus changxingensis* Zone, *Hy.- Hypophiceras* Zone. Legends are same to Fig. 6.2

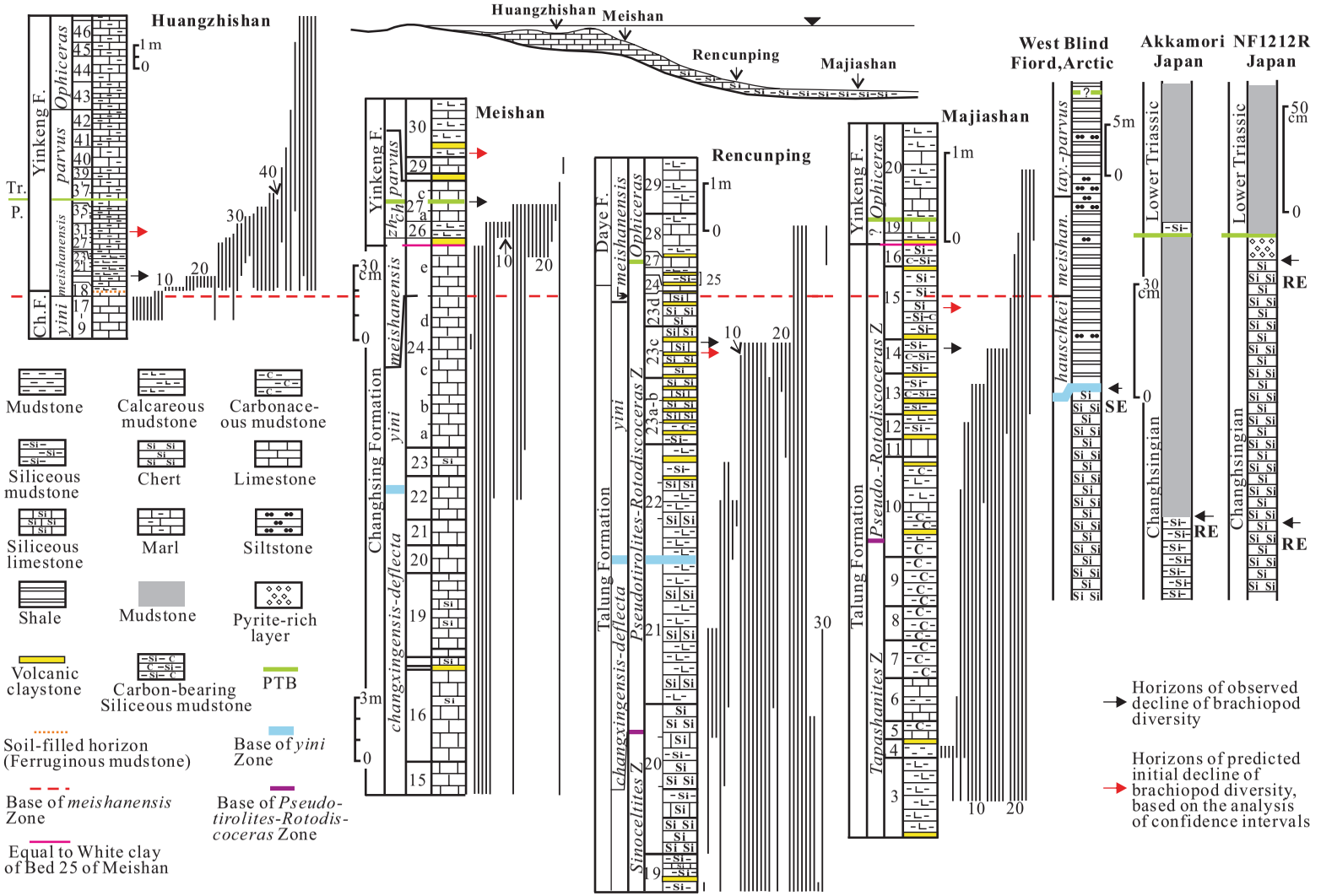

Fig. 6.2 Stratigraphic ranges of brachiopod species (indicated by vertical lines) from the PTB in shallow-water carbonate facies (Huangzhishan and Meishan) and deep-water siliceous facies (Majiashan and Rencunping) (revised after He et al. 2015). The numbers attached to vertical lines refer to species name see He et al. 2015). Details of stratigraphic correlation see Fig. 6.1. Ch.- Changhsing, P.- Permian, Tr.- Triassic, *meishan.- C. meishanensis* Zone, *Pseudo.- Pseudotirolites*, *hauschkei- C. hauschkei* Zone, *taylorae–parvus- C. taylorae* Zone–*H. parvus* Zone, *tay.- C. taylorae*, SE- Siliceous Spongy extinction, RE- Radiolarian extinction, other abbrevations for words see caption of Fig. 6.1

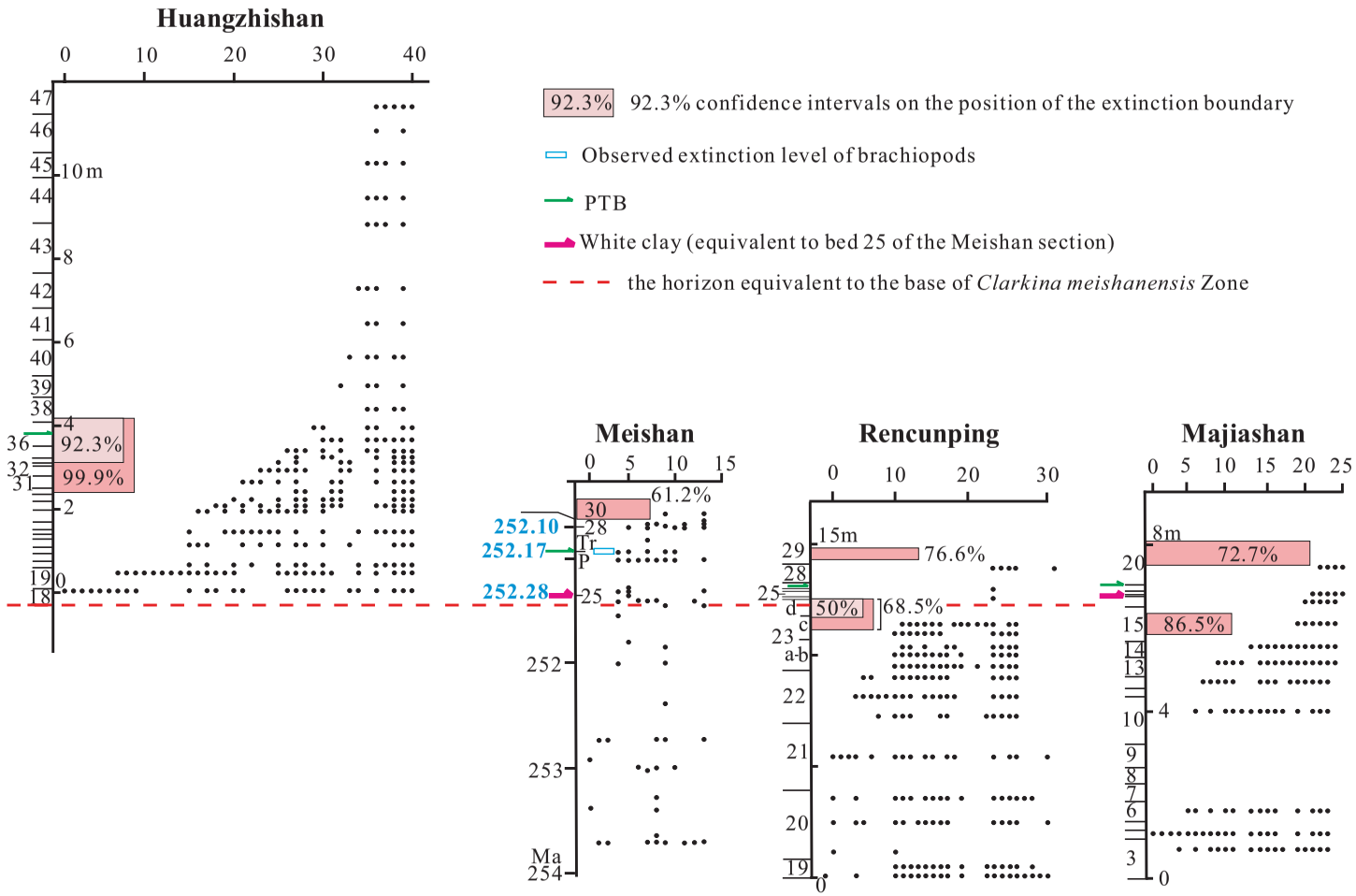

Fig. 6.3 Range chart for the brachiopods at Huangzhishan, Meishan, Rencunping and Majiashan (revised after He et al. 2015). Pink bars indicate the predicted extinction levels at the studied sections. Time (in Ma) is shown on the y axes for the Meishan (Shen et al. 2011) and bed number is shown on the y axes for the Huangzhishan, Rencunping and Majiashan; the number on the x axes for the Meishan indicates the genus number, for Huangzhishan, Rencunping and Majiashan sections indicate the species number (same to the caption of Fig. 6.2). For the Meishan, the position of pink bar and confidence interval on the position of the mass extinction boundary referred to Jin et al. (2000)

of Bed 23c at Rencunping equates to the upper part of Bed 24 of Meishan (Fig. 6.1). Similarly, at Majiashan the first disappearance/extinction pulse began in the middle part of Bed 15, which is equivalent to strata below Bed 25 of the Meishan section (Figs. 6.1 and 6.3).

In contrast, the confidence-interval analysis (50% confidence intervals) revealed that there was one pulse of extinction/disappearance at Huangzhishan (indicated by the distribution of last occurrences of brachiopod species). The disappearance pulse spans the middle part of Bed 30 to the base part of Bed 38 (Fig. 6.3). Thus, the disappearance of brachiopods at Huangzhishan occurred later than the first occurrence of *Clarkina meishanensis* or even possibly occurred in the interval equivalent to Beds 26–27 of the Meishan section (Figs. 6.1 and 6.3). Similarly, adopting the method of confidence-interval analysis (50% confidence intervals), Jin et al. (2000) estimated that the extinction of brachiopods at Meishan might have taken place even later, ~250.6 Ma, which is approximately equivalent to Bed 30 at Meishan (Fig. 6.3). The major mass extinction event occurred in Beds 25–27 at Meishan (Jin et al. 2000). Thus, both the brachiopod extinction and the major mass extinction event at Meishan started later than the first occurrence of *Clarkina meishanensis*. Additionally, the observed disappearance of brachiopods at the shallow-water Zhongzhai section occurred immediately below the PTB (27 cm below) (Zhang et al. 2016) and thus the brachiopod extinction at this section took place approximately in the *Clarkina meishanensis* Zone or later. Therefore, the data from the studied sections revealed that the initial timing of the first pulse of brachiopod disappearance/extinction in deep-water facies occurred earlier than the initial extinction in shallow-water facies (see Figs. 6.2 and 6.3).

References

Algeo TJ, Henderson CM, Tong JN, Feng QL, Yin HF, Tyson RV. 2013. Plankton and productivity during the Permian–Triassic boundary crisis: an analysis of organic carbon fluxes. Global Planetary Change, 105: 52–67.

Basu AR, Petaev MI, Poreda RJ, Jacobsen SB, Becker L. 2003. Chondritic Meteorite Fragments Associated with the Permian–Triassic Boundary in Antarctica. Science, 302: 1388–1392.

Burgess SD, Muirhead JD, Bowring SA. 2017. Initial pulse of Siberian Traps sills as the trigger of the end-Permian mass extinction. Nature Communications, 8: 164.

Chen B, Joachimski MM, Shen SZ, Lambert LL, Lai XL, Wang XD, Chen J, Yuan DX. 2013. Permian ice volume and palaeoclimate history: Oxygen isotope proxies revisited. Gondwana Research, 24: 77–89.

Chen J, Henderson CM, Shen SZ. 2008. Conodont succession around the Permian–Triassic Boundary at the Huangzhishan section, Zhejiang and its stratigraphic correlation. Acta Palaeontologica Sinica, 47: 91–114.

Chen ZQ, Tong JN, Zhang KX, Yang H, Liao ZT, Song HJ, Chen J. 2009. Environmental and biotic turnover across the Permian–Triassic boundary on a shallow carbonate platform in western Zhejiang, South China. Australian Journal of Earth Sciences, 56: 775–797.

Clarkson MO, Kasemann SA, Wood RA, Lenton TM, Daines SJ, Richoz S, Ohnemueller F, Meixner A, Poulton SW, Tipper ET. 2015. Ocean acidification and the Permo–Triassic mass extinction. Science, 348: 229–232.

Clarkson MO, Wood RA, Poulton SW, Richoz S, Newton RJ, Kasemann SA, Bowyer F, Krystyn L. 2016. Dynamic anoxic ferruginous conditions during the end-Permian mass extinction and recovery. Nature Communications, 7: 12236.

Cui Y, Kump LR. 2015. Global warming and the end-Permian extinction event: Proxy and modeling perspectives. Earth-Science Reviews, 149: 5–22.

Feng QL, He WH, Gu SZ, Meng YY, Jin YX, Zhang F. 2007. Radiolarian evolution during the latest Permian in South China. Global and Planetary Change, 55: 177–192.

Foster WJ, Twitchett RJ. 2014. Functional diversity of marine ecosystems after the Late Permian mass extinction event. Nature Geoscience, 7: 233–238.

Grasby SE, Beauchamp B, Bond DPG, Wignall P, Talavera C, Galloway JM, Piepjohn K, Reinhardt L, Blomeier D. 2015. Progressive environmental deterioration in northwestern Pangea leading to the latest Permian extinction. Geological Society of America Bulletin, 127: 1331–1347.

He WH, Twitchett RJ, Zhang Y, Shi GR, Feng QL, Yu JX, Wu SB, Peng XF. 2010. Controls on body size during the Late Permian mass extinction event. Geobiology, 8: 391–402.

He WH, Shi GR, Twitchett RJ, Zhang Y, Zhang KX, Song HJ, Yue ML, Wu SB, Wu HT, Yang TL, Xiao YF. 2015. Late Permian marine ecosystem collapse began in deeper waters: evidence from brachiopod diversity and body size changes. Geobiology, 13: 123–138.

Heydari E, Arzani N, Hassanzadeh J. 2008. Mantle plume: The invisible serial killer–Application to the Permian–Triassic boundary mass extinction. Palaeogeography, Palaeoclimatology, Palaeoecology, 264: 147–162.

Huang YG, Chen ZQ, Wignall PB, Zhao LS. 2017. Latest Permian to Middle Triassic redox condition variations in ramp settings, South China: Pyrite framboid evidence. Geological Society of America Bulletin, 129: 229–243.

Isozaki Y. 2009. Integrated "plume winter" scenario for the double-phased extinction during the Paleozoic–Mesozoic transition: The G–LB and PTB events from a Panthalassan perspective. Journal of Asian Earth Sciences, 36: 459–480.

Jin YG, Wang Y, Wang W, Shang QH, Cao CQ, Erwin DH. 2000. Pattern of marine mass extinction near the Permian–Triassic boundary in South China. Science, 289: 432–436.

Joachimski MM, Lai XL, Shen SZ, Jiang HS, Luo GM, Chen B, Chen J, Sun YD. 2012. Climate warming in the latest Permian and the Permian–Triassic mass extinction. Geology, 40: 195–198.

Li GS, Wang YB, Shi GR, Liao W, Yu LX. 2016. Fluctuations of redox conditions across the Permian–Triassic boundary-new evidence from the GSSP section in Meishan of South China. Palaeogeography, Palaeoclimatology, Palaeoecology, 448: 48–58.

Payne JL, Turchyn AV, Paytan A, DePaolo DJ, Lehrmann DJ, Yu MY, Wei JY. 2010. Calcium isotope constraints on the end-Permian mass extinction. Proceedings of the National Academy of Sciences, 107: 8543–8548.

Retallack GJ, Seyedolali A, Krull ES, Holser WT, Ambers CP, Kyte FT. 1998. Search for evidence of impact at the Permian–Triassic boundary in Antarctica and Australia. Geology, 26: 979–982.

Richards JP, Şengör AMC. 2017. Did Paleo-Tethyan anoxia kill arc magma fertility for porphyry copper formation? Geology, 45: 591–594.

Shen J, Feng QL, Algeo TJ, Li C, Planavsky NJ, Zhou L, Zhang ML. 2016. Two pulses of oceanic environmental disturbance during the Permian–Triassic boundary crisis. Earth and Planetary Science Letters, 443: 139–152.

Shen SZ, Shi GR. 1996. Diversity and extinction patterns of Permian brachiopoda of South China. Historical Biology, 12: 93–110.

Shen SZ, Shi GR. 2002. Paleobiogeographical extinction patterns of Permian brachiopods in the Asian–western Pacific region. Paleobiology, 28: 449–463.

Shen SZ, Crowley JL, Wang Y, Bowring SA, Erwin DH, Sadler PM, Cao CQ, Rothman DH, Henderson CM, Ramezani J, Zhang H, Shen YA, Wang XD, WangW, Mu L, Li WZ, Tang YG, Liu XL, Liu LJ, Zeng Y, Jiang YF, Jin YG. 2011. Calibrating the End-Permian Mass Extinction. Science, 334: 1367–1372.

Song HJ, Wignall PB, Tong JN, Yin HF. 2013. Two pulses of extinction during the Permian–Triassic crisis. Nature Geoscience, 6: 52–56.

Takahashi S, Kaiho K, Hori RS, Gorjan P, Watanabe T, Yamakita S, Aita Y, Takemura A, Sp€orli KB, Kakegawa T, Oba M. 2013. Sulfur isotope profiles in the pelagic Panthalassic deep sea during the Permian–Triassic transition. Global and Planetary Change, 105: 68–78.

Tavakoli V, Naderi-Khujin M, Seyedmehdi Z. 2017. The end-Permian regression in the western Tethys: sedimentological and geochemical evidence from offshore the Persian Gulf, Iran. Geo-Marine Letters, 38: 179–192.

Wang Y, Shen SZ, Zhang YC, Wang XD, Wang W, Sadler PM, Erwin DH, Crowley JL, Henderson CM. 2014. Quantifying the process and abruptness of the end-Permian mass extinction. Paleobiology, 41: 113–129.

Xiang L, Schoepfer SD, Zhang H, Yuan DX, Cao CQ, Zheng QF, Henderson CM, Shen SZ. 2016. Oceanic redox evolution across the end-Permian mass extinction at Shangsi, South China. Palaeogeography, Palaeoclimatology, Palaeoecology, 448: 59–71.

Yang ZY, Yin HF, Wu SB, Yang FQ, Ding MH, Xu GR. 1987. Permian–Triassic boundary stratigraphy and fauna of South China. Geological Publishing House, Beijing, 378 pp. [in Chinese with English abstract].

Yang ZY, Wu SB, Yin HF, Xu GR, Zhang KX. 1991. Permo–Triassic Events of South China. Geological Publishing House, Beijing, 183 pp. [in Chinese with English abstract].

Yin HF, Zhang KX, Tong JN, Yang ZY, Wu SB. 2001. The Global Stratotype Section and Point (GSSP) of the Permian–Triassic boundary. Episodes, 24: 102–114.

Yin HF, Jiang HS, Xia WC, Feng QL, Zhang N, Shen J. 2014. The end-Permian regression in South China and its implication on mass extinction. Earth-Science Reviews, 137: 19–33.

Yuan DX, Shen SZ, Henderson CM, Chen J, Zhang H, Feng HZ. 2014. Revised conodont-based integrated high-resolution timescale for the Changhsingian Stage and end-Permian extinction interval at the Meishan sections, South China. Lithos, 204: 220–245.

Zhang ZY, He WH, Zhang Y, Yang TL, Wu SB. 2009. Late Permian–earliest Triassic ammonoid sequences from the Rencunping section, Sangzhi County, Hunan Province, South China and their regional correlation. Geological Science and Technology Information, 28: 23–30. [in Chinese with English abstract].

Zhang Y, Shi GR, He WH, Wu HT, Lei Y, Zhang KX, Du CC, Yang TL, Yue ML, Xiao YF. 2016. Significant pre-mass extinction animal body-size changes: evidence from the Permian–Triassic boundary brachiopod faunas of South China. Palaeogeography, Palaeoclimatology, Palaeoecology, 448: 85–95.

7 Spatial and Temporal Body-Size Changes of Brachiopods in Relation to Varied Palaeogeographic Settings

Wei-Hong He and G. R. Shi

7.1 Previous Study on the Permian–Triassic Body Sizes and Potential Insights into the Palaeoenvironments

The so-called Lilliput effect refers to a macroevolutionary phonemnon where the surviving animals in the aftermath of a mass extinction tend to be smaller on average than their pre-extinction relatives (Urbanek 1993; Fraiser and Bottjer 2004; Payne 2005; Twitchett 2007; Keller and Abramovich 2009; Zhang et al. 2016). This observation clearly highlights the importance of animal body-size changes in the study of mass extinctions. Body size is a key character of any organism and profoundly affects its biology and ecology (Jablonski 1996). Body size is often controlled by environmental factors, including oxygen fluctuations (Savrda and Bottjer 1986; Payne et al. 2008, 2013), food availability (Hallam 1965; Rheault and Rice 1996; Twitchett 2007; He et al. 2010) and temperature changes (Hunt et al. 2010; Sheridan and Bickford 2011; Edeline et al. 2013), as well as substrate conditions. As many of these factors vary with water depth, the relationship between body size and bathymetry (i.e., spatial body-size changes in this book) is crucial for the study on body-size changes (Anderson 1971; Thiel 1975; Peck and Harper 2010; Shi et al. 2016). For example, the study of spatial body-size changes is useful for examining which factor (or factors) played a more important role in controlling the differences of body sizes, thereby providing insights into the evolution of palaeoenvironments through time. Meanwhile, the study of size changes through past extinction times (i.e., temporal body-size changes in this book) is also of particular importance in understanding the biotic responses to global-scale climatic and environmental evolution (Twitchett 2007; He et al. 2010, 2015).

Numerous researches have been undertaken on the Permian–Triassic body-size changes of conodonts, brachiopods, siliceous sponges, ostracods or foraminifers in South China (He et al. 2007, 2010, 2015, 2016, 2017; Peng et al. 2007; Luo et al. 2008; Song et al. 2011; Liu et al. 2013; Chu et al. 2016; Zhang et al. 2016). Most of these studies have focused on the patterns of body-size changes of individual taxa across time and their possible underlying control mechanisms, and a few (e.g., He et al. 2010; Liu et al. 2013) have addressed the relationship between size changes in relation to primary productivity and redox

W.-H. He (✉)
State Key Laboratory of Biogeology and Environmental Geology, School of Earth Sciences, China University of Geosciences, Wuhan, China
e-mail: whzhang@cug.edu.cn

G. R. Shi
School of Life and Environmental Sciences, Burwood, Victoria, Australia

Deakin University, Geelong, Victoria, Australia
e-mail: grshi@deakin.edu.au

W.-H. He et al. (eds.), *Brachiopods around the Permian-Triassic Boundary of South China*, New Records of the Great Dying in South China, https://doi.org/10.1007/978-981-13-1041-6_7

palaeoproxies in the context of palaeobathymetry. Most recently, based on a global dataset of Changhsingian brachiopod orders, Shi et al. (2016) examined the relationship of Changhsingian brachiopod body-size changes in relation to the onshore–offshore–basin gradient.

7.2 Latest Permian Body-Size Changes in Relation to Varied Palaeogeographic Settings

The palaeogeographic settings of South China are already described in Chap. 2 and the age correlations in Chap. 4. Detailed descriptions of the methodology used for the measurement of body sizes and their analyses including significance testing are given in Chap. 5.

Here we present a summary of body-size changes of latest Permian brachiopods across different bathymetrically controlled palaeoenvironmental settings within the South China basin, extracted from our recent study (He et al. 2017). In this book, we adopted two most commonly found Changhsingian chonetid brachiopod species, *Fusichonetes pygmaea* and *Fusichonetes quadrata* (These two species had been referred to as *Tethyochonetes pygmaea* and *Tethyochonetes quadrata*, respectively, see Wu et al. 2017 for details), from five different sections, which together constituted an approximately-defined basin-wide bathymetric gradient spanning the shallow-water clastic shelf, shallow-water carbonate platform and ramp, and deep-water siliceous basinal settings (see Fig. 7.1; analysis of palaeo-water depths see Chap. 3). The studied five sections include Huangzhishan, Zhongzhai, Daoduishan, Majiashan and Rencunping.

For the study of body sizes, values of X_{mean} and X_{median} were adopted (the definition and reason for selected as parameters sees Chap. 5). The X_{mean} shows that the body sizes at Zhongzhai and Huangzhishan are both close to or greater than 5 mm (see Line **a** in Fig. 7.1a) whereas the same size metric for the Daoduishan, Majiashan and Rencunping sections are all smaller than 4 mm (see Line **b** in Fig. 7.1a) except for *F. quadrata* at Majiashan whose X_{mean} reached larger than 5 mm (Fig. 7.1a).

Additionally, the X_{median} shows that the median body sizes at Huangzhishan and Zhongzhai are close to or larger than 5.0 mm (see Line **c** in Fig. 7.1b). By contrast, the median sizes of brachiopods for the other three deeper-water sections are all close to or smaller than 4.0 mm (see Line **d** in Fig. 7.1b) with the exception of *F. quadrata* at Majiashan whose X_{median} attained larger than 5 mm (Fig. 7.1b). A Mann–Whitney (M–W) test revealed that the difference in median sizes between the two groups of sections (i.e., the Huangzhishan and Zhongzhai as a group representing shallow-water settings while the Daoduishan, Majiashan and Rencunping together representing a group of deeper-water settings) is statistically significant ($P < 0.05$, see Table 5.1), although the difference of medians for *F. quadrata* is not significant between Zhongzhai and Majiashan sections ($P = 0.3622$, see Table 5.1).

Overall, the analysis on body sizes for both species by using different size parameters (X_{mean} and X_{median}) among the studied sections revealed that body sizes at Huangzhishan and Zhongzhai are significantly larger than their counterparts in the Daoduishan, Majiashan and Rencunping sections, with the only exception of *F. quadrata* at Majiashan (see explanation in Chap. 8).

Fig. 7.1 Body-size differences of *F. pygmaea* (black) and *F. quadrata* (purple) in the five studied sections and their comparision with varied palaeo-bathymetry and redox conditions (revised after He et al. 2017). (**a**) Body size (X_{mean}); (**b**) Body size (X_{median}); (**c**) Redox conditions at the studied sections; (**d**) Sketch diagram showing the palaeogeographic settings and palaeo-bathymetry of the studied sections. Note: The division for redox condition in Fig. 7.1c is based on the study of pyrite framboids (see Chap. 8). The estimation for palaeo-bathymetry in Fig. 7.1d sees Chap. 3

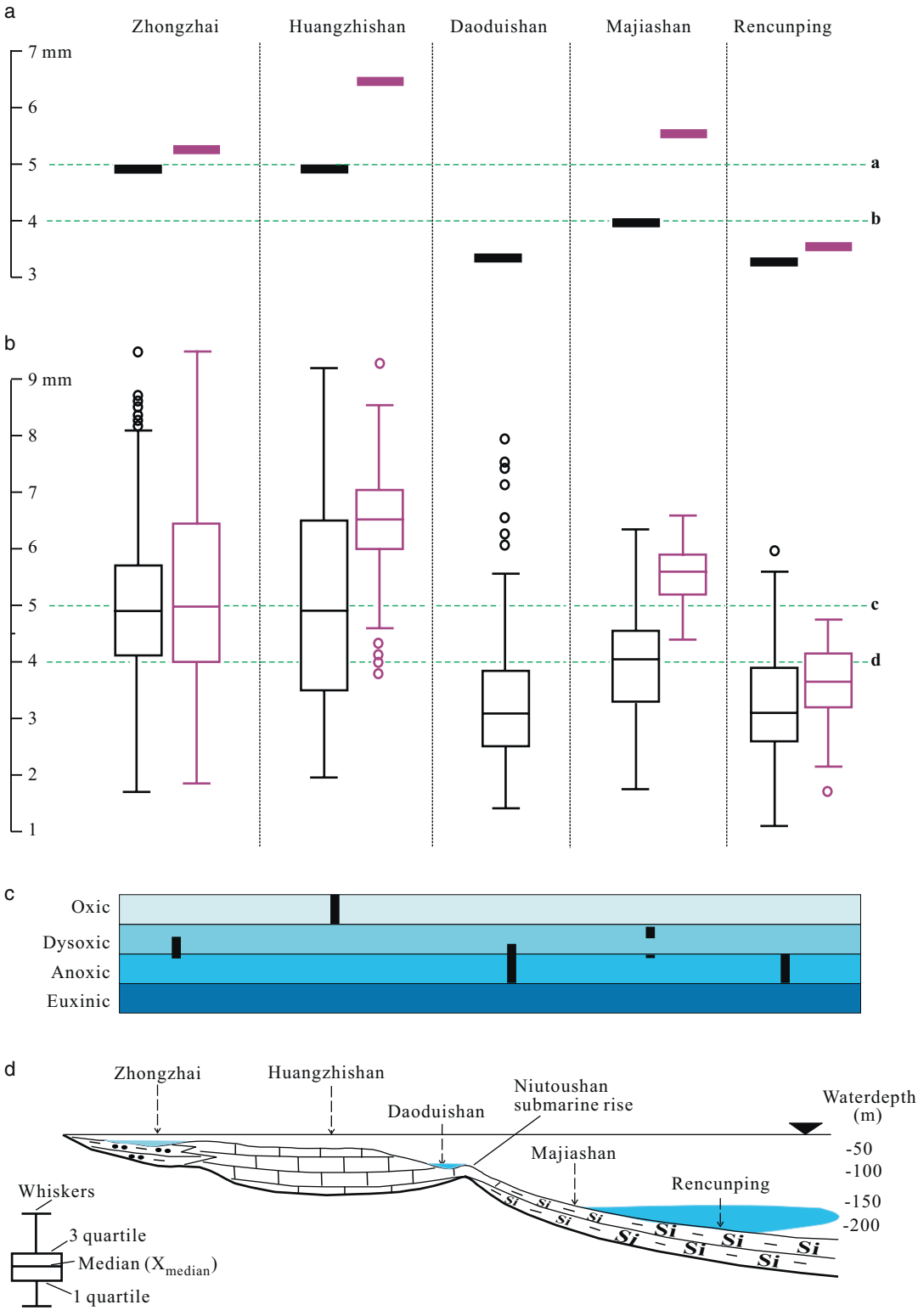
a
Zhongzhai
Huangzhishan
Daoduishan
Majiashan
Rencunping
7 mm
6
5
4
3
a
b
b
9 mm
8
7
6
5
4
3
2
1
c
d
c
Oxic
Dysoxic
Anoxic
Euxinic
d
Zhongzhai
Huangzhishan
Daoduishan
Niutoushan
submarine rise
Majiashan
Rencunping
Waterdepth
(m)
-50
-100
-150
-200
Whiskers
3 quartile
Median (X median)
1 quartile
Si

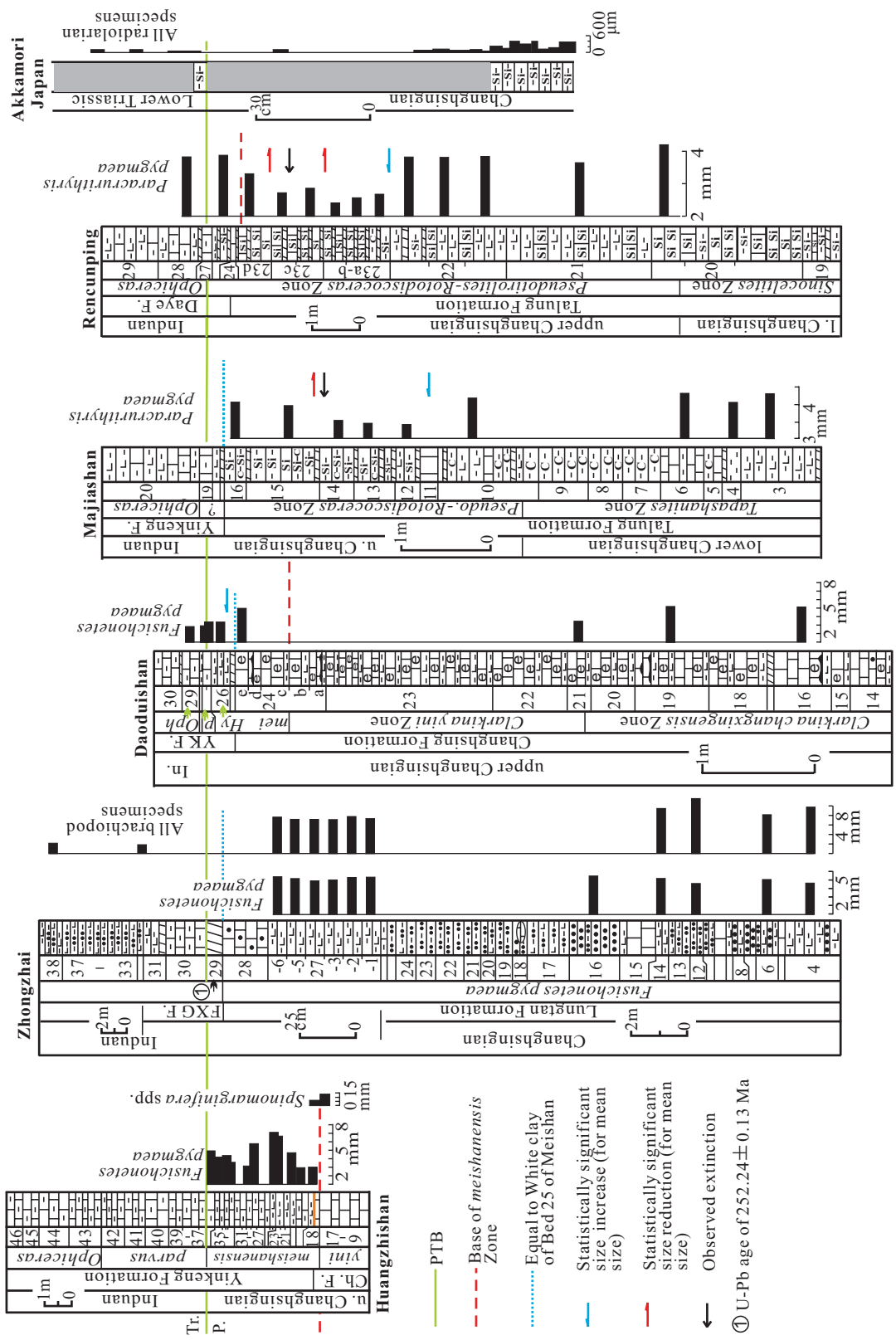
Huangzhishan
Zhongzhai
Daoduishan
Majiashan
Rencunping
Akkamori
Japan
Tr.
P.
PTB
Base of meishanensis Zone
Equal to White clay of Bed 25 of Meishan
Statistically significant size increase (for mean size)
Statistically significant size reduction (for mean size)
Observed extinction
① U-Pb age of 252.24±0.13 Ma

Fig. 7.2 Body-size distribution of varied taxa at the studied sections (revised after He et al. 2017). Widths of thick black bars indicate the size values of brachiopods at Huangzhishan, Zhongzhai, Daoduishan, Majiashan and Rencunping sections of South China or to the size values of radiolarians at the Akkamori of Japan. Meanings of size data: for *Fusichonetes pygmaea* at Huangzhishan refer to the mean size across all specimens in *F. pygmaea* (see He et al. 2017), for *Spinomarginifera* spp. at Huangzhishan refer to the mean size across all specimens in *Spinomarginifera* spp. (see Chen et al. 2009), for *Fusichonetes pygmaea* at Zhongzhai refer to the mean size across all specimens in *F. pygmaea* (see He et al. 2017), for all brachiopod specimens at Zhongzhai refer to the arithmetic mean size (shell width) of all brachiopod species (see Zhang et al. 2016), for *Fusichonetes pygmaea* at Daoduishan represent the mean size across all specimens in *F. pygmaea* (see He et al. 2016), for *Paracrurithyris pygmaea* at Majiashan and Rencunping represent the mean size across all specimens in *P. pygmaea* (see He et al. 2015), and for radiolarian at Akkamori of Japan represent the maximum shell diameter among all specimens (see Takahashi et al. 2009). Biostratigraphy of Huangzhishan, Majiashan and Rencunping after He et al. 2015; U–Pb age of Zhongzhai after Shen et al. 2011; biostratigraphy of Daoduishan after He et al. 2016. Note for abbrevations: u.- upper, l.- lower, FXG- Feixianguan, In.- Induan, YK- Yinkeng, *mei-Clarkina meishanensis* Zone, *Hy- Hypophiceras*, *p- Hindeodus parvus* Zone, *Oph-Ophiceras* Zone, other abbrevations for words see captions of Figs. 6.1 and 6.2

7.3 Temporal Body-Size Changes Through the Permian–Triassic Transition in Varied Palaeogeographic Settings

The studied species for the body-size changes include *Paracrurithyris pygmaea* from the Rencunping and Majiashan sections and *Fusichonetes pygmaea* from the Daoduishan section, with mean size as the studied parameter (see Chap. 5). The reasons for these two species were chosen for study is given in Chap. 5. In addition, body sizes of *Fusichonetes pygmaea* and *Spinomarginifera* spp. from Huangzhishan, *Fusichonetes pygmaea* and all brachiopod specimens from Zhongzhai and all radiolarian specimens from Akkamori of Japan, have also been analyzed for comparison, although their temporal changes could not be tested for significance because of scarcity of specimens (*Fusichonetes pygmaea*) or difference in taxonomy level (e.g., *Spinomarginifera* spp. being at the genus level, all radiolarian specimens being at subclass level).

The analyses revealed the following patterns (Fig. 7.2): *Paracrurithyris pygmaea* at Rencunping significantly reduced its size from Beds 22-3 to 23a and then significantly increased its size from Beds 23b-2 to 23c-1 and again from Beds 23c-2 to 23d–24; *Paracrurithyris pygmaea* at Majiashan shrank from Beds 10–12, followed by a significant increase from Beds 14–15. Thus, it is clear that the mean size of brachiopods from the deep-water Rencunping and Majiashan sections began to decline significantly (in a statistical sense) from the middle *Pseudotirolites–Rotodiscoceras* Zone (≈middle *Clarkina yini* Zone) (Fig. 7.2). In contrast, significant size reduction of brachiopods in the shallower water environment of Daoduishan (shallower, compared to Rencunping and Majiashan) began in the top part of the *C. meishanensis* Zone (Fig. 7.2). As for the compared faunas, the size reduction of radiolarian specimens from the deep-water Akkamori section of Japan (pelagic environment) apparently began to take place far below the PTB, namely earlier than the faunas in the shallow-water settings of South China. The size reduction of *Spinomarginifera* spp. at the shallow-water Huangzhishan took place at the base of *C. meishanensis* Zone and size reduction of *Fusichonetes pygmaea* at this section took place in the upper part of *C. meishanensis* Zone, both later than their counterparts of deep-water environments. At the shallow-water Zhongzhai section, although the mean body size of *Fusichonetes pygmaea* did not appear to have changed significantly, but the body sizes of all brachiopod specimens through the section demonstrate a reduction trend in the Early Triassic (e.g., Beds 32 and 38), and the reduction occurred later than brachiopods living in deep-water environments. In summary, it is evident that size reduction in deep-water environments occurred earlier than in shallow-water environments (Fig. 7.2). This pattern is consistent with the temporal trend of the brachiopod diversity evolution in that the decline of deep-water brachiopod species diversity commenced earlier than in shallow-water settings (the reason and analysis see Chap. 8).

In addition, body sizes of most species which tentatively survived the PTB, attained or demonstrated a reduction trend. For example, *Paryphella orbicularis* and *Chaohochonetes triangusinuata* (=?*Tethyochonetes* sp. of He et al. 2010) at Majiashan reduced their body sizes immediately below the PTB and attained smaller sizes in the Early Triassic. A similar pattern of body-size changes for *Paryphella orbicularis* (=*Paryphella triquetra* of He et al. 2016) has been recorded at Daoduishan. These cases are typical of the Lilliput effect.

References

Anderson EJ. 1971. Environmental models for Paleozoic communities. Lethaia, 4: 287–302.

Chen ZQ, Tong JN, Zhang KX, Yang H, Liao ZT, Song HJ, Chen J. 2009. Environmental and biotic turnover across the Permian–Triassic boundary on a shallow carbonate platform in western Zhejiang, South China. Australian Journal of Earth Sciences, 56: 775–797.

Chu DL, Tong JN, Song HJ, Benton MJ, Song HY, Yu JX, Qiu XC, Huang YF, Tian L. 2016. Lilliput effect in freshwater ostracods during the Permian–Triassic extinction. Palaeogeography, Palaeoclimatology, Palaeoecology, 435: 38–52.

Edeline E, Lacroix G, Delire C, Poulet N, Legendre S. 2013. Ecological emergence of thermal clines in body size. Global Change Biology, 19: 3062–3068.

Fraiser ML, Bottjer DJ. 2004. The Non-Actualistic Early Triassic Gastropod Fauna: A Case Study of the Lower Triassic SinbadLimestone Member. Palaios, 19: 259–275.

Hallam A. 1965. Environmental causes of stunting in living and fossil marine benthonic invertebrates. Palaeontology, 8: 132–155.

He WH, Shi GR, Feng QL, Campi MJ, Gu SZ, Bu JJ, Peng YQ, Meng YY. 2007. Brachiopod miniaturization and its possible causes during the Permian–Triassic crisis in deep water environments, South China. Palaeogeography, Palaeoclimatology, Palaeoecology, 252: 145–163.

He WH, Twitchett RJ, Zhang Y, Shi GR, Feng QL, Yu JX, Wu SB, Peng XF. 2010. Controls on body size during the Late Permian mass extinction event. Geobiology, 8: 391–402.

He WH, Shi GR, Twitchett RJ, Zhang Y, Zhang KX, Song HJ, Yue ML, Wu SB, Wu HT, Yang TL, Xiao YF. 2015. Late Permian marine ecosystem collapse began in deeper waters: evidence from brachiopod diversity and body size changes. Geobiology, 13: 123–138.

He WH, Shi GR, Yang TL, Zhang KX, Yue ML, Xiao YF, Wu HT, Chen B, Wu SB. 2016. Patterns of brachiopod faunal and body-size changes across the Permian–Triassic boundary: evidence from the Daoduishan section in Meishan area, South China. Palaeogeography, Palaeoclimatology, Palaeoecology, 448: 72–84.

He WH, Shi GR, Xiao YF, Zhang KX, Yang TL, Wu HT, Zhang Y, Chen B, Yue ML, Shen J, Wang YB, Yang H, Wu SB. 2017. Body-size changes of latest Permian brachiopods in varied palaeogeographic settings in South China and implications for controls on animal miniaturization in a highly stressed marine ecosystem. Palaeogeography, Palaeoclimatology, Palaeoecolog, 486: 33–45.

Hunt G, Wicaksono SA, Brown JE, Macleod KG. 2010. Climate-driven body-size trends in the Ostracod fauna of the deep Indian Ocean. Palaeontology, 53: 1255–1268.

Jablonski D. 1996. Body size and macroevolution, p. 256–289. In: Jablonski D, Erwin DH, Lipps JH. (Eds), Evolutionary Paleobiology. University of Chicago Press, Chicago and London.

Keller G, Abramovich S. 2009. Lilliput effect in late Maastrichtian planktic foraminifera: Response to environmental stress. Palaeogeography, Palaeoclimatology, Palaeoecology, 284: 47–62.

Liu GC, Feng QL, Shen J, Yu JX, He WH, Algeo T. 2013. Decline of siliceous sponges and spicule miniaturization induced by marine productivity collapse and expanding anoxia during the Permian–Triassic crisis in South China. Palaios, 28: 664–679.

Luo GM, Lai XL, Shi GR, Jiang HS, Yin HF, Xie SC, Tong JN, Zhang KX, He WH, Wignall PB. 2008. Size variation of conodont elements of the *Hindeodus–Isarcicella* clade during the Permian–Triassic transition in South China and its implication for mass extinction. Palaeogeography, Palaeoclimatology, Palaeoecology, 264: 176–187.

Payne JL. 2005. Evolutionary dynamics of gastropod size across the end-Permian extinction and through the Triassic recovery interval. Paleobiology, 31: 269–290.

Payne JL, Boyer AG, Brown JH, Finnegan S, Kowalewski M, Krause Jr RA, Lyons SK, McClain CR, McShea DW, Novack-Gottshall PM, Smith FA, Stempien JA, Wang SC. 2008. Two-phase increase in the maximum size of life over 3.5 billion years reflects biological innovation and environmental opportunity. Proceedings of the National Academy of Sciences of the United States of America, 106: 24–27.

Payne JL, Jost AB, Wang SC, Skotheim JM. 2013. A shift in the long-term mode of foraminiferan size evolution caused by the end-Permian mass extinction. Evolution, 67: 816–827.

Peck LS, Harper EM. 2010. Variation in size of living articulated brachiopods with latitude and depth. Marine Biology, 157: 2205–2213.

Peng YQ, Shi GR, Gao YQ, He WH, Shen SZ. 2007. How and why did the Lingulidae (Brachiopoda) not only survive the end-Permian mass extinction but also thrive in its aftermath? Palaeogeography, Palaeoclimatology, Palaeoecology, 252: 118–131.

Rheault RB, Rice MA. 1996. Food-limited growth and condition index in the eastern oyster, Crassostrea virginica (Gmelin 1791), and the bay scallop, Argopecten irradians irradians (Lamarck 1819). Journal of Shellfish Research, 15: 271–283.

Savrda CE, Bottjer DJ. 1986. Trace fossil model for reconstruction of Paleo-oxygenation in bottom waters. Geology, 14: 3–6.

Shen SZ, Crowley JL, Wang Y, Bowring SA, Erwin DH, Sadler PM, Cao CQ, Rothman DH, Henderson CM, Ramezani J, Zhang H, Shen YA, Wang XD, WangW, Mu L, Li WZ, Tang YG, Liu XL, Liu LJ, Zeng Y, Jiang YF, Jin YG. 2011. Calibrating the End-Permian Mass Extinction. Science, 334: 1367–1372.

Sheridan JA, Bickford D. 2011. Shrinking body size as an ecological response to climate change. Nature Climate Change, 1: 401–406.

Shi GR, Zhang YC, Shen SZ, He WH. 2016. Nearshore–offshore–basin species diversity and body size variation patterns in Late Permian (Changhsingian) brachiopods. Palaeogeography, Palaeoclimatology, Palaeoecology, 448: 96–107.

Song HJ, Tong JN, Chen ZQ. 2011. Evolutionary dynamics of the Permian–Triassic foraminifer size: Evidence for Lilliput effect in the end-Permian mass extinction and its aftermath. Palaeogeography, Palaeoclimatology, Palaeoecology, 308: 98–110.

Takahashi S, Yamakita S, Suzuki N, Kaiho K, Ehiro M. 2009. High organic carbon content and a decrease in radiolarians at the end of the Permian in a newly discovered continuous pelagic section: A coincidence?

Palaeogeography, Palaeoclimatology, Palaeoecology, 271: 1–12.

Thiel H. 1975. The size structure of the deep-sea benthos. Internationale Revue der gesamten Hydrobiologie und Hydrographie, 60: 575–606.

Twitchett RJ. 2007. The Lilliput effect in the aftermath of the end-Permian extinction event. Palaeogeography, Palaeoclimatology, Palaeoecology, 252: 132–144.

Urbanek A. 1993. Biotic crises in the history of upper Silurian graptoloids: a palaeobiological model. Historical Biology, 7: 29–55.

Wu HT, Shi GR, He WH. 2017. A quantitative taxonomic review of *Fusichonetes* and *Tethyochonetes* (Chonetidina, Brachiopoda). Journal of Paleontology, 91: 1296–1305.

Zhang Y, Shi GR, He WH, Wu HT, Lei Y, Zhang KX, Du CC, Yang TL, Yue ML, Xiao YF. 2016. Significant pre-mass extinction animal body-size changes: evidence from the Permian–Triassic boundary brachiopod faunas of South China. Palaeogeography, Palaeoclimatology, Palaeoecology, 448: 85–95.

8 Discussion on Changes of Brachiopod Diversity and Morphologic Features and Their Implications for the Environmental and Biological Crisis of the Great Dying

Wei-Hong He, G. R. Shi, and Jian-Jun Bu

8.1 Why Did the Deep-Water Brachiopod Diversity Decline Earlier Than in Shallow-Water Settings?

As concluded in Chap. 6, the decline of brachiopod diversity in deep-water facies took place earlier than in shallow-water facies during the Permian–Triassic transition. This phenomenon lets us recall the scenario that the upward migration of anoxic deep waters in a stratified ocean caused the radiolarian extinction in a Japanese pelagic environment (Isozaki 2009; Takahashi et al. 2013). Therefore, elsewhere we have proposed that the formation of a stratified ocean and, particularly, upward migration of the chemocline (or Oxygen Minimum Zone) in the stratified ocean was possibly responsible for this bathymetry-dependent differential temporal pattern of brachiopod disappearance across the PTB in South China (Fig. 8.1; He et al. 2015). Furthermore, the ocean stratification and upward migration of the chemocline was most likely linked to contemporaneous sustained volcanism. This was evidenced by the frequent occurrences of volcanic ash beds around the horizons where the diversity declined (Fig. 6.2).

How did this proposed 'killing by volcanism' mechanism unfold in connection to the Permian–Triassic mass extinction? Volcanism on a continental scale could have produced abundant dust and substantially increased atmospheric CO_2. The input of plentiful and sustained CO_2 influx into the atmosphere would cause subsequent long-term global warming (Isozaki et al. 2007; Saunders and Reichow 2009). Isotope data from brachiopods (Kearsey et al. 2009) and conodonts (Joachimski et al. 2012; Sun et al. 2012) revealed that tropical sea surface temperatures were 25–29 °C in the Late Permian and then went through a rapid a rising trend toward the latest Permian. Global warming caused by increased atmospheric CO_2 would have led to ocean stratification and further to anoxic–euxinic deep/bot-

W.-H. He (✉)
State Key Laboratory of Biogeology and Environmental Geology, School of Earth Sciences, China University of Geosciences, Wuhan, China
e-mail: whzhang@cug.edu.cn

G. R. Shi
School of Life and Environmental Sciences, Burwood, Victoria, Australia

Deakin University, Geelong, Victoria, Australia
e-mail: grshi@deakin.edu.au

J.-J. Bu
Wuhan Centre for China Geological Survey, Wuhan, China
e-mail: jianjunbu@cug.edu.cn

W.-H. He et al. (eds.), *Brachiopods around the Permian-Triassic Boundary of South China*, New Records of the Great Dying in South China, https://doi.org/10.1007/978-981-13-1041-6_8

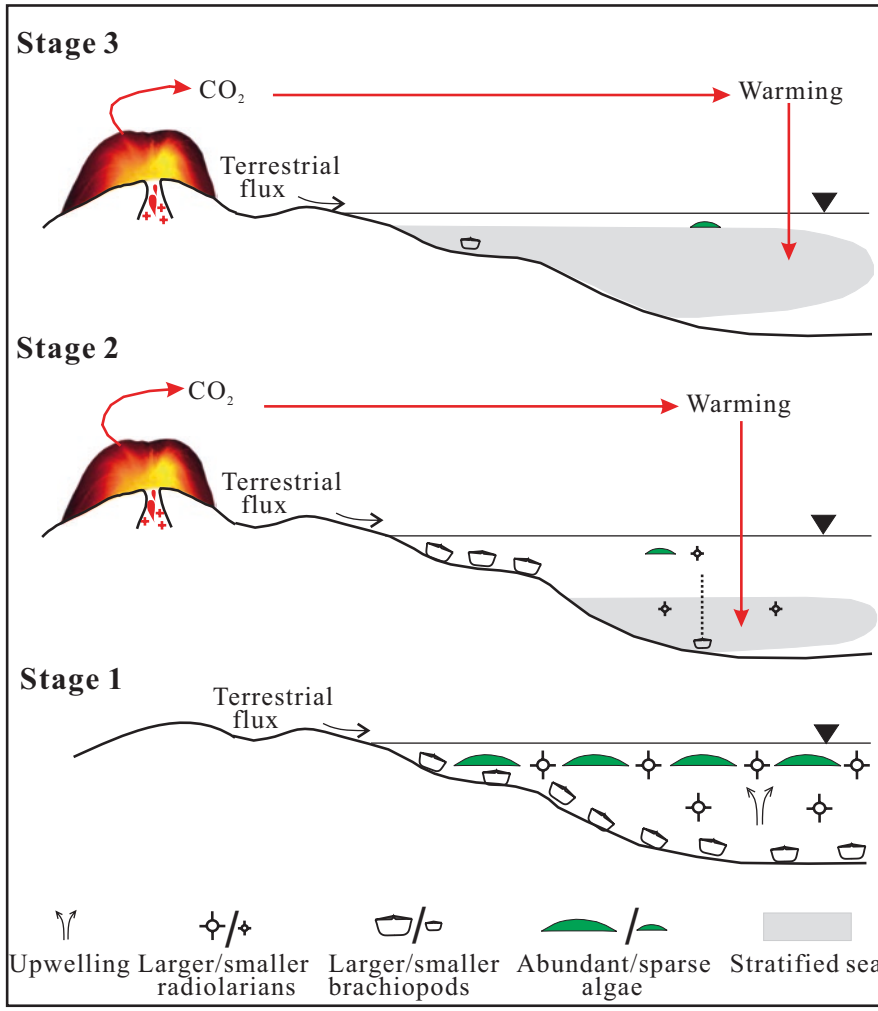

Fig. 8.1 Pattern for depicting 3 hypothesized stages of the end-Permian marine extinction process (revised after He et al. 2015). Stage 1- Pre-extinction environment (upwelling drove by the temperature difference from deep- to shallow-water columns in deep ocean), roughly corresponding to early late Changhsingian (the *C. changxingensis–C. deflecta* Zone to the lower *C. yini* Zone); Stage 2- Stratified sea with the formation of an offshore, wedge-shaped, deep-water chemocline in deep sea triggered by volcanism, roughly corresponding to late late Changhsingian (upper *C. yini* Zone); Stage 3- Expanding of an anoxic sea characterized by hydrogen sulfide gas (H_2S) and rapid shoaling of the chemocline. This stage roughly corresponds to the latest Changhsingian to the basal Triassic (*C. meishanensis* Zone upward)

tom waters with very limited circulations (Zopfi et al. 2001; Jensen et al. 2009). Initially, the chemocline (or Oxygen Minimum Zone) was mainly restricted to the deep sea and affected pelagic and deeper water benthic marine organisms (Stage 2 in Fig. 8.1). Evidence in support of this proposition includes the relatively earlier occurrence of deep-water brachiopod extinction during the *C. yini* Zone in South China, the extinction of the radiolarian Albaillellaria (deep-water dwellers) in South China also during the *C. yini* Zone (Feng et al. 2007; Feng and Algeo

2014), the radiolarian extinction during the late Changhsingian in the Mino terrane (NF1212R section) and North Kitakami Belt (Akkamori section) of Japan (Takahashi et al. 2009; Sano et al. 2012) (Fig. 6.2). In contrast, during this stage (Stage 2 in Fig. 8.1), shallow-water environments (shallow seas and carbonate platforms) largely remained oxygenated and did not exhibit evidence of severe diversity losses. A similar, bathymetry-dependent temporal pattern of brachiopod extinction in the latest Permian has also been observed in the peri-Gondwanan region. For example, at the deep-water Qubu and Tulong PTB sections in southern Tibet, brachiopods disappeared about 40–50 m below the PTB, in contrast to the shallow-water Selong section, also in southern Tibet, where the brachiopod extinction occurred 2.22 m below the PTB (Shen et al. 2006). Further more, a similar temporal pattern of extinction have also been documented in high-latitude Arctic regions (e.g., Arctic Canada, East Greenland) (Twitchett et al. 2001; Beauchamp and Baud 2002; Nabbefeld et al. 2010; Algeo et al. 2012). As one example, the siliceous-sponge chert factory extensively deveopled in deep-water Middle Permian Arctic seas collapsed in the Late Permian, well before the Permian–Triassic mass extinction (Beauchamp and Baud 2002).

With volcanism continued, the global warming became more intensified and tropical sea surface temperature rose up to ~35 °C across the main mass extinction horizon (Kearsey et al. 2009; Joachimski et al. 2012; Sun et al. 2012), leading up to a more stratified ocean system featured by a greatly expanded oxygen minimum zone and upward migration of the chemocline (Stage 3 in Fig. 8.1; see also Algeo et al. 2011). Such a sustained shoaling of chemocline during the latest Changhsingian to the earliest Triassic (i.e., *C. meishanensis* Zone upward) would have triggered a disaster to the shallow-water palaeocommunity which by then had been replaced by a low-diversity, low-provinciality, high-abundance, small-sized assemblage (e.g., survivors of brachiopods, foraminifers) (Stage 3 in Fig. 8.1, see also Zhang et al. 2017). This interpretation is evidenced by the coincidence of timing for the main episode of shallow-water mass extinction (i.e., Bed 25 of the Meishan section), volcanism (Sun et al. 2012; Yang et al. 2012; Pei et al. 2017), and the appearance of widespread anoxic conditions in shallow waters of South China (Yin et al. 2012; Huang et al. 2017).

8.2 Why Were the Latest Permian Body Sizes in Shallow-Water Settings on Average Larger Than in Deep-Water Settings?

As summarized in Chap. 3, the water depths of the studied sections during the latest Permian together constituted an approximately bathymetric gradient, changing from shallow (<50 m or slightly >50 m deep, represented by Zhongzhai and Huangzhishan sections), through moderately deep (50–100 m deep, represented by the Daoduishan section), to deep-water environments (about 100–200 m deep, represented by Majiashan and Rencunping sections) (Fig. 7.1). The overwhelming result of body-size analyses in relation to bathymetry is that the body sizes of the two studied chonetid species are commonly larger in shallow waters than their counterparts in moderately deep to deep waters (Fig. 7.1). This finding is coincided with the study of Shi et al. (2016), which was based on a global dataset using brachiopod orders.

In order to investigate why this was case and whether the bathymetry-related body-size changes were controlled by the oxygen availability in relation to water depths, we studied the pyrite framboids. Generally, in an euxinic condition, framboids are abundant, small (mean diameters 3–5 μm), with a narrow size range; in an anoxic condition, framboids are abundant, mostly small (mean diameters 4–6 μm) mixed

with a few large individuals; in a lower dysoxic condition, framboids are moderately common, 6–10 μm in diameter, with a few large individuals together with some pyrite crystals; in an upper dysoxic condition, framboids commonly or rarely occur (broadly variable in diameters if common, or with a few small individuals (<5 μm) if rare), and the majority of pyrites are crystals; in an oxic condition, framboids are absent and pyrite crystals rarely occur (Bond and Wignall 2010). We examined the pyrite framboids in polished sections and took photos by SEM. The polished sections were made from rocks collected from the Changhsingian (or upper Changhsingian) to the basal part of Triassic at the studied sections. The diameters of framboids were measured and calculated based on SEM images (Fig. 8.2). The studied results show that pyrite framboids are abundant in some intervals of the Changhsingian (or late Changhsingian) at Zhongzhai, Daoduishan and Rencunping (Fig. 8.2; He et al. 2017), but they are absent in the studied intervals of the upper Changhsingian at Huangzhishan. For the Majiashan section, pyrite framboids are very rare except for Bed 9 where they are unusually abundant (Fig. 8.2). Data of measurements for numbers and diameters of pyrite framboids were listed in He et al. (2017).

Applying the above criteria for the pyrite framboids as a proxy of redox conditions, the oxygen condition was probably anoxic (framboid diameters ≤6 μm) throughout the whole late Changhsingian at the deep-water Rencunping (Figs. 7.1C and 8.2). Similarly, it was anoxic to lower dysoxic (framboid diameters being 5–7 μm) in the late Changhsingian at the moderately deep-water Daoduishan (Figs. 7.1C and 8.2). For the deep-water Majiashan section, it was an approximately upper dysoxic condition (framboids rare and the diameters mostly <6 μm) (Figs. 7.1C and 8.2). Summarily, the oxygen conditions were dysoxic to anoxic in moderately deep- to deep-water sections. In contrast, for the shallow-water Huangzhishan section, it was oxic (absent of pyrite framboid) during the late Changhsingian (Fig. 8.2). Interestingly, the oxygen condition for the shallow-water Zhongzhai section, was lower dysoxic (framboids abundant and the diameters being 6–9 μm) for most of the Changhsingian (Figs. 7.1C and 8.2). Thus, it seems that the oxygen availability is not correlated linearly to bathymetry, presumably because of the presence of an expanding OMZ and the emergency of more varied submarine topography in South China (Wu et al. 1986; Zhang et al. 1997; Algeo et al. 2011; Shen et al. 2013; Luo et al. 2014; Song et al. 2014; He et al. 2017). Now we recall the body-size changes at these sections (see Chap. 7).

The values of X_{mean} and X_{median} for both chonetid species (*Fusichonetes pygmaea* and *Fusichonetes quadrata*) at Daoduishan, Majiashan and Rencunping sections are smaller than their counterparts at Huangzhishan; however, the values of X_{mean} and X_{median} for *F. pygmaea* at Zhongzhai are similar to the counterparts at Huangzhishan (Fig. 7.1).

Now, it is appropriate to consider brachiopod body-size changes in relation to oxygen conditions and bathymetry. As a whole, the oxygen variability appears to explain well size variation patterns of both chonetid species (Fig. 7.1). However, it is notable that the apparent oxygen restriction at Zhongzhai (lower dysoxic to anoxic conditions) did not cause size reduction (Fig. 7.1); this could be due to the abundance of food in the nearshore shallow-water environment, offsetting the negative impact of oxygen-poor on body size. If this scenario is followed, it means that food availability must also have played a role in regulating brachiopod body sizes.

8.3 Why Did Size Reduction Take Place and Occur Earlier in Deep Waters Than in Shallow Waters?

As summarized in Chap. 7, the size reduction initially took place below the PTB and occurred earlier in deep waters than in shallow waters. Why was this case? Generally, body-size reduction of animals is considered as a phenotypic

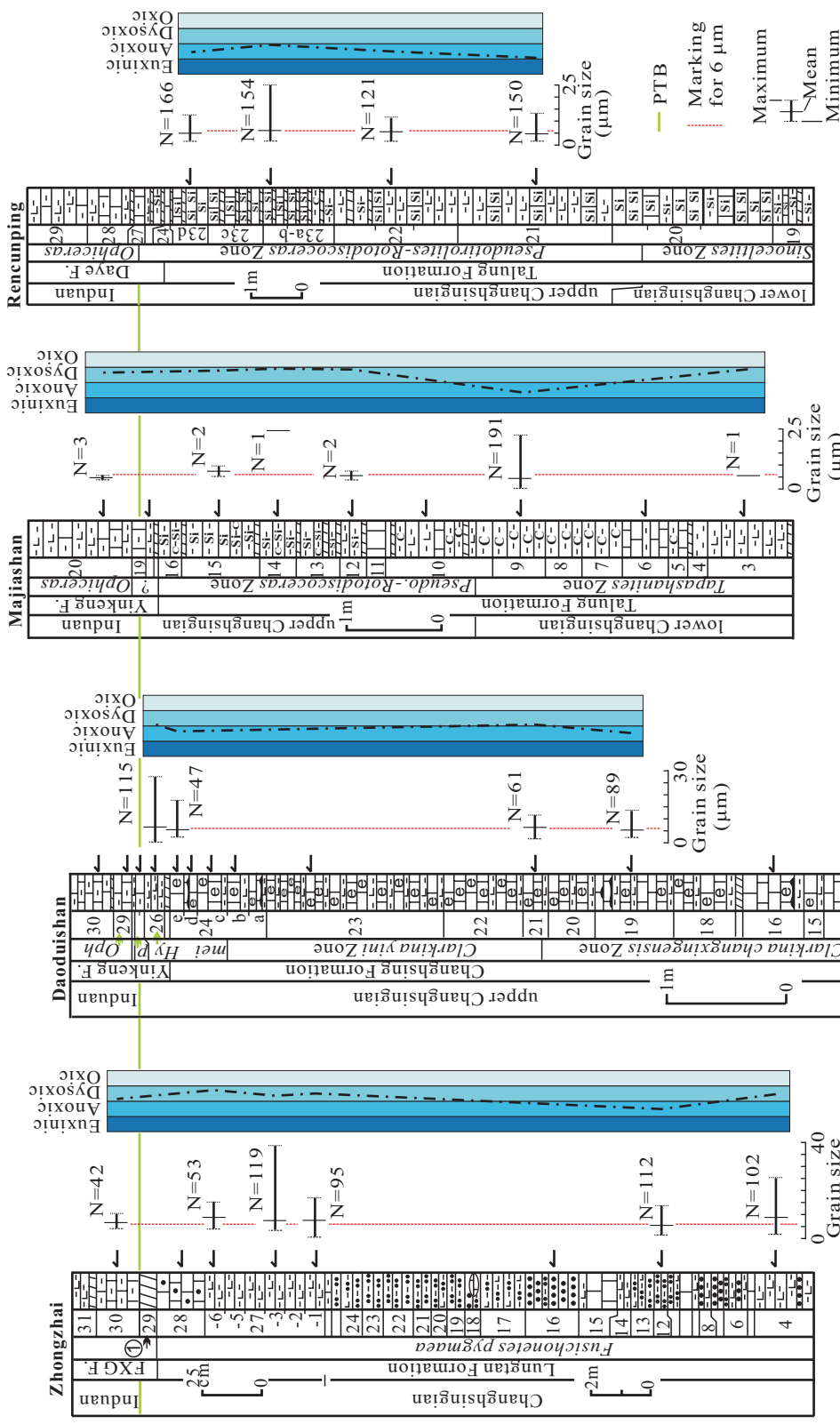

Fig. 8.2 Stratigraphic distribution of pyrite-framboid sizes and the indicated redox conditions along studied sections (after He et al. 2017). "N" represents the number of framboids; black arrows indicate samplings for polished sections of pyrite framboids. Other legends and abbreviations are same to Fig. 7.2

response to stressful or suboptimal environmental conditions, e.g., global warming, marine anoxia, restricted food resources (Twitchett 2007), but their relative impact on body-size changes tend to vary considerably in different cases. If the body-size reduction of brachiopods in the latest Permian of South China is concerned, redox conditions appear to be the primary driver, followed by food availability, as summarized above. The fact that the brachiopods started to significantly reduce their sizes before the PTB suggests that the brachiopod community was already undergoing structural and functional changes at the community level and these changes could be interpreted as possible early warning sygnals for an ecosystem regime shift (Zhang et al. 2017; Wu et al. 2018).

This temporal pattern of brachiopod size reductions may be further explained as follows. Initially, the brachiopods were able to cope with the onset of environmental stress (i.e., marine anoxia, restricted food resources) by first reducing their size, possibly alongside other morphological adaptations and regional biogeographical migrations in South China (e.g., Chen et al. 2011; He et al. 2012, 2014). Subsequently, as environmental deterioration continued, these responses were no longer sufficient to prevent extinction and consequently most species did not survive in the latest Permian mass extinction. Further, the temporal differences in body-size reduction between deep- and shallow-water brachiopods indicate that stressful conditions (e.g., anoxia, restricted food resources) began earlier in deeper water settings, where a stratified ocean (or OMZ) and related deep-water anoxia were emerging and expanding (see the part of 8.1). The small-scale brachiopod body-size increase before the extinction at Rencunping and Majiashan was possibly induced by a short-term, local environmental amelioration. In contrast, the brief size increase after the extinction is attributed to reduced interspecific competition for food resources following the extinction of competitors (He et al. 2010, 2015). The subsequent size reduction in the Early Triassic (i.e., so called Lilliput Effect) should have been owed to the continued stressful environment.

8.4 Discussion on the Morphologic Features of Brachiopods in the Aftermath of Mass Extinction

The brachiopod fauna in the aftermath of mass extinction (= the survival or mixed fauna, see Liao 1979; Chen et al. 2005) mainly comprises *Paryphella*, *Paracrurithyris*, *Fusichonetes*, *Prelissorhynchia*, *Acosarina*, S*peciothyris* (previously assigned to *Crurithyris* or *Orbicoelia*, details given in Chap. 9) and linguloids. These elements have common morphological features, including a small body size, thin and semi-transparent shell, moderately complex lophophore structures or the presence of dense, radially-arranged pseudopunctae within shells.

Geometrically, a small body size would translate to a higher surface area to volume ratio, which in turn would mean a greater potential for oxygen and nutrient uptake (He et al. 2014). Similarly, the possession of a thin, semi-transparent shell by many species of the Permian–Triassic mixed fauna suggests that these brachiopods probably evolved with this feature to aid their respiration and metabolism. Elsewhere, it has also been suggested that both a reduced body size and a thinned shell represent advantageous adaptations to lowered oxygen supply and/or reduced trophic resources (Fürsich and Hurst 1974; Thayer 1986; Levin 2003). Among the survived brachiopods, ambocoeliid brachiopods, *Paracrurithyris pygmaea* and *Speciothyris speciosa*, are good examples in demonstrating these adaptations during the Permian–Triassic boundary life crisis in the ocean. Besides a small size and a thin shell, both *Paracrurithyris pygmaea* and *Speciothyris speciosa* also bear moderately complex lophophore structures inside their shells (Carter et al. in Williams et al. 2006). The function of the lophophore is to enhance the efficiency of filter-feeding or respiration, especially for brachiopod species living in a low-oxygen or nutrition-restricted setting (Fürsich and Hurst 1974; Thayer 1986; Afanasjeva 2009). Thus, it is plausible that the small-bodied, thin-shelled and lophophore-bearing ambocoeliids were adapted

to life in a setting with low dissolved oxygen and restricted food resources (He et al. 2014).

An additional unique feature for the survived brachiopod fauna of South China is the presence of dense, radially-arranged pseudopunctae within their shells (e.g., *Paryphella*, *Fusichonetes*). According to Afanasjeva (2009), the presence of crowded pseudopunctae might indicate the formation of a specialized, much expanded mantle with ridges and pits on the mantle surface. The brachiopod mantle is known to play an important role in transporting and capturing food, sorting particles, pumping water and aiding respiration (Grant 1968; Westbroek et al. 1980; Thayer 1986; Afanasjeva 2008, 2009). Therefore, we can infer that the survived chonetid brachiopods with dense pseudopunctae could also represent another morphological adaptation to a highly-stressed environment where both oxygen and food resources were severely restricted.

To sum up, the morphologic features of brachiopods in the aftermath of mass extinction suggest a setting of anoxia and restricted food availability during the crisis.

8.5 Implications for the Great Dying and Prospects for Future Study

Although previous studies have suggested various modes for the Permian–Triassic mass extinction: one-episode, two-episodes, or multiple-episodes (Yang et al. 1991; Jin et al. 2000; Feng et al. 2007; Shen et al. 2011; Song et al. 2013; Wang et al. 2014; Grasby et al. 2015), we believe that the actual mass extinction involved a much complex process in relation to varied palaeogeographic settings. In view of the spatio–temporal patterns of brachiopod-diversity evolution and body-size changes as outlined above, it is evident that the extinction process initially was coincident with marine anoxia, which was most likely triggered by global warming and upward migration of the chemocline. Subsequently, marine primary productivity declined and food resources became increasingly restricted (Beauchamp and Baud 2002; Algeo et al. 2013). Throughout this process, ocean acidification probably also played a role (Payne et al. 2010; Clarkson et al. 2015), as did with sea-level falling (Yin et al. 2014; Tavakoli et al. 2017). It is possible that all these factors systematically interacted in the lead up to the final Permian–Triassic mass extinction.

In summary, we propose that the latest Permian (Changhsingian) volcanism in relation to formation of Pangaea caused the global warming and formation of an increasingly stratified ocean with an upward migration of chemocline or OMZ. This major environmental crisis first influenced deep-water organisms in pelagic and offshore settings, and then affected shallow-water biotic communities. Thus, during the Late Permian, the environmental and life crisis firstly began in the deeper waters, and then spread to shallow waters.

In terms of the Permian–Triassic palaeoenvironmental conditions, there are still some debates and contradictions. For example, a few researchers have argued against anoxia as one of the primary extinction causes, because of the inconsistency of timing between mass extinction and anoxia events (Chen et al. 2015; Li et al. 2016; Xiang et al. 2016; Zhang et al. 2017). Even if anoxia played a major role, the timing of its onset remains unclear. Also, was anoxia compounded or offset by other environmental/ecological drivers? And was ‘killing by anoxia’ selective in taxonomy? Additionally, the idea of marine acidification leading to the Permian–Triassic mass extinction is still in debate (Payne et al. 2010; Song et al. 2014; Clarkson et al. 2015) and requires more evidence from the fossils themselves as well as from proxy-based studies. Finally, the scenario of marine productivity fluctuations as a contributor to the Permian–Triassic extinction (Algeo et al. 2013; Georgiev et al. 2015) awaits further testing with data from different sections at different palaeogeographical and latitudinal settings. In summary, the study on the evolution of different taxa and multiple environmental indicators in varied palaeogeographic settings will provide important insights into the great dying and more related work are needed in the future.

References

Afanasjeva GA. 2008. Morphological study of the brachiopods of the Order Chonetida. Paleontological Journal, 42: 825–829.

Afanasjeva GA. 2009. Changes in the communities of Paleozoic brachiopods due to their development of their filtering system. Paleontological Journal, 43: 1378–1389.

Algeo TJ, Chen ZQ, Fraiser ML, Twitchett RJ. 2011. Terrestrial–marine teleconnections in the collapse and rebuilding of Early Triassic marine ecosystems. Palaeogeography, Palaeoclimatology, Palaeoecology, 308: 1–11.

Algeo TJ, Henderson CM, Ellwood B, Rowe H, Elswick E, Bates S, Lyons T, Hower JC, Smith C, Maynard B, Hays LE, Summons R, Fulton J, Freeman KH. 2012. Evidence for a diachronous Late Permian marine crisis from the Canadian Arctic region. Geological Society of America Bulletin, 124: 1424–1448.

Algeo TJ, Henderson CM, Tong JN, Feng QL, Yin HF, Tyson RV. 2013. Plankton and productivity during the Permian–Triassic boundary crisis: an analysis of organic carbon fluxes. Global Planetary Change, 105: 52–67.

Beauchamp B, Baud A. 2002. Growth and demise of Permian biogenic chert along northwest Pangea: evidence for end-Permian collapse of thermohaline circulation. Palaeogeography, Palaeoclimatology, Palaeoecology, 184: 37–63.

Bond DPG, Wignall PB. 2010. Pyrite framboid study of marine Permian–Triassic boundary sections: a complex anoxic event and its relationship to contemporaneous mass extinction. Geological Society of America Bulletin, 122: 1265–1279.

Chen J, Chen ZQ, Tong JN. 2011. Environmental determinants and ecologic selectivity of benthic faunas from nearshore to bathyal zones in the end-Permian mass extinction: Brachiopod evidence from South China. Palaeogeography, Palaeoclimatology, Palaeoecology, 308: 84–97.

Chen ZQ, Kaiho K, George AD. 2005. Survival strategies of brachiopod faunas from the end-Permian mass extinction. Palaeogeography, Palaeoclimatology, Palaeoecology, 224: 232–269.

Chen ZQ, Yang H, Luo M, Benton MJ, Kaiho K, Zhao LS, Huang YG, Zhang KX, Fang YH, Jiang HS, Qiu H, Li Y, Tu CY, Shi L, Zhang L, Feng XQ, Chen L. 2015. Complete biotic and sedimentary records of the Permian–Triassic transition from Meishan section, South China: Ecologically assessing mass extinction and its aftermath. Earth-Science Reviews, 149: 63–103.

Clarkson MO, Kasemann SA, Wood RA, Lenton TM, Daines SJ, Richoz S, Ohnemueller F, Meixner A, Poulton SW, Tipper ET. 2015. Ocean acidification and the Permo–Triassic mass extinction. Science, 348: 229–232.

Feng QL, Algeo TJ. 2014. Evolution of oceanic redox conditions during the Permo–Triassic: Evidence from radiolarian deepwater facies. Earth Science Reviews, 137: 34–51.

Feng QL, He WH, Gu SZ, Meng YY, Jin YX, Zhang F. 2007. Radiolarian evolution during the latest Permian in South China. Global and Planetary Change, 55: 177–192.

Fürsich FT, Hurst JM. 1974. Environmental factors determining the distribution of brachiopods. Palaeontology, 17: 879–900.

Georgiev SV, Horner TJ, Stein HJ, Hannah JL, Bingen B, Rehkämper M. 2015. Cadmium-isotopic evidence for increasing primary productivity during the Late Permian anoxic event. Earth and Planetary Science Letters, 410: 84–96.

Grant RE. 1968. Structural adaptation in two Permian brachiopod genera, Salt Range, West Pakistan. Journal of Paleontology, 42: 1–32.

Grasby SE, Beauchamp B, Bond DPG, Wignall P, Talavera C, Galloway JM, Piepjohn K, Reinhardt L, Blomeier D. 2015. Progressive environmental deterioration in northwestern Pangea leading to the latest Permian extinction. Geological Society of America Bulletin, 127: 1331–1347.

He WH, Twitchett RJ, Zhang Y, Shi GR, Feng QL, Yu JX, Wu SB, Peng XF. 2010. Controls on body size during the Late Permian mass extinction event. Geobiology, 8: 391–402.

He WH, Shi GR, Zhang Y, Yang TL, Teng F, Wu SB. 2012. Systematics and palaeoecology of Changhsingian (Late Permian) Ambocoeliidae brachiopods from South China and implications for the end-Permian mass extinction. Alcheringa, 36: 515–530.

He WH, Shi GR, Zhang Y, Yang TL, Zhang KX, Wu SB, Niu ZJ, Zhang ZY. 2014. Changhsingian (latest Permian) deep-water brachiopod fauna from South China. Journal of Systematic Palaeontology, 12: 907–960.

He WH, Shi GR, Twitchett RJ, Zhang Y, Zhang KX, Song HJ, Yue ML, Wu SB, Wu HT, Yang TL, Xiao YF. 2015. Late Permian marine ecosystem collapse began in deeper waters: evidence from brachiopod diversity and body size changes. Geobiology, 13: 123–138.

He WH, Shi GR, Xiao YF, Zhang KX, Yang TL, Wu HT, Zhang Y, Chen B, Yue ML, Shen J, Wang YB, Yang H, Wu SB. 2017. Body-size changes of latest Permian brachiopods in varied palaeogeographic settings in South China and implications for controls on animal miniaturization in a highly stressed marine ecosystem. Palaeogeography, Palaeoclimatology, Palaeoecolog, 486: 33–45.

Huang YG, Chen ZQ, Wignall PB, Zhao LS. 2017. Latest Permian to Middle Triassic redox condition variations in ramp settings, South China: Pyrite framboid evidence. Geological Society of America Bulletin, 129: 229–243.

Isozaki Y. 2009. Integrated "plume winter" scenario for the double-phased extinction during the Paleozoic–Mesozoic transition: The G–LB and PTB events from

a Panthalassan perspective. Journal of Asian Earth Sciences, 36: 459–480.

Isozaki Y, Shimizu N, Yao JX, Ji ZS, Matsuda T. 2007. End-Permian extinction and volcanism-induced environmental stress: The Permian–Triassic boundary interval of lower-slope facies at Chaotian, South China. Palaeogeography, Palaeoclimatology, Palaeoecology 252: 218–238.

Jensen MM, Petersen J, Dalsgaard T, Thamdrup B. 2009. Pathways, rates, and regulation of N_2 production in the chemocline of an anoxic basin, Mariager Fjord, Denmark. Marine Chemistry, 113: 102–113.

Jin YG, Wang Y, Wang W, Shang QH, Cao CQ, Erwin DH. 2000. Pattern of marine mass extinction near the Permian–Triassic boundary in South China. Science, 289: 432–436.

Joachimski MM, Lai XL, Shen SZ, Jiang HS, Luo GM, Chen B, Chen J, Sun YD. 2012. Climate warming in the latest Permian and the Permian–Triassic mass extinction. Geology, 40: 195–198.

Kearsey T, Twitchett RJ, Price GD, Grimes ST. 2009. Isotope excursions and palaeotemperature estimates from the Permian/Triassic Boundary in the Italian Dolomites. Palaeogeography, Palaeoclimatology, Palaeoecology, 279: 29–40.

Levin LA. 2003. Oxygen minimum zone benthos: adaptation and community response to hypoxia. Annual Review of Oceanography and Marine Biology, 41: 1–45.

Li GS, Wang YB, Shi GR, Liao W, Yu LX. 2016. Fluctuations of redox conditions across the Permian–Triassic boundary-new evidence from the GSSP section in Meishan of South China. Palaeogeography, Palaeoclimatology, Palaeoecology, 448: 48–58.

Liao ZT. 1979. Brachiopod Assemblage Zone of Changhsing Stage and brachiopods from Permo–Triassic Boundary Beds in China. Acta Stratigraphica Sinica, 3: 200–208. [in Chinese].

Luo GM, Algeo TJ, Huang JH, Zhou WF, Wang YB, Yang H, Richoz S, Xie SC. 2014. Vertical δ^{13}Corg gradients record changes in planktonic microbial community composition during the end-Permian mass extinction. Palaeogeography, Palaeoclimatology, Palaeoecology, 396: 119–131.

Nabbefeld B, Grice K, Twitchett RJ, Summons RE, Hays L, Böttcher ME, Asif M. 2010. An integrated biomarker, isotopic and palaeoenvironmental study through the Late Permian event at Lusitaniadalen, Spitsbergen. Earth and Planetary Science Letters, 291: 84–96.

Payne JL, Turchyn AV, Paytan A, DePaolo DJ, Lehrmann DJ, Yu MY, Wei JY. 2010. Calcium isotope constraints on the end-Permian mass extinction. Proceedings of the National Academy of Sciences, 107: 8543–8548.

Pei Y, Chen ZQ, Fang YH, Kershaw S, Wu SQ, Luo M. 2017. Volcanism, redox conditions, and microbialite growth linked with the end-Permian mass extinction: Evidence from the Xiajiacao section (western Hubei Province), South China. Palaeogeography, Palaeoclimatology, Palaeoecology, online.

Sano H, Wada T, Naraoka H. 2012. Late Permian to Early Triassic environmental changes in the Panthalassic Ocean: Record from the seamount-associated deep-marine siliceous rocks, central Japan. Palaeogeography, Palaeoclimatology, Palaeoecology, 363–364: 1–10.

Saunders A, Reichow M. 2009. The Siberian Traps and the End-Permian mass extinction: a critical review. Chinese Science Bulletin, 54: 20–37.

Shen J, Lei Y, Algeo TJ, Feng QL, Servais T, Yu JX, Zhou L. 2013. Volcanic effects on microplankton during the Permian–Triassic transition (Shangsi and Xinming, South China). Palaios, 28: 552–567.

Shen SZ, Cao CQ, Henderson CM, Wang XD, Shi GR, Wang Y, Wang W. 2006. End-Permian mass extinction pattern in the northern peri-Gondwanan region. Palaeoworld, 15: 3–30.

Shen SZ, Crowley JL, Wang Y, Bowring SA, Erwin DH, Sadler PM, Cao CQ, Rothman DH, Henderson CM, Ramezani J, Zhang H, Shen YA, Wang XD, WangW, Mu L, Li WZ, Tang YG, Liu XL, Liu LJ, Zeng Y, Jiang YF, Jin YG. 2011. Calibrating the End-Permian Mass Extinction. Science, 334: 1367–1372.

Shi GR, Zhang YC, Shen SZ, He WH. 2016. Nearshore–offshore–basin species diversity and body size variation patterns in Late Permian (Changhsingian) brachiopods. Palaeogeography, Palaeoclimatology, Palaeoecology, 448: 96–107.

Song HJ, Wignall PB, Tong JN, Yin HF. 2013. Two pulses of extinction during the Permian–Triassic crisis. Nature Geoscience, 6: 52–56.

Song HJ, Wignall PB, Chu DL, Tong JN, Sun YD, Song HY. 2014. Anoxia/high temperature double whammy during the Permian-Triassic marine crisis and its aftermath. Scientific Reports. 4(4): 4132.

Song HY, Tong JN, Tian L, Song HJ, Qiu HO, Zhu YY, Algeo TJ. 2014. Paleo-redox conditions across the Permian–Triassic boundary in shallow carbonate platform of the Nanpanjiang Basin, South China. Science China Earth Sciences, 57: 1030–1038.

Sun YD, Joachimski MM, Wignall PB, Yan CB, Chen YL, Jiang HS, Wang LN, Lai XL. 2012. Lethally hot temperatures during the Early Triassic greenhouse. Science, 338: 366–370.

Takahashi S, Yamakita S, Suzuki N, Kaiho K, Ehiro M. 2009. High organic carbon content and a decrease in radiolarians at the end of the Permian in a newly discovered continuous pelagic section: A coincidence? Palaeogeography, Palaeoclimatology, Palaeoecology, 271: 1–12.

Takahashi S, Kaiho K, Hori RS, Gorjan P, Watanabe T, Yamakita S, Aita Y, Takemura A, Sp€orli KB, Kakegawa T, Oba M. 2013. Sulfur isotope profiles in the pelagic Panthalassic deep sea during the Permian–Triassic transition. Global and Planetary Change, 105: 68–78.

Tavakoli V, Naderi-Khujin M, Seyedmehdi Z. 2017. The end-Permian regression in the western Tethys: sedimentological and geochemical evidence from offshore the Persian Gulf, Iran. Geo-Marine Letters, 38: 179–192.

Thayer CW. 1986. Respiration and the function of brachiopod punctae. Lethaia, 19: 23–31.

Twitchett RJ. 2007. The Lilliput effect in the aftermath of the end-Permian extinction event. Palaeogeography, Palaeoclimatology, Palaeoecology, **252**: 132–144.

Twitchett RJ, Looy CV, Morante R, Visscher H, Wignall PB. 2001. Rapid and synchronous collapse of marine and terrestrial ecosystems during the end-Permian mass extinction event. Geology, 29: 351–354.

Wang Y, Shen SZ, Zhang YC, Wang XD, Wang W, Sadler PM, Erwin DH, Crowley JL, Henderson CM. 2014. Quantifying the process and abruptness of the end-Permian mass extinction. Paleobiology, 41: 113–129.

Westbroek P, Yanagida J, Isa Y. 1980. Functional morphology of brachiopod and coral skeletal structures supporting ciliated epithelia. Paleobiology, 6: 313–330.

Williams A, Brunton CHC, Carlson SJ, Baker PG, Carter JL, Curry GB, Dagys AS, Gourvennec R, Hou HF, Jin YG, Johnson JG, Lee DE, MacKinnon DI, Racheboeuf PR, Smirnova TN, Sun DL. 2006. Rhynchonelliformea (part), p. 1689–1937. In: Williams A et al. (Eds), Treatise on Invertebrate Paleontology, Part H, Brachiopoda (revised) 5, Rhynchonelliformea (part). Geological Society of America and University of Kansas, Boulder and Lawrence.

Wu SB, Wei M, Zhang KX. 1986. Facies changes and controlling factors of the Late Permian Changxing limestone in the Changxing area. Geological Review, 32: 419–425. [in Chinese with English abstract].

Wu HT, He WH, Weldon EA. 2018. Prelude of benthic community collapse during the end-Permian mass extinction in siliciclastic offshore sub-basin: Brachiopod evidence from South China. Global and Planetary Change, 163: 158–170.

Xiang L, Schoepfer SD, Zhang H, Yuan DX, Cao CQ, Zheng QF, Henderson CM, Shen SZ. 2016. Oceanic redox evolution across the end-Permian mass extinction at Shangsi, South China. Palaeogeography, Palaeoclimatology, Palaeoecology, 448: 59–71.

Yang JH, Cawood PA, Du YS, Huang H, Huang HM, Tao P. 2012. Large Igneous Province and magmatic arc sourced Permian–Triassic volcanogenic sediments in China. Sedimentary Geology, 261–262: 120–131.

Yang ZY, Wu SB, Yin HF, Xu GR, Zhang KX. 1991. Permo–Triassic Events of South China. Geological Publishing House, Beijing, 183 pp. [in Chinese with English abstract].

Yin HF, Xie SC, Luo G, Algeo TJ, Zhang K. 2012. Two episodes of environmental change at the Permian–Triassic boundary of the GSSP section Meishan. Earth-Science Reviews, 115: 163–172.

Yin HF, Jiang HS, Xia WC, Feng QL, Zhang N, Shen J. 2014. The end-Permian regression in South China and its implication on mass extinction. Earth-Science Reviews, 137: 19–33.

Zhang KX, Tong JN, Yin HF, Wu SB. 1997. Sequence stratigraphy of the Permian–Triassic Boundary Section of Changxing, Zhejiang, southern China. Acta Geologica Sinica, 71: 90–103.

Zhang L, Feng QL, He WH. 2017. Permian radiolarian biostratigraphy. In: Lucas SG, Shen SZ (eds), The Permian timescale, London: Geological Society. 450: 143–163.

Zhang Y, Shi GR, Wu HT, Yang TL, He WH, Yuan AH, Lei Y. 2017. Community replacement, ecological shift and early warning signals prior to the end-Permian mass extinction: A case study from a nearshore clastic-shelf section in South China. Palaeogeography, Palaeoclimatology, Palaeoecology, 487: 118–135.

Zopfi J, Ferdelman TG, Jørgensen BB, Teske A, Thamdrup B. 2001. Influence of water column dynamics on sulfide oxidation and other major biogeochemical processes in the chemocline of Mariager Fjord (Denmark). Marine Chemistry, 74: 29–51.

Systematic Palaeontology

9

Wei-Hong He, G. R. Shi, Shu-Zhong Shen, Ting-Lu Yang, Yang Zhang, Hui-Ting Wu, Han Wang, and Jian-Jun Bu

The classification of Brachiopoda adopted herein follows Williams et al. (2000, 2002, 2006) for Productida, Orthida, Orthotetida, Rhynchonellida, Spiriferida and Lingulida, with exceptions for *Anidanthus* which follows Waterhouse (1968a), *Speciothyris* which follows Jin and Sun, 1981 and Lingulidae which follows Emig (2003). In addition, we revised the classification of *Parapygmochonetes* at the family level based on a parsimony analysis.

All the specimens described in this paper are preserved in the Laboratory of Geobiology, Faculty of Earth Sciences, China University of Geosciences, Wuhan, People's Republic of China, with the prefix of HZS, ZZ (or LZ), DDS, CM, SR, XM, DS, SW, HS, DP, PB, DCB, XJP, LQ, SNM, XC, and DSH. Abbreviations of localities (sections): HZS = Huangzhishan section, ZZ (or LZ) = Zhongzhai section, DDS = Daoduishan section, CM = Majiashan

W.-H. He (✉)
State Key Laboratory of Biogeology and Environmental Geology, School of Earth Sciences, China University of Geosciences, Wuhan, China
e-mail: whzhang@cug.edu.cn

G. R. Shi
School of Life and Environmental Sciences, Burwood, Victoria, Australia

Deakin University, Geelong, Victoria, Australia
e-mail: grshi@deakin.edu.au

S.-Z. Shen
State Key Laboratory of Palaeobiology and Stratigraphy, Nanjing Institute of Geology and Palaeontology and Center for Excellence in Life and Palaeoenvironment, Chinese Academy of Sciences, Nanjing, Jiangsu, China
e-mail: szshen@nigpas.ac.cn

T.-L. Yang
Faculty of Geosciences, East China University of Technology, Nanchang, China
e-mail: yang@geology.hk

Y. Zhang
School of Earth Sciences and Resources, China University of Geosciences, Beijing, China

H.-T. Wu · H. Wang
School of Earth Sciences, China University of Geosciences, Wuhan, China

J.-J. Bu
Wuhan Centre for China Geological Survey, Wuhan, China
e-mail: jianjunbu@cug.edu.cn

W.-H. He et al. (eds.), *Brachiopods around the Permian-Triassic Boundary of South China*, New Records of the Great Dying in South China, https://doi.org/10.1007/978-981-13-1041-6_9

section, SR = Rencunping section, XM = Xinming section, DS = Duanshan section, SW = Shaiwa section, HS = Hushan section, DP = Dongpan section, PB = Paibi section, DCB = Dengcaoba section, XJP = Xiejiaping section, LQ = Liuqiao section, SNM = Shangname section, XC = Xichang section, and DSH = Dushan section. Abbreviations of morphological and anatomical terms see Appendix 2.

Order **Productida** Sarytcheva and Sokolskaya, 1959
Suborder **Productidina** Waagen, 1883
Superfamily **Linoproductoidea** Stehli, 1954
Family **Monticuliferidae** Muir-Wood and Cooper, 1960
Subfamily **Auriculispininae** Waterhouse, 1986
Genus ***Costatumulus*** Waterhouse, 1983a

Type Species *Auriculispina tumida* Waterhouse in Waterhouse et al., 1983. Lower Permian; northern Bowen Basin, Queensland.

Diagnosis Venter swollen; costellae fine; concentric wrinkles developed; spines limited to ventral valve, spine bases quincunxial, elongated, swollen on disk, rows of spines near hingeline or on ears (as emended by He et al., 2014); subelongated pits on dorsal valve (Waterhouse et al., 1983).

Discussion *Cancrinella* was proposed by Fredericks (1928) based on the characteristics of fine radial striae and hollow spines on both valves. Later, Sarytcheva (1937) suggested some additional features also thought to be characteristic of this genus: the surface variably covered with fine radial ribbing and concentric wrinkes, spines covered the ventral valve, and commonly also situated along hingeline and ears. The descriptions of Fredericks (1928) and the supplements of Sarytcheva (1937) suggested that spines covered both ventral and dorsal disks, as well as ventral hingeline and ears. However, Muir-Wood and Cooper (1960) emended the original definition of *Cancrinella*, noting that *Cancrinella* has quincunxial spines only on ventral valve, but with dimples on dorsal valve. If following this definition, *Cancrinella* would become confused with *Costatumulus* (see below). Consequently, we follow the original definition of *Cancrinella* by Fredericks (1928) and Sarytcheva (1937), and consider that the illustration (*Cancrinella*) of Fig. 1–13 in pl. 112 of Muir-Wood and Cooper 1960 and Fig. 370.2g–h of Treatise (Brunton et al. in William et al. 2000) could be a species of *Costatumulus* Waterhouse, 1983a rather than a species of *Cancrinella* (He et al., 2014).

Costatumulus has spines on ventral valve only and subelongate pits (= dimples) on dorsal valve (Waterhouse et al., 1983). Thus, *Cancrinella* species can be readily distinguished from *Costatumulus* by having spines on both valves. *Costatumulus* is similar to *Cancrinelloides* Ustritskhy in Ustritsky and Tschernjak, 1963 in quincunxial and elongated spine bases on ventral disk, and fine costellae, but differs in the latter having a transverse outline and much weaker concentric ornamentation. *Costatumulus* is similar to *Magniplicatina* Waterhouse, 1983b in quincunxial and elongated spine bases on ventral disk, but differs in the latter having spines on dorsal valves and much irregular and stronger rugae on ventral valve (Campbell, 1953; Waterhouse, 1983b).

Costatumulus dongpanensis He and Shen in He et al., 2005
Figs. 9.1, 9.2, 9.3 and 9.4

2005 *Costatumulus dongpanensis* He and Shen in He et al.: 931, Fig. 3.16–3.22.
2012 *Costatumulus dongpanensis* He and Shen; Li et al.: Fig. 7.20–7.25.
2014 *Costatumulus dongpanensis* He and Shen; He et al.: Fig. 19f–q.

Diagnosis Fine, dense, and regular rugae on dorsal valve.

Materials Over 200 specimens. Registered specimens: see below.

Measurements (mm).

Registered number	Width	Length	Width/length	Notes
DP806	28.39	21.18	1.34	External mould of ventral valve
PB-2-293	17.81	12.37	1.44	Ventral valve
DP715	23.06	17.06	1.35	Ventral valve
DP716-dorsal	21.56	15.66	1.38	Conjoined sell
DP-9-291	13.29	11.86	1.12	External mould of ventral valve
DP-10-290	13.79	9.39	1.47	Ventral valve
DS-1-602	15.23	11.48	1.33	External mould of ventral valve
DP-9-283	29.29	19.12	1.53	Ventral valve
DP-7-286	19.90	14.91	1.33	External mould of ventral valve
DP-7-281	21.01	16.30	1.29	External mould of dorsal valve
DP-7-287	30.44	21.96	1.39	External mould of dorsal valve
DP2-0013	17.85	14.04	1.27	External mould of ventral valve
DP-7-288	15.79	13.68	1.15	External mould of dorsal valve
DP710	14.74	6.43	2.29	External mould of dorsal valve
DP711	14.40	6.34	2.27	External mould of dorsal valve
DP803	14.30	13.25	1.08	External mould of dorsal valve
DP9-0035	11.58	8.75	1.32	External mould of dorsal valve
DP10-0037	24.24	15.20	1.59	Internal mould of dorsal valve
DP9-0014	22.75	14.84	1.53	External mould of ventral valve
DP5-0028	8.92	6.28	1.42	Internal mould of dorsal valve
DP9-0010	29.99	19.00	1.58	External mould of ventral valve
DP2-0025	29.20	18.29	1.60	Dorsal valve
DP7-0026	21.53	15.67	1.37	Internal mould of dorsal valve
DP10-0042	21.23	12.33	1.72	Ventral valve
DP3-0033	19.15	14.50	1.32	Internal mould of dorsal valve
DP3-0034	11.73	9.31	1.26	Internal mould of dorsal valve
DP10-0007	21.34	13.79	1.55	Ventral valve
DP-10-290	12.99	8.74	1.49	Ventral valve
DP8-0060	13.17	10.20	1.29	Internal mould of dorsal valve
DP9-0068	8.73	6.15	1.42	Ventral valve (younger adult)
DP9-0064	8.76	6.53	1.34	Ventral valve
DP10-0075	3.49	3.00	1.16	External mould of dorsal valve (juvenile)
DP9-0076	5.50	4.31	1.28	Internal mould of dorsal valve (juvenile)
DP10-0077	4.53	3.66	1.24	Internal mould of dorsal valve (juvenile)
DP9-0080	5.39	3.49	1.54	Ventral valve (juvenile)
DP8-0078	5.70	4.48	1.27	External mould of dorsal valve

Occurrence Upper Changhsingian; Guangxi and Guizhou of South China.

Description Shell 3.5–25.0 mm long and 3.5–30.0 mm wide, subcircular in outline, greatest width slightly anterior to hinge. Ventral valve gently convex, greatest convexity at umbo; beak obtuse, slightly incurved; ears medium, triangular, demarcated from visceral disk by grooves; sulcus absent; flanks gently inclined; shell surface finely costellate, costellae numbering four to five in 2 mm at shell midlength; rugae densely spaced, three in 2 mm, partly irregular on visceral disk; one row of spines along hingeline, the other row of spines situated on ears (Fig. 9.1b, e, f), body spines long, swollen at base, arising at a low angle to shell surface, largely quincunxial in arrangement on visceral disk (body spines weak

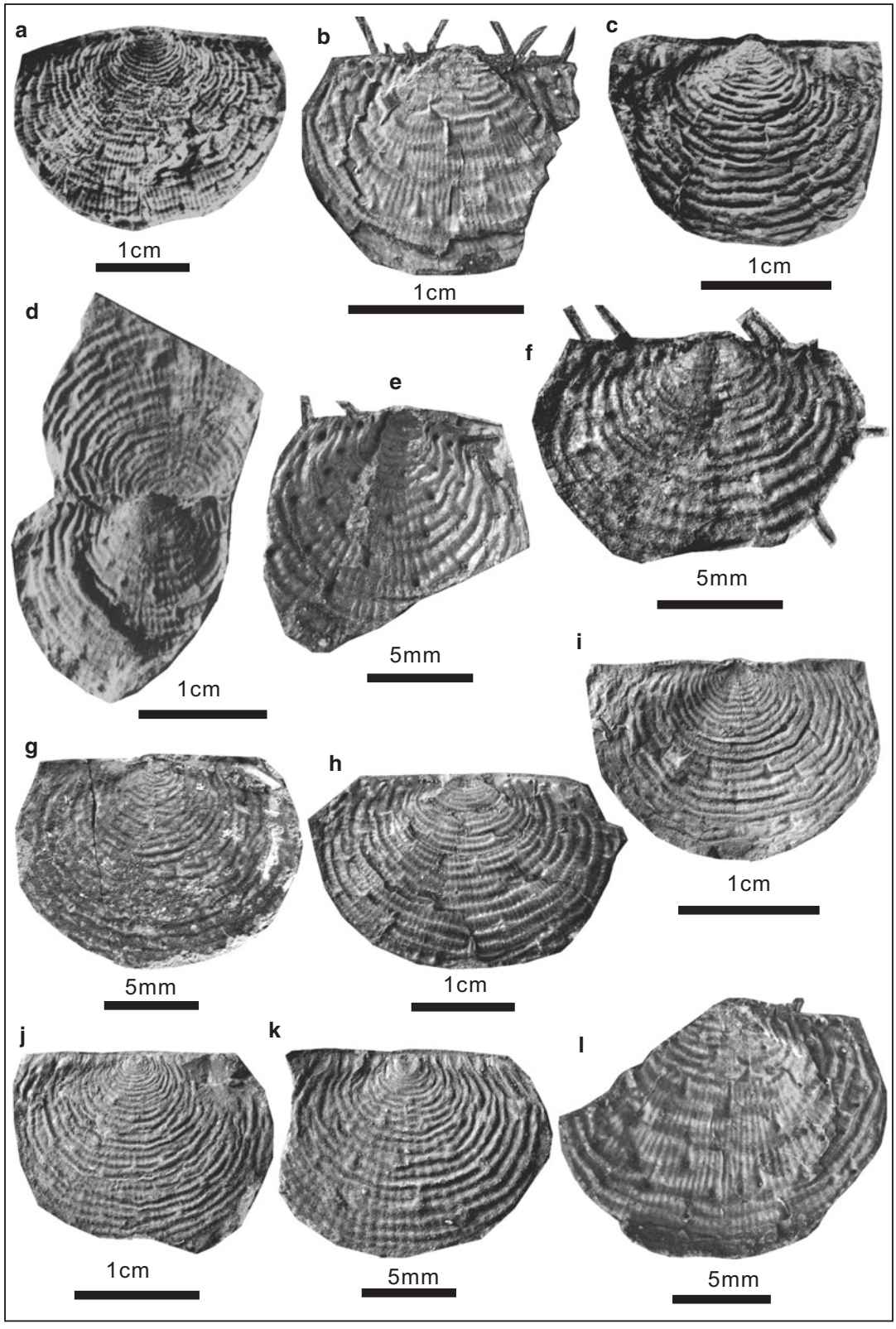
a
1cm
b
1cm
c
1cm
d
1cm
e
5mm
f
5mm
g
5mm
h
1cm
i
1cm
j
1cm
k
5mm
l
5mm

and sparsely spaced on juveniles, see Fig. 9.3f–h). Dorsal visceral disk slightly concave; umbo commonly with a slightly convex cicatrix; ears triangular, well demarcated from visceral disk; rugae strong on ears, becoming weaker on visceral disk; costellae similar to those of ventral valve; dimples largely quincunxial; no spines. Dorsal interior having bilobated cardinal process (marked by *cp*, see Figs. 9.2k, n; 9.3c, g; 9.4), median ridge (*mr*) and endospines (*ens*) on both sides and in front of median ridge (Figs. 9.2e, h, k, m; 9.3g; 9.4).

Discussion This species is similar to *C. occidentalis* Archbold (1993, p. 14, Fig. 9a–i) from the High Cliff Sandstone in Western Australia, in outline and ornament including spines, dimples, and costellae, but the latter is larger in size, has wider and lower rugae, and a more protruding umbo. The present species is somewhat similar to *C. tazawai* Shen et al. (2000, p. 743, Fig. 12.1−12.8, 12.11−12.14) from the Selong Group at the Selong Section in southern Tibet in size and outline, but the latter has a more convex ventral valve, and stronger, wider and irregular rugae. The present species differs from *C. minor* Shen et al. (2002, p. 677, Fig. 5.5−5.17) from the Yongde Formation at the Xiaoxinzhai section, southern Baoshan Block, western Yunnan, in the latter having a small size, fine costellae, more irregular rugae, coarser spines, and larger dimples.

Family **Linoproductidae** Stehli, 1954
Subfamily **Anidanthinae** Waterhouse, 1968a
Genus ***Anidanthus*** Whitehouse, 1928

Type Species *Linoproductus springsurensis* (Booker, 1932). Permian; New South Wales.

Diagnosis Shell usually transverse in outline, ears large, occasionally strongly extended (as emended by He et al. 2014), ribbing on both valves, rugae lamellose dorsally, spines in row near hinge, widely scattered on corpus, trail; dorsal interior with a median septum about half of disk length.

Discussion *Anidanthus* is similar to *Kuvelousia* Waterhouse, 1968b in bifurcated or intercalated costellae, overlapped lamellae on dorsal valve, and extended ears, but differs in the latter having a higher ratio of length to width, finer costellae and a longer dorsal median septum. *Anidanthus* resembles to *Megousia* Muir-Wood and Cooper, 1960 in a transverse outline, bifurcated or intercalated costellae, overlapped lamellae, and dorsal interior, but differs in the former has ears ornamented mainly by concentric rugae, while the latter has larger and crescentic ears ornamented mainly by radials (Muir-Wood and Cooper 1960). *Anidanthus* differs from *Fusiproductus* Waterhouse, 1975 (= *Protanidanthus* Liao, 1979b, as reviewed by Shen et al. in Rong et al., 2017) in the latter having a fusiform outline.

Anidanthus parvimucronata He and Shen *nomen novum*
Figs. 9.5a–k; 9.6

2005 *Anidanthus mucronata* He and Shen in He et al.: 929, Fig. 3.1−3.15.

Fig. 9.1 ***Costatumulus dongpanensis*** He and Shen in He et al., 2005. (**a**), external mold of ventral valve, DP806, (**b**), incomplete ventral valve, PB-2-293, illustrating long hinge spines, two rows of spine bases on the ears, swollen body spines. (**c**), ventral valve, DP715. (**d**), conjoined shell, DP716, illustrating largely quincunxial dimples on dorsal valve. (**e**), external mould of an incomplete ventral valve, DP-9-291. (**f**), a nearly complete ventral valve, DP-10-290. (**g**), external mould of a nearly complete dorsal valve, DS-1-602. (**h**), a nearly complete ventral valve, DP-9-283. (**i**), external mould of a nearly complete ventral valve, DP-7-286. (**j**), external mould of a nearly complete dorsal valve, DP-7-281. (**k**), external mould of a nearly complete dorsal valve, DP-7-287. (**l**), external mould of an incomplete ventral valve, DP2-0013, illustrating body spines swollen at base and arising at the end by a low angle to shell surface

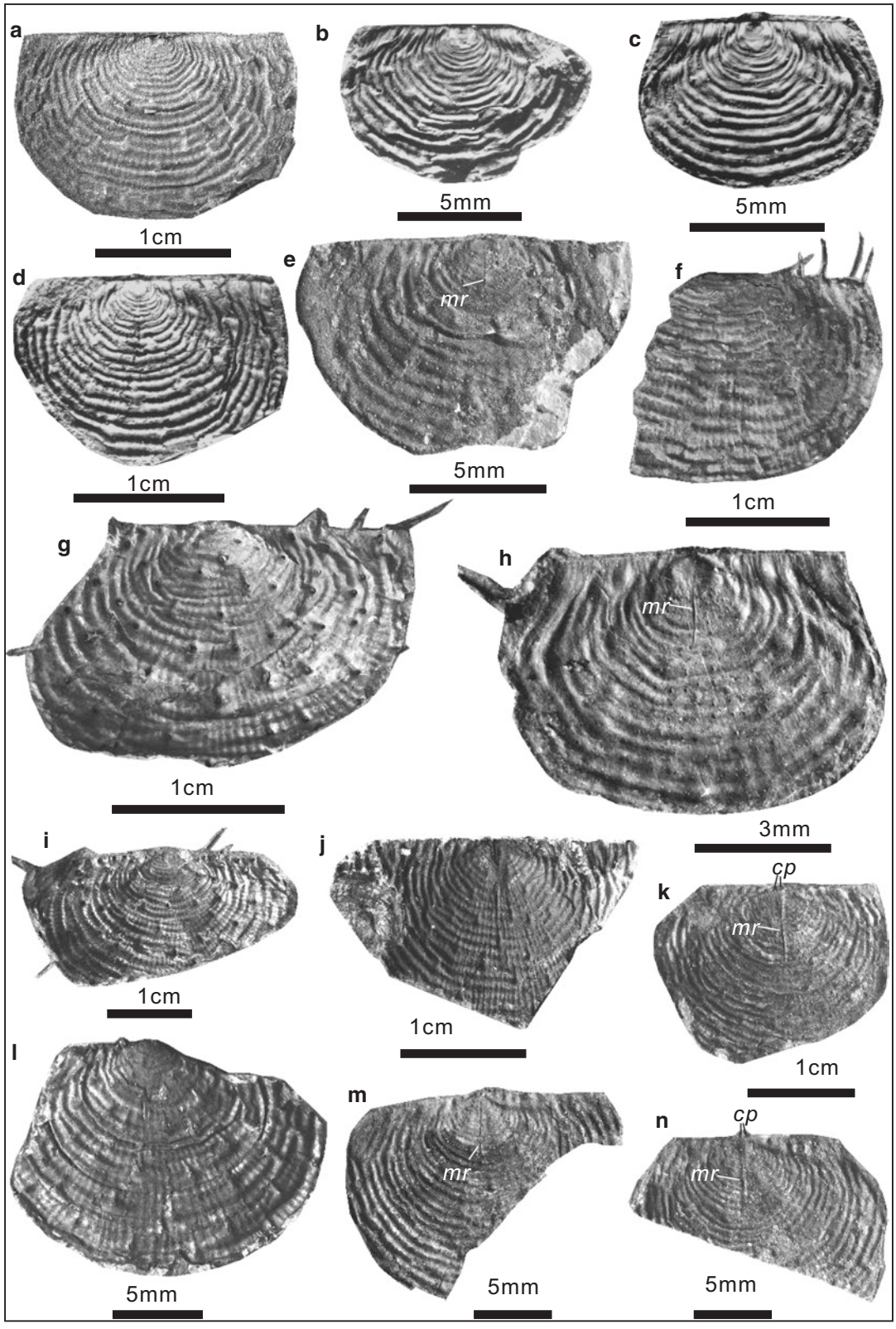
a
1cm
b
5mm
c
5mm
d
1cm
e
mr
5mm
f
1cm
g
1cm
h
mr
3mm
i
1cm
j
1cm
k
cp
mr
1cm
l
5mm
m
mr
5mm
n
cp
mr
5mm

2009 *Anidanthus mucronata* He and Shen; Zhang and He: Fig. 3o–q.
2009a *Anidanthus mucronata* He and Shen; Chen et al.: 172, Fig. 4a, b.
2014 *Anidanthus mucronata* He and Shen; He et al.: Figs. 17j–p, 19a, 19b.

Diagnosis Small *Anidanthus* with mucronate cardinal extremities, strongly extended ears, and strong rugae on ears.

Etymology The name of *Anidanthus mucronatus* had been used for a brachiopod species from the Lower Permian of Jalaid Banner, Heilongjiang Province, northeastern China (Li et al., 1980). Consequently, *Anidanthus mucronata* He and Shen in He et al., 2005 should be re-named and here replaced by the name of *Anidanthus parvimucronata*, referring to a small *Anidanthus* species with mucronate cardinal extremities.

Types As originally illustrated by He et al., 2005, holotype, external mould of a nearly complete dorsal valve (DP707); paratypes, a complete ventral valve (DP802) and external mould of a nearly complete dorsal valve (DP702).

Other Materials Over 100 specimens. Registered specimens: see below.

Measurements (mm):

Registered number	Width	Length	Width/length	Notes
DP707	24.55	7.71	3.18	External mould of dorsal valve
DP708	20.74	8.02	2.58	Internal mould of dorsal valve
DP702	23.97	10.43	2.30	External mould of dorsal valve
PB-5-278	16.83	7.14	2.36	External mould of ventral valve
DP-9-272	26.90	8.23	3.27	Dorsal interior
DP706	24.93	7.45	3.35	External mould of dorsal valve
DP-10-274	23.33	8.81	2.65	Internal mould of dorsal valve
PB-5-279	36.64	11.47	3.19	Ventral valve
DP-9-275	32.90	9.21	3.57	External mould of dorsal valve
PB-5-278	24.57	10.31	2.38	External mould of ventral valve

Fig. 9.2 ***Costatumulus dongpanensis*** He and Shen in He et al., 2005. (**a**), external mould of a nearly complete dorsal valve, DP-7-288. (**b**), external mold of dorsal valve, DP710. (**c**), external mold of dorsal valve, DP711. (**d**), external mold of dorsal valve, DP803. (**e**), internal mould of an incomplete dorsal valve, DP9-0035, illustrating a median ridge (*mr*). (**f**), an incomplete ventral valve, DP10-0037, illustrating hinge spines. (**g**), external mould of a nearly complete ventral valve, DP9-0014, illustrating body spines swollen at base and arising at the end by a low angle to shell surface. (**h**), internal mould of a complete dorsal valve, DP5-0028, illustrating a median ridge (*mr*) and endospines present on both sides and in front of median ridge. (**i**), external mould of an incomplete ventral valve, DP9-0010, illustrating body spines swollen at base and arising at the end by a low angle to shell surface. (**j**), an incomple dorsal valve, DP2-0025, illustrating dimples. (**k**), internal mould of a nearly comple dorsal valve, DP7-0026, illustrating bilobated cardinal process (*cp*), median ridge (*mr*) and endospines. (**l**), an incomplete ventral valve, DP10-0042, illustrating body spines swollen at base and arising at a low angle to shell surface. (**m**), internal mould of an incomplete dorsal valve, DP3-0033, illustrating a median ridge (*mr*). (**n**), internal mould of an incomplete dorsal valve, DP3-0034, illustrating bilobated cardinal process (*cp*) and median ridge (*mr*)

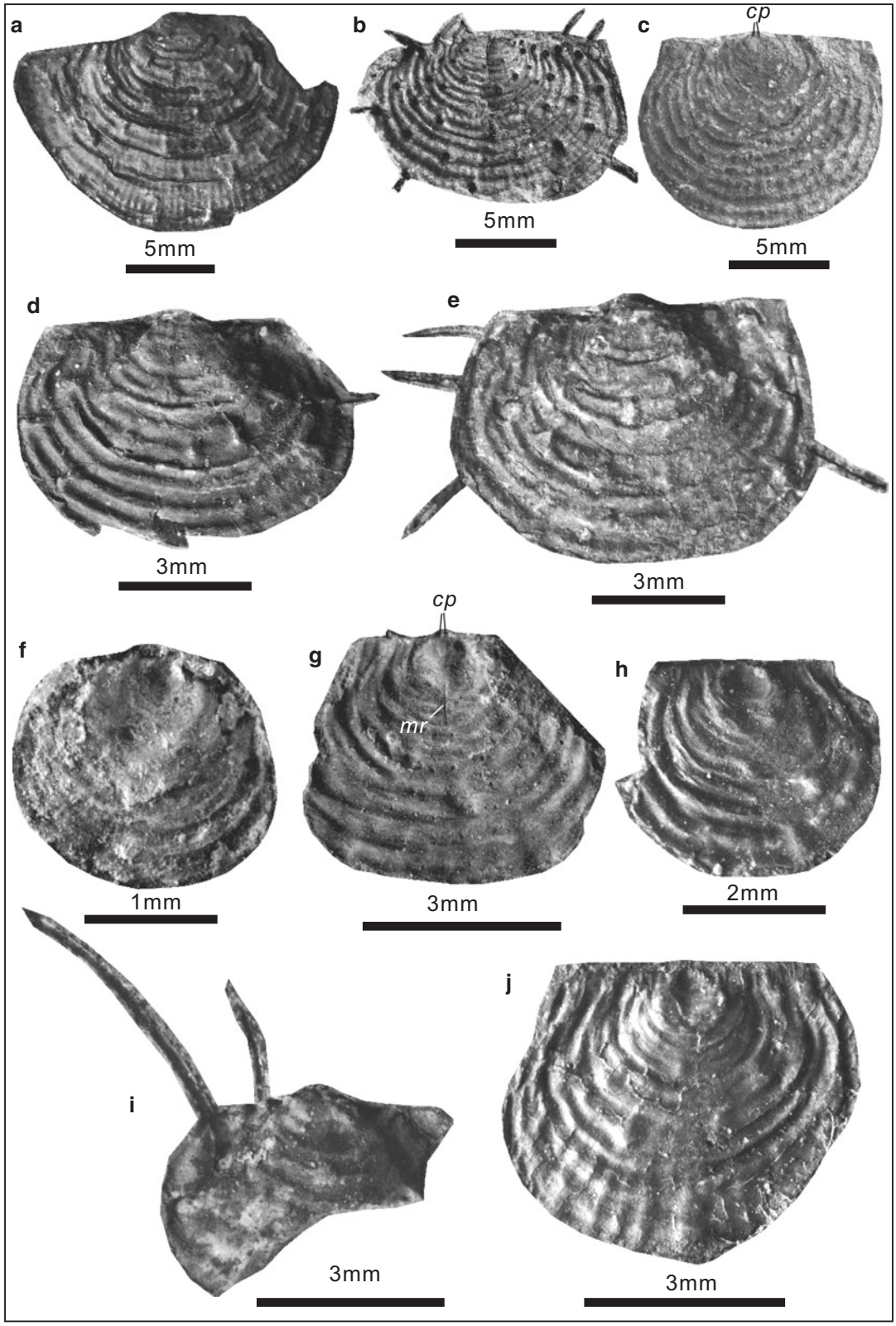
a
5mm
b
5mm
c
cp
5mm
d
3mm
e
3mm
f
1mm
g
cp
mr
3mm
h
2mm
i
3mm
j
3mm

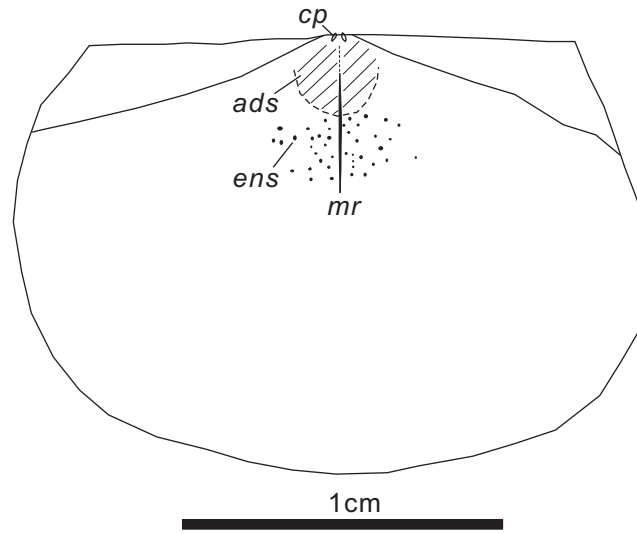

Fig. 9.4 Sketch for the dorsal interior of *Costatumulus dongpanensis*. *cp*- cardinal process; *ads*- adductor scars; *ens*- endospines; *mr*- middle ridge

Occurrence Changhsingian; Guangxi and Guizhou of South China.

Description Shell 5.0–14.0 mm long and 10.0–36.6 mm wide, reversely trapezoid in outline, ratio of width to length generally >2.0, widest at hinge. Ventral valve moderately inflated and geniculate; beak broad and strongly enrolled over hingeline; umbo strongly incurved; ears large, well demarcated from visceral disk by weak depressions, ornamented by concentric rugae and few radials, radials interrupted by rugae (Fig. 9.5d, i, k); sulcus very weak, originating from midvalve, slightly widening anteriorly; venter moderately convex; trail transversely spreading; costellae fine, beginning from umbo, increasing by intercalation and bifurcation, numbering six to nine in 5 mm near anterior margin; rugae strong on ears, weaker on visceral disk; spines in a row near hinge, occasionally sparsely-arranged on visceral disk. Dorsal valve moderately concave and geniculate; ears large, strongley extended and mucronate (Fig. 9.5a, e–g, i, j), ornamented mainly by strong rugae (radials rarely and obscure); trail geniculated; costellae fine and even, interrupted by strong, overlapped lamellose rugae across whole visceral disk; rugae denser on anterior part of visceral disk, but absent on trail. Dorsal interior bearing teeth-like strucutures (*t*) along lateral ridges (Figs. 9.5b, g; 9.6); lateral ridges in dorsal interior extending along hinge from sockets; median septum (*ms*) extending to midvalve (Figs. 9.5b, e, g; 9.6); adductor scars (*ads*) diverging into three pairs, the pair

Fig. 9.3 ***Costatumulus dongpanensis*** He and Shen in He et al., 2005. (**a**), an incomplete ventral valve, DP10-0007, illustrating body spines swollen at base and arising at the end by a low angle to shell surface. (**b**), a nearly complete ventral valve, DP-10-290, illustrating long hinge spines and body spines along lateral margins. (**c**), internal mould of a dorsal valve, DP8-0060, illustrating bilobated cardinal process (*cp*). (**d**), a ventral valve (younger adult), DP9-0068, illustrating fewer body spines. (**e**), a ventral valve, DP9-0064, illustrating long spines along lateral margins. (**f**), external mould of a dorsal valve (juvenile), DP10-0075, illustrating fewer costellae and body spines. (**g**), internal mould of a dorsal valve (juvenile), DP9-0076, illustrating bilobated cardinal process (*cp*), a median ridge (*mr*) and endospines in front of median ridge. (**h**), external mould of a dorsal valve (juvenile), DP10-0077. (**i**), an incomplete ventral valve (juvenile), DP9-0080, illustrating long hingespines. (**j**), external mould of a dorsal valve, DP8-0078, illustrating a few dimples

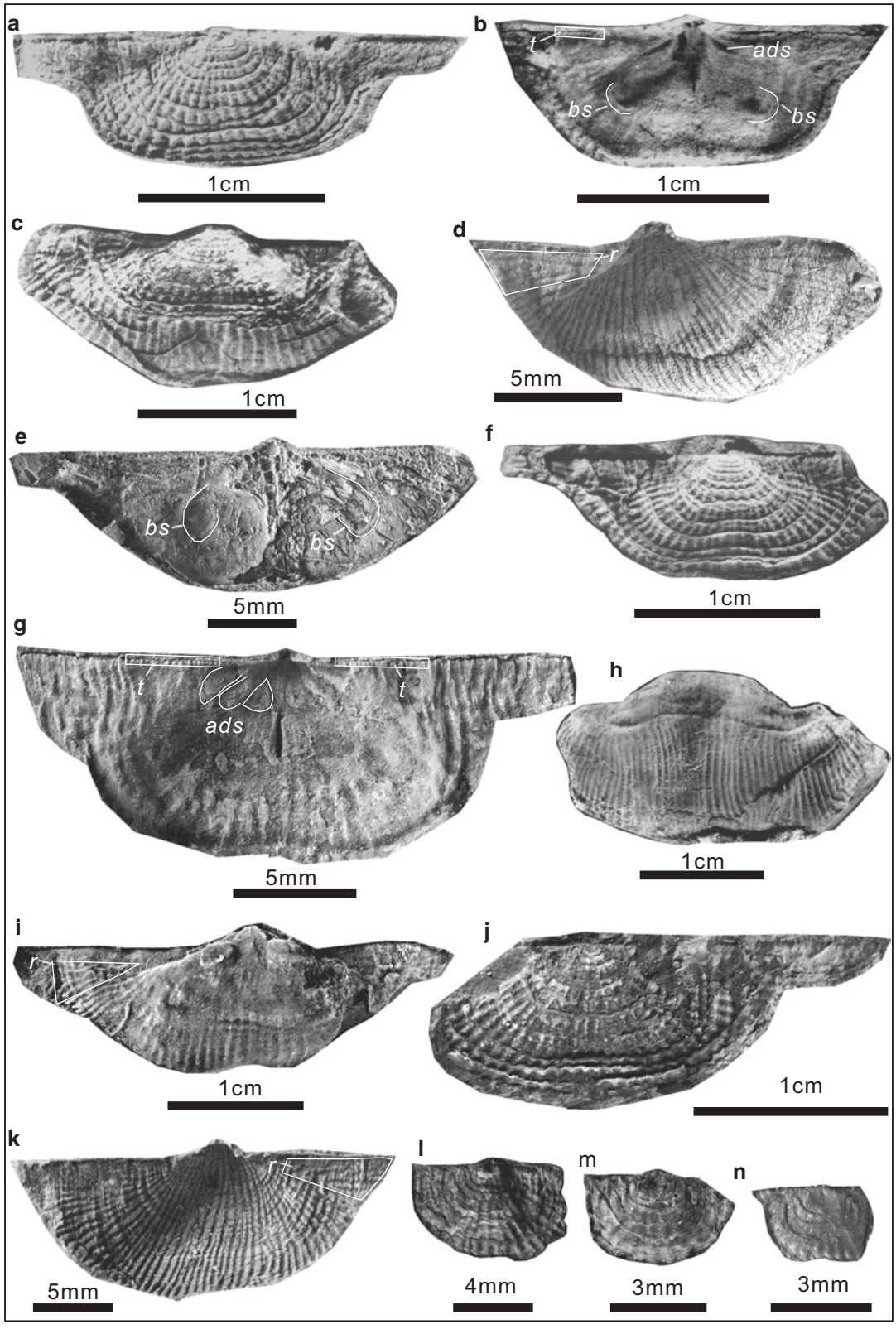
a
1cm
b
t
ads
bs
bs
1cm
c
1cm
d
r
5mm
e
bs
bs
5mm
f
1cm
g
t
t
ads
5mm
h
1cm
i
r
1cm
j
1cm
k
r
5mm
l
4mm
m
3mm
n
3mm

close to median septum crescent or saccate, two other pairs posterolaterally saccate (Figs. 9.5g; 9.6); brachial scars (*bs*) slightly elevated, kidney-shaped (Figs. 9.5b, e; 9.6).

Discussion The new species is similar to *Anidanthus mucronatus* Lee and Gu in Li et al., 1980 from the Lower Permian of northeastern China in mucronate cardinal extremities, but differs in its smaller body size (only a half of shell width of *Anidanthus mucronatus*), a ventral sulcus, sparser costellae, weaker concentric rugae on visceral disk and radials on ears. *Anidanthus parvimucronata* is similar to *A. interruptus* (Huang, 1932, p. 44, pl. 3, Figs. 8, 9) from the Lopingian *Lyttonia* horizon of Panshan, Guizhou, South China in the dorsal ornament, but the latter has nearly subquadrate cardinal extremities. The present species somewhat resembles *Anidanthus ussuricus* (Fredericks, 1924, p. 8, pl. 1, Figs. 2, 3) in the ornamentation, but the latter has a more strongly inflated ventral valve, a larger size, and much more sharply inclined flanks. It is necessary to note that the dorsal muscle scars of this species are very complex and varied (see Fig. 2 of Waterhouse 1968a), and its interiors could not be regarded as offering diagnostic features at either species- or even the genus-level. *Anidanthus parvimucronata* can be readily distinguished from *Anidanthus sinosus* (Huang, 1932, p. 43, pl. 2, Figs. 15, 16) from the Lopingian *Lyttonia* horizon of Panshan, Guizhou, South China, by its less curved lateral profile, shallower sulcus, and stronger lamellose rugae on the dorsal visceral disk.

Anidanthus subquadratus He, Shi and Shen sp. nov.
Figs. 9.5l–n; 9.7

2005? *Cathaysia* sp., He et al.: 933, Fig. 4.7–4.12.

Diagnosis Quadrate to sub-quadrate extremities; ventral ears large, triangular, not extended, ornamented by concentric rugae and few radials; dorsal ears not well demarcated from visceral disk; costellae fine, variably crossed by concentric lines or fila on visceral disk of ventral valve.

Etymology Named for the sub-quadrate outline.

Types Holotype, DP8-0496; paratypes, DP719, DP9-0508.

Other Materials Over 10 specimens. Registered specimens: see below.

Fig. 9.5 (**a**–**k**), ***Anidanthus parvimucronata*** He and Shen *nomen novum*. (**a**), external mould of a complete dorsal valve, DP707 (holotype). (**b**), internal mould of a complete dorsal valve, DP708, *t* showing teeth-like structure along the hingeline, *ads* refers to adductor scars, *bs* refers to scars of brachial ridges. (**c**), external mould of an incomplete dorsal valve, DP702 (paratype). (**d**), external mould of a nearly complete ventral valve, PB-5-278, *r* refers to radial ornaments on ears. (**e**), interior of an incomplete dorsal valve, DP-9-272, *bs*- scars of brachial ridges. (**f**), external mould of an incomplete dorsal valve, DP706, illustrating mucronate cardinal extremities and strong regular rugae. (**g**), internal mould of a complete dorsal valve, DP-10-274, showing the teeth-like structures (*t*) along the hingeline and complex adductor scars (*ads*). (**h**), a nearly complete ventral valve, DP802 (paratype). (**i**), a nearly complete ventral valve, PB-5-279, *r* refers to radial ornaments on ears. (**j**), external mould of an incomplete dorsal valve, DP-9-275. (**k**), external mould of a nearly complete ventral valve, *r* refers to radial ornaments on ears, PB-5-278. (**l**–**n**), ***Anidanthus subquadratus*** He, Shen and Shi sp. nov.. External moulds of three nearly complete dorsal valves, DP7-0096; DP10-0098 (juvenile); DP8-0099 (juvenile)

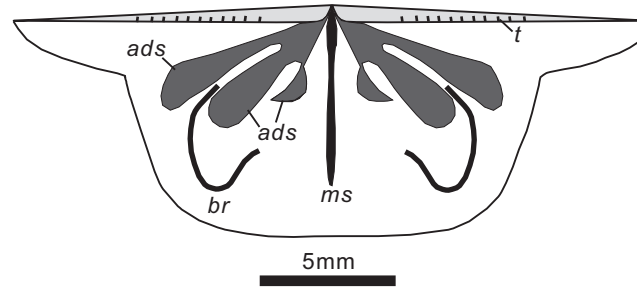

Fig. 9.6 Sketch for the dorsal interior of *Anidanthus parvimucronata* He and Shen *nomen novum*. *t*- teeth-like structures; *ads*- adductor scars; *br*- brachial ridges; *ms*- median septum

Measurements (mm):

Registered number	Width	Length	Width/length	Notes
DP7-0096	8.13	6.39	1.27	External mould of dorsal valve
DP10-0098	5.40	3.61	1.50	External mould of dorsal valve (juvenile)
DP8-0099	3.60	2.69	1.34	External mould of dorsal valve (juvenile)
DP719	15.87	10.60	1.50	External mould of ventral valve
DP720	18.15	10.24	1.77	Ventral exterior
DP7-0494	20.54	12.00	1.71	External mould of ventral valve
LQ-0500	5.53	3.90	1.42	Ventral exterior (juvenile)
DP10-0504	6.73	3.78	1.78	Ventral exterior (juvenile)
LQ5-0501	7.53	5.95	1.27	Ventral exterior
DP10-0506	9.45	6.46	1.46	Ventral exterior
DP9-0511	16.16	8.04	2.01	External mould of dorsal valve
DP9-0508	13.80	7.47	1.85	External mould of dorsal valve
DP9206	15.03	8.14	1.85	External mould of ventral valve
LQ-0497	13.80	8.71	1.58	Ventral exterior
DP9-0495	8.03	6.59	1.22	External mould of ventral valve
DP8-0496	11.58	8.50	1.36	Ventral exterior

Occurrence Changhsingian; Guangxi (Dongpan section) of South China.

Description Shell 2.7–12.0 mm long and 3.6–20.5 mm wide, sub-quadrate in outline, widest at hinge, lateral margins rounded, anterior margin broadly rounded. Ventral valve weakly to moderately convex; beak moderately broad and incurved over hingeline; ears flat, triangular, not extended, well demarcated from visceral disk, variably ornamented by concentric rugae and few radials; sulcus absent; costellae fine, beginning from umbo, increasing by intercalation or bifurcation, numbering 7 to 10 in 5 mm near anterior margin; concentric lines or fila occasionally covered on visceral disk; spines in a row near hinge (Fig. 9.7a, k), occasionally sparsely-arranged on visceral disk (Fig. 9.7d, j, l). Dorsal valve moderately concave; ears not demarcated from visceral disk; costellae low, interrupted by strong, overlapped lamellose rugae across visceral disk (Fig. 9.7h, i, l, m).

Discussion The present specimens are more or less similar to species of *Cathaysia* in outline and concentric rugae on ventral ears, but they have roof-tiled crest for each costellae, unlike the low and rounded costellae in *Cathaysia*. Especially, the presences of lamellose rugae on dorsal valve, spines in row near hinge and large ears of the materials at hand recall *Anidanthus*. New species is similar to *A. sinosus* (Huang, 1932) from the Lopingian *Lyttonia* horizon of Panshan, Guizhou, South China in dorsal ears not well demarcated

from visceral disk, but differs in the latter having strongly inflated ventral valve, a ventral sulcus, fine striae and coarse concentric wrinkles. *A. interruptus* (Huang, 1932) from the Lopingian *Lyttonia* horizon of Panshan, Guizhou, South China shares with the new species a subquadrate outline and dorsal ears not well demarcated from visceral disk, but differs in the former having fine striae and strongly reflexed cincture on the dorsal valve. *Anidanthus parvimucronata* is readily distinguished from *Anidanthus subquadratus* in having extended dorsal ears and a moderately convex, geniculate ventral valve.

Subfamily **Linoproductinae** Stehli, 1954

Genus ***Parapygmochonetes*** He and Shi in He et al., 2014

Type Species *Fusiproductus baoqingensis* Liao in Zhao et al., 1981. Changhsing Formation (Changhsingian); Meishan section, Changxing County, Zhejiang Province, South China.

Diagnosis Semicircular to reversely trapezoid in outline; ears flat to slightly convex; costellae fine with narrower interspaces, irregularly extending anteriorly (sinuose) and increasing by bifurcation; concentric lines irregularly developed; hingespines inclined towards midline at a low angle to hingeline; spines on ears, also inclined towards midline. Ventral interior with a median septum, extending nearly to mid-length; dorsal interior with a trifid cardinal process; median septum fine, short.

Discussion *Parapygmochonetes* is very like *Pygmochonetes* Jin and Hu, 1978 in a hillock umbo, bifurcated costellae in flanks, and a long ventral median septum. Indeed, in some previous works, the materials belonging to *Parapygmochonetes* were identified by Chen et al. (2009a) as *Pygmochonetes*. However, these materials differ significantly from *Pygmochonetes* in having several pairs of hingespines inclined towards midline at an angle of 40–50° to hingeline, spines on ears also inclined towards midline, sinuose costellae, and discontinuous and irregular concentric lines. In comparison, *Pygmochonetes* is characterized by 3 or 4 pairs of hingespines projecting posterolaterally with an angle of about 60°; its ears are covered by fine and weak costellae; costellae straight, lacking any concentric ornamentation on disk (Jin and Hu, 1978).

Chen et al. (2006a) assigned some *Parapygmochonetes*-type materials to *Fanichonetes* sp. on account of their hingespines inclined towards midline. But, it should be noted that these inclined spine canals along the posterior margin (only visiable on internal molds) are not the same as the inclined hingespines on the outer surface of the posterior margin. Sometimes, in well-preserved materials, both of these features can be observed on the same specimen, such as in the case of *Fusichonetes soochowensis* (Chao, 1928) illustrated in this book (see the description of *F. soochowensis*). In this specimen, inclined spine canals along and embedded within the posterior margin and are clearly different from posterolaterally-projecting external hingespines. As already noted by Racheboeuf in Williams et al., 2000 (see p. 405), the inclined spine canals lead to posterolaterally-projecting hingespines. In this light, *Fanichonetes* Xu and Grant, 1994, with inclined spine canals as its key diagnostic feature, is most likely invalid. Actually, the ventral specimen of Fig. 16.12 of Xu and Grant (1994) shows that the hingespines project posterolaterally.

Both *Fusiproductus* Waterhouse, 1975, with *Linoproductus fusiformis* Huang, 1932 as the type species, and *Parapygmochonetes* have a regularly inflated ventral valve with sinuose costellae, but *Fusiproductus* has an enrolled and strongly transversal outline, a pair of subtubular ears, and cardinal extremities with an angle <45°.

As already mentioned above, *Parapygmochonetes* has some features of Caenanopliinae Archbold, 1980, so that it was assigned to the subfamily (He et al., 2014). Meanwhile, the genus has some features of Linoproductinae Stehli, 1954. In order to determine the phylogentic relationship of this genus

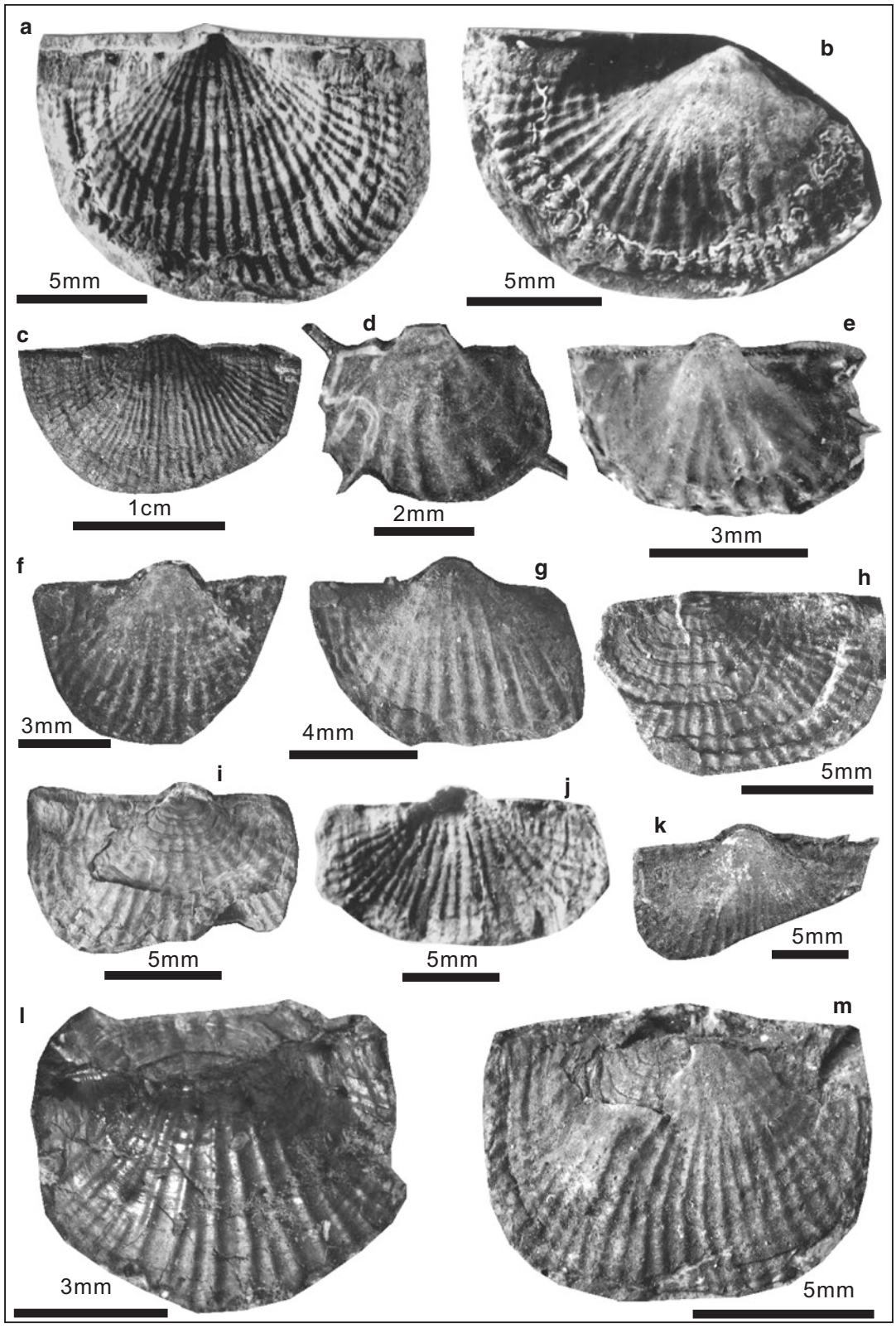
a
5mm
b
5mm
c
1cm
d
2mm
e
3mm
f
3mm
g
4mm
h
5mm
i
5mm
j
5mm
k
5mm
l
3mm
m
5mm

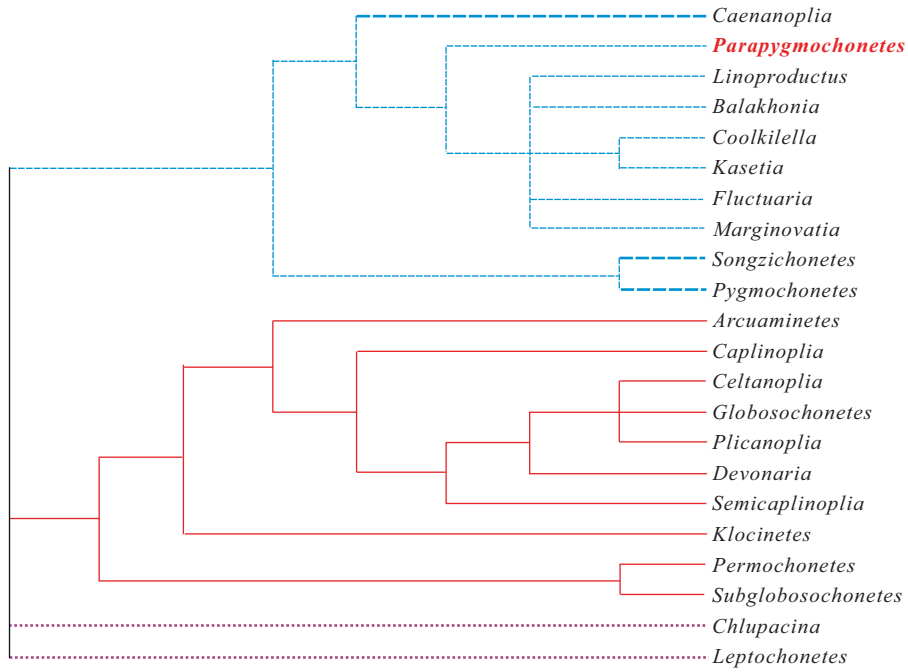

Fig. 9.8 Phylogenetic tree of the subfamilies Caenanopliinae Archbold, 1980 and Linoproductinae Stehli, 1954 obtained by the parsimony analysis. Note: Parsimony analysis was conducted under the software PAUP version 4.0a (Swofford, 2002), including 22 taxa and 23 morphological characters (Table 5.3). Thirteen genera from subfamily Caenanopliinae Archbold, 1980 and six genera from subfamily Linoproductinae Stehli, 1954 were chosen as ingroup taxa. *Chlupacina* and *Leptochonetes* were treated as outgroup. Eight most-parsimonious trees (Tree length = 65; Cosistency index = 0.354; Homoplasy index = 0.646; Retention index = 0.691; Rescaled consistency index = 0.245) were found using heuristic searching with 1000 replicates. The strict consensus tree separated ingroup genera into two main clades. *Parapymochonetes* and all genera from subfamily Linoproductinae belonged to the same clade, indicating that *Parapymochonetes* might have a closer phylogenetic relationship with subfamily Linoproductinae than Caenanopliinae

Fig. 9.7 ***Anidanthus subquadratus*** He, Shen and Shi sp. nov. (**a**), external mold of a complete ventral valve, DP719 (paratype), showing scars of a row of hingspines, costellae and concentric lines/fila. (**b**), exterior of an incomplete ventral valve, DP720, showing costellae with roof-tiled crests. (**c**), external mould of a nearly complete ventral valve, DP7-0494, showing bifurcated costellae, concentric fila and spine scars on disk. (**d**, **e**), exteriors of two complete ventral valves (juveniles), LQ-0500, DP10-0504, showing sparse costellae and spines near margins and hingeline. (**f**, **g**), exteriors of two incomplete ventral valves, LQ5-0501, DP10-0506, showing costellae with roof-tiled crests. (**h**), external mould of an incomplete dorsal valve, DP9-0511, showing costellae interrupted by strong, overlapped lamellose rugae on disk. (**i**), external mould of an incomplete dorsal valve and shell remnant of the conjoined ventral valve, DP9-0508 (paratype), showing lamellose rugae on dorsal disk and costellae with roof-tiled crests. (**j**), external mould of an incomplete ventral valve, DP9206, showing scars of spines along hinge and on disk. (**k**), exterior of an incomplete ventral valve, LQ-0497, showing costellae with roof-tiled crests. (**l**), external mould of an incomplete ventral valve and external mould of posterior part of the conjoined dorsal valve, DP9-0495, showing intercalated costellae with roof-tiled crests on ventral valve and lamellose rugae on dorsal disk. (**m**), exterior of a complete ventral valve (shell decorticated nearby umbo) and external mould of umbo area of the conjoined dorsal valve, DP8-0496 (holotype), showing wavy costellae with roof-tiled crests on ventral valve and lamellose rugae near umbo of the conjoined dorsal valve

with allied genera, a parsimony analysis was conducted (Fig. 9.8). The result shows that the present genus is most allied to the genera of *Linoproductus* Chao, 1927, *Balakhonia* Sarytcheva in Sarytcheva et al., 1963, *Coolkilella* Archbold, 1993, *Fluctuaria* Muir-Wood and Cooper, 1960, *Kasetia* Waterhouse, 1981, *Marginovatia* Gordon and Henry, 1990, the constituents of the subfamily Linoproductinae (Fig. 9.8). Consquently, *Parapygmochonetes* is assigned to Linoproductinae. Moreover, it is interesting to note that *Caenanoplia* Carter, 1968, *Songzichonetes* Yang in Feng et al., 1984, and *Pygmochonetes* Jin and Hu, 1978, which until now have all been assigned to the subfamily Caenanopliinae Archbold, 1980 (see pages 385–388, Racheboeuf in Williams et al., 2000), are in fact more allied to the subfamily Linoproductinae in view of the tree derived from the parsimony analysis (Fig. 9.8).

Parapygmochonetes parvulus He and Shi in He et al., 2014

Figs. 9.9; 9.10a–d

2014 ***Parapygmochonetes parvulus*** He and Shi in He et al.: 931, Figs. 11j–p, 13a–h.

Materials Over 160 specimens. Registered specimens: see below.

Measurements (mm):

Registered number	Width	Length	Width/length	Notes
CM-12-109	9.56	6.51	1.47	Ventral exterior
CM-3-125	8.46	5.45	1.55	Ventral exterior
CM-12-108	6.37	4.47	1.42	Dorsal interior
CM-3-103	8.06	5.44	1.48	Ventral exterior
CM-3-106	6.34	3.51	1.80	Dorsal interior
CM-3-117	5.56	3.51	1.58	Ventral exterior
CM-3-102	8.04	5.02	1.60	Internal mould of ventral valve
CM-3-121	5.03	3.24	1.55	Internal mould of ventral valve
CM-3-120	5.76	3.98	1.44	Ventral exterior
CM-12-537	4.43	2.47	1.80	Ventral exterior
CM-10-110	5.56	4.09	1.36	Ventral exterior
CM-10-114	4.77	3.25	1.47	Ventral exterior
CM-3-119	6.33	4.07	1.56	Dorsal interior
CM-3-122	10.19	6.15	1.66	Ventral exterior
CM-3-118	4.94	2.99	1.65	Dorsal interior

Occurrence Changhsingian; Anhui of South China.

Description Shell 2.5–6.8 mm long and 4.4–10.2 mm wide, semicircular to reversely trapezoid in outline, greatest width at hingeline. Ventral valve moderately convex; umbo round, slightly globular in outline with steep slopes to lateral margin; beak slightly incurved, overhanging hingeline; 3 or 4 pairs of hingespines (*hs*) projecting towards midline at an angle of 40–50° (Figs. 9.9d, j; 9.10c); cardinal extremities with an angle of about 90° on well-preserved specimens; ears large, triangular, occasionally with weak and discontinuous concentric lines and continuous radial costellae, with spines (*es*) inclined towards midline (Figs. 9.9f; 9.10a, c), differentiated from flanks of ventral disk by narrow grooves; sulcus absent; costellae beginning from umbo, commonly bifurcated twice (respectively nearby midlength and commissure) at flanks, irregular in width or sinuose, coarse, with flat crests, numbering 18 to 20 per 5 mm (totally less than 40) near anterior margin; a few concentric lines discontinuously developed. Ventral interior with a short but distinct median septum; papillae nearly radially-arranged, covering the whole internal surface. Dorsal interior with a thin median septum and lateral septa not visible; papillae covering dorsal interior (but smooth on ears), papillae occasionally connected with each other to form radial ridges (Fig. 9.10d).

Discussion *Parapygmochonetes parvulus* is readily distinguished from *P. baoqingensis* Liao in Zhao et al., 1981 of the Changhsing Formation of Meishan, Zhejiang Province, China, as the latter has more costellae (over 50 costellae along the anterior margin).

Parapygmochonetes baoqingensis (Liao in Zhao et al., 1981)
Fig. 9.10e–h

1981 *Fusiproductus baoqingensis* Liao in Zhao et al.: 54, pl. 8, Fig. 30–33.
2006a *Fanichonetes* sp.; Chen et al.: Fig. 3a–f.
2009a? *Pygmochonetes shaiwaensis* Chen in Chen et al.: 166, Fig. 3a–f.
2014 *Parapygmochonetes baoqingensis* (Liao in Zhao et al.); He et al.: 931, Fig. 13i–l.

Materials Four registered specimens: see below.

Measurements (mm):

Registered number	Width	Length	Width/length	Notes
CM-3-104	7.01	4.92	1.43	Ventral exterior
CM-3-101	4.94	5.86	0.84	Ventral exterior
CM-3-123	12.78	7.85	1.63	Ventral exterior
CM-6-115	8.34	5.68	1.47	Ventral exterior

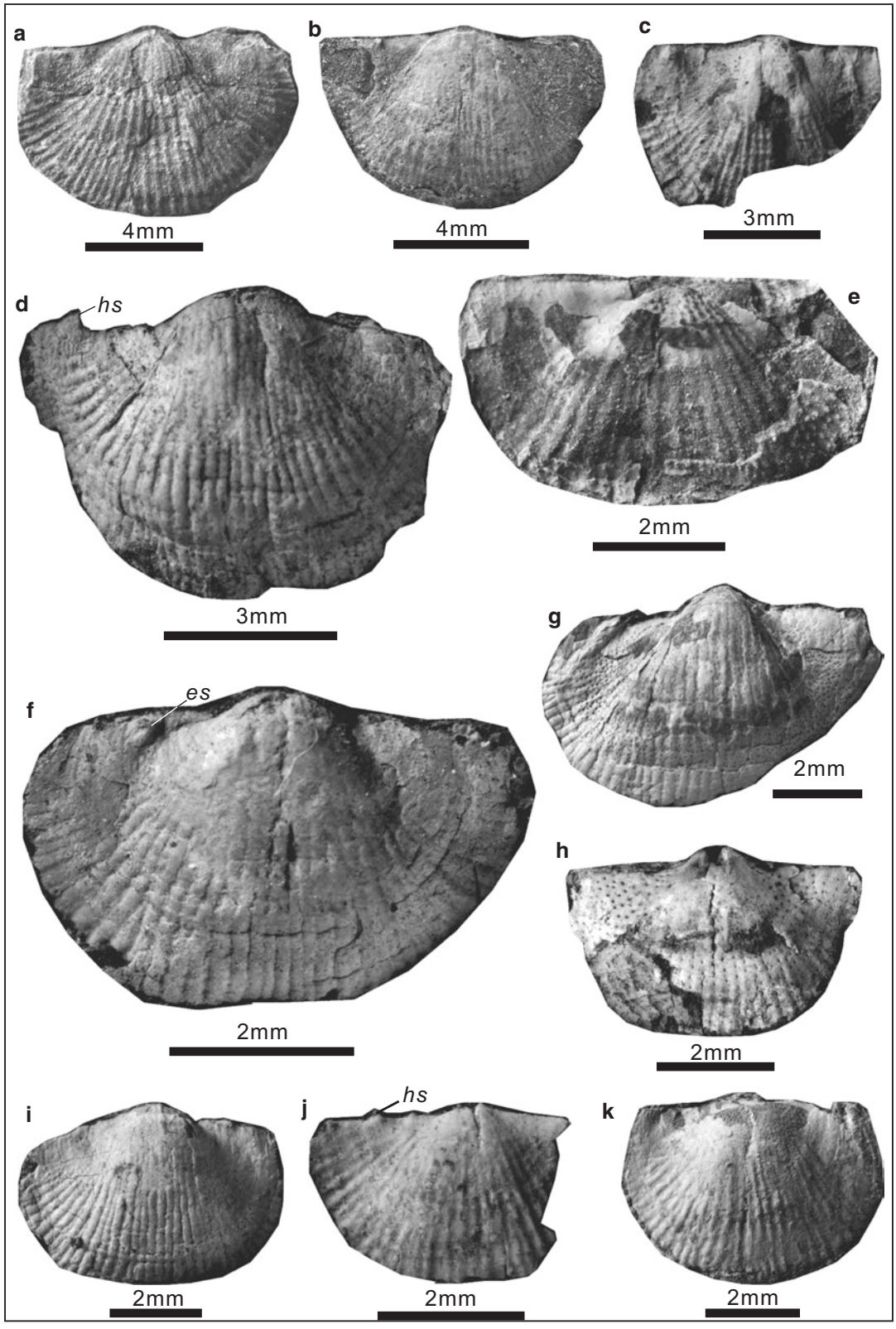
a
4mm
b
4mm
c
3mm
d
hs
3mm
e
2mm
f
es
2mm
g
2mm
h
2mm
i
2mm
j
hs
2mm
k
2mm

Occurrence Changhsingian; Zhejiang, Anhui, Guizhou and Hunan of South China.

Description Shell 4.9–7.9 mm long and 7.0–12.8 mm wide, reversely trapezoid in outline, greatest width at hinge. Ventral valve moderately convex; beak slightly incurved, overhanging hingeline; umbo round, slightly globular; hingespines projecting towards midline; ears slightly convex, not well differentiated from flanks of ventral disk, ornamented by concentric rugae, weak costellae and ear spines; sulcus absent; costellae sinuose, bifurcated at flanks, fine, with flat crests and narrow interspaces, numbering over 50 at anterior margin; concentric rugae regularly covered the ventral surface.

Discussion This species agrees well with *Parapygmochonetes baoqingensis* (Liao in Zhao et al., 1981) from the Changhsing Formation of the Meishan section, Zhejiang Province, China in a semicircular to reversely trapezoid outline, weak and discontinuous concentric lines and typical costellae which is sinuose, fine, dense and bifurcated, with narrower interspaces.

Superfamily **Productoidea** Gray, 1840
Family **Productellidae** Schuchert in Schuchert and LeVene, 1929
Subfamily **Marginiferinae** Stehli, 1954
Genus ***Spinomarginifera*** Huang, 1932

Type Species *Spinomarginifera kueichowensis* Huang, 1932. Upper Permian; Guizhou, southwestern China.

Diagnosis Small to medium, with wide hingeline; weakly concavoconvex with long ventral trail anterior to geniculation, dorsal trail short; ribbing absent; rugae irregular, narrow; spine bases elongate, spines commonly densely spaced, fine, but in some widely spaced anteriorly (spines on dorsal valve variably developed or absent); marginal ridges strong in both valves, but ventrally incomplete anteriorly (Brunton et al. in Williams et al., 2000).

Spinomarginifera kueichowensis Huang, 1932
Fig. 9.11

1932 *Spinomarginifera kueichowensis* Huang: 56, pl. 5, Fig. 1–11.
1960 *Spinomarginifera kueichowensis* Huang; Muir-Wood and Cooper, 215, pl. 65, Fig. 15–22, 24.
1964 *Spinomarginifera kueichowensis* Huang; Wang et al.: 316, pl. 51, Fig. 9–11.
1974 *Spinomarginifera kueichowensis* Huang; Jin et al.: 312, pl. 164, Fig. 13.
1976 *Spinomarginifera kueichowensis* Huang; Tazawa: 184, pl. 2, Fig. 1a, b.
1977 *Spinomarginifera kueichowensis* Huang; Yang et al.: 349, pl. 139, Fig. 9.
1978 *Spinomarginifera kueichowensis* Huang; Feng and Jiang: 252, pl. 89, Fig. 5, 6.
1979 *Spinomarginifera kueichowensis* Huang; Zhan in Hou et al.: 80, pl. 11, Fig. 14–17, 20.
1980a *Spinomarginifera kueichowensis* Huang; Liao: pl.4, Fig. 29.

Fig. 9.9 ***Parapygmochonetes parvulus*** He and Shi in He et al., 2014. (**a**), exterior of a nearly complete but slightly deformed ventral valve, CM-12-109, showing bifurcated costellae. (**b**), exterior of a nearly complete ventral valve, CM-3-125, showing wavy costellae. (**c**), interior of an incomplete dorsal valve and shell remnant of the conjoined ventral valve, CM-12-108, showing numerous papillae. (**d**), exterior of an incomplete ventral valve, CM-3-103, showing bifurcated, wavy costellae and hinge spines (*hs*). (**e**), interior of an incomplete dorsal valve, CM-3-106, showing radially-arranged papillae. (**f**), exterior of a nearly complete ventral valve, CM-3-117, showing bifurcated, wavy costellae and a spine on ear (*es*). (**g**), internal mould of an incomplete ventral and shell remnant, CM-3-102, showing numerous papillae and wavy costellae on shell remnant. (**h**), internal mould of a complete ventral valve, CM-3-121, showing radially-arranged papillae. (**i**), exterior of an incomplete ventral valve, CM-3-120, showing bifurcated costellae. (**j**), exterior of an incomplete ventral valve (shell partly decorticated), CM-12-537, showing bases of hinge spines (*hs*). (**k**), exterior of a nearly complete ventral valve (shell decorticated at umbo), CM-10-110, showing bifurcated, wavy costellae

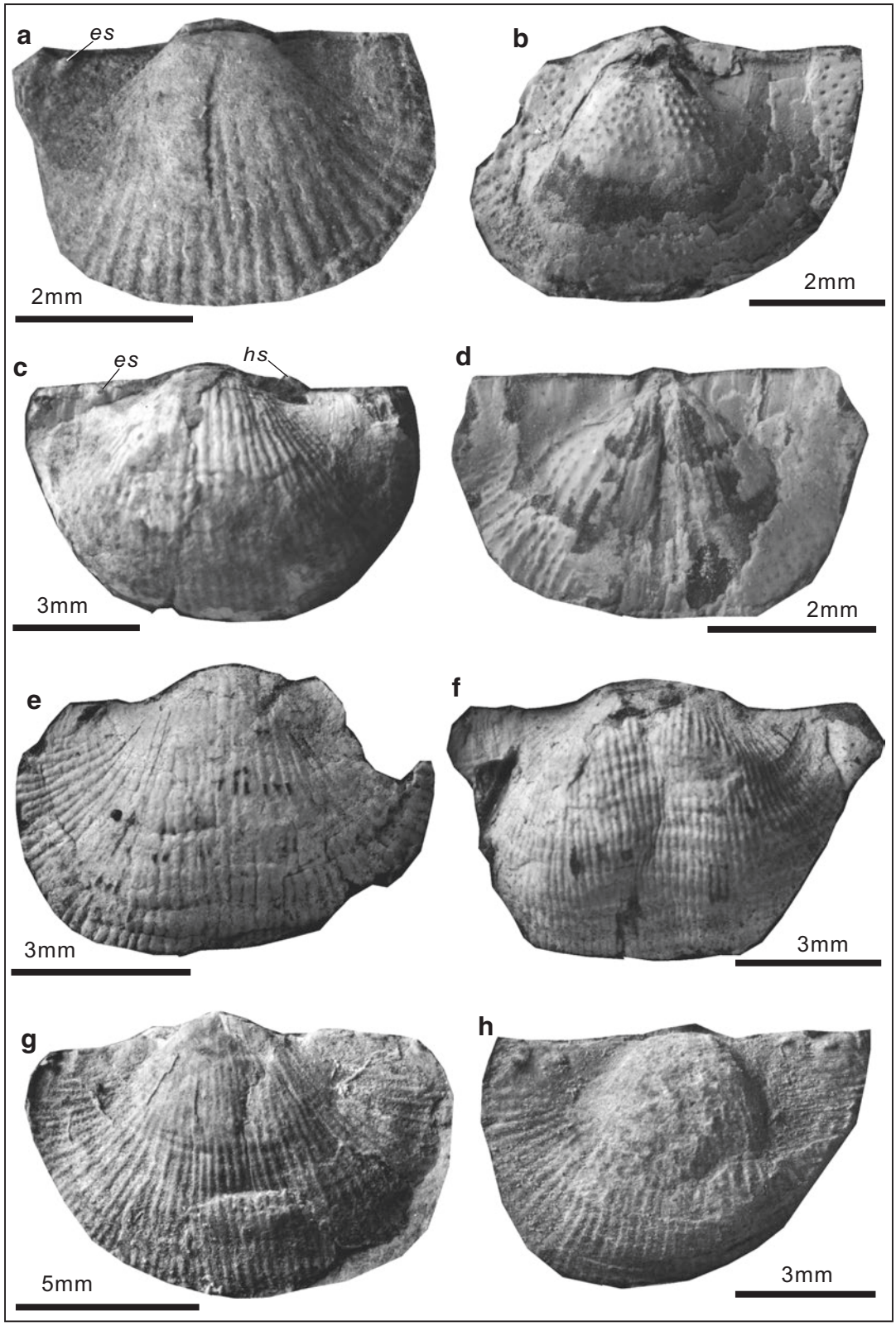
a
es
2mm
b
2mm
c
es
hs
3mm
d
2mm
e
3mm
f
3mm
g
5mm
h
3mm

1981 *Spinomarginifera kueichowensis* Huang; Tian: 57, pl. 32, Fig. 4–10.
1987 *Spinomarginifera kueichowensis* Huang; Xu in Yang et al.: pl. 11, Fig. 7, 10, 11, 13–16.
1987 *Spinomarginifera alpha* (Huang); Xu in Yang et al.: pl. 11, Fig. 3, 4, 8, 12.
1995 *Spinomarginifera kueichowensis* Huang; Zeng et al.: pl. 5, Fig. 10.
2002 *Spinomarginifera kueichowensis* Huang; Tazawa: Fig. 10.11a, b.
2006b *Spinomarginifera kueichowensis* Huang; Chen et al.: 314, Fig. 8a–e.
2009 *Spinomarginifera kuwichowensis* Huang; Shen and Shi: 158, Figs. 3DD, EE, 4I.
2009 *Spinomarginifera kueichowensis* Huang; Zhang and He: 20, Fig. 3e–j.
2015 *Spinomarginifera kueichowensis* Huang; Zhang et al.: 307, Figs. 7a–k, 8i–l.
2015 *Spinomarginifera alpha* (Huang); Zhang et al.: 309, Fig. 7l, 7o–q.
2015 *Spinomarginifera sintanensis* (Chao); Zhang et al.: 310, Fig. 8g.

Diagnosis (emended). Medium shell size, strongly globular. Ventral valve geniculate, median sulcus wide and shallow; dorsal valve geniculate. Surface ornamented by pits and spines and concentric wrinkles on posterior part.

Materials Over 130 specimens. Registered specimens: see below.

Measurements (mm):

Number	Width	Length	Width/length	Notes
LZ2702639	30.46	22.32	1.36	Internal mould of ventral valve
LZ2702631	30.89	23.54	1.31	Internal mould of ventral valve
LZ2702488	31.35	19.59	1.60	Internal mould of ventral valve
LZ1400341	16.44	10.47	1.57	External mould of dorsal valve
LZ2703524	30.02	19.60	1.53	External mould of dorsal valve
LZ1400369	11.10	7.30	1.52	External mould of dorsal valve
LZ2701490	24.61	16.65	1.48	Internal mould of dorsal valve
LZ2704493	28.37	17.43	1.63	Internal mould of dorsal valve
LZ2702640	27.30	17.10	1.60	Internal mould of dorsal valve
LZ1400342	17.44	11.02	1.58	Internal mould of dorsal valve

Fig. 9.10 (**a**–**d**), ***Parapygmochonetes parvulus*** He and Shi in He et al., 2014. (**a**), exterior of a complete ventral valve (shell decorticated), CM-10-114, illustrating the midline-inclined spines on ears (*es*). (**b**), interior of an incomplete dorsal valve and part of internal mould of the conjoined ventral valve, CM-3-119, showing papillae. (**c**), exterior of a complete ventral valve, CM-3-122, illustrating the midline-inclined hinge spines (*hs*) and spines on ears (*es*). (**d**), interior of a complete dorsal valve, CM-3-118, showing papillae connected with each other to form radial ridges. (**e**–**h**), ***Parapygmochonetes baoqingensis*** (Liao in Zhao et al., 1981). (**e**), exterior of an incomplete ventral valve, CM-3-104, showing dense, bifurcated and wavy costellae. (**f**), extererior of a complete ventral valve, CM-3-101, showing dense, wavy costellae interrupted by concentric rugae. (**g**, **h**), exteriors of two nearly complete ventral valves, CM-3-123, CM-6-115, showing dense and wavy costellae

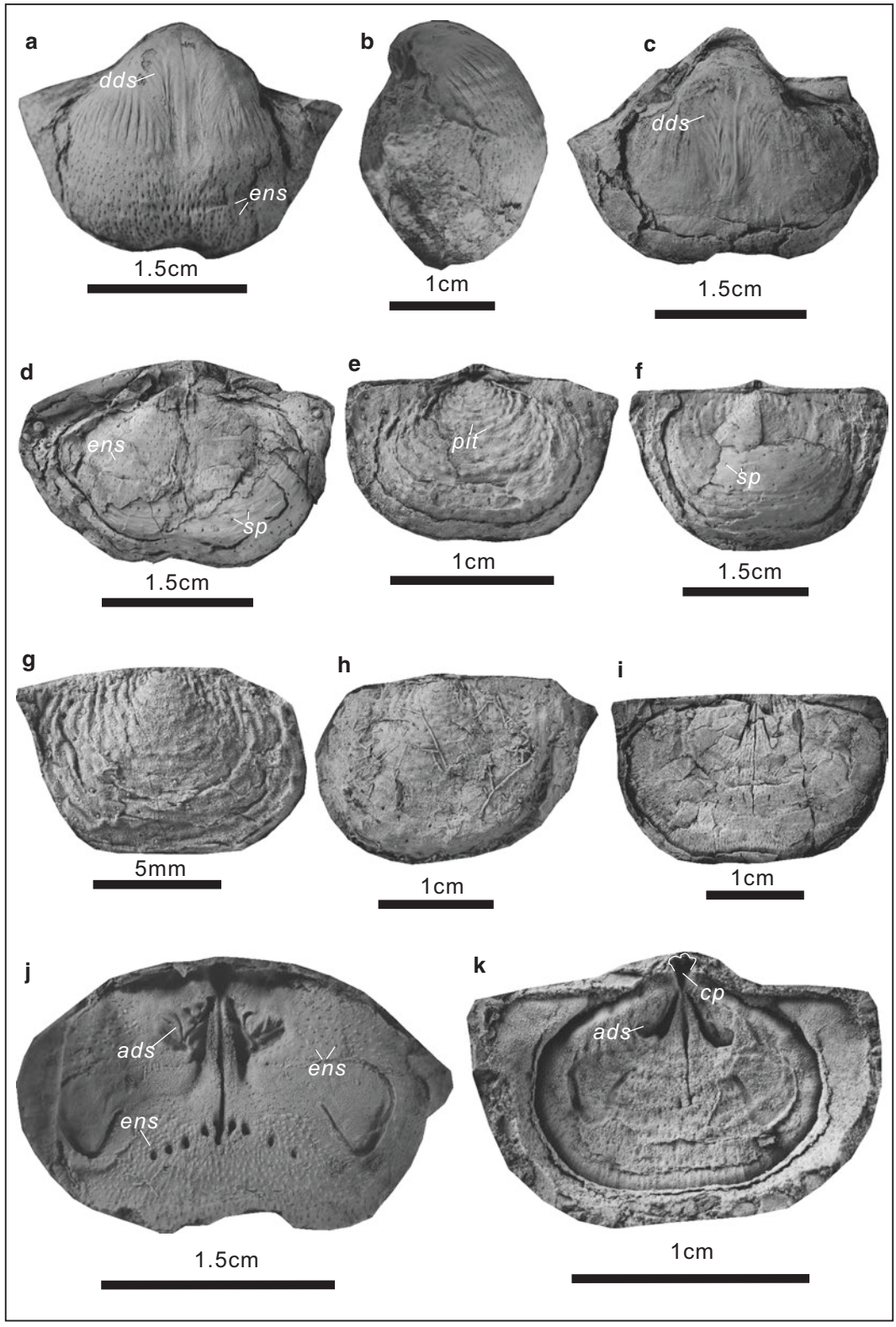
a
dds
ens
1.5cm
b
1cm
c
dds
1.5cm
d
ens
sp
1.5cm
e
pit
1cm
f
sp
1.5cm
g
5mm
h
1cm
i
1cm
j
ads
ens
ens
1.5cm
k
cp
ads
1cm

Occurrence Middle Permian to Lower Triassic; South China (Guizhou, Sichuan, Chongqing, Hunan, Jiangxi, Zhejiang, Guangxi and Guangdong), Japan, Vietnam.

Description Shell 7.3–31.6 mm long and 11.1–38.8 mm wide, strongly globular in outline, maximum width at hingeline. Ventral valve strongly convex, geniculate at midvalve; beak broad, enrolled over hingeline; cardinal extremities forming an angle at around 60–90°; ears convex, triangular, weakly demarcated from visceral region; sulcus originated from midvalve, shallow and wide. Dorsal valve strongly concave, geniculate at anterior; fold indistinct. Dorsal surface with concentric wrinkles, coarse and shallow pits, fine spines (randomly distributed). A row of spines distributed between ears and visceral region.

Ventral interior with pectinate diductor muscle scars (marked by *dds* in Fig. 9.11a) at posterior midvalve and endospines (marked by *ens* in Fig. 9.11a, d). Dorsal interior with a trifid cardinal process (*cp*) (Fig. 9.11k), evenly-distributed fine endospines (Fig. 9.11j) on disk; marginal ridges prominent; median septum long, extending to midlength; lateral septa short, prominent, diverging at an angle of 30–60°; a pair of adductor muscle scars (*ads*) (Fig. 9.11j, k) on both sides of median septum; brachial ridges hook-like, extending to lateral margin; a row of coarse, curved-arranged endospines developed at anterior of midlength (Fig. 9.11j).

Discussion The present species is similar to *Spinomarginifera alpha* Huang, 1932 from the Lungtan Formation (Upper Permian) of Guizhou, southwestern China in outline and interiors, but the latter lacks ventral geniculation. *Spinomarginifera sintanensis* (Chao, 1927) from the Wushan Cherty Limestone (Middle Permian) of Hubei and *S. chengyaoyenensis* Huang, 1932 from the Lungtan Formation of Guizhou, China both are small compared to *Spinomarginifera kueichowensis*, and they are cylindrical in outlines. *Spinomarginifera pseudosintanensis* Huang, 1932 from the Lopingian *Lyttonia* horizon of Guizhou, southwestern China is also small when compared with *Spinomarginifera kueichowensis*; it additionally also lacks a median sulcus.

Subfamily **Productininae** Muir-Wood and Cooper, 1960

Genus ***Rugivestis*** Muir-Wood and Cooper, 1960

Type Species *Proboscidella*? *carinata* Muir-Wood and Cooper in Cooper, 1957. Coyote Butte Formation (Lower Permian); Oregon, North America.

Diagnosis Small, trigonal outline, corpus well separated from trail by cincture, trail generally folded into a nasute extension; disks concavoconvex; reticulate ornamentation distinct on visceral region, ribbing well developed on trails, a row of spines along hingeline, the other row of spines along the cincture, other spines probably symmetrically placed on disks; marginal ridges in both valves (emended here).

Fig. 9.11 ***Spinomarginifera kueichowensis*** Huang, 1932. (**a**), internal mould of a complete ventral valve, LZ2702639, showing diductor muscle scars (*dds*) and endospines (*ens*). (**b**), lateral view of LZ2702639. (**c**), internal mould of an incomplete ventral valve, LZ2702631, showing diductor muscle scars (*dds*). (**d**), internal mould of an incomplete ventral valve and external mould of the conjoined dorsal valve, showing numerous endospines (*ens*) on ventral interior and spines (*sp*) on the surface of dorsal valve, LZ2702488. (**e**), external mould of a nearly complete dorsal valve, LZ1400341, showing coarse pits on disk (*pit*). (**f**), external mould of a nearly complete but deformed dorsal valve, LZ2703524, showing spines (*sp*). (**g**, **h**), external moulds of two incomplete dorsal valves, LZ1400369, LZ2701490. (**i**), internal mould of a nearly complete dorsal valve, LZ2704493, showing a median septum and two lateral septa. (**j**), internal mould of a nearly complete dorsal valve, LZ2702640, showing a pair of adductor muscle scars (*ads*), fine endospines (*ens*) on disk and coarse, curvedly-arranged endospines at anterior of midlength. (**k**), internal mould of a complete dorsal valve, showing the adductor muscle scars (*ads*) and a trifid cardinal process (*cp*), LZ1400342

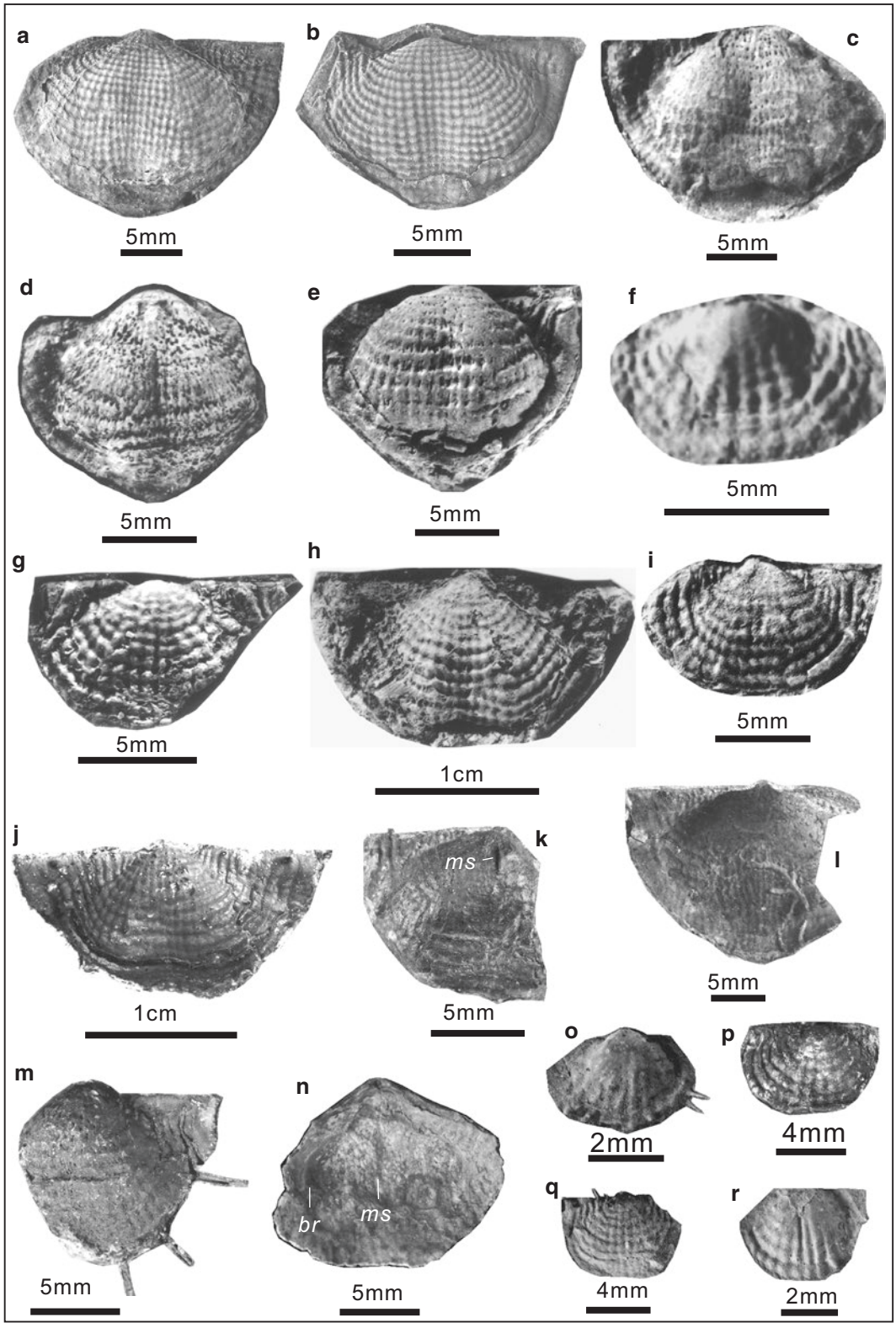
a
5mm
b
5mm
c
5mm
d
5mm
e
5mm
f
5mm
g
5mm
h
1cm
i
5mm
j
1cm
k
ms
5mm
l
5mm
m
5mm
n
br
ms
5mm
o
2mm
p
4mm
q
4mm
r
2mm

Discussion *Dongpanoproductus* He et al. 2005, with *Dongpanoproductus elegans* He et al. 2005 as the type species, was proposed in 2005; however, this genus should be a synonym of *Rugivestis* Muir-Wood and Cooper, 1960, because the typical features shared between them, including the presence of a cincture separating between corpus and trail and reticulate ornamentation, as reviewed by Shen et al. in Rong et al., 2017.

Rugivestis elegans (He and Shen in He et al., 2005)
Fig. 9.12

2005 *Dongpanoproductus elegans* He and Shen in He et al.: 931, Fig. 5.1–5.11.
2014 *Dongpanoproductus elegans* He et al.: 939, Fig. 17a, b.

Materials Over 50 specimens. Registered specimens: see below.

Measurements (mm):

Number	Width	Length	Width/length	Notes
DP-2-270	23.42	15.39	1.52	External mould of dorsal valve
DP-3-271	20.76	12.14	1.71	External mould of dorsal valve
DP728	21.53	14.06	1.53	Ventral valve
DP729	14.09	11.63	1.21	Ventral valve
DP730	16.31	12.33	1.32	Ventral valve
DP731	8.00	5.23	1.53	External mould of dorsal valve
DP811	12.15	6.40	1.90	External mould of dorsal valve
DP812	19.88	10.99	1.81	Ventral valve
DP9601	12.65	7.49	1.69	External mould of dorsal valve
DP10-0153	21.07	10.51	2.00	External mould of ventral valve
DP10-0162	14.33	9.50	1.51	Internal mould of dorsal valve
DP2-0159	25.52	17.18	1.49	Ventral interior
DP7-0156	15.83	10.43	1.52	Ventral valve
DP10-0173	3.98	2.85	1.40	Ventral valve (juvenile)
DP9-0164	8.03	5.38	1.49	Ventral valve (juvenile)
DP10-0171	6.98	5.39	1.30	Ventral valve (juvenile)
DP10-0172	4.97	3.30	1.51	Ventral valve (juvenile)

Fig. 9.12 ***Rugivestis elegans*** (He and Shen in He et al., 2005). (**a**), external mould of an incomplete dorsal valve, DP-2-270, illustrating transverse and semicircular outline. (**b**), external mould of a nearly complete dorsal valve, DP-3-271. (**c**), an incomplete ventral valve, DP728, showing transverse and semicircular outline and distinct cincture. (**d**), an incomplete ventral valve, DP729, showing distinct cincture. (**e**), a nearly complete ventral valve, DP730, showing transverse and semicircular outline, distinct ears, marked reticulation on visceral region, and distinct cincture. (**f**), external mould of a nearly complete dorsal valve, DP731. (**g**), external mould of a nearly complete dorsal valve, DP811, showing transverse and semicircular outline, distinct ears, marked reticulation on visceral region. (**h**), a complete ventral valve, DP812. (**i**), external mould of a nearly complete dorsal valve, DP9601. (**j**), external mould of a complete ventral valve, DP10-0153, illustrating a row of spines on ears and two body spines anterolaterally arranged on the surface. (**k**), internal mould of an incomplete dorsal valve, DP10-0162, illustrating median septum (*ms*). (**l**), interior of an incomplete ventral valve, DP2-0159. (**m**), an incomplete ventral valve, DP7-0156, illustrating long marginal spines. (**n**), internal mould of DP2-0159, illustrating a pair of brachial ridges (*br*) and median septum (*ms*). (**o**), an incomplete ventral valve (juvenile), DP10-0173, showing marginal spines. (**p**), external mould of a nearly complete dorsal valve (juvenile), DP9-0164. (**q**), an incomplete ventral valve (juvenile), DP10-0171, showing hingespines. (**r**), an incomplete ventral valve (juvenile), DP10-0172, showing distinct cincture

Occurrence Upper Changhsingian; Guangxi (Dongpan section) of South China.

Description Shell 2.9–17.2 mm long and 4.0–25.5 mm wide, subquadrate to semicircle in outline, greatest width at hinge. Ventral beak slightly incurved over hingeline; ears large and distinct, triangular, well demarcated from visceral disk by depressions, with strong rugae and occasionally with costellae interrupted by rugae; sulcus weak, originated from anterior to umbo, slightly widening and deepening anteriorly on visceral disk; trail short, separated from corpus by distinct cincture around trail (Fig. 9.12b–e, r); costellae coarse, crossed with strong and regular rugae to form distinct reticulation on visceral disk, slightly converging into sulcus; spines probably arranged in a row along the hingeline (Fig. 9.12j) and the other row between ears and visceral disk (Fig. 9.12e, l), and several long spines along cincture (Fig. 9.12o, m). Dorsal visceral disk slightly concave; ears distinct, well differentiated from visceral disk by depressions; reticulate ornament similar to that on ventral disk. Ventral interior with densely-arranged papillae in internal molds (see He et al., 2005). Dorsal interior with a median septum (Fig. 9.12k, n) and a pair of ear-shaped brachial ridges (Fig. 9.12n).

Discussion Six species have been recognized from the genus of *Rugivestis*, including *R. carinata* (Muir-Wood and Cooper in Cooper, 1957) (type species), *R. kutorgae* (Tschernyschew, 1902), *R. gangiaoensis* Jin and Sun, 1981, *R. tianshanensis* Wang and Yang, 1998, *R. arctica* Shi and Waterhouse, 1996 and the present species *R. elegans* (He and Shen in He et al., 2005). *Rugivestis elegans* differs from *R. carinata* (Muir-Wood and Cooper in Cooper, 1957) of the Coyote Butte Formation of Oregon in the latter lacking a sulcus, and having sparser and thicker reticulate ornamentation, a wider cincture and a wide rim below cincture, and the former having rows of spines near the hingeline (see above). Compared to *Rugivestis elegans*, *R. kutorgae* (Tschernyschew, 1902) from the Lower Permian of southern Ural Mountains lacks a sulcus, has a wider cincture and a wide rim below cincture, and rows of spines near the hingeline. The present species is readily distinguished from *Rugivestis gangiaoensis* Jin and Sun, 1981 of the Permian Gangjiu Limestone of Gangjiu, Zhongba, Tibet in its presence of sulcus. *Rugivestis elegans* resembles to *R. tianshanensis* Wang and Yang, 1998 in having a sulcus and a row of spines between ears and visceral disk, but the latter has much extended ears, a weaker cincture and a wide rim below cincture. This species differs from *Rugivestis arctica* Shi and Waterhouse, 1996 from the Lower Permian of Canada in the latter having weaker costellae and stronger rugae.

Genus ***Paryphella*** Liao in Zhao et al., 1981

Type Species *Cathaysia sulcatifera* Liao, 1980a. Changhsingian; Anshun, Guizhou Province, South China.

Diagnosis Small, sub-quadrate or chonetiform in outline, with ear baffles (= ear curtains); dorsal disks weakly concave; costellae simple, weak posteriorly; rugae strong on ears; two pairs of spines at hinge; low median septum extending to midlength of shell.

Discussion The type species *Cathaysia sulcatifera* Liao, 1980a is a synonym of *Cathaysia sinuata* Chan in Hou et al. (1979), because of their similar sub-quadrate or semicircular outline, sparse but coarse costellae, and deep and narrow ventral sulcus (see Liao, 1980a, p. 261; Hou et al., 1979, p. 76). *Paryphella* is similar to *Chonetella* Waagen, 1884 from the Lower to Middle Permian in a semicircular outline, but the latter has weak ribbing and a narrow, long nasute trail. *Paryphella* shares with *Parachonetella* Liao, 1980a from Upper Permian a semicircular outline, sparse and coarse costellae, but the latter has a deep, stable groove around the disk margin. *Paryphella* is

also close to *Cathaysia* Jin in Wang et al., 1966 in outline, but the latter has finer and denser costellae: 8–11 per 5 mm, in contrast to *Paryphella* with 5–7 per 5 mm. *Paryphella* is possibly the descendent of *Cathaysia*, because they share most morphological similarity and co-occurred in the Upper Permian in South China.

Paryphella transversa Liao, 1984
Fig. 9.13a–i

1984 *Paryphella transversa* Liao: 280, pl. 2, Fig. 10–12.
1984 *Cathaysia transversa* Wang: 180, pl. 73, Fig. 21.
2014 *Paryphella transversa* Liao; He et al.: 935, Fig. 14i–o.
2014 *Paryphella* cf. *nasuta* Liao; He et al.: 935, Fig. 14p, q.

Diagnosis Reversely trapezoid in outline; ventral valve moderately convex; median sulcus beginning from anterior of umbo, shallow and wide.

Materials Over 100 specimens. Registered specimens: see below.

Measurements (mm):

Number	Width	Length	Width/ length	Notes
DCB-34-231	11.44	6.59	1.74	Ventral exterior
CM-12-245	9.00	5.10	1.77	Ventral exterior
CM-13-228	8.23	5.23	1.57	Ventral exterior
CM-4-243	10.11	5.51	1.83	Internal mould of ventral valve
CM-4-248	9.71	5.50	1.76	Ventral exterior
CM-3-237	9.51	5.74	1.66	Ventral exterior
CM-3-241	9.15	5.55	1.65	Ventral exterior
CM-12-222	8.38	5.98	1.40	Ventral exterior
CM-12-223	9.33	6.00	1.55	Ventral exterior

Occurrence Changhsingian (Upper Permian); China.

Description Shell 4.4–7.5 mm long and 6.9–13.0 mm wide, reversely trapezoid in outline. Widest at hinge; ears large, triangular, slightly inflated, with rugae. Ventral valve moderately convex; beak variably incurved, prominently over hingeline; 2–3 pairs of hingespines projecting posterolaterally with an angle of 60–70°; ventral disk nearly flat; sulcus beginning from anterior of umbo, shallow, widening anteriorly; tail variably occurring; costellae beginning from umbo, simple, coarse and round, numbering 5 to 8 per 5 mm near anterior margin. Ventral interior with radially-arranged, fine papillae.

Discussion Although the name of *Paryphella transversa* was used by Liao in Wang et al., 1982 from the Talung Formation of Yongding, Fujian Province, this book considers the species of *Paryphella transversa* of Liao in Wang et al., 1982 is a synonym of *Paryphella corculum* (Liao, 1980a) by sharing features of strong convex ventrals, strongly geniculated along margin of disks and acute cardinal extremities. The present species differs from other species of the genus in a shallow and anteriorly widening median sulcus on the ventral valve (Fig. 9.14).

Paryphella minuta He and Shi in He et al., 2014
Fig. 9.13j–m

2014 *Paryphella minuta* He and Shi in He et al.: 937, Fig. 16U-X.

Diagnosis Small, reversely trapezoid in outline; ventral valve weakly convex; ear flat, well differentiated with disk; median sulcus absent; costellae coarse and covering ventral disk.

Materials 11 specimens. Registered specimens: CM-20-195, CM-20-196, CM-18-200, CM-18-198. Other specimens not well preserved.

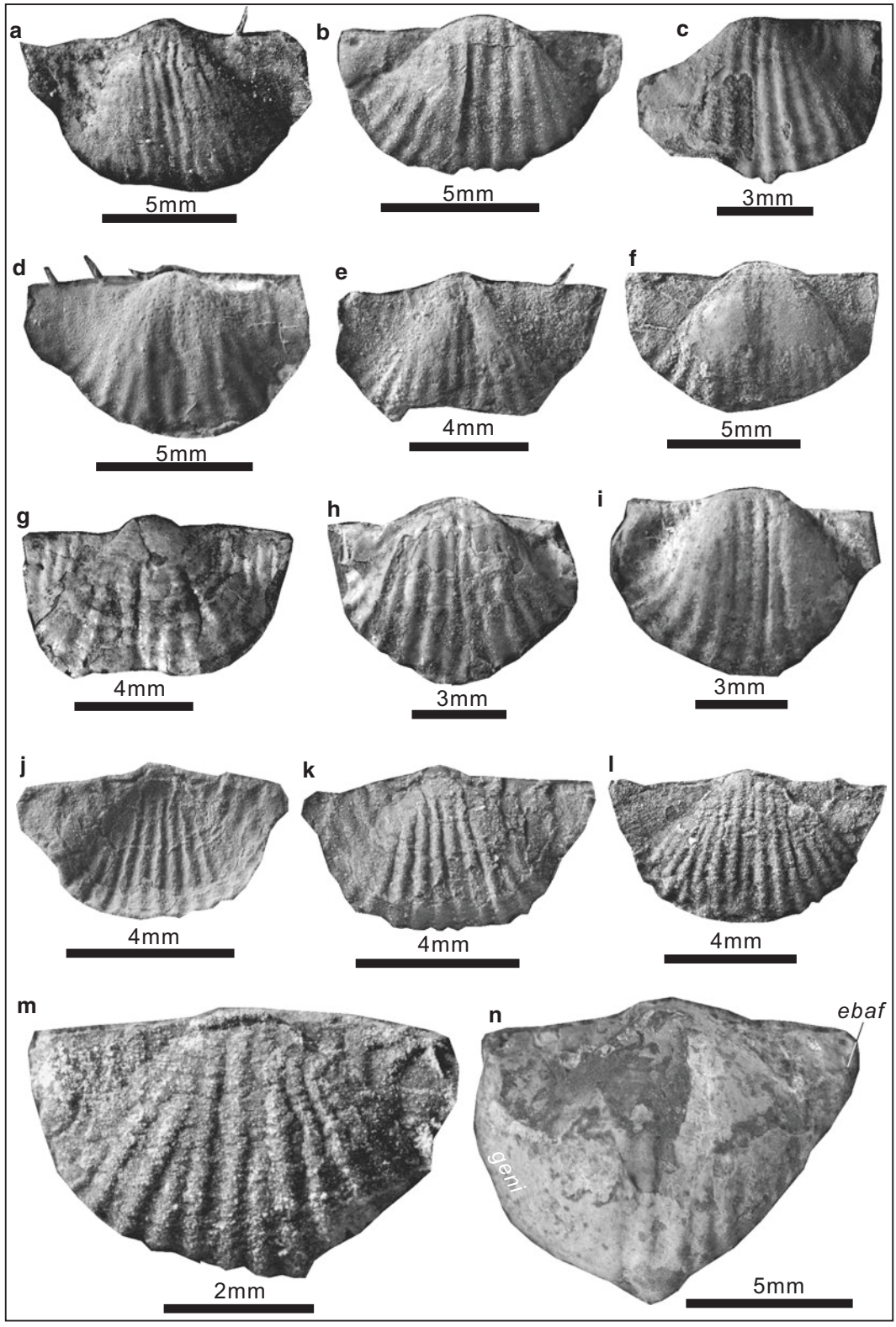
a
5mm
b
5mm
c
3mm
d
5mm
e
4mm
f
5mm
g
4mm
h
3mm
i
3mm
j
4mm
k
4mm
l
4mm
m
2mm
n
ebaf
geni
5mm

Measurements (mm):

Number	Width	Length	Width/ length	Notes
CM-20-196	6.43	3.76	1.71	External mould of dorsal valve
CM-20-195	7.19	4.07	1.77	Ventral exterior
CM-18-200	8.40	4.66	1.80	Ventral exterior
CM-18-198	5.74	3.61	1.59	Ventral exterior

Occurrence Uppermost Changhsingian—lowest Triassic (equivalent to the intervals yielding so-called Permian—Triassic mixed fauna); Anhui (Majiashan section) of South China.

Description Shell small, 3.6—4.7 mm long and 5.7—8.4 mm wide, reversely trapezoid in outline, widest at hinge. Ventral valve flat to weakly convex; beak weakly incurved, slightly over hingeline; cardinal extremities acute, with an angle of about 65—80°; ears triangular, flat, well differentiated from ventral disk, evenly and sparsely covered with rugae; sulcus absent; costellae beginning from umbo, round, coarse, occasionally bifurcated at midlength of shell, 10 to 15 nearby anterior margin; costellae crossed by obscure concentric fila (microornaments, see Fig. 9.13m).

Discussion This species is most similar to *Paryphella sparsiplicata* Liao (1984, p. 280, pl. 2, Fig. 6—8) from the lowest Yinkeng Formation of Zhejiang Province, South China in a small body size and absence of a median sulcus, but differs in its acute cardinal extremities and more costellae (Fig. 9.14). *Paryphella orbicularis* (Liao, 1980a, p. 261, pl. 6, Fig. 1—4) is broadly similar to the present species, but is clearly distinguished by its strongly convex ventral valve (Fig. 9.14).

Paryphella sinuata (Chan in Hou et al., 1979)
Fig. 9.15

1979 *Cathaysia sinuata* Chan in Hou et al.: 76, pl. 8, Fig. 6—9.
1980a *Cathaysia sulcatifera* Liao: 261, pl. 6, Fig. 8—10.
1982 *Paryphella sulcatifera* (Liao); Wang et al., pl. 95, Fig. 3—5.
1984 *Paryphella sulcatifera* (Liao); Liao, pl. 2, Fig. 18.
1984 *Cathaysia sulcatifera* Liao; Wang, 180, pl. 74, Fig. 24.
1984 *Cathaysia sulcatifera* Liao; Yang in Feng et al., 214, pl. 31, Fig. 20.
1987 *Cathaysia sinuata* Chan; Xu in Yang et al.: 223, pl. 10, Fig. 19, 20, 22—23.
1990 *Paryphella sulcatifera* (Liao); Zhu: 67, pl. 18, Fig. 10, 11.

Fig. 9.13 (**a**–**i**), ***Paryphella transversa*** Liao, 1984. (**a**), exterior of a complete ventral valve, DCB-34-231, showing coarse and rounded costellae and a preserved hinge spine. (**b**), exterior of a complete ventral valve, CM-12-245, showing coarse and rounded costellae. (**c**), exterior of an incomplete ventral valve, CM-13-228, showing sparse rugae on ears. (**d**), internal mould of a nearly complete ventral valve, CM-4-243, showing papillae and hinge spines. (**e**), exterior of an incomplete ventral valve, CM-4-248, showing a broad and shallow sulcus. (**f**), exterior of a complete ventral valve (shell partly decorticated), CM-3-237, showing a shallow sulcus. (**g**), exterior of a nearly complete but slightly deformed ventral valve, CM-3-241, showing coarse costellae, few concentric lines and rugae on ears. (**h**), exterior of a nearly complete ventral valve, CM-12-222, showing a very shallow sulcus. (**i**), exterior of a nearly complete ventral valve, CM-12-223, showing a broad and shallow sulcus. (**j**–**m**), ***Paryphella minuta*** He and Shi in He et al. 2014. (**j**), external mould of a complete ventral valve, CM-20-196, showing sparse rugae on ears. (**k**), exterior of a complete ventral valve, CM-20-195. (**l**), exterior of a complete ventral valve, CM-18-200, showing coarse and rounded costellae. (**m**), exterior of a complete ventral valve, CM-18-198, showing occasionally bifurcated costellae and sparse rugae on ears. (**n**), ***Chonetella*** sp., exterior of a deformed ventral valve, CM14-0517, showing ear baffles (*ebaf*) and a geniculation (*geni*)

Species	Shape of umbo	Size mm	Width /length	Ventral sulcus	Umbo angle	Cardinal angle	Costellae	Concentric lines on disc	Rugae on ears	Others	Sketch of outline
P. orbicularis (Liao, 1980a)	Hillock and strongly convex	8.5	1.9	Absent	92¡	90¡	12	Absent	Indistinct		
P. sparsiplicata Liao, 1984	Slightly convex	3.5	1.8	Absent	69	78	5	Weak but densely	3 pairs and strong		
P. transversa Liao, 1984	Broadly triangular and moderately convex	11.0	2.1	Shallow and wide	94	78	16	Absent	4 pairs and weak		
P. nasuta Liao, 1984	Hillock and weakly convex	10.0	1.3	Shallow and narrow	66	90	12	Absent	Indistinct	Nasute -shape tail	
P. sinuata (Chan in Hou et al., 1979)	Hillock and moderately convex	12.1	1.6	Deep and narrow	107	118	15	Absent	Indistinct		
P. undata (Liao, 1984)	Broadly triangular and weakly convex	7.5	3.0	Weak	100	90¡	7	Densely	6 pairs and strong		
P. minuta He and Shi in He et al., 2014	Moderately -broadly triangular and weakly convex	6.6	1.8	Absent	82	65	10	Absent	3 pairs and moderate		
P. corculum Liao, 1980a	Hillock and strongly convex	17.5	1.8	Weak or absent	85	70	17	Absent	3 pairs and weak	Short tail; curved grooves	gr

gr- A pair of curved grooves separated ears and disk

Fig. 9.14 Comparison of some similar *Paryphella* species. Data based on the holotype specimens (ventral valves); size refers to the greatest width of shell; costellae refers to the number of costellae nearby anterior margin

1994 *Cathaysia sinuata* Chan; Xu and Grant: 31, Fig. 17.1–17.22.
2014 *Paryphella sinuata* (Chan); He et al.: 935, Fig. 14r–x.

Diagnosis Semicircle in outline; ventral valve moderately convex; ears weakly inflated; median sulcus narrow but deep, beginning from anterior of umbo, extending nearly to anterior margin.

Materials Over 360 specimens. Registered specimens: see below.

Measurements (mm):

Number	Width	Length	Width/ length	Notes
CM-12-188	6.42	3.86	1.66	Ventral interior
CM-12-193	9.40	7.04	1.34	Internal mould of ventral valve
CM-10-180	10.37	6.14	1.69	External mould of dorsal valve
CM-10-182	9.98	6.58	1.52	Internal mould of ventral valve
CM-10-189	13.26	7.65	1.73	Ventral exterior
DCB-36-190	8.35	6.29	1.33	Internal mould of ventral valve
CM-15-226	13.46	8.04	1.67	Dorsal interior
SR28-0350	6.88	4.62	1.49	Ventral exterior
SR22-0514	10.63	6.98	1.52	Ventral exterior
HZS19-0515	11.17	5.99	1.86	External mould of dorsal valve
HZS19-0516	11.14	7.07	1.58	Ventral exterior
XJP12-0519	11.14	8.12	1.37	Internal mould of ventral valve
HZS19-0522	10.35	6.05	1.71	Ventral exterior
DDS26-0520	10.00	5.92	1.69	Ventral exterior
HZS19-0523	6.89	4.61	1.49	Ventral exterior

Occurrence Changhsingian; South China.

Description Shell 3.8–9.7 mm long and 6.4–15.6 mm wide, semicircle in outline, widest at hingeline; ears large, weakly inflated, covered by weak rugae. Ventral valve moderately convex; 2–3 pairs of hingespines projecting posterolaterally with an angle of 30–60°; ventral sulcus narrow but deep, beginning from anterior of umbo, extending nearly to anterior margin; costellae beginning from umbo, simple and coarse, numbering 5 to 8 per 5 mm at anterior margin. Dorsal valve moderately concave; median fold narrow and prominent, beginning from anterior of umbo, extending nearly to anterior margin. Ventral interior with radially-arranged, fine papillae, with long median septum, extending to anterior margin. Dorsal interior with a median septum, extending over shell midlength; ear baffles (*ebaf*) visible on well-preserved specimens (Fig. 9.15g).

Discussion *Paryphella sulcatifera* (Liao, 1980a, p. 261, pl. 6, Fig. 8–10, from the Talung Formation of Jiaozishan, Anshun, Guizhou), originally proposed as the type species of *Paryphella* by Liao in Zhao et al., 1981, is the junior synonym of *Paryphella sinuata* (Chan in Hou et al., 1979) because they are both semicircle in outline, and have weakly inflated ears, nearly flat ventral disk, sparse and coarse costellae, and especially the deep and narrow ventral sulcus. *Paryphella sinuata* is similar to *Paryphella transversa* Liao, 1984 from the Talung Formation of South China in a moderately convex ventral valve and a nearly flat ventral disk, but differs in having a deep and narrow sulcus and a lower shell width to length ratio (Fig. 9.14).

Paryphella orbicularis (Liao, 1980a)
Figs. 9.16, 9.17 and 9.18

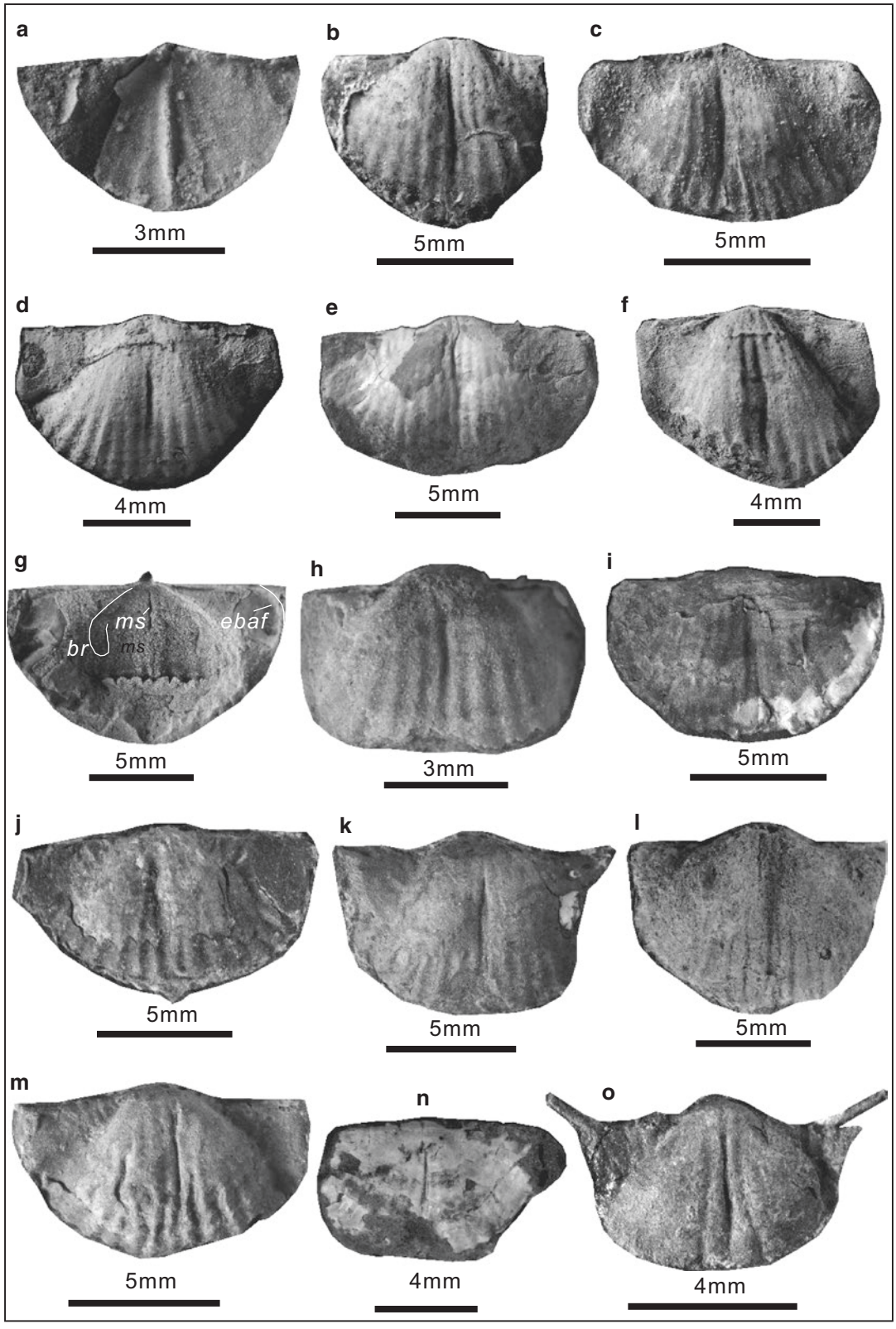
a
3mm
b
5mm
c
5mm
d
4mm
e
5mm
f
4mm
g
br
ms
ms
ebaf
5mm
h
3mm
i
5mm
j
5mm
k
5mm
l
5mm
m
5mm
n
4mm
o
4mm

1980a *Cathaysia orbicularis* Liao: 261, pl. 6, Fig. 1–4.
1981 *Paryphella triquetra* Liao in Zhao et al.: 53, pl. 8, Fig. 18–22.
1982 *Paryphella laohushanensis* Wang et al.: 204, pl. 95, Fig. 2.
1982 *Paryphella triquetra* Liao; Wang et al.: 205, pl. 96, Fig. 14–16.
1984 *Paryphella orbicularis* (Liao); Liao: pl. 2, Fig. 19.
1984 *Paryphella sparsiplicata* Liao: pl. 2, Fig. 9.
1984 *Cathaysia orbicularis* Liao; Wang: 180, pl. 74, Fig. 27.
1994 *Cathaysia orbicularis* Liao; Xu and Grant: 34, Fig. 19.1–19.21.
2005 *Paryphella orbicularis* (Liao); Chen et al.: Fig. 4.4–4.6, 4.13, 4.14.
2009b *Paryphella orbicularis* (Liao); Chen et al.: Fig. 7f.
2014 *Paryphella orbicularis* (Liao); He et al.: 933, Fig. 14a–h.
2014 *Paryphella triquetra* Liao; He et al.: 936, Fig. 16a–j.
2015 *Paryphella orbicularis* (Liao); Zhang et al.: 303, Fig. 4i–r.
2015 *Paryphella triquetra* Liao; Zhang et al.: 304, Fig. 4s–u.
2015 *Paryphella sinuata* (Chan); Zhang et al., 304, Fig. 4v.
2015 *Paryphella elegantula* Zhan in Li et al.; Zhang et al.: Fig. 4w–aa.

Diagnosis Semicircle to reversely trapezoid in outline; ventral valve strongly convex, hillock to roundly triangular in ventral disk; median sulcus absence.

Materials Over 100 specimens. Registered specimens: see below.

Measurements (mm):

Number	Width	Length	Width/length	Notes
DDS29-1-0532	5.53	3.92	1.41	Ventral exterior
DDS29-0541	4.48	3.56	1.26	Ventral exterior
DDS27-2-0545	3.65	2.32	1.57	Ventral exterior
DDS27-2-0533	6.48	4.17	1.55	Ventral exterior
DDS27-2-0535	4.59	3.49	1.32	Ventral exterior
DDS27-0546	2.38	1.36	1.75	Ventral exterior (juvenile)

(continued)

Fig. 9.15 ***Paryphella sinuata*** (Chan in Hou et al., 1979). (**a**), interior of a complete ventral valve (shell decorticated and interior structures not preserved), CM-12-188. (**b**), internal mould of a nearly complete ventral valve, CM-12-193, showing papillae. (**c**), external mould of a complete dorsal valve, CM-10-180, showing a narrow median fold. (**d**), internal mould of a complete ventral valve, CM-10-182. (**e**), exterior of a complete ventral valve, CM-10-189, showing a narrow, deep sulcus. (**f**), internal mould of a complete ventral valve, DCB-36-190, showing a few preserved papillae near umbo. (**g**), interior of a nearly complete dorsal valve, CM-15-226, showing a median septum (*ms*), brachial ridges (*br*) and ear baffles (*ebaf*). (**h**), exterior of a nearly complete ventral valve, SR28-0350, showing a narrow and deep sulcus. (**i**), exterior of a complete ventral valve (shell decorticated on posterior part), SR22-0514, showing a narrow and deep sulcus and concentric fila on observed posterior part of dorsal valve). (**j**), external mould of a complete dorsal valve and shell remnant of the conjoined ventral valve, HZS19-0515, showing a narrow and deep sulcus and rugae on ears. (**k**), exterior of a nearly complete ventral valve, HZS19-0516, showing a narrow and deep sulcus and one preserved spine on ear. (**l**), internal mould of a complete ventral valve, XJP12-0519, showing a narrow and deep sulcus. (**m**), exterior of a complete ventral valve (outer layer of shell mostly decorticated), HZS19-0522, showing a narrow and deep sulcus and rugae on ears. (**n**), exterior of an incomplete ventral valve, DDS26-0520, showing a narrow and deep sulcus. (**o**), exterior of a complete ventral valve (shell mostly decorticated), HZS19-0523, showing two preserved hinge spines

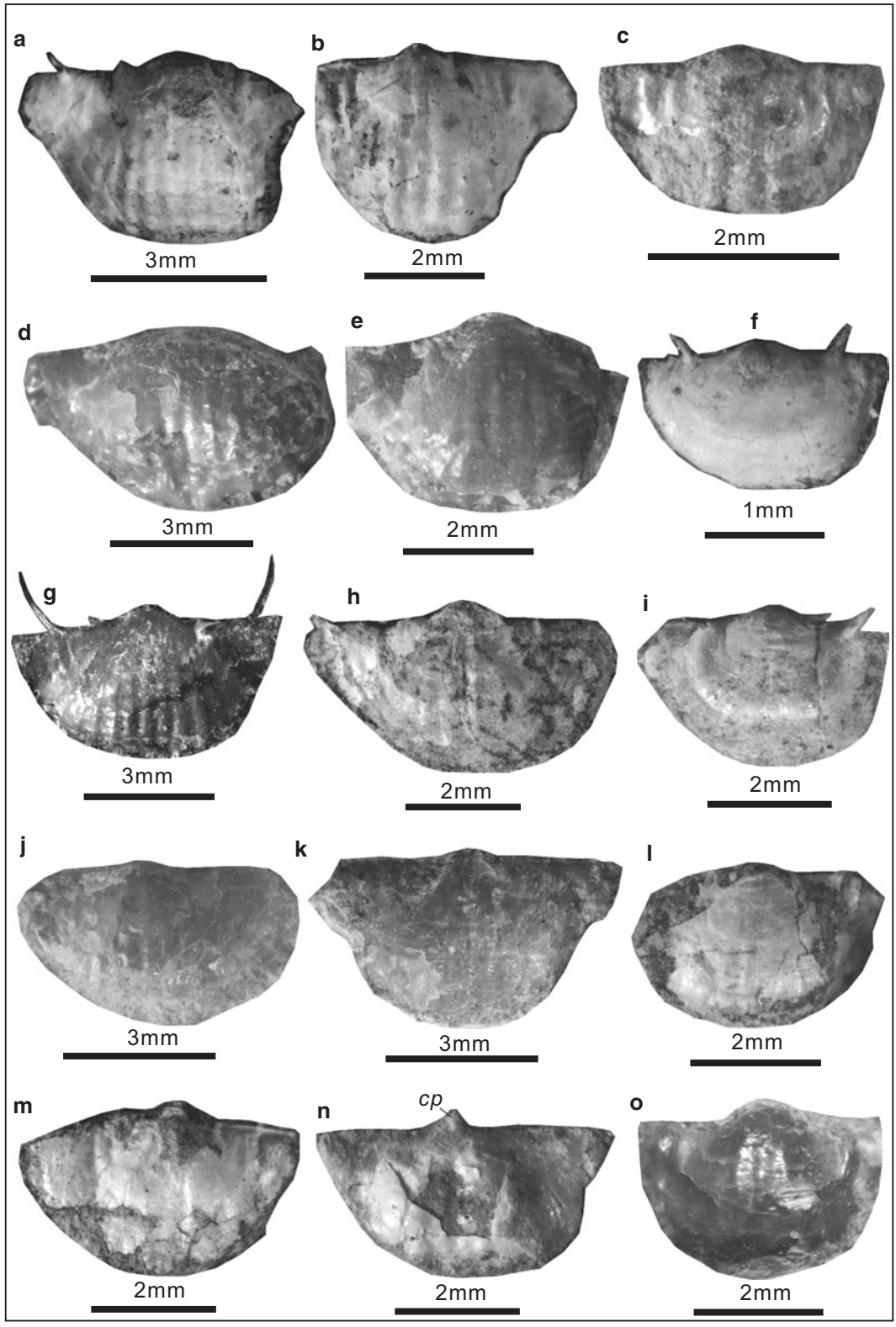
a
3mm
b
2mm
c
2mm
d
3mm
e
2mm
f
1mm
g
3mm
h
2mm
i
2mm
j
3mm
k
3mm
l
2mm
m
2mm
n
cp
2mm
o
2mm

Number	Width	Length	Width/length	Notes
DDS29-0534	5.84	3.41	1.71	Ventral exterior
DDS27-1-0542	5.11	3.23	1.58	Ventral exterior
DDS27-2-0543	3.94	2.81	1.40	Ventral exterior (juvenile)
DDS27-1-0537	5.10	3.36	1.52	Ventral exterior
DDS29-0536	5.80	3.46	1.68	Ventral exterior
DDS27-2-0538	3.93	2.63	1.49	Ventral exterior
DDS27-2-0544	4.48	2.99	1.50	Ventral exterior
DDS27-1-0539	4.95	2.77	1.79	Dorsal interior
DDS27-1	3.78	2.81	1.34	Ventral exterior
CM-20-216	6.53	4.30	1.52	Ventral exterior
CM-13-205	11.84	8.38	1.41	Ventral exterior
CM-13-208	9.49	6.74	1.41	Ventral exterior
CM-13-212	9.07	6.15	1.48	Ventral exterior
CM-13-231	10.72	7.48	1.43	Ventral exterior
CM-4-249	12.86	8.32	1.55	Ventral exterior
CM-12-203	6.26	4.42	1.42	Ventral exterior
CM-12-204	9.15	6.92	1.32	Ventral exterior
CM-10-209	9.35	6.03	1.55	Ventral exterior
CM-12-219	8.40	5.76	1.46	Ventral exterior
CM-10-233	7.97	5.03	1.59	Ventral exterior
CM-10-247	10.00	6.41	1.56	Ventral exterior
CM-10-254	11.35	6.71	1.69	Ventral exterior
CM-13-201	9.83	6.59	1.49	Ventral exterior
CM-12-194	9.09	3.64	2.50	Internal mould of ventral valve
LZ2702676	9.35	6.74	1.39	Ventral exterior
LZ2702646	10.36	6.77	1.53	Internal mould of ventral valve
LZ2702677	10.15	7.38	1.38	Internal mould of ventral valve
LZ2702653	9.06	5.81	1.56	Ventral exterior
LZ2704668	10.92	6.64	1.64	Ventral exterior
LZ2702645	10.52	8.05	1.31	Internal mould of ventral valve
LZ2702651	11.21	7.56	1.48	Ventral valve
LZ2701155	8.42	4.66	1.81	Internal mould of ventral valve
LZ2705531	11.07	7.22	1.53	Ventral exterior
LZ2706170	11.05	7.61	1.45	Ventral exterior
LZ2704160	10.47	7.26	1.44	Ventral exterior
LZ2702644	12.25	8.70	1.41	External mould of dorsal valve

Fig. 9.16 ***Paryphella orbicularis*** (Liao, 1980a). (**a**), exterior of an incomplete ventral valve, DDS29-1-0532, showing concentric fila when shell partly decorticated. (**b**), exterior of an incomplete ventral valve and interior of middle and anterior parts of the conjoined dorsal valve, DDS29-0541, showing rugae on ventral ears and papillae on the observed part of dorsal interior. (**c**–**e**), exteriors of three nearly complete ventral valves, DDS27-2-0545, DDS27-2-0533, DDS27-2-0535, showing low and rounded costellae. (**f**), exterior of a complete ventral valve (juvenile), DDS27-0546, showing two preserved hinge spines and obscure costellae. (**g**), exterior of a complete ventral valve, DDS29-0534, showing two preserved long and curved hinge spines. (**h**), exterior of a nearly complete ventral valve (shell partly decorticated), DDS27-1-0542. (**i**), exterior of a nearly complete ventral valve (juvenile), DDS27-2-0543, showing obscure costellae. (**j**), exterior of an incomplete ventral valve, DDS27-1-0537. (**k**), exterior of a nearly complete ventral valve, DDS29-0536. (**l**), exterior of an incomplete ventral valve, DDS27-2-0538. (**m**), exterior of a deformed ventral valve, DDS27-2-0544, showing rugae on ears. (**n**), interior of a complete dorsal valve, DDS27-1-0539, showing a cardinal process (*cp*). (**o**), exterior of a complete ventral valve, DDS27-1, showing low costellae

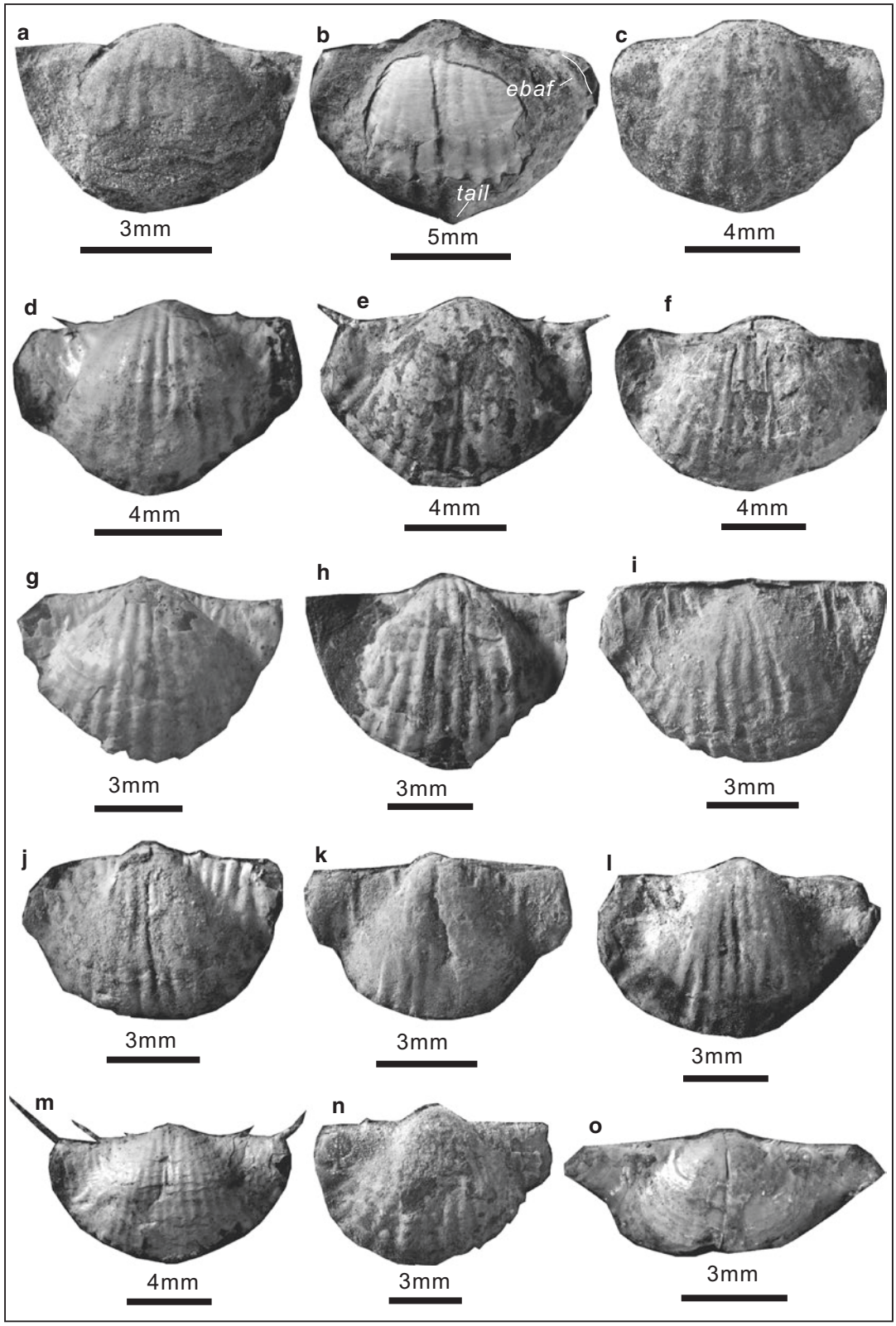
a
3mm
b
ebaf
tail
5mm
c
4mm
d
4mm
e
4mm
f
4mm
g
3mm
h
3mm
i
3mm
j
3mm
k
3mm
l
3mm
m
4mm
n
3mm
o
3mm

Occurrence Changhsingian to the lowest Triassic; South China.

Description Shell 1.4–10.8 mm long and 2.4–14.9 mm wide, semi-orbicular to reversely trapezoid in outline, widest at hingeline; ears slightly inflated, with weak rugae, well differentiated with disk. Ventral valve strongly convex, hillock to roundly triangular in ventral disk; hingespines projecting posterolaterally with an angle of 30–70°; umbo broad, inflated; sulcus absent; costellae beginning from umbo, simple, round and coarse, numbering 4 to 8 per 5 mm nearby anterior margin.

Discussion *Paryphella triquetra* Liao in Zhao et al. (1981, 53, pl. 8, Fig. 18–22) from the Permian–Triassic intervals of South China shares some features with the present species, including a semi-orbicular outline, strongly convex ventral valve, absence of sulcus and usually it is difficult to distinguish between them, and thus we consider *Paryphella triquetra* is a synonym of *Paryphella orbicularis* (Liao, 1980a), as listed by Xu and Grant, 1994. *Paryphella laohushanensis* Wang et al. (1982, 204, pl. 95, Fig. 2) from the Talung Formation, Laohushan, Jiangle, Fujian Province, eastern China also has a semi-orbicular outline and a strongly convex ventral valve, and no sulcus has been observed on disk (despite a broad and shallow sulcus at anterior margin described by Wang). Because of these features, *Paryphella laohushanensis* Wang et al., 1982 has been considered as a synonym of *Paryphella orbicularis* (Liao, 1980a). *Paryphella sinuata* (Chan) of Zhang et al. (2015) (see Fig. 9.18j in this book) and one specimen of *Paryphella elegantula* Zhan of Zhang et al. (2015) (see Fig. 9.18l) are deformed specimens (compressed along midwidth to form a sulcus-shape groove) and apparently can be considered as conspecific with the present species. *Paryphella orbicularis* is distinguished from most other *Paryphella* species in a strongly convex ventral valve and lacking of sulcus (Fig. 9.14).

It is worth noting that the specimens of *Paryphella orbicularis* from the Permian–Triassic transitional beds (equivalent to the intervals yielding Permian–Triassic mixed fauna) of the Daoduishan section, Meishan area are currently the smallest in body size, compared with the Changhsingian specimens of the same species from any other area in South China. Additionally, the specimens from the Changhsingian of Zhongzhai in shallow-water facies are slightly larger than their counterparts from deep-water sections (see Measurements).

Paryphella undata Liao, 1984
Fig. 9.19

1984 *Paryphella sparsiplicata undata* Liao: 281, pl. 2, Fig. 15–17.
2014 *Paryphella undata* Liao; He et al.: 936, pl. 2, Fig. 14y–d′.

Diagnosis Extremely transverse in outline; ears extended, fully covered with coarse rugae; ventral valve weakly convex, disk flat.

Materials Over 20 specimens. Registered specimens: see below.

Fig. 9.17 ***Paryphella orbicularis*** (Liao, 1980a). (**a**), exterior of a complete ventral valve, CM-20-216. (**b**), exterior of a complete ventral valve and part of internal mould of the conjoined dorsal valve, CM-13-205, showing concentric fila on dorsal disk, ear baffles (*ebaf*) and a short tail. (**c**), exterior of a complete ventral valve, CM-13-208. (**d**), exterior of a complete ventral valve, CM-13-212, showing extended ears with rugae, low and rounded costellae. (**e**), exterior of a complete ventral valve, CM-13-231, showing a few preserved hinge spines. (**f**), exterior of a complete ventral valve, CM-4-249. (**g**), exterior of a complete ventral valve, CM-12-203, showing rugae on ears and low, rounded costellae. (**h–k**), exteriors of four complete ventral valves, CM-12-204, CM-10-209, CM-12-219, CM-10-233, showing rugae on ears. (**l**), exterior of a nearly complete ventral valve, CM-10-247, showing occasionally bifurcated costellae. (**m**), exterior of a complete ventral valve, CM-10-254, showing preserved hinge spines, low costellae and weak concentric lines. (**n**), exterior of an incomplete ventral valve, CM-13-201. (**o**), internal mould of an incomplete ventral valve and shell remnant, CM-12-194, showing extended ears

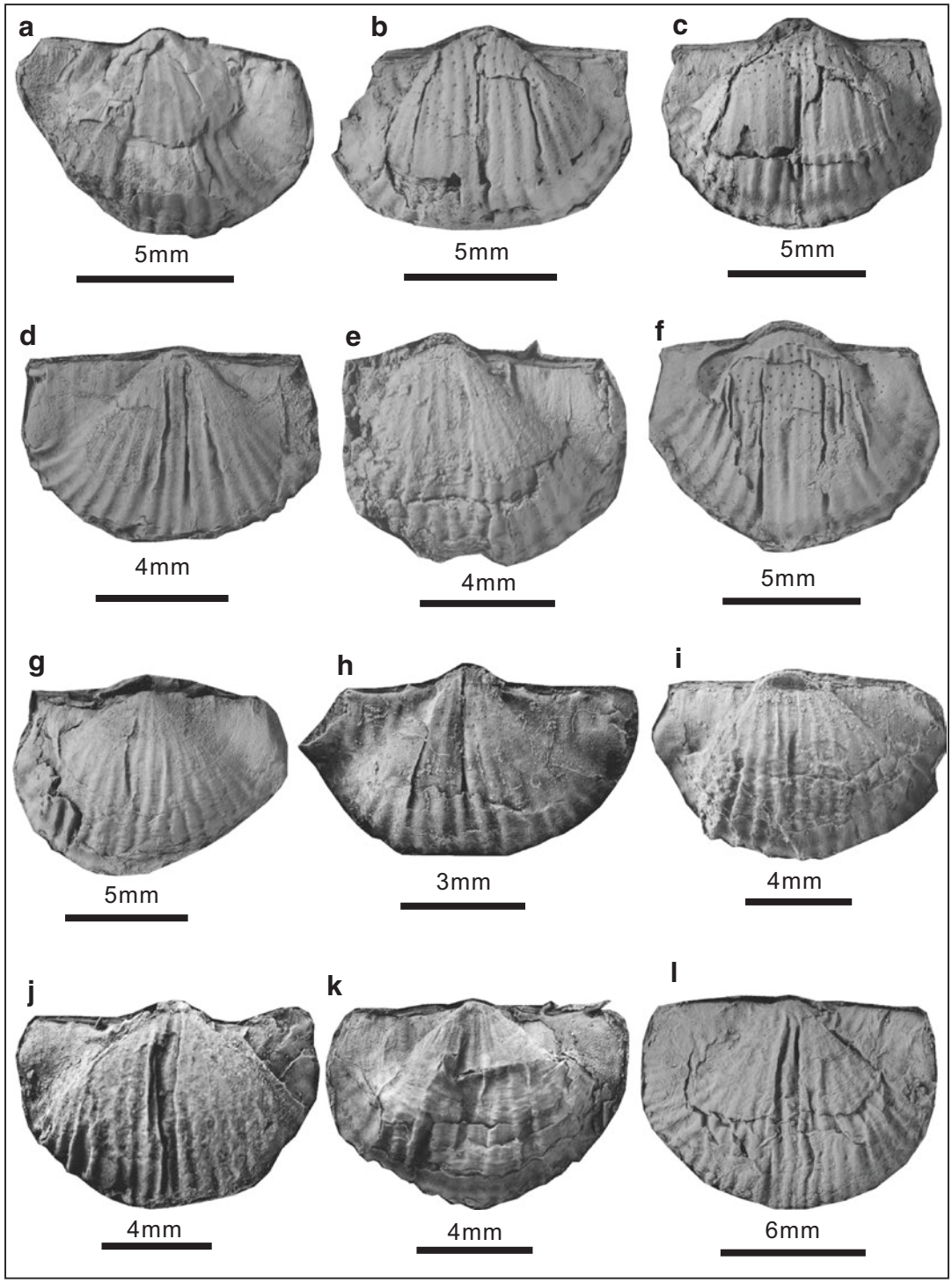

Fig. 9.18 ***Paryphella orbicularis*** (Liao 1980a). (**a**), exterior of a deformed ventral valve, LZ2702676. (**b**), internal mould of an incomplete ventral valve and shell remnant, LZ2702646, showing radially-arranged papillae. (**c**), internal mould of a complete ventral valve and shell remnant, LZ2702677. (**d**), exterior of a slightly deformed ventral valve, LZ2702653, showing simple costellae. (**e**), exterior of an incomplete ventral valve, LZ2704668,

Measurements (mm):

Number	Width	Length	Width/length	Notes
CM-6-266	9.79	5.74	1.70	Ventral exterior
CM-4-258	7.85	4.26	1.84	External mould of dorsal valve
CM-3-268	11.13	5.81	1.92	Internal mould of ventral valve
CM-3-269	7.11	3.35	2.12	Ventral exterior
CM-3-270	12.95	7.11	1.82	External mould of dorsal valve
CM10-0551	9.81	4.91	2.00	External mould of dorsal valve
CM2-0548	8.80	3.17	2.78	Ventral exterior
CM-4-259	7.80	4.00	1.95	Internal mould of dorsal valve
CM2-0549	6.98	2.76	2.53	Ventral exterior
DDS27-2-0555	3.18	1.76	1.81	Dorsal interior (juvenile)
CM2-0550	7.76	3.83	2.03	Dorsal interior
CM10-0553	7.73	4.00	1.93	External mould of dorsal valve
DDS27-2-0552	5.79	2.93	1.98	Ventral exterior
CM2-0547	6.92	3.59	1.93	Ventral interior

Occurrence Changhsingian and lowest Triassic; Anhui (Majiashan section) and Zhejiang (Daoduishan section) of South China.

Description Shell 1.8–7.1 mm long and 3.2–13.0 mm wide, extremely transverse in outline; widest at hingeline; ears large and extended, slightly inflated, fully covered with uneven, coarse rugae, well differentiated with disk. Ventral valve weakly convex; ventral disk elevated but flat, triangular in shape; beak small, straight, slightly over hingeline; umbo flat, with an angle of 70–90° posteriorly; sulcus absent; costellae beginning from umbo, simple and coarse, numbering 7 to 8 per 5 mm near anterior margin. Dorsal valve slightly concave; dorsal disk triangular; umbo flat, moderately wide; costellae numbering 7 per 5 mm. Dorsal interior with a simple cardinal process (marked by *cp* in Fig. 9.19h), a median ridge long, extending anteriorly beyond midlength (marked by *mr* in Fig. 9.19h); endospines sparse, covering mainly muscle-scar area.

Discussion The present species is more or less similar to *Paryphella sparsiplicata* Liao (1984, p. 280, pl. 2, Fig. 9) from the Permian–Triassic transitional beds of Meishan, Zhejiang Province, South China in a weakly convex ventral valve, flat ventral disk and absence of ventral sulcus, but its extended ears and a higher shell width to length ratio separate the two species (Fig. 9.14). Compared with other species of *Paryphella*, *Paryphella undata* differs by its transversely quadrate outline (Fig. 9.14), a flat ventral disk and more rugae on ears.

It is noted that the specimens (with prefix of DDS) from the lowest Triassic in the moderately deep-water Daoduishan section seems to be smaller than those (with prefix of CM) from the Changhsingian in the deep-water Majiashan section in South China (see Measurements).

Fig. 9. 18 (continued) showing concentric fila when outer layer of shell decorticated. (**f**), internal mould of a complete but deformed ventral valve and shell remnant, LZ2702645, showing radially-arranged papillae. (**g**), an incomplete ventral valve, LZ2702651, showing concentric fila when outer layer of shell decorticated. (**h**), internal mould of a nearly complete ventral valve and shell remnant, LZ2701155, showing papillae. (**i**), exterior of a nearly complete ventral valve, LZ2705531. (**j**), exterior of a complete but deformed ventral valve, LZ2706170, showing simple costellae. (**k**), exterior of a complete and slightly deformed ventral valve, LZ2704160, showing concentric fila and hinge spines. (**l**), external mould of a complete dorsal valve and shell remnant of the conjoined ventral valve, LZ2702644, showing rugae on ears

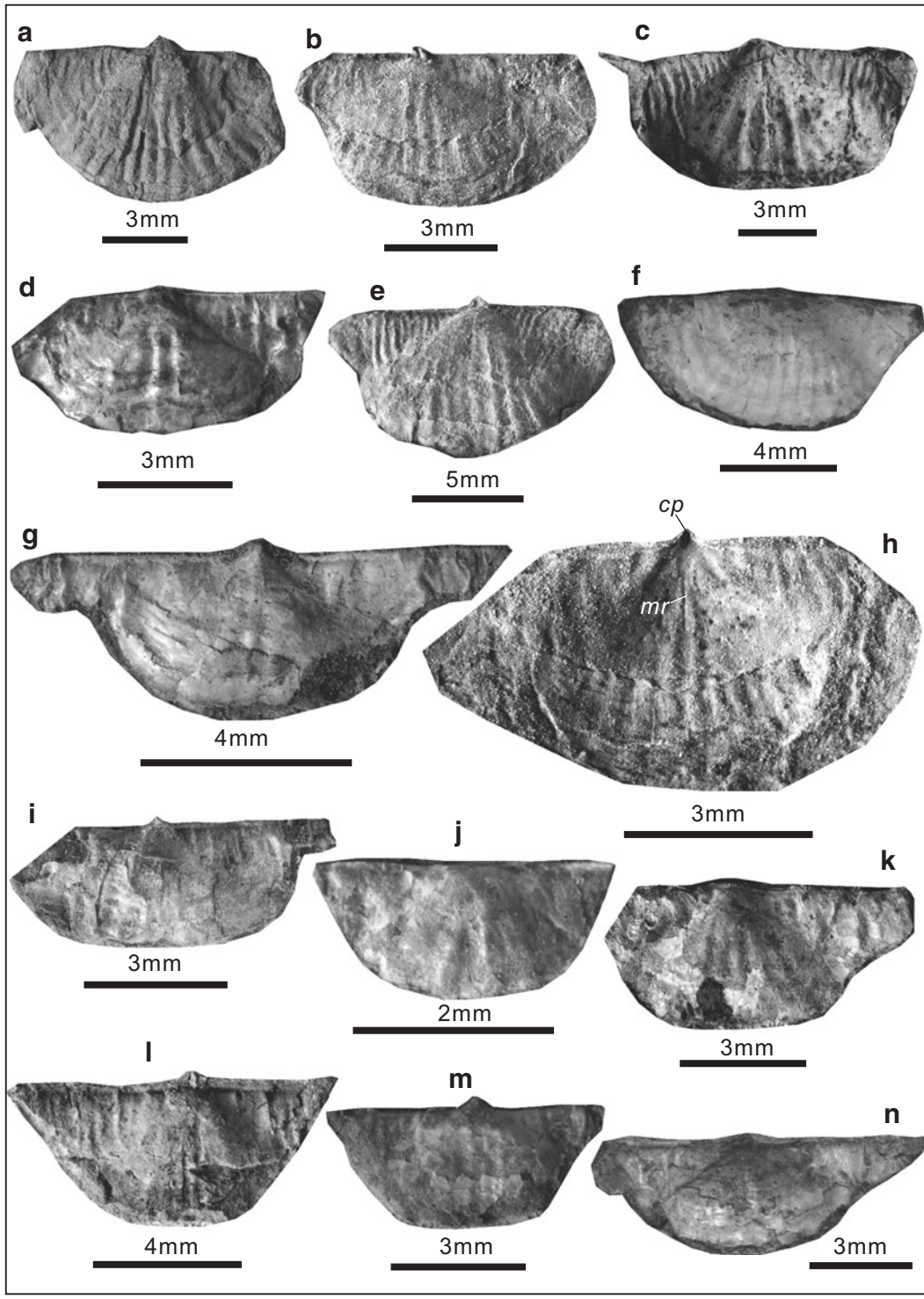

Fig. 9.19 ***Paryphella undata*** Liao, 1984. (**a**), exterior of an incomplete ventral valve, CM-6-266, showing rugae on ears. (**b**), external mould of a nearly complete dorsal valve, CM-4-258. (**c**), internal mould of a complete ventral valve, CM-3-268, showing dense and prominent rugae on ears. (**d**), exterior of an incomplete ventral valve, CM-3-269, showing dense and prominent rugae on ears. (**e**), external mould of a nearly complete dorsal valve, CM-3-270, showing dense rugae on ears. (**f**), external mould of a complete dorsal valve and shell remnant,

Paryphella sparsiplicata Liao, 1984
Fig. 9.20

1984 *Paryphella sparsiplicata* Liao: 280, pl. 2, Fig. 6–8.
2014 *Paryphella majiashanensis* He and Shi in He et al.: 937, Fig. 16k–t.

Diagnosis Subquadrate in outline, ventral valve weakly to moderately convex, ventral umbo slightly convex, ears flat, weakly differentiated from disk, costellae sparse, mainly covering middle part of valves, weak at flanks.

Materials Over 80 specimens. Registered specimens: see below.

Measurements (mm):

Number	Width	Length	Width/length	Notes
CM-4-257	6.25	4.61	1.36	Ventral exterior
CM-4-265	5.77	3.55	1.63	Ventral exterior
CM-4-264	6.01	3.99	1.51	Ventral exterior
CM-4-261	7.93	4.65	1.71	Ventral exterior
CM-4-262	6.23	3.92	1.59	Ventral exterior
CM-10-255	9.95	6.45	1.54	Ventral exterior
CM-4-263	2.98	2.07	1.44	Ventral exterior
CM-4-244	7.21	4.31	1.67	Ventral exterior
CM-10-202	7.29	4.49	1.62	External mould of dorsal valve
DDS26-0568	4.53	3.54	1.28	Ventral exterior
DDS27-1-0567	3.86	2.63	1.47	Ventral exterior
CM9-0559	7.51	4.65	1.62	Ventral exterior
HZS19-0557	5.36	3.51	1.53	Ventral exterior
DDS26-0560	3.58	2.55	1.40	Ventral exterior
DDS27-2-0563	2.67	2.10	1.27	Ventral exterior

Occurrence Changhsingian and lowest Triassic; Anhui (Majiashan section) and Zhejiang (Huangzhishan and Daoduishan sections) of South China.

Description Shell 2.1–6.5 mm long and 2.7–10.0 mm wide, subquadrate in outline, widest at hingeline. Ventral valve weakly to moderately convex; ventral disk nearly flat; beak straight, slightly over hingeline; umbo weakly convex; hingespines projecting vertical to hingeline on juvenile specimens, but generally projecting posterolaterally with an angle of 35–70° on larger adult specimens; cardinal extremities with an angle of about 90°; ears flat or slightly inflated, triangular, weakly differentiated from ventral disk, sulcus absent; costellae beginning from anterior of umbo, simple and coarse, 5 to 9 (commonly 6) costellae covering median portion of valves, weak or absent on flanks of valves. Dorsal valve weakly concave; ears large, flat, weakly differentiated from flanks of ventral disk; fold absent. Concentric microornaments occasionally visible.

Discussion The present species is similar to *Paryphella jianshiensis* (Wang, 1984) from the Talung Formation of Jianshi, Hubei Province, South China in a subquadrate outline, a weakly convex ventral valve and absence of sulcus, but the latter has more costellae (15 costellae). *Paryphella sparsiplicata* can be distinguished with *P. orbicularis* (Liao, 1980a, p. 261, pl. 6, Fig. 1–4) in a weakly or moderately convex ventral valve, slightly convex ventral umbo and sparse costellae. One specimen of *Paryphella sparsiplicata* Liao (1984, p. 280, pl. 2, Fig. 9) has a reversely trapezoid outline, a strongly convex ventral valve and lacks sulcus, suggesting that it may not belong to *Paryphella sparsiplicata*, but rather, conspecific with *Paryphella orbicularis* (see above).

It is note worthy that the specimens from the lowest Triassic in deep to moderately deep waters seem to be smaller than those from the Changhsingian in the deep-water Majiashan section (see Measurements).

Fig. 9. 19 (continued) CM10-0551, showing low costellae. (**g**), exterior of a nearly complete ventral valve, CM2-0548, showing extended ears with rugae and a small, straight beak. (**h**), internal mould of a nearly complete dorsal valve, CM-4-259, showing a simple cardinal process (*cp*) and a median ridge (*mr*). (**i**), exterior of an incomplete ventral valve, CM2-0549, showing extended ears with dense rugae. (**j**), interior of a complete dorsal valve (juvenile, outer layer of shell decorticated), DDS27-2-0555. (**k**), interior of an incomplete dorsal valve, CM2-0550, showing extended ears fully covered with rugae. (**l**), external mould of an incomplete dorsal valve, CM10-0553, showing sparse costellae and rugae on ears. (**m**), exterior of an incomplete ventral valve, DDS27-2-0552. (**n**), interior of a nearly complete ventral valve, CM2-0547, showing extended ears

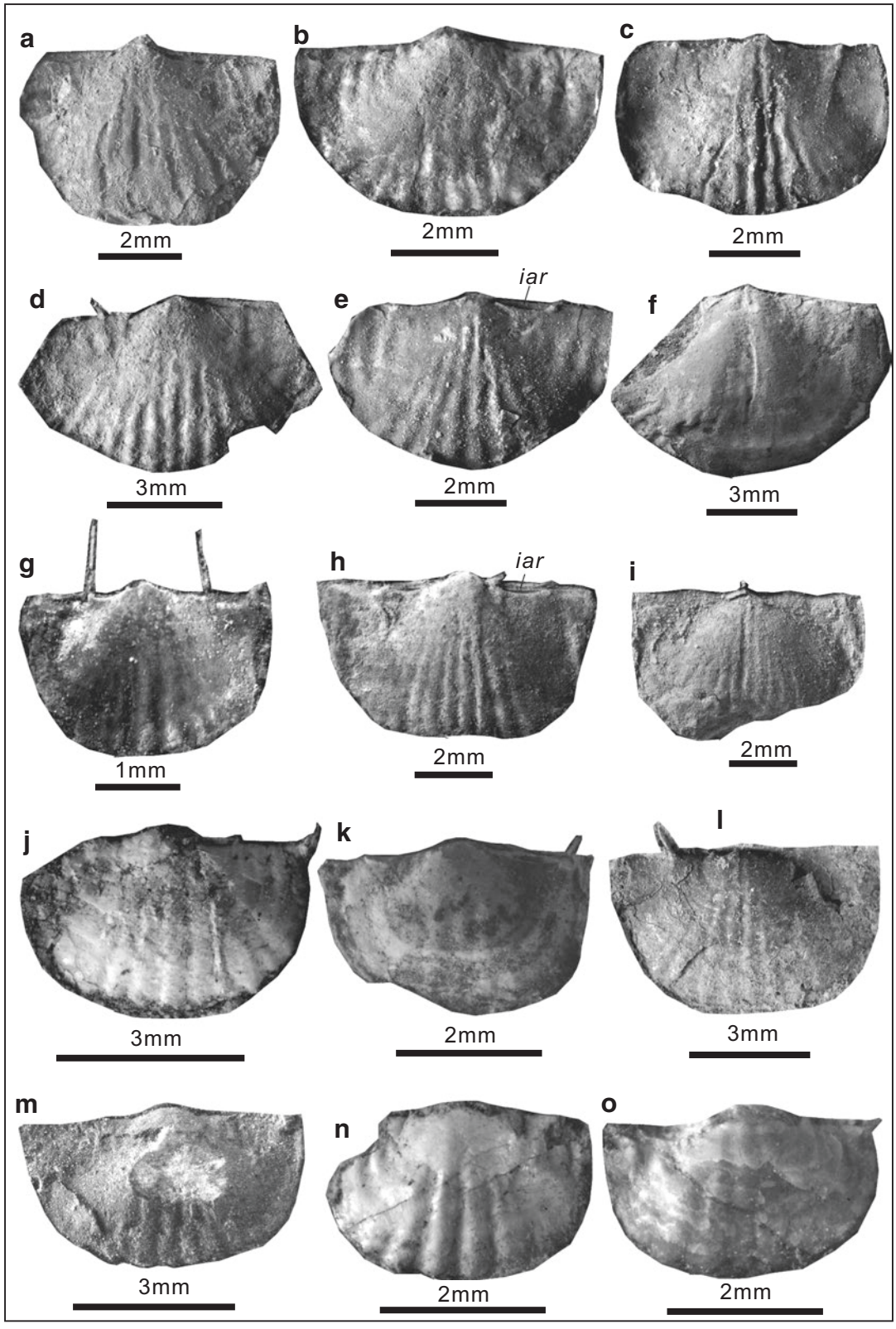
a
2mm
b
2mm
c
2mm
d
3mm
e
iar
2mm
f
3mm
g
1mm
h
iar
2mm
i
2mm
j
3mm
k
2mm
l
3mm
m
3mm
n
2mm
o
2mm

Paryphella corculum (Liao, 1980a)
Fig. 9.21

1980a *Cathaysia corculum* Liao: 260, pl. 6, Fig. 38–41.
1982 *Paryphella transversa* Liao in Wang et al.: 205, pl. 95, Fig. 1.
1989 *Paryphella elegantula* Zhan in Li et al.: 206, pl. 25, Fig. 6, 7, 12, 17, 22.
2015 *Paryphella acutala* Zhang et al.: Figs. 4ab, 6a–m.

Diagnosis (emended). Medium shell size for the genus; reversely trapezoid to rounded pentagonal outline; maximum width at hingeline. Ventral valve strongly convex, groove separated disk from ears, geniculate anteriorly; cardinal extremities acute; sulcus weak or indistinct; dorsal median ridge low, long and thin.

Materials 16 specimens. Registered specimens: see below.

Measurements (mm):

Number	Width	Length	Width/length	Notes
LZ2702168	14.63	9.67	1.51	Ventral exterior
LZ2702675	14.72	10.13	1.45	Ventral exterior
LZ2703169	13.55	9.85	1.38	Ventral exterior
LZ2702650	17.54	10.12	1.73	Ventral exterior
LZ2705534	14.12	10.04	1.41	Ventral exterior
LZ2702673	14.39	9.56	1.50	Ventral exterior
LZ2702672	15.63	8.51	1.84	Ventral exterior
LZ2702163	15.50	10.26	1.51	Ventral exterior
LZ2702656	14.19	9.38	1.51	Internal mould of ventral valve

Occurrence Wujiapingian–Changhsingian; Guizhou, Sichuan and Fujian Provinces, China.

Description Shell 8.5–10.3 mm long and 13.6–17.5 wide; reverse trapezoidal in outline, greatest width at hingeline. Ventral valve strongly convex, ventral disk triangularly hillock; geniculate along disk margin; a groove separating disk from lateral and even anterior margins (or geniculate); beak low, swollen and slightly beyond hingeline; cardinal extremities acute; ears slightly convex, incurved to form ear baffles, covered with weak rugae, and ear baffles (*ebaf*) connected with geniculate (*geni*) to form a skirt-shaped margin (Fig. 9.21b, c, h); sulcus weak or absent; tail variablely developed at middle of anterior margin. Dorsal valve gently concave; fold indistinct. Costellae beginning from anterior of umbo, coarse, occasionally increasing anteriorly by intercalation, numbering 6–8 per 5 mm at anterior margin. Endospines on both valves, becoming larger anteriorly in size, 10–15 per mm^2 at midvalve and 2–3 per mm^2 at anterior; dorsal interior with a low, long and thin median ridge (about half of shell length), and with hook-like brachial ridges.

Discussion This species is more or less similar to *Parachonetella zhongensis* Liao, 1980a from the Lungtan Formation of Zhongying, Guizhou Province in the presence of a tail and a groove between disk and ears, but the tail and groove in the present species are variable, suggesting it may represent a transitional species beween the two genera. Within *Paryphella*, the present species is most like *Paryphella geniculata* Zhan in Li

Fig. 9.20 ***Paryphella sparsiplicata*** Liao, 1984. (**a**), exterior of a nearly complete ventral valve, CM-4-257, showing sparse and weak costellae. (**b**), exterior of a complete ventral valve, CM-4-265, showing sparse costellae and rugae on ears. (**c**), exterior of a nearly complete ventral valve, CM-4-264. (**d**), exterior of an incomplete ventral valve, CM-4-261, showing sparse costellae and weak rugae on ears. (**e**), exterior of a nearly complete ventral valve, CM-4-262, showing a linear interarea (*iar*). (**f**), exterior of an incomplete ventral valve, CM-10-255. (**g**), exterior of a complete ventral valve, CM-4-263, showing sparse and weak costellae and two preserved hinge spines. (**h**), exterior of a complete ventral valve, CM-4-244, showing a linear interarea (*iar*). (**i**), external mould of an incomplete dorsal valve, CM-10-202. (**j**), exterior of a nearly complete ventral valve, DDS26-0568, showing sparse, rounded costellae and a preserved hinge spine. (**k**), exterior of a nearly complete ventral valve, DDS27-1-0567, showing sparse and weak costellae. (**l**), exterior of a complete ventral valve, CM9-0559, showing weak costae and a preserved hinge spine. (**m**), exterior of a complete ventral valve, HZS19-0557, showing weak costae. (**n**), exterior of a nearly complete ventral valve, DDS26-0560, showing weak costae and rugae on ears. (**o**), exterior of a complete ventral valve, DDS27-2-0563, showing weak costae

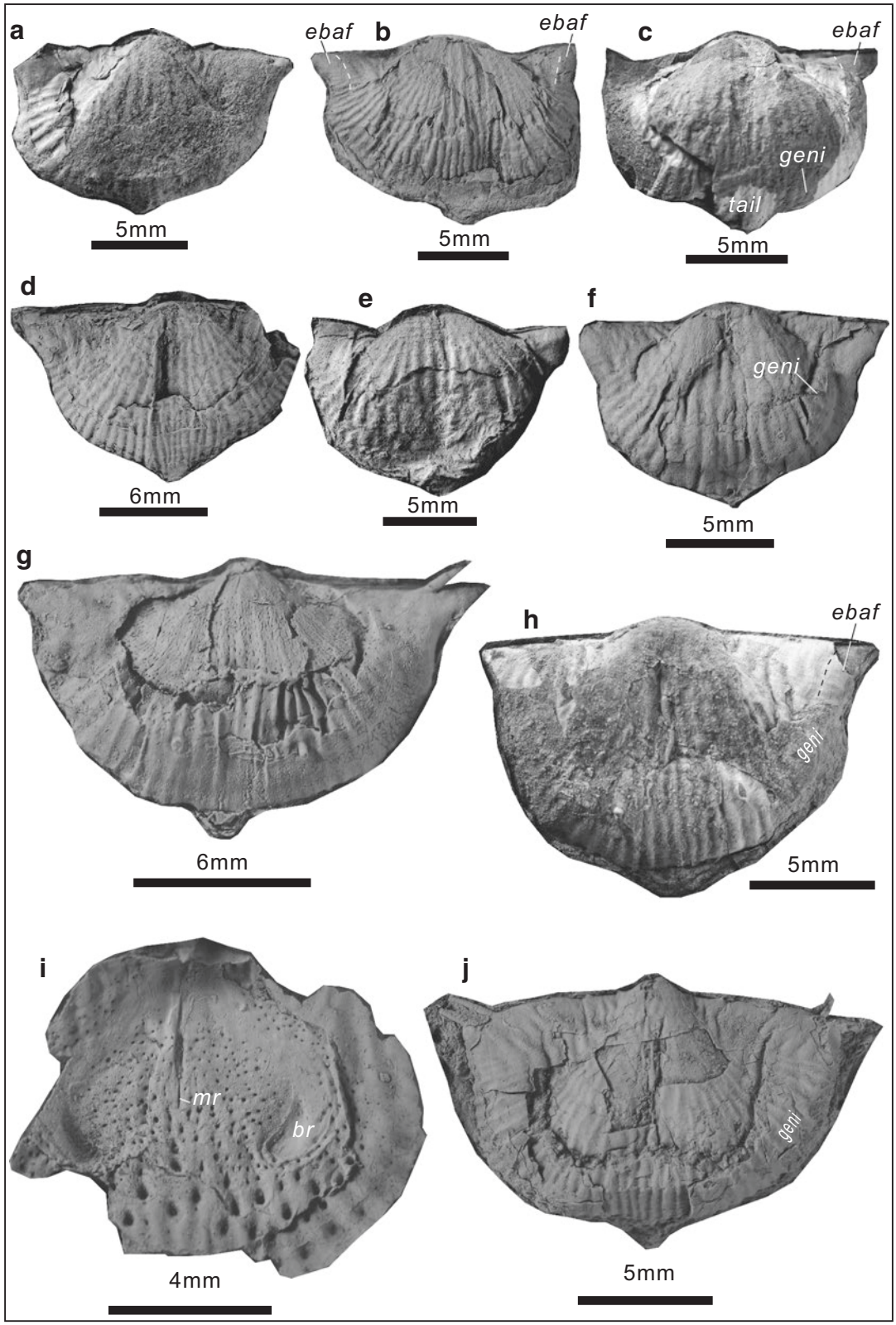
a
b
ebaf
ebaf
c
ebaf
geni
tail
5mm
5mm
5mm
d
e
f
geni
6mm
5mm
5mm
g
h
ebaf
geni
6mm
5mm
i
j
mr
br
geni
4mm
5mm

et al., 1989 from the Talung Formation, Shangsi, Sichuan Province, China in its strongly convex ventral valve with a prominent geniculation, but the latter has convergent costellae nearby the midwidth. *Paryphella nasuta* Liao, 1984 from lowest Triassic of Yixing, Jiangsu Province, South China shares with *Paryphella corculum* a number of features, including the presence of a tail (probably not preserved on the holotype but visible on our specimens) and ear baffles, but they differ in the latter having a prominent geniculation and curved grooves between ears and disk (Fig. 9.14).

Paryphella sp.
Fig. 9.22

Materials Over 100 specimens. Registered specimens: see below.

Measurements (mm):

Number	Width	Length	Width/ length	Notes
HZS20-0574	14.83	9.02	1.64	Ventral exterior
HZS22-0575	12.38	7.81	1.59	Ventral exterior
HZS20-0576	14.40	8.74	1.65	Ventral exterior
HZS27-0577	12.64	8.89	1.42	Ventral exterior
HZS20-0578	13.51	8.60	1.57	Ventral exterior
HZS23-0580	13.04	9.62	1.36	Ventral exterior
HZS20-0582	13.77	8.62	1.60	Ventral exterior
HZS20-0583	10.54	7.12	1.48	Ventral exterior
HZS24-0585	12.62	6.87	1.84	Ventral exterior
HZS20-0587	15.60	8.00	1.95	Ventral exterior
HZS23-0588	13.44	7.95	1.69	Ventral exterior
HZS24-0590	12.19	8.64	1.41	Ventral exterior
HZS24-0584	13.01	8.01	1.62	Ventral exterior
HZS23-0586	13.17	9.24	1.43	Internal mould of ventral valve

Occurrence Lower Yinkeng Formation (uppermost Changhsingian); Zhejiang (Huangzhishan section) of South China.

Description Shell 4.2–9.6 mm long and 10.5–15.6 mm wide, transversely tubulose in outline; widest at hingeline. Ventral ears gently convex, 5–9 coarse rugae, weakly differentiated from visceral disk; ventral valve strongly, evenly convex in latitudinal profile; costellae obscure to weak, simple, numbering 6 per 3 mm at anterior; cardinal extremities with a cardinal angle of about 60° on well-preserved specimens; trail variably developed.

Discussion The present species differs from *Paryphella corculum* Liao, 1980a from the Wujiapingian, Zhijin, Guizhou Province, southwestern China because the latter has more distinct costellae and an geniculation close to the anterior margin. This unnamed species differs from all other *Paryphell*a species in its very weak ornamentation and an evenly convex ventral valve in latitudinal profile.

Chonetella Waagen, 1884

Type Species *Chonetella nasuta* Waagen, 1884. Permian; Khisor Range, Pakistan.

Diagnosis Subcircular to transverse chonetiform, strongly nasute outline; ribbing absent or weak; spines extend posterolaterally from hingeline, but absent from flanks and venter; cardinal process long, but narrow; lateral ridges divegent from hinge, long brachial ridges boardered anteriorly by strong endospines.

Fig. 9.21 ***Paryphella corculum*** (Liao, 1980a). (**a**), exterior of a complete ventral valve (shell partly decorticated), LZ2702168. (**b**), exterior of a complete ventral valve, LZ2702675, showing numerous bifurcated costellae, ear baffles (*ebaf*). (**c**), exterior of a complete ventral valve, LZ2703169, showing ear baffles (*ebaf*), a geniculation (*geni*) and a short tail. (**d**), exterior of an incomplete ventral valve (shell partly decorticated), LZ2702650, showing extended ears. (**e**), exterior of a nearly complete ventral valve (shell partly decorticated), LZ2705534. (**f**), exterior of a complete ventral valve (shell on disk partly decorticated), LZ2702673, showing a geniculation (*geni*). (**g**), exterior of a complete ventral valve (shell on disk decorticated), LZ2702672, showing a geniculation (*geni*) and radially-arranged papillae. (**h**), exterior of a complete ventral valve, LZ2702163, showing ear baffles (*ebaf*) and a geniculation (*geni*). (**i**), internal mould of an incomplete dorsal valve, LZ2702671, showing a median ridge (*mr*) and a pair of brachial ridges (*br*). (**j**), internal mould of a complete ventral valve, LZ2702656, showing a geniculation (*geni*) and rugae on ears

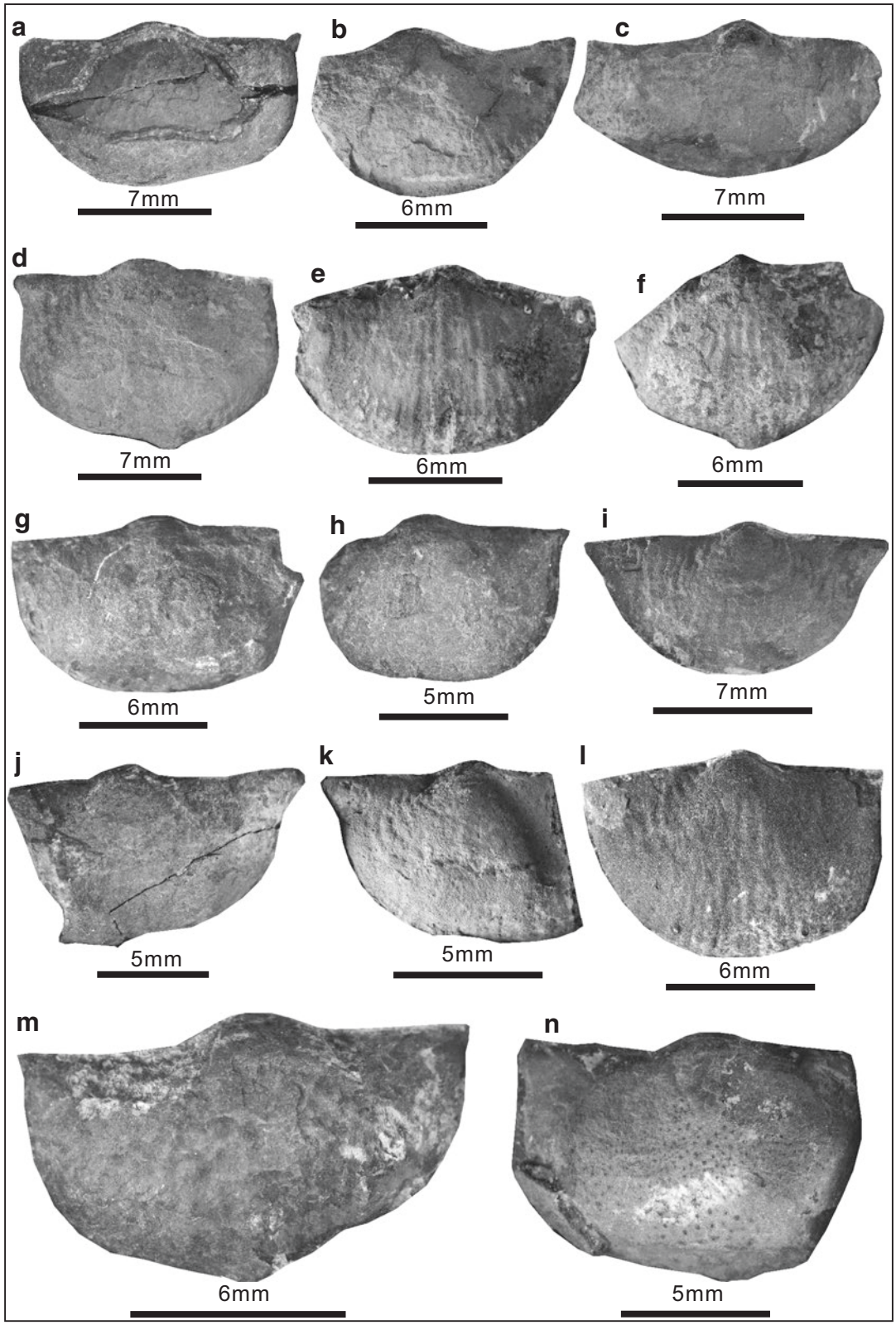
a
7mm
b
6mm
c
7mm
d
7mm
e
6mm
f
6mm
g
6mm
h
5mm
i
7mm
j
5mm
k
5mm
l
6mm
m
6mm
n
5mm

Discussion *Chonetella* Waagen, 1884 is similar to *Paryphella* Liao in Zhao et al., 1981 in a chonetiform outline and the presence of ear baffles (sometimes called as ear-curtain for *Paryphella*), but the former generally has weak ribbing and has no rugae on ears. *Bibatiola* Grant, 1976 from the Lower Permian, Thailand and *Chonetella* share a chonetiform outline and a ribbing pattern, but the former has spines scattered on flanks and venter.

Chonetella sp.
Fig. 9.13n

Material One specimen: CM-14-0517.

Occurrence Changhsingian; Anhui (Majiashan section) of South China.

Description Shell 8.8 mm long and 10.9 mm wide, semicircle in outline; widest at hinge; ears slightly convex, incurved to ear baffles (marked by *ebaf*, see Fig. 9.13n), well differentiated with disk; two pairs of spines at hinge. Ventral valve strongely convex; elevated ventral disk triangular hillock in shape; geniculate nearby anterior part; tail short but prominent; ribbing beginning from umbo, simple, round, numbering 6 per 5 mm near anterior margin.

Discussion This single specimen is similar to the type species *Chonetella nasuta* Waagen, 1884 from the Permian of Khisor Range, Pakistan in a subcircular outline, but it has been slightly deformed; and the absence of a dorsal valve also prevents a more precise identification.

Genus ***Haydenella*** Reed, 1944

Type Species *Productus kiangsiensis* Kayser, 1883. Permian Productus Limestone; Salt Range, Pakistan.

Diagnosis Medium-sized; semi-globose outline; ribbing weak, absent at umbo; rugae only on ears; spines separate disk from posterior ear region, thin spines scattered on ventral disk; marginal ridges absent.

Discussion *Haydenella* Reed, 1944 differs from *Paryphella* Liao in Zhao et al., 1981 in possessing a slightly acute beak and weaker costellae.

Haydenella kiangsiensis (Kayser, 1883)
Fig. 9.23

1883 *Productus kiangsiensis* Kayser: 185, pl. 26, Fig. 6–11.
1932 *Linoproductus kiangsiensis* (Kayser); Huang: 46, pl. 3, Fig. 13–15.
1978 *Haydenella kiangsiensis* (Kayser); Tong: 223, pl. 79, Fig. 10.
1979 *Haydenella kiangsiensis wenganensis* (Huang); Zhan in Hou et al.: 81, pl. 5, Fig. 1–2.
1984 *Haydenella kiangsiensis* (Kayser); Yang in Feng et al.: 218, pl. 33, Fig. 9.
1987 *Haydenella kiangsiensis* (Kayser); Xu in Yang et al.: 223, pl. 10, Fig. 26; pl. 11, Fig. 1, 5, 6.
1990 *Haydenella kiangsiensis* (Kayser); Zhu: 68, pl. 17, Fig. 16–17.

Fig. 9.22 ***Paryphella*** sp.. (**a**), exterior of a complete ventral valve and one part of internal mould of the conjoined dorsal valve (ventral shell partly decorticated), HZS20-0574, showing thick shell and weak costellae on dorsal valve. (**b**), exterior of an incomplete ventral valve, HZS22-0575. (**c**), exterior of an incomplete ventral valve, HZS20-0576, showing a strongly convex (transversal tub-like) valve. (**d**), exterior of a complete ventral valve, HZS27-0577, showing rugae on ears and nearly smooth on disk. (**e**), exterior of a nearly complete ventral valve, HZS20-0578, showing obscure costellae. (**f**), exterior of an incomplete ventral valve, HZS23-0580, showing obscure costellae. (**g**, **h**), exteriors of two nearly complete ventral valves, HZS20-0582, HZS20-0583, showing nearly smooth (obscure) on shell surface. (**i**), exterior of a complete ventral valve, HZS24-0585, showing rugae on ears. (**j**), exterior of a nearly complete ventral valve, HZS20-0587. (**k**), exterior of an incomplete ventral valve, HZS23-0588, showing rugae on ears. (**l**), exterior of a complete ventral valve, HZS24-0590, showing weak rugae on ears and obscure costellae. (**m**), ventral exterior, HZS24-0584, showing a strongly convex (transversal tub-like) valve. (**n**), internal mould of an incomplete ventral valve, HZS23-0586, showing papillae on the surface

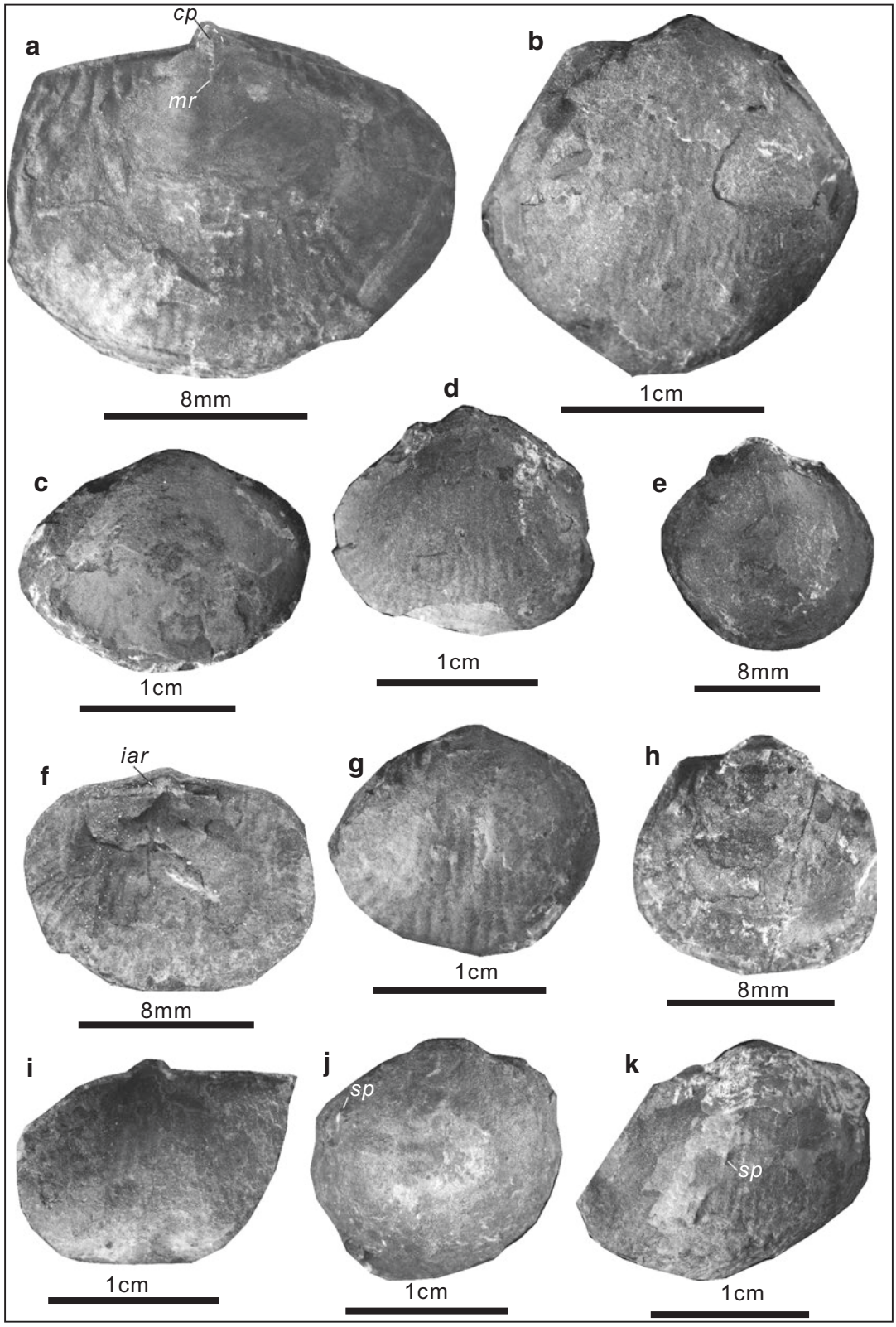
a
cp
mr
8mm
b
1cm
c
1cm
d
1cm
e
8mm
f
iar
8mm
g
1cm
h
8mm
i
1cm
j
sp
1cm
k
sp
1cm

Materials 15 specimens. Registered specimens: see below.

Measurements (mm):

Number	Width	Length	Width/ length	Notes
HZS25-0606	17.20	13.97	1.23	Ventral exterior
HZS24-0611	17.54	17.66	0.99	Ventral exterior
HZS24-0607	17.70	14.36	1.23	Ventral exterior
HZS27-0608	15.72	14.41	1.09	Ventral exterior
HZS24-0609	15.21	13.99	1.09	Ventral exterior
HZS19-0616	14.54	10.46	1.39	Dorsal exterior
HZS24-0612	16.86	14.73	1.14	Ventral exterior
HZS27-0613	12.06	11.03	1.09	Ventral exterior
HZS25-0618	14.61	10.03	1.46	Ventral exterior
HZS24-0615	15.85	15.96	0.99	Ventral exterior
HZS24-0617	16.89	15.42	1.10	Ventral exterior

Occurrence Permian; South China, Pakistan.

Description Medium size, 10.0–17.7 mm long and 12.1–17.7 mm wide, semi-globose in outline, widest at shell midlength. Ventral beak slightly acute and incurved, overhanging hingeline; interarea (*iar*) low (Fig. 23f); ears small, flat, with distinct rugae, well differentiated from visceral disk; cardinal extremities obtuse; ventral valve strongly and evenly convex; geniculate and marginal ridge absent; no median sulcus; trail variably developed at anterior. Dorsal valve moderately and evenly concave. Ribbing weak; spines scattered on ventral disk. Dorsal inerior with a simple cardinal process (marked by *cp* in Fig. 9.23a) and a short median ridge (marked by *mr* in Fig. 9.23a).

Discussion This species is most like *Haydenella chianensis* (Chao, 1927) from the Permian of Susong, Anhui Province in a semi-globose outline, but the latter has a wider and more convex umbo, and prominent costellae. *Haydenella kiangsiensis* (Kayser) of Wang et al. (1982, pl. 91, Fig. 15) from the Lungtan Formation of Jingxian, Anhui Province has a medium size and a strongly convex umbo, more similar to *Haydenella chianensis* (Chao, 1927) from the Permian of Susong, Anhui Province. Thus, owing to these comparisons, *Haydenella kiangsiensis* (Kayser) of Wang et al. (1982) is here considered synonymous with *Haydenella chianensis* (Chao, 1927). *Haydenella subextensa* Chan in Hou et al., 1979 from the Wangpanli Formation (Wuchiapingian) of Damaikong, Lian County, Guangdong Province and *Haydenella longyanensis* Zhu, 1990 from the Tongziyan Formation of Fujian Province, eastern China are both more transverse in outline than *Haydenella kiangsiensis*. *Haydenella wenganensis* (Huang, 1932) from the Lungtan Formation of Wengan, Guizhou Province, southwestern China has coarser and more prominent costellae, when compared to *Haydenella kiangsiensis*. The present species differs from *H. deminuta* Liao, 1980a of the Lungtan Formation of Zhongying, Qinglong County, Guizhou Province in the latter having a moderately convex, narrower umbo and weaker ribbing, and differs from *H. elongata* Liao, 1980a of the Lungtan Formation of Jiaozishan, Anhui City, Guizhou Province as the latter has a longitudinal ovate shell and weaker ribbing.

Fig. 9.23 ***Haydenella kiangsiensis*** (Kayser, 1883). (**a**), exterior of an incomplete ventral valve and posterior part of internal mould of the conjoined dorsal valve, HZS25-0606, showing a cardinal process (*cp*), a short median ridge (*mr*), prominent rugae on ears and weak ribbing on dorsal valve. (**b**), exterior of an incomplete ventral valve, HZS24-0611, showing weak ribbing and coarse spines on the shell surface. (**c**), exterior of an incomplete ventral valve, HZS24-0607, showing nearly smooth shell. (**d**), exterior of an incomplete ventral valve, HZS27-0608, showing weak ribbing and spine bases on the shell surface. (**e**), exterior of an incomplete ventral valve (shell partly decorticated), HZS24-0609. (**f**), exterior of a nearly complete dorsal valve and posterior part of the conjoined ventral valve (dorsal view), HZS19-0616, showing a low interarea (*iar*). (**g**), exterior of an incomplete ventral valve, HZS24-0612, showing weak ribbing. (**h**), exterior of an incomplete ventral valve, HZS27-0613. (**i**), external mould of an incomplete ventral valve, HZS25-0618, showing weak ribbing. (**j**), exterior of an incomplete ventral valve, HZS24-0615, showing a preserved coarse spine base on flank (*sp*). (**k**), exterior of an incomplete, deformed ventral valve, HZS24-0617, showing a preserved spine on disk (*sp*)

Suborder **Strophalosiidina** Schuchert, 1913
Superfamily **Strophalosioidea** Schuchert, 1913
Family **Chonopectidae** Muir-Wood and Cooper, 1960
Genus ***Eileenella*** Racheboeuf in Wongwanich et al., 2004 [The name of genus *Eileenella* will be replaced by a new name in the near future, because of homonym (*Eileenella* had been used for an insect genus)]

Type Species *Eileenella elegans* Racheboeuf in Wongwanich et al., 2004. Carboniferous; Satun Province, southern Thailand.

Diagnosis Leptaenid-like geniculate shells with faint concentric, lamellose growth lines; ventral and dorsal disks almost flat; rounded peripheral ridge bearing a row of stubby, flattened spiny tubercles projecting anterolaterally; ventral valve interior with well-developed diductor muscle field divided by a thin median septum; dorsal interior with a cardinal process; thin, broadly lobate peripheral ridges parallel to the margin of the disk and bending posteriorly medianly.

?Eileenella semicircridge **(**He et al., 2005)
Fig. 9.24

2005 *Spinomarginifera semicircridge* He et al.: 933, Fig. 5.12–5.18.
2014 *Spinomarginifera semicircridge* He et al.: 939, Fig. 17c–i.

Diagnosis (emended). Small, leptaenid-like shells, a pair of ear-shaped adductor scars divided by a short median septum, coarse endospines present in front of adductor scars and a median septum in ventral interior; a pair of circular brachial ridges, coarse endospines around brachial ridges, a pair of thin, broadly lobate peripheral ridges parallel to the margin of the disk and curved posteriorly at midwidth in dorsal interior.

Materials Over 80 specimens. Registered specimens: see below.

Measurements (mm):

Number	Width	Length	Width/ length	Notes
DP9602	5.27	3.19	1.65	External mould of dorsal valve
DP-10-307	6.87	3.82	1.80	External mould of dorsal valve
DP1-0194	6.98	4.12	1.69	External mould of dorsal valve
DP9603	5.32	3.06	1.74	Internal mould of ventral valve
DP9401	6.96	3.37	2.07	Internal mould of ventral valve
DP-8-302	4.72	3.39	1.39	Internal mould of ventral valve
DP-10-315	5.35	3.11	1.72	Internal mould of ventral valve
DP9604	5.27	3.84	1.37	Internal mould of ventral valve
DP-10-313	4.90	3.03	1.62	Internal mould of dorsal valve
DP-10-309	4.52	2.92	1.55	Internal mould of dorsal valve
DP733	3.91	2.73	1.43	Internal mould of dorsal valve
DP-9-304	5.93	3.87	1.53	Internal mould of dorsal valve
DP-8-311	4.41	2.59	1.70	Internal mould of dorsal valve

Occurrence Upper Changhsingian; Guangxi (Dongpan section) of South China.

Description Shell 2.4–4.5 mm long and 3.9–7.2 mm wide, hingeline shorter than greatest

Fig. 9.24 ?***Eileenella semicircridge*** (He and Shen in He et al., 2005). (**a**), external mould of a dorsal valve, DP9602, illustrating fine concentric rugae. (**b**, **c**), external moulds of two dorsal valves, DP-10-307; DP1-0194. (**d**, **e**), internal molds of two incomplete ventral valves, DP9603, DP9401, showing some coarse endospines in front of circular adductor scars. (**f**), internal mould of an incomplete ventral valve, DP-8-302, illustrating the median septum (*ms*), a pair of ear-shaped adductor scars (*ads*) and segment of tail. (**g**), internal mould of an incomplete ventral valve, DP-10-315. (**h**), internal mould of an incomplete ventral valve, DP9604, showing some coarse endospines in front of circular adductor scars, distinct marginal ridge and segment of tail. (**i**–**k**), internal moulds of three incomplete dorsal valves, DP-10-313, DP-10-309, DP733, illustrating circular scars of brachial ridges (*bs*) rounded by coarse endospines. (**l**), internal mould of an incomplete dorsal valve, DP-9-304, showing a pair of scars of brachial ridges (*bs*) and marginal ridge (*mar*). (**m**), DP-8-311, internal mould of an incomplete dorsal valve

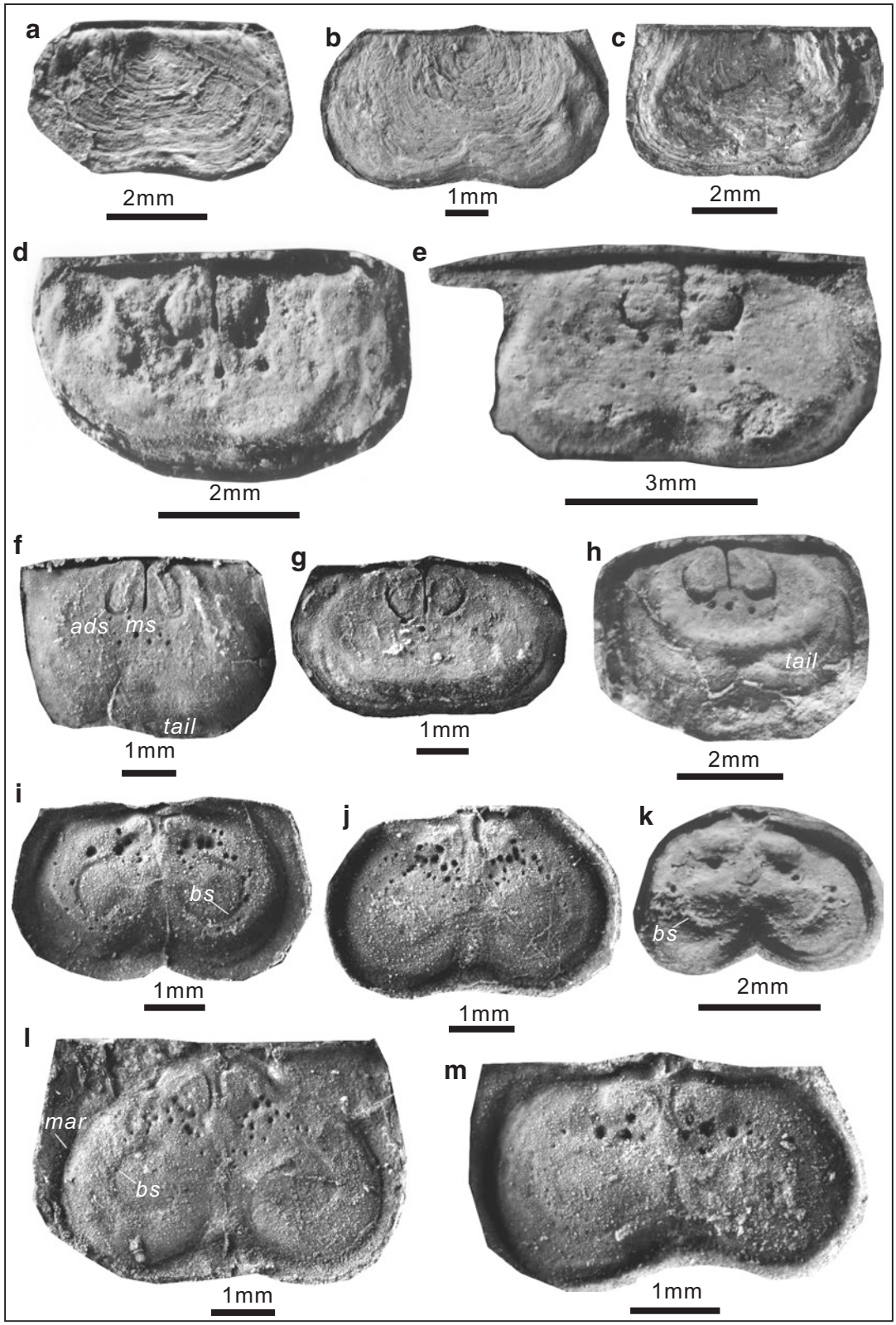
a
2mm
b
1mm
c
2mm
d
2mm
e
3mm
f
ads
ms
tail
1mm
g
1mm
h
tail
2mm
i
bs
1mm
j
1mm
k
bs
2mm
l
mar
bs
1mm
m
1mm

width at shell midlength, elliptical to globular in outline; strongly geniculate in profile. Ventral valve in our materials commonly broken along margin of corpus, except of several specimens with part of tails (Fig. 9.24d, f, g). Dorsal visceral disk nearly flat or slightly convex (emended here, see Fig. 9.24a–c); ears very small; dorsal surface with fine and irregular concentric lines and occasionally with lamellose rugae; spines absent or not preserved.

Dorsal interior with a pair of thin, broadly lobate marginal ridges (*mar*) parallel to the margin of the disk and curved posteriorly at midwidth (Fig. 9.24l); a few coarse endospines present at posterior of disk; brachial scars (*bs*) strong and circular in outline, slightly elevated and covered by numerous endospines (Fig. 9.24i, l). Ventral interior with short median septum (*ms*), extending anteriorly to one-third of valve (Fig. 9.24f); a pair of ear-shaped adductor scars (*ads*) well developed, surrounded by ridges (Fig. 9.24f); a few coarse endospines present in front of adductor scars (Fig. 9.24d–h).

Discussion Although this species was originally assigned to *Spinomarginifera* (He et al. 2005, 2014), it shares more features with the genus of *Eileenella*, including a leptaenid-like outline, ventral interior and a pair of thin, broadly lobate marginal ridges parallel to the margin of the disk in the doral interior. On the other hand, the dorsal interiors of these specimens appear to show some difference with the interior of *Eileenella*, including more prominent brachial scars and coarser endospines. In view of these comparisons, we temporarily assign this species in *Eileenella*. The present species differs from the type species *Eileenella elegans* Racheboeuf in Wongwanich et al., 2004 from the Carboniferous of southern Thailand in possessing more distinct brachial scars and a weaker median ridge in the dorsal interior.

Suborder **Chonetidina** Muir-Wood, 1955
Superfamily **Chonetoidea** Bronn, 1862
Family **Anopliidae** Muir-Wood, 1962
Subfamily **Caenanopliinae** Archbold, 1980
Genus ***Pygmochonetes*** Jin and Hu, 1978

Type Species *Pygmochonetes jingxianensis* Jin and Hu, 1978. Lower Permian; Jingxian, Anhui, South China.

Diagnosis Semicircular to roundly triangular in outline, strongly concavoconvex; ears with fine, indistinct costellae; 3 or 4 pairs of hingespines, extending posterolaterally with an angle of 60° to hingeline; sulcus absent; costellae fine, simple in the middle of shell, but bifurcated at flanks; ventral interior with a median septum; dorsal interior with a thin median septum and two parallel lateral septa.

Pygmochonetes jingxianensis Jin and Hu, 1978
Fig. 9.25a–m

1978 *Pygmochonetes jingxianensis* Jin and Hu: 111, pl. 1, Fig. 29–31.
2005 *Pygmochonetes* sp.; He et al.: 933, Fig. 4.13, 4.14.
2014 *Pygmochonetes jingxianensis* Jin and Hu: He et al., Fig. 14m–p.

Fig. 9.25 (**a**–**m**), ***Pygmochonetes jingxianensis*** Jin and Hu, 1978. (**a**), external mould of an incomplete, deformed dorsal valve, DP-7-294. (**b**), internal mould of a ventral valve and one part of the conjoined dorsal valve, DP-7-295. (**c**), incomplete and deformed ventral valve, DP-5-297. (**d**), internal mould of a ventral valve and segments of shell, DP-10-298. (**e**), internal mould of an incomplete, deformed ventral valve, DP3-0214. (**f**), internal mould of an incomplete ventral valve, DP10-0216, showing radially arranged papillae (*pap*). (**g**), internal mould of a nearly complete ventral valve and segment of shell, DP7-0217. (**h**), posterior of DP7-0217, showing a short median septum (*ms*). (**i**, **j**), external moulds of two incomplete dorsal valves, DP10-0219, PB5-0220. (**k**), interior of a dorsal valve and segment of a conjoined ventral valve, DP10-0221. (**l**), external mould of a dorsal valve, DP3-0223. (**m**), internal mould of an incomplete ventral valve, DP10-0233. (**n**, **o**), ***Pygmochonetes*** sp.. (**n**), internal mould of a ventral valve, DP5-0224, showing a short median septum (*ms*). (**o**), internal mould of a nearly complete ventral valve and segment of shell, DP3-0231

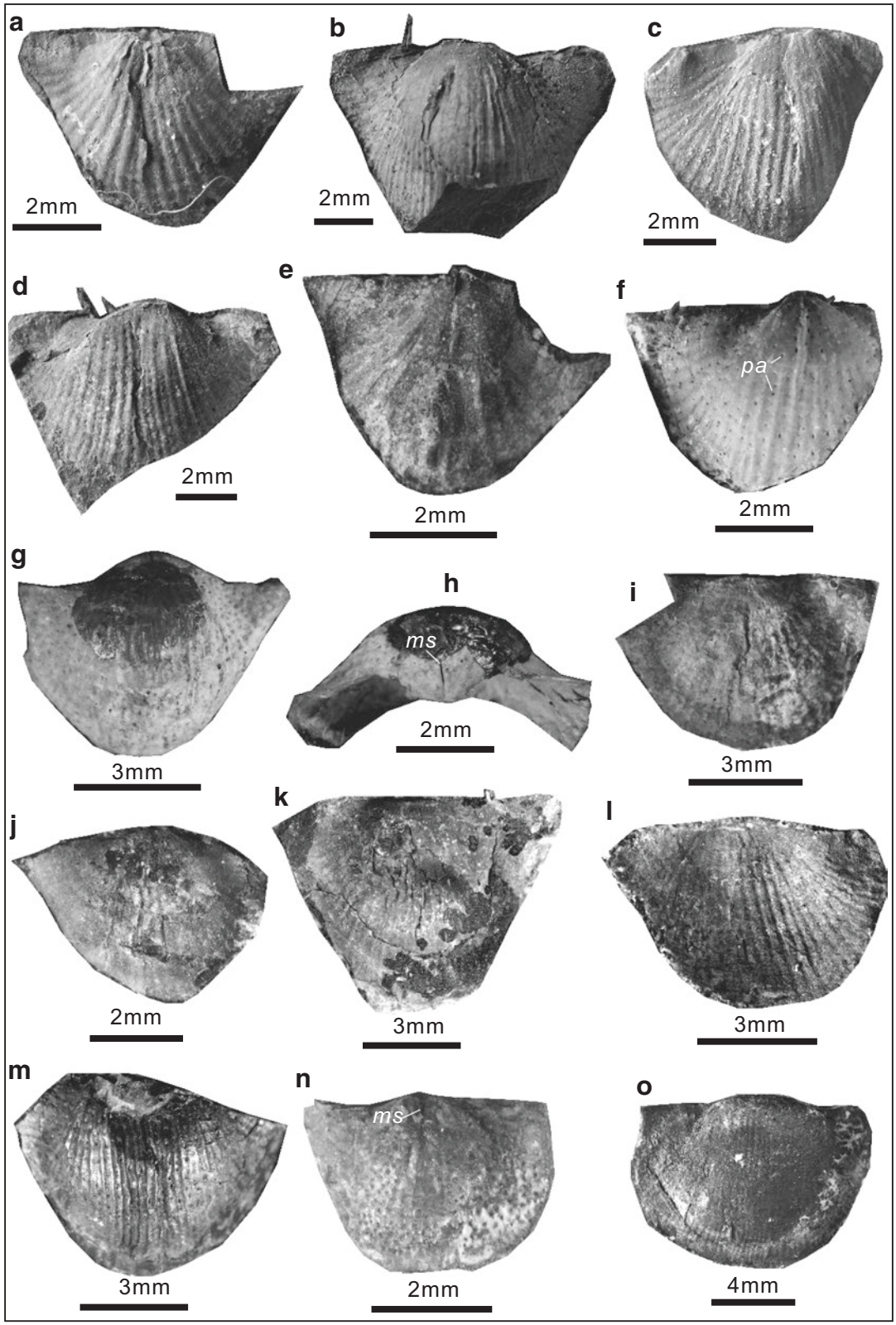
a
2mm
b
2mm
c
2mm
d
2mm
e
2mm
f
pa
2mm
g
3mm
h
ms
2mm
i
3mm
j
2mm
k
3mm
l
3mm
m
3mm
n
ms
2mm
o
4mm

Materials Over 15 specimens. Registered specimens: see below.

Measurements (mm):

Number	Width	Length	Width/ length	Notes
DP-7-294	5.98	4.53	1.32	External mould of dorsal valve
DP-7-295	9.72	6.88	1.41	Internal mould of ventral valve
DP-5-297	7.68	5.95	1.29	Ventral valve
DP-10-298	8.93	7.12	1.25	Internal mould of ventral valve
DP3-0214	5.26	3.86	1.36	Internal mould of ventral valve
DP10-0216	5.48	4.57	1.20	Internal mould of ventral valve
DP7-0217	6.99	5.61	1.25	Internal mould of ventral valve
DP10-0219	5.09	4.89	1.04	External mould of dorsal valve
PB5-0220	6.72	4.32	1.56	External mould of dorsal valve
DP10-0221	9.85	6.89	1.43	Dorsal interior
DP3-0223	7.25	5.68	1.28	External mould of dorsal valve
DP10-0233	8.02	6.13	1.31	Internal mould of ventral valve

Occurrence Changhsingian; China.

Description Shell 3.9–7.1 mm long and 5.1–9.9 mm wide, roundly triangular in outline, strongly-elevated middle part of ventral valve, flanks steep, widest at hinge. Ventral visceral disk highly elevated; ears acute, gently convex, costellae indistinct, well differentiated from visceral disk by depressions; hingespines extending posterolaterally with an angle of 40–60° to hingeline; costellae fine, simple in the middle part of shell, numbering 4 in 1 mm on umbo, increasing anteriorly by intercalation and bifurcation at flanks; cardinal extremities acute, with a cardinal angle of about 45–60°; anterior margin regularly rounded. Dorsal visceral disk strongly concave. Ventral interior with a short median septum (*ms*) (Fig. 9.25h) and radially arranged papillae (*pap*) (Fig. 9.25f).

Discussion The present species is comparable with *P. jingxianensis* Jin and Hu (1978, 111, pl. 1, Fig. 28–31) from the Kuhfeng Formation at the Yangongtang section in Jingxian County, Anhui Province, in terms of its appearance (a strongly elevated middle part of shell width and a roundly-triangular outline), ventral costellation, and absence of sulcus. The present species differs from *P. taniantawengica* Jin and Shi in Jin et al., 1985 from the Lower Permian of Mangkang, Tibet in the latter having nonbifurcated costellae.

Pygmochonetes sp.
Figs. 9.25n, o; 9.26

1978 *Pygmochonetes jingxianensis* Jin and Hu: 111, pl. 1, Fig. 28.
1984 *Pygmochonetes jingxianensis* Jin and Hu; Yang in Feng et al.: 210, pl. 31, Fig. 6.

Materials Seven registered specimens: see below.

Measurements (mm):

Number	Width	Length	Width/ length	Notes
DP5-0224	4.65	3.64	1.28	Internal mould of ventral valve
DP3-0231	12.74	8.19	1.56	Internal mould of ventral valve
PB10-0232	12.20	7.06	1.73	Ventral valve
DP10-0228	5.52	3.42	1.61	Ventral valve (juvenile)
DP10-0235	8.63	5.71	1.51	Internal mould of ventral valve
DP10-0236	10.56	6.18	1.71	External mould of ventral valve
DP10-0238	4.18	2.98	1.40	Ventral valve (juvenile)

Occurrence Upper Changhsingian; Guangxi (Dongpan section) of South China.

Description Shell 3.0–8.2 mm long and 4.2–12.7 mm wide, semicircular in outline; strongly-elevated, globose ventral disk, flanks gently sloping, widest at hinge. Ventral visceral disk highly elevated; ears gently convex, costellae indistinct, differentiated from visceral disk by weak depressions; hingespines extending posterolaterally with an angle of 60–70° to hingeline; costellae fine, simple in the middle part of

shell, numbering 3–5 in 1 mm on umbo, increasing anteriorly by intercalation and bifurcation at flanks; cardinal extremities with a cardinal angle of about 70–90°; anterior margin regularly rounded.

Ventral interior with a median septum (*ms*) and radially arranged papillae (Fig. 25n).

Discussion The present species is similar to *Pygmochonetes jingxianensis* Jin and Hu, 1978 from the Lower Permian of Jingxian, Anhui, South China in its strongly convex ventral valve, costellation, and lacking of sulcus, but differs in the former has a semi-circular outline, gently-sloping flanks and a larger cardinal angle. This species resembles to *Pygmochonetes subjingxianensis* Zhao and Tan, 1984 from the Middle Permian Chihsia Formation of Sangzhi, Hunan Province, South China in a larger cardinal angle and simple costellae in the middle part of shell width, but *P. subjingxianensis* has a smaller umbo angle and a narrower middle part of the shell width.

Subfamily **Anopliinae** Muir-Wood, 1962
Genus ***Tornquistia*** Paeckelmann, 1930

Type Species *Leptaena* (*Chonetes*) *polita* McCoy, 1855. Lower Carboniferous; Scotland.

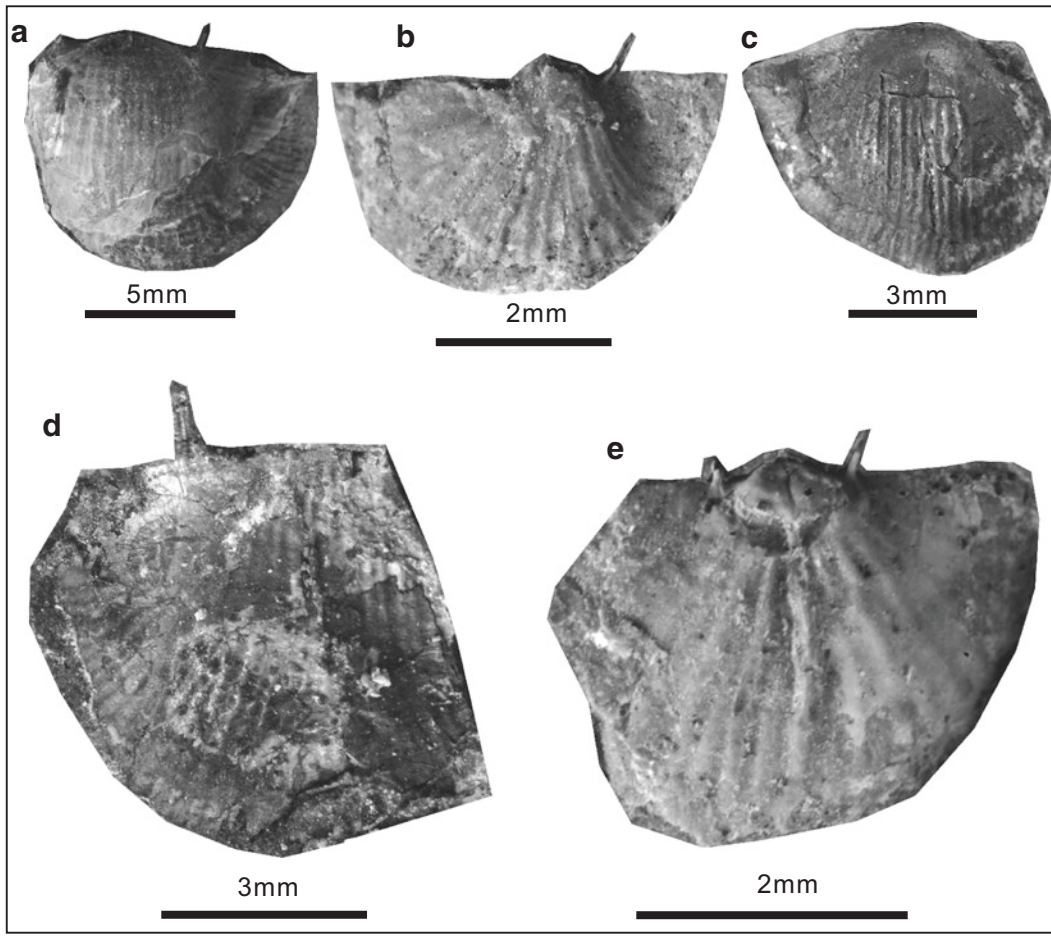

Fig. 9.26 ***Pygmochonetes*** sp.. (**a**), a deformed ventral valve, PB10-0232. (**b**), a deformed ventral valve (juvenile), DP10-0228. (**c**), internal mould of an incomplete ventral valve, DP10-0235. (**d**), external mould of an incomplete ventral valve and segment of shell, DP10-0236. (**e**), a ventral valve (juvenile), DP10-0238

Diagnosis (emended). Small, ventral valve highly convex medianly, greatest width along hinge; ears well demarcated; dorsal valve correspondingly concave; shell smooth or faintly capillate, occasionally with concentric lines, scattered spinule apertures; row of spines extending at high angle to hinge. Ventral interior with variable median septum, long or short; teeth variable, large to obscure; few papillae along marginal area. Dorsal interior with small cardinal process; two lateral septa anteriorly divergent at 25–35°; median septum obscure or absent; sockets laterally extending, almost parallel to hinge; papillae in radial rows.

Discussion To date, the occurrences of Permian *Tornquistia* are restricted from the Lower to Middle Permian in Western Australia (Archbold, 1980, 1981, 1990), southern Thailand (Grant, 1976), eastern Siberia (Zavodowsky, 1960, 1971; Afanasjeva, 1977), Arctic Canada (Bamber and Waterhouse, 1971). The presence of the genus at the Dongpan section is the first discovery of this genus in the uppermost Permian in the world. The genus is quite similar to *Fusichonetes* in ventral interior, but differs in having a pair of long lateral septa, and its dorsal median septum is weak or absent. *Tornquistia* differs from the Lower Devonian *Anoplia* Hall and Clarke, 1892 as the latter is characterized by long curved socket ridges and a prominent median septum in the dorsal interior. Compared to *Tornquistia*, *Demonedys* Grant, 1976 from the Lower Permian in southern Thailand has a higher and narrower median fold beginning at beak and rising anteriorly on the ventral valve. *Songzichonetes* Yang in Feng et al., 1984 from the Middle Permian of South China shares with *Tornquistia* a pair of thick, anteriorly-divergent lateral septa in the dorsal interior, but the former has longer lateral septa and posterolateral ridges in the dorsal interior, as well as prominent, bificuated costellae.

Tornquistia changhsingia He, Shi and Shen sp. nov.
Figs. 9.27; 9.28

Diagnosis Small, shield-like outline; minute teeth; short ventral median septum; a pair of thick, long lateral septa in dorsal interior; dorsal median septum absent.

Etymology Named for the age of Changhsingian for the species.

Types Holotype, PB2-MC070; paratypes, DP5-MC027, DP5-MC015.

Other Materials Over 130 specimens. Registered specimens: see below.

Measurements (mm):

Number	Width	Length	Width/length	Notes
DP7-MC001	5.26	3.37	1.56	Internal mould of ventral valve
PB5-MC003-1	4.06	2.68	1.51	Ventral interior
DP9-MC006-1	3.92	2.85	1.38	Ventral interior
DP3-MC017	4.70	3.12	1.51	Internal mould of ventral valve
DP10-MC007-1	4.01	2.64	1.52	External mould of ventral valve
DP3-MC018	4.27	2.57	1.66	Internal mould of dorsal valve
DP3-MC004-1	3.73 (ventral)	2.24 (ventral)	1.67 (ventral)	Internal mould of conjoined shell
DP3-MC004-1	3.04 (dorsal)	1.78 (dorsal)	1.75 (dorsal)	Internal mould of conjoined shell
DP5-MC027	3.86 (ventral)	2.20 (ventral)	1.62 (ventral)	Internal mould of conjoined shell
DP3-MC012	3.62	2.24	1.70	Internal mould of ventral valve
DP8-MC021	4.17	2.46	1.40	Internal mould of dorsal valve
DP5-MC015	3.35	2.39	1.49	Internal mould of dorsal valve
DP7-MC043-1	4.20	2.81	1.61	Ventral exterior
DP8-MC026	4.01	2.49	1.61	Internal mould of ventral valve
DP10-MC007-2	3.44	2.14	1.61	Internal mould of dorsal valve

(continued)

Number	Width	Length	Width/length	Notes
DP5-MC035	4.26	3.10	1.37	External mould of dorsal valve
DP5-MC033-1	4.22	2.81	1.50	External mould of dorsal valve
DP8-MC037	4.24	2.95	1.44	External mould of dorsal valve
DP8-MC041	3.46	2.31	1.50	External mould of dorsal valve
DP8-MC046	4.65	3.20	1.45	External mould of dorsal valve
PB2-MC070	3.99	2.66	1.50	Ventral exterior
PB8-MC038	4.23	2.60	1.63	Ventral exterior
PB5-MC039	3.36	2.08	1.62	Ventral exterior
PB8-MC047	4.23	2.93	1.44	Ventral exterior
DP5-MC014	3.94	2.10	1.88	Dorsal interior
DP7-MC040	4.58	2.90	1.58	Ventral interior
DP7-MC034-2	5.30	3.72	1.42	Internal mould of dorsal valve
DP7-MC071	5.17	3.38	1.53	Ventral exterior

Occurrence Upper Changhsingian; Guangxi (Dongpan section) of South China.

Description Shell small, 1.8–3.7 mm long and 3.0–5.3 mm wide, shield-like outline, highly concavoconvex in profile; greatest width at hingeline; surface smooth except for the presence of weak growth lines and radial lines when shell surface is decorticated (Fig. 9.27l); interareas low, ventral interarea only slightly higher than dorsal interarea.

Ventral interior with a short median septum (marked by *ms*, e.g., Fig. 9.27a, g, h) and few papillae along marginal area. Dorsal interior with a small, quadrilobate cardinal process (marked by *cp*, see Fig. 9.27e); sockets laterally extending, almost parallel to hingeline (marked by *soc*, see Fig. 9.27k, n); a pair of long, thick lateral septa anteriorly divergent at 30–50° (marked by *ls*, see Fig. 9.27f–h); papillate elongate along lateral septa (marked by *pap*, see Fig. 9.27g); median septum obscure or absent.

Discussion The new species is most like *T. tropicalis* Grant, 1976 from the Artinskian of Ko Muk in southern Thailand in a small body size and shield-shaped outline, but differs in the latter having large teeth, a median ridge anterior to median septum in the ventral interior, and a bilobed cardinal process in the dorsal interior. *T. orthogona* Wongwanich et al., 2004 from the Carboniferous in southern Thailand is larger (6.0–9.4 mm in wide) than the new species and it has a well-defined median ridge anterior to the median septum within the ventral interior. Comapred to the new species, both *Tornquistia occidentalis* Archbold, 1980 from the Sakmarian and *T. magna* Archbold, 1980 from the Artinskian in Western Australia have a larger body size (for *T. occidentalis*, 8.2–12.0 mm wide; for *T. magna*, 6.0–14.0 mm wide), larger teeth and a long median septum in the ventral interior. *Tornquistia subquadratus* Archbold, 1990 from the Sakmarian in western Autralia is also a relatively large species (10.8–14.0 mm wide), with large teeth, a long median septum in the ventral interior, a short but prominent median septum and weaker lateral septa in the dorsal interior. *T. tricorporum* Waterhouse, 1981 from the Lower Permian in southern Thailand has a high and narrow median fold beginning at beak and rising anteriorly on ventral valve and thus should be assigned to the genus of *Demonedys* Grant, 1976.

Family **Rugosochonetidae** Muir-Wood, 1962
Subfamily **Rugosochonetinae** Muir-Wood, 1962
Genus ***Fusichonetes*** Liao in Zhao et al., 1981

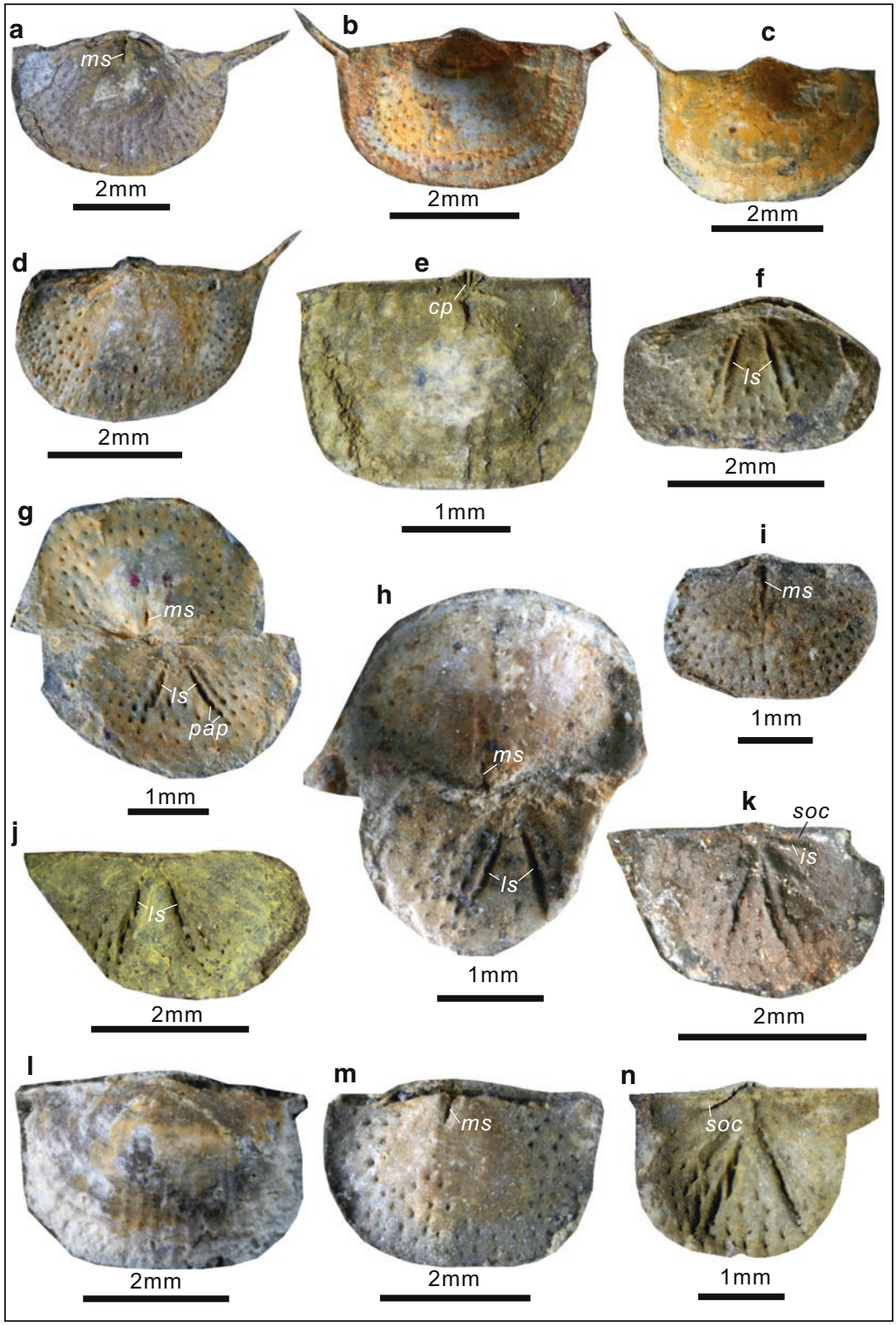
a
ms
2mm
b
2mm
c
2mm
d
2mm
e
cp
1mm
f
ls
2mm
g
ms
ls
pap
1mm
h
ms
ls
1mm
i
ms
1mm
j
ls
2mm
k
soc
is
2mm
l
2mm
m
ms
2mm
n
soc
1mm

Type Species *Plicochonetes nayongensis* Liao, 1980a. Changhsingian (Upper Permian); Guizhou Province, southwestern China.

Diagnosis Small to medium in size, about 1.0–12.0 mm length and 2.0–21.0 mm width; transversely rectangular to reverse trapezoidal in outline; concavoconvex to almost planoconvex; ears normally smooth, flattened or slightly swollen; external surface usually with simple costellae, occasionally bifurcated or intercalated, with micro-ornament of tubes on well-preserved specimens; sulcus and fold variable. Ventral interior with median septum; dorsal interior with median septum, lateral septa (possibly) and brachial scars, cardinal process bilobate to quadrilobate; internal surface of both valves with radially-, almost evenly-distributed papillae.

Discussion The genus *Fusichonetes* (Liao in Zhao et al., 1981) was first recorded by Liao in Zhao et al., 1981 with a brief description, with *Plichonetes nayongensis* Liao, 1980a as the type species. Subsequently, Chen et al. (2000) proposed *Tethyochonetes*, to include many species originally assigned to "*Waagenites*" as well as some of the species assigned to *Fusichonetes* (e.g., *Fusichonetes pigmaea* Liao, 1979a). The main justification Chen et al. employed to distinguish *Tethyochonetes* from *Fusichonetes* was that the former has a lower ratio of shell width to length and less costellae at midvalve (Chen et al., 2000). He et al. (2014) also pointed out that *Fusichonetes* Liao in Zhao et al., 1981 has a more transversely outline than *Tethyochonetes*. However, a recent study by Wu et al. (2017) using both quantitative morphometrics (Fig. 9.29) and a cladistic analysis of over 1000 specimens from the Xinmin section, revealed that *Tethyochonetes* should be a synonym of *Fusichonetes*.

Fusichonetes differs from *Neochonetes* Muir-Wood, 1962 because the latter has two parallel lateral septa (*ls*); typical papillae which are radially arranged, usually increased in the number and decreased in size towards margin (namely so-called "*Neochonetes*-like papillae", see He et al., 2014); and more, bifurcated costellae. *Fusichonetes* is readily distinguished from *Waterhouseiella* Archbold, 1983 as the latter has more hingespines (7–9), and from *Sulcirugaria* Waterhouse, 1983b as the latter has *Neochonetes*-like papillae in the dorsal valve. *Fusichonetes* is more or less similar to *Quinquenella* Waterhouse, 1975 in a subquadrata outline and the ventral interior, but differs in the latter having concentric stria and long accessory septa in the dorsal interior, and lacking costellae.

Fig. 9.27 ***Tornquistia changhsingia*** He, Shi and Shen sp. nov.. (**a**), internal mould of a nearly complete ventral valve, DP7-MC001, showing a short median septum (*ms*), a preserved hinge spine and papillae. (**b**), interior of a nearly complete ventral valve, PB5-MC003-1, showing the preserved two hinge spines and papillae. (**c**), interior of a nearly complete ventral valve, DP9-MC006-1, showing a few preserved papillae. (**d**), internal mould of a nearly complete ventral valve, DP3-MC017, showing radially-arranged papillae. (**e**), external mould of an incomplete dorsal valve and posterior of the internal mould, DP10-MC007-1, showing quadrilobate cardinal process (*cp*) and nearly smooth ornamentation. (**f**), internal mould of an incomplete dorsal valve, DP3-MC018, showing lateral septa (*ls*) and papillae on the surface. (**g**), internal mould of an incomplete dorsal valve and internal mould of the conjoined, complete ventral valve, DP3-MC004-1, showing a short ventral median septum (*ms*), a pair of dorsal lateral septa (*ls*) and elongated papillae along lateral septa (*pap*). (**h**), internal mould of an incomplete dorsal valve and internal mould of the conjoined, nearly complete dorsal valve, DP5-MC027 (paratype), showing a short ventral median septum (*ms*), a pair of dorsal lateral septa (*ls*) and a few preserved papillae. (**i**), internal mould of an incomplete ventral valve, DP3-MC012, showing a well-preserved median septum (*ms*) and papillae. (**j**), internal mould of an incomplete dorsal valve, DP8-MC021, showing lateral septa (*ls*) and papillae. (**k**), internal mould of an incomplete dorsal valve, DP5-MC015 (paratype), showing a pair of lateral septa, sockets (*soc*) and inner socket ridges (*is*). (**l**), exterior of a nearly complete ventral valve, DP7-MC043-1, showing weak costellae. (**m**), internal mould of a nearly complete ventral valve, DP8-MC026, showing a short median septum (*ms*). (**n**), internal mould of an incomplete dorsal valve, DP10-MC007-2, showing lateral septa and deep sockets (*soc*)

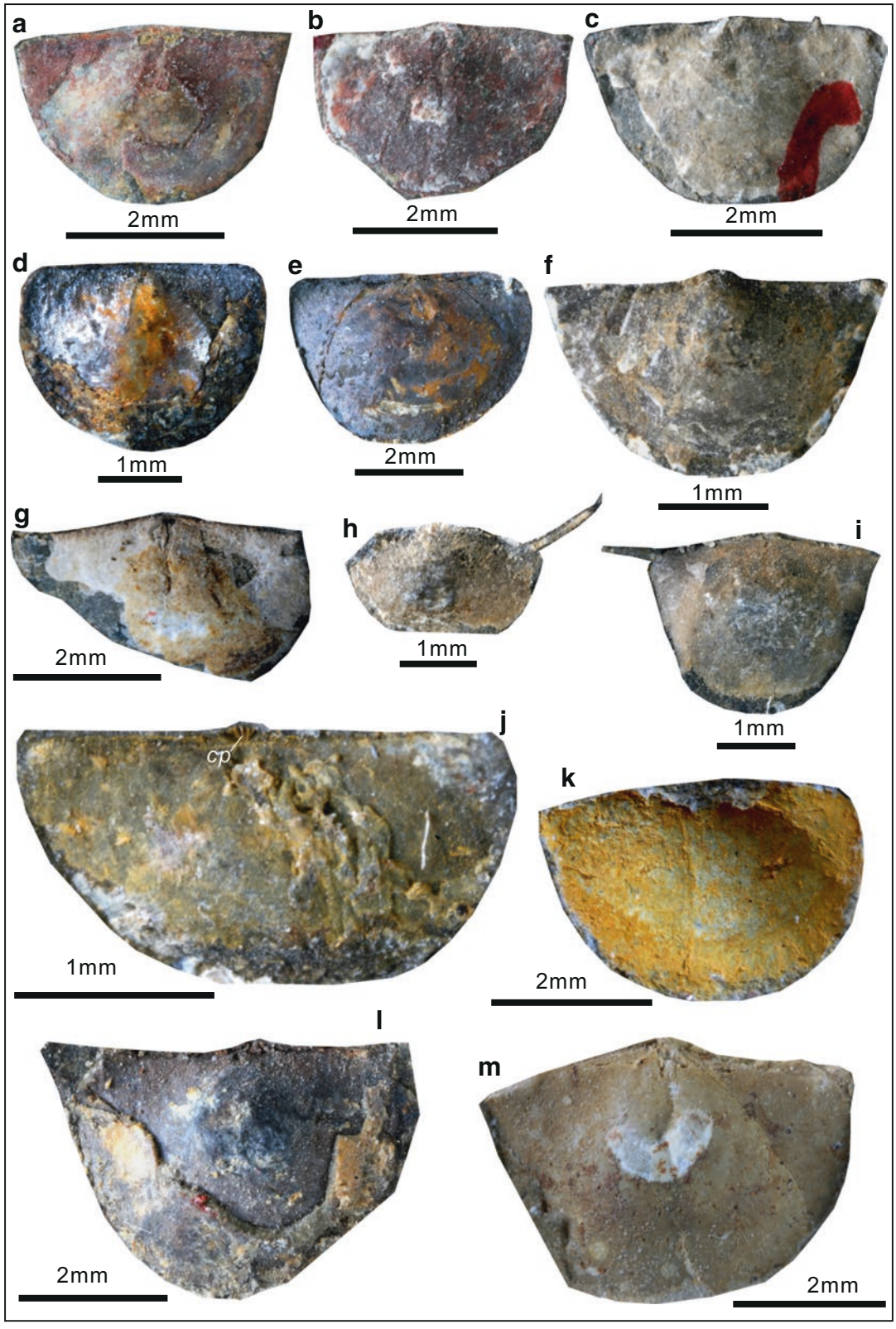
a
2mm
b
2mm
c
2mm
d
1mm
e
2mm
f
1mm
g
2mm
h
1mm
i
1mm
j
cp
1mm
k
2mm
l
2mm
m
2mm

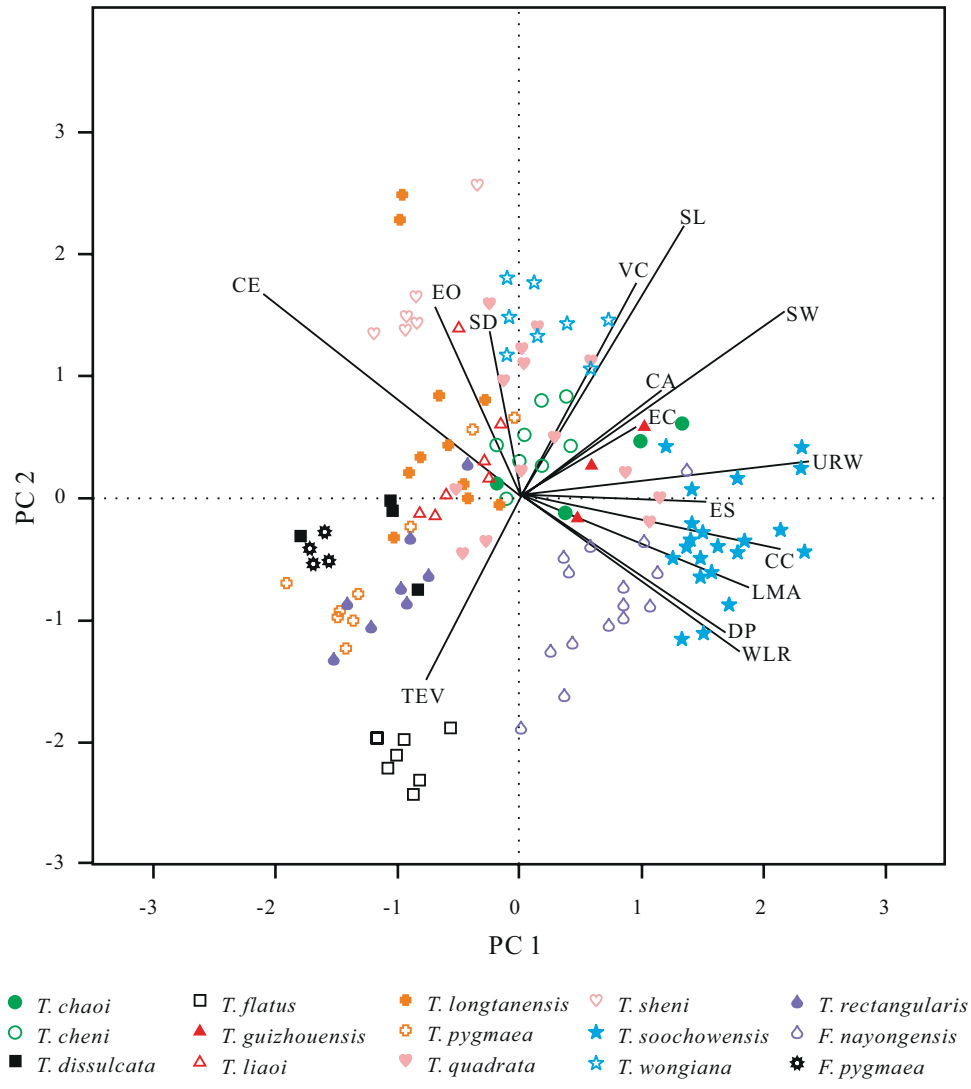

Fig. 9.29 Categorical Principle Component Analysis (CATPCA) for specimens of 15 species which were previously assigned to the genera of *Tethyochonetes* and *Fusichonetes* from publications (revised after Wu et al., 2017). Note: Results show *F. nayongensis* and *F. pygmaea* are well merged with those of *Tethyochonetes* and both genera should be the same genus

Fig. 9.28 ***Tornquistia changhsingia*** He, Shi and Shen sp. nov.. (**a**), external mould of a nearly complete dorsal valve and shell remnant, DP5-MC035, showing smooth ornamentation. (**b**), external mould of an incomplete dorsal valve and shell remnant, DP5-MC033-1. (**c**), external mould of a nearly complete dorsal valve and shell remnant, DP8-MC037, showing the base of a preserved hinge spine. (**d**), external mould of a complete dorsal valve and shell remnant, DP8-MC041. (**e**), external mould of a complete dorsal valve, DP8-MC046. (**f**), exterior of a nearly complete ventral valve, PB2-MC070 (holotype), showing smooth ornamentation. (**g**), exterior of an incomplete ventral valve, PB8-MC038. (**h**), exterior of an incomplete ventral valve, PB5-MC039, showing a preserved long hinge spine. (**i**), exterior of a nearly complete ventral valve, PB8-MC047, showing a preserved hinge spine. (**j**), interior of an incomplete dorsal valve (shell mostly decorticated), DP5-MC014, showing a quadrilobate cardinal process (*cp*). (**k**), interior of a complete ventral valve (shell mostly decorticated), DP7-MC040. (**l**), internal mould of an incomplete dorsal valve and shell remnant, DP7-MC034-2. (**m**), exterior of an incomplete ventral valve, DP7-MC071

Fusichonetes nayongensis (Liao, 1980a)
Fig. 9.30

1980a *Plicochonetes nayong ensis* Liao: 256, pl. 4, Fig. 7–9.
1980b *Fusichonetes nayongensis* (Liao); Liao: pl. 1, Fig. 3, 4.
1981 *Fusichonetes nayongensis* (Liao); Liao in Zhao et al.: pl. 8, Fig. 13.
1984 *Fusichonetes nayongensis* (Liao): pl. 1, Fig. 15.
2002 *Fusichonetes nayongensis* (Liao); Shen and Archbold: 340, Fig. 6q.

Holotype *Plicochonetes nayongensis* Liao, 1980a, pl. 4, Fig. 8, deposited in the Nanjing Institute of Geology and Palaeontology, Chinese Academy of Sciences, a ventral valve, from Talung Formation (Lopingian), Nayong, Guizhou Province, China.

Diagnosis (simplified from Wu et al., 2017). Extremely transverse outline (average of width/length = 2.1), strongly acute cardinal extremities, ventral sulcus shallow. Ventral interior with median septum; dorsal interior with median septum, lateral septa (possibly) and brachial scars, cardinal process quadrilobate; internal surface of both valves with radially distributed papillae.

Materials Over 50 specimens. Registered specimens: see below.

Measurements (mm):

Number	Width	Length	Width/length	Notes
XM2-0393	3.82	1.87	2.04	Dorsal interior
XM2-0390	5.37	2.57	2.09	Dorsal exterior
XM4-0392	4.91	2.72	1.81	Dorsal interior
XM10-0398	3.97	1.85	2.15	Ventral valve
XM9-0410	5.35	3.04	1.76	Ventral valve
XM2-0384	5.10	2.92	1.75	Ventral valve
XM24-280	4.36	1.63	2.67	External mould of dorsal valve
XM24-252	11.63	4.79	2.43	External mould of dorsal valve
XM2-0383	5.27	2.99	1.76	Internal mould of ventral valve
XM24-248	10.98	3.88	2.83	Ventral exterior
XM10-0400	5.77	3.03	1.90	Dorsal interior
XM10-0406	3.53	2.14	1.65	Ventral exterior
XM24-258	12.23	4.87	2.51	Internal mould of ventral valve

Occurrence Upper Permian; commonly in western Guizhou, occasionally in Hunan, Jiangsu and Zhejiang Provinces, China.

Description Shell 1.6—4.9 mm long and 3.5—14.0 mm wide, extremely transverse in outline (ratio of shell width to length > 1.6), concavoconvex to planoconvex; widest at hinge; usually four pairs of hinge spines posterolaterally projecting; cardinal extremities very acute, cardinal angle about 40 to 60°; ears flat to slightly inflated, smooth, well differentiated from flanks of ventral disk; costellae distinctly originating

Fig. 9.30 ***Fusichonetes nanyongensis*** (Liao, 1980a). (**a**), interior of a complete dorsal valve, XM2-0393, showing a trilobed process (*cp*) and a short median septum (*ms*). (**b**), exterior of a complete dorsal valve, XM2-0390. (**c**), interior of a complete dorsal valve, XM4-0392, showing radially-arranged papillae papillae. (**d**, **e**), exteriors of two nearly complete ventral valves, XM10-0398, XM9-0410. (**f**), exterior of a nearly complete ventral valve, showing posterolaterally-projecting hinge spines, XM2-0384. (**g**, **h**), external moulds of two nearly complete dorsal valves, XM24-280, XM24-252. (**i**), internal mould of an incomplete ventral valve and shell remnant, showing a few preserved papillae and hinge spines, XM2-0383. (**j**), ventral exterior, XM24-248, showing well-preserved hingespines. (**k**), dorsal interior, showing well-preserved papillae, XM10-0400. (**l**), ventral exterior, showing costellae on the surface and hinge spines XM10-0406. (**m**), internal mould of a ventral valve, XM24-258, radially-arranged papillae (not well-preserved)

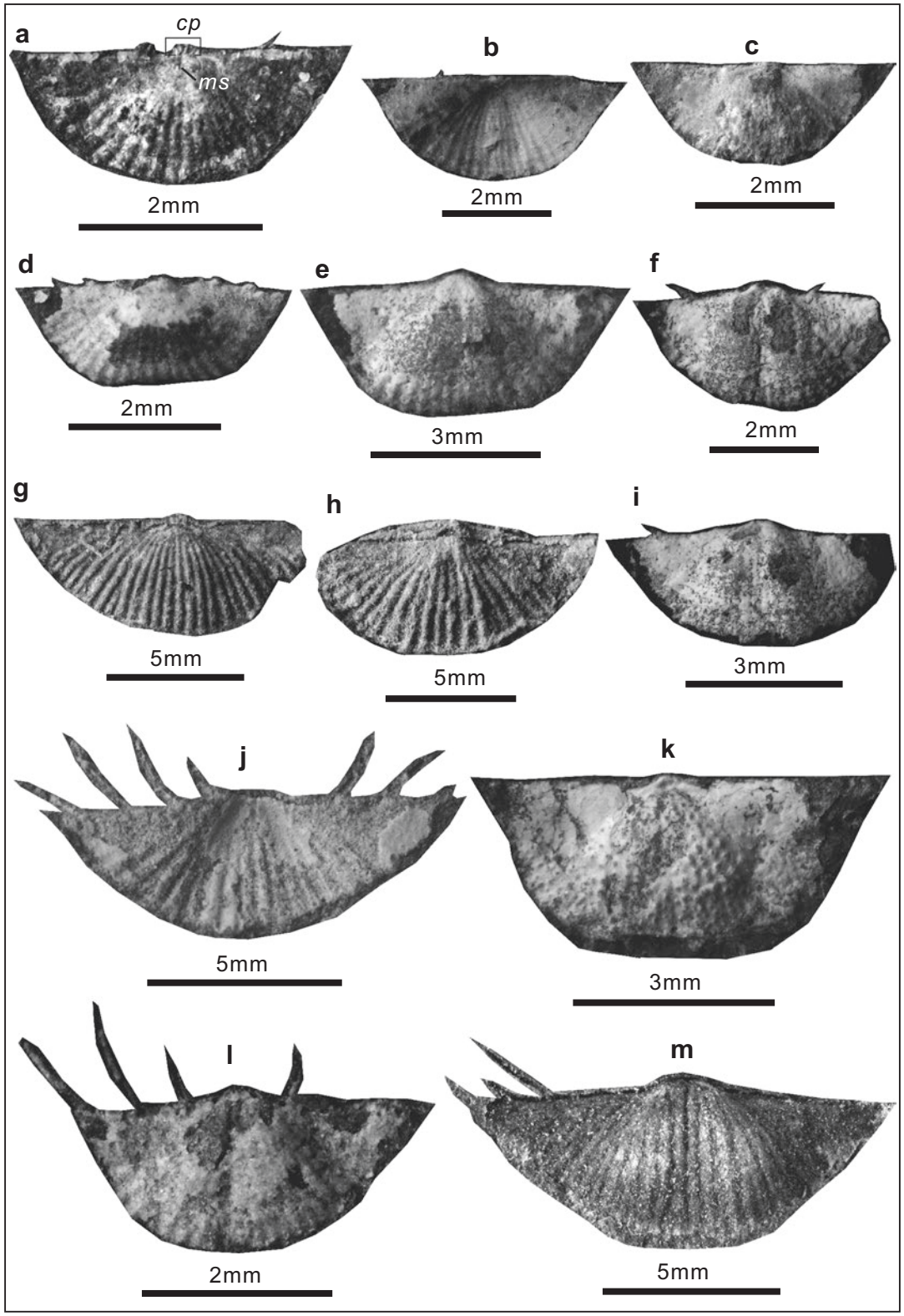
a
cp
ms
2mm
b
2mm
c
2mm
d
2mm
e
3mm
f
2mm
g
5mm
h
5mm
i
3mm
j
5mm
k
3mm
l
2mm
m
5mm

from umbo, with a few bifurcation near umbo and few intercalation near anterior or lateral margins, numbering about 14–26 at margin.

Ventral valve moderately to strongly convex; umbonal region swollen, overhanging hingeline; maximum convexity in the middle part of the shell; sulcus shallow, beginning from umbo, widening anteriorly. Dorsal valve slightly or prominently concave; beak low; fold weak.

Ventral interior with radially-, almost evenly-arranged papillae. Dorsal interior with a trilobed process (*cp*); distinct inner socket ridges, extending laterally at an angle of 10−20° to hingeline; a short median septum (*ms*) (Fig. 9.30a).

Discussion This species is similar to *Fusichonetes soochowensis* (Chao, 1928) from the Permian of Yanwashan area, Jiangsu Province, China in its transvese outline, but differs in the former having acuter cardinal angles.

Fusichonetes soochowensis (Chao, 1928)
Fig. 9.31

1928 *Chonetes soochowensis* Chao: 31, pl. 1, Fig. 14−16.
1932 *Chonetes soochowensis* Chao; Huang: 5, pl. 1, Fig. 8a, 8b.
1964 *Chonetes soochowensis* Chao; Wang et al.: 241, pl. 37, Fig. 20, 21.
1974 *Waagenites barusiensis* (Davidson); Jin et al.: pl. 164, Fig. 8.
1977 *Waagenites soochowensis* (Chao); Yang et al.: 332, pl. 135, Fig. 22.
1978 *Waagenites soochowensis* (Chao); Feng and Jiang: 243, pl. 88, Fig. 4.
1979 *Waagenites soochowensis* (Chao); Chan in Hou et al.: 72, pl. 11, Fig. 7.
1980a *Waagenites soochowensis* (Chao); Liao: pl. 5, Fig. 4.
1980a *Waagenites guizhouensis* Liao: 258, pl. 5, Fig. 5−7.
1980a *Waagenites barusiensis* (Davidson); Liao: pl. 5, Fig. 24−26.
1980b *Waagenites* cf. *soochowensis* (Chao); Liao: pl. 1, Fig. 2.
1982 *Waagenites soochowensis* (Chao); Wang et al.: 197, pl. 91, Fig. 3, 4.
1984 *Waagenites soochowensis* (Chao); Liao: pl. 1, Fig. 10.
1987 *Waagenites soochowensis* (Chao); Xu in Yang et al.: pl. 8, Fig. 15, 16.
1990 *Waagenites soochowensis* (Chao); Zhu: 64, pl. 18, Fig. 1, 2.
1998 *Waagenites soochowensis* (Chao); Shi and Shen: 509, Fig. 4.6.
2002 *Tethyochonetes soochowensis* (Chao); Shen and Archbold: 338, Fig. 5q−r.
2013 *Tethyochonetes soochowensis* (Chao); Zhang et al., 2013, 232, 233, Fig. 5o–p.
2014 *Tethyochonetes soochowensis* (Chao); He et al., 2014, 918, Fig. 4x, y–a', c′−e'.

Holotype *Chonetes soochowensis* Chao, 1928, pl. 1, Fig. 14, an external mould of dorsal valve, from Permian shale, Yanwashan area, Jiangsu Province, China.

Diagnosis (emended). Shell very transverse (average of width/length = 2.0), acute cardinal extremities, costellae bifurcated or widening anteriorly for adults, but rarely bifurcated for juveniles.

Materials Over 10 specimens. Registered specimens: see below.

Measurements (mm):

Number	Width	Length	Width/length	Notes
CM10-0352	8.96	5.16	1.74	External mould of ventral valve
SR23b-0419	4.50	2.53	1.78	Internal mould of ventral valve
LZ2702263	11.96	6.19	1.93	Ventral exterior
LZ2702235	10.55	5.63	1.87	Dorsal interior
DS-1-475	7.42	3.61	2.06	Internal mould of ventral valve
CM-4-459	6.47	3.26	1.98	Internal mould of ventral valve
CM-10-482	10.29	4.31	2.39	External mould of dorsal valve
DS-1-485	13.69	6.28	2.18	External mould of dorsal valve
DS-1-478	6.26	2.81	2.22	External mould of ventral valve
SR-16-481	9.51	4.46	2.13	External mould of dorsal valve
XM24110	6.14	2.86	2.15	Internal mould of ventral valve

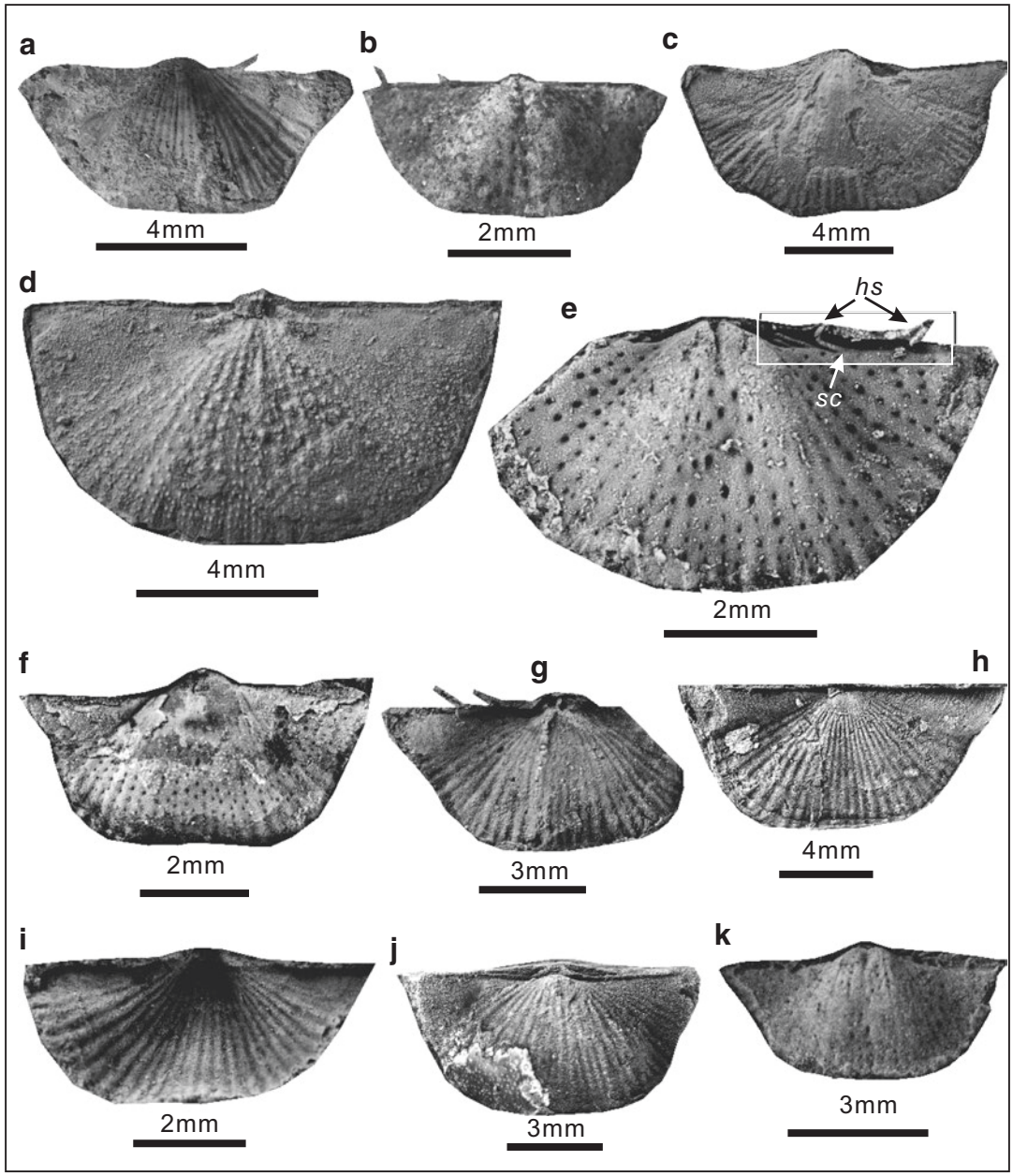

Fig. 9.31 ***Fusichonetes soochowensis*** (Chao, 1928). (**a**), external mould of a nearly complete ventral valve, CM10-0352, showing hinge spines and bifurcated costellae on flanks. (**b**), internal mould of ventral valve, SR23b-0419. (**c**), exterior of an incomplete ventral valve, LZ2702263, showing numerous costellae. (**d**), interior of a complete dorsal valve, LZ2702235, showing papillae arranged in rows (row bifurcated at midlength and anterior and probably corresponding to bifurcated costellae). (**e**), internal mould of an incomplete ventral valve, DS-1-475, illustrating hinge spines (*hs*) extending posterolaterally and spine canals (*sc*) inclined midline. (**f**), internal mould of a complete ventral valve, CM-4-459. (**g**), external mould of an incomplete dorsal valve, CM-10-482, showing two preserved hinge spines. (**h**), external mould of a complete dorsal valve, DS-1-485, showing numerous costellae and transversely broad outline. (**i**), external mould of a complete ventral valve, DS-1-478, showing numerous costellae. (**j**), external mould of a complete dorsal valve, SR-16-481, showing numerous, bifurcated costellae. (**k**), internal mould of a nearly complete ventral valve, XM24110, showing transversely broad outline

Occurrence Wuchiapingian–Changhsingian; Guizhou, Sichuan, Hunan, Jiangsu and Zhejiang Provinces, China.

Description Shell 2.5–6.3 mm long and 4.5–14.0 mm wide, transverse (ratio of shell width/length 1.74–2.39), reversely trapezoid in outline, widest at hinge; ears large, smooth, prominently convex, well differentiated from visceral disk by a groove. Ventral valve moderately to strongly convex; beak slightly incurved, overhanging hingeline; 3 to 4 pairs of hingespines projecting posterolaterally with an angle of 30–50°; cardinal extremities with an angle of 60–70°; sulcus beginning from anterior of umbo, about one third of shell width near anterior margin; costellae beginning from umbo, firstly bifurcated near umbo and secondly bifurcated anteriorly (middle length or anterior margin), numbering 22 to 28 at anterior margin. Dorsal valve moderately concave; median fold weak.

Ventral interior spine canals (the definition see Racheboeuf in Williams et al., 2000) hollow, inclined toward midline along posterior margin and connected to the mantle directly; hingespines projecting posterolaterally (projecting at a reverse direction with the project direction of spine canals, see Fig. 9.31e); median septum short; papillae radially-arranged. Dorsal interior with a pair of distinct inner socket ridges; papillae radially arranged in rows, decreasing in size and increased in rows towards margin (apparently related to the bifurcation of costellae and different from the "*Neochonetes*-like papillae).

Discussion *Waagenites guizhouensis* Liao, 1980a is considered as a synonym of the present species, because its costellae near the margin are prominently bifurcated although the number of bifurcated costellae is less than the holotype of *F. soochowensis* (probably because the "*Waagenites guizhouensis*" specimens are not adults). Additionally, it is difficult to distinguish between "*T.*" *guizhouensis* and "*T.*" *soochowensis*, based on the Categorical Principle Component Analysis (see Fig. 9.29). *Waagenites barusiensis* (Davidson) in Jin et al., 1974 (see pl. 164, Fig. 8) was considered as the holotype of *Tethyochonetes chaoi* Chen et al. 2000 by Chen et al. (2000). This specimen is the external mould of a dorsal valve (because the beak does not overhang the hingeline), from the Lungtan Formation (Wuchiapingian), Wenxing Village, Chongqing, southwestern China. This specimen is featured by costellae prominently widening anteriorly and most like a juvenile of *F. soochowensis*. And thus, the specimen should belong to *F. soochowensis* and *Tethyochonetes chaoi* Chen et al. (2000) could be invalid. *Waagenites barusiensis* (Davidson) in Liao, 1980a (see pl. 5, Fig. 26) was considered as the holotype of *Tethyochonetes*? *liaoi* Chen e al. 2000 in Chen et al. (2000). This specimen is an external mould of a conjoined shell with both valves, but the acute cardinal extremities were not well preserved (indicated by the remanent shell), suggesting that the specimen has a larger shell width to length ratio; and this specimen has bifurcated costellae widening anteriorly. All these features coincide with *F. soochowensis* and thus *Tethyochonetes*? *liaoi* Chen et al. 2000 could be another synonym of *F. soochowensis*.

The present species differs from *Fusichonetes wongiana* (Chao, 1928, p. 28, pl. 1, Fig. 17b) from the Lungtan Formation of Langdai, Guizhou, southwestern China in the latter having a more distinct dorsal fold, a smaller shell width to length ratio and less costellae.

Fusichonetes cheni (Zhang et al., 2013)
Figs. 9.32; 9.33

Fig. 9.32 ***Fusichonetes cheni*** (Zhang et al. 2013). (**a–f**), exteriors of six incomplete ventral valves, XM-1-0375, XM-1-0370, XM-1-0372, XM-1-0379, XM-1-0380, XM-1-0378. (**g**), internal mould of ventral valve and shell remnant, XM-1-0382, showing small papillae on ventral inner surface. (**h**), ventral exterior, showing costellae on the surface XM-7-0368. (**i**), exterior of a deformed ventral valve, XM-7-0374, showing hinge spines. (**j**), exterior of an incomplete ventral valve, XM-10-0376, showing a preserved long hinge spine. (**k**), exterior of a nearly complete ventral valve, XM-1-0367, showing obscure costellae. (**l–n**), exteriors of three complete ventral valves, XM22202, XM23801, XM20-701. (**o**), a conjoined shell (dorsal view), XM20-402, showing a pseudodeltidium (*psd*) on the low, triangular interarea (*iar*)

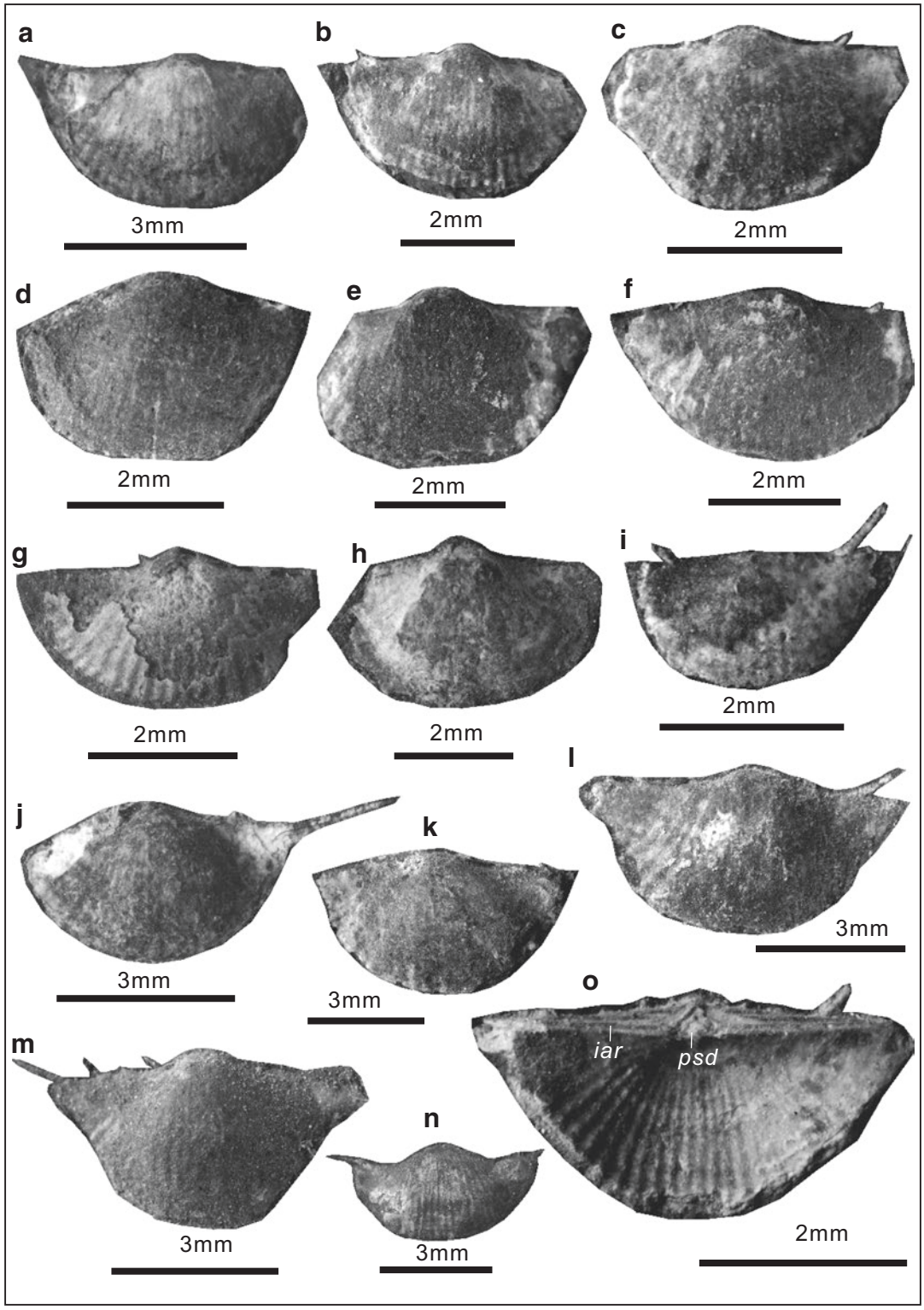
a
3mm
b
2mm
c
2mm
d
2mm
e
2mm
f
2mm
g
2mm
h
2mm
i
2mm
j
3mm
k
3mm
l
3mm
m
3mm
n
3mm
o
iar
psd
2mm

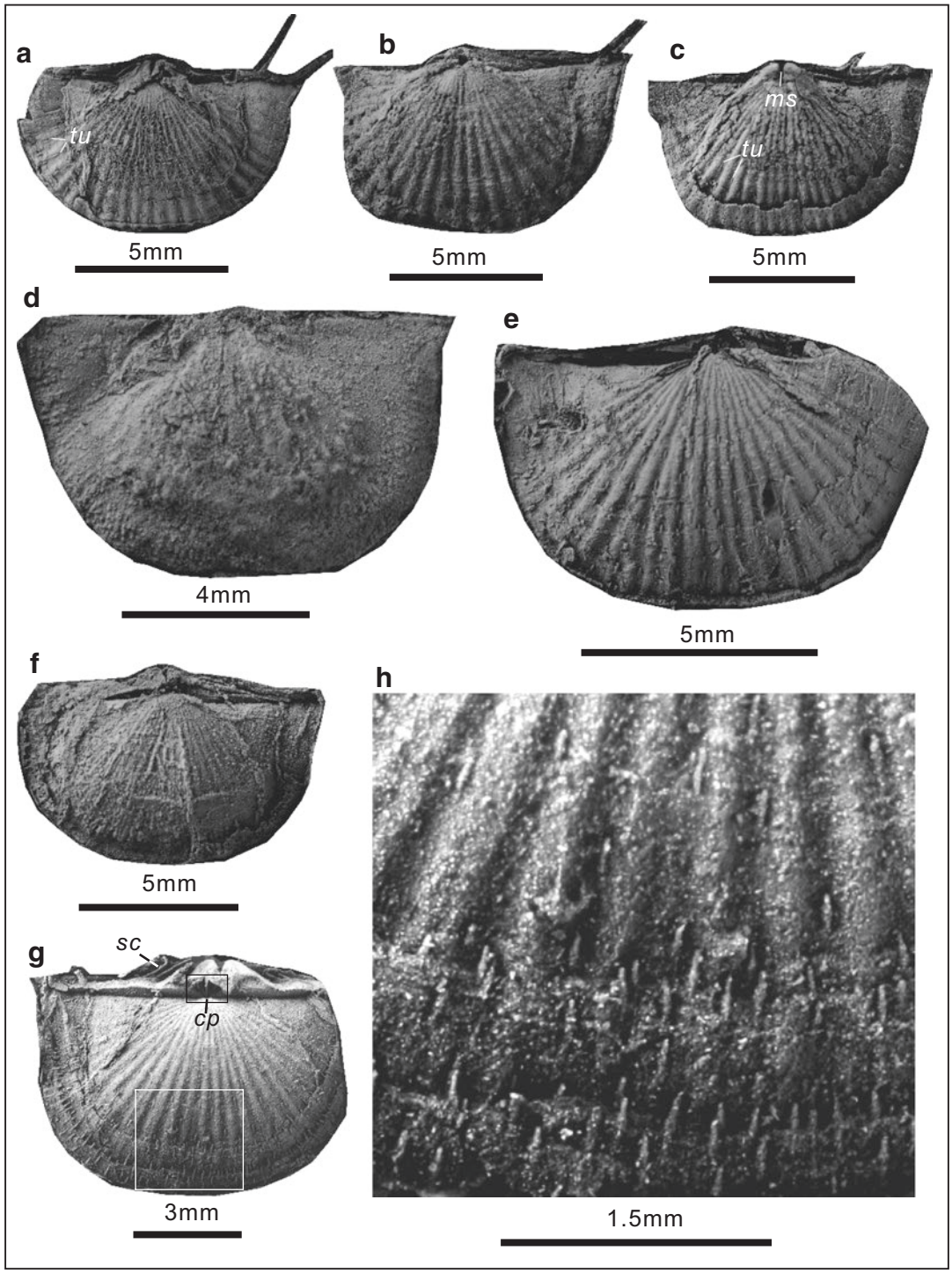

Fig. 9.33 ***Fusichonetes cheni*** (Zhang et al., 2013). (**a**), external mould of a nearly complete dorsal valve, LZ2703265, showing small tubes (*tu*) on dorsal external surface and hinge spines. (**b**), external mould of an incomplete dorsal valve, LZ2706254. (**c**), external mould of a dorsal valve and internal mould of the conjoined ventral valve, LZ2706032, showing small tubes (*tu*) on dorsal external surface, radially-arranged papillae on anterior margin of ventral interior and a median septum (*ms*). (**d**), dorsal interior, showing papillae and elevated muscle scars, LZ2702223. (**e**), external mould of an incomplete dorsal valve, LZ2703266, showing small tubes on dorsal external surface. (**f**), external mould of a dorsal valve and internal mould of the conjoined ventral valve, LZ2701034. (**g**), external mould of a dorsal valve and internal mould of the conjoined ventral valve, LZ2702071, showing small tubes and concentric lamellae on dorsal external surface, quadrilobate cardinal process (*cp*) and spine canals (*sc*). (**h**), enlarged rectangular area of LZ2702071, showing small tubes on dorsal external surface

2013 *Tethyochonetes cheni* (Zhang, He, Shi and Zhang): 234, Figs. 5aa, 5ab, 9a–9k.

Diagnosis Small to medium, transverse or reversely trapezoid; ventral ears variedly convex, dorsal ears nearly flat; cardinal extremities moderately acute, fold absent, strongly convex at about middle shell length (emended after Zhang et al., 2013).

Materials Over 50 specimens. Registered specimens: see below.

Measurements (mm):

Number	Width	Length	Width/ length	Notes
XM-1-0375	4.82	3.01	1.60	Ventral exterior
XM-1-0370	4.70	2.87	1.64	Ventral exterior
XM-1-0372	3.54	2.55	1.39	Ventral exterior
XM-1-0379	4.65	3.14	1.48	Ventral exterior
XM-1-0380	5.78	3.34	1.73	Ventral exterior
XM-1-0378	4.04	2.69	1.50	Ventral exterior
XM-1-0382	4.44	2.69	1.65	Internal mould of ventral valve
XM-7-0368	4.84	3.39	1.43	Ventral exterior
XM-7-0374	2.90	2.03	1.43	Ventral exterior
XM-10-0376	4.99	3.06	1.63	Ventral exterior
XM-1-0367	7.07	4.29	1.65	Ventral exterior
XM22202	3.66	2.55	1.44	Ventral exterior
XM23801	5.89	3.26	1.80	Ventral exterior
XM20-701	4.98	2.65	1.88	Ventral exterior
XM20-402	4.26	2.09	2.04	Dorsal valve
LZ2703265	9.20	5.57	1.65	External mould of dorsal valve
LZ2706254	9.64	5.90	1.63	External mould of dorsal valve
LZ2706032	9.96	6.05	1.65	Internal mould of ventral valve
LZ2702223	9.36	5.79	1.62	Dorsal interior
LZ2703266	9.20	5.79	1.59	External mould of dorsal valve
LZ2701034	9.34	5.33	1.75	Internal mould of ventral valve
LZ2702071	9.63	5.69	1.69	Internal mould of ventral valve

Occurrence Upper Changhsingian; Guizhou (Zhongzhai and Xinmin sections) of southwestern China.

Description Shell 2.0–6.8 mm long and 2.9–10.3 mm wide, reversely trapezoid or transverse in outline, widest at hinge; ears smooth. Ventral valve strongly and evenly convex, highest at about middle shell length; beak incurved, overhanging hingeline; 3 to 4 pairs of hingespines projecting posterolaterally; cardinal extremities with an angle of 55–75°; umbo evenly convex; sulcus absent; costellae beginning from umbo, not bifurcated or rarely bifurcated, round and coarse, numbering 20 to 25 nearby anterior margin. Dorsal valve slightly to moderately concave; cardinal extremities with an angle of 60–90°; microornamented with fine concentric lamellae and very small tubes (marked by *tu*, see Fig. 9.33c, g) along costellae, each tube about 0.3–0.4 mm long and 0.05 mm wide, with a density of 5–6 per mm^2 at anterior (Fig. 9.33h).

Ventral interior spine canals inclined toward midline at about middle part of posterior margin (marked by *sc*, see Fig. 9.33g); interarea low, triangular, with pseudodeltidium (interarea marked by *iar*, pseudodeltidium marked by *psd*, see Fig. 9.32o); median septum anteriorly thinning; papillae radially arrandged, with a density of 15 per mm^2 at anterior. Dorsal interior with a trilobed cardinal process (marked by *cp* in Fig. 9.33g); papillate radially arranged.

Discussion The present species similar to *Fusichonetes soochowensis* (Chao, 1928) from the Permian shale, Yanwashan area, Jiangsu Province, China in a transversely wide outline, but differs in being more convex in the middle shell length, rarely having bifurcated costellae and a lack of sulcus. This species differs from *F. nayongensis* in a lower shell width to length ratio and a larger convexity at middle shell length.

Fusichonetes quadrata (Chan in Hou et al., 1979)
Figs. 9.34, 9.35 and 9.36

1979 *Waagenites soochowensis quadrata* Chan in Hou et al.: 70, pl. 4, Fig. 16–19.
1984 *Waagenites longtanensis* Liao: 279, pl. 1, Fig. 8, 9.
2000 *Tethyochonetes quadrata* (Chan); Chen et al.: 9, Fig. 4a–d, g.
2002 *Tethyochonetes quadrata* (Chan); Shen and Archbold: 339, Fig. 6a–e.
2009b *Tethyochonetes longtanensis* (Liao); Chen et al.: Fig. 7e.
2013 *Tethyochonetes* sp. cf. *T. quadrata* (Chan); Zhang et al.: 233, Fig. 5q–t.
2013 *Tethyochonetes longtanensis* (Liao); Zhang et al.: 227, Fig. 5d–e.
2014 *Tethyochonetes quadrata* (Chan); He et al.: 914, Fig. 4a–h.
2014 *Tethyochonetes longtanensis* (Liao); He et al.: 915, Fig. 4i–o.

Holotype *Waagenites soochowensis quadrata* Chan in Hou et al., 1979, pl. 4, Fig. 17, a ventral valve, from the Shuizhutang Formation, Shuizhutang Village, Lian County, Guangdong Province, South China.

Diagnosis (this paper). Subquadrate (width/length ratio prominently <2), ears slightly convex, ventral valve extremely convex, sulcus varying from indistinct to deep, costellae bifurcated, median septum half of or one third of shell length (on well-preserved specimens).

Materials Over 1000 specimens. Registered specimens: see below.

Measurements (mm):

Number	Width	Length	Width/length	Notes
CM-4-541	8.18	4.80	1.70	Internal mould of ventral valve
CM-4-469	2.68	2.04	1.32	Internal mould of ventral valve
CM-4-471	4.79	3.67	1.30	Internal mould of ventral valve
CM-4-470	4.53	3.72	1.22	Internal mould of ventral valve
CM-4-457	5.69	4.08	1.40	Internal mould of ventral valve
CM-4-458	5.60	3.84	1.46	Internal mould of ventral valve
CM-4-466	7.66	5.27	1.45	Ventral interior
CM2-0321	5.05	3.60	1.40	External mould of dorsal valve
SR20-0325	4.23	3.34	1.27	Ventral exterior
SR20-0323	4.79	3.88	1.23	Ventral exterior
SR20-0324	4.23	3.59	1.18	Ventral exterior
SR20-0340	7.49	5.67	1.32	Ventral exterior
ZZ2702-0327	9.24	6.38	1.45	Internal mould of ventral valve
ZZ2702-0328	7.46	4.79	1.56	Ventral exterior
ZZ2705-0329	8.32	5.58	1.49	Internal mould of ventral valve
ZZ2702-0330	7.86	4.73	1.66	Ventral exterior
ZZ2703-0334	8.24	5.85	1.41	Internal mould of ventral valve
HZS36-0336	6.59	4.52	1.46	Ventral exterior

(continued)

Fig. 9.34 (continued) complete ventral valves, CM-4-457, CM-4-458. (**g**), interior of a nearly complete ventral valve, CM-4-466, showing a thin median septum. (**h**), external mould of an incomplete dorsal valve, CM2-0321, showing the deeply concave dorsal valve and bifurcated costellae. (**i**), exterior of an incomplete ventral valve, SR20-0325, showing bifurcated costellae. (**j**), exterior of a complete ventral valve, SR20-0323, showing two preserved hinge spines. (**k**), exterior of an incomplete ventral valve, SR20-0324. (**l**), exterior of a complete ventral valve, showing costellae, SR20-0440

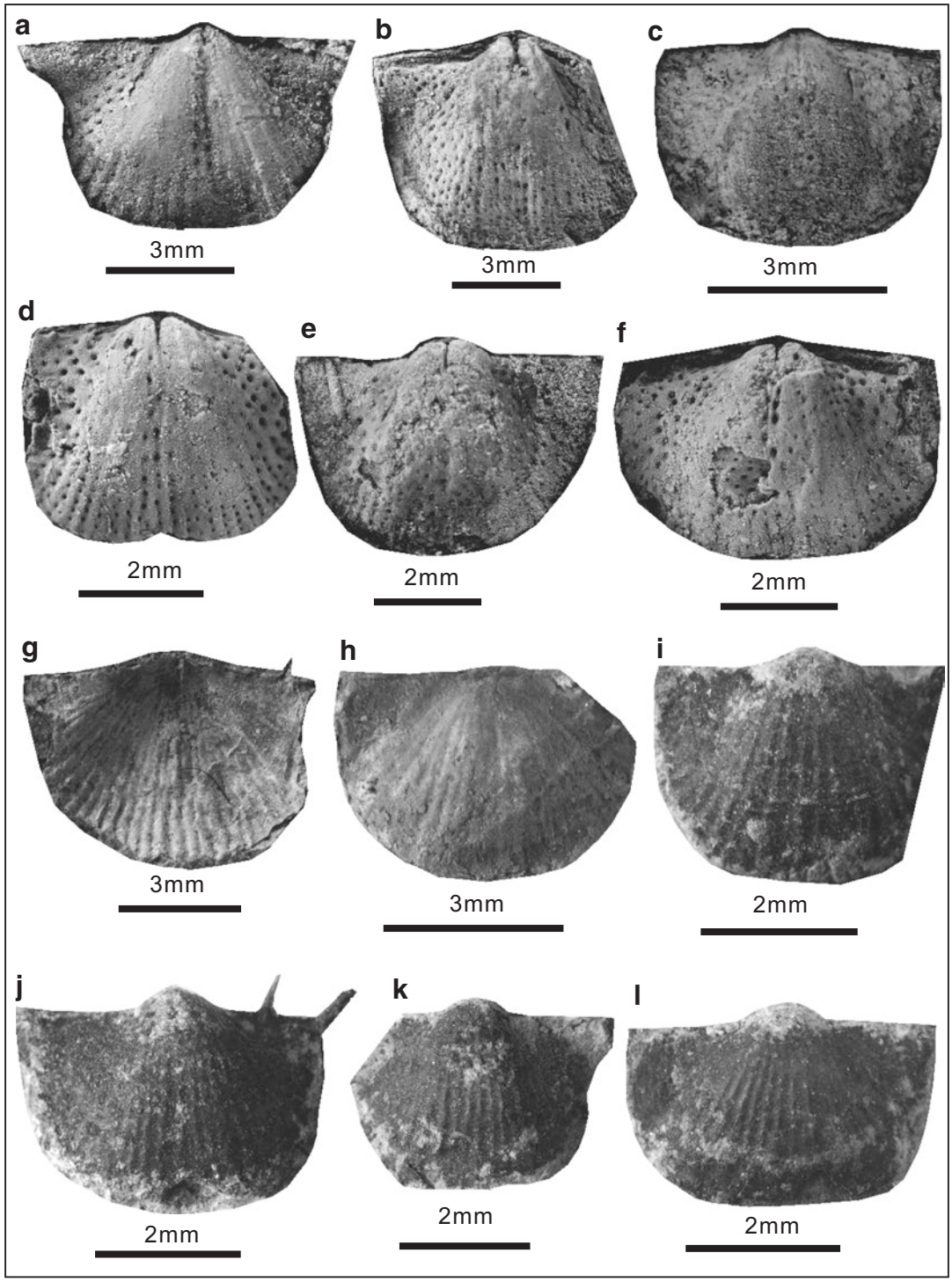

Fig. 9.34 ***Fusichonetes quadrata*** (Chan in Hou et al., 1979). (**a**), internal mould of a complete ventral valve, CM-4-541. (**b**), internal mould of an incomplete ventral valve, CM-4-469, showing radially-arranged papillae and a median septum. (**c**), internal mould of a complete ventral valve, CM-4-471. (**d**), internal mould of an incomplete ventral valve, CM-4-470, showing evenly-arranged papillae and a median septum. (**e**, **f**), internal moulds of two

Number	Width	Length	Width/length	Notes
HZS24-0337	8.88	5.62	1.58	External mould of dorsal valve
HZS24-0338	7.62	5.79	1.32	Dorsal exterior
HZS24-0339	8.55	6.99	1.22	Dorsal exterior
HZS23-0341	6.71	5.67	1.18	Dorsal exterior
HZS27-0343-1	8.01	5.75	1.39	Dorsal exterior
HZS27-0343-2	8.00	4.84	1.65	Dorsal exterior
ZZ2706-0333	10.01	5.81	1.72	Internal mould of ventral valve
LZ0400278	2.45 (ventral)	1.60 (ventral)	1.53 (ventral)	Internal mould of conjoined shell
LZ0400281	2.73 (ventral)	1.59 (ventral)	1.72 (ventral)	Internal mould of conjoined shell (juvenile)
CM-4-460	4.97	3.53	1.41	Internal mould of ventral valve
CM-3-408	3.57	2.26	1.58	Internal mould of dorsal valve
CM-3-409	3.51	2.06	1.70	Internal mould of dorsal valve
CM-10-425	4.73	2.67	1.77	Internal mould of dorsal valve
CM-3-464	4.97	3.10	1.61	Internal mould of dorsal valve
CM-3-465	5.56	3.57	1.56	Dorsal interior
HZS34-0344	7.08	4.50	1.57	Ventral exterior
HZS24-0345	10.01	6.29	1.59	Ventral exterior
HZS31-0347	8.50	6.05	1.40	Ventral exterior
HZS24-0346	9.50	7.61	1.25	Ventral exterior
LZ2705303	6.64	4.57	1.45	Ventral exterior
LZ2701231	9.47	5.66	1.67	Dorsal interior
CM-12-455	5.09	2.83	1.80	Internal mould of dorsal valve

Occurrence Upper Wuchiapingian to Changhsingian; South China.

Description Shell small, 1.6–7.6 mm long and 2.5–10.0 mm wide, subquadrate in outline, widest at hinge; ears acute, slightly convex, gradually differentiated from flanks of ventral disk. Ventral valve strongly convex; beak strongly incurved, overhanging hingeline; umbo extremely convex; sulcus varying from shallow to indistinct; costellae bifurcated, numbering 22 to 30 at anterior margin. Dorsal valve moderately to strongly concave; median fold weak to absent. Ventral interior with spine canals (*sc*) inclined toward midline along posterior margin, a median septum extending to one third of shell length; papillae radially arranged in rows, decreasing in size and increased in rows towards margin (Fig. 9.35m). Dorsal interior with a pair of distinct inner socket ridges (*is* in Fig. 9.36b, l, m).

Fig. 9.35 ***Fusichonetes quadrata*** (Chan in Hou et al., 1979). (**a**), internal mould of a complete ventral valve and shell remnant, ZZ2702-0327, showing papillae and hinge spines. (**b**), exterior of a nearly complete ventral valve, ZZ2702-0328, showing bifurcated costellae. (**c**), external mould of a dorsal valve and internal mould of the conjoined ventral valve, ZZ2705-0329, showing preserved small tubes (near anterior margin) on dorsal valve and a median septum of ventral valve. (**d**), exterior of a complete ventral valve, ZZ2702-0330, showing costellae on the surface and hinge spines. (**e**), internal mould of an incomplete ventral valve and shell remnant, ZZ2703-0334, showing papillae. (**f**), exterior of a ventral valve (not well preserved), HZS36-0336. (**g**), external mould of an incomplete dorsal valve, HZS24-0337, showing bifurcated costellae. (**h**–**k**), exteriors of four nearly complete ventral valves, HZS24-0338, HZS24-0339, HZS23-0341, HZS27-0343-1, showing the varied preservation of costellae (from obscurely to moderately well). (**l**), exterior of a complete dorsal valve and posterior of the conjoined ventral valve, HZS27-0343-2, showing bifurcated costellae. (**m**), internal mould of an incomplete ventral valve, ZZ2706-0333, showing the spine canals (*sc*) inclined toward midline, a median septum and papillae (the papillae near to margins seems to be finer, but differs from the Neochonetes-like papillae and apparently resulted from preservational bias, because the finer-papillae zone is variable in width along margins). (**n**, **o**), internal moulds of two conjoined ventral-dorsal valves, LZ0400278, LZ0400281 (juveniles)

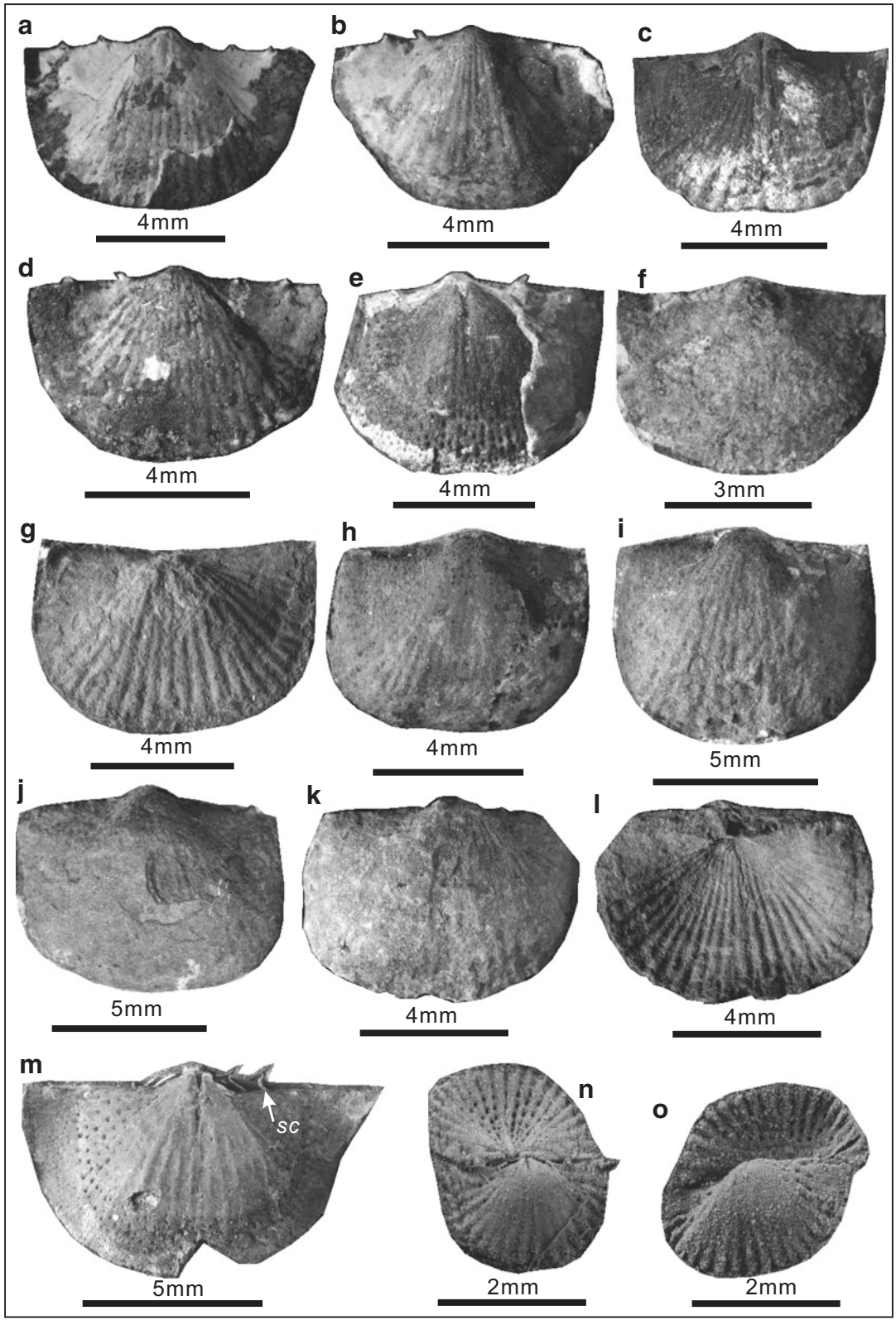
a
4mm
b
4mm
c
4mm
d
4mm
e
4mm
f
3mm
g
4mm
h
4mm
i
5mm
j
5mm
k
4mm
l
4mm
m
sc
5mm
n
2mm
o
2mm

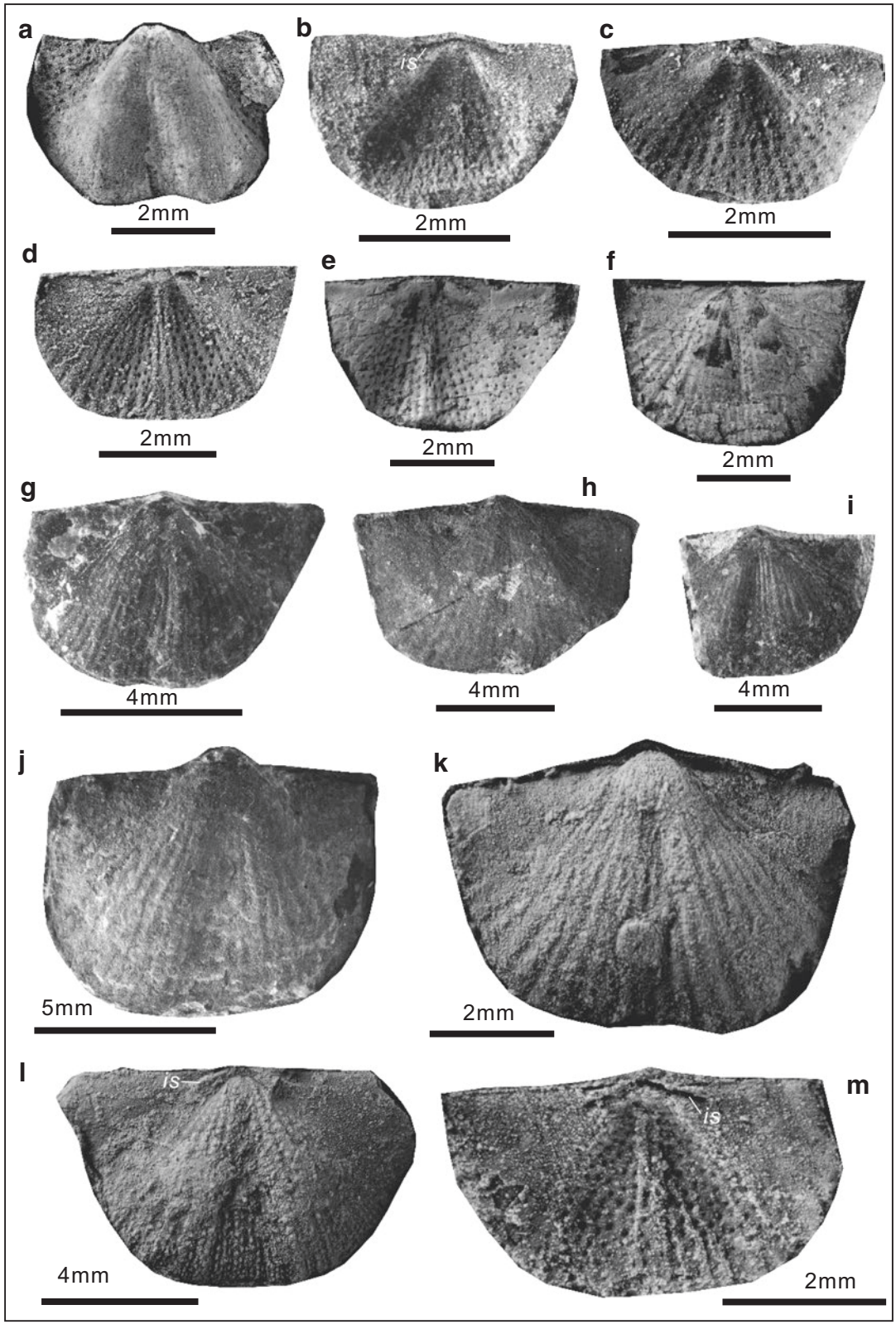
a
2mm
b
is
2mm
c
2mm
d
2mm
e
2mm
f
2mm
g
4mm
h
4mm
i
4mm
j
5mm
k
2mm
l
is
4mm
m
is
2mm

Discussion *Waagenites longtanensis* Liao, 1984 was first defined by Liao in 1984. This species was revised as *Tethyochonetes longtanensis* (Liao, 1984) by Chen et al. (2000), with the proposition of their new genus *Tethyochonetes* (here considered as the junior synonym of *Fusichonetes*, see above). This species has a subquadrate outline, an extremely convex ventral valve and commonly bifurcated costellae. All these features overlap the original description of *F. quadrata* (Chan in Hou et al., 1979), although the latter species additionally was said to have "narrower" ventral sulcus and less bifurcated costellae. However, authors recently observed the holotype specimen (Fig. 9.37) and considered that these small differences are intraspecific variations. On this basis, *Waagenites longtanensis* Liao, 1984 should be regarded as a junior synonym of *F. quadrata* (Chan in Hou et al., 1979). The specimens of *Tethyochonetes* cf. *quadrata* of Zhang et al. (2013, Fig. 5q–t) share features with *Fusichonetes quadrata* (Chan in Hou et al., 1979), including a subquadrate outline, an extremely convex ventral valve, and commonly bifurcated costellae, although the former has a smaller body size (possibly represented by juveniles); thus the former is conspecific with *Fusichonetes quadrata*.

Fusichonetes quadrata is similar to *F. soochowensis* (Chao, 1928) from the Permian shale, Yanwashan area, Jiangsu Province, China in bifurcated costellae, but differs in the former having a subquadrate outline and larger acute-angle cardinal extremities (cardinal angles 70–80°). *Fusichonetes quadrata* shares with *F. convexa* (Fan in Yang et al., 1962, p. 48, pl. 14, Fig. 11–13) from the Upper Permian of Delinha, Qinghai Province, northwestern China a width to length ratio, a strongly convex ventral disk, a deep sulcus, as well as the ornamentation, but may be distinguishable by the latter has a larger body size (twice of the former), a more convex ventral valve and a less curved overhanging beak. *F. quadrata* differs from *F. cheni* in a subquadrate outline, more convex umbo and bifurcated costellae; and from *F. wongiana* (Chao, 1928) of the Wuchiapingian of Guizhou, southwestern China in the latter having a larger ratio of shell width to length (about 2.0).

It is worth noting that the specimens of *Fusichonetes quadrata* from the Changhsingian of Huangzhishan and Zhongzhai in shallow-water facies are commonly larger their counterparts from Majiashan in deep-water facies (see Measurements).

Fusichonetes flatus (Shen and Archbold, 2002) Fig. 9.38

2002 *Tethyochonetes flatus* Shen and Archbold: 342, Fig. 6h–n.
2014 *Tethyochonetes flatus* Shen and Archbold; He et al.: 919, Fig. 6o–b′.

Holotype *Tethyochonetes flatus* Shen and Archbold, 2002, Fig. 6l, external mould of a ventral valve, from the Douling Formation, Xiaoyuanchong section, Jiahe County, Hunan Province, South China.

Fig. 9.36 ***Fusichonetes quadrata*** (Chan in Hou et al., 1979). (**a**), internal mould of an incomplete ventral valve, CM-4-460, showing inflated umbo and deep sulcus. (**b**), internal mould of a nearly complete dorsal valve, CM-3-408, showing a pair of strong inner socket ridges (*is*). (**c**, **d**), internal moulds of two complete dorsal valves, CM-3-409, CM-10-425. (**e**), internal mould of an incomplete dorsal valve, CM-3-464, showing radially-arranged papillae. (**f**), interior of a complete dorsal valve, CM-3-465, showing a few preserved papillae. (**g**), exterior of a complete ventral valve, HZS34-0344, showing weak costellae (due to preservational bias). (**h**), exterior of a nearly complete ventral valve, HZS24-0345, showing weak costellae. (**i**), exterior of an incomplete ventral valve, HZS31-0347. (**j**), exterior of a complete ventral valve, HZS24-0346, showing a deep sulcus and quadrate outline. (**k**), exterior of a nearly complete ventral valve, LZ2705303. (**l**), interior of a nearly complete dorsal valve, LZ2701231, showing papillae arranged in rows (row bifurcated at midlength and anterior and probably corresponding to bifurcated costellae) and prominent inner socket ridges (*is*). (**m**), internal mould of a nearly complete dorsal valve, CM-12-455, showing prominent inner socket ridges (*is*)

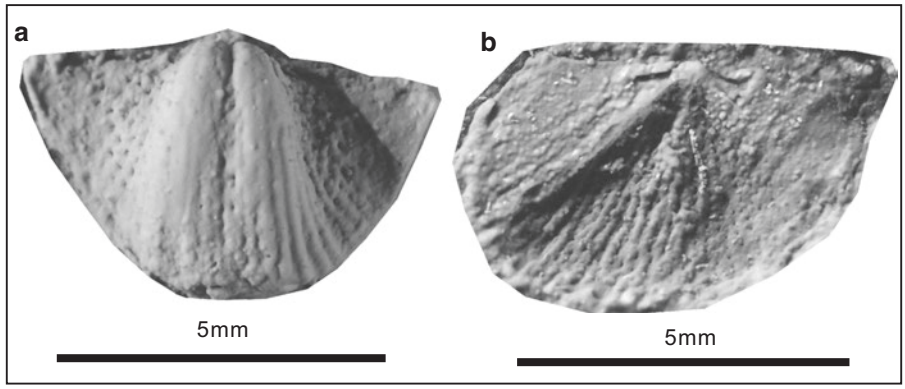

Fig. 9.37 ***Fusichonetes quadrata*** (Chan in Hou et al., 1979). (**a**), internal mould of a slightly deformed ventral valve (previously regarded as the holotype specimen of *Waagenites longtanensis* (Liao, 1984), re-photoed), 71125. (**b**), internal mould of a nearly complete dorsal valve (previously examined as *Waagenites longtanensis* (Liao, 1984), re-photoed), 71124

Diagnosis Very small for the genus, ventral valve nearly flat, ears smooth, costellae simple, 14–17 in numbering, ventral sulcus absent.

Materials Over 100 specimens. Registered specimens: see below.

Measurements (mm):

Number	Width	Length	Width/ length	Notes
CM-12-509	4.87	2.96	1.64	Ventral exterior
CM-12-522	6.42	3.12	2.06	Ventral exterior
CM-12-532	3.69	2.02	1.82	Dorsal interior
CM-12-529	2.84	1.60	1.77	Internal mould of ventral valve
CM-12- 530	5.32	2.52	2.11	Internal mould of ventral valve
CM-12-204	5.50	3.03	1.82	Dorsal interior
SR22-0358	4.65	3.43	1.36	External mould of dorsal valve
CM3-0360	5.39	3.81	1.41	External mould of dorsal valve
CM-12-525	5.29	2.94	1.80	Ventral exterior
CM10-0362	5.09	3.06	1.66	Internal mould of ventral valve
XM9-0357	5.27	3.16	1.67	Ventral exterior
CM14-0361	6.43	3.48	1.85	External mould of ventral valve
CM12-0363	6.10	3.96	1.54	Ventral interior
CM12-0364	7.00	4.29	1.63	Dorsal exterior

Occurrence Changhsingian; South China.

Description Shell 1.6–4.3 mm long and 2.8–7.5 mm wide, subquadrate to reversely trapezoid in outline, widest at hinge; cardinal extremities acute, with an angle of 70–80°. Ventral valve nearly flat, hingespines projecting posterolaterally with an angle of 30–60°; ears flat, smooth, not well differentiated from flanks of ventral disk; sulcus absent; costellae beginning from umbo, rarely bifurcated, round and coarse, numbering 17 to 25 near anterior margin. Dorsal valve flat or slightly concave; fold absent.

Ventral interior spine canals (*sc*) inclined toward midline along posterior margin (Fig. 9.38e); papillae sparse and radially arranged; a thin median septum (Fig. 9.38j, m). Dorsal interior cardinal process pit small; outer sockets coalescing with cardinal process, parallel to hingeline; inner sockets coalescing with cardinal process, extending laterally at an angle of 15° with hingeline (Fig. 9.38f); papillae radially arranged.

Discussion These specimens are nearly identical to *F. flatus* (Shen and Archbold, 2002) from the Douling Formation (Upper Permian) of the Xiaoyuanchong section, Hunan Province, South China in a small size, the absence of both ventral sulcus and dorsal fold, and flat ventral and dorsal valves. Among the present specimens, a few have

more costellae than in the holotype of *F. flatus*, but this may be explained as reflecting a degree of intraspecific variation for the same species from different sedimentary facies. The present species differs from other known species of *Fusichonetes* in its flat ventral and dorsal valves and the absence of sulcus.

Fusichonetes pygmaea (Liao, 1980a)
Figs. 9.39; 9.40

1964 *Chonetes barusiensis* (Davidson); Wang et al.: 240–241, pl. 37, Fig. 27.
1977 *Waagenites barusiensis* (Davidson); Yang et al.: 332, pl. 135, Fig. 4.
1978 *Waagenites barusiensis* (Davidson); Feng and Jiang: 244, pl. 88, Fig. 6.
1979a *Fusichonetes pigmaea* (Liao): pl. 1, Fig. 14.
1980a *Plicochonetes pigmaea* (Liao); Liao: 257, pl, 4, Fig. 4–6.
1980b *Fusichonetes pigmaea* (Liao); Liao: pl. 1, Fig. 5, 6.
1981 *Fusichonetes pigmaea* (Liao); Liao in Zhao et al.: pl. 8, Fig. 7, 8.
1982 *Fusichonetes pigmaea* (Liao); Wang et al.: 200, pl. 96, Fig. 8, 9.
1984 *Waagenites pigmaea* (Liao); Liao: 279, pl. 1, Fig. 7.
1987 *Fusichonetes pigmaea* (Liao); Liao: 100, pl. 3, Fig. 24.
1989 *Waagenites barusiensis* (Davidson); Zhan in Li et al.: pl. 25, Fig. 9.
2013 *Tethyochonetes pygmaea* (Liao 1980); Zhang et al.: 229, Fig. 5f.
2013 *Tethyochonetes chaoi* (Davidson); Zhang et al.: 227, Fig. 5a.
2014 *Tethyochonetes pigmaea* (Liao 1980); He et al.: 918, Fig. 6a–h.
2014 *Tethyochonetes chaoi* (Davidson); He et al.: 915, Fig. 4p–w, b′.

Holotype *Plicochonetes pigmaea* Liao, 1980a, pl. 4, Fig. 6, deposited in the Nanjing Institute of Geology and Palaeontology, Chinese Academy of Sciences, a ventral valve, from Talung Formation (Lopingian), Jiaozishan section, Anshun, Guizhou Province, China.

Diagnosis (this paper). Small, reversely trapezoid (width/length < 2), cardinal extremities generally with an angle of 60–90°, ventral sulcus weak or moderate; costellae simple or slightly bifurcated; ventral median septum short but distinct.

Materials Over 400 specimens. Registered specimens: see below.

Measurements (mm):

Number	Width	Length	Width/length	Notes
SR28-0349-1	7.92	4.74	1.67	Internal mould of ventral valve
SR28-0351	7.45	4.98	1.50	Ventral interior
XM2-0435	3.18	2.39	1.33	External mould of dorsal valve
DDS26-0468	4.73	2.91	1.63	Ventral exterior
DDS26-0470	8.04	4.14	1.94	Internal mould of ventral valve
DDS29-0471	4.72	2.80	1.69	Ventral exterior
DDS29-0472	3.38	2.21	1.53	Ventral exterior
DDS29-0474	4.39	2.26	1.94	Dorsal exterior
DDS29-0475	4.89	3.44	1.42	Dorsal exterior
XM2-0478	5.28	3.23	1.63	Internal mould of ventral valve
SR22-0477	3.01	1.68	1.79	Internal mould of ventral valve
SR22-0479	5.51	3.69	1.49	Internal mould of ventral valve
SR23a-0480	6.55	4.32	1.52	External mould of dorsal valve
SR2202-0489	6.92	3.39	2.04	External mould of dorsal valve
SR2202-0490	4.04	3.77	1.07	Internal mould of dorsal valve
HZS20-0442-1	8.70	5.30	1.64	Ventral exterior
HZS20-0442-2	6.10	3.60	1.69	External mould of dorsal valve
HZS29-0443	8.05	5.33	1.51	Ventral exterior
HZS20-0444	8.76	5.61	1.56	Ventral exterior
HZS24-0445	9.52	6.19	1.54	External mould of dorsal valve
HZS28-0446	7.97	4.86	1.64	Dorsal exterior
ZZ2705-0457	8.50	4.26	2.00	Dorsal internal mould of conjoined shell
ZZ2705-0457	7.73	3.79	2.04	Ventral internal mould of conjoined shell (incomplete)

(continued)

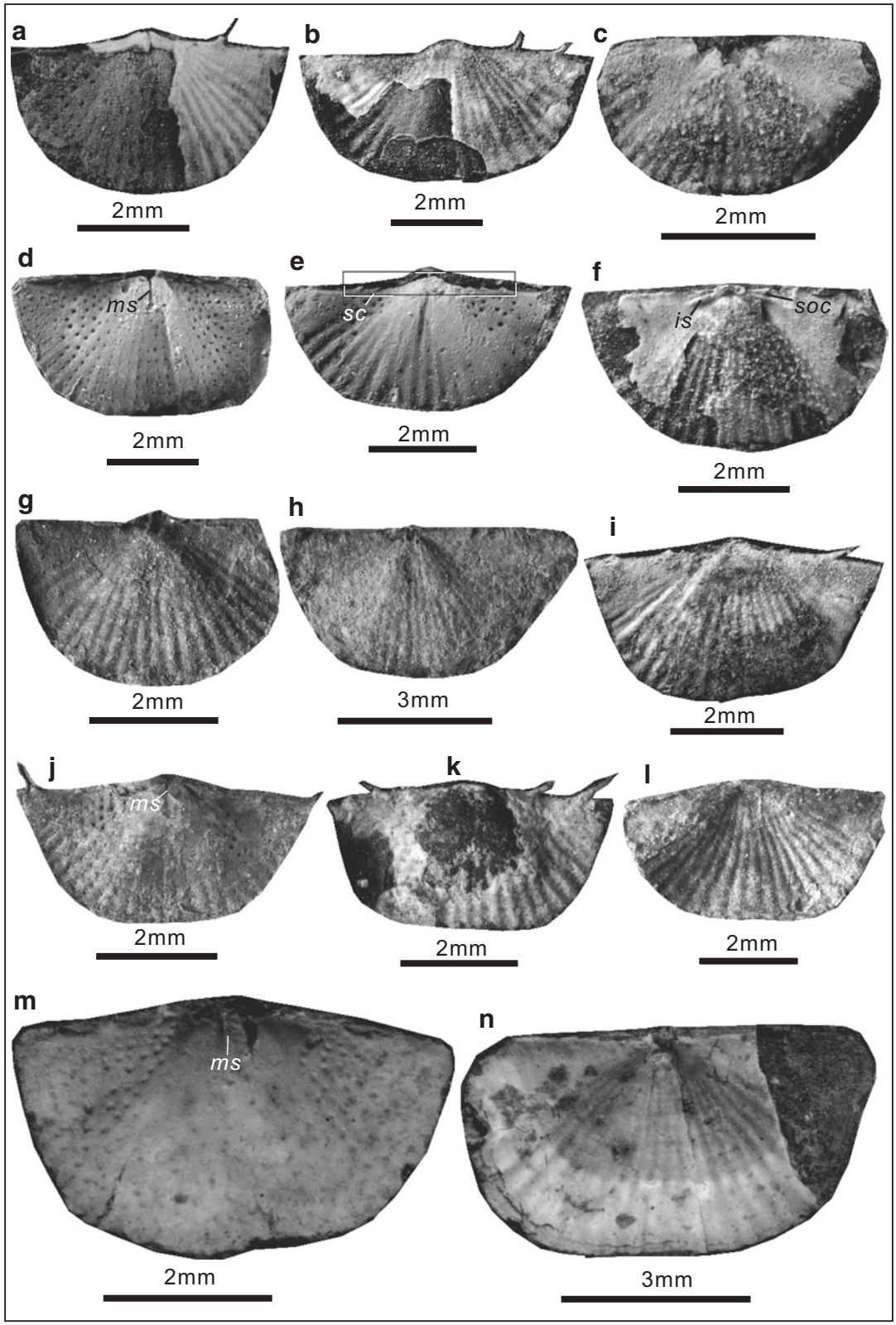
a
2mm
b
2mm
c
2mm
d
ms
2mm
e
sc
2mm
f
is
soc
2mm
g
2mm
h
3mm
i
2mm
j
ms
2mm
k
2mm
l
2mm
m
ms
2mm
n
3mm

Number	Width	Length	Width/ length	Notes
ZZ2701-0454	7.76	4.77	1.63	Ventral exterior
ZZ2705-0455	7.11	4.14	1.72	Internal mould of ventral valve
ZZ2705-0460	7.63	4.08	1.87	External mould of dorsal valve
ZZ6-0456-2	7.15	4.03	1.77	Ventral internal mould of conjoined shell (incomplete)
ZZ6-0456-2	6.65	3.90	1.71	Dorsal internal mould of conjoined shell (incomplete)
ZZ2703-0459	8.98	6.50	1.38	External mould of dorsal valve

Occurrence Changhsingian–lowest Triassic; South China.

Description Shell 1.7–6.5 mm long and 3.0–9.5 mm wide on average, reversely trapezoid or transversely quadrate in outline, widest at hingeline; ears small, triangular, smooth, well differentiated from visceral disk. Ventral valve moderately convex; beak slightly incurved, overhanging hingeline; cardinal extremities with an angle of 80–90°; sulcus present but weak, slightly widening anteriorly; costellae beginning from umbo, simple, numbering 22 to 24 at anterior margin. Dorsal valve slightly concave; median fold weak; microornamented by tubes (*tu*) on well-preserved specimens (Fig. 9.40j).

Ventral interior with a short but distinct median septum (*ms* in Fig. 9.40i, k); papillae radially-arranged, coarser near ears. Dorsal interior with trifid cardinal process (*cp* in Fig. 9.39m); inner socket ridges coarse and coalescing with cardinal process, extending latterally at an angle of 20° to hingeline (Fig. 9.40k); papillae radially-arranged, even in size.

Discussion *Fusichonetes pigmaea* was named by Liao (1979a), without description and holotype but with illustration (Liao, 1979a, pl. 1, Fig. 14, the specimen from the Permian–Triassic interval of Meishan, Zhejiang, South China). As noted by Wu et al. (2017), the lack of description had subsequently resulted in this species being referred to a number of genera: *Plicochonetes* Paeckelmann, 1930 by Liao (1980a, only with a simple description), *Waagenites* Paeckelmann, 1930 by Liao (1984, without description) and *Tethyochonetes* (Chen et al., 2000). Fortunately, Wu et al. (2017) recently clarified this issue.

Fusichonetes pygmaea is more or less similar to *F. cheni* in a reversely trapezoid or transversely quadrate outline, but differs in having a sulcus and a smaller ratio of shell width to length. *Fusichonetes quadrata* has a smaller ratio of shell width to length and bifurcated costellae, when compared with *F. pygmaea*. The flat dorsal and ventral valves and fewer costellae of *F. flatus* clearly separate this species from the

Fig. 9.38 ***Fusichonetes flatus*** (Shen and Archbold, 2002). (**a**), exterior of a complete ventral valve (shell mostly decorticated), CM-12-509, showing a preserved hinge spine. (**b**), exterior of an incomplete ventral valve, CM-12-522. (**c**), interior of a nearly complete dorsal valve, CM-12-532, showing radially-arranged papillae. (**d**), internal mould of a nearly complete ventral valve, CM-12-529, showing a median septum (*ms*) and papillae. (**e**), internal mould of a nearly complete ventral valve, CM-12- 530, showing the spine canals (*sc*) inclined midline. (**f**), interior of a nearly complete dorsal valve, CM-12-204, showing sockets (*soc*) and inner socket ridges (*is*). (**g**), external mould of a nearly complete dorsal valve, SR22-0358, showing costellae. (**h**), external mould of a nearly complete dorsal valve, CM3-0360, showing obscure costellae (due to preservational bias). (**i**), exterior of a complete ventral valve, CM-12-525. (**j**), internal mould of a complete ventral valve, CM10-0362, showing hinge spines, median septum (*ms*) and papillae. (**k**), exterior of a nearly complete ventral valve, XM9-0357, showing hinge spines. (**l**), external mould of a nearly complete ventral valve, CM14-0361, showing coarse, simple costellae. (**m**), interior of a nearly complete ventral valve, CM12-0363, showing papillae and a thin median septum (*ms*). (**n**), exterior of a complete dorsal valve, CM12-0364, showing coarse, simple costellae

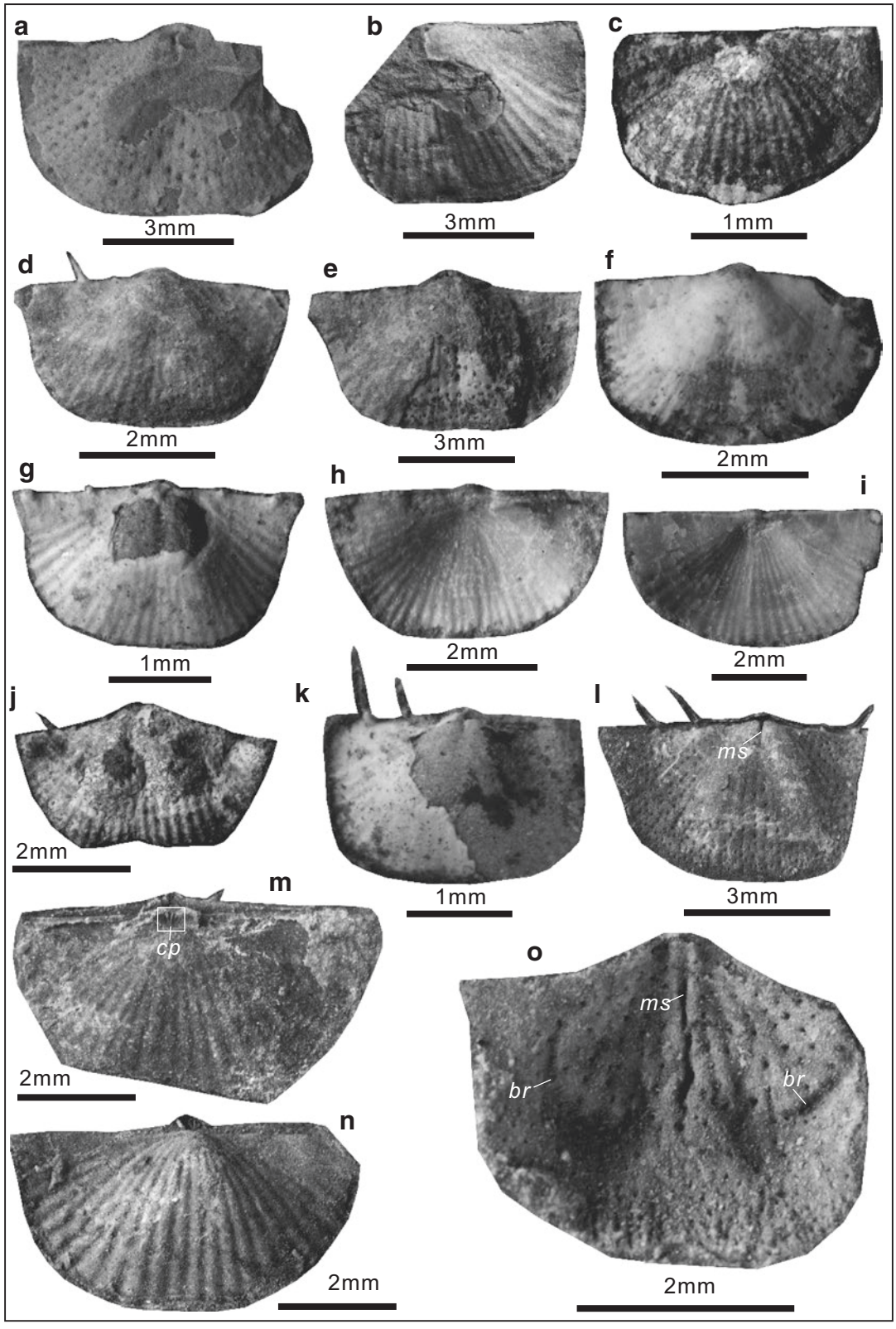
a
3mm
b
3mm
c
1mm
d
2mm
e
3mm
f
2mm
g
1mm
h
2mm
i
2mm
j
2mm
k
1mm
l
ms
3mm
m
cp
2mm
n
2mm
o
ms
br
br
2mm

present species. Both *F. soochowensis* and *F. nayongensis* have a larger shell width to length ratio than in *F. pygmaea*, with *F. soochowensis* being additionally distinguishable by its bifurcated costellae.

Fusichonetes rectangularis (He and Shi in He et al., 2014)
Fig. 9.41

2014 *Tethyochonetes rectangularis* He and Shi in He et al.: 915, Fig. 7a–j.

Holotype *Tethyochonetes rectangularis* He and Shi in He et al., 2014, Fig. 7b, deposited in the Laboratory of Geobiology, Faculty of Earth Sciences, China University of Geosciences, Wuhan, People's Republic of China, external mould of a dorsal valve, from upper part of the Talung Formation (uppermost Changhsingian), Majiashan section, Chaohu, Anhui Province, China.

Diagnosis Small and transversely rectangular (width twice of length) in outline. Ventral valve slightly convex; cardinal extremities nearly right-angled or large acute-angled; median sulcus shallow, beginning to rapidly widen from anterior of umbo. Dorsal valve slightly concave; median fold weak, rapidly widening from anterior of umbo. Costellae simple, rarely bifurcated.

Materials Eight registered specimens: see below.

Measurements (mm):

Number	Width	Length	Width/ length	Notes
CM-14-91	10.95	6.07	1.80	External mould of dorsal valve
CM-13-350	5.25	2.73	1.92	Ventral exterior
SR-23-393	5.90	2.81	2.10	Internal mould of ventral valve
CM-12-359	5.63	3.23	1.75	Internal mould of ventral valve
CM-14-355	7.21	4.27	1.69	Ventral interior
CM-12-357	8.04	4.06	1.98	Ventral interior
CM-14-358	7.86	4.16	1.89	Ventral interior
CM-12-354	7.15	3.62	1.98	Ventral interior

Occurrence Changhsingian; South China.

Description Shell small to medium for genus, 2.7–6.1 mm long and 5.3–12.0 mm wide, transversely rectangular, greatest width at hinge. Ventral valve slightly convex, beak small, slightly overhanging hingeline; ears large, flat or slightly convex; cardinal extremities sub-quadrate, cardinal angle 70–90°; median sulcus shallow, widening anteriorly from umbo. Dorsal slightly concave, median fold weak, widening anteriorly from umbo; costellae simple, rarely bifurcated, numbering 20–24 nearby anterior margin. Ventral median septum short, distinct; radially-arranged papillae covering the ventral interior. Dorsal median septum short, distinct.

Discussion *Fusichonetes rectangularis* is somewhat similar to species of *Neochonetes* Muir-Wood, 1962 in a transversely rectangular outline,

Fig. 9.39 ***Fusichonetes pygmaea*** (Liao, 1980a). (**a**), internal mould of an incomplete ventral valve, SR28-0349-1, showing radially-arranged papillae. (**b**), interior of the incomplete ventral valve, SR28-0351 (= SR28-0349-1). (**c**), external mould of a complete dorsal valve, XM2-0435, showing simple costellae. (**d**), exterior of a complete ventral valve, DDS26-0468. (**e**), internal mould of a complete ventral valve and shell remnant, DDS26-0470, partly showing papillae. (**f**), exterior of an incomplete ventral valve, DDS29-0471, showing weak costellae. (**g**), exterior of a complete ventral valve, DDS29-0472, showing bases of hinge spines. (**h**), exterior of a complete dorsal valve, DDS29-0474, showing linear interarea. (**i**), exterior of a complete dorsal valve, DDS29-0475. (**j**), internal mould of a slightly deformed but nearly complete ventral valve and shell remnant, XM2-0478. (**k**), internal mould of a nearly complete ventral valve and shell remnant, SR22-0477, showing weak costellae. (**l**), internal mould of an incomplete ventral valve, SR22-0479, showing a median septum (*ms*), hinge spines and papillae. (**m**), external mould of an incomplete dorsal valve, SR23a-0480, showing a quadrilobate cardinal process (*cp*). (**n**), external mould of a nearly complete dorsal valve, SR2202-0489, showing simple costellae. (**o**), internal mould of an incomplete dorsal valve, SR2202-0490, showing a long median septum (*ms*) and scars of brachial ridges (*br*)

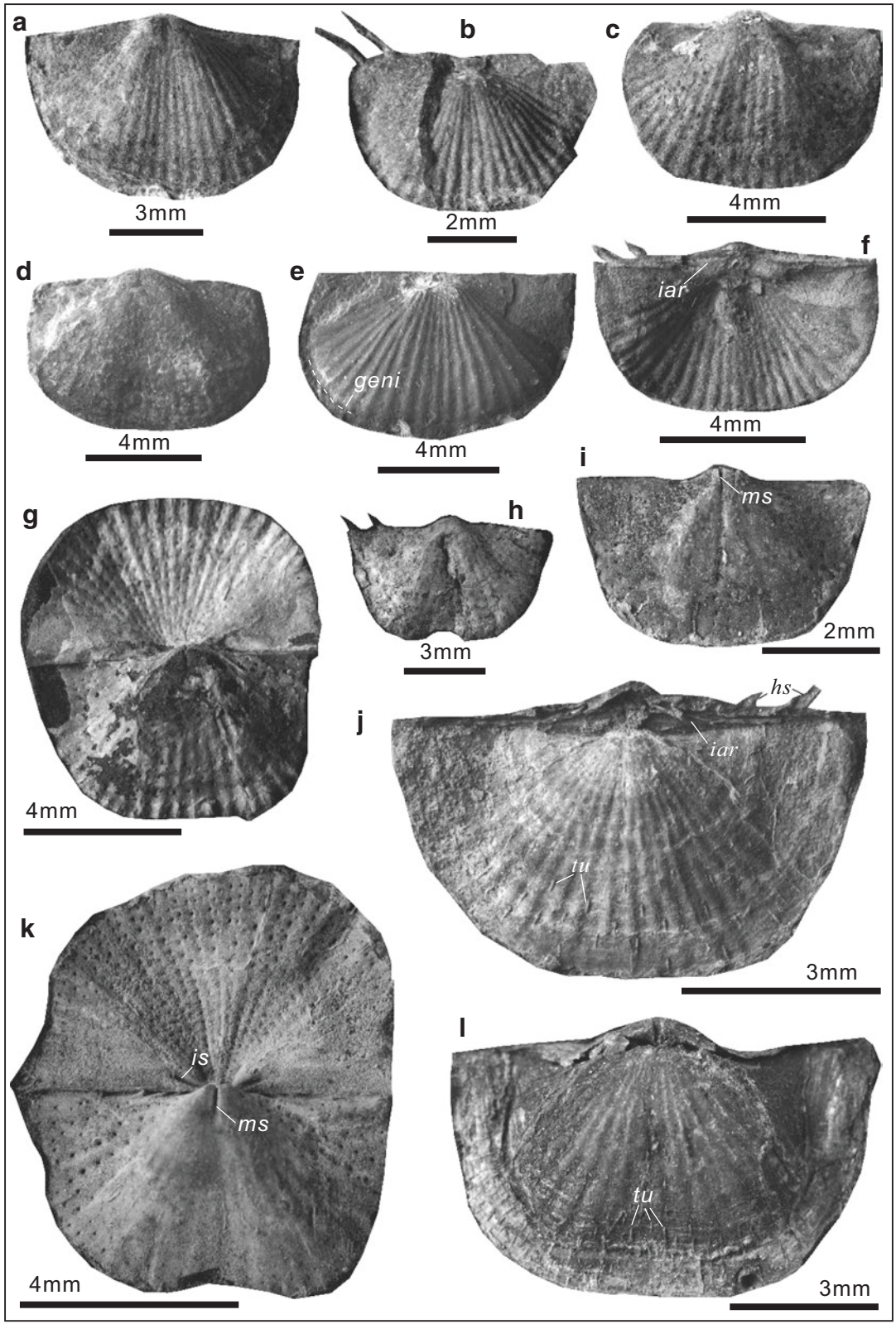
a
3mm
b
2mm
c
4mm
d
4mm
e
geni
4mm
f
iar
4mm
g
4mm
h
3mm
i
ms
2mm
j
hs
iar
tu
3mm
k
is
ms
4mm
l
tu
3mm

but differs from *Neochonetes* in the details of its ventral interior, characterized by lacking parallel lateral septa and absence of *Neochonetes*-like papillae. The present species resembles to *Fusichonetes nayongensis* (Liao, 1980a) in a strongly transverse outline, slightly convex ventral valve, rarely bifurcated costellae, but differs from the latter in having sub-quadrate cardinal extreminites and a more prominent sulcus. This species is more or less similar to *Fusichonetes soochowensis* (Chao, 1928, p. 31, pl. 1, Fig. 14–16) in a transverse outline, but the former has sub-quadrate cardinal extreminites and simple costellae.

Fusichonetes sinuata (He and Shi in He et al., 2014)
Fig. 9.42

2014 *Tethyochonetes*? *sinuata* He and Shi in He et al.: 921, Fig. 7k–m.

Diagnosis Small, reversely trapezoid in outline. Ventral valve strongly and evenly convex; cardinal extremities acute; median sulcus narrow, deep, slightly widening anteriorly, beginning from the anterior of umbo. Dorsal slightly and evenly concave, median fold narrow but distinct. Costellae straight, begin to bifurcate nearby beak.

Materials Four specimens. Registered specimens: see below.

Measurements (mm):

Number	Width	Length	Width/ length	Notes
CM-10-16	7.93	4.34	1.83	Internal mould of dorsal valve
CM-10-27	7.51	4.01	1.87	External mould of dorsal valve
HZS19-0605	3.39	2.30	1.47	Dorsal interior

Occurrence Changhsingian; South China.

Description Reversely trapezoid, greatest width at hinge; shell 2.3–6.7 mm long and 3.4–12.7 mm wide. Dorsal valve slightly concave, median fold narrow, distinct, slightly widening anteriorly to about one fifth of shell width, costellae bifurcated from umbo, numbering 29 at anterior. Dorsal median ridge weak but extending anteriorly to one third of shell length; sockets shallow; inner socket ridges coarse, extending latterally at an angle of 25° to hingeline; radially-arranged papillae covering dorsal interior, papillae absent towards ears.

Discussion Although He et al. (2014) described these specimens as having "*Neochonetes*-like" papillae in the dorsal interior, here we still think the species is best to be placed in *Fusichonetes*. The reason is that the presence of "*Neochonetes*-like" papillae may be due to varied preservation (see Fig. 9.42a, c), rather than typical *Neochonetes*-like papillae (because these papillae near the margins do not form a prominent

Fig. 9.40 ***Fusichonetes pygmaea*** (Liao, 1980a). (**a**), exterior of a complete ventral valve, HZS20-0442-1, showing well-preserved costellae. (**b**), external mould of a nearly complete dorsal valve and remnant of the conjoined ventral valve, HZS20-0442-2, showing the preserved two hinge spines. (**c**), exterior of a complete ventral valve, HZS29-0443. (**d**), exterior of a complete ventral valve, HZS20-0444, showing obscure costellae (due to badly preserved). (**e**), external mould of a nearly complete dorsal valve, HZS24-0445, showing well-preserved costellae and a geniculation (*geni*). (**f**), exterior of a complete dorsal valve and posterior of the conjoined ventral valve (dorsal view), HZS28-0446, showing a narrow interarea (*iar*). (**g**), internal mould of a nearly complete ventral and internal mould of the conjoined dorsal valve (shell remnant observed), ZZ2705-0457, showing radially-arranged papillae. (**h**), exterior of a deformed ventral valve, ZZ2701-0454, showing the preserved two hinge spines. (**i**), internal mould of a complete ventral valve, ZZ2705-0455, showing a median septum (*ms*). (**j**), external mould of a complete dorsal valve and posterior of the conjoined ventral valve (dorsal view), ZZ2705-0460, showing small tubes (*tu*), interarea (*iar*) and hinge spines (*hs*). (**k**), internal mould of an incomplete ventral valve and internal mould of the conjoined dorsal valve, ZZ6-0456-2, showing a ventral median septum (*ms*) and inner socket ridges (*is*). (**l**), external mould of a complete dorsal valve and posterior of internal mould of the conjoined ventral valve, ZZ2703-0459, showing small tubes (*tu*) and concentric lamellae near margins

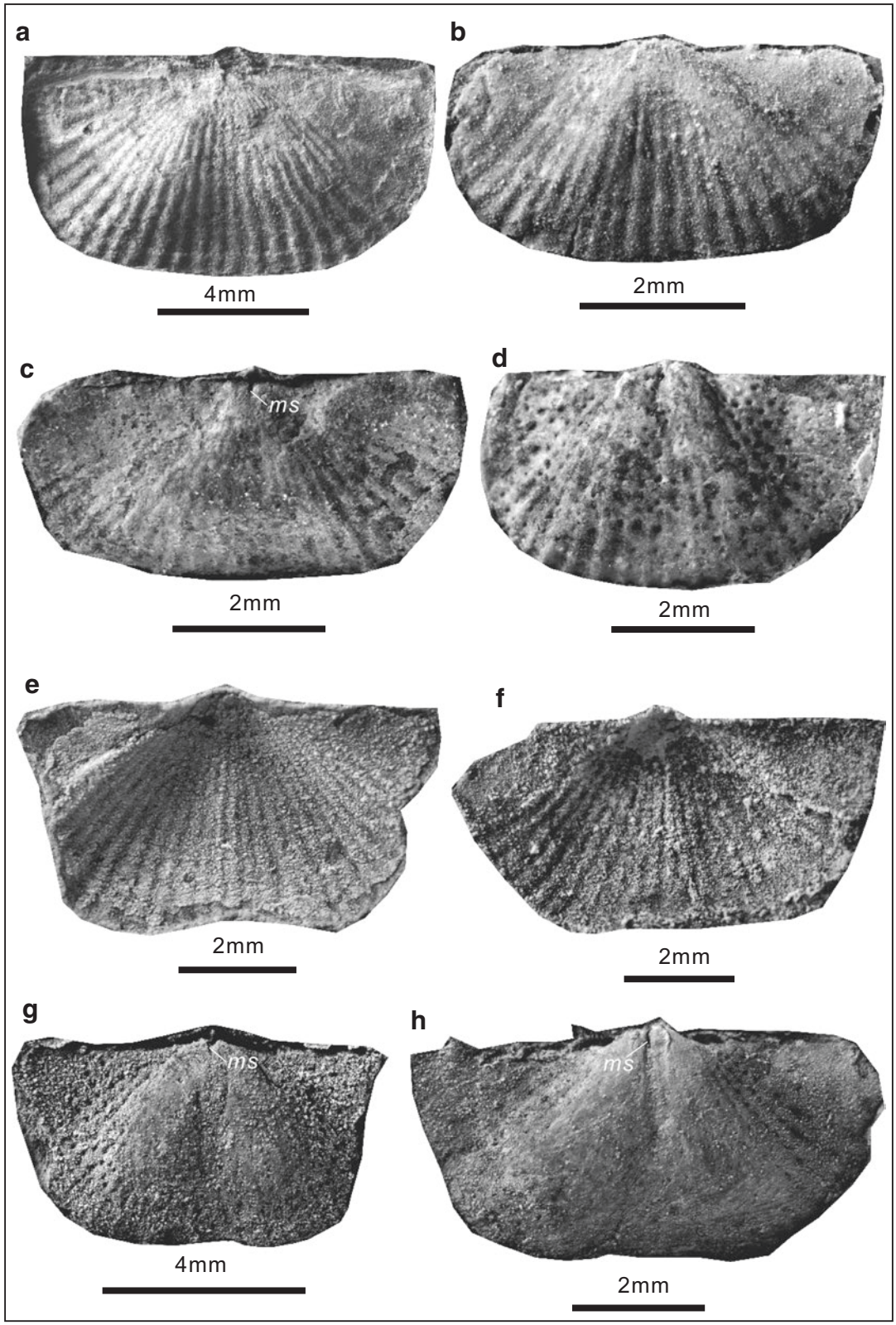
a
4mm
b
2mm
c
ms
2mm
d
2mm
e
2mm
f
2mm
g
ms
4mm
h
ms
2mm

band). Additionally, the reversely trapezoid outline and the internal feature of these specimens are more typical of *Fusichonetes*. This species differs from all other species of *Fusichonetes* by its narrow but distinct dorsal fold.

Genus ***Neochonetes*** Muir-Wood, 1962

Type Species *Chonetes dominus* King, 1938. Upper Carbonaceous Marble Falls limestone; West Texas.

Diagnosis (emended). Transversely quadrate in outline, plano- to moderately concavo-convex in profile. Ventral interior generally with a median septum or median ridge; lateral septa parallel, usually extending anteriorly to a half of shell length; papillae covering ventral interior, increasing in number and decreasing in size towards margin (Densy papillae arranged around margins and formed a band, unique to this genus, described as "*Neochonetes*-like papillae" by He et al., 2014). Dorsal interior with prominent inner socket ridges; generally with a median septum or median ridge, extending anteriorly to two thirds of shell length; lateral septa short, distinct; papillae similar to ventral interior.

Discussion *Neochonetes* differs from both *Rugaria* Cooper and Grant, 1969 from the Permian (Asselian) of Hess Canyon and *Waterhouseiella* Archbold, 1983 from the Permian of Southern Thailand in its finer costellae. Additionally, *Waterhouseiella* with a stout dorsal median septum is easily distinguished with *Neochonetes* which lacks a dorsal median septum. Six subgenera, *N.* (*Neochonetes*) Muir-Wood, 1962; *N.* (*Huangichonetes*) Shen and Archbold, 2002; *N.* (*Nongtaia*) Archbold, 1999; *N.* (*Sommeriella*) Archbold, 1982; *N.* (*Zechiella*) Archbold, 1999 and *N.* (*Zhongyingia*) Shen and Archbold, 2002, have been included in *Neochonetes*. Four of these, *N.* (*Nongtaia*), *N.* (*Sommeriella*), *N.* (*Zechiella*) and *N.* (*Neochonetes*), all have nearly quadrate cardinal extremities and are thus easily distinguished from other two subgenera, *N.* (*Zhongyingia*) and *N.* (*Huangichonetes*) (Fig. 9.43). The ornamentation of *N.* (*Nongtaia*), *N.* (*Sommeriella*), *N.* (*Zechiella*) and *N.* (*Neochonetes*) are different to each other (Fig. 9.43). *N.* (*Zhongyingia*) has a broad, shallow sulcus and fasciculatedly bifurcated costellae and thus slightly differs from *N.* (*Huangichonetes*) which has a moderately wide (rapidly widening anteriorly) sulcus and evenly bifurcated costellae (Fig. 9.43).

Subgenus ***Neochonetes*** (***Huangichonetes***) Shen and Archbold, 2002

Type Species *Chonetes substrophomenoides* Huang, 1932. Upper Permian; South China.

Diagnosis Small *Neochonetes*, reverse trapezoid in outline, cardinal extremities acute (ears small, acute), disk strongly convex, sulcus moderately wide, costellae fine, numbering 30–50 near margin. Ventral interior with a very short median septum.

Neochonetes (***Huangichonetes***) ***substrophomenoides*** (Huang, 1932)
Fig. 9.44

1932 *Chonetes substrophomenoides* Huang: 3, pl. 1, Fig. 3–7.
1964 *Chonetinella substrophomenoides* (Huang); Wang et al.: 243, pl. 37, Fig. 31.
1977 *Neochonetes substrophomenoides* (Huang); Yang et al.: 331, pl. 135, Fig. 20.
1978 *Chonetinella substrophomenoides* (Huang); Feng and Jiang: 242, pl. 88, Fig. 1.

Fig. 9.41 ***Fusichonetes rectangularis*** (He and Shi in He et al., 2014). (**a**), external mould of a complete dorsal valve, CM-14-91, showing simple costellae and concentric fila. (**b**), exterior of a nearly complete ventral valve, CM-13-350. (**c**), internal mould of a nearly complete ventral valve, SR-23-393, showing a short median septum (*ms*). (**d**), internal mould of a nearly complete ventral valve, CM-12-359, showing papillae. (**e**, **f**), interiors of two incomplete ventral valves, CM-14-355, CM-12-357. (**g**, **h**), internal moulds of two nearly complete ventral valves, CM-14-358, CM-12-354, showing a short median septum (*ms*) for each specimen

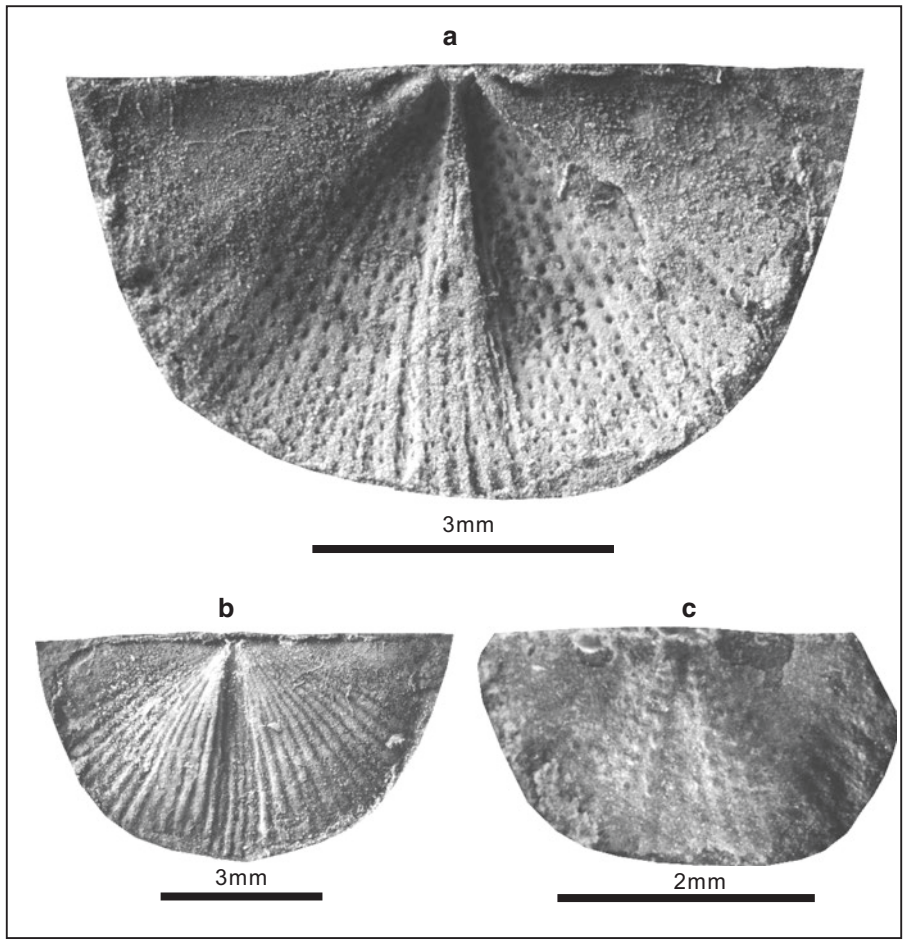

Fig. 9.42 ***Fusichonetes sinuata*** (He and Shi in He et al., 2014). (**a**), internal mould of a complete dorsal valve, CM-10-16. (**b**), listed as holotype by He et al., 2014, external mould of a complete dorsal valve, CM-10-27, showing a distinct, narrow median fold. (**c**), interior of a nearly complete dorsal valve, HZS19-0605, showing radially-arranged papillae

Subgenus	Cardinal extremity	Ventral sulcus	Median septum	Papillae	Ornament	Sketch of outline
N. (*Nongtaia*) Archbold, 1999	Quadrate	Distinct, narrow	Long	Distinct	Costellae	
N. (*Sommeriella*) Archbold, 1982	Quadrate	Moderately wide	Long	Distinct	Capillae	
N. (*Zechiella*) Archbold, 1999	Quadrate	Absent	?	Obsole-scent	Poorly developed	
N. (*Neochonetes*) Muir-Wood, 1962	Quadrate	Weak, only at anterior margin	Long	Distinct	Fine costellae	
N. (*Zhongyingia*) Shen and Archbold, 2002	More acute	Broad, shallow	Long	Distinct	Costellae fasciculatedly bifurcated	
N. (*Huangichonetes*) Shen and Archbold, 2002	Acute	Moderately wide	Short	Distinct	Costellae	

Fig. 9.43 Comparison of six subgenera of *Neochonetes*

1979 *Neochonetes sublatesinuata* Chan in Hou et al.: 70, pl. 11, Fig. 5, 6, 8.
1980a *Neochonetes elegans* Liao: 257, pl. 5, Fig. 1–3.
1982 *Neochonetes substrophomenoides* (Huang); Wang et al.: 200, pl. 96, Fig. 10, 11.
1987 *Neochonetes substrophomenoides* (Huang); Xu in Yang et al.: 221, pl. 9, Fig. 14–20, 26, 27.
1987 *Neochonetes convexa* Liao; Xu in Yang et al.: 221, pl. 9, Fig. 25; pl. 10, Fig. 7, 9.
1989 *Neochonetes* cf. *substrophomenoides* (Huang); Zhan in Li et al.: pl. 25, Fig. 16.
2002 *Neochonetes* (*Huangichonetes*) *substrophomenoides* (Huang); Shen and Archbold: 337, Fig. 5e–j, l, m.
2013 *Neochonetes* (*Huangichonetes*) *substrophomenoides* (Huang, 1932); Zhang et al.: Fig. 9m–p, x, z.
2013 *Neochonetes* (*Huangichonetes*) *archboldi* Zhang et al.: Figs. 9aa, 11a–l, 11n–o.
2013 *Neochonetes* (*Sommeriella*) *strophomenoides* (Waagen); Zhang et al.: Fig. 11r.
2013 *Neochonetes* (*Zhongyingia*) *zhongyingensis* Liao; Zhang et al.: Fig. 12x.

Materials Over 1000 specimens. Registered specimens: see below.

Measurements (mm):

Number	Width	Length	Width/ length	Notes
LZ0400110	13.95	7.62	1.83	Ventral internal mould of a conjoined shell
LZ2702387	15.33	8.51	1.80	Internal mould of ventral valve
LZ1400530	14.46	8.59	1.68	Internal mould of ventral valve
LZ2705142	10.70	6.78	1.58	External mould of dorsal valve
LZ1400368	11.24	7.05	1.59	Internal mould of ventral valve
LZ2704059	9.79	6.45	1.52	Internal mould of ventral valve
LZ2704108	11.76	6.58	1.79	External mould of dorsal valve
LZ2705143	10.34	5.93	1.74	External mould of dorsal valve
LZ2703148	10.73	6.03	1.78	External mould of dorsal valve

Occurrence Changhsingian; China.

Description Reverse trapezoid in outline, greatest width at hingeline; medium size for the subgenus, 5.3–9.5 mm long and 9.2–15.3 mm wide; cardinal extremities with an angle *ca* 60–70°; ears slightly inflated, well demarcated from visceral region.

Ventral valve strongly convex; beak slightly extending beyond hingeline; sulcus originating from umbo anterior, widening and deepening anteriorly; four pairs of hingespines: the pairs close to midhingeline projected initially posteromedially, then changed direction and projected posterolaterally; the pairs close to cardinal extremities directly projected posterolaterally (Fig. 9.44b). Dorsal valve strongly concave; costellae fine, rounded, commonly bifurcating, 35–40 near anterior margin; very small tubes (*tu*) along costellae and open posteriorly (Fig. 9.44h, i), about 0.2–0.3 mm long and 0.05 mm cross, with a density of 7–8 per mm^2 at anterior.

Ventral interior with a median septum; papillae, radially arranged, increasing in number but distinctly decreasing in size towards margin (so called "*Neochonetes*-like papillae"), with a density of 13–14 per mm^2 at midvalve and 32–36 per mm^2 at anterior (Fig. 9.44a, b).

Discussion The specimen of *Neochonetes* (*Sommeriella*) *strophomenoides* of Zhang et al. (2013, Fig. 11r) has acute cardinal extremities (trimmed it as to having quadrate cardinal extremities by Zhang et al. 2013), unparallel lateral margins and a moderately wide fold, and so should be assigned to the present species. *Neochonetes* (*Huangichonetes*) *archboldi* Zhang et al., 2013 is synonymous with the present species, because they have many common features, including a reverse trapezoidal outline, acute cardinal extremities, a moderately wide sulcus and similar costellae. *Neochonetes* (*Zhongyingia*) *zhongyingensis* of Zhang et al. (2013, Fig. 12x) has a more convex ventral valve and a more concave dorsal valve and thus more possibly coincides with the present species.

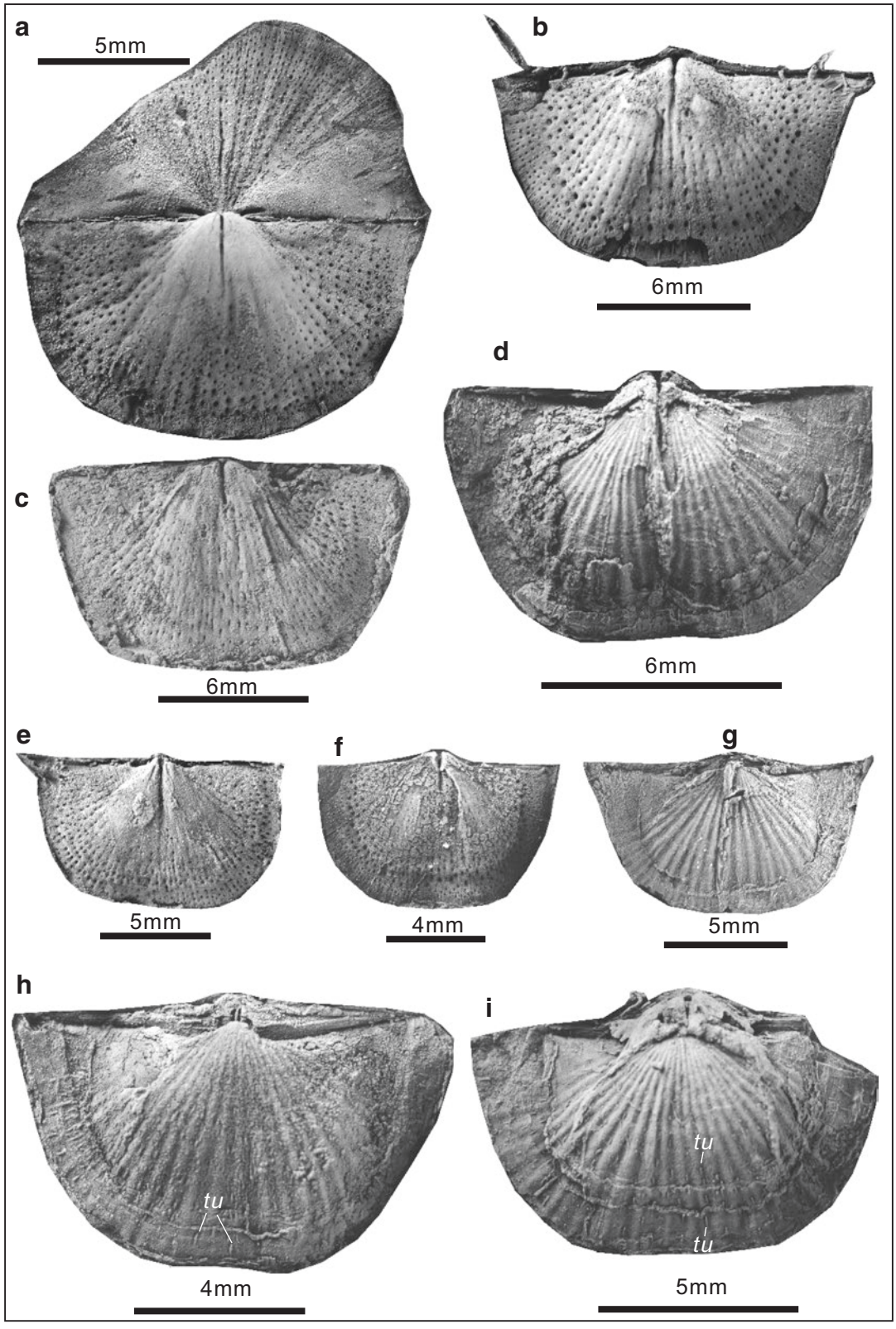
a
5mm
b
6mm
c
6mm
d
6mm
e
5mm
f
4mm
g
5mm
h
tu
4mm
i
tu
tu
5mm

Neochonetes (*Huangichonetes*) *inflatus* Shen in Shen et al., 2002 from the Middle Permian Yongde Formation of western Yunnan, China differs from the present species in having finer costellae and slightly larger cardinal angles (about 85–87°), and that the former was considered to have a hingeline shorter than greatest shell width (this case actually due to preservation bias, e.g., if referred to Fig. 3.1 of Shen et al., 2002, then the greatest width of the shell at hingeline). The present species is easily distinguished from *Neochonetes* (*Huangichonetes*) *geniculatus* Campi and Shi, 2005 from the Changhsing Formation and lowermost Feixianguan Formation (Changhsingian) of Sichuan Province, China in the latter having a geniculate ventral valve and smaller body size.

Subgenus ***Neochonetes*** (***Sommeriella***) Archbold, 1982

Type Species *Chonetes prattii* Davidson, 1859. Sakmarian; Western Australia.

Diagnosis Medium to large for *Neochonetes*, transversely quadrate in outline, cardinal extremities quadrate; disk strongly convex; sulcus prominent, moderately wide; fine capillae or costellae. Ventral interior with a long median septum, extending to a half of midlength; a pair of parallel vascular trunks, closely positioned each side of median septum. Dorsal interior with a long median septum, extending to/over a half of midlength; a pair of short lateral septa anteriorly diverged.

Neochonetes (***Sommeriella***) ***wufengensis*** (He and Shi in He et al., 2014)
Fig. 9.45a–e

2014 *Neochoetes* (*Huangichonetes*?) *wufengensis* He and Shi in He et al.: 927, Fig. 9h–l.

Materials Over 20 specimens. Registered specimens: DCB-34-395, DCB-35-398, DCB-35-399, DCB-35-400, DCB-34-394.

Measurements (mm):

Number	Width	Length	Width/ length	Notes
DCB-34-395	7.54	4.46	1.69	Internal mould of ventral valve
DCB-35-398	5.47	3.53	1.55	Ventral interior
DCB-35-400	6.19	3.81	1.62	Internal mould of ventral valve
DCB-34-394	7.32	4.92	1.49	Ventral interior

Occurrence Changhsingian; Wufeng in Hubei Province, South China.

Description Transversely quadrate in outline, widest at hinge; shell small for the subgenus, 3.4–4.9 mm long and 5.5–8.4 mm wide; lateral margins parallel, ears triangular, flat, smooth, not extended. Ventral valve strongly convex, elevated part triangular (equal to one-third of shell width); beak slightly overhanging hingeline; cardinal

Fig. 9.44 ***Neochonetes*** (***Huangichonetes***) ***substrophomenoides*** (Huang, 1932). (**a**), internal mould of a complete ventral valve and part of internal mould of the conjoined dorsal valve, LZ0400110. (**b**), internal mould of a complete ventral valve, LZ2702387, showing *Neochonetes*-like papillae. (**c**), internal mould of an incomplete ventral valve, LZ1400530. (**d**), external mould of a complete dorsal valve and posterior part of internal mould of the conjoined ventral valve, LZ2705142. (**e**, **f**), internal moulds of two complete ventral valves, LZ1400368, LZ2704059, showing a thick median septum and *Neochonetes*-like papillae for each specimen. (**g**), external moulds of dorsal valves, LZ2704108, showing bifurcated costellae. (**h**), external mould of a complete dorsal valve, LZ2705143, showing small tubes (*tu*). (**i**), external mould of a nearly complete dorsal valve and posterior part of internal mould of the conjoined ventral valve, LZ2703148, showing small tubes (*tu*)

extremities with an angle of about 90°; sulcus deep, originating from umbo and widening anteriorly; costellae fine, dense, numbering 3 per 1 mm. Dorsal valve strongly concave, concave part triangular. Ventral interior with a short median septum (*ms* in Fig. 9.45a); a pair of parallel vascular trunks (*vt* in Fig. 9.45a); papillae radially-arranged. Dorsal interior with a thick median septum.

Discussion Although initially tentatively assigned to the subgenus of *Huangichonetes* (He et al., 2014), these specimens have quadrate cardinal extremities, a moderately wide median sulcus and fine costellae, all characteristics of *Sommeriella*. Comapred to the present species, *Neochonetes* (*Sommeriella*) *strophomenoides* (Waagen 1884) from the Permian of Salt Range has a wider umbo, more extended ears and acute extremities. *Neochonetes* (*Sommeriella*) *regularis* Shen et al., 2000 from the Selong Group (Upper Permian) of Xishan, Tibet, China has more and finer costellation in comparison with *N.* (*Sommeriella*) *wufengensis*.

Subgenus ***Neochonetes*** (***Zhongyingia***) Shen and Archbold, 2002

Type Species *Neochonetes zhongyingensis* Liao, 1980a. Changhsingian (Upper Permian), South China.

Diagnosis Reversely trapezoidal outline, greatest width at hingeline; ears acute, cardinal extremities extended; ventral valve slightly convex; sulcus broad and shallow; surface ornamented by fine costellae. Dorsal interior with long lateral ridges parallel to hingeline.

Neochonetes (***Zhongyingia***) ***zhongyingensis*** Liao, 1980a
Fig. 9.45f–h

1980a *Neochonetes zhongyingensis* Liao: 257, pl. 5, Fig. 10–13.
2002 *Neochonetes* (*Zhongyingia*) *zhongyingensis* Liao; Shen and Archbold: 333, Fig. 4a–q.
2013 *Neochonetes* (*Zhongyingia*) *zhongyingensis* Liao; Zhang et al.: 243, Fig. 12y–aa.

Materials Over 10 specimens. Registered specimens: see below.

Measurements (mm):

Number	Width	Length	Width/ length	Notes
LZ1200082	11.10	5.65	1.97	External mould of dorsal valve
LZ0400085	15.12	7.94	1.90	External mould of dorsal valve
LZ0400127	11.98	6.35	1.89	External mould of dorsal valve

Occurrence Upper Permian; Hunan and Guizhou in South China.

Description Reversely trapezoidal in outline, greatest width at hingeline; shell medium size for the subgenus, 5.7–7.9 mm long and 9.9–15.1 mm wide; cardinal extremities acute, with an angle of 60–80°; ears large, nearly flat, well demarcated from visceral region. Dorsal valve slightly concave; fold indistinct. Costellae fine, increasing by bifurcatiuon and forming fasciculated, numbering 30–36 near anterior margin; hinge spines projecting posterolaterally at about 0–40°.

Discussion The specimen of *Neochonetes* (*Zhongyingia*) *zhongyingensis* Liao of Zhang et al. (2013, Fig. 12w) has a strongly convex ventral valve, quadrate cardinal extremities and a sulcus which is weak and only positioned near anterior margin, unlike features of *Neochonetes* (*Zhongyingia*), but rather like those in *Neochonetes* (*Neochonetes*) (Fig. 9.43) (see below).

Subgenus ***Neochonetes*** (***Neochonetes***) Muir-Wood, 1962

Type Species *Chonetes dominus* King, 1938. Upper Carbonaceous Marble Falls limestone; West Texas.

Diagnosis Transversely quadrate in outline, cardinal extremities quadrate; small to medium for the genus; slightly concavoconvex in profile. Ventral valve with a weak sulcus near anterior

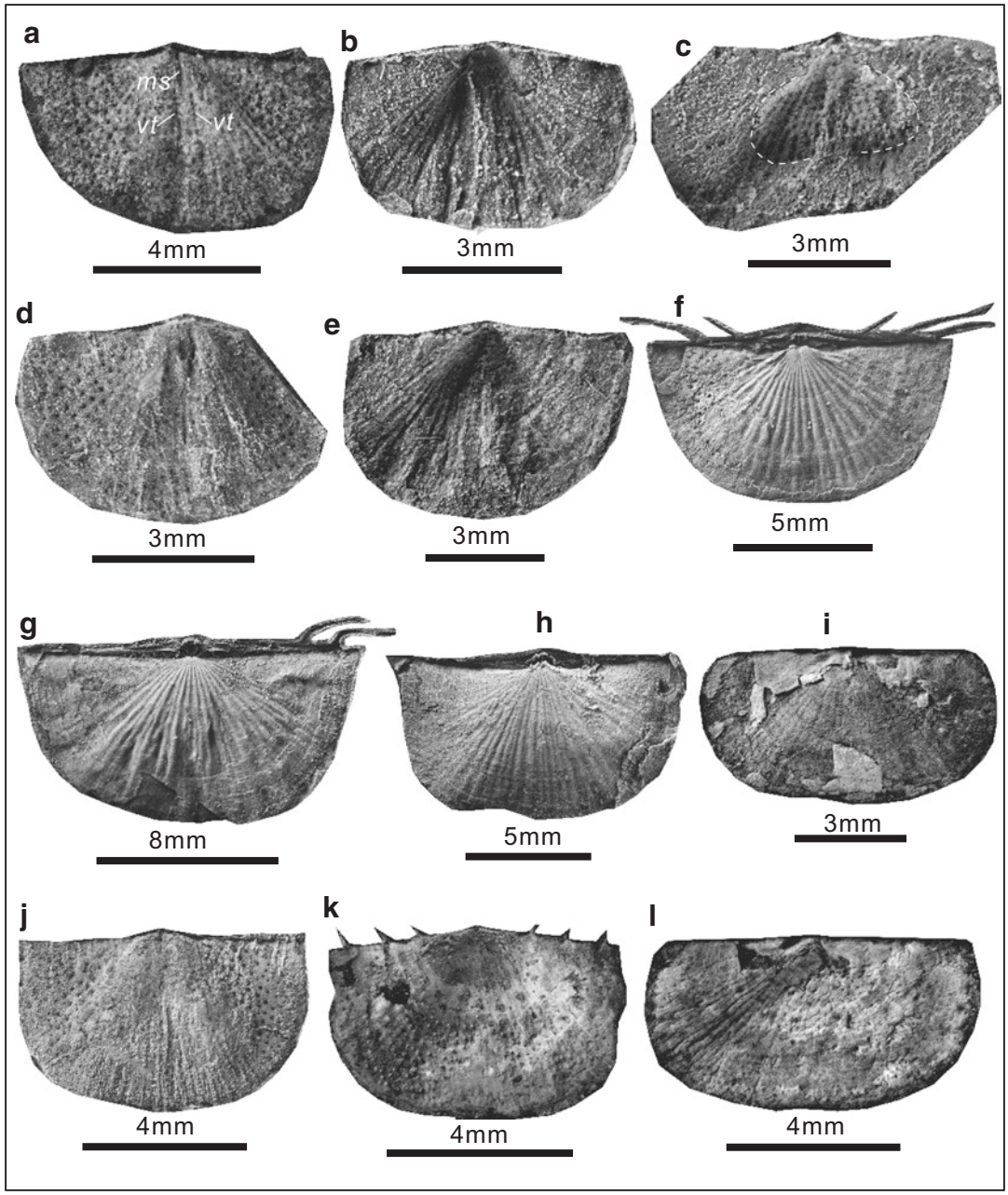

Fig. 9.45 (**a**–**e**), ***Neochonetes*** (***Sommeriella***) ***wufengensis*** (He and Shi in He et al., 2014). (**a**), internal mould of a complete ventral valve, DCB-34-395, showing a median septum (*ms*) and vascular trunks (*vt*). (**b**), interior of a nearly complete ventral valve, DCB-35-398. (**c**), internal mould of an incomplete dorsal valve, DCB-35-399, showing scars of brachial ridges. (**d**), internal mould of an incomplete ventral valve, DCB-35-400. (**e**), interior of a complete ventral valve, DCB-34-394. (**f**–**h**), ***Neochonetes*** (***Zhongyingia***) ***zhongyingensis*** Liao, 1980a. (**f**), external mould of a complete dorsal valve, LZ1200082, showing bifurcated costellae and hinge spines. (**g**), external mould of a complete dorsal valve, LZ0400085, showing bifurcated costellae. (**h**), external mould of a complete but slightly deformed dorsal valve, LZ0400127, showing bifurcated costellae. (**i**–**l**), ***Neochonetes*** (***Neochonetes***) ***liaoi*** (He and Shi in He et al., 2014). (**i**), interior of a nearly complete dorsal valve (shell mostly decorticated), CM-1-373. (**j**), internal mould of a complete ventral valve, CM-1-372, showing quadrate cardinal extremities. (**k**), interior of an incomplete ventral valve, CM-1-364 (holotype as originally illustrated by He et al., 2014), showing radially-arranged papillae and quadrate cardinal extremities. (**l**), internal mould of a complete dorsal valve, CM-1-376 (paratype as originally illustrated by He et al., 2014)

margin. Surface ornamented by fine costellae. Ventral interior generally with a long median septum or median ridge; vascular trunks parallel; *Neochonetes*-like papillae. Dorsal interior with a long septum septum and prominent inner socket ridges.

Neochonetes* (*Neochonetes*) *liaoi (He and Shi in He et al., 2014)
Fig. 9.45i–l

2014 *Neochonetes* (?*Zhongyingia*) *liaoi* He and Shi in He et al., 2014: 927, Figs. 9m–o, 11a–f.

Materials Over 20 specimens. Registered specimens: see below.

Measurements (mm):

Number	Width	Length	Width/ length	Notes
CM-1-373	7.98	4.23	1.89	Dorsal interior
CM-1-372	7.19	4.47	1.61	Internal mould of ventral valve
CM-1-364	6.39	4.19	1.52	Ventral interior
CM-1-376	7.72	4.06	1.90	Internal mould of dorsal valve

Occurrence Wuchiapingian (more commonly) to Changhsingian; South China.

Description Shell small for the subgenus, 3.7–5.6 mm long and 6.3–8.9 mm wide, transversely quadrate in outline, widest at hingeline, lateral margins parallel, ears large, triangular, flat, smooth, not extended. Ventral valve slightly convex; umbo broad, with an angle of 110°; 3 pairs of hingespines projecting posterolaterally; cardinal extremities with an angle of about 90°; sulcus weak to absent, only at anterior margin when present. Dorsal valve slightly concave; umbo broad, with an angle of 110°; fold absent; capillae dense, numbering 4 per 1 mm. Ventral interior with fine *Noechonetes*-like papillae. Dorsal interior median septum coarse; lateral septa thick, coalescing with a median septum; inner socket ridges distinct, coalescing with a cardinal process, extending latterally at an angle of 30° to hingeline (see He et al., 2014).

Discussion Although these specimens were originally assigned to the subgenus of *Zhongyingia*, they prominently have quadrate cardinal extremities and an indistinct (or even absent) median sulcus, suggesting features of subgenus *Neochonetes*. This species differs from *Neochonetes* (*Neochonetes*) *dominus* (King, 1938, p. 259, pl. 36, Fig. 1–7) from the Upper Carbonaceous Marble Falls limestone of West Texas in the latter prominently having parallel vascular trunks in the ventral interior, concentric lines and a larger size. The present species differs from *Neochonetes* (*Sommeriella*) *wufengensis* in a wider umbo and absence of a deep sulcus.

Neochonetes* (*Neochonetes*) *convex Liao, 1980a
Fig. 9.46

1980a *Neochonetes convexa* Liao: 257, pl. 5, Fig. 19–22.
1982 *Neochonetes convexa* Liao; Wang et al.: 200, pl. 95, Fig. 13.

Fig. 9.46 ***Neochonetes* (*Neochonetes*) *convex*** Liao, 1980a. (**a**), internal mould of a complete ventral valve, LZ0400128, showing a median septum (*ms*) and vascular trunks (*vt*). (**b**, **c**), internal moulds of two complete ventral valves, LZ1200074, LZ0400124, showing a median septum and radially-arranged papillae for each specimen. (**d**), internal mould of a nearly complete ventral valve, LZ2704210. (**e**–**h**), internal moulds of four complete ventral valves, LZ0400100, LZ1200132, LZ1200102 (*ms*-median septum, *vt*- vascular trunks), LZ1400033. (**i**), internal mould of a complete ventral valve and shell remnant, LZ2705020. (**j**), internal mould of a complete ventral valve, LZ2702212, showing spine canals (*sc*) inclined toward midline and a median septum (*ms*). (**k**), internal mould of a nearly complete ventral valve, LZ2702049. (**l**), internal mould of a complete dorsal valve, LZ1200133, showing sockets (*soc*), inner socket ridges (*is*), median septum (*ms*), lateral septa (*ls*). (**m**), external mould of a complete dorsal valve, LZ0400105, showing bifurcated costellae. (**n**), external mould of an incomplete dorsal valve and part of internal mould of the conjoined ventral valve, LZ2702289, showing a distinct fold. (**o**), exterior of a complete ventral valve, LZ0400096, showing a broad and shallow sulcus

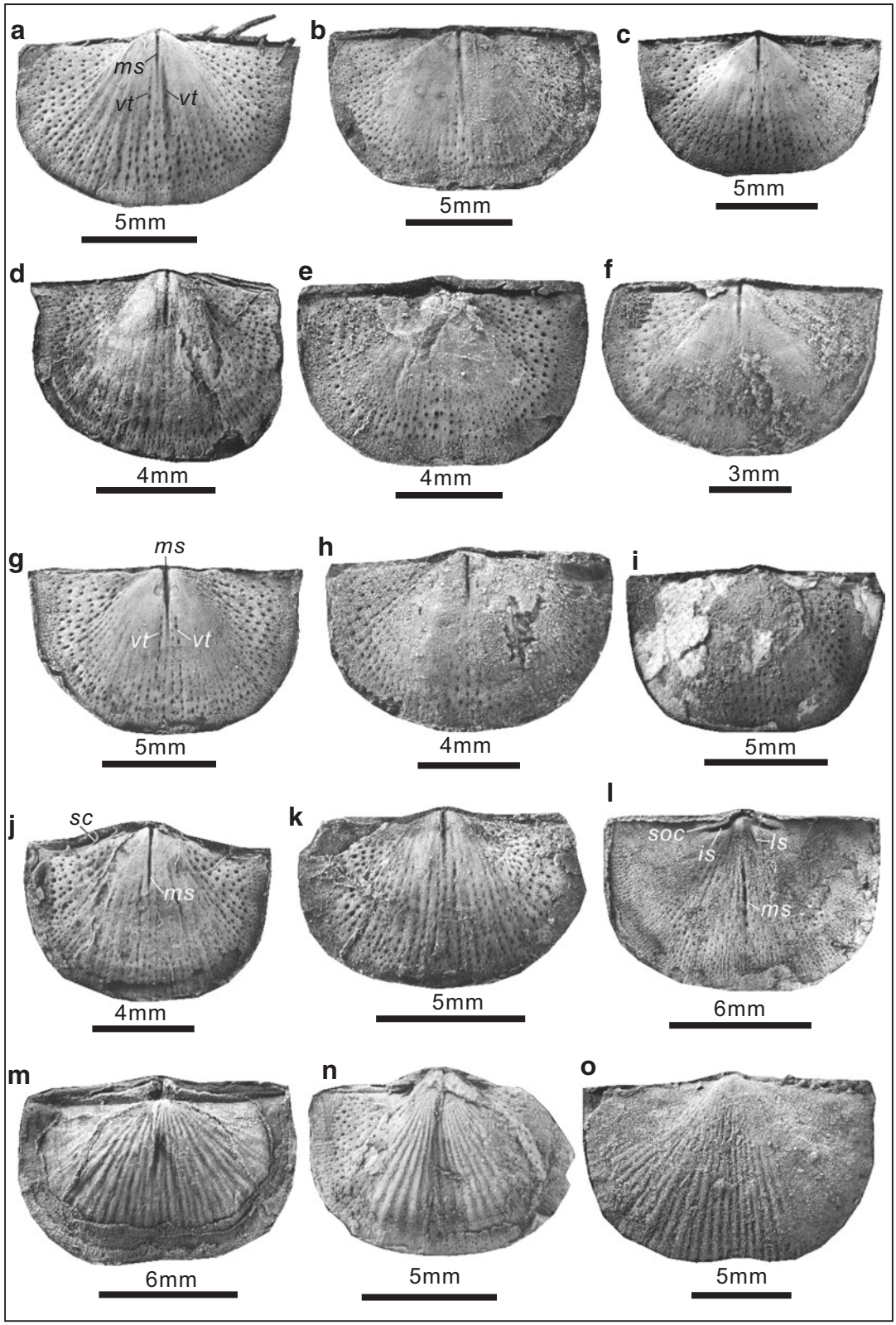
a
ms
vt
vt
5mm
b
5mm
c
5mm
d
4mm
e
4mm
f
3mm
g
ms
vt
vt
5mm
h
4mm
i
5mm
j
sc
ms
4mm
k
5mm
l
soc
is
ls
ms
6mm
m
6mm
n
5mm
o
5mm

2001 *Neochonetes* (*Sommeriella*) *strophomenoides* (Waagen); Shen et al.: 277, Fig. 3.10–3.15.
2002 *Neochonetes* (*Sommeriella*) *strophomenoides* (Waagen); Shen and Archbold: 334, Fig. 5a, c, d.
2013 *Neochonetes* (*Huangichonetes*) *substrophomenoides* (Huang, 1932); Zhang et al.: Fig. 9q–w, y.
2013 *Neochonetes* (*Huangichonetes*) *archboldi* Zhang et al.: Fig. 11m.
2013 *Neochonetes* (*Sommeriella*) *strophomenoides* (Waagen, 1884); Zhang et al.: Fig. 11t, v.
2013 *Neochonetes* (*Sommeriella*) *regularis* Shen, Archbold, Shi and Chen; Zhang et al.: Fig. 11x, y.
2013 *Neochonetes* (*Sommeriella*) *waterhousei* Zhang et al.: 241, Fig. 12c–l.
2013 *Neochonetes* (*Sommeriella*) *rectangularis* Zhang et al.: 242, Fig. 12m–v.
2013 *Neochonetes* (*Zhongyingia*) *zhongyingensis* Liao, 1980a; Zhang et al.: Fig. 12w.
2013 *Neochonetes semicircularis* Zhang et al.: Fig. 14c, d.

Materials Over 100 specimens. Registered specimens: see below.

Measurements (mm):

Number	Width	Length	Width/length	Notes
LZ0400128	12.31	7.69	1.60	Internal mould of ventral valve
LZ1200074	12.82	7.49	1.71	Internal mould of ventral valve
LZ0400124	11.98	7.24	1.65	Internal mould of ventral valve
LZ2704210	9.06	6.50	1.39	Internal mould of ventral valve
LZ0400100	10.91	6.72	1.62	Internal mould of ventral valve
LZ1200132	10.23	6.52	1.57	Internal mould of ventral valve
LZ1200102	12.08	7.45	1.62	Internal mould of ventral valve
LZ1400033	11.26	7.22	1.56	Internal mould of ventral valve
LZ2705020	10.48	6.81	1.54	Internal mould of ventral valve
LZ2702212	9.73	6.84	1.42	Internal mould of ventral valve
LZ2702049	9.70	6.14	1.58	Internal mould of ventral valve
LZ1200133	11.71	7.69	1.52	Internal mould of dorsal valve
LZ0400105	12.04	7.32	1.64	External mould of dorsal valve
LZ2702289	9.88	7.01	1.41	External mould of dorsal valve
LZ0400096	14.95	9.31	1.61	Ventral exterior

Occurrence Changhsingian; Guizhou of South China.

Description Shell subquadrate, greatest width at hinge; small to medium for the subgenus, 6.1–9.9 mm long and 9.1–15.0 mm wide.

Ventral valve slightly convex; beak low, broad, slightly overhanging hingeline; sulcus weak, developed at anterior margin. Dorsal valve moderately concave; fold weak. Costellae fine, increasing by bifurcation, numbering about 35 near anterior margin; 3 to 4 pairs of hinge spines projecting posterolaterally.

Ventral interior with a short median septum, extending to about one-third of shell length; a pair of parallel vascular trunks (*vt*), closely positioned each side of median septum (*ms*) (Fig. 9.46a, g); inner surface with radial papillae, larger and rare in visceral region and ears, and then becoming smaller and densely packed to form a band near margins, with a density of 6–8 per mm^2 at midvalve and 20–25 per mm^2 at anterior. Dorsal interior with deep sockets (*soc*), inner socket ridges (*is*) diverging at an angle about 160°; a median septum (*ms*) anteriorly extending to two-thirds of shell length; a pair of lateral septa (*ls*); radial papillae, sparse but larger in disk, and becoming more dense and smaller near margins (Fig. 9.46l).

Discussion Several *Neochonetes* (*Neochonetes*) specimens have been assigned to other subgenera (*Sommeriella*, *Zhongyingia* or *Huangichonetes*) by Zhang et al. (2013) (see the above synonym). However, these specimens all have quadrata cardinal extremities, parallel lateral margins and

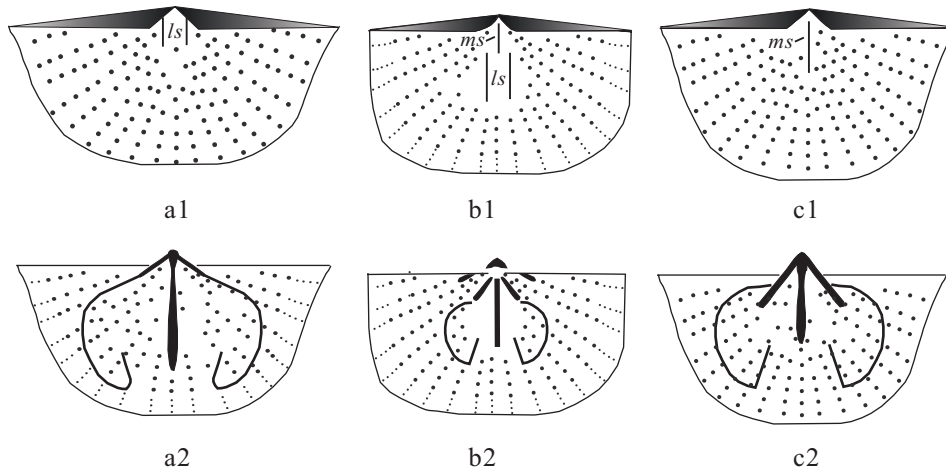

Fig. 9.47 Comparison of *Chaohochonetes* He and Shi in He et al., 2014, *Neochonetes* Muir-Wood, 1962 and *Fusichonetes* Liao in Zhao et al., 1981 (after He et al., 2014). (**a1**)- Ventral interior of *Chaohochonetes*, (**a2**)- Dorsal interior of *Chaohochonetes*, (**b1**)- Ventral interior of *Neochonetes*, (**b2**)- Dorsal interior of *Neochonetes*, (**c1**)- Ventral interior of *Fusichonetes*, (**c2**)- Dorsal interior of *Fusichonetes*. Note: *ls*- lateral septa; *ms*- median septum

therefore should not be assigned to *Zhongyingia* or *Huangichonetes*. Additionally, these specimens commonly have typical features, e.g., costellae coarse, sulcus weak or lacking; therefore, they cannot be assigned to *Sommeriella* (*Sommeriella* prominently has capillae ornamentation and a moderately wide sulcus, Fig. 9.43). We prefer to assign these specimens to the subgenus *Neochonetes*, based on their subquadrate outline, presence of costellae and basically lacking of sulcus. *Neochonetes* (*Sommeriella*) *rectangularis* Zhang et al., 2013 and *Neochonetes* (*Sommeriella*) *waterhousei* Zhang et al., 2013 should be synonymous with the present species, because they share morphological features, including a subquadrate outline, quadrate cardinal extremities, greatest width at hinge, absence of sulcus and a slightly convex ventral valve.

The present species differs from *Neochonetes* (*Neochonetes*) *liaoi* (He and Shi in He et al., 2014) in the latter has a more transverse outline, and differs from *Neochonetes* (*Sommeriella*) *regularis* Shen et al., 2000 from the Selong Group (Upper Permian) of Xishan, Tibet, China in the latter has fine capillae.

Genus ***Chaohochonetes*** He and Shi in He et al., 2014

Type Species *Chaohochonetes triangusinuata* He and Shi in He et al., 2014. Uppermost Changhsingian to the lowest Triassic; China.

Diagnosis Small, reversely trapezoid rugosochonetids, profile weakly concavo-convex; greatest width at hinge; ventral valve moderately convex; ventral sulcus varying from triangular to absent; dorsal fold narrowly triangular to absent; round and coarse radial costellae on shell surface. Ventral median septum absent, lateral septa parallel and thin, radially-arranged papillae covering ventral interior and extending towards margin with the same diameter size; *Neochonetes*-like papillae covering dorsal interior, but absent towards and over the interior areas of ears.

Discussion The present genus is like *Neochonetes* Muir-Wood, 1962 in the radially-ranged papillae in dorsal interior, but differs in the latter having a ventral median septum (Fig. 9.47). *Chaohochonetes* is also like *Fusichonetes* Liao in Zhao et al., 1981 in outline and ornamentation, but the former has two lateral

septa in the ventral valve and *Neochonetes*-like papillae within the dorsal interior (Fig. 9.47). Currently, specimens for the present genus have only been found in the horizons near the PTB of Chaohu, Anhui Province, China.

Chaohochonetes triangusinuata He and Shi in He et al., 2014
Figs. 9.48; 9.49a–i, m, n

2014 *Tethyochonetes triangusinuata* He and Shi in He et al.: 923, Figs. 8a–o, 9a–d.

Holotype *Tethyochonetes triangusinuata* He and Shi in He et al., 2014, Fig. 8a, deposited in the Laboratory of Geobiology, Faculty of Earth Sciences, China University of Geosciences, Wuhan, People's Republic of China, external mould of a dorsal valve, from upper part of the Talung Formation (uppermost Changhsingian), Majiashan section, Chaohu, Anhui Province, China.

Diagnosis Sulcus prominent, narrow, beginning from umbo, extending anteriorly to middle valve, then widening rapidly to one third or one fourth of the shell width near anterior margin.

Materials 71 specimens. Registered specimens: see below.

Measurements (mm):

Number	Width	Length	Width/ length	Notes
CM-15-8	9.42	6.30	1.50	Internal mould of ventral valve
CM-15-7	10.95	6.85	1.60	Internal mould of ventral valve
CM-15-1	5.48	3.19	1.72	Internal mould of ventral valve
CM-15-2	12.39	5.77	2.15	Internal mould of ventral valve
CM-15-3	12.06	6.91	1.74	Internal mould of ventral valve
CM-14-9	8.11	4.80	1.69	Internal mould of ventral valve
CM-15-5	10.57	6.10	1.73	Internal mould of ventral valve
CM-18-20	6.74	4.18	1.61	Ventral exterior
CM-16-23	7.16	3.74	1.92	Ventral exterior
CM-18-24	6.72	3.89	1.73	Ventral exterior
CM-16-14	9.50	4.43	2.14	Dorsal interior
CM-13-26	5.58	3.41	1.63	External mould of dorsal valve
CM-15-17	9.42	4.83	1.95	Internal mould of dorsal valve
CM-14-18	10.23	4.61	2.22	Internal mould of dorsal valve
CM-15-13	9.16	5.34	1.72	External mould of dorsal valve
CM14-0599	7.79	4.12	1.89	Ventral valve
CM-15-6	8.51	5.10	1.67	Internal mould of ventral valve

Occurrence Uppermost Changhsingian to the lowest Triassic; Anhui (Majiashan section) of South China.

Description Shell 3.0–7.1 mm long and 5.1–12.4 mm wide, reversely trapezoid, widest at hingeline. Ventral valve moderately convex, median convex portion being widely triangular in shape; beak slightly incurved, overhanging hingeline; hingespines projecting posterolaterally at a varied angle of 40–70°; cardinal extremities with an angle of 70–90°; ears smooth, not well differentiated from flanks of ventral disk; sulcus originating from umbo, narrow, prominent, and extending anteriorly to middle valve, then widening rapidly to one third or one fourth of shell width near anterior margin; costellae

Fig. 9.48 ***Chaohochonetes triangusinuata*** He and Shi in He et al., 2014. (**a**), internal mould of complete ventral valve, CM-15-8. (**b**), enlarged portion of CM-15-8, illustrating a pair of lateral septa (*ls*). (**c**), internal mould of ventral valve, CM-15-7. (**d**), enlarged portion of CM-15-7, illustrating a pair of lateral septa (*ls*). (**e**), internal mould of a complete ventral valve, CM-15-1 (as the Holotype by He et al. 2014), showing a pair of lateral septa (*ls*). (**f**), internal mould of a complete ventral valve, CM-15-2, showing hinge spines. (**g**, **h**), internal moulds of two complete ventral valves, CM-15-3, CM-14-9

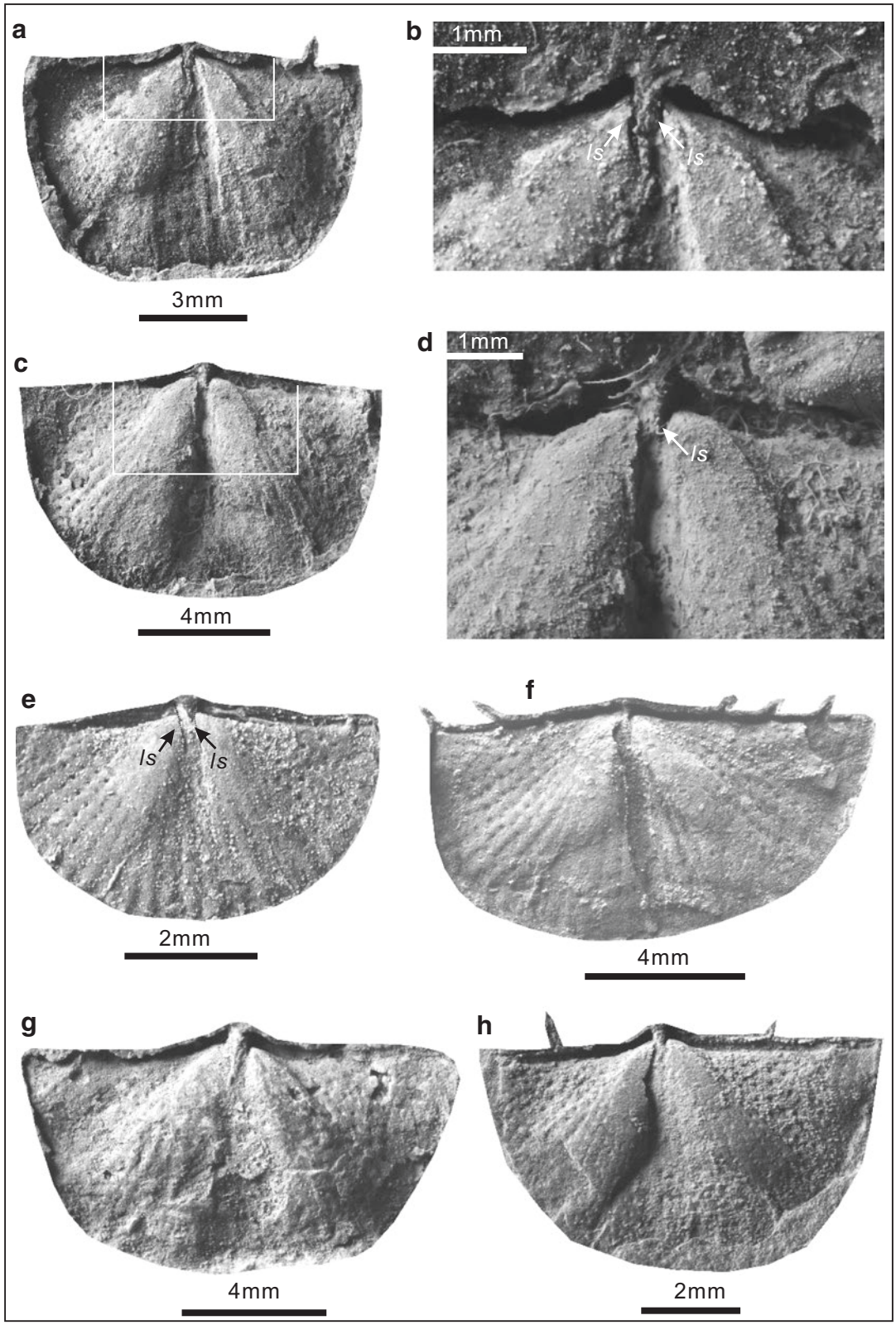
a
3mm
b
1mm
ls
ls
c
4mm
d
1mm
ls
e
ls
ls
2mm
f
4mm
g
4mm
h
2mm

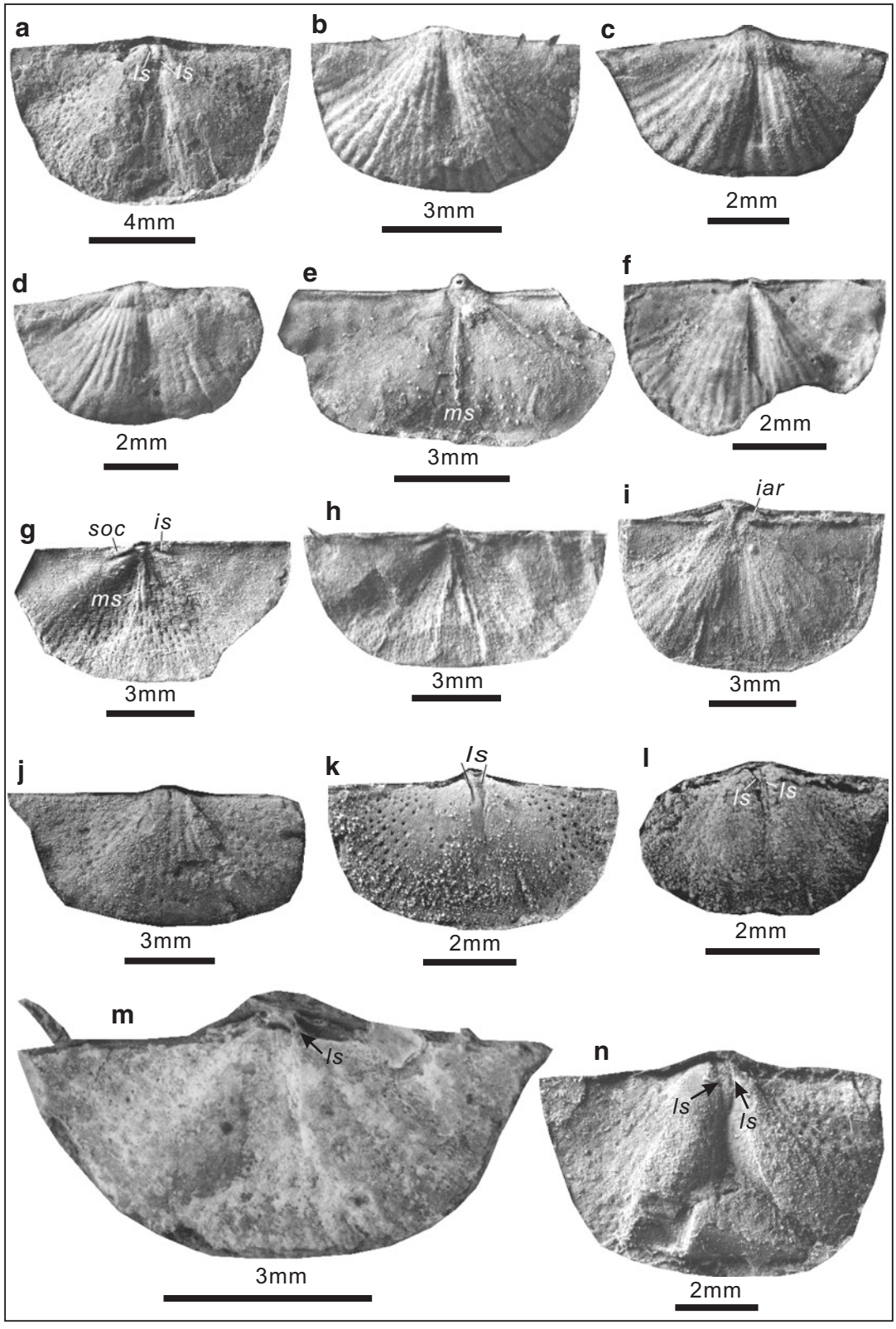
a
ls
ls
4mm
b
3mm
c
2mm
d
2mm
e
ms
3mm
f
2mm
g
soc
is
ms
3mm
h
3mm
i
iar
3mm
j
3mm
k
ls
2mm
l
ls
ls
2mm
m
ls
3mm
n
ls
ls
2mm

originating from umbo, round and coarse, rarely bifurcated, numbering 18 to 20 near anterior margin. Dorsal valve slightly concave; median concave portion being widely triangular in shape; ears flat, triangular, smooth, well differentiated from flanks of ventral disk; fold prominent, originating from umbo, narrowly triangular, and extending anteriorly to middle valve, then rapidly widening anteriorly; costellae beginning from umbo, bifurcated near anterior margin.

Ventral median septum absent, lateral septa short, parallel, weak or ill-defined near beak (*ls* refers to lateral septa, see Figs. 9.48b, d, e; 9.49m); papillae radially-arranged. Dorsal interior median septum long, extending to at least half of shell length; sockets (*soc*) shallow, inner socket ridges (*is*) coarse and coalescing with cardinal process, extending latterally at an angle of 10° to hingeline (Fig. 9.49g); *Neochonetes*-like papillae covering dorsal interior (Fig. 9.49g, h), papillae absent towards ears in dorsal interior.

Discussion These specimens are assignable to *Chaohochonetes* in terms of the absence of a median septum, and having two short parallel lateral septa in the ventral interior, and *Nechonetes*-like papillae in the dorsal interior. This species is characteristically defined by its conspicuous triangular sulcus.

Chaohochonetes sp.
Fig. 9.49j–l

Materials Three registered specimens: CM-12-378, XM-2-410, CM-15-87.

Measurements (mm):

Number	Width	Length	Width/ length	Notes
CM-15-87	11.01	4.72	2.33	Internal mould of ventral valve
CM-12-378	6.31	3.40	1.86	Internal mould of ventral valve
XM-2-410	4.40	2.63	1.67	Internal mould of ventral valve

Occurrence Upper Changhsingian; Anhui (Majiashan section) and Guizhou (Xinmin) of South China.

Description Shell 2.6–4.7 mm long and 4.4–11.0 mm wide, reversely trapezoid, widest at hingeline. Ventral valve moderately convex, median convex portion being widely triangular; beak slightly overhanging hingeline; cardinal extremities with an angle of 80–90°; ears triangular, smooth, not well differentiated from flanks of ventral disk; sulcus absent; costellae coarse. Ventral median septum absent, lateral septa parallel (*ls*) (Fig. 9.49k, l) and extending anteriorly to one fourth to one third of length; papillae radially-arranged.

Discussion The present species is similar to *Chaohochonetes triangusinuata* in a widely triangular, convex median portion on the ventral

Fig. 9.49 (**a**–**i**, **m**, **n**), ***Chaohochonetes triangusinuata*** He and Shi in He et al., 2014. (**a**), internal mould of ventral valve, CM-15-5, showing a pair of lateral septa (*ls*). (**b**–**d**), exteriors of three complete ventral valves, CM-18-20, CM-16-23, CM-18-24, showing a narrow triangular sulcus for each specimen. (**e**), interior of a dorsal valve, CM-16-14, showing a long median septum (*ms*). (**f**), external mould of an incomplete dorsal valve, CM-13-26. (**g**), internal mould of an incomplete dorsal valve, CM-15-17, showing a long median septum (*ms*), deep sockets (*soc*) and prominent inner socket ridges (*is*). (**h**), internal mould of a nearly complete dorsal valve, CM-14-18. (**i**), external mould of an incomplete dorsal valve, CM-15-13, showing a low interarea (*iar*). (**m**), a complete ventral valve (outer layer of shell mostly decorticated), CM14-0599, showing one preserved lateral septum (*ls*). (**n**), internal mould of a nearly complete ventral valve, CM-15-6, showing a pair of lateral septa (*ls*). (**j**–**l**), ***Chaohochonetes*** sp.. (**j**), internal mould of a neary complete ventral valve, CM-15-87. (**k**), internal mould of a complete ventral valve, CM-12-378, showing a pair of lateral septa (*ls*). (**l**), internal mould of an incomplete ventral valve, XM-2-410, showing a pair of lateral septa (*ls*)

valve, but differs in its slightly longer lateral septa and the absence of a ventral sulcus.

Suborder **Lyttoniidina** Williams, Harper and Grant in Williams et al., 2000
Superfamily **Lyttoninoidea** Waagen, 1883
Family **Lyttoniidae** Waagen, 1883
Subfamily **Lyttoniinae** Waagen, 1883
Genus ***Leptodus*** Kayser, 1883

Type Species *Leptodus richthofeni* Kayser, 1883. Wujiapingian (Upper Permian); China.

Diagnosis Ventral valve scoop shaped, normally transversely oval; lateral septa in ventral interior arcuate, convex anteriorly; muscle scars large, bounded laterally by high, medianly concave ridges.

Discussion *Leptodus* differs from *Collemataria* Cooper and Grant, 1974 of the Upper Permian of Texas in its transversely oval outline (the latter has a narrowly triangular outline). Compared to *Leptodus*, *Oldhamina* Waagen, 1883 has a more convex ventral valve, lateral septa extending anterolaterally and crossed with the median septum at an acute angle in the ventral interior.

Leptodus richthofeni Kayser, 1883
Fig. 9.50a–g, j

1883 *Leptodus richthofeni* Kayser: 161, pl. 21, Fig. 9–11.
1977 *Leptodus richthofeni* Kayser; Yang et al.: 372, pl. 147, Fig. 10.
1995 *Leptodus richthofeni* Kayser; Zeng et al.: pl. 11, Fig. 6.

Materials Seven registered specimens: see below.

Measurements (mm):

Number	Width	Length	Width/ length	Notes
CM-4-62	20.33	>15.63		Internal mould of ventral valve
CM-4-60	31.68	>24.28		Internal mould of ventral valve
XM-4-615	>17.09	>11.35		Internal mould of ventral valve
HZS19-0620	>37.08	>23.76		Internal mould of ventral valve
HZS19-0621	>23.28	>15.32		Internal mould of ventral valve
XM18525-1	26.61	28.71	0.93	Internal mould of ventral valve
XM18525	26.96	28.59	0.94	Internal mould of ventral valve

Occurrence Upper Permian; Guangxi, Hubei and Sichuan of South China.

Description Shell transversely oval in outline, widest at midlength; posterolateral margins meet at an angle of 130–140°. Ventral interior with a long median septum originated from umbo and extending to anterior margin; 12 pairs of lateral septa preserved, evenly convex anteriorly.

Discussion These specimens are assigned to *Leptodus*, because of the presence of a transversely oval outline and arcuate, convex anteriorly lateral septa. The present species differs from *L. nobilis* Waagen 1883 of the Upper Permian of Pakistan as the latter has subparallel lateral margins and more lateral septa (over 30), and from *L. deminutus* Liao, 1980a of the Lungtan Formation of Puding, Guizhou Province in the latter having fewer lateral septa (6–8).

Genus ***Oldhamina*** Waagen, 1883

Fig. 9.50 (**a**–**g**, **j**), ***Leptodus richthofeni*** Kayser, 1883, internal moulds of eight incomplete ventral valves, CM-4-62, CM-4-60, XM-4-615, HZS19-0620, HZS19-0621, XM18525-1, XM18525, XM18024, showing a long median septum and anteriorly convex lateral septa for each specimen. (**h**), ***Oldhamina interrupta*** Chan in Hou et al. 1979, internal mould of an incomplete ventral valve, LZ1200363, showing a long median septum interrupted by long warts and anterolatterally extended lateral septa. (**i**, **k**), ***Matanoleptodus*** sp., internal moulds of two incomplete ventral valves, HZS18-0622, HZS18-0623, showing a broad median septum and widely-grooved lateral septa

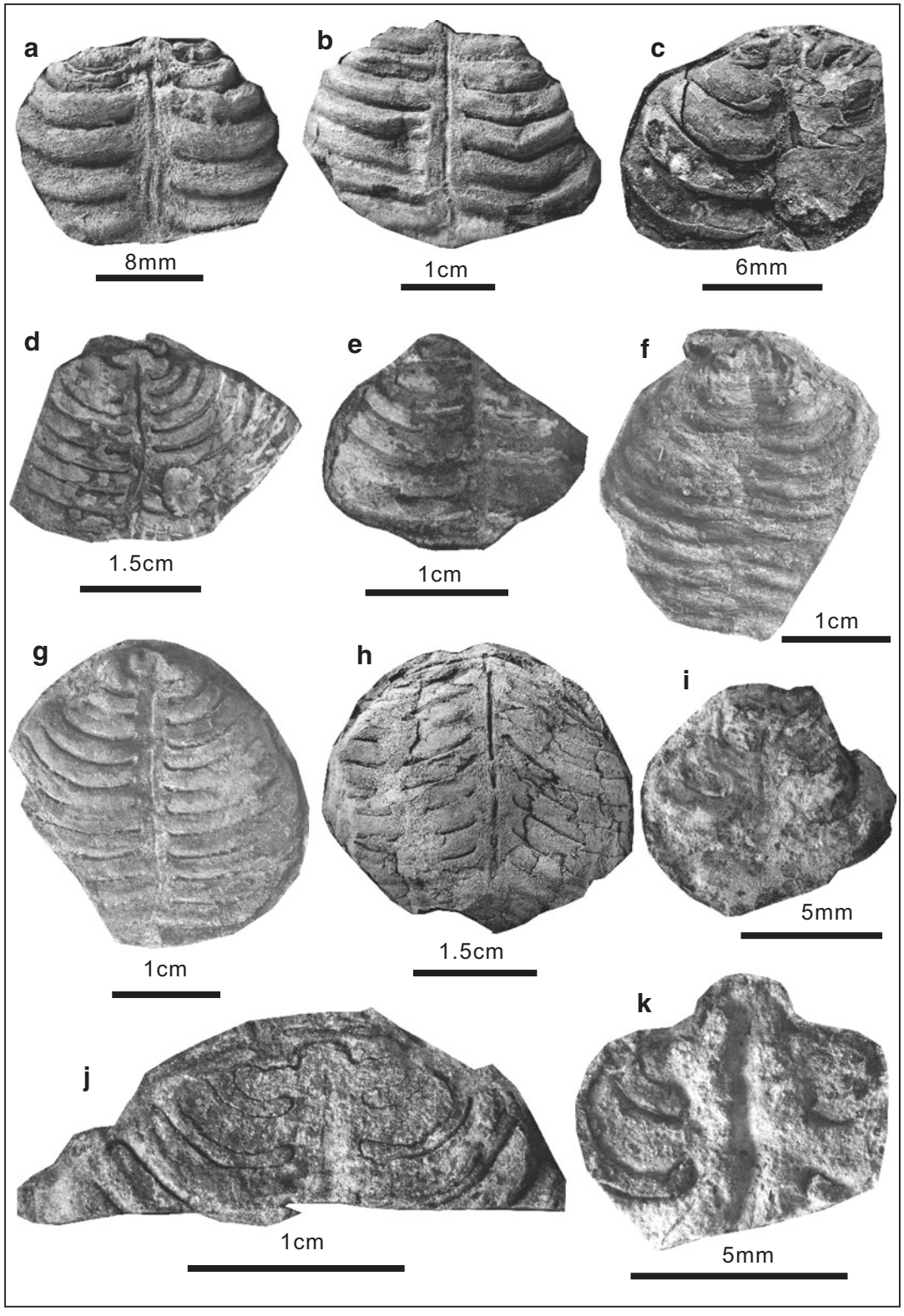
a
8mm
b
1cm
c
6mm
d
1.5cm
e
1cm
f
1cm
g
1cm
h
1.5cm
i
5mm
j
1cm
k
5mm

Type Species *Bellerophon decipiens* De Koninck, 1863. Upper Permian; Paskistan.

Diagnosis Ventral valve strongly convex; distal ends of lateral septa in ventral interior strongly convex, arcuate anteriorly.

Oldhamina interrupta Chan in Hou et al., 1979
Fig. 9.50h

1979 *Oldhamina interrupta* Chan in Hou et al.: 92, pl. 12, Fig. 9, 10.
1980a *Oldhamina subsquamosa* Liao: 262, pl. 7, Fig. 25–28.
2015 *Oldhamina interrupta* Chan in Hou et al.; Zhang et al.: 311, Fig. 8h.

Material One registered specimen: LZ1200363.

Measurement (mm):

Number	Width	Length	Width/ Length	Notes
LZ1200363	37.72	35.31	1.07	Internal mould of ventral valve

Occurrence Changhsingian; Guizhou Province, southwestern China.

Description Shell semicircular in outline, widest at midlength; posterolateral margins meet at an angle of 150°. Ventral interior with a long median septum originated from umbo, extending to anterior margin, and interrupted by long warts; at least 10 pairs of lateral septa preserved, extended anterolatterally, slightly convex towards anterior and formed a angle of 50–60° with median septum.

Discussion The specimen is assigned to *Oldhamina* on accounts of the presence of a strongly convex ventral valve and anteriorly convex lateral septa at distal ends. The present species differs from *O. squamosa* Huang, 1932 and *O. anshunensis* Huang, 1932 from the Lungtan Formation of Guizhou Province in its median septum being interrupted by long warts. Compared to *Oldhamina interrupta*, *O. regularis* Huang, 1932 from the Upper Permian Baoan Formation (Wushan Limestone) of Xintan, Hubei Province, South China has thin and nearly straight lateral septa.

Genus ***Matanoleptodus*** Liao, 1983

Type Species *Matanoleptodus punctatus* Liao, 1983. Upper Permian; Guangxi Zhuang Autonomous Region in South China.

Diagnosis Shell small, suboval in outline; median septum strong, flanked by 5 or 6 pairs of arcuate, widely-grooved lateral septa.

Matanoleptodus sp.
Fig. 9.50i, k

Materials Two registered specimens: see below.

Measurements (mm):

Number	Width	Length	Width/ length	Notes
HZS18-0622	10.72	9.29	1.15	Internal mould of ventral valve
HZS18-0623	9.09	7.71	1.18	Internal mould of ventral valve

Occurrence Changhsingian; Zhejiang Province, China.

Description Shell suboval in outline, widest at midlength. Ventral interior with a strong (broad) median septum originated from umbo, extending to anterior margin; 3 pairs of widely-grooved lateral septa preserved, convex towards anterior and nearly formed at a right angle with the median septum.

Discussion The presence of a small, suboval shell, a strong median septum and less arcuate lateral septa recalls *Matanoleptodus*, but the shell width (7–8 mm) in our material is smaller than the type species *M. punctatus* Liao, 1983. Besides, limited material and incomplete preservation prevent further examination and comparison.

Order **Spiriferida** Waagen, 1883
Superfamily **Martinioidea** Waagen, 1883
Family **Martiniidae** Waagen, 1883
Subfamily **Martiniinae** Waagen, 1883
Genus ***Martinia*** McCoy, 1844

Type Species *Spirifer glaber* Sowerby, 1820. Lower Carboniferous; England.

Diagnosis Suboval to subpentagonal in outline, ventral sulcus and dorsal fold variabley developed. Ventral interior simple, with dental flanges and impressed muscle scar bisected by long and narrow median groove, pinnate vascular markings (Carter and Gourvennec in Williams et al. 2006), or partly ramiform to netlike pallial markings (emend. here).

Discussion *Martinia* differs from *Spinomartinia* Waterhhouse, 1968c in the latter having microornament of small spinules. Additionally, according to Shi and Waterhouse (1996), strong ramiform to netlike pallial markings in the ventral interior are typical of *Spinomartinia* Waterhouse, 1968c and pinnate pallial markings in the ventral interior are typical of *Martinia* McCoy, 1844. *Spinomartinia* has so far only been found in the Cisuralian (Lower Permian) of Thailand and Australia and the Lopingian (Upper Permian) of New Zealand, whereas *Martinia* is long known from the Carboniferous to the Permian throughout the world (Carter and Gourvennec in Williams et al., 2006). However, the materials from China show that ramiform pallial markings were found in the ventral interior, as evident, for example, from *Martinia lopingensis* Chao, 1929 of the coal-bearing sequence (Wuchiapingian of Upper Permian) of Jiangxi and Guizhou and of the Changhsingian (Upper Permian) in Hubei (Chao, 1929; Huang, 1933; Yang et al., 1987). It is therefore possible that the feature of pallial markings within the ventral valve can not be regarded as a key difference between these two genera.

Martinia liuqiaoiensis He, Shen and Shi sp. nov. Figs. 9.51, 9.52, 9.53 and 9.54

2014 *Martinia* sp. of He et al.: 949, Fig. 22A–N.
2014 *Cleiothyridina*? sp. 1 of He et al.: Fig. 23C–E.
2014 *Cleiothyridina*? sp. 3 of He et al.: Fig. 23N–R.

Diagnosis Shell suboval, greatest width at shell midlength, ventral beak slightly incurved, both sulcus and fold absent; smooth except a few concentric lines.

Etymology Named for Liuqiao Town, nearby the type locality of this species.

Types Holotype, DP-1-56; parytypes, DP3-0140, DP7-0310.

Other Materials Over 200 specimens. Registered specimens: see below.

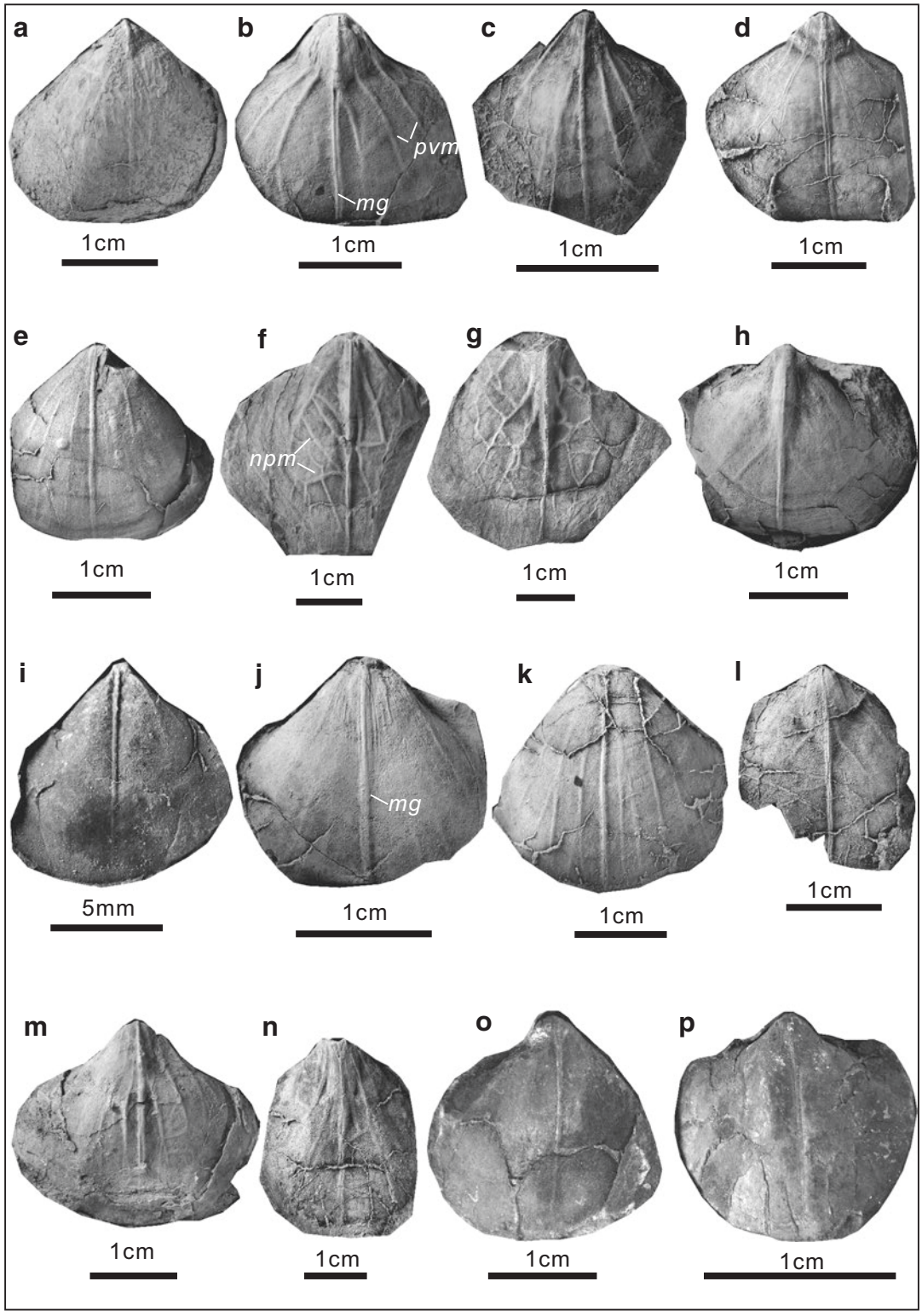

Fig. 9.51 ***Martinia liuqiaoiensis*** He, Shen and Shi sp. nov.. (**a**), internal mould of a nearly complete ventral valve, DP-1-55. (**b**–**d**), internal moulds of three incomplete ventral valves, DP-1-56 (holotype, *mg*- median groove, *pvm*- pinnate vascular markings), DP-2-57-2, DP-2-57-1. (**e**–**h**), internal moulds of four incomplete

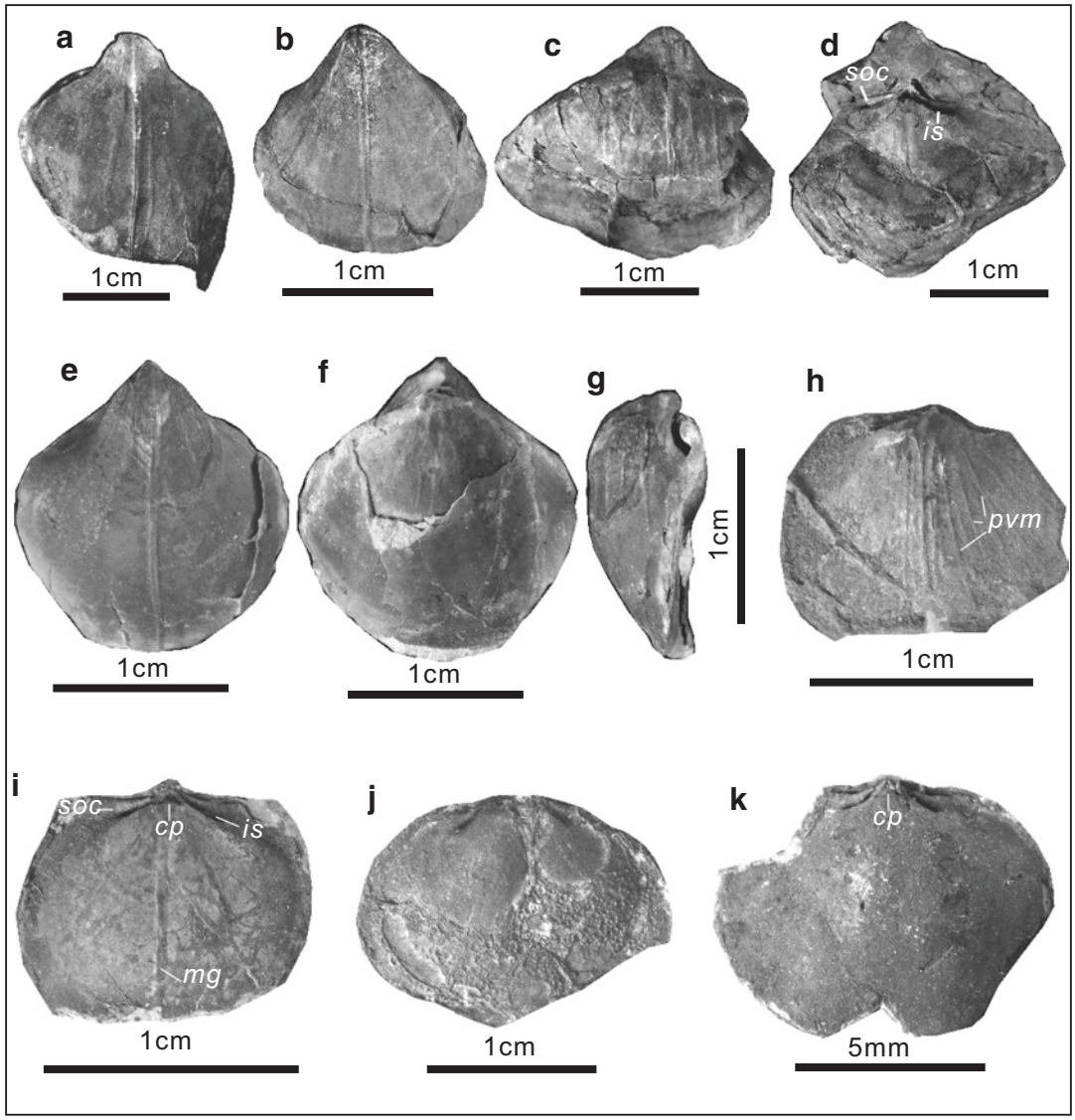

Fig. 9.52 ***Martinia liuqiaoiensis*** He, Shen and Shi sp. nov.. (**a**), internal mould of an incomplete ventral valve, DP10-0107. (**b**), internal mould of a complete ventral valve, DP3-0111, showing obscure ramiform vascular markings. (**c**), internal mould of an incomplete conjoined shell (ventral view), DP2-0114. (**d**), dorsal view of DP2-0114, *soc*- sockets, *is*- inner socket ridges. (**e**), internal mould of a complete conjoined shell (ventral view), DP5-0118. (**f**), dorsal view of DP5-0118. (**g**), lateral view of DP5-0118 (dorsal valve deformed). (**h**), internal mould of an incomplete dorsal valve, DP7-0121-2, *pvm* showing pinnate vascular markings. (**i**), internal mould of a nearly complete dorsal valve, DP2-0121, *cp*- trifid cardinal process, *soc*- sockets, *is*- inner socket ridges, *mg*- median groove. (**j**), internal mould of an incomplete dorsal valve, DP7-0122. (**k**), internal mould of an incomplete dorsal valve, DP10-0126, *cp*- cardinal process

ventral valves, **Fig. 9.51** (continued) DS-1-51, SNM-47 (*npm*- netlike pallial markings), SNM-49, SNM-54. (**i**, **j**), internal moulds of two nearly complete ventral valves, DP-9-321, DS-1-53 (*mg*- median groove). (**k**, **l**), internal moulds of two incomplete ventral valves, DS-1-52, SW-5-46-1. (**m**), internal mould of a nearly complete ventral valve, DP-2-59. (**n**), internal mould of an incomplete ventral valve, SNM-48. (**o**), internal mould of a complete ventral valve, DP2-0108, showing obscure ramiform vascular markings. (**p**), internal mould of a complete ventral valve, DP2-0117

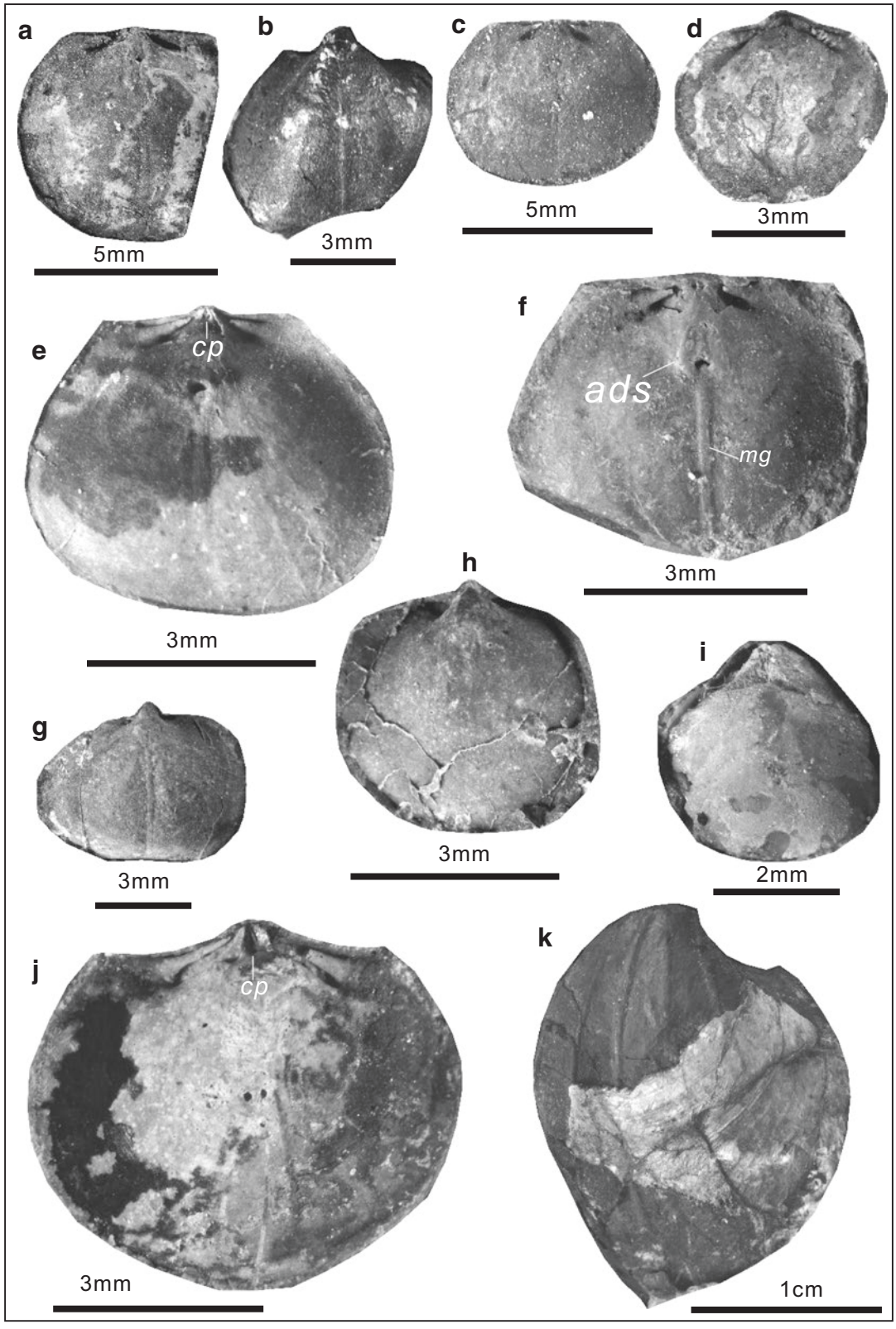
a
5mm
b
3mm
c
5mm
d
3mm
e
cp
3mm
f
ads
mg
3mm
g
3mm
h
3mm
i
2mm
j
cp
3mm
k
1cm

Measurements (mm):

Number	Width	Length	Width/length	Notes
DP-1-55	25.44	21.48	1.18	Internal mould of ventral valve
DP-1-56	21.49	20.75	1.04	Internal mould of ventral valve
DP-2-57-2	15.13	16.03	0.94	Internal mould of ventral valve
DP-2-57-1	25.50	22.34	1.14	Internal mould of ventral valve
DS-1-51	18.86	20.06	0.94	Internal mould of ventral valve
SNM-47	37.67	34.60	1.09	Internal mould of ventral valve
SNM-49	38.32	38.85	0.99	Internal mould of ventral valve
SNM-54	24.20	21.10	1.15	Internal mould of ventral valve
DP-9-321	20.39	20.54	0.99	Internal mould of ventral valve
DS-1-53	18.46	17.05	1.08	Internal mould of ventral valve
DS-1-52	26.06	24.89	1.05	Internal mould of ventral valve
DP-2-59	28.28	45.83	0.62	Internal mould of ventral valve
SNM-48	24.84	32.32	0.77	Internal mould of ventral valve
DP2-0108	22.28	21.28	1.05	Internal mould of ventral valve
DP2-0117	13.19	12.61	1.05	Internal mould of ventral valve
DP10-0107	20.25	21.43	0.94	Internal mould of ventral valve
DP3-0111	16.34	15.31	1.07	Internal mould of ventral valve
DP2-0114	35.30	21.90	1.61	Ventral internal mould of a conjoined shell
DP2-0114	29.40	17.40	1.69	Dorsal internal mould of a conjoined shell
DP5-0118	15.41	17.50	0.88	Dorsal internal mould of a conjoined shell
DP5-0119	15.68	14.56	1.08	Ventral internal mould of a conjoined shell
DP7-0121-2	12.95	10.61	1.22	Internal mould of dorsal valve
DP2-0121	14.02	10.94	1.28	Internal mould of dorsal valve
DP7-0122	17.17	14.72	1.17	Internal mould of dorsal valve
DP10-0126	9.91	7.38	1.34	Internal mould of dorsal valve
DP2-0124	7.38	6.56	1.13	Internal mould of dorsal valve (juvenile)
DP7-0145	6.33	6.98	0.91	Internal mould of ventral valve
DP10-0125	6.86	4.79	1.43	Internal mould of dorsal valve (juvenile)
DP3-0129	5.55	4.62	1.20	Internal mould of dorsal valve (juvenile)
DP10-0131	5.62	4.69	1.20	Internal mould of dorsal valve (juvenile)
DP10-0127	5.29	4.30	1.23	Internal mould of dorsal valve (juvenile)
DP3-0146	6.19	5.08	1.22	Internal mould of ventral valve
PB-0144	4.41	4.25	1.04	Internal mould of dorsal valve (juvenile)
DP7-0139	7.97	6.65	1.20	Conjoined shell (juvenile)
DP3-0140	6.57	5.06	1.30	Internal mould of dorsal valve (juvenile)
DP7-0310	24.32	21.26	1.14	Internal mould of ventral valve

Fig. 9.53 ***Martinia liuqiaoiensis*** He, Shen and Shi sp. nov.. (**a**), internal mould of an incomplete dorsal valve (juvenile), DP2-0124. (**b**), internal mould of an incomplete ventral valve (juvenile), DP7-0145, showing lack of vascular markings. (**c**), internal mould of a complete dorsal valve (juvenile), DP10-0125. (**d**), internal mould of a complete dorsal valve (juvenile), DP3-0129. (**e**), internal mould of a complete dorsal valve (juvenile), DP10-0131, *cp*- cardinal process. (**f**), internal mould of an incomplete dorsal valve (juvenile), DP10-0127, *ads*- adductor scars, *mg*- median groove. (**g**), internal mould of an incomplete ventral valve, DP3-0146. (**h**), internal mould of a complete ventral valve (juvenile), PB-0144, showing lack of vascular markings. (**i**), a nearly complete conjoined shell (juvenile, dorsal view), DP7-0139. (**j**), internal mould of a complete dorsal valve (juvenile), DP3-0140 (paratype), *cp*- trifid cardinal process. (**k**), internal mould of a complete ventral valve and segment of shell, DP7-0310 (paratype), showing fine concentric lines

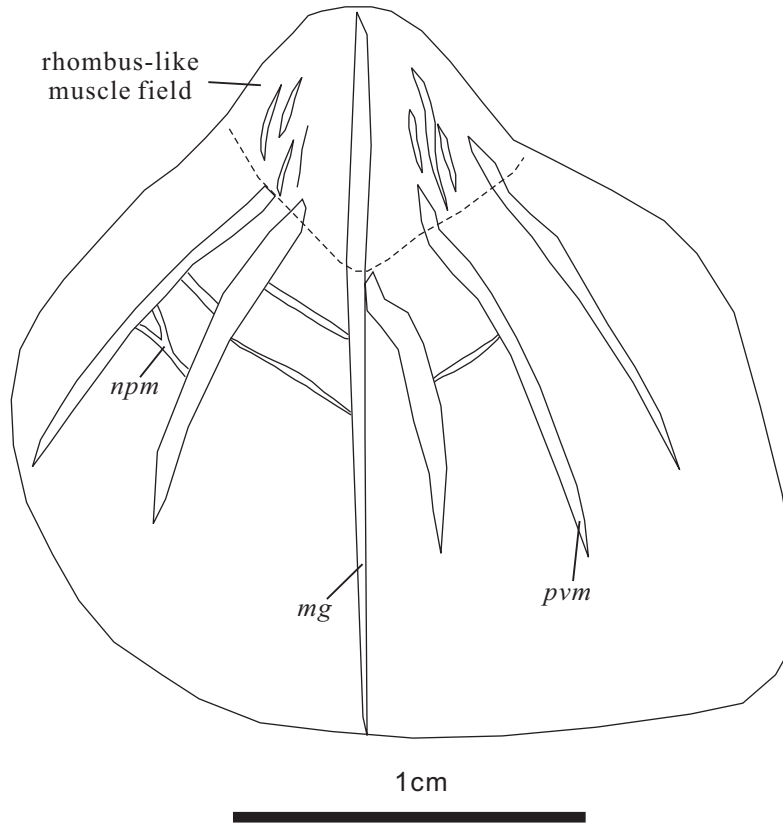

Fig. 9.54 Sketch diagram showing ventral interior of ***Martinia liuqiaoiensis*** He, Shen and Shi sp. nov.. Note: *mg*- median groove; *npm*- netlike pallial markings; *pvm*- pinnate vascular markings

Occurrence Upper Permian; Guangxi and Guizhou of South China.

Description Shell suboval, 4.3–45.8 mm long and 4.4–40.0 mm wide for adults on average, ventral valve moderately convex and dorsal valve weakly convex in profile, hingeline shorter than greatest width at shell midlength. Ventral valve beak slightly incurved; sulcus absent; external surface ornamented by concentric lines (Fig. 9.53k); microornamentation absent. Dorsal valve with rounded cardinal extremities; median fold absent.

Ventral interior generally with a deeply depressed, longitudinally rhombus-like, and apically-located muscle field, numerous ramiform, pinnate to netlike pallial markings anterior and lateral to (around) muscle field (pinnate vascular markings marked by *pvm*, netlike pallial markings marked by *npm*, see Figs. 9.51 and 9.54; pallial markings occasionally lack, especially on juveniles, see Fig. 9.53g, h), a median groove (*mg*) beginning from beak, extending through muscle field and anteriorly to near anterior margin (Figs. 9.51; 9.54). Dorsal interior with deep sockets (*soc*), thick inner socket ridges (*is*), and a trifid cardinal process (*cp*) (Figs. 9.52; 9.53); occasionally with ramiform pallial markings (Fig. 9.52h) and median groove (Figs. 9.52i; 9.53F).

Discussion Most specimens have a longitudinally rhombus-like muscle field at ventral umbo, ramiform to netlike pallial markings anteriorly and laterally around the muscle field, a median groove cut across the muscle field and extending nearly to anterior margin. These features are consistent with the type species *Spinomartinia spinosa* Waterhouse (1968c, pl. 9, Fig. 1, 7) and also consistent with the diagnosis of *Martinia*. However, the present specimens lack of microor-

nament of erect spines and thus belong to *Martinia*.

The new species is similar to *M. semiplana glossoexserta* Zeng et al. 1995 from the Changhsing Formation of Huayingshan, Sichuan Province, South China as both lack sulcus and fold, but differs in the latter having a rhombic outline and a tongue-shaped anterior margin. *Martinia triquetra* Gemmellaro, 1899 from the Permian of Sicily is characterized by plications, comprising a median fold and a fold in each lateral margin in the dorsal valve, none of which presents in the new species. The new species differs from other species of *Martinia* in lacking of sulcus and fold.

Superfamily **Reticularioidea** Waagen, 1883
Family **Elythidae** Fredericks, 1924
Subfamily **Phricodothyridinae** Caster, 1939
Genus ***Phricodothyris*** George, 1932

Type Species *Phricodothyris lucerna* George, 1932. Visean of the Lower Carboniferous, Great Britain.

Diagnosis Small to medium size; unequally biconvex; subovate outline; fold and sulcus absent; ventral interarea well defined, vertically finely striated; short, flat deltidial plates nearly at right angle to interarea. Ventral interior with very low dental flanges; dorsal interior with dental sockets nearly parallel to cardinal margin, dorsal septum and adminicula absent (Carter and Gourvennec in William et al., 2006). Concentric lamellae with double-hooklet or double-spore spines (so-called double-barrelled spines), or with finely interspinous pustules (George, 1932).

Discussion *Phricodothyris* differs from *Squamularia* Gemmellaro, 1899 in the latter having a nearly equally biconvex outline and closely spaced uniramous spines.

Phricodothyris sp.
Figs. 9.55; 9.56

Materials Over 50 specimens. Registered specimens: see below.

Measurements (mm):

Number	Width	Length	Width/ length	Notes
PB5-0262	7.73	7.37	1.05	Ventral valve
PB5-0268	7.19	7.65	0.94	Ventral valve
PB7-0257	9.33	9.31	1.00	Ventral valve
PB8-0265	8.71	9.90	0.88	Ventral valve
PB7-0267	8.15	8.71	0.94	Ventral valve
PB7-0260	9.81	7.83	1.25	External mould of ventral valve
PB9-001	3.95	4.31	0.92	External mould of dorsal valve

Occurrence Changhsingian (Upper Permian); Guangxi (Paibi section) of South China.

Description Shell transversely subovate, 4.3–9.9 mm long and 4.0–9.8 mm wide. Ventral valve moderately convex and dorsal valve weakly convex in profile, hingeline shorter than greatest width at shell midlength. Ventral valve beak slightly incurved; sulcus absent; dorsal valve without fold. External surface with concentric lamellae (Figs. 9.55h; 9.56), double-spore spines (Figs. 9.55i; 9.56) and more finely interspinous pustules nearby the anterior margin of each lamella (Figs. 9.55h; 9.56).

Discussion The presence of concentric lamellae with double-spores spines in the present specimens recalls *Phricodothyris*, but absence of interiors prevents further comparison at present.

Superfamily **Ambocoelioidea** George, 1931
Family **Ambocoeliidae** George, 1931
Subfamily **Ambocoeliinae** George, 1931
Genus ***Attenuatella*** Stehli, 1954

Type Species *Attenuatella texana* Stehli, 1954.

Diagnosis Shell small, ventral valve strongly inflated, longitudinally elongated, with strongly incurved beak and shallow sulcus; dorsal valve nearly flat; ventral interior with diductor scars

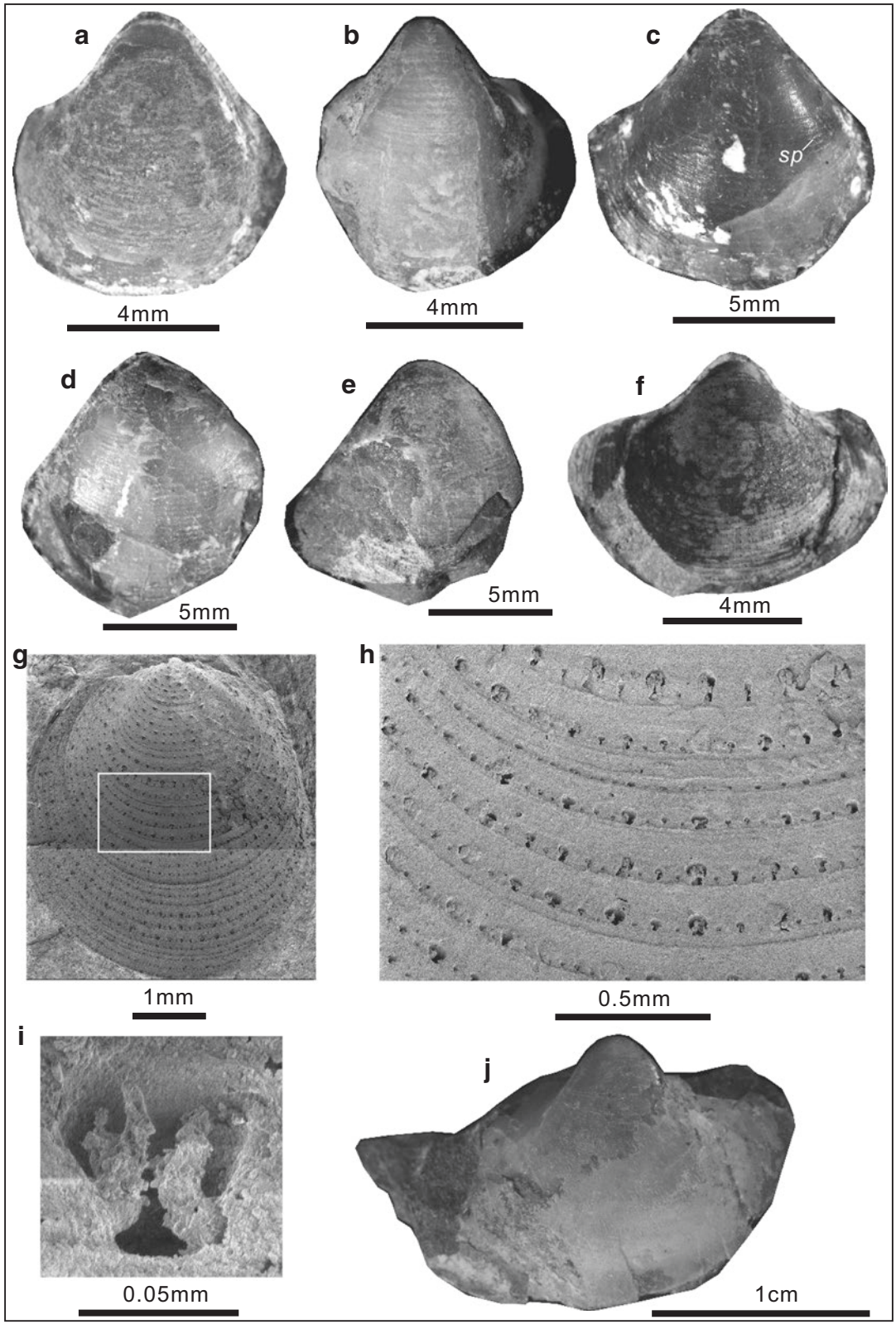
a
4mm
b
4mm
c
sp
5mm
d
5mm
e
5mm
f
4mm
g
1mm
h
0.5mm
i
0.05mm
j
1cm

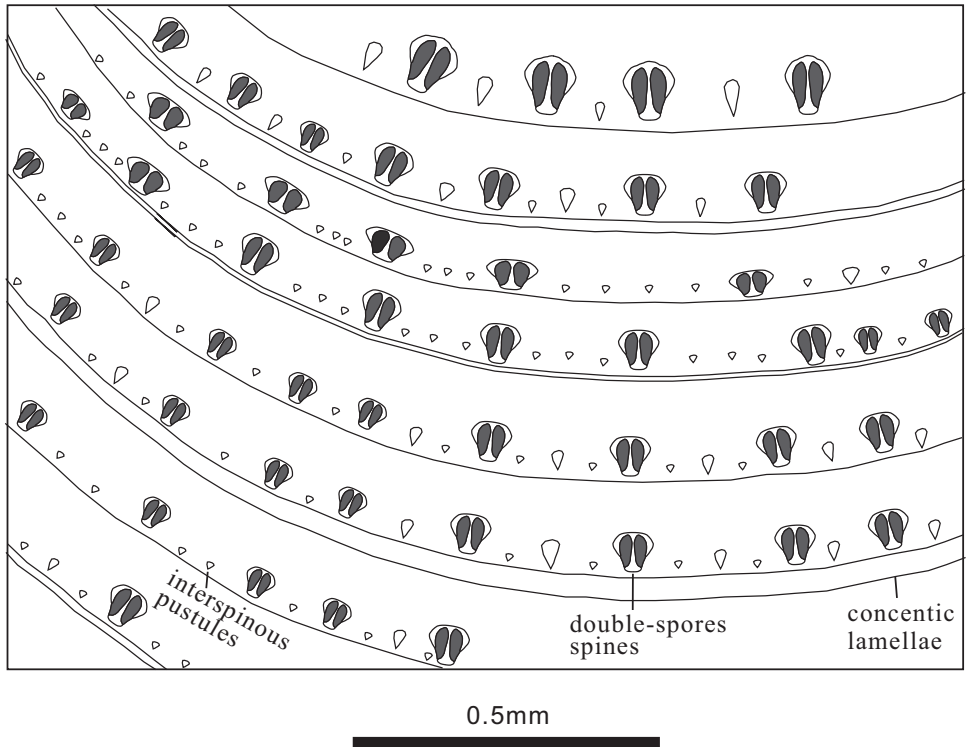

Fig. 9.56 Sketch diagram showing ornaments of ***Phricodothyris*** sp.

raised on long, low narrow ridge with low lateral flanges; dorsal interior with short, triangular, anteriorly diverging crural plates; primary spinose micro-ornamentation (spinose structures above the primary shell layer and easily visible).

Discussion *Attenuatella* differs from other genera of Ambocoeliidae in its extremely elongate outline (Fig. 9.57). *Attenuatella* is more or less similar to *Biconvexiella* Waterhouse, 1983a from the Permian in an elongate outline and interiors, but the latter has a moderately incurved umbo and slightly higher ratio of shell width to length (Fig. 9.57).

Attenuatella mengi He and Shi in He et al., 2007
Figs. 9.58, 9.59 and 9.60a–e

2005 *Paracrurithyris pygmaea* (Liao); He et al.: 935, Fig. 6.6–6.15.
2006a *Attenuatella* sp.; Chen et al.: Fig. 4v, w.
2007 *Attenuatella mengi* He and Shi in He et al.: 276, Figs. 5a–p, 6a–h.
2009 *Attenuatella mengi* He and Shi in He et al.; Zhang and He: 20, Fig. 4s–r.
2009a *Attenuatella mengi* He and Shi in He et al.; Chen et al.: 178, Fig. 7a–c.
2012 *Attenuatella mengi* He and Shi in He et al.; He et al.: 517, Figs. 3a–i, 4a–p.

Fig. 9.55 ***Phricodothyris*** sp.. (**a**), a complete ventral valve, PB5-0262. (**b**), an incomplete ventral valve, PB5-0268. (**c**), a nearly complete ventral valve, PB7-0257, showing spines (*sp*) nearby the anterior margin of each lamella. (**d**, **e**), two incomplete ventral valves, PB8-0265, PB7-0267. (**f**), external mould of a slightly deformed ventral valve, PB7-0260. (**g**), external mould of an incomplete dorsal valve, PB9-001, showing lamellae and spines (SEM). (**h**), portion of PB9-001 (marked by a white rectangle, SEM). (**i**), enlargement of a spine of PB9-001 (SEM). (**j**), an incomplete, deformed ventral valve, PB5-0266

Genera	Ventral interior		Dorsal interior	Exterior				Micro-ornamentation
	Adductor scar	Diductor scar	Crural plate	Shape	Sulcus	Dorsal hingline	Dorsal cardinal extremity	
Attenuatella Stehli, 1954	Adductor scars prominent, narrow, elongate, raised, bisected by a median groove.	Diductor scars prominent, narrow, elongate, raised, lateralto the adductor scars, separated from adductor scars by grooves.	Short, triangular, diverged at a moderately acute angle anteriorly.	Longitudinal-ly elongate	Presence	Nearly straight	Obtuse angled	Spinose
Crurithyris George, 1931	Adductor scars narrow, elongate, depressed, bisected by a median ridge.	Diductor scars narrow, elongate, depressed, lateral position, separated from adductor scars by a pair of ridges.	Long, extending anteriorly and parallel to each other.	Subrounded	Presence	Nearly straight	Rounded	Spinose
Paracruri-thyris Liao in Zhao et al., 1981	Adductor scars weak, narrow, elongate, depressed, bisected by a median ridge.	Diductor scars ill-defined.	Short, triangular, diverged at a moderately acute angle anteriorly.	Subrounded	Presence	Nearly straight	Obtuse angled	Spinose or smooth
Ogilviecoelia Shi and Waterhouse, 1996	Adductor scars elongate, depressed, bisected by a median ridge.	Diductor scars elongate, oval,depressed, posterolateral position, separated from adductor scars by a pair of ridges.	Short, triangular, diverged at a moderately acute angle anteriorly.	Subrounded	Presence	Nearly straight	Rounded	Sparse, short and elongate grooves, no spines
Biconvexiella Waterhouse, 1983b	Adductor scars elongate, depressed, bisected by a median ridge.	Diductor scars wide, short, depressed, posterolateral position, separated from adductor scars by a pair of ridges.	Short, triangular, diverged at a moderately acute angle anteriorly.	Slightly elongate	Presence	Nearly straight	Obtuse angled	Spinose
Orbicoelia Waterhouse and Piyasin, 1970	Muscle scars obscure/invisible.		Short, triangular, diverged at a moderately acute angle anteriorly.	Subrounded	Absence	Convex posteri-orly	Rounded	Finely spinose
Cruricella Grant, 1976	Muscle scars obscure/invisible.		Moderately long, extending anteriorly and parallel to each other.	Subrounded	Absence	Nearly straight	Obtuse angled	Smooth or fine pustules
Speciothyris Jin and Sun, 1981	Muscle scars obscure/invisible.		Short, extending anteriorly, nearly parallel to each other.	Subrounded	Absence	Nearly straight	Rounded	Smooth or weak pustules

Fig. 9.57 Comparison of some similar genera of Ambocoeliidae George, 1931 (revised after He et al., 2014)

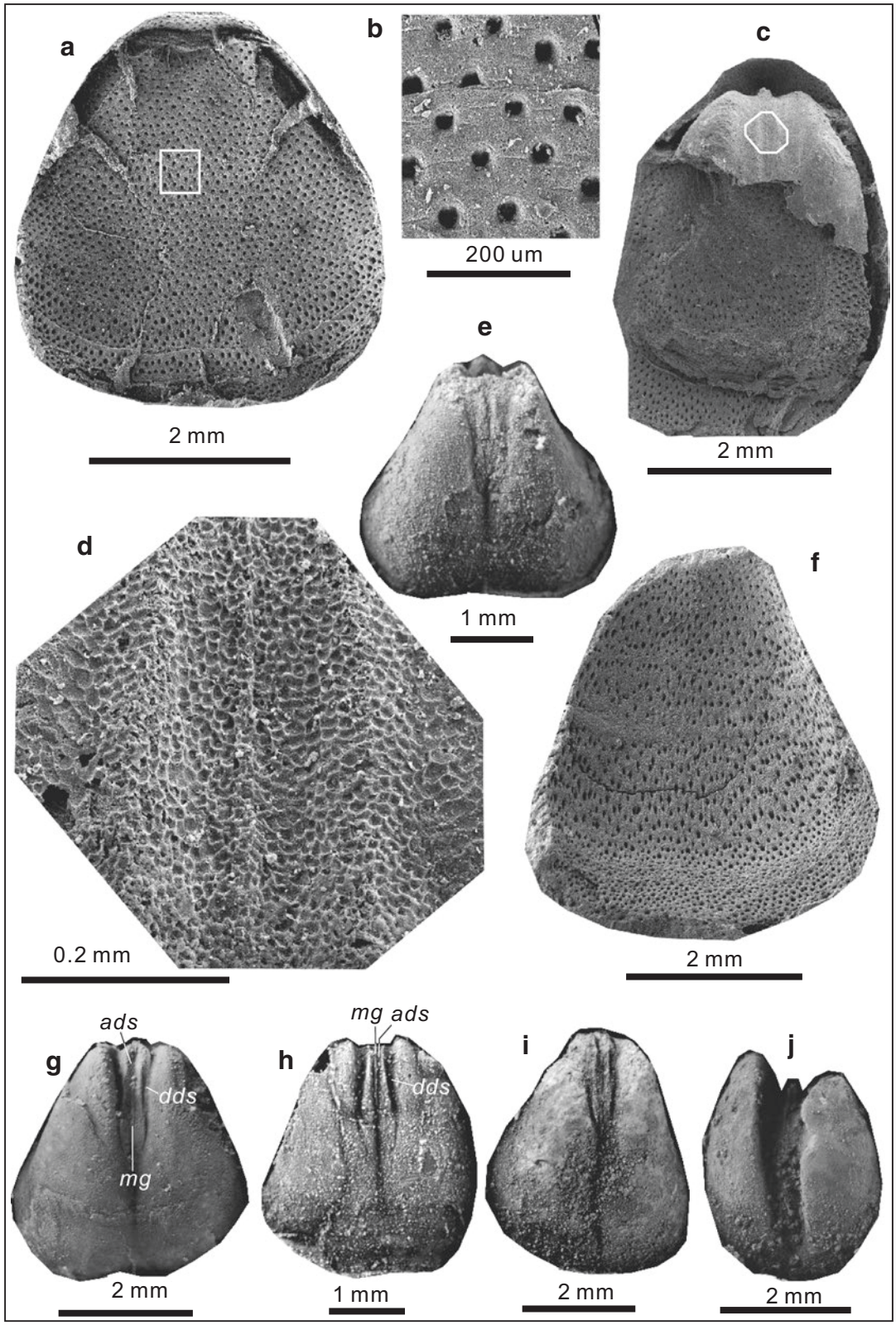
a
2 mm
b
200 um
c
2 mm
e
1 mm
d
0.2 mm
f
2 mm
g
ads
dds
mg
2 mm
h
mg ads
dds
1 mm
i
2 mm
j
2 mm

Materials Over 300 specimens. Registered specimens: see below.

Measurements (mm):

Number	Width	Length	Width/length	Notes
DP-7-1063	3.68	3.93	0.94	External mould of ventral valve
DP-10-1062	3.02	3.93	0.77	Internal mould of ventral valve
DP-9-2-351	3.11	2.96	1.05	Internal mould of ventral valve
DP-5-1070				External mould of ventral valve
DP-2-350	3.55	3.65	0.97	Internal mould of ventral valve
DP-9-8-354	2.84	3.22	0.88	Internal mould of ventral valve
DP-9-353	4.24	4.36	0.97	Internal mould of ventral valve
DP-5-349	2.76	3.55	0.78	Internal mould of ventral valve (juvenile)
DP-5-356	3.52	2.90	1.21	External mould of dorsal valve
DP-5-1071	4.85	4.15	1.17	Internal mould of dorsal valve
DP-7-1066	3.58	2.93	1.22	Internal mould of dorsal valve

Occurrence Changhsingian; Guizhou and Guangxi of South China.

Description Shell 1.4–6.0 mm long, 1.0–5.0 mm wide; hingeline shorter than greatest width at the anterior third, extremely elongate in outline, nearly plano-convex in profile.

Ventral valve strongly inflated; beak and umbo strongly incurved; interarea (*iar*) high, delthyrium (*del*) open (Fig. 9.59d, e); sulcus weakly developed; flanks sharply inclined. Concentric lamellae variable on visceral disk; two orders of spine bases locally quincunxially-arranged, larger ones alternated with smaller ones commonly concentrically as a whole (Fig. 9.58a, f); numbering of larger spine bases about 6–12 per mm, smaller spine bases about 14–18 per mm, spine base 0.03–0.05 mm in diameter; spine bases tapering to the end, with a groove (*gs*) on the posterior of each spine base and two ridges (*rs*) on the anterior of each spine base (Fig. 9.59f).

Dorsal valve nearly flat, slightly convex on umbo, sulcus weak (Fig. 9.60a). Cardinal extremities obtusely rounded, cardinal angle of 120–140°; greatest width at anterior third. Concentric lamellae variable on visceral disk; two orders of spine bases; spine bases close to edges of concentric lamellae smaller, larger spine bases alternated with smaller spine bases concentrically as a whole; numbering of smaller spine bases (close to edges of concentric lamellae) about 15 to 18 per mm, larger spine bases (located further away from edges of concentric lamellae) about 8 to 12 per mm.

Ventral interior with distinct, narrow and long adductor scars (*ads*); adductor scars extending anteriorly to middle or two thirds of valve length, posteriorly bisected by a narrow median groove (*mg*) that extends anteriorly to midvalve (Fig. 9.58g, h). Diductor scars prominent, narrow, elongate and lateral to adductor scars (Fig. 9.58g–i). Tiny net-like vesicles preserved on muscle scars (Fig. 9.58d).

Dorsal interior with deep sockets; cardinal process trilobate; crural plates short, triangular,

Fig. 9.58 ***Attenuatella mengi*** He and Shi in He et al., 2007. (**a**), external mould of a nearly complete ventral valve, DP-7-1063, showing quincunxially-arranged spine bases. (**b**), enlarged portion of DP-7-1063. (**c**), internal mould of an incomplete ventral valve and external mould of the conjoined dorsal valve, DP-10-1062. (**d**), enlarged portion of DP-10-1062, showing net-like vesicles on muscle scars. (**e**), internal mould of a ventral valve, DP-9-2-351. (**f**), external mould of a ventral valve, DP-5-1070, showing two orders (large and small) of spine bases. (**g**, **h**), internal moulds of two nearly complete ventral valves, DP-2-350, DP-9-8-354, showing a median groove (*mg*), a pair of distinct and long adductor scars (*ads*) and a pair of diductor scars (*dds*). (**i**), internal mould of a complete ventral valve, DP-9-353. (**j**), internal mould of a complete ventral valve (juvenile), DP-5-349

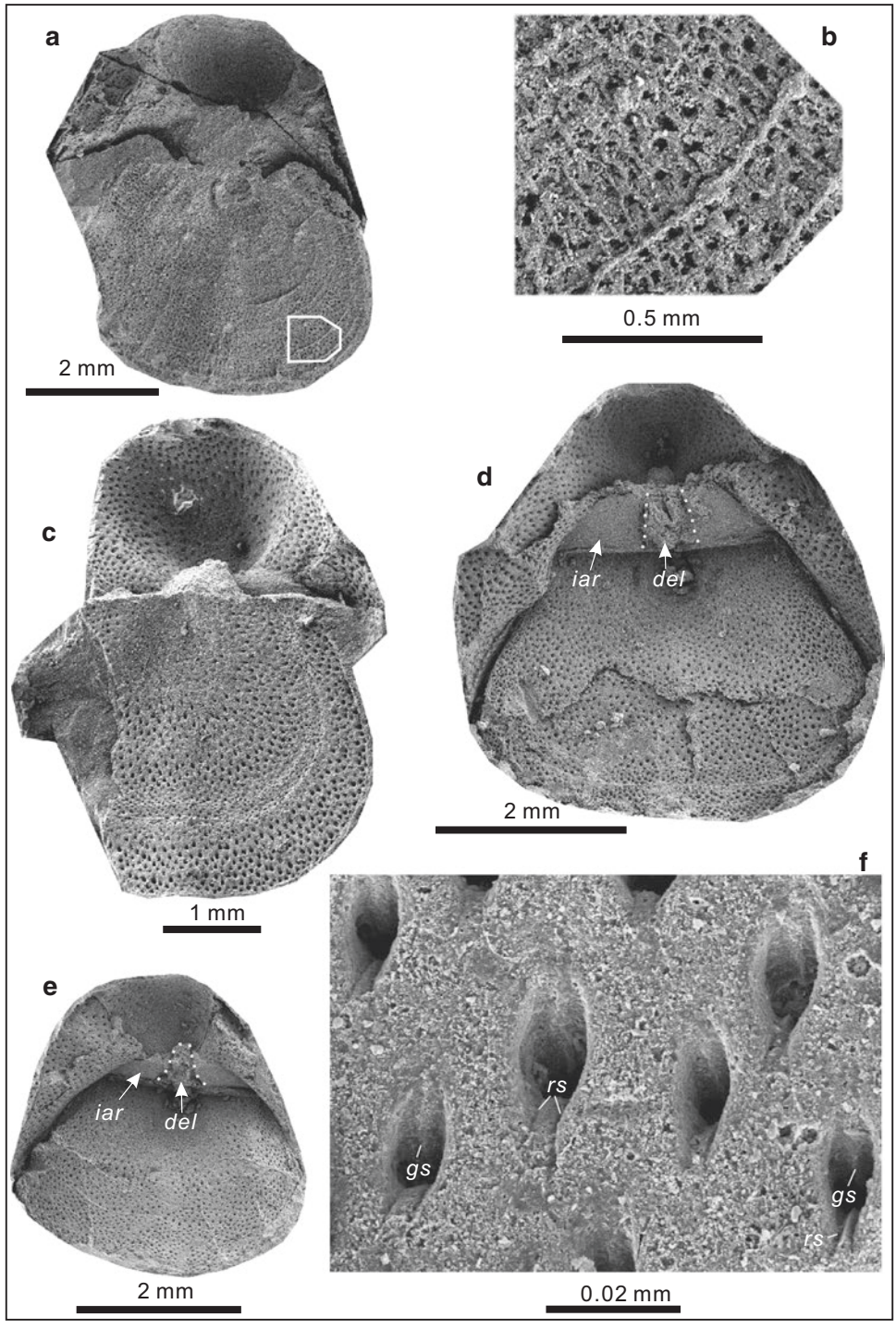

Fig. 9.59 ***Attenuatella mengi*** He and Shi in He et al., 2007. (**a**), external mould of an incomplete dorsal valve and posterior part of external mould of the conjoined ventral valve, SW-4–1003, showing prominent spines despite of heavy diagenesis and deformation. (**b**), enlarged portion of SW-4–1003. (**c**), external mould of an incomplete dorsal valve and posterior part of external mould of the conjoined ventral valve, DP-7-1069, prominently showing two orders of spine bases. (**d**, **e**), external moulds of two complete dorsal valves and posterior parts of external moulds of the conjoined ventral valves, DP-8-1061, DP-8-1068, illustrating an open delthyrium (*del*) and a high interarea (*iar*). (**f**), external mould of a ventral valve, DP-10-1, illustrating groove (*gs*) and ridge (*rs*) at the spine base

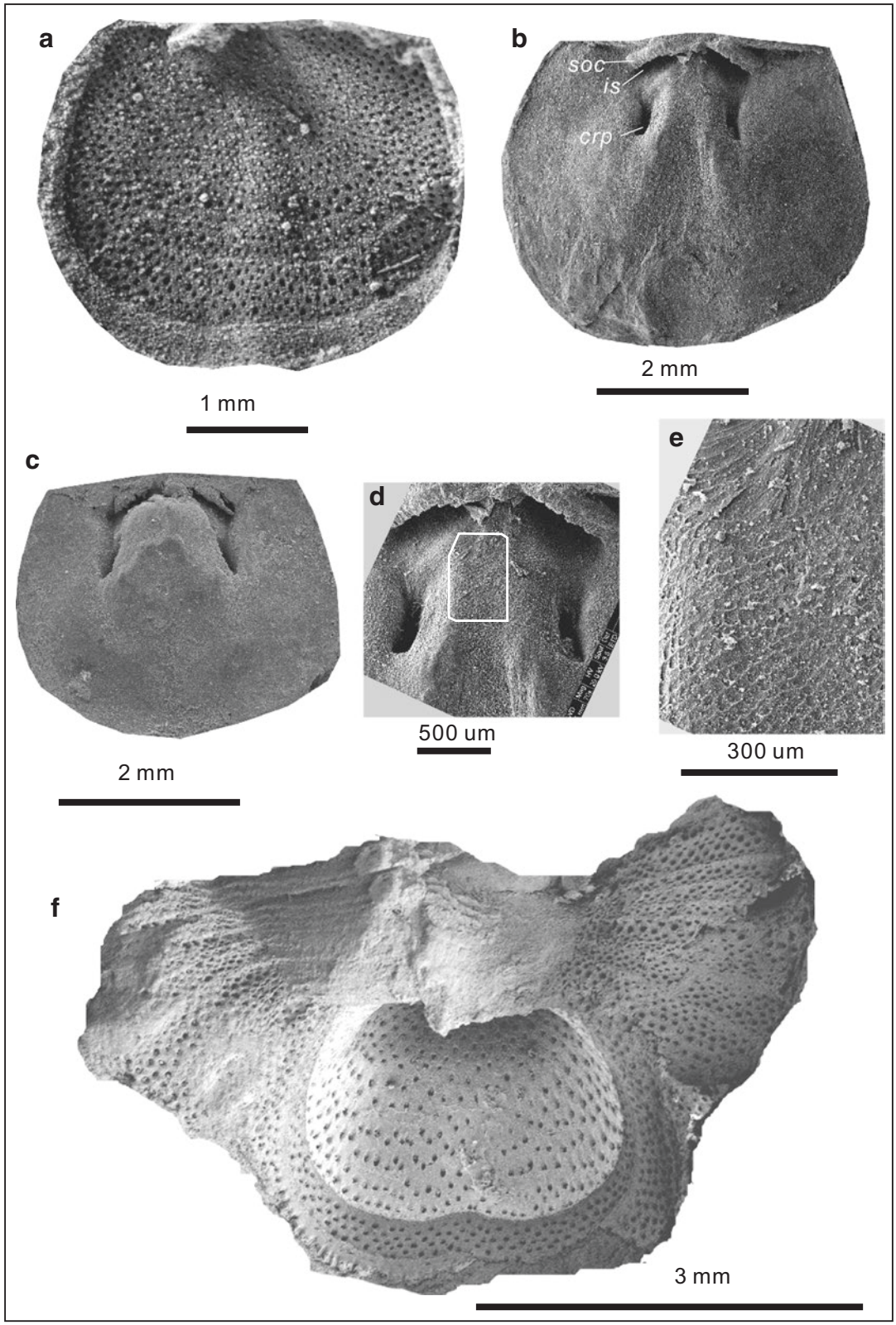
a
1 mm
b
soc
is
crp
2 mm
c
2 mm
d
500 um
e
300 um
f
3 mm

free anteriorly from floor of valve, diverging anteriorly at a moderately acute angle (Fig. 9.60b). Muscle scars generally obscure; adductor scars clearly differentiated into posterior and anterior portions, posterior adductor scars small and oval, bisected by weak median ridge, anterior adductor scars larger and crescent, separated from adjacent posterior adductor scar by a weak ridge (observed on well-preserved specimens occasionlly). Tiny net-like vesicles preserved on muscle scars (Fig. 9.60e).

Discussion An extremely elongate outline and a pair of long, raised adductor scars ("median ridge" called by Stehli, 1954) suggest the diagnostic features of *Attenuatella* Stehli, 1954. *Attenuatella mengi* differs from *A. texana* Stehli (1954, p. 343) of the Early Permian of Texas, southwestern USA in its smaller body size and a median groove bisected adductor scars, and from *A. incurvata* Waterhouse (1964, p. 108–110, pls 20, 21) of the Middle Permian of New Zealand in having a smaller body size and slightly wider outline. Compared with the present species, *Attenuatella multispinosa* Waterhouse, 1967 of the Middle Permian, New South Wales, Australia has a more elongate outline. In addition, *Attenuatella mengi* was only discovered at deeper water sections, including Dongpan in Guangxi, Shaiwa and Duanshan in southern Guizhou and therefore differs from *Paracrurithyris pygmaea* in palaeogeographic distribution (the latter commonly discovered in the Talung Formation of South China but not found in the counterpart at Dongpan).

Attenuatella sp.
Fig. 9.60f

Material One registered specimen: DP-9-12.

Occurrence Changhsingian; Guangxi of South China.

Description Shell small, 3.0 mm long and 3.1 mm wide, hingeline shorter than greatest width at anterior third, oval in outline. Ventral valve strongly convex; sulcus near anterior margin, shallow; flanks sharply inclined (external moulds of flanks formed and look like two wing-like structures); ventral surface with a prominent concentric lamella near anterior margin; spine bases quincunxially arranged, two orders of spine bases present, those on visceral disk large, measuring about 8 per mm; spine bases located near anterior margin relatively small, with 10 per mm, all spine bases tapering to the end and with two ridges protruding from the anterior.

Genus ***Paracrurithyris*** Liao in Zhao et al., 1981

Type Species *Crurithyris pygmaea* Liao, 1980a.

Diagnosis (emended). Shell small, subrounded in outline; widest at midvalve; planoconvex to unequally biconvex. Ventral valve strongly convex, with incurved beak; interarea high with narrowly triangular delthyrium without cover; sulcus beginning from near umbo to anterior margin. Dorsal valve flat or slightly convex with small beak; interarea low or uneasily observed; sulcus shallow but visible, extending from beak to ante-

Fig. 9.60 (**a–e**), ***Attenuatella mengi*** He and Shi in He et al., 2007. (**a**), external mould of a complete dorsal valve, DP-5-356, showing quincunxially-arranged spine bases. (**b**), internal mould of a complete dorsal valve, DP-5-1071, showing deep sockets (*soc*), prominent inner socket ridges (*is*) and crural plates (*crp*). (**c**), internal mould of a complete dorsal valve, DP-7-1066. (**d**), enlarged muscle scar of DP-5-1071. (**e**), further enlarged portion of DP-5-1071, showing tiny net-like vesicles. (**f**), ***Attenuatella*** sp., external mould of a complete dorsal valve and external mould of flanks of the conjoined ventral valve, DP-9-12, showing quincunxially-arranged spine bases and concentric lines

rior margin. Shell surface ornamented with concentric lamellae, smooth or with secondary spinose micro-ornamentation (spinose structures embedded in the primary shell layer and visible on partly weathered specimens when the primary shell layer around spines decorticated). Ventral interior without any plates; teeth short, knoblike; ventral muscle area weak, or adductor scars elongate, located beside medium ridge, diductor scars obscure. Dorsal interior with small, triangular cardinal process; sockets deep with thick ridges; crural plates short, free anteriorly from floor of valve; adductor scars small, quadrate and obscure; median ridge weak.

Discussion *Paracrurithyris* was named and illustrated by Liao (1979a), and shortly after, described by Liao, 1980a. The name of *Paracrurithyris pigmaea* was changed to *Paracrurithyris pygmaea* considering the spelling rule in Ladin by Johnson, Carter and Hou in Williams et al. (2006).

Paracrurithyris is very similar to *Crurithyris* George, 1931 in its ovate outline and ventral interior, but the former has shorter crural plates, obtuse angled cardinal extremities (Fig. 9.57) and occurred only in the Changhsingian to the Induan; by contrast, the latter has rounded cardinal extremities (Fig. 9.57) and originated from the Upper Devonian. *Paracrurithyris* differs from *Ogilviecoelia* Shi and Waterhouse, 1996 in the latter having grooves as the micro-ornamentation (Fig. 9.57). *Paracrurithyris* is distinguished from *Orbicoelia* Waterhouse and Piyasin, 1970 in the former has a nearly straight dorsal hingline, relatively prominent muscle scars in the ventral interior and sulcus on both valves; while the latter has a posteriorly convex dorsal hingeline, obscure muscle scars and lacks sulcus (Fig. 9.57). Compared with *Cruricella* Grant, 1976, *Paracrurithyris* would differ in having ventral and dorsal sulcuses and relatively prominent muscle scars in the ventral interior (Fig. 9.57).

Paracrurithyris pygmaea (Liao in Zhao et al., 1981)

Figs. 9.61, 9.62a–h and 9.63

1979a *Paracrurithyris pygmaea* Liao: 207, Fig. 4–7.
1979 *Crurithyris pusilla* Chan in Hou et al.: 96, pl. 13, Fig. 24–26.
1980a *Crurithyris pygmaea* Liao: 264, pl. 8, Fig. 1–4.
1984 *Crurithyris pygmaea* (Liao); Liao, 285, pl. 2, Fig. 26, 27.
1984 *Crurithyris pusilla* Chan in Hou et al.; Wang: 224, pl. 89. Fig. 24, 25, 28.
2012 *Crurithyris tazawai* He and Shi in He et al.: 521, Figs. 5a–s, 6a–j.
2012 *Paracrurithyris pygmaea* (Liao in Zhao et al.); He et al.: 523, Fig. 7a–n.

Materials Over 3000 specimens. Registered specimens: see below.

Fig. 9.61 ***Paracrurithyris pygmaea*** (Liao in Zhao et al., 1981). (**a**), external mould of an incomplete dorsal valve, CM-1-1005, showing tiny spine bases and sparsely-arranged concentric lines. (**b**), enlarged portion of CM-1-1005, showing quincunxially-arranged spine bases. (**c**), external mould of an incomplete ventral valve, CM-13-1007. (**d**), enlarged portion of CM-13-1007, showing quincunxially-arranged spine bases. (**e**), external mould of a complete ventral valve, CM-13-1018. (**f**), enlarged portion of CM-13-1018, showing quincunxially-arranged spine bases. (**g**), interior of an incomplete ventral valve (shell partly decorticated), SR-23b-1014, showing spine bases when shell decorticated (marked by white square). (**h**), enlarged portion of SR-23b-1014, showing quincunxially-arranged spine bases. (**i**), internal mould of a complete ventral valve, SR-23b-1011, showing obscure muscle scars. (**j**, **k**), internal moulds of two complete dorsal valves, CM-14-1016, SR-23b-1023, showing deep sockets, thick inner socket ridges and crural plates

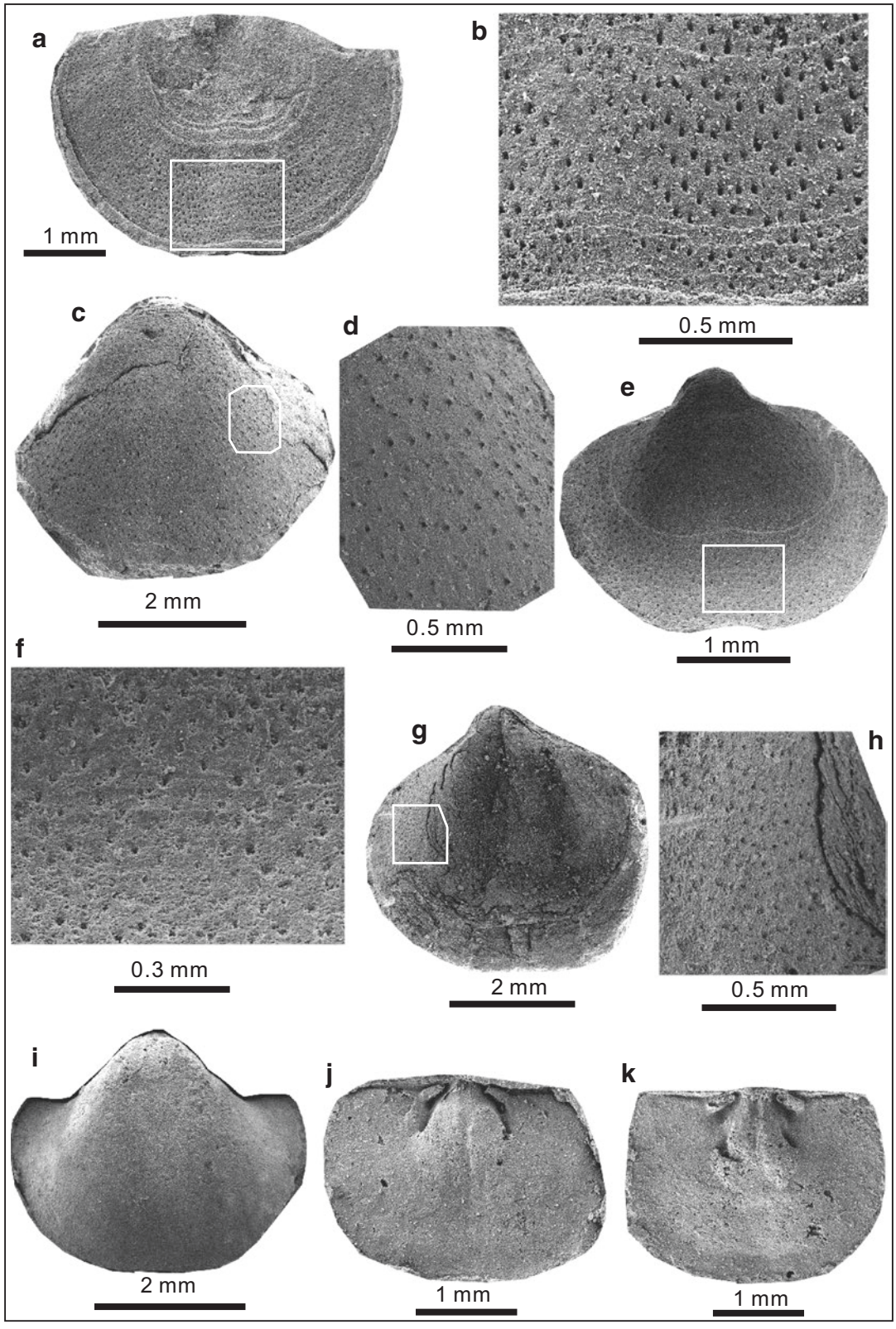
a
1 mm
b
0.5 mm
c
2 mm
d
0.5 mm
e
1 mm
f
0.3 mm
g
2 mm
h
0.5 mm
i
2 mm
j
1 mm
k
1 mm

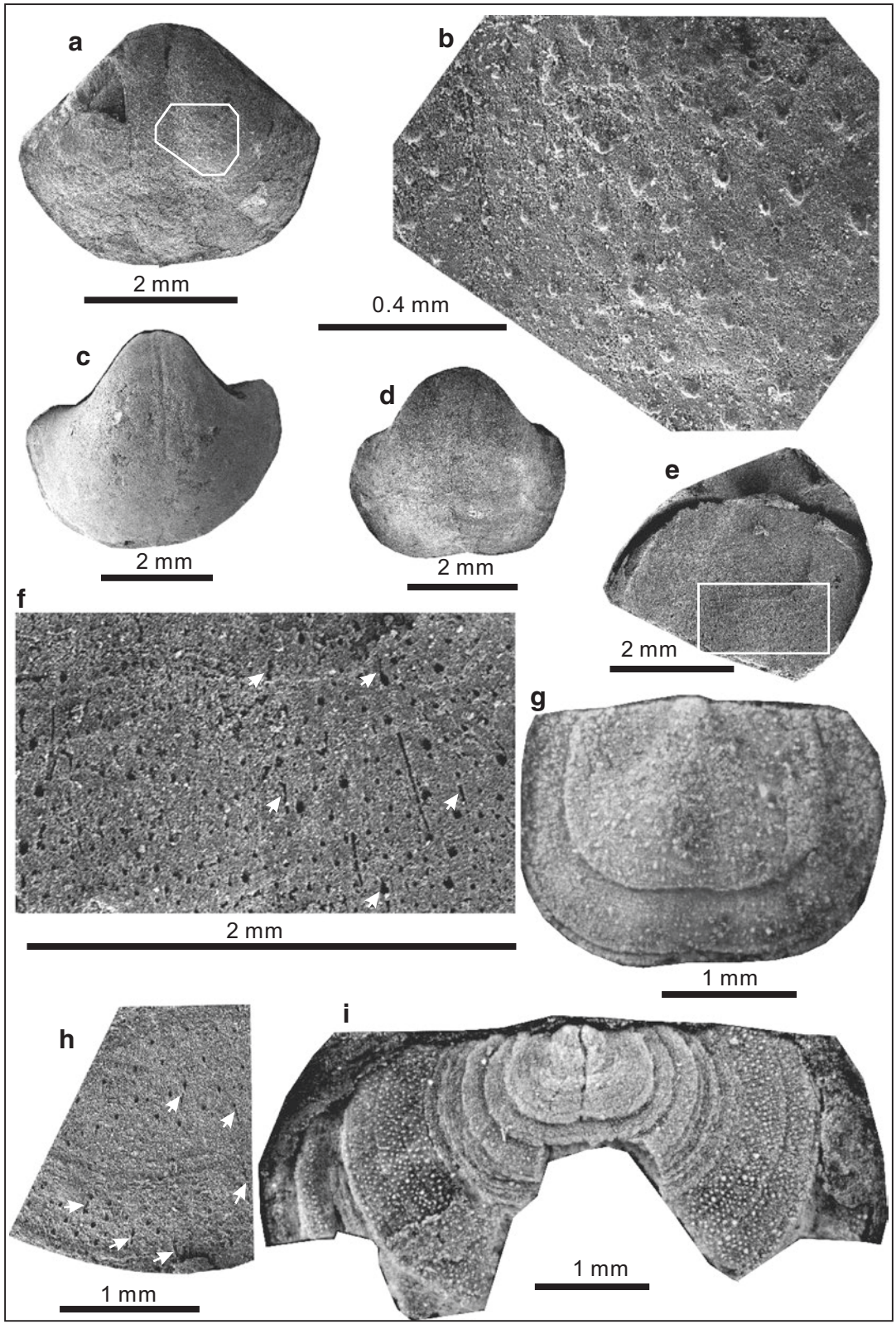
a
2 mm
b
0.4 mm
c
2 mm
d
2 mm
e
2 mm
f
2 mm
g
1 mm
h
1 mm
i
1 mm

Measurements (mm):

Number	Width	Length	Width/length	Notes
CM-1-1005	4.29	2.92	1.47	External mould of dorsal valve
CM-13-1007	4.34	3.84	1.13	External mould of ventral valve
CM-13-1018	2.89	2.35	1.23	External mould of ventral valve
SR-23b-1014	4.50	4.25	1.06	Ventral interior
SR-23b-1011	3.93	3.22	1.22	Internal mould of ventral valve
CM-14-1016	2.79	2.06	1.35	Internal mould of dorsal valve
SR-23b-1023	2.92	2.20	1.33	Internal mould of dorsal valve
CM-14-1021	3.93	3.20	1.23	Ventral valve
SR-23b-1028	4.57	3.93	1.16	Internal mould of ventral valve
SR-23c-1027	3.94	3.48	1.13	Internal mould of ventral valve
CM-12-508	2.71	2.03	1.34	External mould of dorsal valve
CM-16-1052	4.50	4.18	1.08	Internal mould of ventral valve
CM-15-1056	3.05	2.53	1.20	Internal mould of ventral valve
XM-1-1037	2.44	1.85	1.32	Dorsal exterior
CM-16-1045	3.61	3.38	1.07	Internal mould of ventral valve
CM-13-1040	4.15	3.34	1.24	Internal mould of dorsal valve
CM-12-1039	2.34	1.89	1.24	Dorsal exterior
CM-14-1036	3.53	2.72	1.30	Internal mould of dorsal valve
CM-14-1041	4.23	3.25	1.30	Internal mould of dorsal valve
CM-16-1047	3.98	3.05	1.30	Internal mould of ventral valve
CM-16-1044	3.96	3.20	1.24	Ventral interior

Occurrence Changhsingian (Upper Permian) to Induan (lowest Triassic); South China.

Description Shell tiny, 3.5 mm long and 4.2 mm wide on average, smallest specimen 1.72 mm long and 1.72 mm wide, and largest specimen 6.74 mm long and 7.98 mm wide; subrounded in outline, hingeline shorter than greatest width at shell midlength, nearly plano-convex in profile.

Ventral valve moderately inflated, beak strongly incurved; ventral interarea high, delthyrium open; sulcus weak. Number of concentric laminae variable on visceral disk, smooth or spinose micro-ornamentation, spine bases quincunxially arranged, numbering of spine bases about 40–250 per mm^2 (if spinose).

Dorsal valve nearly flat; sulcus absent or weak. Concentric lamellae variable on visceral disk; smooth or spinose micro-ornamentation, spine bases approximately concentrically-arranged as a whole and quincunxially-arranged locally (Fig. 9.61a, b), numbering of spine bases about 20–180 per mm^2 (if spinose); scars of tiny spines occasionally visible on specimens (see Fig. 9.62e, f, h).

Ventral interior with obscure, elongated muscle scars, bisected by median ridge. Dorsal interior with deep sockets; thick inner socket ridges, crural plates short, triangular, diverging at a moderately acute angle anteriorly.

Discussion *Crurithyris tazawai* He and Shi in He et al., 2012 is here considered as synonymous

Fig. 9.62 (**a**–**h**), ***Paracrurithyris pygmaea*** (Liao in Zhao et al., 1981). (**a**), an incomplete ventral valve (shell partly decorticated), CM-14-1021. (**b**), enlarged portion of CM-14-1021, showing quincunxially-arranged spine bases. (**c**, **d**), internal moulds of two complete ventral valves, SR-23b-1028, SR-23c-1027, showing obscure muscle scars. (**e**), external mould of an incomplete dorsal valve and posterior part of external mould of the conjoined ventral valve, CM-14-1016-2. (**f**), enlarged portion of CM-14-1016-2, white arrows showing scars of tiny spines. (**g**), a complete dorsal valve, CM-12-508, showing pustule-like spine bases and sparsely-distributed concentric lamellae. (**h**), external mould of a part of dorsal valve, CM-15-1022, white arrows showing scars of tiny spines. (**i**), ***Paracrurithyris*** sp., an incomplete dorsal valve, CM-15-542, showing quincunxially-arranged pustule-like spine bases

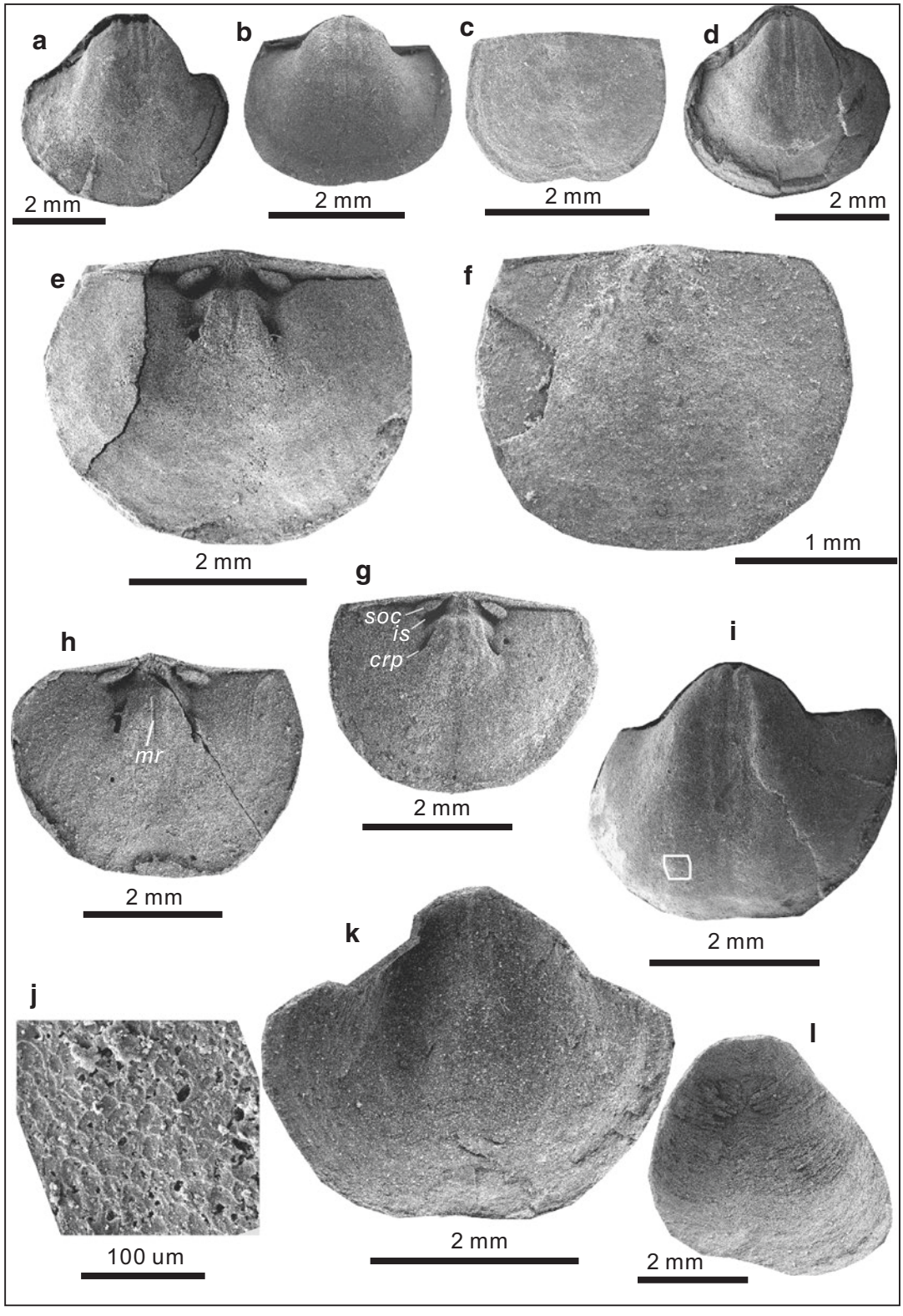
a
2 mm
b
2 mm
c
2 mm
d
2 mm
e
2 mm
f
1 mm
g
soc
is
crp
2 mm
h
mr
2 mm
i
2 mm
j
100 um
k
2 mm
l
2 mm

with *Paracrurithyris pygmaea* (Liao in Zhao et al., 1981). The reasons are two fold. Firstly, spinose ornamentation is locally visible on most shells, especially on those shells that have been partly weathered, as already noted by Baliński (1975). In all likelihood, these spines are micro-ornaments, most (or even all) of them are embedded within the outer layer of the shell and they would have been exposed when shell was partly decorticated due to weathering. Secondly, "*Crurithyris tazawai*" is usually found to co-occur with *Paracurithyris pygmaea*, in the same sedimentary environment and geological age, suggesting that they probably belong to the same species. If this is correct, the character of spinose micro-ornamentation should be added to the definition of *Paracrurithyris* Liao in Zhao et al., 1981 (see Diagnosis of *Paracrurithyris*).

Paracrurithyris sp.
Fig. 9.62i

Material One incomplete dorsal valve (CM-15-542).

Occurrence Uppermost Changhsingian; Anhui (Majiashan section) of South China.

Description Shell 5.5 mm wide, hingeline slightly shorter than greatest width. Dorsal valve flat, slightly convex on umbo. Cardinal extremities obtusely rounded, cardinal angle of 135°. Shell surface ornamented with strong, unevenly-arranged concentric lamellae, two orders of pustule-like spine bases; spine bases irregularly concentric as a whole and locally quincunxially-arranged; numbering of fine spine bases, numbering about 300 per mm^2.

Discussion The present species differs from *Paracrurithyris pygmaea* in its dense spine bases and more concentric lamellae.

Genus ***Speciothyris*** Jin and Sun, 1981

Type Species *Crurithyris speciosa* Wang, 1955a.

Diagnosis Shell small to medium, nearly rounded in outline, hingeline shorter than greatest width. Ventral valve moderately inflated, with moderately incurved beak; delthyrium high, wide and bridged at apex by short delthyrial plate; sulcus absent. Dorsal valve weakly convex; cardinal extremities rounded; lack of sulcus or fold. Anterior commissure rectimarginate. Surface smooth or may be weakly pustulose. Ventral interior with short teeth, no internal plates, muscle area smooth or obscure. Dorsal interior with globose cardinal process; crural plates short, extending anteriorly and nearly parallel to each other; coiled spiralia have more than 10 volutions and their axes directed posterolaterally toward the hinge ends (Shen et al. in Rong et al., 2017).

Discussion *Speciothyris* was proposed with *Crurithyris speciosa* Wang, 1955a as the type species, sketched (interiors) and compared with *Crurithyris* George, 1931 by Jin and Sun (1981), despite lacking a detailed description. We agree that *Crurithyris speciosa* Wang, 1955 from the Changhsingian and earliest Triassic of South China is different from typical *Crurithyris*, a long-ranging genus characterized by possessing weak sulcus on both valves (Johnson et al. in Williams et al., 2006, p. 1733) and well-developed delthyrial covering-plates (Jin and Sun, 1981). Also, *Crurithyris speciosa* Wang, 1955 can not be assigned to *Paracrurithyris* Liao in Zhao et al., 1981, because it completely lacks of sulcus, and has obscure/

Fig. 9.63 ***Paracrurithyris pygmaea*** (Liao in Zhao et al., 1981). (**a**, **b**), internal moulds of two complete ventral valves, CM-16-1052, CM-15-1056, showing obscure muscle scars. (**c**, **f**), exteriors of two complete dorsal valves, XM-1-1037, CM-12-1039, showing smooth ornamentation. (**d**), internal mould of a ventral valve and remnant shell, CM-16-1045. (**e**), internal mould of a complete dorsal valve and shell remnant, CM-13-1040. (**g**), internal mould of a complete dorsal valve, CM-14-1036, showing socket (*soc*), inner socket ridge (*is*) and crural plates (*crp*). (**h**), internal mould of a complete dorsal valve, CM-14-1041, showing a median ridge (*mr*). (**i**), internal mould of a complete ventral valve, CM-16-1047. (**j**), enlarged portion of CM-16-1047, showing net-like vesicles. (**k**), interior of a nearly complete ventral valve, CM-16-1044. (**l**), interior of an incomplete ventral valve and shell remnant, XM-4-1059

invisible muscle scars and rounded dorsal cardinal extremities (Fig. 9.57) (despite the author S. Z. Shen still regards *Speciothyris* as a synonym of *Paracrurithyris*, as reviewed by Shen et al. in Rong et al., 2017). Another difference between *Speciothyris* and *Paracrurithyris* is of note is that, based on our observation of numerous specimens from varied sedimentary facies, specimens here assigned to *Speciothyris* are all from shallow-water carbonate and silty mudstone facies (e.g., Huangzhishan of Zhejiang, Zhongzhai and Zhongying of western Guizhou), whereas those of *Paracrurithyris* are restricted to deep-water siliceous mudstone facies and moderately deep-water ramp facies of carbonate platform (e.g., Majiashan of Anhui, Rencunping of Hunan, Meishan of Zhejiang). *Speciothyris* is also similar to *Cruricella* Grant, 1976 and *Orbicoelia* Waterhouse and Piyasin, 1970 in interiors (specifically obscure or invisible muscle scars), outline and lacking of sulcus on both valves. However, *Speciothyris* differs from *Cruricella* Grant, 1976 in rounded dorsal extremities (Fig. 9.57), and from *Orbicoelia* Waterhouse and Piyasin, 1970 in the latter having a longer, more incurved dorsal beak and posteriorly convex dorsal hingeline (Fig. 9.57). Because of the absence of a sulcus in *Crurithyris speciosa* Wang, 1955a, type species of *Speciothyris*, Chen et al. (2006b) assigned it to *Orbicoelia*, but we believe it is not *Orbicoelia* in view of the comparisons offered here.

Speciothyris speciosa (Wang, 1955a)
Fig. 9.64

1955a *Crurithyris speciosa* Wang: 146, pl. 83, Fig. 1–4.
1956 *Crurithyris speciosa* Wang: 389, pl. 6, Fig. 1–6.
1964 *Crurithyris speciosa* Wang; Wang et al.: 546, pl. 104, Fig. 13–16.
1978 *Crurithyris speciosa* Wang; Tong: 254, pl. 89, Fig. 6.
1978 *Crurithyris speciosa* Wang; Feng and Jiang: 283, pl. 102, Fig. 10.
1980a *Crurithyris speciosa* Wang; Liao, pl. 8, Fig. 16, 17.
1984 *Crurithyris speciosa* Wang; Wang: 225, pl. 66, Fig. 12, 18.
1995 *Crurithyris speciosa* Wang; Zeng et al.: pl. 12, Fig. 19.
2006b *Orbicoelia speciosa* (Wang); Chen et al.: 317, Figs. 9a–f, 10.
2014 *Orbicoelia speciosa* (Wang); Zhang et al.: 498, Fig. 10a–i, l–s.

Materials Over 700 specimens. Registered specimens: see below.

Measurements (mm):

Number	Width	Length	Width/ length	Notes
LZ2704642	13.61	12.61	1.08	Internal mould of ventral valve
LZ1400444	11.54	9.13	1.27	Internal mould of ventral valve
LZ1400482	14.48	9.52	1.52	Internal mould of dorsal valve
LZ0400463	9.60	7.94	1.21	Internal mould of dorsal valve
LZ1400452	18.22	15.67	1.16	Internal mould of ventral valve
LZ0400641	14.63	10.51	1.39	Internal mould of dorsal valve
LZ0400454	15.56	15.34	1.01	Internal mould of ventral valve
HZS20-0683	7.83	6.92	1.18	Ventral valve of a conjoined shell
HZS20-0683	7.77	6.57	1.18	Dorsal valve of a conjoined shell
HZS23-0679	9.99	8.15	1.23	Ventral valve
HZS20-0682	8.38	8.10	1.03	Ventral valve

Fig. 9.64 (continued) LZ0400463. (**f**), internal mould of a complete ventral valve, LZ1400452. (**g**), internal mould of a complete dorsal valve and posterior part of the conjoined ventral valve, LZ0400641, showing a pair of subparallel crural plates (*crp*). (**h**), internal mould of a complete ventral valve, LZ0400454, showing weak muscle scars. (**i**), internal mould of an incomplete dorsal valve and posterior part of internal mould of the conjoined ventral valve, LZ0400486, showing triangular ventral interarea (*iar*) and a cardinal process (*cp*). (**j**), conjoined valves, HZS20-0683, showing smooth ornamentation (ventral view). (**k**), dorsal view of HZS20-0683, showing a nearly straight hingeline. (**l**), lateral view of HZS20-0683, showing a ventribiconvex profile. (**m**, **n**), two conjoined valves (ventral views), HZS23-0679, HZS20-0682. (**o**), lateral view of HZS20-0682

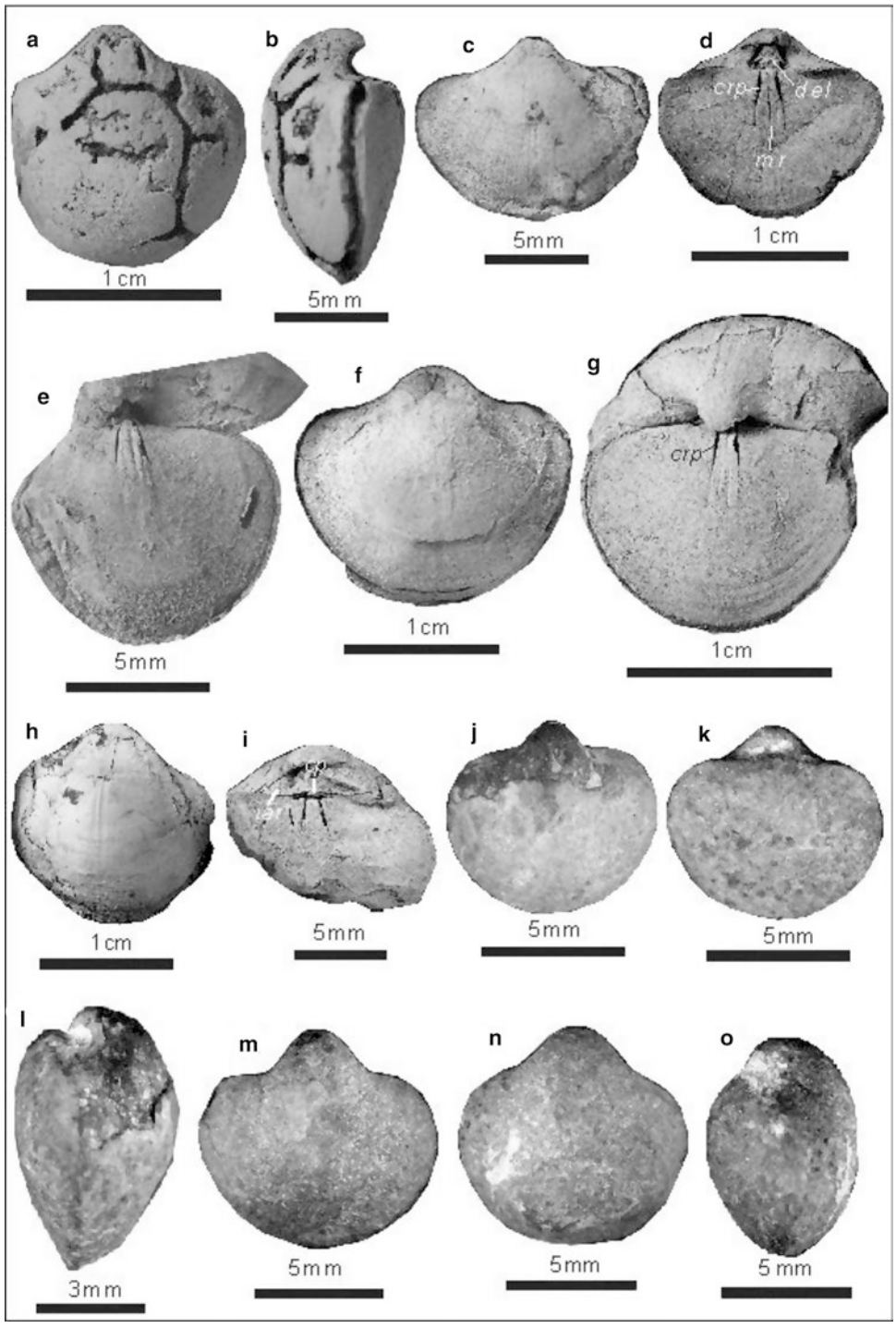

Fig. 9.64 ***Speciothyris speciosa*** (Wang, 1955a). (**a**), internal mould of a complete ventral valve, LZ2704642. (**b**), lateral view of LZ2704642, showing a ventribiconvex profile. (**c**), internal mould of a complete ventral valve, LZ1400444. (**d**), internal mould of a complete dorsal valve and posterior part of internal mould of the conjoined ventral valve, LZ1400482, showing an open delthyrium (*del*), sub-parallel crural plates (*crp*) and a median ridge (*mr*). (**e**), internal mould of a complete dorsal and posterior part of internal mould of the conjoined ventral valve,

Occurrence Changhsingian (Upper Permian) to Induan (lowest Triassic); South China.

Description Shell small to medium, 6.6–15.7 mm long and 7.8–17.3 mm wide; subrounded in outline, hingeline shorter than greatest width at shell midlength, ventribiconvex in profile.

Ventral valve moderately inflated; beak incurved, overhanging delthyrium; ventral interarea (*iar*) high, delthyrium (*del*) open (Fig. 9.64d, i); sulcus absent. Dorsal valve nearly flat or weakly convex; hingeline nearly straight, cardinal extremities rounded; sulcus or fold absent. Smooth, concentric lines occasionally visible on disks.

Ventral interior with weak muscle scars. Dorsal interior with a simple cardinal process (Fig. 9.64i); deep sockets; crural plates (*crp*) short, triangular, extending anteriorly and nearly parallel to median ridge (*mr*) (Fig. 9.64d).

Discussion Probably the type species is the only species for the genus at present. However, "*Crurithyris*" *longa* Liao, 1980a from the Changhsingian silty mudstone of Qinglong, western Guizhou, South China is convex along midwidths for both valves despite with an anterior tongue nearby the anterior margin, this feature differs from the sulcus on both valves for *Crurithyris*, and probably "*Crurithyris*" *longa* Liao, 1980a is a species of *Speciothyris*.

Order **Orthida** Schuchert and Cooper, 1932
Suborder **Dalmanellidina** Moore, 1952
Superfamily **Dalmanelloidea** Schuchert, 1913
Family **Rhipidomellidae** Schuchert, 1913
Subfamily **Rhipidomellinae** Schuchert, 1913
Genus ***Rhipidomella*** Oehlert, 1890

Type Species *Terebratula michelini* Léveillé, 1835. Visean of Lower Carboniferous of Belgium.

Diagnosis Dorsibiconvex, rectimarginate to weakly unisulcate valves; ventral interior with extended, flabellate muscle scars, bisected in front of adductor scar by short median ridge; dorsal interior with brachiophores.

Discussion *Rhipidomella* Oehlert, 1890 is similar to *Schuchertella* Girty, 1904 in a thick median ridge which bisects muscle scar in the ventral interior and a simple, prominent cardinal process, but the latter has a more transverse outline and lacks brachiophores. *Rhipidomella* resembles to *Clavodalejina* Havlíček, 1977 in a wide (or thick) median ridge in the dorsal interior, a simple cardinal process and a pair of brachiophores, but differs in the latter has dental plates and lacks a median ridge in the ventral interior.

Occurrence *Rhipidomella* Oehlert, 1890 has mainly been found in Carbonifeous to Lower Permian, although it is also known sparsely from the Middle Permian in Timor and Cambodia (Broili, 1916; Chi-Thuan, 1961; Grant, 1976) and from the Upper Permian (Changhsing Formation) in South China (Shen and He, 1994).

Rhipidomella parvula He, Shi and Shen sp. nov. Figs. 9.65, 9.66 and 9.67

2005 *Schuchertella* sp.; He et al., p. 935, Fig. 6.1–6.5.

Diagnosis Small *Rhipidomella* with coarse costae and rugae, and micro-ornamentation of fine tubes and lamellae.

Etymology Refers to its very small body size.

Fig. 9.65 (continued) internal mould of a nearly complete dorsal valve, DP9-0243, showing a pair of sockets (*soc*) and a pair of brachial ridges (*br*). (**c**), internal mould of an incomplete dorsal valve, DP8-0242 (paratype), showing sockets (*soc*), brachial ridges (*br*), depressed and semilunar adductor scars (*ads*), a thick median ridge (*mr*), radially-striated vascular markings (*vm*). (**d**), external mould of a nearly complete but not well-preserved ventral valve, DP10-0249. (**e**), external mould of an incomplete dorsal valve, DP10-0247. (**f**), external mould of a nearly complete dorsal valve, DP10-0246. (**g**), external mould of a nearly complete dorsal valve, DP10-0245. (**h**), internal mould of a nearly complete ventral valve, DP10-0250. (**i**), internal mould of a complete ventral vavle, DP10-0241. (**j**, **k**), internal moulds of two incomplete dorsal vavles, DP10-0244 (*cp*- cardinal process, *br*- brachial ridges, *vm*- vascular markings), DP10-0252

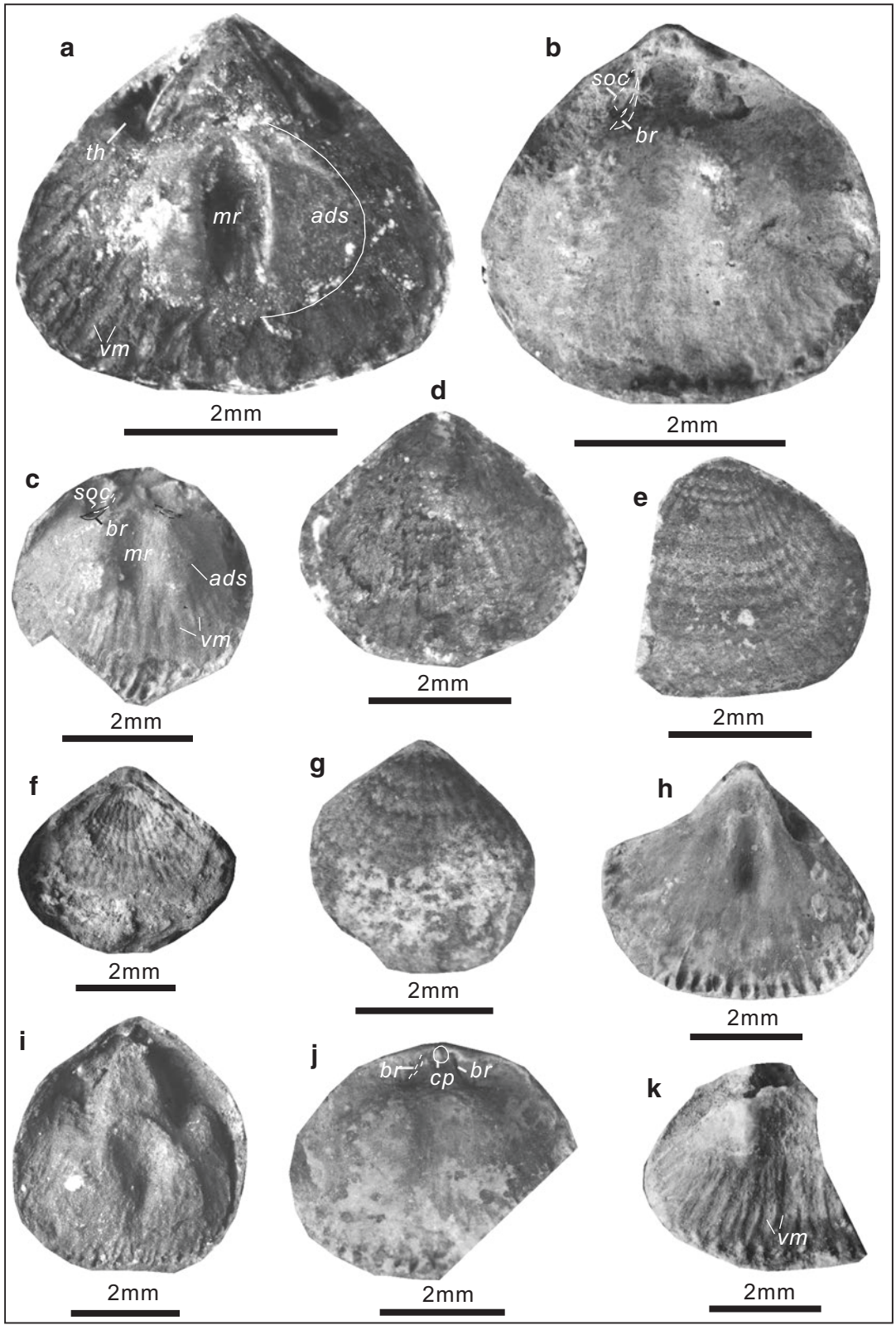

Fig. 9.65 ***Rhipidomella parvula*** He, Shi and Shen sp. nov.. (**a**), internal mould of a complete ventral valve, DP10-0240 (holotype), showing a thick median ridge (*mr*) developed in the middle of shell length, a pair of depressed, semilunar adductor scars (*ads*), a pair of teeth (*th*), and radially-striated vascular markings (*vm*). (**b**),

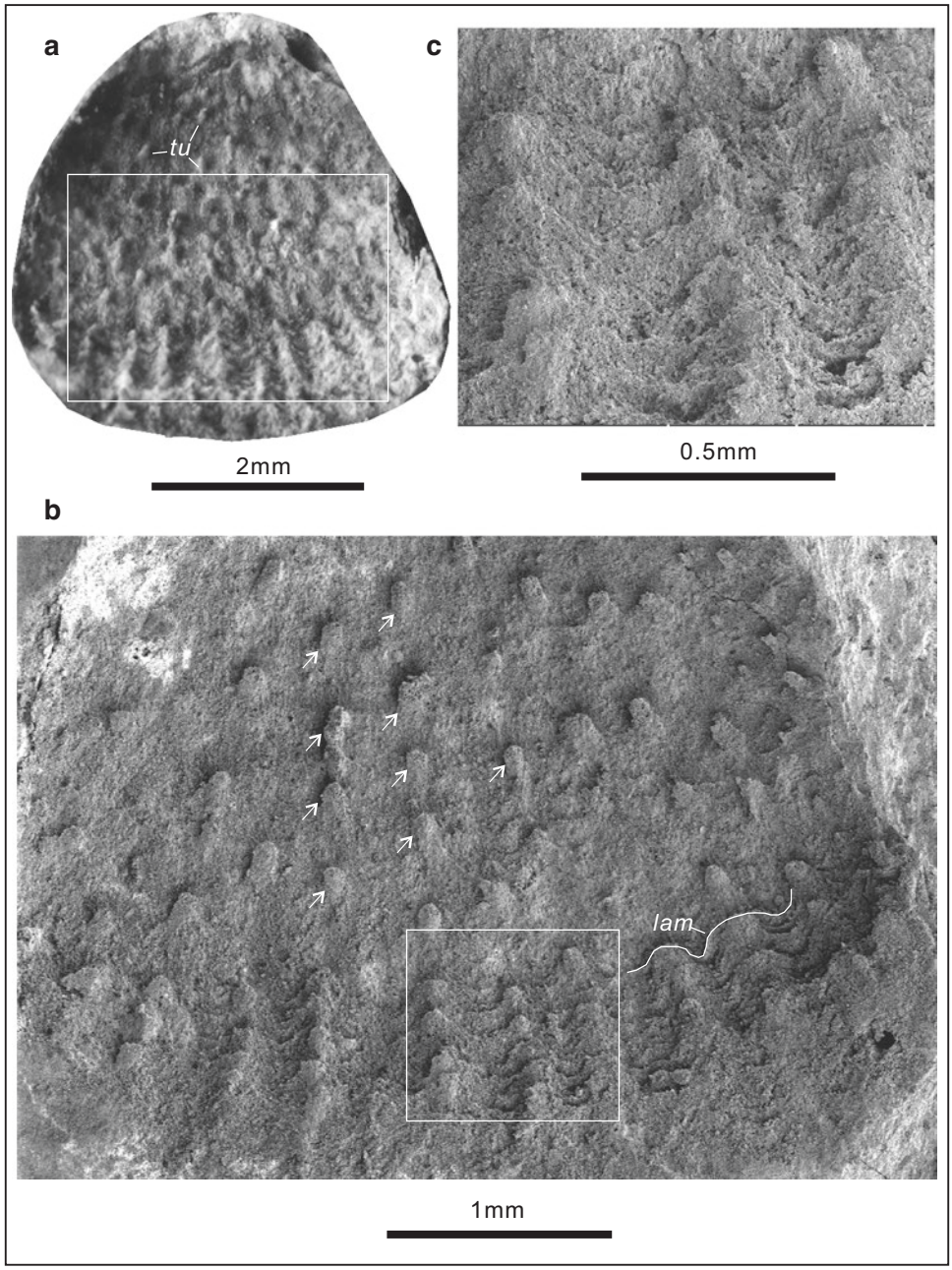

Fig. 9.66 SEM micrographs of ***Rhipidomella parvula*** He, Shi and Shen sp. nov.. (**a**), external mould of a nearly complete dorsal valve, DP10-0248 (paratype), showing micro-ornamentation of fine tubes (*tu*). (**b**), enlargement of DP10-0248, showing fine tubes (indicated by white arrows) and finely concentric lamellae (*lam*). **c**, portion of DP10-0248, showing finely concentric lamellae

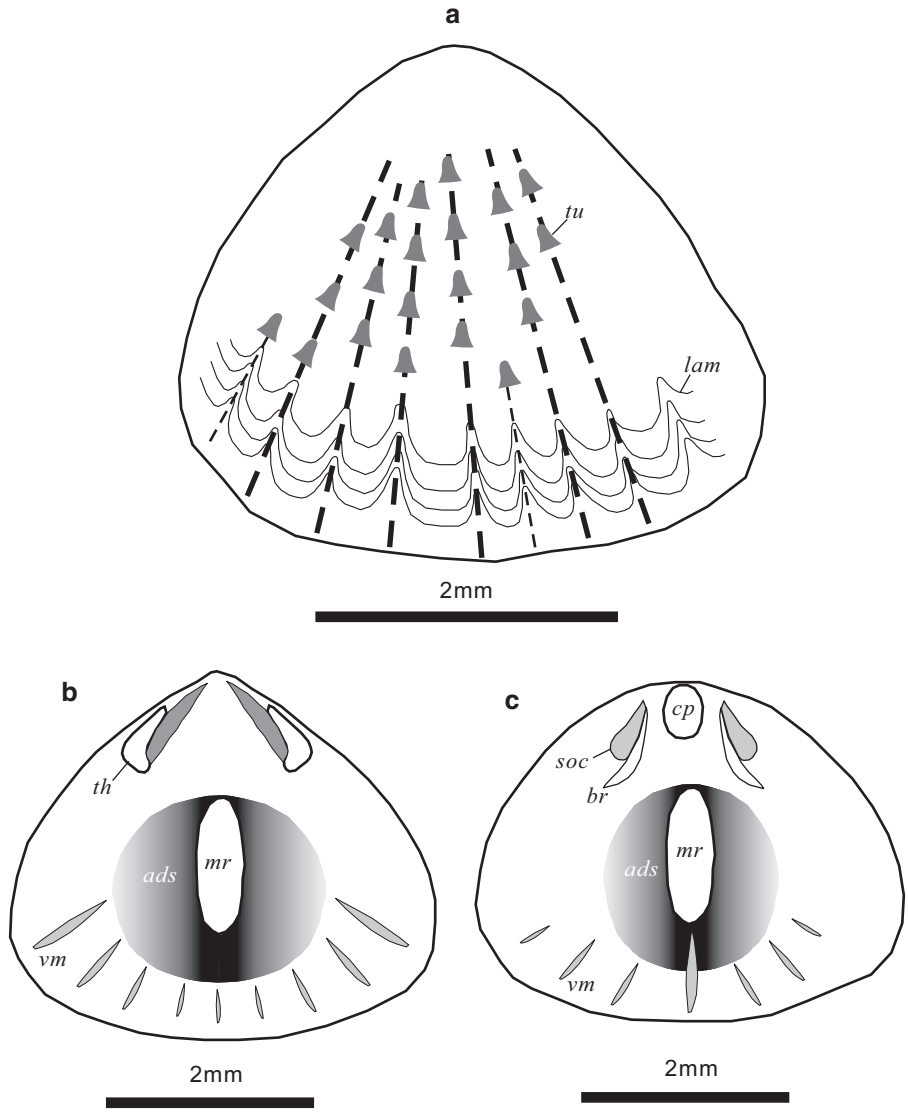

Fig. 9.67 Sketch diagram of ***Rhipidomella parvula*** He, Shi and Shen sp. nov.. (**a**)- Ornamentation (concentric lamellae and fine tubes along the interspace between costae. (**b**)- Ventral interior. (**c**)- Dorsal interior. Note: *tu*- fine tubs, *lam*- finely concentric lamellae, *th*- tooth, *vm*- vascular markings, *ads*- adductor scars, *mr*- thick median ridge, *cp*- cardinal process, *soc*- sockets, *br*- bladed brachiophores

Types Holotype DP10-0240; paratypes DP8-0242, DP10-0248.

Other Materials Over 10 specimens. Registered specimens: see below.

Measurements (mm):

Number	Width	Length	Width/ length	Notes
DP10-0240	4.20	3.63	1.16	Interior mould of ventral valve
DP10-0241	4.65	4.80	0.97	Interior mould of ventral valve
DP8-0242	3.69	2.88	1.28	Interior mould of dorsal valve
DP9-0243	4.38	3.56	1.23	Interior mould of dorsal valve

(continued)

Number	Width	Length	Width/ length	Notes
DP10-0244	4.97	4.17	1.19	Interior mould of dorsal valve
DP10-0245	4.66	3.51	1.33	External mould of dorsal valve
DP10-0246	4.98	3.87	1.29	External mould of dorsal valve
DP10-0247	?	3.66		External mould of dorsal valve
DP10-0248	5.23	4.32	1.21	External mould of dorsal valve
DP10-0249	4.08	3.96	1.03	External mould of ventral valve
DP10-0250	5.09	4.71	1.08	Interior mould of ventral valve
DP10-0251	4.31	3.53	1.22	Interior mould of dorsal valve
DP10-0252	?	4.31		Interior mould of dorsal valve

Occurrence Uppermost Changhsingian; Guangxi (Dongpan section) of South China.

Description Shell very small, 2–5 mm long and 3–6 mm wide, rounded triangular in outline; greatest width at about middle shell length or anterior third of shell length; gently biconvex in lateral profile. Ventral valve moderately convex, interarea moderately high, rounded triangular; sulcus absent. Dorsal valve circular in outline, moderately convex; fold absent. Shell surface with coarse costae and rugae; costae numbering 8 in 2 mm, rugae about 6 in 2 mm in the middle shell length; costae becoming thicker anteriorly, rugae becoming weaker anteriorly; with microornamentation of fine tubes (*tu*) along the interspace between costae (Figs. 9.66a, b; 9.67a) and fine concentric lamellae (*lam*) near anterior margin (Figs. 9.66b, c; 9.67a).

Ventral interior with a pair of teeth (*th*) (Figs. 9.65a; 9.67b); a pair of depressed, semilunar adductor scars (*ads*) (Figs. 9.65a; 9.67b); a thick median ridge (*mr*) (Figs. 9.65a; 9.67b); vascular markings radially striated (*vm*) (Figs. 9.65a; 9.67b). Dorsal interior with a simple cardinal process (*cp*), a pair of bladed brachiophores (*br*), a pair of depressed, semilunar adductor scars (*ads*) bisected by a thick median ridge (*mr*) (Figs. 9.65c, j; 9.67c).

Discussion The new species is similar to *Rhipidomella cordialis* Grant, 1976 from the Lower Permian limestone of Ko Muk, southern Thailand in a pair of strong teeth and a thick median ridge in the ventral interior, and a prominent cardinal process, a pair of brachiophores, a thick median ridge in the dorsal interior, but differs in the latter has a larger adult size (> 1 cm in shell width), a lower median ridge in the dorsal valve, and anteriorly opening hollow pits on the dorsal vavle, and the former has rugae on shell surface. Compared to the new species, *R. hessensis* King 1930 from the upper Hess Formation (Lower Permian) of Glass Mountains, Texas is larger (> 1.5 cm in shell width) and lacks rugae on shell surface. The new species can be distinguished from *R. leonardensis* King, 1930 of the Leonard Formation (Middle Permian) in Glass Mountains, Texas because the latter has a pentagonal outline, dental flanges and intercalated costae which are uneven in width. *R. mesoplatys* King, 1930 from the Leonard Formation (Middle Permian) and *R. transversa* King, 1930 from the Hess Formation (Lower Permian) of Glass Mountains, Texas, both are more transverse and larger (> 1 cm in shell width) than the new species. *R. subcircularis* Shen and He, 1994 from the Changhsing Formation of Changhsingian (Upper Permian) of Guiding, Guizhou Province, South China is also a large species (> 1 cm in shell width), and has a shallow sulcus on the dorsal valve and fine costae, which together make it very different from the new species.

Genus ***Permorhipidomella*** He, Shi and Shen gen. nov.

Type Species *Permorhipidomella ovatus* He, Shi and Shen gen. and sp. nov.

Diagnosis Biconvex, unisulcate valves; ventral interior with short, nearly parallel dental plates,

lacking of prominent median ridge or septum; dorsal interior with short crural plates and weak median ridge.

Etymology Named for a Permian genus of Rhipidomellinae.

Discussion The subfamily Rhipidomellinae Shuchert, 1913 currently includes 13 genera, most of which occurred in the Silurian and Devonian, with only *Rhipidomella* Oehlert, 1890 sparsely known from the Permian (and *Rhipidomella* mostly recorded in the Devonian to Carboniferous up to now). The new genus is more or less similar to some genera of Rhipidomellinae Shuchert, 1913 in interiors and ornamentation. Thus the new genus is assigned to the subfamily Rhipidomellinae. *Permorhipidomella* is most like *Strixella* Boucot and Amsden, 1958 in reticulated ornamention and a pair of dental plates, but the latter has a thick cardinal process, divergent brachiophores, a pair of triangular dentals. *Permorhipidomella* is similar to *Rhipidomella* Oehlert, 1890 in a pair of deep sockets and finely reticulated ornamentation, but differs in having a pair of crural plates and lacking of thick median ridges in ventral and dorsal interiors. *Pseudodicoelosia* Boucot and Amsden, 1958 also bears finely reticulated ornamentation, but its stronger brachiophores and thicker teeth easily separate it apart from the new genus.

Permorhipidomella ovatus He, Shi and Shen gen. and sp. nov.
Figs. 9.68, 9.69 and 9.70

Diagnosis Ovate, finely reticulated-ornamentation on both valves; ventral interior with parallel or slightly divergent dental plates; dorsal interior with deep sockets and moderately divergent crural plates.

Etymology Named for the ovate outline.

Types Holotype DP3-0277; paratypes, DP3-0289, DP3-0285.

Other Materials Over 10 specimens. Registered specimens: see below.

Measurements (mm):

Number	Width	Length	Width/length	Notes
DP7-0276	13.14	10.71	1.25	External mould of dorsal valve
DP3-0277	6.79	6.36	1.07	Internal mould of dorsal valve
DP9-0279	10.16	8.98	1.13	Internal mould of dorsal valve
DP8-0280	14.54	12.23	1.19	Internal mould of dorsal valve
XC1-0283	13.34	10.25	1.30	Internal mould of ventral valve
DP3-0285	13.08	11.81	1.11	Internal mould of ventral valve
DP10-0286	10.24	9.22	1.11	Internal mould of ventral valve
DP10-0288	8.50	8.00	1.06	Dorsal interior
DP3-0290	4.62	4.30	1.07	External mould of ventral valve
DP2-0292	8.10	8.63	0.94	Internal mould of ventral valve
DP10-0284	8.54	6.46	1.32	Dorsal interior
DP3-0278	12.16	9.49	1.28	Internal mould of ventral valve
DP3-0289	6.49	5.16	1.26	Internal mould of ventral valve
DP9-0282	9.70	7.51	1.29	External mould of dorsal valve
DP8-0281	11.32	6.80	1.66	Internal mould of dorsal valve
DP10-0291	9.59	10.08	0.95	Dorsal interior
DP9-0287	8.22	7.59	1.08	Internal mould of dorsal valve

Occurrence Uppermost Changhsingian; Guangxi of South China.

Description Shell about 4.3–12.2 mm long and 4.6–14.5 mm wide, ovate in outline; greatest width at about middle shell length or anterior third of shell length; weakly biconvex in lateral profile. Ventral valve weakly convex, interarea moderately high, triangular; fold weak, originated from middle shell length, widening anteriorly. Dorsal valve ovate in outline, weakly convex; sulcus originated from umbo, widening anteriorly to one third or one fourth of shell width. Shell surface with fine costellae and concentric lines, together forming fine reticulation on shell surface (Figs. 9.68f, h; 9.69b, d; 9.70c); costellae or concentric lines numbering 10–12 in 2 mm in the middle shell.

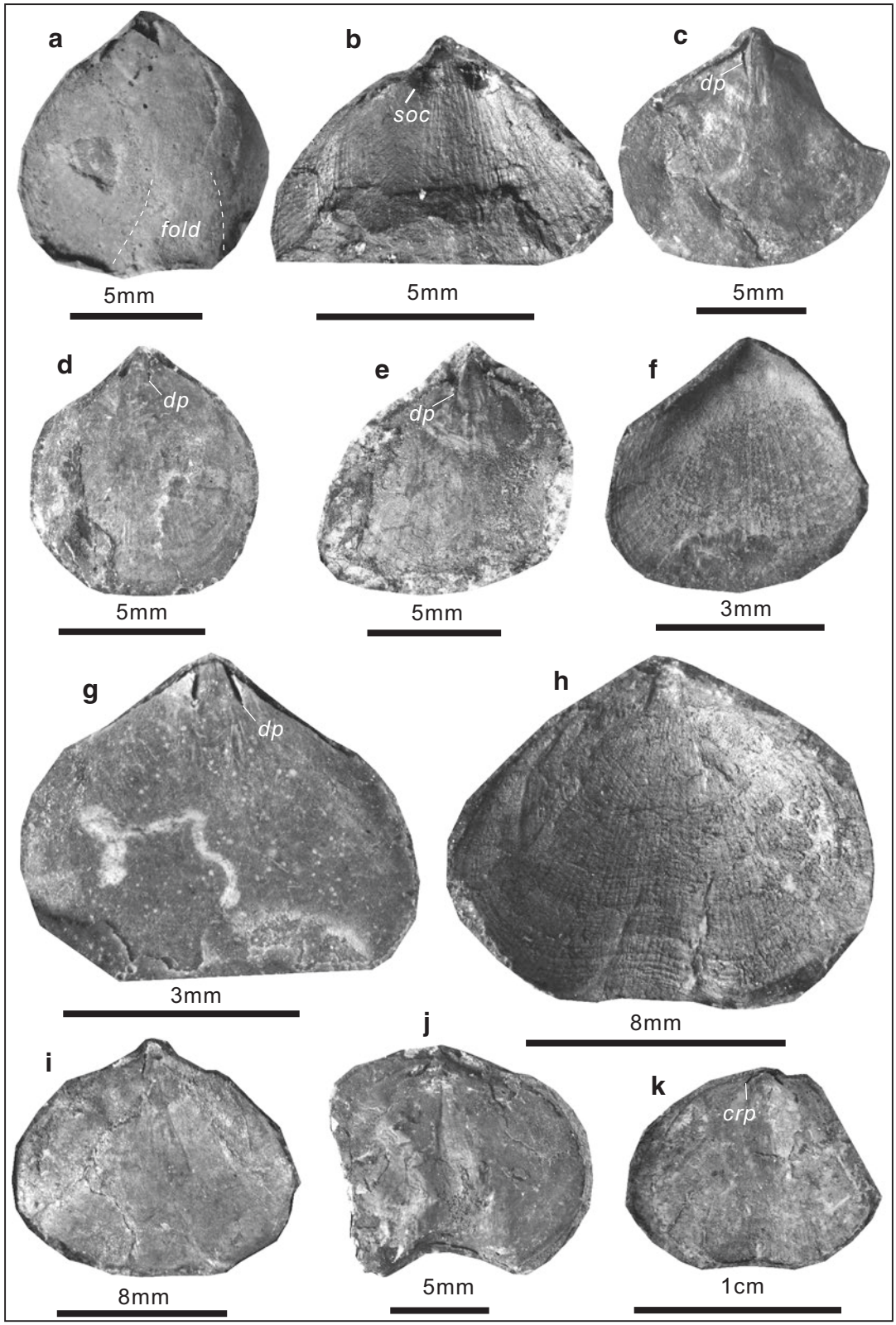
a
fold
5mm
b
soc
5mm
c
dp
5mm
d
dp
5mm
e
dp
5mm
f
3mm
g
dp
3mm
h
8mm
i
8mm
j
5mm
k
crp
1cm

Ventral interior with a pair of nearly parallel to slightly divergent dental plates (*dp*) (Figs. 9.68c–e, g; 9.70a). Dorsal interior with deep sockets (*soc*) (Figs. 9.68b; 9.69d; 9.70b) and moderately divergent crural plates (*crp*) (Figs. 9.69a, c, g, h; 9.70b).

Discussion Within the Rhipidomellinae, we are not aware of any species that can be closely compared to the new species, perhaps except *Rhipidomella parvula* He, Shen and Shi sp. nov. is somewhat similar to this species in the reticulated ornamentation, but the new species has finer ornaments.

Superfamily **Enteletoidea** Waagen, 1884
Family **Enteletidae** Waagen, 1884
Genus ***Enteletes*** Fischer de Waldheim, 1825

Type Species *Enteletes glabra* Fischer de Waldheim, 1830. Pennsylvanian of Upper Carboniferous of Russia.

Diagnosis Uniplicate, capillate valves; ventral interior with high, subparallel to slightly convergent dental plates, bisected by a high, thin median septum, length of dental plates nearly equivalent to length of median septum; dorsal interior with well-developed tusklike brachiophores, divergent crural plates, a median ridge.

Discussion *Enteletes* is similar to *Enteletina* Schuchert and Cooper, 1931 in interiors, but the former has uniplicate valves while the latter has unisulcate valves. *Enteletes* resembles to *Parenteletes* King, 1931 in the subparallel median septum and dental plates, but the latter has unisulcate valves and an anteriorly-forked median septum.

Enteletes subaequivalis Gemmellaro, 1899
Figs. 9.71; 9.72a–c

1899 *Enteletes subaequivalis* Gemmellaro: 140, pl. 28, Fig. 25–32.
1964 *Enteletes subaequivalis* Gemmellaro; Wang et al.: 148, pl. 19, Fig. 1–4.
1979 *Enteletes subaequivalis* Gemmellaro; Jin and Ye: 74, pl. 36, Fig. 10–12, 16–18.
1979 *Enteletes subaequivalis obscura* Ching and Ye; Jin and Ye: 74, pl. 36, Fig. 19–22.
2014 *Meekella*? *sparsiplicata* He and Shi in He et al.: 946, Fig. 21h, i.

Materials 14 registered specimens: see below.

Measurements (mm):

Number	Width	Length	Width/length	Notes
DSH-0294	12.01	11.54	1.04	Internal mould of dorsal valve
DP7-0295	19.71	13.44	1.47	External mould of ventral valve
DP8-0297	7.61	6.24	1.22	Internal mould of dorsal valve
DP2-0300	12.02	8.90	1.35	Internal mould of dorsal valve
DP2-0306	13.47	9.89	1.36	Internal mould of dorsal valve
DP3-0307	10.42	7.03	1.48	Internal mould of dorsal valve
DP3-0301	16.63	12.74	1.31	Internal mould of dorsal valve

(continued)

Fig. 9.68 ***Permorhipidomella ovatus*** He, Shi and Shen sp. nov.. (**a**), internal mould of a deformed ventral valve, XC1-0283, showing a fold widening anteriorly. (**b**), interior of an incomplete dorsal valve, DP10-0284, showing deep sockets (*soc*). (**c**), internal mould of an incomplete ventral valve, DP10-0286, showing a pair of nearly parallel dental plates (*dp*). (**d**), internal mould of a nearly complete ventral valve, DP2-0292, showing a preserved dental plate (*dp*). (**e**), internal mould of an incomplete ventral valve, DP3-0278, showing a pair of nearly parallel dental plates (*dp*). (**f**), external mould of a deformed ventral vavle, DP3-0290. (**g**), internal mould of a nearly complete ventral valve, DP3-0289 (paratype), showing a pair of slightly divergent dental plates (*dp*). (**h**), external mould of a ventral valve, DP3-0285, showing finely reticulated ornamentation. (**i**), internal mould of DP3-0285 (paratype). (**j**), internal mould of an incomplete dorsal valve, DP8-0280. (**k**), internal mould of an incomplete dorsal valve, DP9-0279, showing a pair of thin crural plates (*crp*)

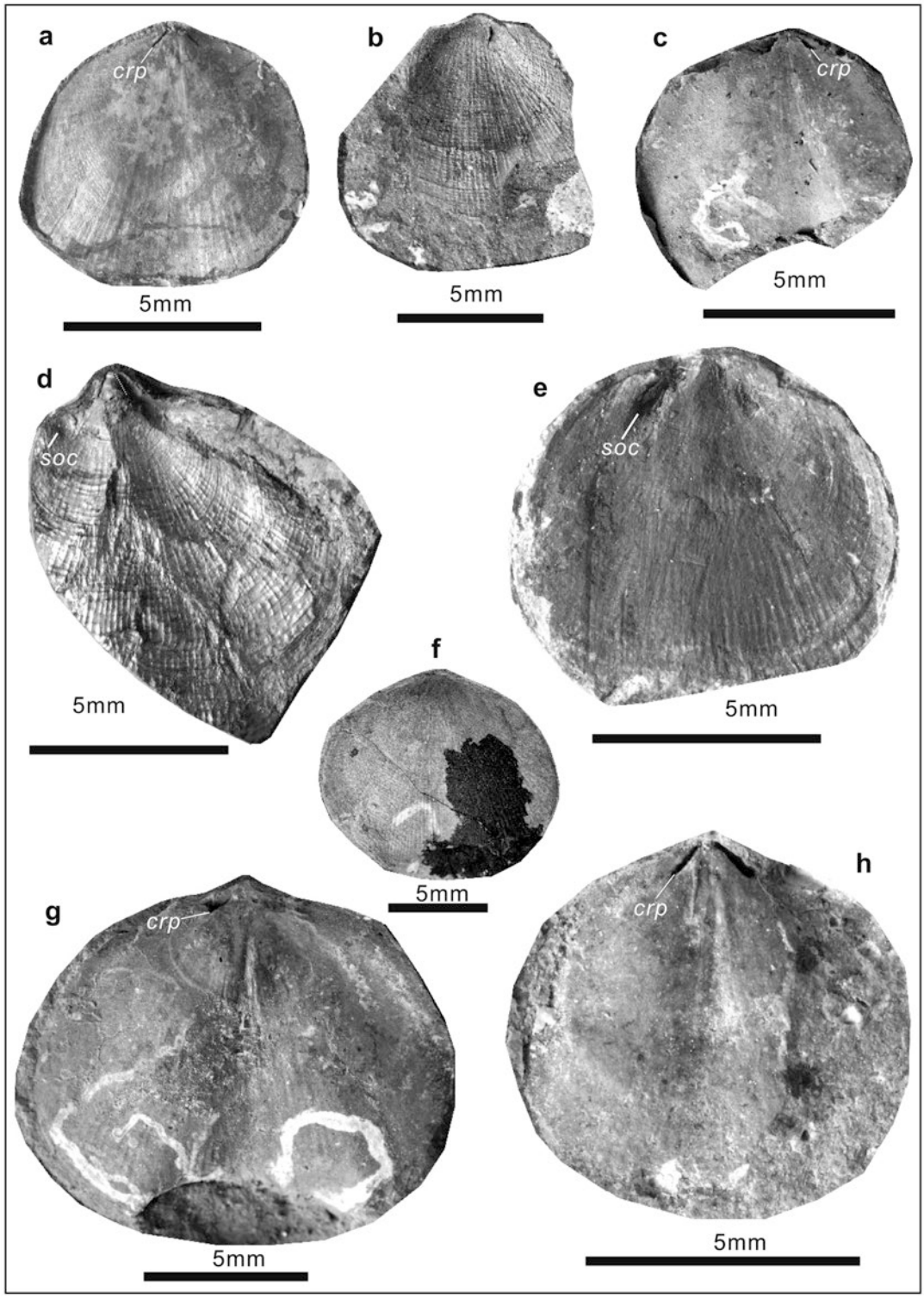
a
crp
5mm
b
5mm
c
crp
5mm
d
soc
5mm
e
soc
5mm
f
5mm
g
crp
5mm
h
crp
5mm

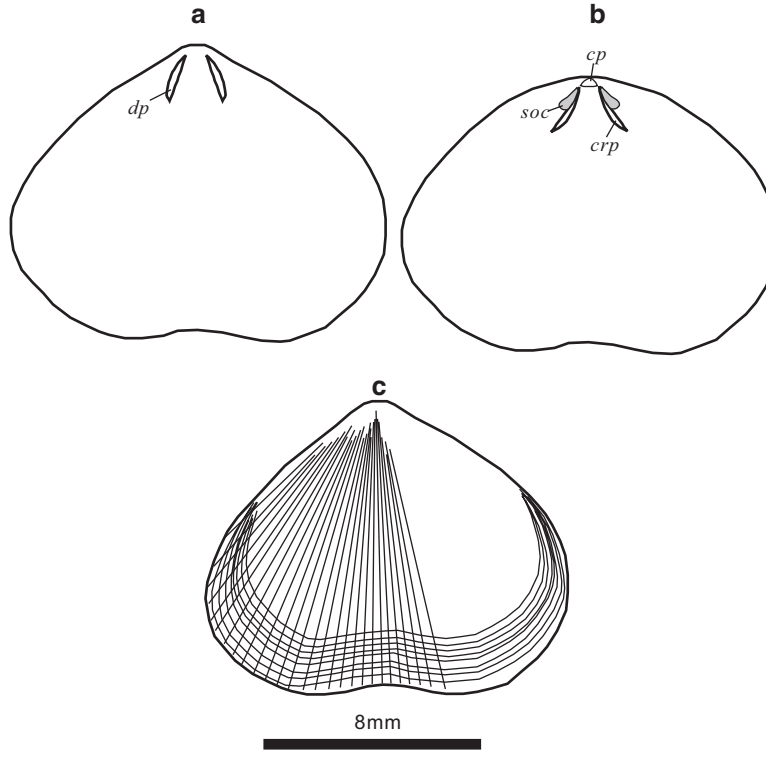

Fig. 9.70 Sketch diagram of ***Permorhipidomella ovatus*** He, Shi and Shen sp. nov.. (**a**)- Ventral interior. (**b**)- Dorsal interior. (**c**)- Finely reticulated ornamentation. Note: *dp*- dental plates, *cp*- cardinal process, *soc*- sockets, *crp*- crural plates

Number	Width	Length	Width/length	Notes
DP5-0302	10.99	9.28	1.18	Internal mould of dorsal valve
PB5-0303	19.95	13.87	1.44	Dorsal valve
PB5-0298	12.58	11.37	1.11	Internal mould of dorsal valve
DP10-0299	7.58	7.20	1.05	Internal mould of dorsal valve
DP3-0304	12.81	9.33	1.37	Internal mould of dorsal valve
DP3-0308	18.74	11.03	1.70	Dorsal valve
DP5-0309	20.60	15.77	1.31	Internal mould of dorsal valve

Occurrence Changhsingian; Guangxi of South China.

Description Shell 6.2–15.8 mm long and 7.6–20.6 mm wide, subcircular in outline, biconvex, greatest width at shell midlength. Ventral valve beak slightly incurved; sulcus originated from middle length, slightly widening and deepening anteriorly; external surface ornamented by coarse plication and fine costellae, number of plication variable (1–3) on each flank, plication with slightly angulated crest, fine costellae evenly dis-

Fig. 9.69 ***Permorhipidomella ovatus*** He, Shi and Shen sp. nov.. (**a**), internal mould of a complete dorsal valve, DP3-0277 (holotype), showing thin crural plates (*crp*). (**b**), external mould of an incomplete dorsal valve, DP9-0282, showing finely reticulated ornamentation. (**c**), internal mould of an incomplete dorsal valve, DP8-0281, showing slightly divergent crural plates (*crp*). (**d**), interior of an incomplete dorsal valve, DP10-0291, showing deep sockets (*soc*). (**e**), interior of a nearly complete dorsal valve, DP10-0288, showing a preserved deep socket (*soc*). (**f**), external mould of a complete dorsal valve, DP7-0276. (**g**), internal mould of DP7-0276, showing a pair of crural plates (*crp*). (**h**), internal mould of an incomplete dorsal valve, DP9-0287, showing a pair of thin crural plates (*crp*)

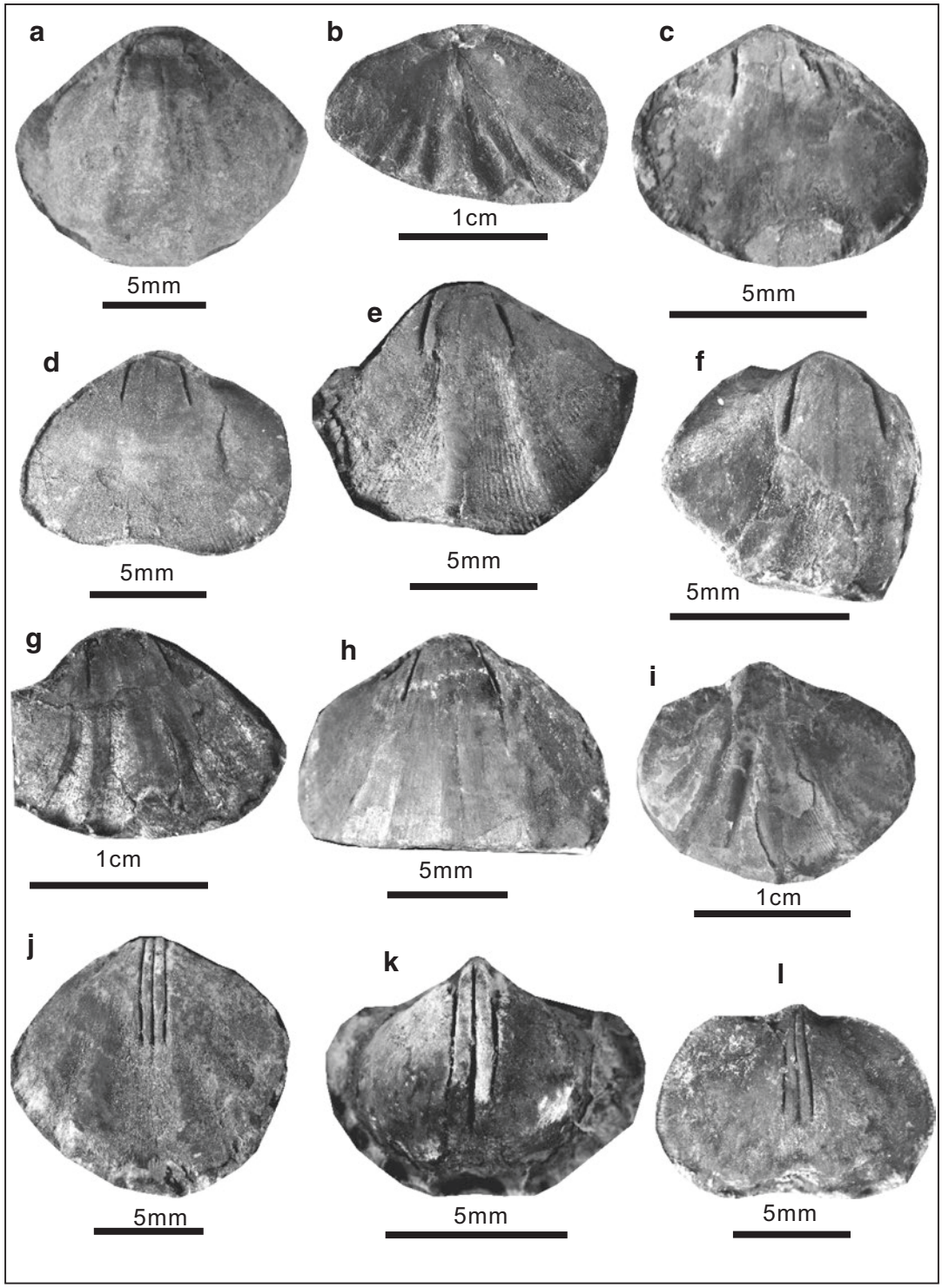

Fig. 9.71 ***Enteletes subaequivalis*** Gemmellaro, 1899. (**a**), internal mould of a dorsal valve, DSH-0294. (**b**), external mould an incomplete ventral valve, DP7-0295. (**c**-**e**), internal moulds of three nearly complete dorsal valves, DP8-0297, DP2-0300, DP2-0306. (**f**–**h**), internal moulds of three incomplete dorsal valves, DP3-0307, DP3-0301, DP5-0302. (**i**), a slightly deformed dorsal valve, PB5-0303. (**j**–**l**), internal moulds of three nearly complete dorsal valves, PB5-0298, DP10-0299, DP3-0304

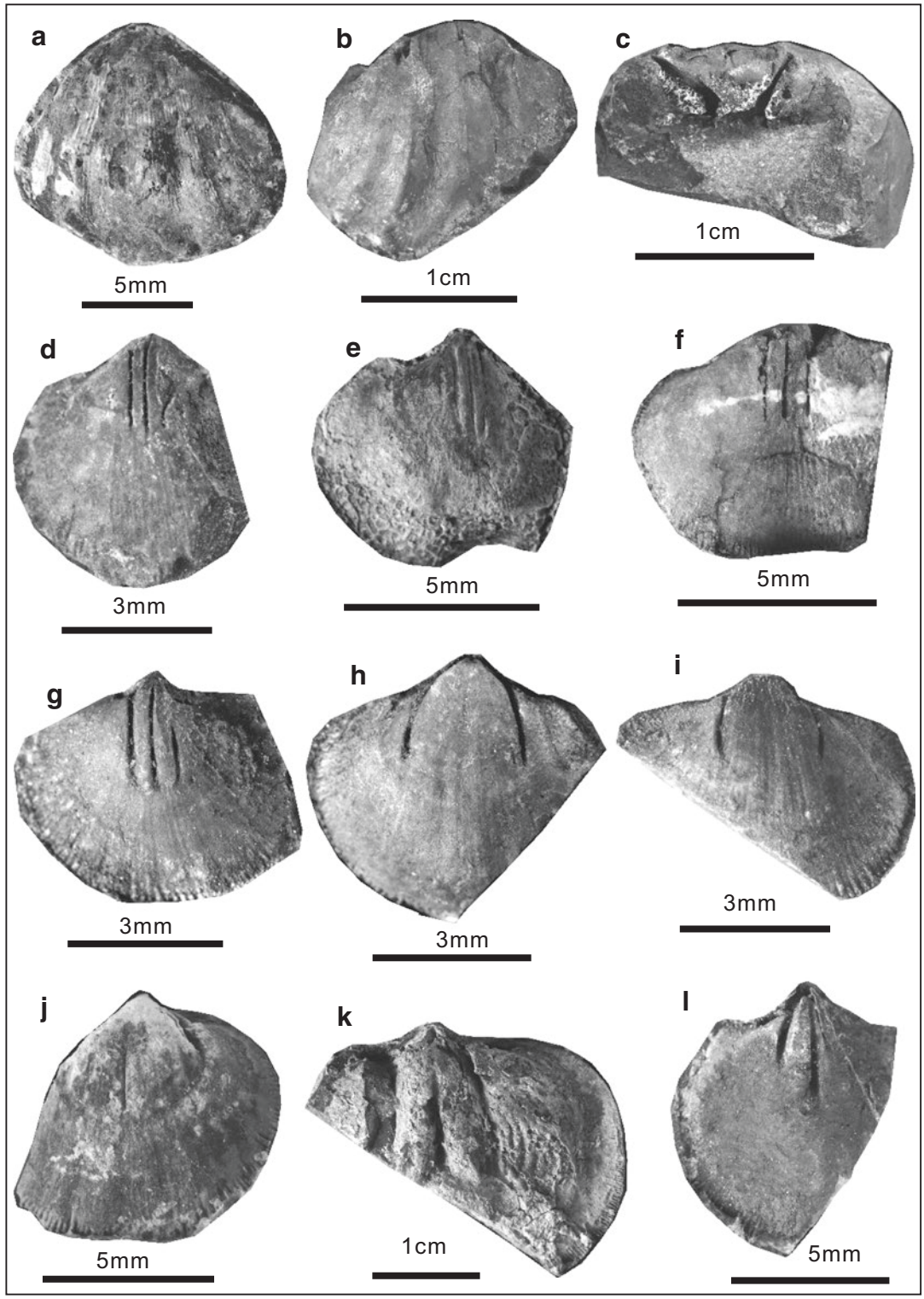

Fig. 9.72 (**a**–**c**), ***Enteletes subaequivalis*** Gemmellaro, 1899. (**a**), a nearly complete and slightly deformed dorsal valve, DP3-0308. (**b**), internal mould of an incomplete dorsal valve, DP5-0309. (**c**), posterior view of DP5-0309. (**d**–**i**), ***Orthotichia*** sp. 1, (**d**–**g**), internal moulds of four incomplete ventral valves, PB2-0317, DP5-0313, DP3-0314, DP3-0315. (**h**, **i**), internal moulds of two incomplete dorsal valves, DP2-0320, DP3-0319. (**j**), ***Orthotichia*** sp. 2, internal mould of an incomplete dorsal valve, DP7-0318. (**k**), ***Orthotichia*** sp. 3, internal mould of an incomplete ventral valve, DP5-0311. (**l**), ***Orthotichia*** sp. 4, internal mould of an incomplete dorsal valve, DP5-0316

tributed on shell surface (Figs. 9.71b, g, i; 9.72a, b). Dorsal valve beak slightly incurved; fold originated from middle length, slightly widening anteriorly.

Ventral interior with high, subparallel dental plates, bisected by a high, thin median septum (Fig. 9.71j–l). Dorsal interior with divergent crural plates and a weak median ridge (Figs. 9.71c–h; 9.72b, c).

Discussion The present species is like *E. nucleola* Grabau, 1931 from the Permian Jisu Honguer limestone of Inner Mongolia in weak plications, but the latter has plications with nearly flat crests. Comparing with the present species, *E. obesa* Grabau, 1931 from the Permian *Martinia* bed of Mongolia has a globoser outline in profile and sharper crest plications. *E. retardate* Huang, 1933 from the Permian limestone of Guizhou Province, southwestern China has a pair of slightly divergent dental plates and weaker placations, if compared to *Enteletes subaequivalis*. *E. asymmatrosis* Xu and Grant, 1994 from the Changhsingian Longdongchuan Formation of Xikou section, Zhenan, Shaanxi, China and *E. wannanensis* Zhang and Jin, 1961 from the Wuchiapingian Lungtan Formation of Jinxian, Anhui Province, China are more globose than *Enteletes subaequivalis*, and *E. wannanensis* is additionally distinguished by its sharper crest plications. Additionally, *E. bisulcata* Liao and Meng, 1986 from the Changhsingian Changhsing Formation of Huatang, Hunan Province has a dorsal sulcus and thus should not be assigned to *Enteletes*.

Family **Schizophoriidae** Schuchert and LeVene, 1929

Genus ***Orthotichia*** Hall and Clarke, 1892

Type Species *Orthis*? *morganiana* Derby, 1874. Carboniferous of Brazil.

Diagnosis Weak uniplicate, finely capillate valves; ventral interior with long, high, subparallel dental plates, bisected by a long, high, thin median septum, length of dental plates nearly equivalent to length of median septum; dorsal interior with divergent crural plates, a median ridge.

Discussion *Orthotichia* is similar to *Enteletes* Fischer de Waldheim, 1825 in interiors, but the former lacks coarse plications. *Orthotichia* is like *Acosarina* Cooper and Grant, 1969 in a subcircular outline, a long median septum in the ventral interior and divergent crural plates, but the latter has shorter dental plates. *Orthotichia* resembles to *Schizophoria* (*Paraschizophoria*) King, 1850 in a median septum parallel to dental plates and a pair of divergent crural plates, but the latter has shorter dental plates and a globoser outline.

Orthotichia sp. 1
Fig. 9.72d–i

Materials Six registered specimens: see below.

Measurements (mm):

Number	Width	Length	Width/ length	Notes
PB2-0317	6.22	5.47	1.14	Internal mould of ventral valve
DP5-0313	7.21	6.67	1.08	Internal mould of ventral valve
DP3-0314	8.27	6.56	1.26	Internal mould of ventral valve
DP3-0315	6.08	4.35	1.40	Internal mould of ventral valve
DP2-0320	6.79	5.93	1.15	Internal mould of dorsal valve
DP3-0319	6.42	5.30	1.21	Internal mould of dorsal valve

Occurrence Changhsingian; Guangxi of South China.

Description Shell 4.4–6.7 mm long and 6.1–8.3 mm wide, subcircular in outline, biconvex, greatest width at shell midlength. Ventral valve beak slightly incurved; sulcus shallow, nearby anterior margin; external surface ornamented by fine costellae. Dorsal valve beak slightly incurved; fold weak, nearby anterior margin.

Ventral interior with high, subparallel dental plates, bisected by a high, thin median septum, length of dental plates nearly equivalent to length of median septum (Fig. 9.72d–g). Dorsal interior

with moderately divergent crural plates and a weak median ridge (Fig. 9.72h, i).

Discussion These specimens have a pair of dental plates parallel to a median septum, the length of dental plates nearly equivalent to length of median septum in the ventral valve, and a pair of divergent crural plates in the dorsal valve. All these features strongly suggest a species of *Orthotichia*, but the lack of external features prevent us from further comparing with other species.

Orthotichia sp. 2
Fig. 9.72j

Material One incomplete dorsal valve, DP7-0318.

Measurement (mm):

Number	Width	Length	Width/ Length	Notes
DP7-0318	8.68	8.09	1.07	Internal mould of dorsal valve

Occurrence Changhsingian; Guangxi of South China.

Description Subcircular in outline, greatest width at shell midlength. Dorsal valve beak slightly incurved; fold weak, nearby anterior margin. Dorsal interior with a pair of widely divergent crural plates and a prominent median ridge.

Discussion The present species is similar to *Orthotichia* sp. 1 of this book in outline and ornamentation, but the former has a more widely divergent crural plates (divergent angle twice of the latter).

Orthotichia sp. 3
Fig. 9.72k

Material One incomplete ventral valve, DP5-0311.

Measurement (mm):

Number	Width	Length	Width/ Length	Notes
DP5-0311	32.33	24.94	1.30	Internal mould of ventral valve

Occurrence Changhsingian; Guangxi of South China.

Description Transversely subcircular in outline. Ventral external surface ornamented by fine costellae. Ventral interior with high, slightly divergent (subparallel) dental plates, bisected by a high, thin median septum; length of dental plates nearly equivalent to length of median septum; median septum forked anteriorly.

Discussion *Orthotichia* sp. 3 differs from *Orthotichia* sp. 1 of this book as the latter has closer triple plates in the ventral interior.

Orthotichia sp. 4
Fig. 9.72l

Material One incomplete dorsal valve, DP-0316.

Measurement (mm):

Number	Width	Length	Width/ Length	Notes
DP5-0316	7.37	8.64	0.85	Internal mould of dorsal valve

Occurrence Changhsingian; Guangxi of South China.

Description Circular in outline, greatest width at shell midlength. Dorsal external surface ornamented by fine costellae (based on the anterior margin of dorsal interior). Dorsal interior with a pair of slightly divergent crural plates and a median septum.

Discussion The species differs from *Orthotichia* sp. 1 of this book in a pair of divergent crural plates in the dorsal interior.

Genus ***Acosarina*** Cooper and Grant, 1969

Type Species *Acosarina dorsisulcata* Copper and Grant, 1969. Middle Permian of West Texas (*Acosarina minuta* (Abich, 1878)).

Diagnosis Shell small to medium, subcircular, biconvex, widest at midlength; anterior commissure rectimarginate to sulcate. Pedicle valve interior with low but long median septum, extending to or slightly beyond midlength; dental plates short; dorsal interior with widely divergent brachiophore plates and deep sockets.

Discussion As mentioned by Campi and Shi (2005) and Zhang et al. (2014), *Sunacoarina* Liang, 1990 from the Middle Permian of Zhejiang Province, China is synonymous with *Acosarina*, because both of them have similar interiors, including a long median septum and two short, divergent plates in the ventral interior, and two divergent, curved brachiophore plates. *Acosarina* is similar to *Schizophoria* (*Paraschizophoria*) King, 1850 in a pair of divergent crural plates, but the latter has a shorter median septum and subparallel dental plates, and a globoser outline.

Acosarina minuta (Abich, 1878)
Fig. 9.73

1878 *Streptorhynchus peregrinus* var. *minutus* Abich: 78, pl. 9, Fig. 1a.
1884 *Orthis indica* Waagen: 568, pl. 56, Figs. 7, 8, 14–16.
1931 *Schizophoria indica* Ozaki: 167, pl. 15, Fig. 3.
1962 *Orthotichia indica* (Waagen); Zhan and Li: 443, pl. 1, Fig. 1, 2.
1964 *Schizophoria indica* (Waagen); Wang et al.: 134, pl. 16, Fig. 28.
1969 *Acosarina dorsisulcata* Cooper and Grant: 2, pl. 5, Fig. 19–23.
1976a *Acosarina dorsisulcata* Cooper and Grant; Cooper and Grant: 2621, pl. 667, Fig. 1–26
1977 *Acosarina indica* (Waagen); Yang et al.: 311, pl. 130, Fig. 3.
1978 *Orthotichia indica* (Waagen); Tong: 211, pl. 27, Fig. 3.
1978 *Acosarina dorsisulcata* Cooper and Grant; Feng and Jiang: 235, pl. 85, Fig. 10.
1979 *Acosarina indica* (Waagen); Jin and Ye: 74, pl. 36, Fig. 6–9.
1982 *Acosarina indica* (Waagen); Wang et al.: 190, pl. 180, Fig. 7.
1986 *Acosarina dorashamensis* Cooper and Grant; Liao and Meng: pl. 1, Fig. 14.
1987 *Acosarina dorashamensis* Cooper and Grant; Liao: pl. 1, Fig. 3–8.
1988 *Acosarina* sp.; Yanagida: pl. 29, Fig. 1–12.
1990 *Acosarina indica* (Waagen); Liang: 354, pl. 1. Fig. 6–10.
1990 *Acosarina indica* (Waagen); Zhu: 62, pl. 9, Fig. 5–7.
1993 *Kotlaia capilosa* Grant: 5, Fig. 4.1–4.6.
1995 *Acosarina minuta* (Abich); Zeng et al.: pl. 3, Fig. 10.
1998 *Acosarina minuta* (Abich); Shi and Shen: 506, Fig. 3.5–3.11.
2007 *Acosarina minuta* (Abich); Shen and Shi: 39, pl. 14, Fig. 27–38; pl. 15, Fig. 1–21.
2014 *Acosarina minuta* (Abich); He et al.: 950, Fig. 21a–d.
2014 *Acosarina minuta* (Abich); Zhang et al.: 488, Figs. 7x–ac, 9a–d.

Materials Over 70 specimens. Registered specimens: see below.

Fig. 9.73 ***Acosarina minuta*** (Abich, 1878). (**a**), internal mould of an incomplete ventral valve, LZ1200379, showing a long median septum (*ms*) and a pair of dental plates (*dp*). (**b**), internal mould of a complete ventral valve, LZ1400371. (**c**), internal mould of an incomplete ventral valve, LZ1400377. (**d**), internal mould of a complete dorsal valve, LZ1400378, showing a pair of crural plates (*crp*). (**e**), internal mould of an incomplete dorsal valve, LZ1400376, showing a pair of complex adductor scars (*ads*). (**f**), internal mould of a complete but slightly deformed dorsal valve, LZ1400375, showing a pair of crural plates (*crp*) and a cardinal process (*cp*). (**g**), internal mould of an incomplete ventral valve, XM140C01. (**h**), internal mould of an incomplete dorsal valve, XM15115. (**i**), internal mould of a complete dorsal valve, LZ1400372, showing a well-preserved adductor scars (*ads*). (**j**), enlarged portion of LZ1400372, showing the crenulated cardinal process

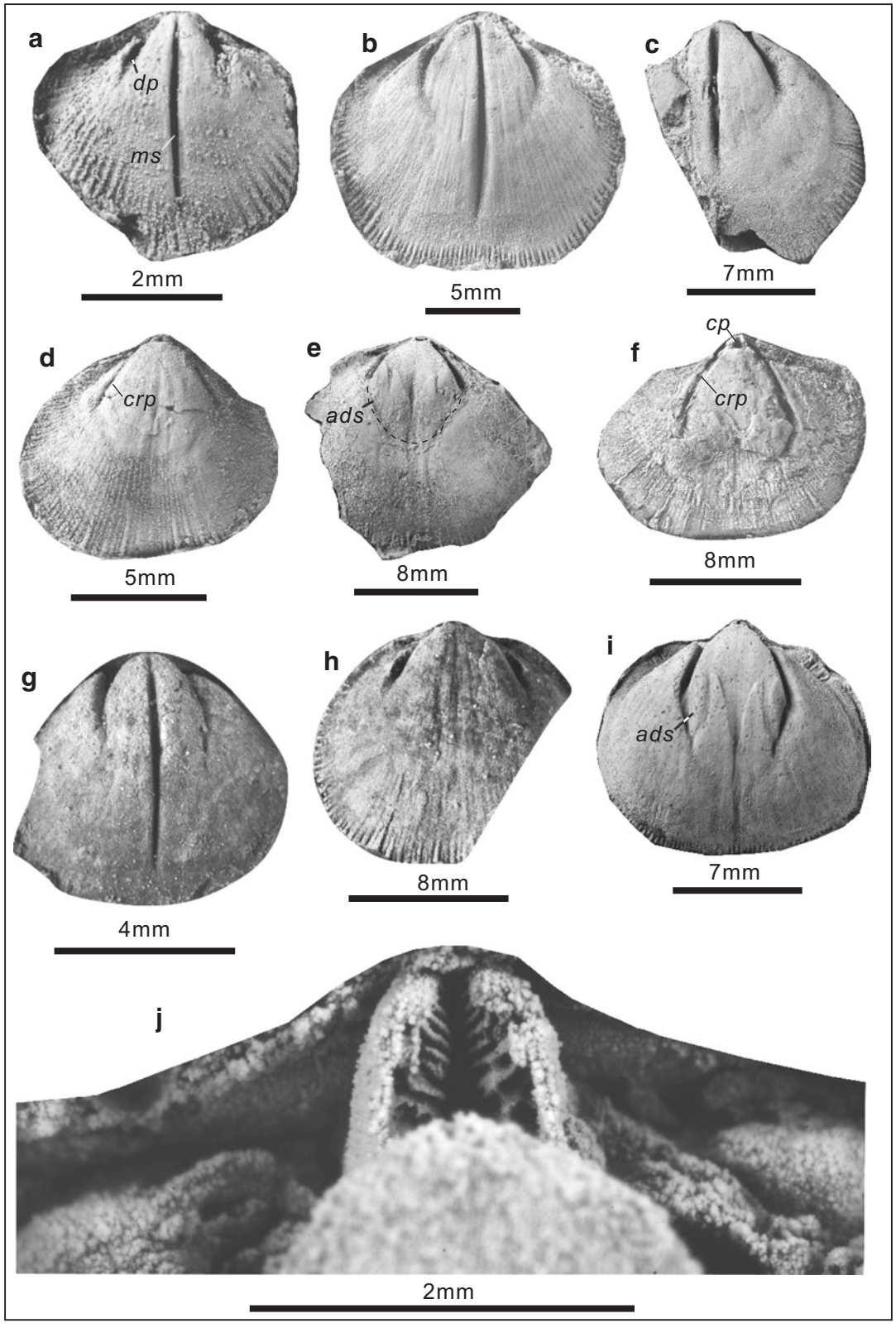
a
dp
ms
2mm
b
5mm
c
7mm
d
crp
5mm
e
ads
8mm
f
cp
crp
8mm
g
4mm
h
8mm
i
ads
7mm
j
2mm

Measurements (mm):

Number	Width	Length	Width/ length	Notes
LZ1200379	4.12	3.55	1.16	Internal mould of ventral valve
LZ1400371	15.54	13.69	1.14	Internal mould of ventral valve
LZ1400377	16.60	13.33	1.25	Internal mould of ventral valve
LZ1400378	10.27	8.36	1.23	Internal mould of dorsal valve
LZ1400376	17.10	14.43	1.18	Internal mould of dorsal valve
LZ1400375	14.24	10.95	1.30	Internal mould of dorsal valve
XM140C01	6.06	5.61	1.08	Internal mould of ventral valve
XM15115	13.76	12.14	1.13	Internal mould of dorsal valve
LZ1400372	14.84	12.76	1.16	Internal mould of dorsal valve

Occurrence Permian to lowest Triassic; Russia, Pakistan, Thailand, United States, Vietnam and China.

Description Shell small to medium for the genus, subcircular in outline, subequally biconvex, greatest width at midlength, 2.9–14.4 mm long, 4.0–17.1 mm wide; anterior commissure rectimarginate to weakly sulcate. Surface multicostellae, costellae fine, 7–8 per 2 mm at anterior margin.

Ventral interior with a long median septum (*ms*), extending anteriorly to over half of shell length or nearby anterior margin; dental plates (*dp*) short, straight or curved, anteriorly divergent at a large acute angle (close to 90°) (Fig. 9.73a).

Dorsal interior with with a crenulated cardinal process (Fig. 9.73j); a pair of brachiophore plates (*bp*) anteriorly divergent at a large acute angle (70−80°) (Fig. 9.73d); two pairs of prominent muscle scars (*ads*), one pair small, elongated and posteriorly located close to brachiophores, the other pair much larger, triangular, distributed anteriorly to the small pair (Fig. 9.73i).

Discussion The present species slightly differs from *Acosarina strophiria* Xu and Grant, 1994 from the Changhsing Formation of Huangzhishan, Zhejiang Province, South China because the latter has a coarser dorsal median ridge. *Acosarina rectimarginata* Cooper and Grant, 1976a from the Neal Ranch Formation (Permian) of West Texas possesses a shorter ventral median septum, when compared with the present species. This species differs from *Acosarina antesulcate* Waterhouse, 1983c of the Upper Permian of Thailand as the latter has acutely diverging posterior margins and coarse costellae, and from *A. mesoplatys* (King, 1931) of the Cathedral Mountain Formation of West Texas as the latter has tubular costellae.

Order **Rhynchonellida** Kuhn, 1949
Superfamily **Wellerelloidea** Licharew, 1956
Family **Pontisiidae** Cooper and Grant, 1976b
Subfamily **Pontisiinae** Cooper and Grant, 1976b
Genus ***Prelissorhynchia*** Xu and Grant, 1994

Type Species *Pugnax pseudoutah* Huang, 1933. Lungtan Formation; Guizhou Province, southwestern China.

Diagnosis Shell small, semicircular to subtriangular, dorsibiconvex in profile, strongly uniplicate with distinct indentation at anterior commissure. Costae coarse, rounded, simple. Interiors with slightly divergent (subparallel) dental plates and undivided arched hinge plate.

Discussion *Neowellerella* Dagys, 1974 is synonymous with *Lissorhynchia* Yang and Xu, 1966, according to Savage et al. in Williams et al., 2002. The difference between *Prelissorhynchia* and *Lissorhynchia* is that the former has a subcircular outline and lacks a dorsal median ridge and the latter has a subtriangular outline and a median ridge in the dorsal interior (Savage et al. in Williams et al., 2002). However, such a difference may be intrageneric variations, because those specimens with subcircular outlines (character of the former) variably have dorsal median ridges (see Fig. 9.74a, b, g). Considering this, it is possible that *Prelissorhynchia* and *Lissorhynchia* are synonymous, because both are dorsibiconvex, with a prominent ventral sulcus and a dorsal fold, as well as subparallel dental plates. However, the

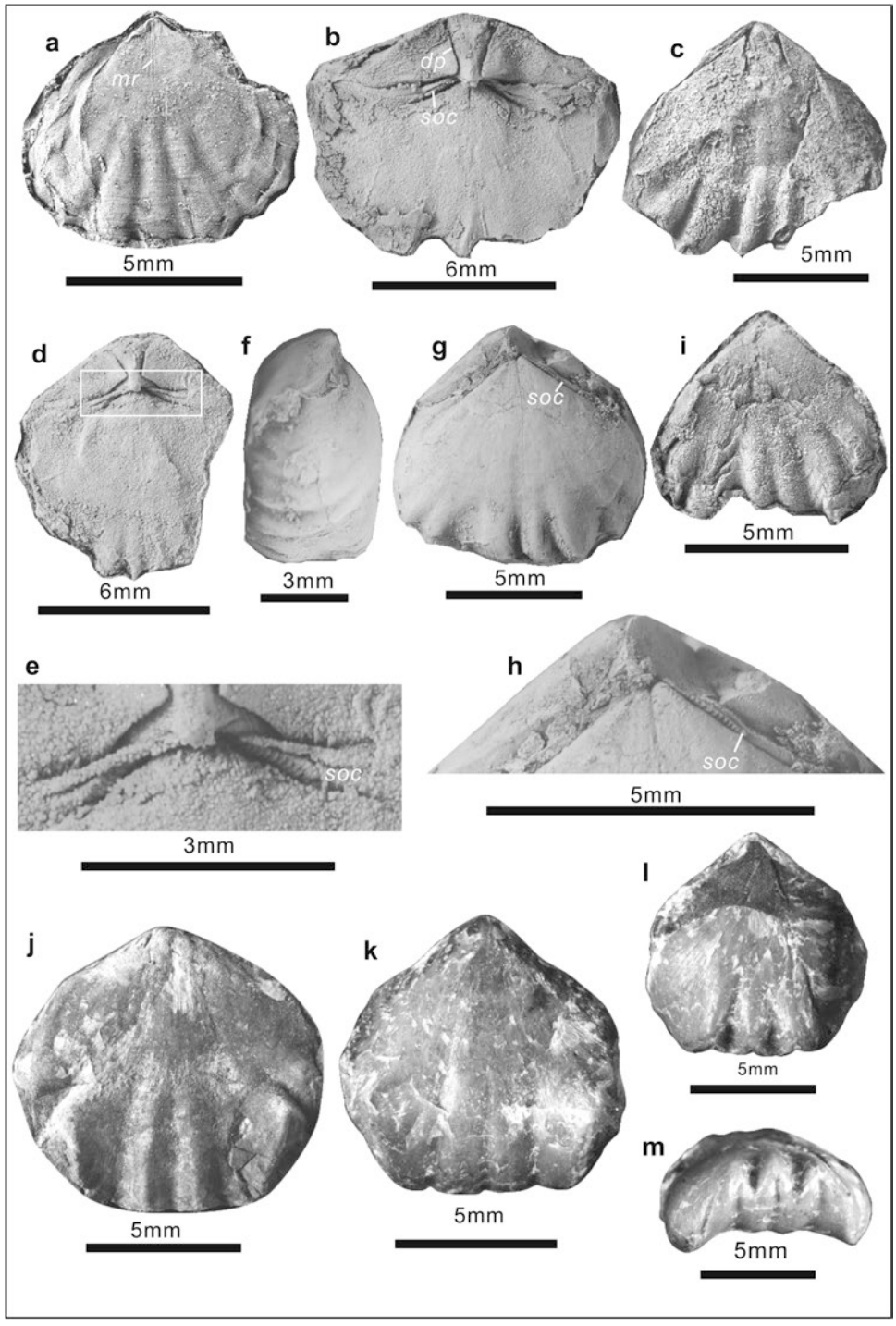

Fig. 9.74 ***Prelissorhynchia pseudoutah*** (Huang, 1933). (**a**), internal mould of a dorsal valve, LZ1400334, showing a median ridge (*mr*). (**b**), internal mould of conjoined shells, LZ2702680, showing dental plates (*dp*) and sockets (*soc*). (**c**), internal mould of an incomplete ventral valve, LZ2700385, illustrating dental plates. (**d**), internal mould of incomplete conjoined shells, LZ2702679. (**e**), enlarged portion of LZ2702679, showing denticulate hinge sockets (*soc*). (**f**), lateral view of internal mould of conjoined valves, LZ2702681. (**g**), dorsal view of LZ2702681, showing sockets (*soc*). (**h**), enlarged portion of LZ2702681, showing denticulate hinge sockets (*soc*). (**i**), exterior of a nearly complete ventral valve (shell partly decorticated), LZ1600336. (**j**), exterior of a complete ventral valve (shell partly decorticated), XM16709. (**k**–**m**), complete, conjoined valves, XM283C08, showing ventral, dorsal and anterior views

species that have so far been assigned to these two genera are concerned, they seem to be of very different age ranges: *Prelissorhynchia* is from the Late Permian to the earliest Triassic and *Lissorhynchia* is typical for the Early to Middle Triassic (Rong et al., 2017). With this consideration in mind, we tentatively assign the Upper Permian specimens to *Prelissorhynchia*.

Prelissorhynchia pseudoutah (Huang, 1933)
Fig. 9.74

1933 *Pugnax pseudoutah* Huang: 64, pl. 10, Fig. 1–8.
1977 *Pugnax pseudoutah* Huang; Yang et al.: 381, pl. 151, Fig. 3a–d.
1978 *Pugnax pseudoutah* Huang; Tong: 241, pl. 85, Fig. 11.
1979 *Pugnax pseudoutah* Huang; Zhan in Hou et al.: 95, pl. 13, Fig. 21, 22.
1980a *Neowellerella pseudoutah* (Huang); Liao: 276, pl. 7, Fig. 38, 39.
1987 *Lissorhynchia pseudoutah* (Huang); Xu in Yang et al.: 229, pl. 13, Fig. 15, 16; pl. 14, Fig. 10, 12.
1987 *Neowellerella pseudoutah* (Huang); Liao: pl. 8, Fig. 1.
1994? *Prelissorhynchia pseudoutah* (Huang); Xu and Grant: 38, Fig. 22.28–22.48.
1999 *Prelissorhynchia pseudoutah* (Huang); Chen and Shi: 20, Fig. 6a–f, h–j, l–r.
1999 *Prelissorhynchia xui* Chen and Shi: 23, Fig. 4.
2007 *Prelissorhynchia pseudoutah* (Huang); Shen and Shi: 53, pl. 20, Fig. 32–35; pl. 21, Fig. 1–27.
2009b *Prelissorhynchia pseudoutah* (Huang); Chen et al.: Fig. 7t–u.
2014 *Prelissorhynchia pseudoutah* (Huang); Zhang et al.: 490, Fig. 9j–u.
2014 *Prelissorhynchia pseudoutah* (Huang); He et al.: 490, Fig. 9j–u.

Materials Over 170 specimens. Registered specimens: see below.

Measurements (mm):

Number	Width	Length	Width/ length	Notes
LZ1400334	7.87	6.73	1.17	Internal mould of dorsal valve
LZ2702680	10.28	5.79	1.78	Internal mould of dorsal valve
LZ2700385	10.36	8.75	1.18	Internal mould of ventral valve
LZ2702679	8.58	6.69	1.28	Internal mould of dorsal valve
LZ2702681	9.33	7.95	1.17	Dorsal internal mould of a conjoined shell
LZ2702681	9.33	8.84	1.06	Ventral internal mould of a conjoined shell
LZ1600336	7.25	6.58	1.10	Ventral exterior
XM16709	10.02	9.26	1.08	Ventral exterior
XM283C08	8.86	8.63	1.03	Ventral valve of a conjoined shell
XM283C08	8.81	8.20	1.07	Dorsal valve of a conjoined shell

Occurrence Upper Permian–lowest Triassic; South China (more abundant in shallow-water facies).

Description Shell subtriangular to subcircular, 5.7–9.3 mm long and 5.3–10.8 mm wide, greatest width at/anterior to shell midlength, lateral margins anteriorly diverging at about 80–120°; anterior commissure strongly uniplicate with sharp zigzag outline; costae usually developed only near margins, simple, with rounded to roof-tiled crests, 1–3 on fold or sulcus, 1–3 pairs on flanks. Ventral valve gently convex; beak acute, erect; sulcus beginning from slightly anterior to midlength, distinctly deepening anteriorly, forming a distinctly elevated tongue. Ventral interior with subparallel (slightly anteriorly-diverging) dental plates (*dp*), dental plates anteriorly extending to fourth of shell length (Fig. 9.74b–d). Dorsal interior with denticulate hinge sockets (*soc*) (Fig. 9.74e, h; mistakenly described as "denticulate hinge teeth" of ventral interior in Zhang et al., 2014) and a variable median ridge (*mr*) (Fig. 9.74a).

Discussion This species is identical to *Prelissorhynchia pseudoutah* (Huang, 1933, p. 64, pl. 10, Fig. 1–8) from the Lungtan Formation of Guizhou, South China in all observed external and internal features, as illustrated by Xu and Grant, 1994. Compared to the present species, *Prelissorhynchia triplicatioid* Xu and Grant, 1994 from the Changhsing Formation of Sichuan Province in southwestern China has a more circular outline and a shallower sulcus. *Prelissorhynchia plena* Shen and Shi, 2007 from the Changhsing Formation of Sichuan Province in southwestern China has a much less convex lateral profile when compared with *Prelissorhynchia pseudoutah*.

Order **Orthotetida** Waagen, 1884
Suborder **Orthotetidina** Waagen, 1884
Superfamily **Orthotetoidea** Waagen, 1884
Family **Meekellidae** Stehli, 1954
Subfamily **Meekellinae** Stehli, 1954
Genus ***Orthothetina*** Schellwien, 1900

Type Species *Orthotetes persicus* Schellwien, 1900. Guadalupian (Middle Permian); Iran.

Diagnosis Shell medium in size, subcircular, with a strong monticulus in flat pseudodeltidium; a pair of subparallel dental plates; a pair of strong brachiophore plates, diverging at an obtuse angle; costellation fine, increased by intercalation or bifurcation.

Discussion *Orthothetina* differs from *Perigeyerella* Wang, 1955b in having a pair of subparallel dental plates that do not converge anteriorly to form a spondylium, and a pair of brachiophore plates which diverge at an obtuse angle. *Orthothetina* is easily distinguished from *Meekella* White and St John, 1867 in finer costellae and lacking of plicae. Compared to *Orthothetina*, *Paraorthotetina* He and Zhu, 1985 differs in having greatest width at hingeline and a dorsal median septum. *Orthothetina* differs from *Orthotetes* Fischer de Waldheim, 1829 and *Derbyia* Waagen, 1884 in lacking of a median septum, and from *Schellwienella* Thomas, 1910 in the longer and more closely spaced dental plates.

Orthothetina frechi (Huang 1933)
Fig. 9.75a–j

1933 *Schuchertella frechi* Huang: 21, pl. 3, Fig. 2–6.
1978 *Orthotetina ruber* (Frech); Feng and Jiang: 238, pl. 87, Fig. 9.
1980a *Orthotetina frechi* (Huang); Liao: pl. 2, Fig. 12.
1987 *Orthothetina frechi* (Huang); Liao: pl. 3, Fig. 8–12.
2007 *Orthothetina frechi* (Huang); Shen and Shi: 24, pl. 7, Fig. 25–29.
2014 *Orthothetina frechi* (Huang); Zhang et al.: 486, Fig. 7a–h.

Materials Over 230 specimens. Registered specimens: see below.

Measurements (mm):

Number	Width	Length	Width/length	Notes
LZ1200356	26.55	19.61	1.35	External mould of dorsal valve
LZ0400122	19.66	13.57	1.45	Internal mould of dorsal valve
LZ1200353	25.71	18.48	1.39	Internal mould of dorsal valve
LZ1200354	22.28	16.48	1.35	Internal mould of ventral valve
LZ1200351	27.12	19.18	1.41	Internal mould of dorsal valve
LZ1600352	26.30	18.21	1.44	Internal mould of dorsal valve
LZ1600350	28.83	18.48	1.56	Internal mould of dorsal valve
XM14907	9.38	7.65	1.23	Dorsal interior

Occurrence Upper Permian; South China.

Description Shell medium in size for genus, 7.7–20.5 mm long and 9.4–28.6 mm wide, transversely subcircular in outline. Ventral valve slightly concave, umbo weakly convex; interarea low, broadly triangular. Dorsal valve slightly convex, umbo gently convex; hingeline straight, shorter than maximum width at/posterior to midlength; cardinal extremities and lateral margins rounded. Shell surface with costellae, costellae fine and increased

anteriorly by bifurcation, 14–17 per 5 mm near anterior margin; concentric fila fine and weak, about 10 per 2 mm near anterior margin.

Ventral interior with very short dental plates (about one nineth of shell length), dental plates diverging at an angle of about 40–50°; ventral interior ornamented with fine and dense papillae (Fig. 9.75e). Dorsal interior with crural plates; crural plates short, strong, diverging at an angle of about 100–110°; dorsal interior ornamented with fine and dense papillae (Fig. 9.75j).

Discussion The present species is similar to *Orthothetina ruber* (Frech, 1911) in a transversely subcircular outline and fine costellation, but the latter has a higher interarea and longer dental plates. *Orthothetina frechi* is also very similar to *O. regularis* (Huang, 1933) in a transversely subcircular outline and interiors, but the latter exhibits coarser costellation and is smaller in shell size. The specimen of *Orthotetina ruber* (Frech) illustrated by Feng and Jiang, 1978 (pl. 87, Fig. 9) has a transversely subcircular outline, low interarea and fine costellation, suggesting it should belong to *Orthothetina frechi* (Huang 1933).

Orthothetina regularis (Huang, 1933)
Figs. 9.75o; 9.76

1933 *Schellwienella regularis* Huang: 25, pl. 3, Fig. 10–11.
1961 *Schellwienella regularis* Huang; Shimizu: 247, pl. 9, Fig. 6–9.
1979 *Lopingia regularis* (Huang); Zhan in Hou et al.: 66, pl. 4, Fig. 22, 23.
1980a *Orthothetina regularis* (Huang); Liao: pl. 1, Fig. 39–42.
1986 *Orthothetina regularis* (Huang); Liao and Meng: pl. 1, Fig. 16.
1987 *Orthothetina regularis* (Huang); Liao: pl. 3, Fig. 1–7.
1987 *Orthothetina regularis* (Huang); Xu in Yang et al.: pl. 7, Fig. 19–22, 26.
1990 *Orthothetina ruber* (Frech); Zhu: 64, pl. 9, Fig. 21.
2007 *Orthothetina regularis* (Huang); Shen and Shi: 21, pl. 6, Fig. 19–24.
2008 *Orthothetina regularis* (Huang); Li and Shen: 317, Fig. 6.12–6.16.
2014 *Goniarina* sp.; He et al.: 947, Fig. 21k.
2014 *Orthothetina regularis* (Huang); Zhang et al.: 487, Fig. 7i—w.

Materials Over 60 specimens. Registered specimens: see below.

Measurements (mm):

Number	Width	Length	Width/ length	Notes
XM-2-75	3.59	2.77	1.30	External mould of dorsal valve
LZ1400355	12.45	8.53	1.46	Internal mould of dorsal valve
LZ1400327	11.24	8.36	1.34	External mould of ventral valve
LZ1400328	5.17	3.77	1.37	External mould of dorsal valve
LZ1400324	12.69	8.43	1.51	External mould of ventral valve
LZ0400329	6.62	4.58	1.45	Internal mould of ventral valve

Fig. 9.75 (**a**–**j**), ***Orthothetina frechi*** (Huang, 1933). (**a**), external mould of a complete dorsal valve, LZ1200356, showing bifurcated costellae. (**b**, **c**), internal moulds of two nearly complete dorsal valves, LZ0400122, LZ1200353, showing anteriorly-diverged crural plates (*crp*). (**d**), internal mould of a nearly complete ventral valve, LZ1200354, showing short dental plates. **e**, enlarged portion of LZ1200354, showing fine and dense papillae. (**f**–**h**), internal moulds of three incomplete dorsal valves, LZ1200351, LZ1600352, LZ1600350. (**i**), interior of a complete dorsal valve, XM14907. (**j**), enlarged portion of XM14907, showing fine and dense papillae. (**k**, **l**), ***Orthothetina ruber*** (Frech, 1911). (**k**), internal mould of a broken ventral valve, SR-21-143, showing slightly anteriorly-diverged dental plates. (**l**), exterior of an incomplete dorsal valve, SR-20-133, showing intercalated costellae. (**m**, **n**), ***Goniarina*** sp.. (**m**), external mould of a complete dorsal valve, DP-2-342, showing coarse, rounded, bifurcated costellae and concentric fila. (**n**), internal mould of an incomplete dorsal valve, LQ-3-343, showing a fork-shaped cardinal process (*cp*). (**o**), ***Orthothetina regularis*** (Huang, 1933), external mould of a complete dorsal valve, XM-2-75, showing coarse, rounded costellae. (**p**, **q**), ***Streptorhynchus*** sp.. (**p**), internal mould of an incomplete dorsal valve, XM-2-74. (**q**), external mould of an incomplete dorsal valve and posterior part of external mould of the conjoined ventral valve, SR-23-145, showing a high ventral apsacline interarea (*iar*) and micro-protuberances (*pr*) along crests of costellae

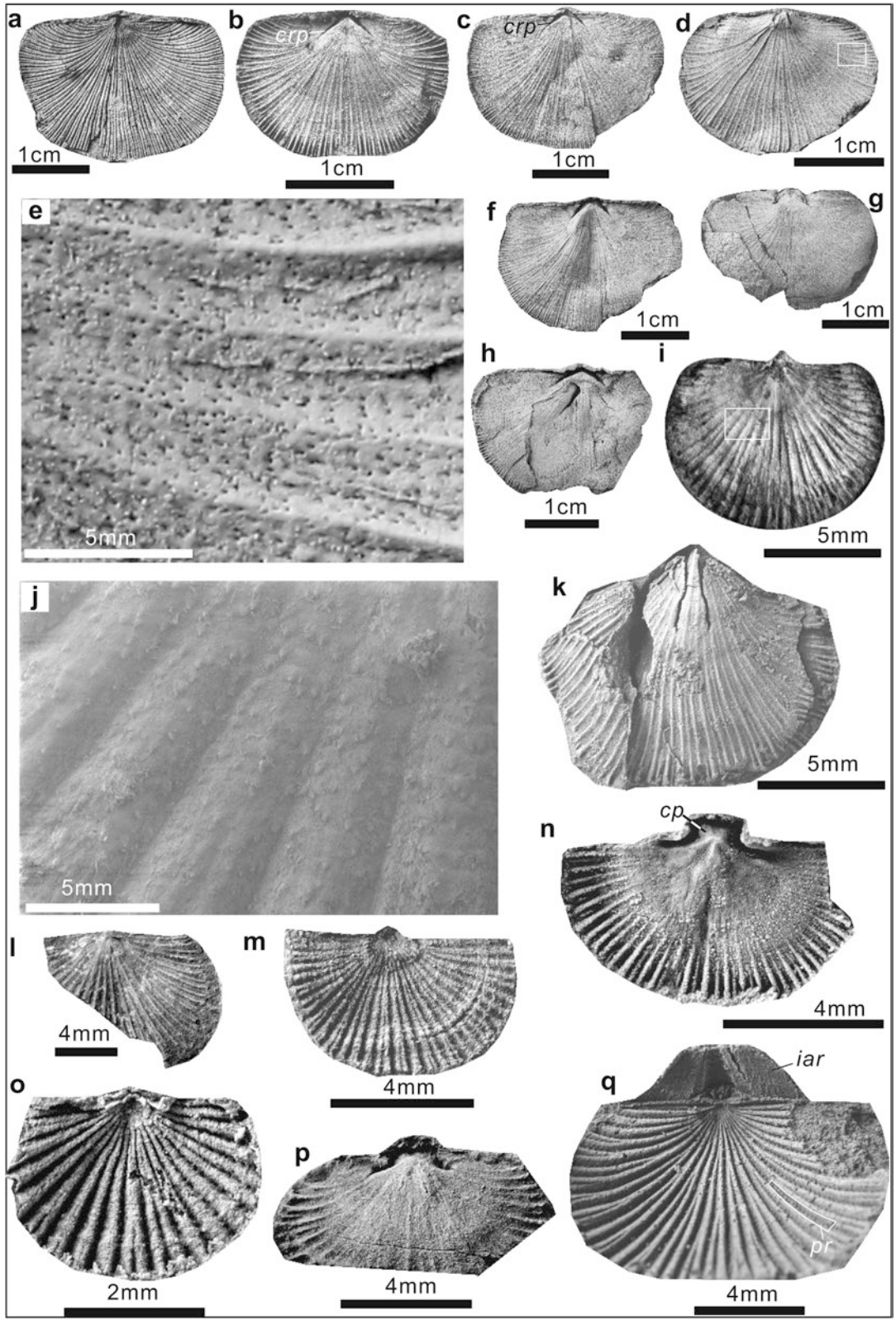
a
1cm
b
crp
1cm
c
crp
1cm
d
1cm
e
5mm
f
1cm
g
1cm
h
1cm
i
5mm
j
5mm
k
5mm
n
cp
4mm
l
4mm
m
4mm
o
2mm
p
4mm
q
iar
pr
4mm

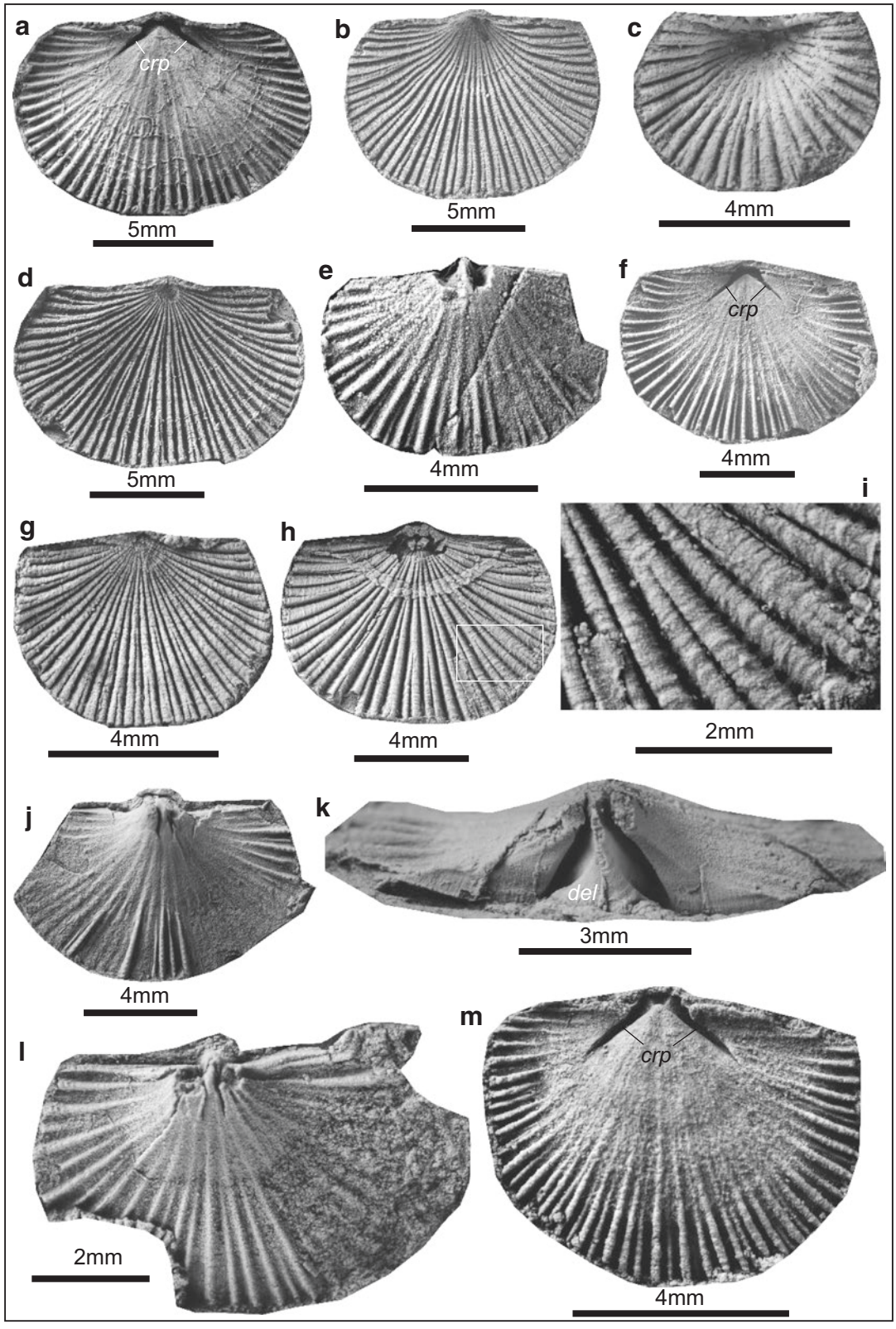
a
crp
5mm
b
5mm
c
4mm
d
5mm
e
4mm
f
crp
4mm
g
4mm
h
4mm
i
2mm
j
4mm
k
del
3mm
l
2mm
m
crp
4mm

Number	Width	Length	Width/ length	Notes
LZ1200322	10.86	7.75	1.40	Internal mould of dorsal valve
LZ1400321	6.11	4.61	1.33	External mould of ventral valve
LZ0400326	9.64	7.06	1.37	External mould of ventral valve
LZ0400330	10.63	6.69	1.59	Internal mould of ventral valve
LZ1600331	6.32	4.60	1.37	Internal mould of dorsal valve
LZ1400325	6.99	5.56	1.26	Internal mould of ventral valve

Occurrence Upper Permian; South China.

Description Shell small for genus, 2.8–8.7 mm long and 3.6–12.7 mm wide, transversely subcircular in outline. Ventral valve nearly flat, umbo gently convex; interarea moderately high, broadly triangular. Dorsal valve flat or slightly convex, umbo gently convex; hingeline straight, shorter than maximum width at midlength; cardinal extremities bluntly rounded, lateral margins rounded. Shell surface with costellae, costellae fine and increased anteriorly by intercalation, 10–16 per 5 mm near anterior margin; concentric fila fine and weak, about 10 per 2 mm near anterior margin.

Ventral interior with short dental plates (about one-sixth of shell-length), dental plates diverging at an angle of about 20°. Dorsal interior with brachiophore plates, brachiophore plates short, strong, diverging at an angle of about 100–120°.

Discussion The species is closest to *Orthothetina frechi* (Huang, 1933), but the difference is still evident (see above). The specimen of *Orthothetina ruber* (Frech) illustrated by Zhu, 1990 (pl. 9, Fig. 21) has a small body size and transversely subcircular outline, suggesting it is conspecific with the present species.

Orthothetina ruber (Frech, 1911)
Fig. 9.75k, l

1911 *Orthothetes ruber* Frech: 124, pl. 26, Fig. 4a, b.
1933 *Schellwienella ruber* (Frech); Huang: 23, pl. 3, Fig. 8, 9.
1978 *Orthotetina ruber* (Frech); Feng and Jiang: 238, pl. 87, Fig. 10.
1978 *Orthotetina ruber* (Frech); Tong: 214, pl. 78, Fig. 3–6.
1979 *Lopingia ruber* (Frech); Zhan in Hou et al.: 65, pl. 4, Fig. 3, 4.
1980a *Orthotetina ruber* (Frech); Liao: pl. 2, Fig. 1–3.
1987 *Orthotetina ruber* (Frech); Xu in Yang et al.: 218, pl. 7, Fig. 10–15, 17, 18.
1990 *Orthotetina ruber* (Frech); Zhu: 64, pl. 18, Fig. 29–32.
1990 *Orthotetina ruber* (Frech); Liang: 109, pl. 15, Fig. 9, 10.
2007 *Orthotetina ruber* (Frech); Shen and Shi: 20, pl. 6, Fig. 4—18.

Materials Two registered specimens: see below.

Measurements (mm):

Number	Width	Length	Width/ length	Notes
SR-21-143	11.85	9.68	1.22	Internal mould of ventral valve
SR-20-133	14.64	8.88	1.65	Dorsal exterior

Occurrence Upper Permian; South China.

Fig. 9.76 ***Orthothetina regularis*** (Huang, 1933). (**a**), internal mould of a complete dorsal valve, LZ1400355, showing anteriorly-diverged crural plates (*crp*, at an obtuse angle). (**b**), external mould of a complete ventral valve, LZ1400327, showing bifurcated costellae and concentric fila. (**c**), external mould of a complete dorsal valve, LZ1400328. (**d**), external mould of a complete ventral valve, LZ1400324. (**e**), internal moulds of ventral valves, LZ0400329, showing short dental plates. (**f**), internal mould of a dorsal valve, LZ1200322, showing anteriorly-diverged crural plates (*crp*). (**g**), external mould of a complete ventral valve, LZ1400321, showing bifurcated costellae. (**h**), external mould of a ventral valve, LZ0400326. (**i**), enlarged portion of LZ0400326, showing concentric fila. (**j**), internal mould of an incomplete ventral valve, LZ0400330, showing short dental plates. (**k**), enlarged posterior view of LZ0400330, showing the delthyrium (*del*). (**l**), internal mould of an incomplete ventral valve, LZ1600331. (**m**), internal mould of a nearly complete dorsal valve, LZ1400325, showing anteriorly-diverged crural plates (*crp*, at an obtuse angle)

Description Shell medium in size for genus, 8.9–9.7 mm long and 11.9–14.6 mm wide, subcircular in outline, convex-concave in profile. Ventral valve weakly convex; interarea moderately high, broadly triangular. Dorsal valve flat, umbo gently convex; hingeline straight, shorter than maximum width at midlength; cardinal extremities bluntly rounded, lateral margins rounded. Shell surface with fine costellae, costellae increased anteriorly by intercalation, 14 per 5 mm near anterior margin.

Ventral interior with a pair of dental plates, dental plates diverged anteriorly with an angle of 20°, extending to third of shell length.

Discussion The present species is similar to *Orthothetina regularis* (Huang, 1933) in outline, but differs in possessing finer costellation and slightly longer dental plates.

Family **Schuchertellidae** Williams, 1953
Subfamily **Schuchertellinae** Williams, 1953
Genus ***Goniarina*** Cooper and Grant, 1969

Type Species *Goniarina pyelodes* White, 1862. Neal Ranch Formation (Lower Permian); Glass Mountains, Texas, USA.

Diagnosis A subconical outline, ventribiconvex, relatively coarse costellate crossed by concentric lines, nearly straight costellae on the part of posterolateral valves; ventral interarea apsacline, pseudodeltidium with monticulus.

Discussion *Goniarina* is distinguished from *Streptorhynchus* by its relatively straight costellae on the part of posterolateral valves and quadrate dorsal cardinal extremities, contrasted respectively to the distinctly curved (and trending to parallel to hingeline) costellate on the part of posterolateral valves and rounded dorsal extremities in *Streptorhynchus*. *Goniarina* differs from *Schuchetella* Girty, 1904 in a more conical outline, a smaller size, coarser costellae and a longer median ridge.

Goniarina sp.
Fig. 9.75m, n

Materials Four specimens. Registered specimens: see below.

Measurements (mm):

Number	Width	Length	Width/ length	Notes
DP-2-342	7.26	4.18	1.74	External mould of dorsal valve
LQ-3-343	7.70	4.83	1.60	Internal mould of dorsal valve

Occurrence Changhsingian; Guangxi of South China.

Description Shell small for genus, 2.8–5.0 mm long and 3.6–8.0 mm wide. Dorsal costellae coarse, with rounded crests, increasing by intercalation, 22 per 5 mm at anterior margin, costellae on the part of posterolateral valves distinctly straight; concentric fila fine, obscure. Dorsal interior with a fork-shaped cardinal process (*cp*) (Fig. 9.75n); sockets deep; socket plates diverged laterally, nearly parallel to hingeline; adductor field bisected a weak median ridge, median ridge extending beyond the muscle field.

Discussion Coarse, straight costellae (the distinctly curved costellae on the part of posterolateral valves absent), quadrate dorsal cardinal extremities, socket plates diverged at a large abtuse angle and a long median ridge are all features characteristic of *Goniarina*, but the absence of ventral valve hinders further examination.

Subfamily **Streptorhynchinae** Stehli, 1954
Genus ***Streptorhynchus*** King, 1850

Type Species *Terebratulites pelargonatus* Schlotheim, 1816. Kazanian (Middle Permian); Gera, Germany.

Diagnosis (emended). A subconical outline, ventribiconvex; relatively coarse costellae crossed by concentric fila, costellae on part of posterolateral valves curved and trending to be parallel to hingeline; ventral interarea apsacline, pseudodeltidium with monticulus.

Discussion *Streptorhynchus* differs from *Goniarina* Cooper and Grant, 1969 in its rounded dorsal extremities, curved costellae on the part of posterolateral valves and longer teeth. This genus differs from *Orthothetina* Schellwien, 1900 in its coarser costellae.

Streptorhynchus sp.
Fig. 9.75p, q

Materials Four specimens. Registered specimens: see below.

Measurements (mm):

Number	Width	Length	Width/ length	Notes
XM-2-74	8.52			Internal mould of dorsal valve
SR-23-145	11.57	6.53	1.77	External mould of dorsal valve

Occurrence Changhsingian; South China.

Description Subconical in outline, 4.8–8.0 mm long and 6.6–11.6 mm wide, hingeline straight, shorter than greatest width at shell midlength, lateral margins evenly rounded. Ventral valve with a high apsacline interarea, pseudodeltidium with monticulus (Fig. 9.75q). Dorsal valve with coarse costellae, costellae increasing by several bifurcations from umbo to anterior margin, costellae on the part of posterolateral valves curved posteriorly and nearly parallel to hingeline (Fig. 9.75q); microscopic protuberances (marked by *pr*, see Fig. 9.75q) along crests of costellae to form concentric fila. Dorsal interior with deep sockets, thick inner socket ridges extending anteriorly at an angle of 120°.

Discussion A subconical outline, curved (and nearly parallel to hingeline) costellae on the part of posterolateral valves, a high and apsacline ventral interarea and a pseudodeltidium with monticulus agree well with the genus *Streptorhynchus*, but absence of ventral interior hinders further examination.

Class **Lingulata** Gorjansky and Popov, 1985
Order **Lingulida** Waagen, 1884
Superfamily **Discinoidea** Gray, 1840
Family **Discinidae** Gray, 1840
Genus ***Orbiculoidea*** d'Orbigny, 1847

Type Species *Orbicula forbesii* Davidson, 1848. Wenlock (Silurian); West Midlands, England.

Diagnosis Shell strongly dorsibiconvex, subcircular; shell thin-walled; concentric lines separated by broader interspaces. Dorsal valve conical to subconical with subcentral apex; ventral valve depressed, conical with subcentral apex. Pedicle track narrow, tapering posteriorly, anteriorly closed by shallow listrium; foramen in posterior end of listrium with short internal tube (Mergl, 2006).

Discussion *Orbiculoidea* differs from *Acrosaccus* Willard, 1928 of the Ordovician as the latter has a submarginal dorsal apex, and from *Roemerella* Hall and Clarke, 1890 of the Devonian as the latter has a central apex and a pedicle track on a broadly elevated area.

Orbiculoidea nucleola Liao, 1980a
Fig. 9.77a–h, l–o

1980a *Orbiculoidea nucleola* Liao: 252, pl. 1, Fig. 10–16.
2014 *Orbiculoidea elegans* Liao; Zhang et al.: 484, Fig. 4a–o.
2014 *Orbiculoidea nucleola* Liao; Zhang et al.: 484, Fig. 5a–o.

Diagnosis Shell medium to large for genus, subcircular in outline; nearly equally biconvex; apex eccentric, marginal area partly flat; pedicle track narrow, tapering at posterior margin, extending to front of posterior margin; posterior slope slightly concave.

Materials 29 specimens. Registered specimens: see below.

Measurements (mm):

Number	Width	Length	Width/ length	Notes
LZ1200182	8.74	9.72	0.90	Dorsal exterior
LZ1200203	8.37	9.81	0.85	Internal mould of dorsal valve
LZ1200625	9.12	10.67	0.85	External mould of ventral valve
LZ1200623	7.17	8.58	0.84	Ventral exterior
LZ1200622	8.84	10.47	0.84	Ventral exterior
LZ1200606	9.25	10.75	0.86	Ventral exterior
LZ1600208	16.28	17.99	0.90	Dorsal exterior
LZ1200611	15.05	14.71	1.02	Internal mould of ventral valve
LZ0200199	10.56	11.20	0.94	Dorsal exterior

Occurrence Changhsingian; Guizhou Province, South China.

Description Medium to large, 8.5–18.0 mm long, 7.2–17.1 mm wide; subcircular in outline, nearly equally biconvex (dorsal convexity slightly stronger than ventral).

Ventral valve low conical, apex from slightly eccentric to strongly eccentric (at third of shell posterior), marginal area gently convex or nearly flat; pedicle track narrow and shallow, tapering at one half or two-thirds of shell posterior.

Dorsal valve low conical, slightly more convex than ventral valve, apex strongly eccentric. Concentric lines fine, interspace about two to three times wider than concentric lines, about 8−12 lines per 2 mm near anterior margin.

Discussion This species differs from *Orbiculoidea elegans* Liao, 1980a of the Lower Triassic of Guizhou, southwestern China in the latter having a longer pedicle track (extending to posterior margin). The specimens of *Orbiculoidea elegans* of Zhang et al., 2014 have a short pedicle track (extending to a half of shell posterior, see Fig. 4e, g, i, k of Zhang et al., 2014) and therefore should not belong to *Orbiculoidea elegans* Liao, 1980a, but to the present species. *Orbiculoidea anhuiensis* Jin and Hu, 1978 from the Middle Permian of southern Anhui Province, China has a narrower pedicle track than in the present species.

Orbiculoidea liaoi Zhang et al., 2014
Fig. 9.77i−k, p

1978 *Orbiculoidea minor* Liao (MS); Feng and Jiang: 232, pl. 85, Fig. 1.
2014 *Orbiculoidea qinglongensis* Liao; Zhang et al.: 485, Fig. 5r.
2014 *Orbiculoidea liaoi* Zhang et al.: 485, Figs. 5p, t, q, u; 6a.

Diagnosis (emended). Small for genus, circular in outline; concentric lines between apex and midlength circular; pedicle track wide and shallow, extending to front of posterior margin.

Materials Four registered specimens: see below.

Fig. 9.77 (**a**–**h**, **l**–**o**), ***Orbiculoidea nucleola*** Liao, 1980a. (**a**), exterior of a complete dorsal valve (shell decorticated near umbo), LZ1200182. (**b**), internal mould of a complete dorsal valve, LZ1200203. (**c**), external mould of a complete ventral valve and shell remnant, LZ1200625. (**d**), enlarged portion of LZ1200625, illustrating a pedicle track tapering posteriorly. (**e**), exterior of an incomplete ventral valve (shell decorticated near umbo), LZ1200623. (**f**), exterior of a complete ventral valve (shell decorticated near umbo), LZ1200622. (**g**), enlarged portion of LZ1200622, showing a pedicle track tapering posteriorly. (**h**), exterior of an incomplete ventral valve (shell decorticated near umbo), LZ1200606. (**l**, **o**), exteriors of two incomplete dorsal valves, LZ1600208, LZ0200199, showing elliptical concentric lines between apex and midlength. (**m**), internal mould of an incomplete ventral valve and shell remnant, LZ1200611, showing a pedicle track. (**n**), Enlarged portion of LZ1200611, illustrating the pedicle track extending to two-thirds of shell posterior. (**i**–**k**, **p**), ***Orbiculoidea liaoi*** Zhang et al., 2014. (**i**, **j**), external moulds of two complete dorsal valves, LZ2702628, LZ2702614, showing circular concentric lines between apex and midlength. (**k**), internal mould of a complete ventral valve and shell remnant, LZ2701198, showing a pedicle track extending to front of posterior margin. (**p**), exterior of a complete ventral vavle (shell decorticated at umbo), LZ0700187

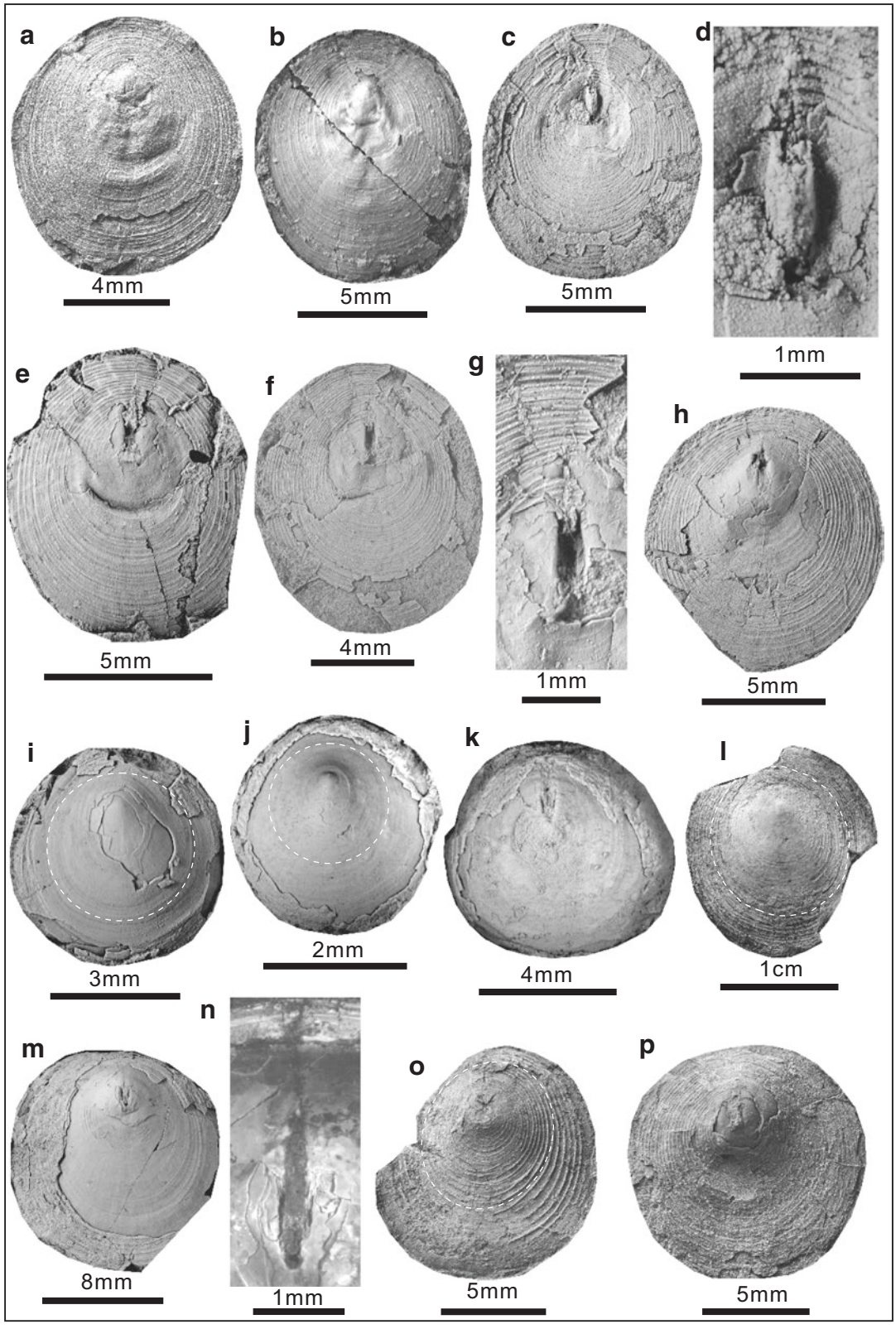
a
4mm
b
5mm
c
5mm
d
1mm
e
5mm
f
4mm
g
1mm
h
5mm
i
3mm
j
2mm
k
4mm
l
1cm
m
8mm
n
1mm
o
5mm
p
5mm

Measurements (mm):

Number	Width	Length	Width/ length	Notes
LZ2702628	4.92	5.05	0.98	External mould of dorsal valve
LZ2702614	2.97	3.07	0.97	External mould of dorsal valve
LZ2701198	6.73	5.98	1.13	Internal mould of ventral valve
LZ0700187	11.15	10.89	1.02	Ventral exterior

Occurrence Changhsingian; Guizhou Province, South China.

Description Shell small, 3.1–10.9 mm long and 3.0–11.2 mm wide; circular in outline, gently dorsibiconvex. Ventral valve low conical, apex slightly eccentric; pedicle track wide and shallow, extending to front of posterior margin. Dorsal valve low conical, slightly more convex than ventral vavle, apex eccentric, at one-third of shell posterior. Shell surface with concentric lines, concentric lines between apex and midlength circular, whereas those between midlength and anterior margin slightly elliptical.

Discussion This species differs from *Orbiculoidea nucleola* Liao, 1980a in its circular outline and circular concentric lines between apex and midlength, from *Orbiculoidea elegans* Liao, 1980a in a shorter pedicle track, and from *Orbiculoidea anhuiensis* Jin and Hu, 1978 in a wider pedicle track.

Superfamily **Linguloidea** Menke, 1828
Family **Lingulidae** Menke, 1828
Genus ***Lingularia*** Biernat and Emig, 1993

Type Species *Lingularia similis* Biernat and Emig, 1993. Lower Jurassic (Brentskardhaugen Bed); Wimanfjellet in the Sassenfjorden area, Central Spitsbergen.

Diagnosis Shell longitudinally oval in outline, lateral margins subparallel, anterior margin broadly rounded. Dorsal interior with a narrow median ridge bisecting anterior lateral muscle scars. Ventral valve with a small pseudointerarea, a pedicle groove, heart-shaped umbonal muscle scar bisected by impression of a pedicle nerve. Vascula lateralia in both valves convergent.

Discussion *Lingularia* resembles to *Semilingula* Popov in Egorov and Popov, 1990 from the Permian, but the latter has dorsal vascular media (Egorov and Popov, 1990). The present genus is distinguished from *Glottidia* Dall, 1870 of the Cretaceous to Holocene by its nearly straight anterior margin and a higher length to width ratio. *Lingularia* differs from *Argentiella* Archbold et al., 2005 of the Lower Permian of Argentina in the latter having a broad median ridge in the ventral interior and acute posterior parts of shells. Peng and Shi (2008) proposed two new genera, *Sinolingularia* Peng and Shi, 2008 (with *S. huananensis* Peng and Shi, 2008 as the type species) and *Sinoglottidia* Peng and Shi, 2008 (with *S. archboldi* Peng and Shi, 2008 as the type species), based on the variations of anterior lateral muscle scars which were regarded as the intrageneric characteristic (Posenato et al., 2014; Holmer et al., 2016), and therefore *Sinolingularia* and *Sinoglottidia* had been considered as synonymous with *Lingularia* (Posenato et al., 2014; Holmer et al., 2016).

?Lingularia borealis (Bittner, 1899)
Figs. 9.78a–h; 9.79a

2014 *Sinoglottidia* sp. of He et al.: 954, Fig. 21P–U.

Materials 10 specimens. Registered specimens: see below.

Measurements (mm):

Number	Width	Length	Width/ length	Notes
SR-17-88	3.65	6.00	0.61	Ventral interior
SR-15-89	2.53	4.12	0.61	Ventral interior
SR-17-90	1.82	2.96	0.62	Internal mould of ventral valve
CM-13-97	2.10	3.63	0.58	Ventral valve
CM-10-98	2.82	4.72	0.60	Dorsal interior
XJP-11-93	2.99	4.93	0.61	Dorsal exterior
XJP-2f-87	3.24	4.94	0.66	Ventral exterior

Occurrence Upper Permian; Hunan, Hubei and Anhui Provinces, China.

Description Shell longitudinally ovate, 3.0–7.0 mm long and 1.8–4.6 mm wide; lateral margins subparallel; anterior margin broadly rounded. Numerous fine concentric lines intercalated by thick growth ridges. Ventral umbo elliptical, with pseudointerarea (*pa*) separated by a deep pedicle groove (*pg*) (Fig. 9.78b); greatest width around midlength. Ventral interior with a V-shaped nerve groove (*ng*) and a pair of central muscle scars (*cms*) at one third of length (Figs. 9.78b, c; 9.79a).

Discussion The presence of a small pseudointerarea, a deep pedicle groove separating a pair of central muscle scars in the ventral interior and a broadly-rounded anterior margin generally suggests some features of *Lingularia* Biernat and Emig, 1993. However, we could tentatively assign them to *Lingularia*, because of the sparsity of dorsal information.

Lingularia sp. 1
Figs. 9.78i; 9.79b

Material One registered specimen (HZS44-0699).

Occurrence Lower Triassic; Huangzhishan of Zhejiang Province, China.

Description Shell longitudinally ovate, 7.10 mm long and 4.81 mm wide (the width/length ratio being 0.68); lateral margins subparallel; anterior margin broadly rounded. Numerous fine concentric lines intercalated by thick growth ridges. Dorsal interior with a pair of central muscle scars (*cms*) and an anterolateral muscle scar (*alms*) (Fig. 9.78i).

Discussion The specimen has a pair of central muscle scars and an anterolateral muscle scar in the dorsal interior and a broadly-rounded anterior margin, all these features basically suggest *Lingularia* Biernat and Emig, 1993. The present specimen is more or less similar to *Lingularia borealis* (Bittner, 1899) in doral interior, but lacking of information on ventral valve prevents further comparison.

Lingularia sp. 2
Figs. 9.78j; 9.79c

Material One registered specimen (HZS37-0701).

Occurrence Lowest Triassic; Huangzhishan of Zhejiang Province, China.

Description Shell longitudinally ovate, 5.77 mm long and 3.94 mm wide (the width/length ratio being 0.68); lateral margins subparallel; anterior margin broadly rounded. Fine concentric lines intercalated by thick growth ridges. Dorsal interior with a pair of central muscle scars (*cms*) and an anterolateral muscle scar extending anteriorly and forming two oval parts (*alms*).

Discussion The presence of a pair of central muscle scars (*cms*) and an anterolateral muscle scar (*alms*) in the dorsal interior and a broadly-rounded anterior margin suggests characteristics of *Lingularia* Biernat and Emig, 1993. This specimen is more or less similar to *Lingularia similis* Biernat and Emig, 1993 in a dorsal anterolateral muscle scar probably bisected by a median ridge anteriorly (so forming two oval parts). The present specimen differs from *Lingularia* sp. 1 (see above) in having a more complex anterolateral muscle scar and smaller central muscle scars in the dorsal interior.

Genus ***Semilingula*** Popov in Egorov and Popov, 1990

Type Species *Lingula arctica* Miloradovich, 1936. Kungurian (Lower Permian); Russia.

Diagnosis Shell longitudinally ovate, lateral margins subparallel; ventral pseudointerarea small, with broadly triangular pedicle groove and vestigial propareas; umbonal muscle scars heart-

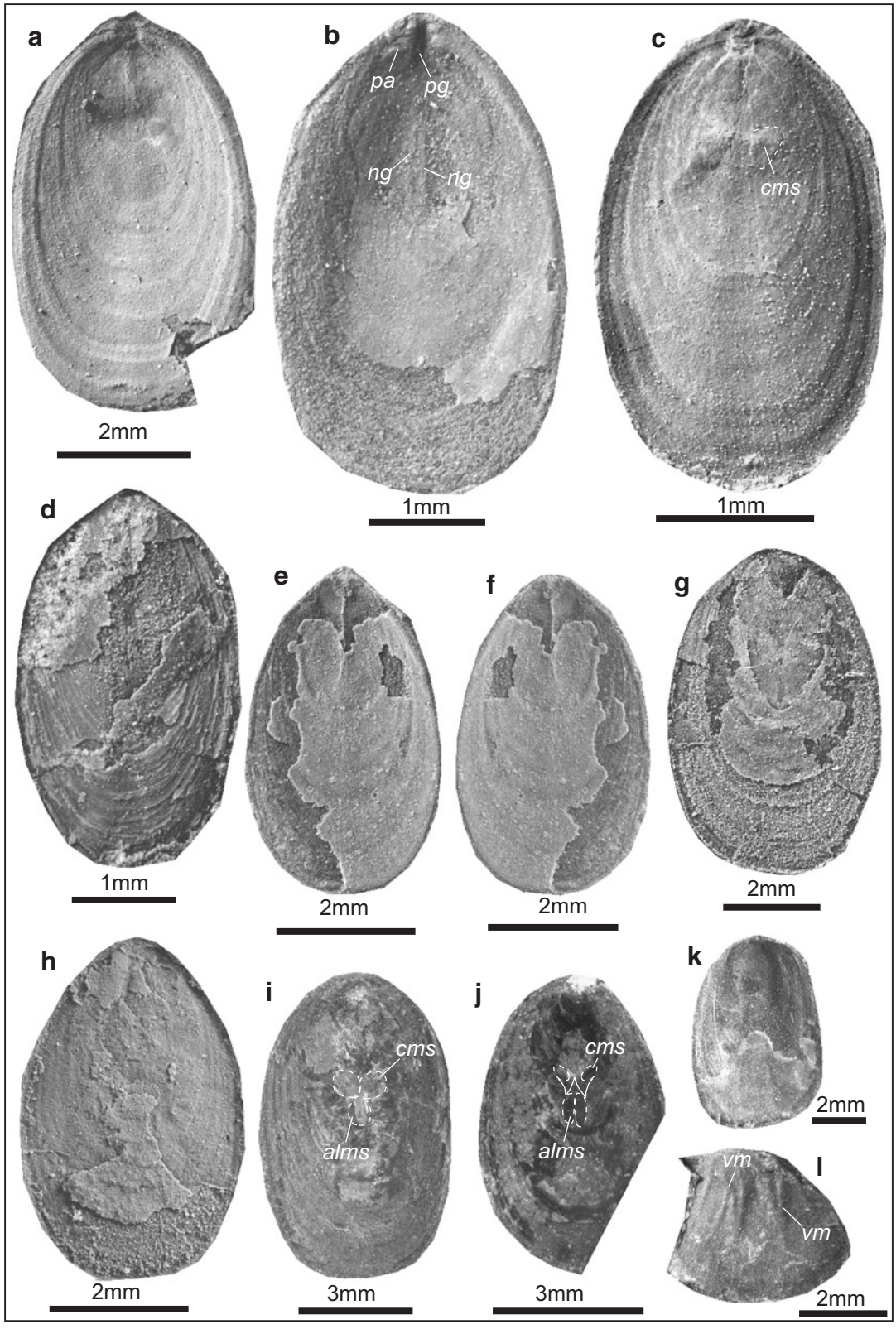
a
2mm
b
pa
pg
ng
ng
1mm
c
cms
1mm
d
1mm
e
2mm
f
2mm
g
2mm
h
2mm
i
cms
alms
3mm
j
cms
alms
3mm
k
2mm
l
vm
vm
2mm

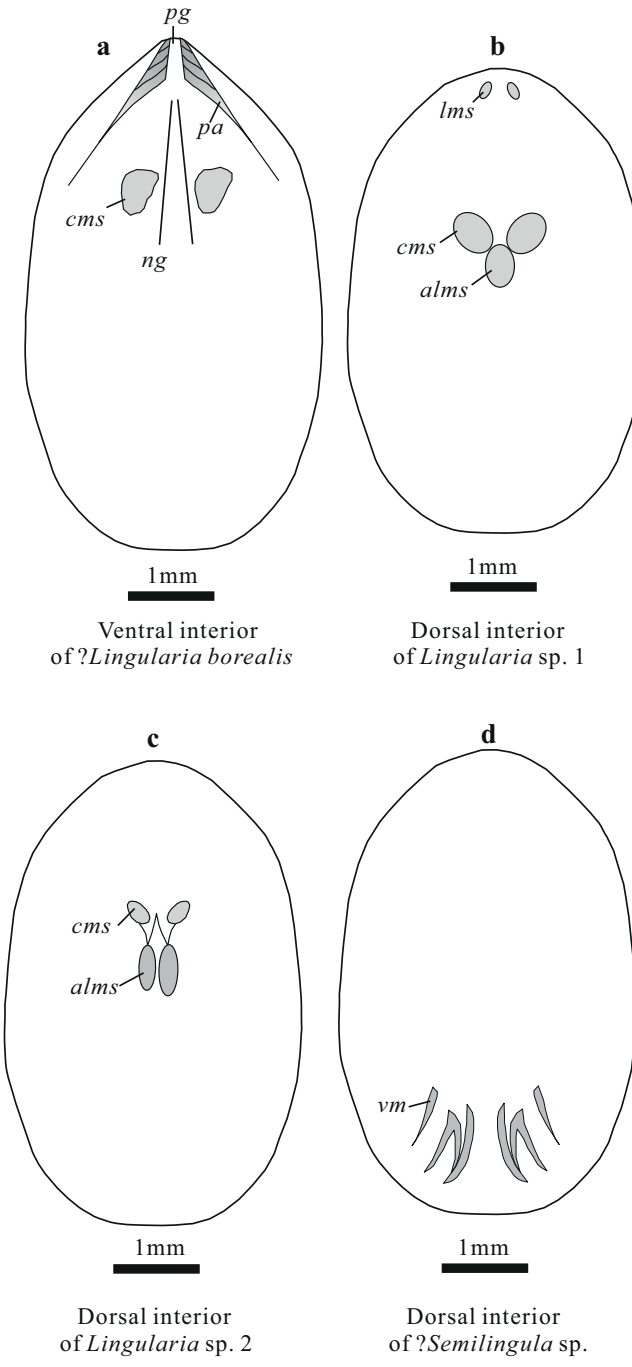

Fig. 9.79 Sketch diagrams of?***Lingularia borealis*** (Bittner, 1899) (**a**), ***Lingularia*** sp. 1 (**b**), ***Lingularia*** sp. 2 (**c**), and?***Semilingula*** sp. (**d**). Note: *pg*- pedicle groove, *pa*- propareas, *ng*- nerve groove, *cms*- central muscle scars, *alms*- anterolateral muscle scar, *vm*- vasculas median

Fig. 9.78 (**a**–**h**),?***Lingularia borealis*** (Bittner, 1899). (**a**), interior of nearly complete ventral valve, SR-17-88. (**b**), interior of complete ventral valve, SR-15-89, showing propareas (*pa*), pedicle groove (*pg*), nerve grooves (*ng*). (**c**), internal mould of a complete ventral valve, SR-17-90, showing a pair of central muscle scars (*cms*). (**d**), a nearly complete ventral valve (shell partly decorticated), CM-13-97. (**e**), interior of a complete dorsal valve, CM-10-98. (**f**), internal mould of CM-10-98. (**g**), exterior of a complete dorsal valve (shell mostly decorticated), XJP-11-93. (**h**), exterior of a complete ventral valve (shell mostly decorticated), XJP-2f-87. (**i**), ***Lingularia*** sp. 1. internal mould of a complete dorsal valve, HZS44-0699, showing a pair of central muscle scars (*cms*) and anterolateral muscle scar (*alms*). (**j**), ***Lingularia*** sp. 2. interior of an incomplete dorsal valve, HZS37-0701, showing a pair of central muscle scars (*cms*) and a complex anterolateral muscle scar extending anteriorly and forming two oval parts (*alms*). (**k**, **l**),?***Semilingula*** sp.. (**k**), external mould of a dorsal valve, HZS37-0698, showing fine concentric lines. (**l**), internal mould of an incomplete dorsal valve, HZS37-0702, showing vasculas median (*vm*)

shaped, bisected by pedicle nerve; dorsal interior with vestigial vasculas median and a short median ridge bisecting anterior lateral muscle scars.

?*Semilingula* sp.
Figs. 9.78k, l; 9.79d

Materials Two registered specimens (HZS37-0698, HZS37-0702).

Occurrence Lowest Triassic; Zhejiang Province (Huangzhishan section), South China.

Description Shell longitudinally ovate, 7.23 long and 4.75 mm wide (the width/length ratio being 0.66), greatest width around midlength, lateral margins subparallel. Numerous fine concentric lines intercalated by thick growth ridges. Dorsal interior with a vasculas median (*vm*) (see Figs. 9.78l; 9.79d).

Discussion The presence of vasculas median is reminiscent of *Semilingula* Popov in Egorov and Popov, 1990; however, sparsity of other features prevents further examination.

References

Abich OWH. 1878. Geologische Forschungen in den Kaukasischen Ländern. Th. 1. Eine Bergkaok fauna aus der Araxesenge bei Djoulfa in Armenien, Wien, 7: 1–126.

Afanasjeva GA. 1977. Suborder Chonetidina. In: Sarycheva, TG (Ed.), Pozdiepaleozoiskie Productidy Sibiri i Arktiki. Akademiia Nauk SSSR, Paleozoologicheskii Institute, Trudy (Moscow), 161: 5–41 [in Russian].

Archbold NW. 1980. Studies on western Australian Permian brachiopods. 1. The family Anopliidae (Chonetidina). Proceedings of the Royal Society of Victoria, 91: 181–192.

Archbold NW. 1981. A new species of *Tornquistia* (Brachiopoda: Chonetidina) from the Artinskian (Permian) of Western Australia. Memoirs of the National Museum of Victoria, 42: 7–14.

Archbold NW. 1982. *Sommeriella*, a new name for the Permian chonetacean brachiopod subgenus *Sommeria* Archbold 1981. Proceedings of the Royal Society of Victoria, 94: 10.

Archbold NW. 1983. Permian marine invertebrate provinces of the Gondwanan Realm. Alcheringa, 7: 59–73.

Archbold NW. 1990. Studies on Western Australian Permian brachiopods 9. The Sterlitamakian brachiopod fauna the Cuncudgerie Sandstone, Canning Basin. Proceedings of the Royal Society of Victoria, 102: 1–13.

Archbold NW. 1993. Studies on Western Australian Permian brachiopods 11. New genera, species and records. Proceedings of the Royal Society of Victoria, 105: 1–29.

Archbold NW. 1999. Additional records of Permian brachiopods from near Rat Buri, Thailand. Proceedings of the Royal Society of Victoria, 111: 71–86.

Archbold NW, Cisterna GA, Sterren AF. 2005. Lingulida (Brachiopoda) from the Early Permian of Argentina. Proceedings of the Royal Society of Victoria, 112: 307–317.

Baliński A. 1975. Secondary changes in microornamentation of some Devonian Ambocoeliid brachiopods. Palaeontology, 18: 179–189.

Bamber EW, Waterhouse JB. 1971. Carboniferous and Permian Stratigraphy and Paleontology, northern Yukon Territory, Canada. Bulletin of Canadian Petroleum *Geology, 19: 29–250.*

Biernat G, Emig CC. 1993. Anatomical distinctions of the Mesozoic lingulide brachiopods. Acta Palaeontologica Polonica, 38: 1–20.

Bittner A. 1899. Versteinerungen aus den Trias—Abladerungen des Süd-Ussuri-Gebietes in der ostsibirischen Küstenprovinz. Mémoires du Comité Géologique, 7: 1—35.

Booker FW. 1932. A new species of *Productus* from the Lower Bowen Series–Queensland. Proceedings of the Royal Society of Queensland, 43: 66–72.

Boucot AJ, Amsden TW. 1958. New genera of brachiopods. Bulletin of the Oklahoma Geological Survey, 78: 159–170.

Broili F. 1916. Die Permischen Brachiopoden von Timor. In: Wanner J, Weber F (Eds), Erggebnisse der Expeditionen G.A.F. Molengraaff, VII, 104 pp.

Bronn HG. 1862. Die Klassen und Ordnungen der Weichthiere. C. F. Winter'sche Verlagshandlung Press, Leipzig and Heidelberg, 518 pp.

Campbell KSW. 1953. The fauna of the Permo–Carboniferous Ingelara Beds of Queensland. Papers of Department of Geology of University of Queensland, 3: 1–43.

Campi MJ, Shi GR. 2005. New Lopingian (Late Permian) rugosochonetid species from Sichuan, South China. Alcheringa, 29: 275–285.

Carter JL. 1968. New genera and species of early Mississippian brachiopods from the Burlington Limestone. Journal of Paleontology, 42: 1140–1152.

Caster KE. 1939. A Devonian fauna from Colombia. Bulletin of American Paleontology, 24: 1–218.

Chao YT. 1927. Productidae of China, Part 1. Palaeontologia Sinica, Series B, 5: 1–244.

Chao YT. 1928. Productidae of China. Palaeontologia Sinica, Series B, 5: 1–85.

Chao YT. 1929. Carboniferous and Permian Spiriferids of China. Palaeontologia Sinica, Series B, 11: 1–133.

Chen ZQ, Shi G R. 1999. Revision of *Prelissorhynchia* Xu & Grant, 1994 (Brachiopoda) from the Upper Permian of South China. Proceedings of the Royal Society of Victoria, 111: 15–26.

Chen ZQ, Shi GR, Shen SZ, Archbold NW. 2000. *Tethyochonetes* gen. nov. (Chonetida, Brachiopoda) from the Lopingian (Late Permian) of China. Proceedings of the Royal Society of Victoria, 112: 1–15.

Chen ZQ, Kaiho K, George AD. 2005. Survival strategies of brachiopod faunas from the end-Permian mass extinction. Palaeogeography, Palaeoclimatology, Palaeoecology, 224: 232–269.

Chen ZQ, Shi GR, Yang FQ, Gao YQ, Tong JN, Peng YQ. 2006a. An ecologically mixed brachiopod fauna from Changhsingian deep-water basin of South China: consequence of end-Permian global warming. Lethaia, 39: 79–90.

Chen ZQ, Kaiho K, George AD, Tong JN. 2006b. Survival brachiopod faunas of the end-Permian mass extinction from the Southern Alps (Italy) and South China. Geological Magazine, 143: 301–327.

Chen ZQ, Shi GR, Gao YQ, Tong JN, Yang FQ, Peng YQ. 2009a. A late Changhsingian (latest Permian) deep-water brachiopod fauna from Guizhou, South China. Alcheringa, 33: 163–183.

Chen ZQ, Tong JN, Zhang KX, Yang H, Liao ZT, Song HJ, Chen J. 2009b. Environmental and biotic turnover across the Permian–Triassic boundary on a shallow carbonate platform in western Zhejiang, South China. Australian Journal of Earth Sciences, 56: 775–797.

Chi-Thuan TT. 1961. Les brachiopodes permiens du Phnom-Tup (Sisophon-Cambodge). Annales de la Faculté des Sciences, Université de Saigon, 1961: 267–308.

Cooper GA. 1957. Permian brachiopods from central Oregon. Smithsonian Miscellaneous Collections, 134: 1–79.

Cooper GA, Grant RE. 1969. New Permian Brachiopoda from West Texas. Smithsonian Contributions to Paleobiology, 1: 1–20.

Cooper GA, Grant RE. 1974. Permian brachiopods of West Texas. Smithsonian Contributions to Paleobiology, 15: 233–793.

Cooper GA, Grant RE. 1976a. Permian brachiopods of West Texas, V. Smithsonian Contributions to Paleobiology, 24: 2609–3159.

Cooper GA, Grant RE. 1976b. Permian brachiopods of West Texas, IV. Smithsonian Contributions to Paleobiology, 21: 1923–2607.

d'Orbigny A. 1847. Considérations zoologiques et géologiques sur les Brachiopodes ou Palliobranches. Comptes Rendus Hebdomadaires des Séances de l'Académie des Sciences, 25: 266–269.

Dagys AS. 1974. Triasovye brakhiopody (Morfologiia, sistema, filogeniia, stratigraficheskoe znachenie I biogeografiia) [Triassic brachiopods (Morphology, classification, phylogeny, stratigraphical significance and biogeography)]. Sibirskoe Otdelenie Izdatel'stvo "Nauka." Novosibirsk, 387 pp.

Dall WH. 1870. A revision of the Terebratulidae ad Lingulidae. American Journal of Conchology, 6: 177–204.

Davidson T. 1848. Mémoire sur les Brachiopodes du Système Silurien supérieur de l'Angleterre. Société Géologique de France, Bulletin (series 2), 5: 309–338.

Davidson T. 1859. Palaeontological notes on the Brachiopoda. 2. On the families Strophomenidae and Productidae. Geologist, 2: 97–117.

De Koninck LG. 1863. Mémoire sur les fossiles paléozoïques recueillis dans l'Inde par M. le Docteur Fleming. H. Dessain. Liège, 44 pp.

Derby OA. 1874. On the Carboniferous Brachiopoda of Itaituba, Rio Tapajos, Province of Para, Brazil. Cornell University Scientific Bulletin, 2: 1–63.

Egorov AN, Popov LE. 1990. Novyi rod lingulid iz nizhnepermskikh otlozhenii Sibirskoi Platformy. Paleontologicheskii Zhurnal, 4: 111–115.

Emig CC. 2003. Proof that *Lingula* (Brachiopoda) is not a living-fossil, and emended diagnoses of the family Lingulidae. Notebooks on Geology, Letter 2003/01. Updated at http://paleopolis.rediris.es/cg/CG2003_L01_CCE/.

Feng RL, Jiang ZL. 1978. Brachiopoda, p. 231–305. In: Guizhou Working Group of Paleontology (Ed.), Paleontological atlas of southwest China. Geological Publishing House, Beijing. [In Chinese].

Feng SN, Xu SY, Lin JX, Yang DL. 1984. Biostratigraphy of the Yangtze Gorge Area (3), p. 63–239. In: Yichang Institution of Geology and Mineral Resources (Ed.), Late Palaozoic Era. Geological Publishing House, Beijing. [in Chinese].

Fischer de Waldheim G. 1825. Notice sur la Choristite. Programme d'invitation à la Société Impériale des Naturalistes de Moscou, Moscow, 12 pp.

Fischer de Waldheim G. 1829. Quelques fossiles de gouvernement de Moscou. Société Impériale des Naturalistes de Moscou Bulletin, 1: 375–376.

Fischer de Waldheim G. 1830. Oryctographie du gouvernement de Moscou, 1st ed. A. Semen, Moscow, 202 pp.

Frech F. 1911. Das Obercarbon Chinas, die Dyas, p. 64–193. In: von Richthofen F (Ed.), China, Volume 5, Dietrich Reimer, Berlin.

Fredericks G. 1924. Ussuriiskii verkhnii paleozoi. I. Brachiopoda. Materialy po Geologii I Poleznym Iskopaemym Dal'nego Vostoka, 28: 1–53.

Fredericks G. 1928. Materialy dlya klassifiatsii roda Productus Sow. Izvestiia Geologicheskogo Komiteta Leningrad, 46: 773–792.

Gemmellaro GG. 1899. La fauna dei calcari con Fusulina della valle del fiume Sosio nella Provincia di Palermo. Parte IV Brachiopoda. Giornale di Scienze Naturali ed Economiche di Palermo, 22: 95–214.

George TN. 1931. Ambocoelia Hall and certain similar British Spiriferidae. Geological Society of London Quarterly Journal, 87: 30–61.

George TN. 1932. The British Carboniferous reticulate Spiriferidae. Geological Society of London Quarterly Journal, 88: 516–575.

Girty GH. 1904. New molluscan genera from the Carboniferous. United States National Museum Proceedings, 27: 721–736.

Gordon M, Henry TW. 1990. Marginovatia, a mid-Carboniferous genus of linoproductid brachiopods. Journal of Paleontolog, 64: 532–551.

Gorjansky VI, Popov LE. 1985. Morfologiia, systematicheskoe polozhenie i proiskhozhdenie bezzamkovykh brachiopods karbonatnoi rakovinoi. Paleontologicheskii Zhurnal, 3: 3–14.

Grabau AW. 1931. The Permian of Mongolia. American Museum of Natural History, Natural History of Central Asia, 4: 1–665.

Grant RE. 1976. Permian brachiopods from southern Thailand. Journal of Paleontology, 50 (supplement to No. 3, Paleontological Society Memoir 9): 1–269.

Grant RE. 1993. Permian brachiopods from Khios Island, Greece. Journal of Paleontology, 67: 1–21.

Gray JE. 1840. Synopsis of the contents of the British Museum, 42 edition. British Musuem, London, 370 pp.

Hall J, Clarke JM. 1890. Extract. Palaeontology of New York. Charles van Benthuysen and Sons, Albany, 8: 120–137.

Hall J, Clarke JM. 1892. An introduction to the study of the genera of Palaeozoic brachiopoda. Natural History of New York, Palaeontology, 8: 1–367.

Havlíček V. 1977. Brachiopods of the order Orthida in Czechoslovakia. Rozpravy ÚstřednÍho Ústavu Geologického, 44: 1–327.

He WH, Shen SZ, Feng QL, Gu SZ. 2005. A late Changxingian (Late Permian) deep-water brachiopod fauna from the Talung Formation at the Dongpan Section, Southern Guangxi, in South China. Journal of Paleontology, 79: 927–938.

He WH, Shi GR., Feng QL., Peng YQ. 2007. Discovery of late Changhsingian (latest Permian) brachiopod *Attenuatella* species from South China. Alcheringa, 31: 271–284.

He WH, Shi GR, Zhang Y, Yang TL, Teng F, Wu SB. 2012. Systematics and palaeoecology of Changhsingian (Late Permian) Ambocoeliidae brachiopods from South China and implications for the end-Permian mass extinction. Alcheringa, 36: 515–530.

He WH, Shi GR, Zhang Y, Yang TL, Zhang KX, Wu SB, Niu ZJ, Zhang ZY. 2014. Changhsingian (latest Permian) deep-water brachiopod fauna from South China. Journal of Systematic Palaeontology, 12: 907–960.

He XL, Zhu ML. 1985. Some Upper Permian new genera and species of Orthotetacea in south west China. Acta Palaeontologia Sinica, 24: 198–204. [in Chinese with English abstract].

Holmer LE, Popov LE, Klishevich I, Ghobadi PM. 2016. Reassessment of the early Triassic lingulid brachiopod '*Lingula*' *borealis* Bittner, 1899 and related problems of lingulid taxonomy. GFF, 138: 519–525.

Hou HF, Zhan LP, Chen BW, Others. 1979. The coal-bearing strata and fossils of the Late Permian from Guangdong. Geological Publishing House, Beijing, 166 pp. [in Chinese].

Huang TK. 1932. Late Permian brachiopoda of southwestern China, Part 1. Palaeontologia Sinica, Series B, 9: 1–138.

Huang TK. 1933. Late Permian brachiopoda of southwestern China, Part 2. Palaeontologia Sinica, Series B, 9: 1–172.

Jin YG, Hu SZ. 1978. Brachiopods of the Kuhfeng Formation in South Anhui and Nanking Hills. Acta Palaeontologica Sinica, 17: 101–127. [in Chinese].

Jin YG, Ye SL. 1979. Brachiopoda, p. 60–217. In: Nanjing Institute of Geology and Palaeontology and Geological Institute of Qinghai Province (Ed.). Paleontological Atlas of northwest China-Qinghai. Volumn 1. Geological Publishing House, Beijing. [in Chinese].

Jin YG, Sun DL. 1981. Palaeozoic brachiopods from Xizang, p. 127–176, pls. 1–12. In: Nanjing Institute of Geology and Palaeontology (Ed.), Palaeontology of Xizang, Book 3 (The series of the Scientific Expedition to the Qinghai–Xizang Plateau). Science Press, Beijing. [In Chinese with English abstract].

Jin YG, Liao ZT, Fang BX. 1974. Brachiopoda (Permian), p. 308–314. In: Nanjing Institute of Geology and Palaeontology (Ed.), A handbook of the Stratigraphy and Palaeontology in Southwest China. Science Press, Beijing. [in Chinese].

Jin YG, Wang Y, Sun DL. 1985. Late Paleozoic and Triassic brachiopods from the East of the Qinghai–Xizang Plateau, p. 182–249, pls. 1–20. In: Nanjing Institute of Geology and Palaeontology, Academia Sinica and Regional Geological Surveying Team, Sichuan Province (Eds), Stratigraphy and Palaeontology in W. Sichuan and E. Xizang, China, Part 3. Sichuan Science and Technology Press, Chengdu. [In Chinese with English abstract]

Kayser E. 1883. Obercarbonische Fauna von Loping, p. 160–208. In: von Richthofen F (Ed.), China. Band 4. D. Reimer, Berlin.

King RH. 1930–1931. The geology of the Glass Mountain, Texas, Part 2: Faunal summary and correlation of the Permian formations with descriptions of brachiopods. University of Texas Bulletin, 3042: 1–245.

King RH. 1938. New Chonetidae and Productidae from Pennsylvanian and Permian strata of North-Central Texas. Journal of Paleontolog, 12: 257–279.

King W. 1850. A monograph of the Permian fossils of England. Palaeontographical Society, Monography, 3: 1–258.

Kuhn O. 1949. Lehrbuch der Paläozoologie. E. Schweizerbart'sche Verlagsbuchhandlung, Stuttgart, 326 pp.

Léveillé C. 1835. Aperçu géologique de quelques localités très riches en coquilles sur les frontières de France et de Belgique. Mémoire de la Société Géologique de la France, 2: 29–40.

Li L, Gu F, Su YZ. 1980. Brachiopoda, p. 327–428. In: Shenyang Institute of Geology and Mineral Resources (Ed.), Palaeontological Atlas of Northeast China 1, Paleozoic Volume. Geological Publishing House, Beijing. [in Chinese].

Li WZ, Shen SZ. 2008. Lopingian (Late Permian) brachiopods around the Wuchiapingian–Changhsingian boundary at the Meishan sections C and D, Changxing, South China. Geobios, 41: 307–320.

Li ZS, Zhan LP, Zhu XF, Zhang JH, Huang HQ, Xu DY, Yan Z, Li HM. 1989. Study on the Permian–Triassic biostratigraphy and event stratigraphy of northern Sichuan and southern Shaanxi. Geological Publishing House, Beijing, 435 pp. [in Chinese].

Li WZ, Shi GR, Yarinpil A, He WH, Shen SZ. 2012. *Cancrinella* and *Costatumulus* (Brachiopoda) from the Permian of South Monglia and South China: Their morphology, biostratigraphy and distribution. Geobios, 45: 297–309.

Liang WP. 1990. Lengwu Formation of Permian and its brachiopod fauna in Zhejiang Province. Geological Publishing House, Beijing, 435 pp. [in Chinese].

Liao ZT. 1979a. Brachiopod Assemblage Zone of Changhsing Stage and brachiopods from Permo–Triassic Boundary Beds in China. Acta Stratigraphica Sinica, 3: 200–208. [in Chinese].

Liao ZT. 1979b. Uppermost Carboniferous brachiopods from western Guizhou. Acta Palaeontologica Sinica, 18: 527–546. [in Chinese with English abstract].

Liao ZT. 1980a. Upper Permian Brachiopods from western Guizhou, p. 241–277. In: Nanjing Institute of Geology and Paleontology (Ed.), Stratigraphy and Palaeontology of Upper Permian Coal-Bearing Formations in western Guizhou and eastern Yunnan, China. Science Press, Beijing. [in Chinese].

Liao ZT. 1980b. Brachiopod assemblages from the Upper Permian and Permian–Triassic boundary beds, South China. Canadian Journal of Earth Sciences, 17: 289–295.

Liao ZT. 1983. Two new genera of Brachiopoda from the Heshan Formation (Upper Permian) of Guangxi. Acta Palaeontologica Sinica, 22: 637–641. [in Chinese with English abstract].

Liao ZT. 1984. New genus and species of Late Permian and earliest Triassic brachiopods from Jiangsu, Zhejiang and Anhui Provinces. Acta of Palaeontologica Sinica, 23: 276–285. [in Chinese with English abstract].

Liao ZT. 1987. Paleoecological characters and stratigraphic significance of silified brachiopods of the Upper Permian from Heshan, Laibin, Guangxi, p. 81–125. In: Nanjing Institute of Geology and Paleontology (Ed.), Stratigraphy and Palaeontology of Systemic Boundares in China Perman and Triassic Boundary (1). Nanjing University Press, Nanjing. [in Chinese].

Liao ZT, Meng FY. 1986. Late Changhsingian brachiopods from Huatang of Chen Xian County, southern Hunan. Memoir of Nanjing Institution of Geology and Palaeontology, Academia Sinica, 22: 71–94. [in Chinese with English abstract].

Licharew BK. 1956. Nadsemeistvo Rhynchonellacea Gray, 1848, p. 56–61. In: Kiparisova LD, Markowskii BP, Radchenko GP (Eds), Materialy po Paleontologii, Novye Semeistva I Rody. Volume 12. Vsesoiuznyi Nauchnolssledovatel'skii Geologicheskii Institut (VSEGEI), Materialy (Paleontologiia).

McCoy F. 1844. A Synopsis of the Character of the Carboniferous Fossils of Ireland. University Press, Dobin, 207 pp.

McCoy F. 1855. Systematic descriptions of the British Palaeozoic fossils in the Geological Museum of the University of Cambridge, London, 3: 407–661.

Menke CT. 1828. Synopsis methodica molluscorum generum omnium et specierum earum quae in Museo Menkeano adservantur. G. Uslar. Pyrmonti, 91 pp.

Mergl M. 2006. A review of Silurian discinoid brachiopods from historical British localities. Bulletin of Geosciences, 81: 215–236.

Miloradovich BV. 1936. Nizhnepermskaia fauna ostrova Mezhdusharskogo (Iuzhnyi Ostrov Novoy Zemli). Transactions of the Arctic Institute, 37: 37–82.

Moore RC. 1952. Brachiopod, p. 197–267. In: Moore RC, Lalicker CG, Fischer AG (Eds), Invertebrate fossils. McGraw-Hill, New York.

Muir-Wood HM. 1955. A history of the classification of the phylum Brachiopoda. British Museum, Natural History, London, 124 pp.

Muir-Wood HM. 1962. On the morphology and classification of the brachiopod suborder Chonetoidea. British Museum, National History, London, 132 pp.

Muir-Wood HM, Cooper GA. 1960. Morphology, classification and life habits of the Productoidea (Brachiopoda). Geological Society of America Memoir, 81: 1–447.

Oehlert DP. 1890. Note sur différents groupes établis dans le genre Orthis et en particulier sur *Rhipidomella* Oehlert (= *Rhipidomys* Oehlert, olim). Journal de Conchyliologie, 30: 366–374.

Ozaki KE. 1931. Upper Carboniferous brachiopods from North China. Shanghai Science Institute Bulletin, 1: 1–205.

Paeckelmann W. 1930. Die fauna des deutschen Untercarbons. Die Brachiopoden, I: die Orthiden, Strophomeniden und Choneten des mittleren und oberen Unterkarbons. Königliche-Preussische Geologische Landesanstalt, Abhandlungen (new series), 122: 143–326.

Peng YQ, Shi GR. 2008. New Early Triassic Lingulidae (Brachiopoda) genera and species from South China. Alcheringa, 32: 149–170.

Posenato R, Holmer LE, Prinoth H. 2014. Adaptive stratigies and environmental significance of lingulid brachiopods across the late Permian extinction. Palaeogeography, Palaeoclimatology, Palaeoecology, 399: 373–384.

Reed FRC. 1944. Brachiopoda and Mollusca from the Productus limestones of the Salt Range. Memoirs of Geological Survey of India, Palaeontologia Indica, 23: 1–678.

Rong JY, Jin YG, Shen SZ, Zhan RB. 2017. Phanerozoic Brachiopod Genera of China. Science Press, Beijing, 1096 pp.

Sarytcheva TG. 1937. Nizhnekamennougol'nye produktidy podmoskovnogo basseina (Rody Striatifera, Linoproductus I Cancrinella). Akademiia Nauk SSSR, Paleozoologicheskii Institute, Trudy (Moscow), 6: 7–123 [in Russian].

Sarytcheva TG, Sokolskaya AN. 1959. O Klassificatsin lozhnoporistykh brachiopod. Akademiia Nauk SSSR, Doklady (Moscow), 125: 181–184 [in Russian].

Sarytcheva TG, Sokolskaya AN, Beznosova GA, Maksimova SV. 1963. Brakhiopody i paleografiia Karbona Kuznetskoi kotloviny. Akademiia Nauk SSSR, Paleontologicheskii Institut, Trudy (Moscow), 95: 1–547 [in Russian].

Schellwien E. 1900. Beiträge zur Systematik der Strophomeniden des oberen Paläozoicum. Neues Jahrbuch für Mineralogie, Geologie und Paläontologie, 1: 1–15.

von Schlotheim EF. 1816. Beitrage zur Naturgeschichte der Versteinerungen in geognostischer Hinsicht. Akademi Wissenschaften Munchen Mathematischephysike Klasse Denkschriften, 6: 13–36.

Schuchert C. 1913. Class Brachiopoda, p. 290–449. In: The Lower Devonian deposits of Maryland. Maryland Geological Survey, Baltimore.

Schuchert C, Levene CM. 1929. Brachiopoda (Generum et Genotyporum Index et Bibliographia), p. 1–140. In: Pompeckj JF (Ed.), Fossilium Catalogus. I: Animalia. Part 42, W. Junk, Berlin.

Schuchert C, Cooper GA. 1931. Synopsis of the brachiopod genera of the suborders Orthoidea and Pentameroidea, with notes on the Telotremata. American Journal of Science (series 5), 22: 241–255.

Schuchert C, Cooper GA. 1932. Brachiopod genera of the suborders Orthoidea and Pentameroidea. Memoirs of the Peabody Museum of Natural History, 4: 1–270.

Shen SZ, He XL. 1994. Changhsingian brachiopod fauna from Guiding, Guizhou. Acta Palaeontologica Sinica, 33: 440–454. [in Chinese with English abstract].

Shen SZ, Archbold NW. 2002. Chonetoidea (Brachiopoda) from the Lopingian (Late Permian) of South China. Alcheringa, 25: 327–349.

Shen SZ, Shi GR. 2007. Lopingian (Late Permian) brachiopods from South China, Part 1, Orthotetida, Orthida and Rhynchonellida. Bulletin of the Tohoku University Museum, 6: 1–102.

Shen SZ, Shi GR. 2009. Latest Guadalupian brachiopods from the Guadalupian/Lopingian boundary GSSP section at Penglaitan in Laibin, Guangxi, South China and implications for the timing of the pre-Lopingian crisis. Palaeoworld, 18: 152–161.

Shen SZ, Archbold NW, Shi GR, Chen ZQ. 2000. Permian brachioipods from the Selong Xishan Section, Xizang (Tibet), China, Part 1, Stratigraphy, Strophomenida, Productida and Rhynchonellida. Geobios, 33: 725–752.

Shen SZ, Archbold NW, Shi GR. 2001. A Lopingian (Late Permian) brachiopod fauna from the Qubuerga Formation at Shengmi in the Mount Qomolangma Region of southern Xizang (Tibet), China. Journal of Paleontology, 75: 274–283.

Shen SZ, Shi GR, Fang ZJ. 2002. Permian brachiopods from the Baoshan and Simao Blocks in western Yunnan, China. Journal of Asian Earth Sciences, 20: 665–682.

Shi GR, Waterhouse JB. 1996. Lower Permian brachiopods and mollusks from the upper Jungle Creek Formation, northern Yukon, Canada. Geological Survey of Canada Bulletin, 424: 119–123.

Shi GR, Shen SZ. 1998. A Changhsingian (Late Permian) brachiopod fauna from Son La, northwest Vietnam. Journal of Asian Earth Sciences, 16: 501–511.

Shimizu D. 1961. Brachiopod fossils from the Upper Permian Gujo Formation of the Maizuru Group, Kyoto Prefecture, Japan. Kyoto University, College of Science, Geology and Mineralogy, Memoirs, Series B, 28: 243–254.

Sowerby J. 1818–1821. The mineral conchology of Great Britain. W. Ardling, London, 184 pp.

Stehli FG. 1954. Lower Leonardian brachiopoda of the Sierra Diablo. Bulletin of the American Museum of National History, 105: 257–358.

Swofford L. 2002, PAUP: phylogenetic analysis using parsimony (and other methods), 4.0 beta 10, programme and documentation, Sunderland, Massachusetts, Sinauer Associates, 140 pp.

Tazawa J. 1976. The Permian of Kesennuma, Kitakami Mountains: A preliminary report. Earth Science, Journal of the Association for Geological Collaboration in Japan, 30: 175–185.

Tazawa J. 2002. Late Paleozoic brachiopod faunas of the South Kitakami Belt, northeast Japan, and their paleobiogeographic and tectonic implications. The Island Arc, 11: 287–301.

Thomas I. 1910. The British Carboniferous Orthotetinae. Great Britain Geological Survey Memoir, 1: 83–134.

Tian BL. 1981. Fossil Atlas of Wangjiazhai Coal Field, Shuicheng County, Guizhou Province. Geological Publishing House, Beijing, 98 pp. [in Chinese].

Tong ZX. 1978. Brachiopoda, p. 210–267. In: Geological Institute of Southwest China (Ed.), Paleontological Atlas of Southwest China, Sichuan. Volume 2, Geological Publishing House, Beijing. [in Chinese].

Tschernyschew TN. 1902. Verkhnekamennougol'nye brakhiopody Urala i Timana [Upper Carboniferous brachiopods of the Urals and the Timann]. Trudy Geologicheskogo Komiteta, 16: 1–749. [In Russian].

Ustritsky VI, Tschernjak GE. 1963. Biostratigrafia I brakhiopody verkhnego Paleozoia Taimyra. Nauchno-Issledovatel'skii Institut Geologii Arktiki (NIIGA), Trudy (Moscow), 134: 1–139 [in Russian].

Waagen W. 1882–85. Salt Range Fossils I. *Productus* Limestone Fossils. Palaeontologia Indica, Series 13, 4: 329–728.

Wang CW, Yang SP. 1998. Study on Late Carboniferous–Early Permian brachiopod fauna in central Xinqiang and biostratigraphy. Geological Publishing House, Beijing, 156 pp. [in Chinese].

Wang GP, Liu QZ, Jin YG, Hu SZ, Liang WP, Liao ZT. 1982. Brachiopoda, p. 186–256. In: Nanjing Institution of Geology and Mineral Resources (Ed.), Paleontological atlas of southeast China, Late Paleozoic 2. Geological Publishing House, Beijing. [in Chinese].

Wang SM. 1984. Brachiopoda, p. 128–236. In: Regional Geological Surveying Team of Hubei (Ed.), Palaeontological Atlas of Hubei Province, Hubei Science and Technology Press, Wuhan. [in Chinese].

Wang Y. 1955a. Phylum Brachiopoda, p. 109–171. In: Index Fossils of China (Invertebratea), Book 2. Science Press, Beijing. [in Chinese].

Wang Y. 1955b. New genera of brachiopods. Acta Palaeontologica Sinica, 4: 327–357. [in Chinese].

Wang Y. 1956. New species of brachiopods (II). Acta Palaeontologica Sinica, 4: 387–407. [in Chinese].

Wang Y, Jin YG, Fang DW. 1964. Brachiopod fossils of China. Science Press, Beijing, 777 pp. [in Chinese].

Wang Y, Jin YG, Fang DW. 1966. Fossil Brachiopoda. Scientific Press, Beijing, 373 pp. [in Chinese].

Waterhouse JB. 1964. Permian brachiopods of New Zealand. New Zealand Geological Survey, Paleontological Bulletin, 35: 1–285.

Waterhouse JB. 1967. A new species of *Attenuatella* (Brachiopoda) from Permian beds near Drake, New South Wales. Records of Australian Museum, 27: 167–173.

Waterhouse JB. 1968a. Redescription of the Permian brachiopod *Anidanthus springsurensis* Booker. Transactions of the Society of New Zealand Geology, 5: 235–243.

Waterhouse JB. 1968b. New species of *Megousia* Muir-Wood and Cooper and allied new genus from the Permian of Australia and North America. Journal of Paleontology, 42: 1171–1185.

Waterhouse JB. 1968c. The classification and descriptions of Permian Spiriferida (Brachiopoda) from New Zealand. Palaeontographica (A), 129: 1–94.

Waterhouse JB. 1975. New Permian and Triassic brachiopod taxa. Paper of Department of Geology of University of Queensland, 7: 1–23.

Waterhouse JB. 1981. Early Permian brachiopods from Ko Yao Noi and near Krabi, southern Thailand, p. 47–213. In: Waterhouse JB, Pitakpaivan K, Mantajit N (Eds), The Permian Stratigraphy and Palaeontology of southern Thailand. Geological Survey Division Department of Mineral Resources, Bangkok.

Waterhouse JB. 1983a. New Permian invertebrate genera from East Australian segment of Gondwana. Bulletin of the Indian Geologists' Association, 16: 153–158.

Waterhouse JB. 1983b. Permian brachiopods from Pija Member, Senja Formation in Manang district of Nepal, with new brachiopod genera and species from other regions. Bulletin of the Indian Geologists' Association, 16: 111–151.

Waterhouse JB. 1983c. A Late Permian lyttoniid fauna from northwest Thailand. Paper of Department of Geology of University of Queensland, 10: 111–153.

Waterhouse JB. 1986. New late Paleozoic invertebrate taxa. Bulletin of the Indian Geologists' Association, 19: 1–8.

Waterhouse JB, Piyasin S. 1970. Mid-Permian brachiopods from Khao Phrik, Thailand. Palaeontographica (Abt. A), 135: 83–197.

Waterhouse JB, Briggs DJC, Parfrey SM. 1983. Major fauna assemblages in the Early Permian Tiverton Formation nearly Homevale Homestead, northern Bowen basin, Queensland, p. 121–138. In: Foster CB (Ed.), Permian Geology of Queensland. Geological Society of Australia, Brisbane.

White CA. 1862. Description of new species of fossils from the Devonian and Carboniferous rocks of the Mississippi Valley. Boston Society of Natural History Proceedings, 9: 8–33.

White CA, St John O. 1867. Descriptions of new Subcarboniferous and coal measure fossils, collected upon the Geological Survey of Iowa together with a notice of new generic characters involved in two species of brachiopods. Chicago Academy of Science, Transactions, 1: 115–127.

Whitehouse FW. 1928. Notes on upper Paleozoic marine horizons in eastern and western Australia. Australian Association for the Advancement of Science. Report, 18: 281–283.

Willard B. 1928. The brachiopods of the Ottosee and Holston formations of Tennessee and Virginia. Bulletin of the Harvard Museum of Comparative Zoology, 68: 255–292.

Williams A. 1953. The classification of the strophomenoid brachiopods. Washington Academy of Sciences Journal, 43: 1–13.

Williams A, Carlson SJ, Brunton CHC, Holmer LE, Popov LE, Mergl M, Laurie JR, Bassett MG, Cocks LRM, Rong JY, Lazarev SS, Grant RE, Racheboeuf PR, Jin YG, Wardlaw BR, Harper DAT, Wright AD, Rubel M. 2000. Linguliformea, Craniiforemea, and Rhynchonelliformea (part), p. 350–688, 714–846. In: Williams A et al. (Eds), Treatise on Invertebrate Paleontology, Part H, Brachiopoda (revised) 2, 3, Linguliformea, Craniiforemea, and Rhynchonelliformea (part). The Geological Society of America, and the University of Kansas, Lawrence.

Williams A, Brunton CHC, Carlson SJ, Alvarez F, Blodgett RB, Boucot AJ, Copper P, Dagys AS, Grant RE, Jin YG, MacKinnon DI, MancenÑido MO, Owen EF, Rong JY, Savage NM, Sun DL. 2002. Rhynchonelliformea (part), p. 1027–1376, 1496–1583. In: Williams A et al. (Eds), Treatise on Invertebrate Paleontology, Part H, Brachiopoda (revised) 4, Rhynchonelliformea (part). The Geological Society of America, and the University of Kansas, Lawrence.

Williams A, Brunton CHC, Carlson SJ, Baker PG, Carter JL, Curry GB, Dagys AS, Gourvennec R, Hou HF, Jin YG, Johnson JG, Lee DE, MacKinnon DI, Racheboeuf PR, Smirnova TN, Sun DL. 2006. Rhynchonelliformea (part), p. 1689–1937. In: Williams A et al. (Eds), Treatise on Invertebrate Paleontology,

Part H, Brachiopoda (revised) 5, Rhynchonelliformea (part). Geological Society of America and University of Kansas, Boulder and Lawrence.

Wongwanich T, Boucot AJ, Brunton CHC, House MR, Racheboeuf PR. 2004. Namurian fossils (brachiopods, goniatites) from Satun Province, Southern Thailand. Journal of Paleontology, 78: 1072–1085.

Wu HT, Shi GR, He WH. 2017. A quantitative taxonomic review of *Fusichonetes* and *Tethyochonetes* (Chonetidina, Brachiopoda). Journal of Paleontology, 91: 1296–1305.

Xu GR, Grant RE. 1994. Brachiopods near the Permian–Triassic boundary in south China. Smithsonian Contributions to paleobiology, 76: 1–68.

Yanagida J. 1988. Biostratigraphic study of Paleozoic and Mesozoic groups in central and northern Thailand, An Interim Report. Kyushu University, Kyushu, 47 pp.

Yang DL, Ni SZ, Chang ML, Chao RX. 1977. Brachiopoda, p. 303–470. In: Hubei Institution of Geological Science and others (Eds), Paleontological atlas of central South China 2. Geological Publishing House, Beijing. [in Chinese].

Yang ZY, Xu GR. 1966. Triassic brachiopods of central Guizhou Province, China. Geological Publishing House, Beijing, 151 pp. [in Chinese].

Yang ZY, Ding PZ, Yin HF, Zhang SX, Fan JS. 1962. The brachiopod fauna of Carboniferous, Permian, and Triassic in the Chilianshan region. Monograph on the geology of the Chilianshan Mountains 4(4). Science Press, Beijing, 134 pp. [in Chinese].

Yang ZY, Yin HF, Wu SB, Yang FQ, Ding MH, Xu GR. 1987. Permian–Triassic boundary stratigraphy and fauna of South China. Geological Publishing House, Beijing, 378 pp. [in Chinese with English abstract].

Zavodowsky VM. 1960. Novye vidy permskikh brachiopod basseina Kolymy i Ohhotskogo poberazh'ya. Materialy po Geologii Poleznym Iskopaemym Severo-Vostoka SSSR, 14: 61–73.

Zavodowsky VM. 1971. Brachiopoda, p. 70–182. In: Kulikov MV (Ed.), Field Atlas of the Permian fauna and flora of Northeast of USSR. Izd-Vo Magadan Kn.

Zeng Y, He XL, Zhu ML. 1995. Brachiopod communities and their succession and replacement in the Permian of Huayingshan Area. China University of Mining and Technology Press, Xuzhou, 187 pp. [in Chinese with English summary].

Zhan LP, Li L. 1962. Early Permian brachiopods from the Maokou Suite of the eastern Qinling Mountain. Acta Palaeontologica Sinica, 10: 472–483. [in Chinese].

Zhang Y, Jin YG. 1961. An Upper Permian brachiopoda fauna from Jingxian, Anhui Province. Acta Palaeontologica Sinica, 9: 401–417. [in Chinese with English abstract].

Zhang Y, He WH. 2009. Brachiopod fauna of Duanshan Section in Guizhou Province, and its geological significance. Geological Science and Technology Information, 28: 15–37. [in Chinese with English abstract].

Zhang Y, He WH, Shi GR, Zhang KX. 2013. A new Changhsingian (Late Permian) Rugosochonetidae (Brachiopoda) fauna from the Zhongzhai section, southwestern Guizhou Province, South China. Alcheringa, 37: 223–247.

Zhang Y, Shi GR, He WH, Zhang KX, Wu HT. 2014. A new Changhsingian (Late Permian) brachiopod fauna from the Zhongzhai section (South China), Part 2: Lingulida, Orthida, Orthotetida and Spiriferida. Alcheringa, 38: 480–503.

Zhang Y, He WH, Shi GR, Zhang KX, Wu HT. 2015. A new Changhsingian (Late Permian) brachiopod fauna from the Zhongzhai section (South China) Part 3: Productida. Alcheringa, 39: 295–314.

Zhao JK, Sheng JZ, Yao ZQ, Liang XL, Chen CZ, Rui L, Liao ZT. 1981. The Changhsingian and the Permian–Triassic Boundary in South China. Nanjing Institute of Geology and Palaeontology, Bulletin, 2: 1–112. [in Chinese with English abstract].

Zhao RX, Tan ZX. 1984. Lower Permian brachiopods from Sangzhi, Hunan. Acta Palaeontologica Sinica, 23: 20–31. [in Chinese with English abstract].

Zhu T. 1990. The Permian coal-bearing strata and palaeobiocoenosis of Fujian. Geological Publishing House, Beijing, 127 pp. [in Chinese].

Appendices

Appendix 1: Index and Occurrence Information for All Fossils Illustrated in the Book

The materials published elsewhere are noted here with the original figure number(s) in the reference in the column of "Source of Materials". We have obtained copyright permission from the relevant publishers for the reuse of these published materials, as detailed below:

1. He WH, Shen SZ, Feng QL, Gu SZ. 2005. A late Changxingian (Late Permian) deep-water brachiopod fauna from the Talung Formation at the Dongpan Section, Southern Guangxi, in South China. Journal of Paleontology, 79 (5), figures 3–5 (reprinted by permission of Cambridge University Press).
2. He WH, Shi GR., Feng QL., Peng YQ. 2007. Discovery of late Changhsingian (latest Permian) brachiopod *Attenuatella* species from South China. Alcheringa, 31, figure 5 (reprinted by permission of Taylor and Francis Ltd, www.tandfonline.com).
3. He WH, Shi GR, Zhang Y, Yang TL, Teng F, Wu SB. 2012. Systematics and palaeoecology of Changhsingian (Late Permian) Ambocoeliidae brachiopods from South China and implications for the end-Permian mass extinction. Alcheringa, 36, figures 3–7 (reprinted by permission of Taylor and Francis Ltd, www.tandfonline.com).
4. He WH, Shi GR, Zhang Y, Yang TL, Zhang KX, Wu SB, Niu ZJ, Zhang ZY. 2014. Changhsingian (latest Permian) deep-water brachiopod fauna from South China. Journal of Systematic Palaeontology, 12 (8), figures 4, 6–9, 11, 13, 14, 16, 17, 19, 21, 22 (reprinted by permission of Cambridge University Press).
5. Wu HT, He WH, Zhang Y, Yang TL, Xiao YF, Chen B, Weldon EA. 2016. Palaeobiogeographic distribution patterns and processes of Neochonetes and Fusichonetes (Brachiopoda) in the late Palaeozoic and earliest Mesozoic. Palaeoworld, 25, figure 1. (reprinted by permission of Elseier).
6. Wu HT, Shi GR, He WH. 2017. A quantitative taxonomic review of *Fusichonetes* and *Tethyochonetes* (Chonetidina, Brachiopoda). Journal of Paleontology, 91 (6), figure 3 (reprinted by permission of Cambridge University Press).
7. Zhang Y, He WH, Shi GR, Zhang KX. 2013. A new Changhsingian (Late Permian) Rugosochonetidae (Brachiopoda) fauna from the Zhongzhai section, southwestern Guizhou Province, South China. Alcheringa, 37, figures 5, 9, 11. 12, 14 (reprinted by permission of Taylor and Francis Ltd, www.tandfonline.com).
8. Zhang Y, Shi GR, He WH, Zhang KX, Wu HT. 2014. A new Changhsingian (Late Permian) brachiopod fauna from the Zhongzhai section (South China), Part 2: Lingulida, Orthida, Orthotetida and Spiriferida. Alcheringa, 38, figures 4, 5, 7, 9, 10 (reprinted by permission of Taylor and Francis Ltd, www.tandfonline.com).
9. Zhang Y, He WH, Shi GR, Zhang KX, Wu HT. 2015. A new Changhsingian (Late Permian) brachiopod fauna from the Zhongzhai section (South China) Part 3: Productida. Alcheringa, 39, figures 4, 6–8 (reprinted by permission of Taylor and Francis Ltd, www.tandfonline.com).

W.-H. He et al. (eds.), *Brachiopods around the Permian-Triassic Boundary of South China*, New Records of the Great Dying in South China, https://doi.org/10.1007/978-981-13-1041-6

Fossil name in the book	Registered number	Page and figure numbers in the book	Source of Materials	Occurences	Others
Costatumulus dongpanensis	DP806	Fig. 9.1a	Fig. 4.3; He et al. (2005)	Bed 8; *Pseudotirolites–Rotodiscoceras* Z	
Costatumulus dongpanensis	PB-2-293	Fig. 9.1b	Fig. 19Q; He et al. (2014)	Bed 2; *Pseudotirolites–Rotodiscoceras* Z	
Costatumulus dongpanensis	DP715	Fig. 9.1c	Fig. 4.2; He et al. (2005)	Bed 7; *Pseudotirolites–Rotodiscoceras* Z	Paratype
Costatumulus dongpanensis	DP716	Fig. 9.1d	Fig. 4.5; He et al. (2005)	Bed 7; *Pseudotirolites–Rotodiscoceras* Z	
Costatumulus dongpanensis	DP-9-291	Fig. 9.1e	Fig. 19P; He et al. (2014)	Bed 9; *Pseudotirolites–Rotodiscoceras* Z	
Costatumulus dongpanensis	DP-10-290	Fig. 9.1f	Fig. 19O; He et al. (2014)	Bed 10; *Pseudotirolites–Rotodiscoceras* Z	
Costatumulus dongpanensis	DS-1-602	Fig. 9.1g	Fig. 19N; He et al. (2014)	Bed 1; *Pseudotirolites–Rotodiscoceras* Z	
Costatumulus dongpanensis	DP-9-283	Fig. 9.1h	Fig. 19H; He et al. (2014)	Bed 9; *Pseudotirolites–Rotodiscoceras* Z	
Costatumulus dongpanensis	DP-7-286	Fig. 9.1i	Fig. 19K; He et al. (2014)	Bed 7; *Pseudotirolites–Rotodiscoceras* Z	
Costatumulus dongpanensis	DP-7-281	Fig. 9.1j	Fig. 19G; He et al. (2014)	Bed 7; *Pseudotirolites–Rotodiscoceras* Z	
Costatumulus dongpanensis	DP-7-287	Fig. 9.1k	Fig. 19L; He et al. (2014)	Bed 7; *Pseudotirolites–Rotodiscoceras* Z	
Costatumulus dongpanensis	DP2-0013	Fig. 9.1l	In this book	Bed 2; *Pseudotirolites–Rotodiscoceras* Z	
Costatumulus dongpanensis	DP-7-288	Fig. 9.2a	Fig. 19M; He et al. (2014)	Bed 7; *Pseudotirolites–Rotodiscoceras* Z	
Costatumulus dongpanensis	DP710	Fig. 9.2b	Fig. 3.16; He et al. (2005)	Bed 7; *Pseudotirolites–Rotodiscoceras* Z	
Costatumulus dongpanensis	DP711	Fig. 9.2c	Fig. 3.19; He et al. (2005)	Bed 7; *Pseudotirolites–Rotodiscoceras* Z	
Costatumulus dongpanensis	DP803	Fig. 9.2d	Fig. 3.17; He et al. (2005)	Bed 8; *Pseudotirolites–Rotodiscoceras* Z	
Costatumulus dongpanensis	DP9-0035	Fig. 9.2e	In this book	Bed 9; *Pseudotirolites–Rotodiscoceras* Z	
Costatumulus dongpanensis	DP10-0037	Fig. 9.2f	In this book	Bed 10; *Pseudotirolites–Rotodiscoceras* Z	
Costatumulus dongpanensis	DP9-0014	Fig. 9.2g	In this book	Bed 9; *Pseudotirolites–Rotodiscoceras* Z	
Costatumulus dongpanensis	DP5-0028	Fig. 9.2h	In this book	Bed 5; *Pseudotirolites–Rotodiscoceras* Z	
Costatumulus dongpanensis	DP9-0010	Fig. 9.2i	In this book	Bed 9; *Pseudotirolites–Rotodiscoceras* Z	
Costatumulus dongpanensis	DP2-0025	Fig. 9.2j	In this book	Bed 2; *Pseudotirolites–Rotodiscoceras* Z	
Costatumulus dongpanensis	DP7-0026	Fig. 9.2k	In this book	Bed 7; *Pseudotirolites–Rotodiscoceras* Z	
Costatumulus dongpanensis	DP10-0042	Fig. 9.2l	In this book	Bed 10; *Pseudotirolites–Rotodiscoceras* Z	
Costatumulus dongpanensis	DP3-0033	Fig. 9.2m	In this book	Bed 3; *Pseudotirolites–Rotodiscoceras* Z	
Costatumulus dongpanensis	DP3-0034	Fig. 9.2n	In this book	Bed 3; *Pseudotirolites–Rotodiscoceras* Z	
Costatumulus dongpanensis	DP10-0007	Fig. 9.3a	In this book	Bed 10; *Pseudotirolites–Rotodiscoceras* Z	
Costatumulus dongpanensis	DP-10-290	Fig. 9.3b	In this book	Bed 10; *Pseudotirolites–Rotodiscoceras* Z	
Costatumulus dongpanensis	DP8-0060	Fig. 9.3c	In this book	Bed 8; *Pseudotirolites–Rotodiscoceras* Z	
Costatumulus dongpanensis	DP9-0068	Fig. 9.3d	In this book	Bed 9; *Pseudotirolites–Rotodiscoceras* Z	
Costatumulus dongpanensis	DP9-0064	Fig. 9.3e	In this book	Bed 9; *Pseudotirolites–Rotodiscoceras* Z	
Costatumulus dongpanensis	DP10-0075	Fig. 9.3f	In this book	Bed 10; *Pseudotirolites–Rotodiscoceras* Z	

Costatumulus dongpanensis	DP9-0076	Fig. 9.3g	In this book	Bed 9; *Pseudotirolites–Rotodiscoceras* Z	
Costatumulus dongpanensis	DP10-0077	Fig. 9.3h	In this book	Bed 10; *Pseudotirolites–Rotodiscoceras* Z	
Costatumulus dongpanensis	DP9-0080	Fig. 9.3i	In this book	Bed 9; *Pseudotirolites–Rotodiscoceras* Z	
Costatumulus dongpanensis	DP8-0078	Fig. 9.3j	In this book	Bed 8; *Pseudotirolites–Rotodiscoceras* Z	
Anidanthus parvimucronata	DP707	Fig. 9.5a	Fig. 3.12; He et al. (2005)	Bed 7; *Pseudotirolites–Rotodiscoceras* Z	Holotype
Anidanthus parvimucronata	DP708	Fig. 9.5b	Fig. 3.14; He et al. (2005)	Bed 7; *Pseudotirolites–Rotodiscoceras* Z	
Anidanthus parvimucronata	DP702	Fig. 9.5c	Fig. 3.3; He et al. (2005)	Bed 7; *Pseudotirolites–Rotodiscoceras* Z	Paratype
Anidanthus parvimucronata	PB-5-278	Fig. 9.5d	Fig. 19A; He et al. (2014)	Bed 5; *Pseudotirolites–Rotodiscoceras* Z	
Anidanthus parvimucronata	DP-9-272	Fig. 9.5e	Fig. 17M; He et al. (2014)	Bed 9; *Pseudotirolites–Rotodiscoceras* Z	
Anidanthus parvimucronata	DP706	Fig. 9.5f	Fig. 3.9; He et al. (2005)	Bed 7; *Pseudotirolites–Rotodiscoceras* Z	
Anidanthus parvimucronata	DP-10-274	Fig. 9.5g	Fig. 17K; He et al. (2014)	Bed 10; *Pseudotirolites–Rotodiscoceras* Z	
Anidanthus parvimucronata	DP802	Fig. 9.5h	Fig. 3.11; He et al. (2005)	Bed 8; *Pseudotirolites–Rotodiscoceras* Z	Paratype
Anidanthus parvimucronata	PB-5-279	Fig. 9.5i	Fig. 17O; He et al. (2014)	Bed 5; *Pseudotirolites–Rotodiscoceras* Z	
Anidanthus parvimucronata	DP-9-275	Fig. 9.5j	Fig. 17N; He et al. (2014)	Bed 9; *Pseudotirolites–Rotodiscoceras* Z	
Anidanthus parvimucronata	PB-5-278	Fig. 9.5k	Fig. 17P; He et al. (2014)	Bed 5; *Pseudotirolites–Rotodiscoceras* Z	
Anidanthus subquadratus	DP7-0096	Fig. 9.5l	In this book	Bed 7; *Pseudotirolites–Rotodiscoceras* Z	
Anidanthus subquadratus	DP10-0098	Fig. 9.5m	In this book	Bed 10; *Pseudotirolites–Rotodiscoceras* Z	
Anidanthus subquadratus	DP8-0099	Fig. 9.5n	In this book	Bed 8; *Pseudotirolites–Rotodiscoceras* Z	
Anidanthus subquadratus (=?*Cathaysia* sp. of He et al. 2005)	DP719	Fig. 9.7a	Fig. 4.10; He et al. (2005)	Bed 7; *Pseudotirolites–Rotodiscoceras* Z	Paratype
Anidanthus subquadratus (=?*Cathaysia* sp. of He et al. 2005)	DP720	Fig. 9.7b	Fig. 4.12; He et al. (2005)	Bed 7; *Pseudotirolites–Rotodiscoceras* Z	
Anidanthus subquadratus	DP7-0494	Fig. 9.7c	In this book	Bed 7; *Pseudotirolites–Rotodiscoceras* Z	
Anidanthus subquadratus	LQ-0500	Fig. 9.7d	In this book	Bed 5; *Pseudotirolites–Rotodiscoceras* Z	
Anidanthus subquadratus	DP10-0504	Fig. 9.7e	In this book	Bed 10; *Pseudotirolites–Rotodiscoceras* Z	
Anidanthus subquadratus	LQ5-0501	Fig. 9.7f	In this book	Bed 5; *Pseudotirolites–Rotodiscoceras* Z	
Anidanthus subquadratus	DP10-0506	Fig. 9.7g	In this book	Bed 10; *Pseudotirolites–Rotodiscoceras* Z	
Anidanthus subquadratus	DP9-0511	Fig. 9.7h	In this book	Bed 9; *Pseudotirolites–Rotodiscoceras* Z	
Anidanthus subquadratus	DP9-0508	Fig. 9.7i	In this book	Bed 9; *Pseudotirolites–Rotodiscoceras* Z	Paratype
Anidanthus subquadratus (=?*Cathaysia* sp. of He et al. 2005)	DP9206	Fig. 9.7j	Fig. 4.9; He et al. (2005)	Bed 9; *Pseudotirolites–Rotodiscoceras* Z	
Anidanthus subquadratus	LQ-0497	Fig. 9.7k	In this book	Bed 5; *Pseudotirolites–Rotodiscoceras* Z	
Anidanthus subquadratus	DP9-0495	Fig. 9.7l	In this book	Bed 9; *Pseudotirolites–Rotodiscoceras* Z	

(continued)

Fossil name in the book	Registered number	Page and figure numbers in the book	Source of Materials	Occurences	Others
Anidanthus subquadratus	DP8-0496	Fig. 9.7m	In this book	Bed 8; *Pseudotirolites–Rotodiscoceras* Z	Paratype
Parapygmochonetes parvulus	CM-12-109	Fig. 9.9a	Fig. 11J; He et al. (2014)	Bed 12; *Pseudotirolites–Rotodiscoceras* Z	
Parapygmochonetes parvulus	CM-3-125	Fig. 9.9b	Fig. 11K; He et al. (2014)	Bed 3; *Tapashanites* Z	
Parapygmochonetes parvulus	CM-12-108	Fig. 9.9c	Fig. 11O; He et al. (2014)	Bed 12; *Pseudotirolites–Rotodiscoceras* Z	
Parapygmochonetes parvulus	CM-3-103	Fig. 9.9d	Fig. 11L; He et al. (2014)	Bed 3; *Tapashanites* Z	
Parapygmochonetes parvulus	CM-3-106	Fig. 9.9e	Fig. 11M; He et al. (2014)	Bed 3; *Tapashanites* Z	
Parapygmochonetes parvulus	CM-3-117	Fig. 9.9f	Fig. 13F; He et al. (2014)	Bed 3; *Tapashanites* Z	Holotype
Parapygmochonetes parvulus	CM-3-102	Fig. 9.9g	Fig. 11P; He et al. (2014)	Bed 3; *Tapashanites* Z	
Parapygmochonetes parvulus	CM-3-121	Fig. 9.9h	Fig. 11N; He et al. (2014)	Bed 3; *Tapashanites* Z	
Parapygmochonetes parvulus	CM-3-120	Fig. 9.9i	Fig. 13C; He et al. (2014)	Bed 3; *Tapashanites* Z	
Parapygmochonetes parvulus	CM-12-537	Fig. 9.9j	Fig. 13B; He et al. (2014)	Bed 12; *Pseudotirolites–Rotodiscoceras* Z	
Parapygmochonetes parvulus	CM-10-110	Fig. 9.9k	Fig. 13A; He et al. (2014)	Bed 10; *Pseudotirolites–Rotodiscoceras* Z	
Parapygmochonetes parvulus	CM-10-114	Fig. 9.10a	Fig. 13D; He et al. (2014)	Bed 10; *Pseudotirolites–Rotodiscoceras* Z	
Parapygmochonetes parvulus	CM-3-119	Fig. 9.10b	Fig. 13E; He et al. (2014)	Bed 3; *Tapashanites* Z	
Parapygmochonetes parvulus	CM-3-122	Fig. 9.10c	Fig. 13H; He et al. (2014)	Bed 3; *Tapashanites* Z	
Parapygmochonetes parvulus	CM-3-118	Fig. 9.10d	Fig. 13G; He et al. (2014)	Bed 3; *Tapashanites* Z	
Parapygmochonetes baoqingensis	CM-3-104	Fig. 9.10e	Fig. 13I; He et al. (2014)	Bed 3; *Tapashanites* Z	
Parapygmochonetes baoqingensis	CM-3-101	Fig. 9.10f	Fig. 13J; He et al. (2014)	Bed 3; *Tapashanites* Z	
Parapygmochonetes baoqingensis	CM-3-123	Fig. 9.10g	Fig. 13K; He et al. (2014)	Bed 3; *Tapashanites* Z	
Parapygmochonetes baoqingensis	CM-6-115	Fig. 9.10h	Fig. 13L; He et al. (2014)	Bed 6; *Tapashanites* Z	
Spinomarginifera kueichowensis	LZ2702639	Fig. 9.11a	Fig. 7A; Zhang et al. (2015)	Bed 27-2; *Fusichonetes pygmaea* Z	
Spinomarginifera kueichowensis	LZ2702639	Fig. 9.11b	Fig. 7C; Zhang et al. (2015)	Bed 27-2; *Fusichonetes pygmaea* Z	
Spinomarginifera kueichowensis	LZ2702631	Fig. 9.11c	Fig. 7H; Zhang et al. (2015)	Bed 27-2; *Fusichonetes pygmaea* Z	
Spinomarginifera kueichowensis	LZ2702488	Fig. 9.11d	Fig. 7G; Zhang et al. (2015)	Bed 27-2; *Fusichonetes pygmaea* Z	
Spinomarginifera kueichowensis (=*Spinomarginifera* cf. *sintanensis* of Zhang et al. 2015)	LZ1400341	Fig. 9.11e	Fig. 8G; Zhang et al. (2015)	Bed 14; *Fusichonetes pygmaea* Z	
Spinomarginifera kueichowensis	LZ2703524	Fig. 9.11f	Fig. 7K; Zhang et al. (2015)	Bed 27-3; *Fusichonetes pygmaea* Z	

Spinomarginifera kueichowensis (=*Spinomarginifera* cf. *sintanensis* of Zhang et al. 2015)	LZ1400369	Fig. 9.11g	Fig. 8A; Zhang et al. (2015)	Bed 14; *Fusichonetes pygmaea* Z	
Spinomarginifera kueichowensis	LZ2701490	Fig. 9.11h	Fig. 7I; Zhang et al. (2015)	Bed 27-1; *Fusichonetes pygmaea* Z	
Spinomarginifera kueichowensis (=*Spinomarginifera alpha* of Zhang et al. 2015)	LZ2704493	Fig. 9.11i	Fig. 7O; Zhang et al. (2015)	Bed 27-4; *Fusichonetes pygmaea* Z	
Spinomarginifera kueichowensis	LZ2702640	Fig. 9.11j	Fig. 7E; Zhang et al. (2015)	Bed 27-2; *Fusichonetes pygmaea* Z	
Spinomarginifera kueichowensis	LZ1400342	Fig. 9.11k	Fig. 7J; Zhang et al. (2015)	Bed 14; *Fusichonetes pygmaea* Z	
Rugivestis elegans (=*Dongpanoproductus elegans* of He et al. 2014)	DP-2-270	Fig. 9.12a	Fig. 17A; He et al. (2014)	Bed 2; *Pseudotirolites*–*Rotodiscoceras* Z	
Rugivestis elegans (=*Dongpanoproductus elegans* of He et al. 2014)	DP-3-271	Fig. 9.12b	Fig. 17B; He et al. (2014)	Bed 3; *Pseudotirolites*–*Rotodiscoceras* Z	
Rugivestis elegans (=*Dongpanoproductus elegans* He et al. 2005)	DP728	Fig. 9.12c	Fig. 5.5; He et al. (2005)	Bed 7; *Pseudotirolites*–*Rotodiscoceras* Z	
Rugivestis elegans (=*Dongpanoproductus elegans* He et al. 2005)	DP729	Fig. 9.12d	Fig. 5.7; He et al. (2005)	Bed 7; *Pseudotirolites*–*Rotodiscoceras* Z	
Rugivestis elegans (=*Dongpanoproductus elegans* He et al. 2005)	DP730	Fig. 9.12e	Fig. 5.8; He et al. (2005)	Bed 7; *Pseudotirolites*–*Rotodiscoceras* Z	Holotype
Rugivestis elegans (=*Dongpanoproductus elegans* He et al. 2005)	DP731	Fig. 9.12f	Fig. 5.10; He et al. (2005)	Bed 7; *Pseudotirolites*–*Rotodiscoceras* Z	
Rugivestis elegans (=*Dongpanoproductus elegans* He et al. 2005)	DP811	Fig. 9.12g	Fig. 5.1; He et al. (2005)	Bed 8; *Pseudotirolites*–*Rotodiscoceras* Z	Paratype
Rugivestis elegans (=*Dongpanoproductus elegans* He et al. 2005)	DP812	Fig. 9.12h	Fig. 5.3; He et al. (2005)	Bed 8; *Pseudotirolites*–*Rotodiscoceras* Z	
Rugivestis elegans (=*Dongpanoproductus elegans* He et al. 2005)	DP9601	Fig. 9.12i	Fig. 5.6; He et al. (2005)	Bed 9; *Pseudotirolites*–*Rotodiscoceras* Z	

(continued)

Fossil name in the book	Registered number	Page and figure numbers in the book	Source of Materials	Occurences	Others
Rugivestis elegans	DP10-0153	Fig. 9.12j	In this book	Bed 10; *Pseudotirolites–Rotodiscoceras* Z	
Rugivestis elegans	DP10-0162	Fig. 9.12k	In this book	Bed 10; *Pseudotirolites–Rotodiscoceras* Z	
Rugivestis elegans	DP2-0159	Fig. 9.12l	In this book	Bed 2; *Pseudotirolites–Rotodiscoceras* Z	
Rugivestis elegans	DP7-0156	Fig. 9.12m	In this book	Bed 7; *Pseudotirolites–Rotodiscoceras* Z	
Rugivestis elegans	DP2-0159	Fig. 9.12n	In this book	Bed 2; *Pseudotirolites–Rotodiscoceras* Z	
Rugivestis elegans	DP10-0173	Fig. 9.12o	In this book	Bed 10; *Pseudotirolites–Rotodiscoceras* Z	
Rugivestis elegans	DP9-0164	Fig. 9.12p	In this book	Bed 9; *Pseudotirolites–Rotodiscoceras* Z	
Rugivestis elegans	DP10-0171	Fig. 9.12q	In this book	Bed 10; *Pseudotirolites–Rotodiscoceras* Z	
Rugivestis elegans	DP10-0172	Fig. 9.12r	In this book	Bed 10; *Pseudotirolites–Rotodiscoceras* Z	
Paryphella transversa	DCB-34-231	Fig. 9.13a	Fig. 14I; He et al. (2014)	Bed 34; *Pseudotirolites* Z	
Paryphella transversa	CM-12-245	Fig. 9.13b	Fig. 14J; He et al. (2014)	Bed 12; *Pseudotirolites–Rotodiscoceras* Z	
Paryphella transversa	CM-13-228	Fig. 9.13c	Fig. 14K; He et al. (2014)	Bed 13; *Pseudotirolites–Rotodiscoceras* Z	
Paryphella transversa	CM-4-243	Fig. 9.13d	Fig. 14L; He et al. (2014)	Bed 4; *Tapashanites* Z	
Paryphella transversa	CM-4-248	Fig. 9.13e	Fig. 14M; He et al. (2014)	Bed 4; *Tapashanites* Z	
Paryphella transversa	CM-3-237	Fig. 9.13f	Fig. 14N; He et al. (2014)	Bed 3; *Tapashanites* Z	
Paryphella transversa	CM-3-241	Fig. 9.13g	Fig. 14O; He et al. (2014)	Bed 3; *Tapashanites* Z	
Paryphella transversa	CM-12-222	Fig. 9.13h	Fig. 14P; He et al. (2014)	Bed 12; *Pseudotirolites–Rotodiscoceras* Z	
Paryphella transversa	CM-12-223	Fig. 9.13i	Fig. 14Q; He et al. (2014)	Bed 12; *Pseudotirolites–Rotodiscoceras* Z	
Paryphella minuta	CM-20-196	Fig. 9.13j	Fig. 16U; He et al. (2014)	Bed 20; *Ophiceras* Z	
Paryphella minuta	CM-20-195	Fig. 9.13k	Fig. 16V; He et al. (2014)	Bed 20; *Ophiceras* Z	Holotype
Paryphella minuta	CM-18-200	Fig. 9.13l	Fig. 16W; He et al. (2014)	Bed 18; Uppermost Permian	
Paryphella minuta	CM-18-198	Fig. 9.13m	Fig. 16X; He et al. (2014)	Bed 18; Uppermost Permian	
Chonetella sp.	CM14-0517	Fig. 9.13n	In this book	Bed 14; *Pseudotirolites–Rotodiscoceras* Z	
Paryphella sinuata	CM-12-188	Fig. 9.15a	Fig. 14R; He et al. (2014)	Bed 12; *Pseudotirolites–Rotodiscoceras* Z	
Paryphella sinuata	CM-12-193	Fig. 9.15b	Fig. 14S; He et al. (2014)	Bed 12; *Pseudotirolites–Rotodiscoceras* Z	
Paryphella sinuata	CM-10-180	Fig. 9.15c	Fig. 14T; He et al. (2014)	Bed 10; *Pseudotirolites–Rotodiscoceras* Z	
Paryphella sinuata	CM-10-182	Fig. 9.15d	Fig. 14U; He et al. (2014)	Bed 10; *Pseudotirolites–Rotodiscoceras* Z	
Paryphella sinuata	CM-10-189	Fig. 9.15e	Fig. 14V; He et al. (2014)	Bed 10; *Pseudotirolites–Rotodiscoceras* Z	
Paryphella sinuata	DCB-36-190	Fig. 9.15f	Fig. 14W; He et al. (2014)	Bed 36; *Pseudotirolites* Z	
Paryphella sinuata	CM-15-226	Fig. 9.15g	Fig. 14X; He et al. (2014)	Bed 15; *Pseudotirolites–Rotodiscoceras* Z	
Paryphella sinuata	SR28-0350	Fig. 9.15h	In this book	Bed 28; *Ophiceras* Z	
Paryphella sinuata	SR22-0514	Fig. 9.15i	In this book	Bed 22; *Clarkina yini* Z	

Paryphella sinuata	HZS19-0515	Fig. 9.15j	In this book	Bed 19; *Clarkina meishanensis* Z	
Paryphella sinuata	HZS19-0516	Fig. 9.15k	In this book	Bed 19; *Clarkina meishanensis* Z	
Paryphella sinuata	XJP12-0519	Fig. 9.15l	In this book	Bed 12; Upper Permian	
Paryphella sinuata	HZS19-0522	Fig. 9.15m	In this book	Bed 19; *Clarkina meishanensis* Z	
Paryphella sinuata	DDS26-0520	Fig. 9.15n	In this book	Bed 26; *Hypophiceras* Z	
Paryphella sinuata	HZS19-0523	Fig. 9.15o	In this book	Bed 19; *Clarkina meishanensis* Z	
Paryphella orbicularis	DDS29-1-0532	Fig. 9.16a	In this book	Bed 29; *Ophiceras* Z	
Paryphella orbicularis	DDS29-0541	Fig. 9.16b	In this book	Bed 29; *Ophiceras* Z	
Paryphella orbicularis	DDS27-2-0545	Fig. 9.16c	In this book	Bed 27; *Hindeodus parvus* Z	
Paryphella orbicularis	DDS27-2-0533	Fig. 9.16d	In this book	Bed 27; *Hindeodus parvus* Z	
Paryphella orbicularis	DDS27-2-0535	Fig. 9.16e	In this book	Bed 27; *Hindeodus parvus* Z	
Paryphella orbicularis	DDS27-0546	Fig. 9.16f	In this book	Bed 27; *Hindeodus parvus* Z	
Paryphella orbicularis	DDS29-0534	Fig. 9.16g	In this book	Bed 29; *Ophiceras* Z	
Paryphella orbicularis	DDS27-1-0542	Fig. 9.16h	In this book	Bed 27-1; immediately below *Hindeodus parvus* Z	
Paryphella orbicularis	DDS27-2-0543	Fig. 9.16i	In this book	Bed 27-2; *Hindeodus parvus* Z	
Paryphella orbicularis	DDS27-1-0537	Fig. 9.16j	In this book	Bed 27-1; immediately below *Hindeodus parvus* Z	
Paryphella orbicularis	DDS29-0536	Fig. 9.16k	In this book	Bed 29; *Ophiceras* Z	
Paryphella orbicularis	DDS27-2-0538	Fig. 9.16l	In this book	Bed 27-2; *Hindeodus parvus* Z	
Paryphella orbicularis	DDS27-2-0544	Fig. 9.16m	In this book	Bed 27-2; *Hindeodus parvus* Z	
Paryphella orbicularis	DDS27-1-0539	Fig. 9.16n	In this book	Bed 27-1; immediately below *Hindeodus parvus* Z	
Paryphella orbicularis	DDS27-1	Fig. 9.16o	In this book	Bed 27-1; immediately below *Hindeodus parvus* Z	
Paryphella orbicularis	CM-20-216	Fig. 9.17a	Fig. 14B; He et al. (2014)	Bed 20; *Ophiceras* Z	
Paryphella orbicularis	CM-13-205	Fig. 9.17b	Fig. 14C; He et al. (2014)	Bed 13; *Pseudotirolites–Rotodiscoceras* Z	
Paryphella orbicularis	CM-13-208	Fig. 9.17c	Fig. 14D; He et al. (2014)	Bed 13; *Pseudotirolites–Rotodiscoceras* Z	
Paryphella orbicularis	CM-13-212	Fig. 9.17d	Fig. 14E; He et al. (2014)	Bed 13; *Pseudotirolites–Rotodiscoceras* Z	
Paryphella orbicularis	CM-13-231	Fig. 9.17e	Fig. 14F; He et al. (2014)	Bed 13; *Pseudotirolites–Rotodiscoceras* Z	
Paryphella orbicularis	CM-4-249	Fig. 9.17f	Fig. 14H; He et al. (2014)	Bed 4; *Tapashanites* Z	
Paryphella orbicularis (=*Paryphella triquetra* of He et al. 2014)	CM-12-203	Fig. 9.17g	Fig. 16A; He et al. (2014)	Bed 12; *Pseudotirolites–Rotodiscoceras* Z	
Paryphella orbicularis (=*Paryphella triquetra* of He et al. 2014)	CM-12-204	Fig. 9.17h	Fig. 16B; He et al. (2014)	Bed 12; *Pseudotirolites–Rotodiscoceras* Z	

(continued)

Fossil name in the book	Registered number	Page and figure numbers in the book	Source of Materials	Occurences	Others
Paryphella orbicularis (=*Paryphella triquetra* of He et al. 2014)	CM-10-209	Fig. 9.17i	Fig. 16D; He et al. (2014)	Bed 10; *Pseudotirolites*–*Rotodiscoceras* Z	
Paryphella orbicularis (=*Paryphella triquetra* of He et al. 2014)	CM-12-219	Fig. 9.17j	Fig. 16E; He et al. (2014)	Bed 12; *Pseudotirolites*–*Rotodiscoceras* Z	
Paryphella orbicularis (=*Paryphella triquetra* of He et al. 2014)	CM-10-233	Fig. 9.17k	Fig. 16F; He et al. (2014)	Bed 10; *Pseudotirolites*–*Rotodiscoceras* Z	
Paryphella orbicularis (=*Paryphella triquetra* of He et al. 2014)	CM-10-247	Fig. 9.17l	Fig. 16G; He et al. (2014)	Bed 10; *Pseudotirolites*–*Rotodiscoceras* Z	
Paryphella orbicularis (=*Paryphella triquetra* of He et al. 2014)	CM-10-254	Fig. 9.17m	Fig. 16H; He et al. (2014)	Bed 10; *Pseudotirolites*–*Rotodiscoceras* Z	
Paryphella orbicularis (=*Paryphella triquetra* of He et al. 2014)	CM-13-201	Fig. 9.17n	Fig. 16I; He et al. (2014)	Bed 13; *Pseudotirolites*–*Rotodiscoceras* Z	
Paryphella orbicularis (=*Paryphella triquetra* of He et al. 2014)	CM-12-194	Fig. 9.17o	Fig. 16J; He et al. (2014)	Bed 12; *Pseudotirolites*–*Rotodiscoceras* Z	
Paryphella orbicularis	LZ2702676	Fig. 9.18a	Fig. 4I; Zhang et al. (2015)	Bed 27-2; *Fusichonetes pygmaea* Z	
Paryphella orbicularis	LZ2702646	Fig. 9.18b	Fig. 4Q; Zhang et al. (2015)	Bed 27-2; *Fusichonetes pygmaea* Z	
Paryphella orbicularis	LZ2702677	Fig. 9.18c	Fig. 4J; Zhang et al. (2015)	Bed 27-2; *Fusichonetes pygmaea* Z	
Paryphella orbicularis (=*Paryphella triquetra* of Zhang et al. 2015)	LZ2702653	Fig. 9.18d	Fig. 4S; Zhang et al. (2015)	Bed 27-2; *Fusichonetes pygmaea* Z	
Paryphella orbicularis	LZ2704668	Fig. 9.18e	Fig. 4K; Zhang et al. (2015)	Bed 27-4; *Fusichonetes pygmaea* Z	
Paryphella orbicularis	LZ2702645	Fig. 9.18f	Fig. 4P; Zhang et al. (2015)	Bed 27-2; *Fusichonetes pygmaea* Z	
Paryphella orbicularis	LZ2702651	Fig. 9.18g	Fig. 4L; Zhang et al. (2015)	Bed 27-2; *Fusichonetes pygmaea* Z	
Paryphella orbicularis (=*Paryphella triquetra* of Zhang et al. 2015)	LZ2701155	Fig. 9.18h	Fig. 4T; Zhang et al. (2015)	Bed 27-1; *Fusichonetes pygmaea* Z	
Paryphella orbicularis	LZ2705531	Fig. 9.18i	Fig. 4O; Zhang et al. (2015)	Bed 27-5; *Fusichonetes pygmaea* Z	
Paryphella orbicularis (=*Paryphella sinuata* of Zhang et al. 2015)	LZ2706170	Fig. 9.18j	Fig. 4V; Zhang et al. (2015)	Bed 27-6; *Fusichonetes pygmaea* Z	
Paryphella orbicularis (=*Paryphella triquetra* of Zhang et al. 2015)	LZ2704160	Fig. 9.18k	Fig. 4U; Zhang et al. (2015)	Bed 27-4; *Fusichonetes pygmaea* Z	
Paryphella orbicularis (=*Paryphella elegantula* of Zhang et al. 2015)	LZ2702644	Fig. 9.18l	Fig. 4X; Zhang et al. (2015)	Bed 27-2; *Fusichonetes pygmaea* Z	
Paryphella undata	CM-6-266	Fig. 9.19a	Fig. 14Y; He et al. (2014)	Bed 6; *Tapashanites* Z	

Paryphella undata	CM-4-258	Fig. 9.19b	Fig. 14Z; He et al. (2014)	Bed 4; *Tapashanites* Z	
Paryphella undata	CM-3-268	Fig. 9.19c	Fig. 14A'; He et al. (2014)	Bed 3; *Tapashanites* Z	
Paryphella undata	CM-3-269	Fig. 9.19d	Fig. 14B'; He et al. (2014)	Bed 3; *Tapashanites* Z	
Paryphella undata	CM-3-270	Fig. 9.19e	Fig. 14C'; He et al. (2014)	Bed 3; *Tapashanites* Z	
Paryphella undata	CM10-0551	Fig. 9.19f	In this book	Bed 10; *Pseudotirolites–Rotodiscoceras* Z	
Paryphella undata	CM2-0548	Fig. 9.19g	In this book	Bed 2; Upper Permian	
Paryphella undata	CM-4-259	Fig. 9.19h	Fig. 14D'; He et al. (2014)	Bed 4; *Tapashanites* Z	
Paryphella undata	CM2-0549	Fig. 9.19i	In this book	Bed 2; Upper Permian	
Paryphella undata	DDS27-2-0555	Fig. 9.19j	In this book	Bed 27-2; *Hindeodus parvus* Z	
Paryphella undata	CM2-0550	Fig. 9.19k	In this book	Bed 2; Upper Permian	
Paryphella undata	CM10-0553	Fig. 9.19l	In this book	Bed 10; *Pseudotirolites–Rotodiscoceras* Z	
Paryphella undata	DDS27-2-0552	Fig. 9.19m	In this book	Bed 27-2; *Hindeodus parvus* Z	
Paryphella undata	CM2-0547	Fig. 9.19n	In this book	Bed 2; Upper Permian	
Paryphella sparsiplicata (=*Paryphella majiashanensis* He and Shi in He et al. 2014)	CM-4-257	Fig. 9.20a	Fig. 16K; He et al. (2014)	Bed 4; *Tapashanites* Z	
Paryphella sparsiplicata (=*Paryphella majiashanensis* He and Shi in He et al. 2014)	CM-4-265	Fig. 9.20b	Fig. 16L; He et al. (2014)	Bed 4; *Tapashanites* Z	
Paryphella sparsiplicata (=*Paryphella majiashanensis* He and Shi in He et al. 2014)	CM-4-264	Fig. 9.20c	Fig. 16M; He et al. (2014)	Bed 4; *Tapashanites* Z	
Paryphella sparsiplicata (=*Paryphella majiashanensis* He and Shi in He et al. 2014)	CM-4-261	Fig. 9.20d	Fig. 16N; He et al. (2014)	Bed 4; *Tapashanites* Z	
Paryphella sparsiplicata (=*Paryphella majiashanensis* He and Shi in He et al. 2014)	CM-4-262	Fig. 9.20e	Fig. 16O; He et al. (2014)	Bed 4; *Tapashanites* Z	
Paryphella sparsiplicata (=*Paryphella majiashanensis* He and Shi in He et al. 2014)	CM-10-255	Fig. 9.20f	Fig. 16R; He et al. (2014)	Bed 10; *Pseudotirolites–Rotodiscoceras* Z	
Paryphella sparsiplicata (=*Paryphella majiashanensis* He and Shi in He et al. 2014)	CM-4-263	Fig. 9.20g	Fig. 16P; He et al. (2014)	Bed 4; *Tapashanites* Z	

(continued)

Fossil name in the book	Registered number	Page and figure numbers in the book	Source of Materials	Occurences	Others
Paryphella sparsiplicata (=*Paryphella majiashanensis* He and Shi in He et al. 2014)	CM-4-244	Fig. 9.20h	Fig. 16S; He et al. (2014)	Bed 4; *Tapashanites* Z	Holotype
Paryphella sparsiplicata (=*Paryphella majiashanensis* He and Shi in He et al. 2014)	CM-10-202	Fig. 9.20i	Fig. 16Q; He et al. (2014)	Bed 10; *Pseudotirolites–Rotodiscoceras* Z	Paratype
Paryphella sparsiplicata	DDS26-0568	Fig. 9.20j	In this book	Bed 26; *Hypophiceras* Z	
Paryphella sparsiplicata	DDS27-1-0567	Fig. 9.20k	In this book	Bed 27-1; immediately below *Hindeodus parvus* Z	
Paryphella sparsiplicata	CM9-0559	Fig. 9.20l	In this book	Bed 9; *Tapashanites* Z	
Paryphella sparsiplicata	HZS19-0557	Fig. 9.20m	In this book	Bed 19; *Clarkina meishanensis* Z	
Paryphella sparsiplicata	DDS26-0560	Fig. 9.20n	In this book	Bed 26; *Hypophiceras* Z	
Paryphella sparsiplicata	DDS27-2-0563	Fig. 9.20o	In this book	Bed 27-2; *Hindeodus parvus* Z	
Paryphella corculum (=*Paryphella autala* Zhang et al. 2015)	LZ2702168	Fig. 9.21a	Fig. 6G; Zhang et al. (2015)	Bed 27-2; *Fusichonetes pygmaea* Z	
Paryphella corculum (=*Paryphella autala* Zhang et al. 2015)	LZ2702675	Fig. 9.21b	Fig. 6E; Zhang et al. (2015)	Bed 27-2; *Fusichonetes pygmaea* Z	
Paryphella corculum (=*Paryphella autala* Zhang et al. 2015)	LZ2703169	Fig. 9.21c	Fig. 6A; Zhang et al. (2015)	Bed 27-3; *Fusichonetes pygmaea* Z	
Paryphella corculum (=*Paryphella autala* Zhang et al. 2015)	LZ2702650	Fig. 9.21d	Fig. 6H; Zhang et al. (2015)	Bed 27-2; *Fusichonetes pygmaea* Z	
Paryphella corculum (=*Paryphella autala* Zhang et al. 2015)	LZ2705534	Fig. 9.21e	Fig. 6J; Zhang et al. (2015)	Bed 27-5; *Fusichonetes pygmaea* Z	
Paryphella corculum (=*Paryphella autala* Zhang et al. 2015)	LZ2702673	Fig. 9.21f	Fig. 6C; Zhang et al. (2015)	Bed 27-2; *Fusichonetes pygmaea* Z	
Paryphella corculum (=*Paryphella autala* Zhang et al. 2015)	LZ2702672	Fig. 9.21g	Fig. 6D; Zhang et al. (2015)	Bed 27-2; *Fusichonetes pygmaea* Z	
Paryphella corculum (=*Paryphella autala* Zhang et al. 2015)	LZ2702163	Fig. 9.21h	Fig. 6B; Zhang et al. (2015)	Bed 27-2; *Fusichonetes pygmaea* Z	
Paryphella corculum (=*Paryphella autala* Zhang et al. 2015)	LZ2702671	Fig. 9.21i	Fig. 6L; Zhang et al. (2015)	Bed 27-2; *Fusichonetes pygmaea* Z	
Paryphella corculum (=*Paryphella autala* Zhang et al. 2015)	LZ2702656	Fig. 9.21j	Fig. 4AB; Zhang et al. (2015)	Bed 27-2; *Fusichonetes pygmaea* Z	
Paryphella sp.	HZS20-0574	Fig. 9.22a	In this book	Bed 20; *Clarkina meishanensis* Z	
Paryphella sp.	HZS22-0575	Fig. 9.22b	In this book	Bed 22; *Clarkina meishanensis* Z	

Paryphella sp.	HZS20-0576	Fig. 9.22c	In this book	Bed 20; *Clarkina meishanensis* Z	
Paryphella sp.	HZS27-0577	Fig. 9.22d	In this book	Bed 27; *Clarkina meishanensis* Z	
Paryphella sp.	HZS20-0578	Fig. 9.22e	In this book	Bed 20; *Clarkina meishanensis* Z	
Paryphella sp.	HZS23-0580	Fig. 9.22f	In this book	Bed 23; *Clarkina meishanensis* Z	
Paryphella sp.	HZS20-0582	Fig. 9.22g	In this book	Bed 20; *Clarkina meishanensis* Z	
Paryphella sp.	HZS20-0583	Fig. 9.22h	In this book	Bed 20; *Clarkina meishanensis* Z	
Paryphella sp.	HZS24-0585	Fig. 9.22i	In this book	Bed 24; *Clarkina meishanensis* Z	
Paryphella sp.	HZS20-0587	Fig. 9.22j	In this book	Bed 20; *Clarkina meishanensis* Z	
Paryphella sp.	HZS23-0588	Fig. 9.22k	In this book	Bed 23; *Clarkina meishanensis* Z	
Paryphella sp.	HZS24-0590	Fig. 9.22l	In this book	Bed 24; *Clarkina meishanensis* Z	
Paryphella sp.	HZS24-0584	Fig. 9.22m	In this book	Bed 24; *Clarkina meishanensis* Z	
Paryphella sp.	HZS23-0586	Fig. 9.22n	In this book	Bed 23; *Clarkina meishanensis* Z	
Haydenella kiangsiensis	HZS25-0606	Fig. 9.23a	In this book	Bed 25; *Clarkina meishanensis* Z	
Haydenella kiangsiensis	HZS24-0611	Fig. 9.23b	In this book	Bed 24; *Clarkina meishanensis* Z	
Haydenella kiangsiensis	HZS24-0607	Fig. 9.23c	In this book	Bed 24; *Clarkina meishanensis* Z	
Haydenella kiangsiensis	HZS27-0608	Fig. 9.23d	In this book	Bed 27; *Clarkina meishanensis* Z	
Haydenella kiangsiensis	HZS24-0609	Fig. 9.23e	In this book	Bed 24; *Clarkina meishanensis* Z	
Haydenella kiangsiensis	HZS19-0616	Fig. 9.23f	In this book	Bed 19; *Clarkina meishanensis* Z	
Haydenella kiangsiensis	HZS24-0612	Fig. 9.23g	In this book	Bed 24; *Clarkina meishanensis* Z	
Haydenella kiangsiensis	HZS27-0613	Fig. 9.23h	In this book	Bed 27; *Clarkina meishanensis* Z	
Haydenella kiangsiensis	HZS25-0618	Fig. 9.23i	In this book	Bed 25; *Clarkina meishanensis* Z	
Haydenella kiangsiensis	HZS24-0615	Fig. 9.23j	In this book	Bed 24; *Clarkina meishanensis* Z	
Haydenella kiangsiensis	HZS24-0617	Fig. 9.23k	In this book	Bed 24; *Clarkina meishanensis* Z	
?*Eileenella semicircridge* (=*Spinomarginifera semicircridge* He et al. 2005)	DP9602	Fig. 9.24a	Fig. 5.14; He et al. (2005)	Bed 9; *Pseudotirolites–Rotodiscoceras* Z	Paratype
?*Eileenella semicircridge* (=*Spinomarginifera semicircridge* of He et al. 2014)	DP-10-307	Fig. 9.24b	Fig. 17E; He et al. (2014)	Bed 10; *Pseudotirolites–Rotodiscoceras* Z	
?*Eileenella semicircridge*	DP1-0194	Fig. 9.24c	In this book	Bed 1; *Pseudotirolites–Rotodiscoceras* Z	
?*Eileenella semicircridge* (=*Spinomarginifera semicircridge* He et al. 2005)	DP9603	Fig. 9.24d	Fig. 5.16; He et al. (2005)	Bed 9; *Pseudotirolites–Rotodiscoceras* Z	

(continued)

Fossil name in the book	Registered number	Page and figure numbers in the book	Source of Materials	Occurences	Others
?*Eileenella semicircridge* (=*Spinomarginifera semicircridge* He et al. 2005)	DP9401	Fig. 9.24e	Fig. 5.17; He et al. (2005)	Bed 9; *Pseudotirolites–Rotodiscoceras* Z	
?*Eileenella semicircridge* (=*Spinomarginifera semicircridge* of He et al. 2014)	DP-8-302	Fig. 9.24f	Fig. 17C; He et al. (2014)	Bed 8; *Pseudotirolites–Rotodiscoceras* Z	
?*Eileenella semicircridge* (=*Spinomarginifera semicircridge* of He et al. 2014)	DP-10-315	Fig. 9.24g	Fig. 17D; He et al. (2014)	Bed 10; *Pseudotirolites–Rotodiscoceras* Z	
?*Eileenella semicircridge* (=*Spinomarginifera semicircridge* He et al. 2005)	DP9604	Fig. 9.24h	Fig. 5.18; He et al. (2005)	Bed 9; *Pseudotirolites–Rotodiscoceras* Z	Holotype
?*Eileenella semicircridge* (=*Spinomarginifera semicircridge* of He et al. 2014)	DP-10-313	Fig. 9.24i	Fig. 17F; He et al. (2014)	Bed 10; *Pseudotirolites–Rotodiscoceras* Z	
?*Eileenella semicircridge* (=*Spinomarginifera semicircridge* of He et al. 2014)	DP-10-309	Fig. 9.24j	Fig. 17G; He et al. (2014)	Bed 10; *Pseudotirolites–Rotodiscoceras* Z	
?*Eileenella semicircridge* (=*Spinomarginifera semicircridge* He et al. 2005)	DP733	Fig. 9.24k	Fig. 5.13; He et al. (2005)	Bed 7; *Pseudotirolites–Rotodiscoceras* Z	
?*Eileenella semicircridge* (=*Spinomarginifera semicircridge* of He et al. 2014)	DP-9-304	Fig. 9.24l	Fig. 17H; He et al. (2014)	Bed 9; *Pseudotirolites–Rotodiscoceras* Z	
?*Eileenella semicircridge* (=*Spinomarginifera semicircridge* of He et al. 2014)	DP-8-311	Fig. 9.24m	Fig. 17I; He et al. (2014)	Bed 8; *Pseudotirolites–Rotodiscoceras* Z	
Pygmochonetes jingxianensis	DP-7-294	Fig. 9.25a	Fig. 13M; He et al. (2014)	Bed 7; *Pseudotirolites–Rotodiscoceras* Z	
Pygmochonetes jingxianensis	DP-7-295	Fig. 9.25b	Fig. 13N; He et al. (2014)	Bed 7; *Pseudotirolites–Rotodiscoceras* Z	
Pygmochonetes jingxianensis	DP-5-297	Fig. 9.25c	Fig. 13O; He et al. (2014)	Bed 5; *Pseudotirolites–Rotodiscoceras* Z	
Pygmochonetes jingxianensis	DP-10-298	Fig. 9.25d	Fig. 13P; He et al. (2014)	Bed 10; *Pseudotirolites–Rotodiscoceras* Z	
Pygmochonetes jingxianensis	DP3-0214	Fig. 9.25e	In this book	Bed 3; *Pseudotirolites–Rotodiscoceras* Z	
Pygmochonetes jingxianensis	DP10-0216	Fig. 9.25f	In this book	Bed 10; *Pseudotirolites–Rotodiscoceras* Z	
Pygmochonetes jingxianensis	DP7-0217	Fig. 9.25g	In this book	Bed 7; *Pseudotirolites–Rotodiscoceras* Z	

Pygmochonetes jingxianensis	DP7-0217	Fig. 9.25h	In this book	Bed 7; *Pseudotirolites–Rotodiscoceras* Z	
Pygmochonetes jingxianensis	DP10-0219	Fig. 9.25i	In this book	Bed 10; *Pseudotirolites–Rotodiscoceras* Z	
Pygmochonetes jingxianensis	PB5-0220	Fig. 9.25j	In this book	Bed 5; *Neoalbaillella optima* Z	
Pygmochonetes jingxianensis	DP10-0221	Fig. 9.25k	In this book	Bed 10; *Pseudotirolites–Rotodiscoceras* Z	
Pygmochonetes jingxianensis	DP3-0223	Fig. 9.25l	In this book	Bed 3; *Pseudotirolites–Rotodiscoceras* Z	
Pygmochonetes jingxianensis	DP10-0233	Fig. 9.25m	In this book	Bed 10; *Pseudotirolites–Rotodiscoceras* Z	
Pygmochonetes sp.	DP5-0224	Fig. 9.25n	In this book	Bed 5; *Pseudotirolites–Rotodiscoceras* Z	
Pygmochonetes sp.	DP3-0231	Fig. 9.25o	In this book	Bed 3; *Pseudotirolites–Rotodiscoceras* Z	
Pygmochonetes sp.	PB10-0232	Fig. 9.26a	In this book	Bed 10; *Neoalbaillella optima* Z	
Pygmochonetes sp.	DP10-0228	Fig. 9.26b	In this book	Bed 10; *Pseudotirolites–Rotodiscoceras* Z	
Pygmochonetes sp.	DP10-0235	Fig. 9.26c	In this book	Bed 10; *Pseudotirolites–Rotodiscoceras* Z	
Pygmochonetes sp.	DP10-0236	Fig. 9.26d	In this book	Bed 10; *Pseudotirolites–Rotodiscoceras* Z	
Pygmochonetes sp.	DP10-0238	Fig. 9.26e	In this book	Bed 10; *Pseudotirolites–Rotodiscoceras* Z	
Tornquistia changhsingia	DP7-MC001	Fig. 9.27a	In this book	Bed 7; *Pseudotirolites–Rotodiscoceras* Z	
Tornquistia changhsingia	PB5-MC003-1	Fig. 9.27b	In this book	Bed 5; *Neoalbaillella optima* Z	
Tornquistia changhsingia	DP9-MC006-1	Fig. 9.27c	In this book	Bed 9; *Pseudotirolites–Rotodiscoceras* Z	
Tornquistia changhsingia	DP3-MC017	Fig. 9.27d	In this book	Bed 3; *Pseudotirolites–Rotodiscoceras* Z	
Tornquistia changhsingia	DP10-MC007-1	Fig. 9.27e	In this book	Bed 10; *Pseudotirolites–Rotodiscoceras* Z	
Tornquistia changhsingia	DP3-MC018	Fig. 9.27f	In this book	Bed 3; *Pseudotirolites–Rotodiscoceras* Z	
Tornquistia changhsingia	DP3-MC004-1	Fig. 9.27g	In this book	Bed 3; *Pseudotirolites–Rotodiscoceras* Z	
Tornquistia changhsingia	DP5-MC027	Fig. 9.27h	In this book	Bed 5; *Pseudotirolites–Rotodiscoceras* Z	Paratype
Tornquistia changhsingia	DP3-MC012	Fig. 9.27i	In this book	Bed 3; *Pseudotirolites–Rotodiscoceras* Z	
Tornquistia changhsingia	DP8-MC021	Fig. 9.27j	In this book	Bed 8; *Pseudotirolites–Rotodiscoceras* Z	
Tornquistia changhsingia	DP5-MC015	Fig. 9.27k	In this book	Bed 5; *Pseudotirolites–Rotodiscoceras* Z	Paratype
Tornquistia changhsingia	DP7-MC043-1	Fig. 9.27l	In this book	Bed 7; *Pseudotirolites–Rotodiscoceras* Z	
Tornquistia changhsingia	DP8-MC026	Fig. 9.27m	In this book	Bed 8; *Pseudotirolites–Rotodiscoceras* Z	
Tornquistia changhsingia	DP10-MC007-2	Fig. 9.27n	In this book	Bed 10; *Pseudotirolites–Rotodiscoceras* Z.	
Tornquistia changhsingia	DP5-MC035	Fig. 9.28a	In this book	Bed 5; *Pseudotirolites–Rotodiscoceras* Z	
Tornquistia changhsingia	DP5-MC033-1	Fig. 9.28b	In this book	Bed 5; *Pseudotirolites–Rotodiscoceras* Z	
Tornquistia changhsingia	DP8-MC037	Fig. 9.28c	In this book	Bed 8; *Pseudotirolites–Rotodiscoceras* Z	
Tornquistia changhsingia	DP8-MC041	Fig. 9.28d	In this book	Bed 8; *Pseudotirolites–Rotodiscoceras* Z	
Tornquistia changhsingia	DP8-MC046	Fig. 9.28e	In this book	Bed 8; *Pseudotirolites–Rotodiscoceras* Z	
Tornquistia changhsingia	PB2-MC070	Fig. 9.28f	In this book	Bed 2; *Neoalbaillella optima* Z	Holotype

(continued)

Fossil name in the book	Registered number	Page and figure numbers in the book	Source of Materials	Occurences	Others
Tornquistia changhsingia	PB8-MC038	Fig. 9.28g	In this book	Bed 8; *Neoalbaillella optima* Z	
Tornquistia changhsingia	PB5-MC039	Fig. 9.28h	In this book	Bed 5; *Neoalbaillella optima* Z	
Tornquistia changhsingia	PB8-MC047	Fig. 9.28i	In this book	Bed 8; *Neoalbaillella optima* Z	
Tornquistia changhsingia	DP5-MC014	Fig. 9.28j	In this book	Bed 5; *Pseudotirolites–Rotodiscoceras* Z	
Tornquistia changhsingia	DP7-MC040	Fig. 9.28k	In this book	Bed 7; *Pseudotirolites–Rotodiscoceras* Z	
Tornquistia changhsingia	DP7-MC034-2	Fig. 9.28l	In this book	Bed 7; *Pseudotirolites–Rotodiscoceras* Z	
Tornquistia changhsingia	DP7-MC071	Fig. 9.28m	In this book	Bed 7; *Pseudotirolites–Rotodiscoceras* Z	
Fusichonetes nanyongensis	XM2-0393	Fig. 9.30a	In this book	Bed 2; *Clarkina changxingensis* Z	
Fusichonetes nanyongensis	XM2-0390	Fig. 9.30b	In this book	Bed 2; *Clarkina changxingensis* Z	
Fusichonetes nanyongensis	XM4-0392	Fig. 9.30c	In this book	Bed 4; *Clarkina yini* Z	
Fusichonetes nanyongensis	XM10-0398	Fig. 9.30d	In this book	Bed 1; *Clarkina changxingensis* Z	
Fusichonetes nanyongensis	XM9-0410	Fig. 9.30e	In this book	Bed 1; *Clarkina changxingensis* Z	
Fusichonetes nanyongensis	XM2-0384	Fig. 9.30f	In this book	Bed 2; *Clarkina changxingensis* Z	
Fusichonetes nanyongensis	XM24-280	Fig. 9.30g	Fig. 1D; Wu et al. (2016)	Bed 4; *Clarkina changxingensis* Z	
Fusichonetes nanyongensis	XM24-252	Fig. 9.30h	Fig. 1C; Wu et al. (2016)	Bed 4; *Clarkina changxingensis* Z	
Fusichonetes nanyongensis	XM2-0383	Fig. 9.30i	In this book	Bed 2; *Clarkina changxingensis* Z	
Fusichonetes nanyongensis	XM24-248	Fig. 9.30j	Fig. 1A; Wu et al. (2016)	Bed 4; *Clarkina changxingensis* Z	
Fusichonetes nanyongensis	XM10-0400	Fig. 9.30k	In this book	Bed 1; *Clarkina changxingensis* Z	
Fusichonetes nanyongensis	XM10-0406	Fig. 9.30l	In this book	Bed 1; *Clarkina changxingensis* Z	
Fusichonetes nanyongensis	XM24-258	Fig. 9.30m	Fig. 1B; Wu et al. (2016)	Bed 4; *Clarkina changxingensis* Z	
Fusichonetes soochowensis	CM10-0352	Fig. 9.31a	In this book	Bed 10; *Pseudotirolites–Rotodiscoceras* Z	
Fusichonetes soochowensis	SR23b-0419	Fig. 9.31b	In this book	Bed 23; *Clarkina yini* Z	
Fusichonetes soochowensis (=*Tethyochonetes soochowensis* of Zhang et al. 2013)	LZ2702263	Fig. 9.31c	Fig. 5P; Zhang et al. (2013)	Bed 27-2; *Fusichonetes pygmaea* Z	
Fusichonetes soochowensis (=*Tethyochonetes soochowensis* of Zhang et al. 2013)	LZ2702235	Fig. 9.31d	Fig. 5O; Zhang et al. (2013)	Bed 27-2; *Fusichonetes pygmaea* Z	
Fusichonetes soochowensis (=*Tethyochonetes soochowensis* of He et al. 2014)	DS-1-475	Fig. 9.31e	Fig. 4X; He et al. (2014)	Bed 1; *Pseudotirolites–Rotodiscoceras* Z	
Fusichonetes soochowensis (=*Tethyochonetes soochowensis* of He et al. 2014)	CM-4-459	Fig. 9.31f	Fig. 4Y; He et al. (2014)	Bed 4; *Tapashanites* Z	

Fusichonetes soochowensis (=*Tethyochonetes soochowensis* of He et al. 2014)	CM-10-482	Fig. 9.31g	Fig. 4Z; He et al. (2014)	Bed 10; *Pseudotirolites–Rotodiscoceras* Z	
Fusichonetes soochowensis (=*Tethyochonetes soochowensis* of He et al. 2014)	DS-1-485	Fig. 9.31h	Fig. 4A'; He et al. (2014)	Bed 1; *Pseudotirolites–Rotodiscoceras* Z	
Fusichonetes soochowensis (=*Tethyochonetes soochowensis* of He et al. 2014)	DS-1-478	Fig. 9.31i	Fig. 4C'; He et al. (2014)	Bed 1; *Pseudotirolites–Rotodiscoceras* Z	
Fusichonetes soochowensis (=*Tethyochonetes soochowensis* of He et al. 2014)	SR-16-481	Fig. 9.31j	Fig. 4E'; He et al. (2014)	Bed 16; *Konglingites* Z	
Fusichonetes soochowensis	XM24110(=CUG24110 of Wu et al. 2017)	Fig. 9.31k	Fig. 3.9; Wu et al. (2017)	Bed 4; *Clarkina changxingensis* Z	
Fusichonetes cheni	XM-1-0375	Fig. 9.32a	In this book	Bed 1; *Clarkina changxingensis* Z	
Fusichonetes cheni	XM-1-0370	Fig. 9.32b	In this book	Bed 1; *Clarkina changxingensis* Z	
Fusichonetes cheni	XM-1-0372	Fig. 9.32c	In this book	Bed 1; *Clarkina changxingensis* Z	
Fusichonetes cheni	XM-1-0379	Fig. 9.32d	In this book	Bed 1; *Clarkina changxingensis* Z	
Fusichonetes cheni	XM-1-0380	Fig. 9.32e	In this book	Bed 1; *Clarkina changxingensis* Z	
Fusichonetes cheni	XM-1-0378	Fig. 9.32f	In this book	Bed 1; *Clarkina changxingensis* Z	
Fusichonetes cheni	XM-1-0382	Fig. 9.32g	In this book	Bed 1; *Clarkina changxingensis* Z	
Fusichonetes cheni	XM-7-0368	Fig. 9.32h	In this book	Bed 1; *Clarkina changxingensis* Z	
Fusichonetes cheni	XM-7-0374	Fig. 9.32i	In this book	Bed 1; *Clarkina changxingensis* Z	
Fusichonetes cheni	XM-10-0376	Fig. 9.32j	In this book	Bed 1; *Clarkina changxingensis* Z	
Fusichonetes cheni	XM-1-0367	Fig. 9.32k	In this book	Bed 1; *Clarkina changxingensis* Z	
Fusichonetes cheni	XM22202 (=CUG22202 of Wu et al. 2017	Fig. 9.32l	Fig. 3.3; Wu et al. (2017)	Bed 3; *Clarkina changxingensis* Z	
Fusichonetes cheni	XM23801 (=CUG23801 of Wu et al. 2017)	Fig. 9.32m	Fig. 3.4; Wu et al. (2017)	Bed 3; *Clarkina changxingensis* Z	
Fusichonetes cheni	XM20-701	Fig. 9.32n	In this book	Bed 3; *Clarkina changxingensis* Z	
Fusichonetes cheni	XM20-402	Fig. 9.32o	In this book	Bed 3; *Clarkina changxingensis* Z	

(continued)

Fossil name in the book	Registered number	Page and figure numbers in the book	Source of Materials	Occurences	Others
Fusichonetes cheni (=*Tethyochonetes cheni* Zhang et al. 2013)	LZ2703265	Fig. 9.33a	Fig. 9H; Zhang et al. (2013)	Bed 27-3; *Fusichonetes pygmae*a Z	Holotype
Fusichonetes cheni (=*Tethyochonetes cheni* Zhang et al. 2013)	LZ2706254	Fig. 9.33b	Fig. 9D; Zhang et al. (2013)	Bed 27-6; *Fusichonetes pygmae*a Z	
Fusichonetes cheni (=*Tethyochonetes cheni* Zhang et al. 2013)	LZ2706032	Fig. 9.33c	Fig. 5AA; Zhang et al. (2013)	Bed 27-6; *Fusichonetes pygmae*a Z	
Fusichonetes cheni (=*Tethyochonetes cheni* Zhang et al. 2013)	LZ2702223	Fig. 9.33d	Fig. 9A; Zhang et al. (2013)	Bed 27-2; *Fusichonetes pygmae*a Z	
Fusichonetes cheni (=*Tethyochonetes cheni* Zhang et al. 2013)	LZ2703266	Fig. 9.33e	Fig. 9F; Zhang et al. (2013)	Bed 27-3; *Fusichonetes pygmae*a Z	
Fusichonetes cheni (=*Tethyochonetes cheni* Zhang et al. 2013)	LZ2701034	Fig. 9.33f	Fig. 5AB; Zhang et al. (2013)	Bed 27-1; *Fusichonetes pygmae*a Z	
Fusichonetes cheni (=*Tethyochonetes cheni* Zhang et al. 2013)	LZ2702071	Fig. 9.33g	Fig. 9I; Zhang et al. (2013)	Bed 27-2; *Fusichonetes pygmae*a Z	
Fusichonetes cheni (=*Tethyochonetes cheni* Zhang et al. 2013)	LZ2702071	Fig. 9.33h (enlarged portion of Fig. 9.33g in the book)	Fig. 9I; Zhang et al. (2013)	Bed 27-2; *Fusichonetes pygmae*a Z	
Fusichonetes quadrata (=*Tethyochonetes quadrata* of He et al. 2014)	CM-4-541	Fig. 9.34a	Fig. 4A; He et al. (2014)	Bed 4; *Tapashanites* Z	
Fusichonetes quadrata (=*Tethyochonetes quadrata* of He et al. 2014)	CM-4-469	Fig. 9.34b	Fig. 4B; He et al. (2014)	Bed 4; *Tapashanites* Z	
Fusichonetes quadrata (=*Tethyochonetes quadrata* of He et al. 2014)	CM-4-471	Fig. 9.34c	Fig. 4C; He et al. (2014)	Bed 4; *Tapashanites* Z	
Fusichonetes quadrata (=*Tethyochonetes quadrata* of He et al. 2014)	CM-4-470	Fig. 9.34d	Fig. 4D; He et al. (2014)	Bed 4; *Tapashanites* Z	

Fusichonetes quadrata (=*Tethyochonetes quadrata* of He et al. 2014)	CM-4-457	Fig. 9.34e	Fig. 4E; He et al. (2014)	Bed 4; *Tapashanites* Z	
Fusichonetes quadrata (=*Tethyochonetes quadrata* of He et al. 2014)	CM-4-458	Fig. 9.34f	Fig. 4F; He et al. (2014)	Bed 4; *Tapashanites* Z	
Fusichonetes quadrata (=*Tethyochonetes quadrata* of He et al. 2014)	CM-4-466	Fig. 9.34g	Fig. 4H; He et al. (2014)	Bed 4; *Tapashanites* Z	
Fusichonetes quadrata	CM2-0321	Fig. 9.34h	In this book	Bed 2; Upper Permian	
Fusichonetes quadrata	SR20-0325	Fig. 9.34i	In this book	Bed 20; basal *Pseudotirolites–Rotodiscoceras* Z	
Fusichonetes quadrata	SR20-0323	Fig. 9.34j	In this book	Bed 20; basal *Pseudotirolites–Rotodiscoceras* Z	
Fusichonetes quadrata	SR20-0324	Fig. 9.34k	In this book	Bed 20; basal *Pseudotirolites–Rotodiscoceras* Z	
Fusichonetes quadrata	SR20-0440	Fig. 9.34l	In this book	Bed 20; basal *Pseudotirolites–Rotodiscoceras* Z	
Fusichonetes quadrata	ZZ2702-0327	Fig. 9.35a	In this book	Bed 27-2; *Fusichonetes pygmaea* Z	
Fusichonetes quadrata	ZZ2702-0328	Fig. 9.35b	In this book	Bed 27-2; *Fusichonetes pygmaea* Z	
Fusichonetes quadrata	ZZ2705-0329	Fig. 9.35c	In this book	Bed 27-5; *Fusichonetes pygmaea* Z	
Fusichonetes quadrata	ZZ2702-0330	Fig. 9.35d	In this book	Bed 27-2; *Fusichonetes pygmaea* Z	
Fusichonetes quadrata	ZZ2703-0334	Fig. 9.35e	In this book	Bed 27-3; *Fusichonetes pygmaea* Z	
Fusichonetes quadrata	HZS36-0336	Fig. 9.35f	In this book	Bed 36; *Clarkina meishanensis* Z	
Fusichonetes quadrata	HZS24-0337	Fig. 9.35g	In this book	Bed 24; *Clarkina meishanensis* Z	
Fusichonetes quadrata	HZS24-0338	Fig. 9.35h	In this book	Bed 24; *Clarkina meishanensis* Z	
Fusichonetes quadrata	HZS24-0339	Fig. 9.35i	In this book	Bed 24; *Clarkina meishanensis* Z	
Fusichonetes quadrata	HZS23-0341	Fig. 9.35j	In this book	Bed 23; *Clarkina meishanensis* Z	
Fusichonetes quadrata	HZS27-0343-1	Fig. 9.35k	In this book	Bed 27; *Clarkina meishanensis* Z	
Fusichonetes quadrata	HZS27-0343-2	Fig. 9.35l	In this book	Bed 27; *Clarkina meishanensis* Z	
Fusichonetes quadrata	ZZ2706-0333	Fig. 9.35m	In this book	Bed 27-6; *Fusichonetes pygmaea* Z	
Fusichonetes quadrata (=*Tethyochonetes* cf. *quadrata* of Zhang et al. 2013)	LZ0400278	Fig. 9.35n	Fig. 5Q; Zhang et al. (2013)	Bed 4; *Fusichonetes pygmaea* Z	
Fusichonetes quadrata (=*Tethyochonetes* cf. *quadrata* of Zhang et al. 2013)	LZ0400281	Fig. 9.35o	Fig. 5S; Zhang et al. (2013)	Bed 4; *Fusichonetes pygmaea* Z	
Fusichonetes quadrata (=*Tethyochonetes longtanensis* of He et al. 2014)	CM-4-460	Fig. 9.36a	Fig. 4I; He et al. (2014)	Bed 4; *Tapashanites* Z	

(continued)

Fossil name in the book	Registered number	Page and figure numbers in the book	Source of Materials	Occurences	Others
Fusichonetes quadrata (=*Tethyochonetes longtanensis* of He et al. 2014)	CM-3-408	Fig. 9.36b	Fig. 4J; He et al. (2014)	Bed 3; *Tapashanites* Z	
Fusichonetes quadrata (=*Tethyochonetes longtanensis* of He et al. 2014)	CM-3-409	Fig. 9.36c	Fig. 4K; He et al. (2014)	Bed 3; *Tapashanites* Z	
Fusichonetes quadrata (=*Tethyochonetes longtanensis* of He et al. 2014)	CM-10-425	Fig. 9.36d	Fig. 4L; He et al. (2014)	Bed 10; *Pseudotirolites*–*Rotodiscoceras* Z	
Fusichonetes quadrata (=*Tethyochonetes longtanensis* of He et al. 2014)	CM-3-464	Fig. 9.36e	Fig. 4N; He et al. (2014)	Bed 3; *Tapashanites* Z	
Fusichonetes quadrata (=*Tethyochonetes longtanensis* of He et al. 2014)	CM-3-465	Fig. 9.36f	Fig. 4O; He et al. (2014)	Bed 3; *Tapashanites* Z	
Fusichonetes quadrata	HZS34-0344	Fig. 9.36g	In this book	Bed 34; *Clarkina meishanensis* Z	
Fusichonetes quadrata	HZS24-0345	Fig. 9.36h	In this book	Bed 24; *Clarkina meishanensis* Z	
Fusichonetes quadrata	HZS31-0347	Fig. 9.36i	In this book	Bed 31; *Clarkina meishanensis* Z	
Fusichonetes quadrata	HZS24-0346	Fig. 9.36j	In this book	Bed 24; *Clarkina meishanensis* Z	
Fusichonetes quadrata (=*Tethyochonetes longtanensis* of Zhang et al. 2013)	LZ2705303	Fig. 9.36k	Fig. 5E; Zhang et al. (2013)	Bed 27-5; *Fusichonetes pygmaea* Z	
Fusichonetes quadrata (=*Tethyochonetes longtanensis* of Zhang et al. 2013)	LZ2701231	Fig. 9.36l	Fig. 5D; Zhang et al. (2013)	Bed 27-1; *Fusichonetes pygmaea* Z	
Fusichonetes quadrata (=*Tethyochonetes longtanensis* of He et al. 2014)	CM-12-455	Fig. 9.36m	Fig. 4M; He et al. (2014)	Bed 12; *Pseudotirolites*–*Rotodiscoceras* Z	
Fusichonetes quadrata (=*Waagenites longtanensis* Liao 1984)	71125	Fig. 9.37a	Liao (1984)	Upper part of Talung Formation	Holotype
Fusichonetes quadrata (=*Waagenites longtanensis* Liao 1984)	71124	Fig. 9.37b	Liao (1984)	Upper part of Talung Formation	

Fusichonetes flatus (=*Tethyochonetes flatus* of He et al. 2014)	CM-12-509	Fig. 9.38a	Fig. 6Q; He et al. (2014)	Bed 12; *Pseudotirolites–Rotodiscoceras* Z	
Fusichonetes flatus (=*Tethyochonetes flatus* of He et al. 2014)	CM-12-522	Fig. 9.38b	Fig. 6T; He et al. (2014)	Bed 12; *Pseudotirolites–Rotodiscoceras* Z	
Fusichonetes flatus (=*Tethyochonetes flatus* of He et al. 2014)	CM-12-532	Fig. 9.38c	Fig. 6U; He et al. (2014)	Bed 12; *Pseudotirolites–Rotodiscoceras* Z	
Fusichonetes flatus (=*Tethyochonetes flatus* of He et al. 2014)	CM-12-529	Fig. 9.38d	Fig. 6V; He et al. (2014)	Bed 12; *Pseudotirolites–Rotodiscoceras* Z	
Fusichonetes flatus (=*Tethyochonetes flatus* of He et al. 2014)	CM-12- 530	Fig. 9.38e	Fig. 6Y; He et al. (2014)	Bed 12; *Pseudotirolites–Rotodiscoceras* Z	
Fusichonetes flatus (=*Tethyochonetes flatus* of He et al. 2014)	CM-12-204	Fig. 9.38f	Fig. 6Z; He et al. (2014)	Bed 12; *Pseudotirolites–Rotodiscoceras* Z	
Fusichonetes flatus	SR22-0358	Fig. 9.38g	In this book	Bed 22; *Clarkina yini* Z	
Fusichonetes flatus	CM3-0360	Fig. 9.38h	In this book	Bed 3; *Tapashanites* Z	
Fusichonetes flatus (=*Tethyochonetes flatus* of He et al. 2014)	CM-12-525	Fig. 9.38i	Fig. 6A'; He et al. (2014)	Bed 12; *Pseudotirolites–Rotodiscoceras* Z	
Fusichonetes flatus	CM10-0362	Fig. 9.38j	In this book	Bed 10; *Pseudotirolites–Rotodiscoceras* Z	
Fusichonetes flatus	XM9-0357	Fig. 9.38k	In this book	Bed 1; *Clarkina changxingensis* Z	
Fusichonetes flatus	CM14-0361	Fig. 9.38l	In this book	Bed 14; *Pseudotirolites–Rotodiscoceras* Z	
Fusichonetes flatus	CM12-0363	Fig. 9.38m	In this book	Bed 12; *Pseudotirolites–Rotodiscoceras* Z	
Fusichonetes flatus	CM12-0364	Fig. 9.38n	In this book	Bed 12; *Pseudotirolites–Rotodiscoceras* Z	
Fusichonetes pygmaea	SR28-0349-1	Fig. 9.39a	In this book	Bed 28; *Ophiceras* Z	
Fusichonetes pygmaea	SR28-0351	Fig. 9.39b	In this book	Bed 28; *Ophiceras* Z	
Fusichonetes pygmaea	XM2-0435	Fig. 9.39c	In this book	Bed 2; *Clarkina changxingensis* Z	
Fusichonetes pygmaea	DDS26-0468	Fig. 9.39d	In this book	Bed 26; *Hypophiceras* Z	
Fusichonetes pygmaea	DDS26-0470	Fig. 9.39e	In this book	Bed 26; *Hypophiceras* Z	
Fusichonetes pygmaea	DDS29-0471	Fig. 9.39f	In this book	Bed 29; *Ophiceras* Z	
Fusichonetes pygmaea	DDS29-0472	Fig. 9.39g	In this book	Bed 29; *Ophiceras* Z	
Fusichonetes pygmaea	DDS29-0474	Fig. 9.39h	In this book	Bed 29; *Ophiceras* Z	

(continued)

Fossil name in the book	Registered number	Page and figure numbers in the book	Source of Materials	Occurences	Others
Fusichonetes pygmaea	DDS29-0475	Fig. 9.39i	In this book	Bed 29; *Ophiceras* Z	
Fusichonetes pygmaea	XM2-0478	Fig. 9.39j	In this book	Bed 2; *Clarkina changxingensis* Z	
Fusichonetes pygmaea	SR22-0477	Fig. 9.39k	In this book	Bed 22; *Clarkina yini* Z	
Fusichonetes pygmaea	SR22-0479	Fig. 9.39l	In this book	Bed 22; *Clarkina yni* Z	
Fusichonetes pygmaea	SR23a-0480	Fig. 9.39m	In this book	Bed 23; *Clarkina yini* Z	
Fusichonetes pygmaea	SR2202-0489	Fig. 9.39n	In this book	Bed 22; *Clarkina yini* Z	
Fusichonetes pygmaea	SR2202-0490	Fig. 9.39o	In this book	Bed 22; *Clarkina yini* Z	
Fusichonetes pygmaea	HZS20-0442-1	Fig. 9.40a	In this book	Bed 20; *Clarkina meishanensis* Z	
Fusichonetes pygmaea	HZS20-0442-2	Fig. 9.40b	In this book	Bed 20; *Clarkina meishanensis* Z	
Fusichonetes pygmaea	HZS29-0443	Fig. 9.40c	In this book	Bed 29; *Clarkina meishanensis* Z	
Fusichonetes pygmaea	HZS20-0444	Fig. 9.40d	In this book	Bed 20; *Clarkina meishanensis* Z	
Fusichonetes pygmaea	HZS24-0445	Fig. 9.40e	In this book	Bed 24; *Clarkina meishanensis* Z	
Fusichonetes pygmaea	HZS28-0446	Fig. 9.40f	In this book	Bed 28; *Clarkina meishanensis* Z	
Fusichonetes pygmaea	ZZ2705-0457	Fig. 9.40g	In this book	Bed 27-5; *Fusichonetes pygmaea* Z	
Fusichonetes pygmaea	ZZ2701-0454	Fig. 9.40h	In this book	Bed 27-1; *Fusichonetes pygmaea* Z	
Fusichonetes pygmaea	ZZ2705-0455	Fig. 9.40i	In this book	Bed 27-5; *Fusichonetes pygmaea* Z	
Fusichonetes pygmaea	ZZ2705-0460	Fig. 9.40j	In this book	Bed 27-5; *Fusichonetes pygmaea* Z	
Fusichonetes pygmaea	ZZ6-0456-2	Fig. 9.40k	In this book	Bed 6; *Fusichonetes pygmaea* Z	
Fusichonetes pygmaea	ZZ2703-0459	Fig. 9.40l	In this book	Bed 27-3; *Fusichonetes pygmaea* Z	
Fusichonetes rectangularis (=*Tethyochonetes rectanularis* He and Shi in He et al. 2014)	CM-14-91	Fig. 9.41a	Fig. 7B; He et al. (2014)	Bed 14; *Pseudotirolites*–*Rotodiscoceras* Z	Holotype
Fusichonetes rectangularis (=*Tethyochonetes rectanularis* He and Shi in He et al. 2014)	CM-13-350	Fig. 9.41b	Fig. 7C; He et al. (2014)	Bed 13; *Pseudotirolites*–*Rotodiscoceras* Z	Paratype
Fusichonetes rectangularis (=*Tethyochonetes rectanularis* He and Shi in He et al. 2014)	SR-23-393	Fig. 9.41c	Fig. 7A; He et al. (2014)	Bed 23; *Clarkina yini* Z	
Fusichonetes rectangularis (=*Tethyochonetes rectanularis* He and Shi in He et al. 2014)	CM-12-359	Fig. 9.41d	Fig. 7E; He et al. (2014)	Bed 12; *Pseudotirolites*–*Rotodiscoceras* Z	
Fusichonetes rectangularis (=*Tethyochonetes rectanularis* He and Shi in He et al. 2014)	CM-14-355	Fig. 9.41e	Fig. 7F; He et al. (2014)	Bed 14; *Pseudotirolites*–*Rotodiscoceras* Z	

Fusichonetes rectangularis (=*Tethyochonetes rectanularis* He and Shi in He et al. 2014)	CM-12-357	Fig. 9.41f	Fig. 7H; He et al. (2014)	Bed 12; *Pseudotirolites–Rotodiscoceras* Z	
Fusichonetes rectangularis (=*Tethyochonetes rectanularis* He and Shi in He et al. 2014)	CM-14-358	Fig. 9.41g	Fig. 7I; He et al. (2014)	Bed 14; *Pseudotirolites–Rotodiscoceras* Z	
Fusichonetes rectangularis (=*Tethyochonetes rectanularis* He and Shi in He et al. 2014)	CM-12-354	Fig. 9.41h	Fig. 7J; He et al. (2014)	Bed 12; *Pseudotirolites–Rotodiscoceras* Z	
Fusichonetes sinuata (=*Tethyochonetes*? *sinuata* He and Shi in He et al. 2014)	CM-10-16	Fig. 9.42a	Fig. 7L; He et al. (2014)	Bed 10; *Pseudotirolites–Rotodiscoceras* Z	
Fusichonetes sinuate (=*Tethyochonetes*? *sinuata* He and Shi in He et al. 2014)	CM-10-27	Fig. 9.42b	Fig. 7K; He et al. (2014)	Bed 10; *Pseudotirolites–Rotodiscoceras* Z	Holotype
Fusichonetes sinuata	HZS19-0605	Fig. 9.42c	In this book	Bed 19; *Clarkina meishanensis* Z	
Neochonetes (*Huangichonetes*) *substrophomenoides* (=*N.* (*Zhongyingia*) *zhongyingensis* of Zhang et al. 2013)	LZ0400110	Fig. 9.44a	Fig. 12X; Zhang et al. (2013)	Bed 4; *Fusichonetes pygmaea* Z	
Neochonetes (*Huangichonetes*) *substrophomenoides*	LZ2702387	Fig. 9.44b	Fig. 9P; Zhang et al. (2013)	Bed 27-2; *Fusichonetes pygmaea* Z	
Neochonetes (*Huangichonetes*) *substrophomenoides*	LZ1400530	Fig. 9.44c	Fig. 9X; Zhang et al. (2013)	Bed 14; *Fusichonetes pygmaea* Z	
Neochonetes (*Huangichonetes*) *substrophomenoides* (=*N.* (*Huangichonetes*) *archboldi* Zhang et al. 2013)	LZ2705142	Fig. 9.44d	Fig. 11I; Zhang et al. (2013)	Bed 27-5; *Fusichonetes pygmaea* Z	
Neochonetes (*Huangichonetes*) *substrophomenoides*	LZ1400368	Fig. 9.44e	Fig. 9Z; Zhang et al. (2013)	Bed 14; *Fusichonetes pygmaea* Z	
Neochonetes (*Huangichonetes*) *substrophomenoides* (=*N.* (*Huangichonetes*) *archboldi* Zhang et al. 2013)	LZ2704059	Fig. 9.44f	Fig. 11B; Zhang et al. (2013)	Bed 27-4; *Fusichonetes pygmaea* Z	
Neochonetes (*Huangichonetes*) *substrophomenoides* (=*N.* (*Huangichonetes*) *archboldi* Zhang et al. 2013)	LZ2704108	Fig. 9.44g	Fig. 11F; Zhang et al. (2013)	Bed 27-4; *Fusichonetes pygmaea* Z	

(continued)

Fossil name in the book	Registered number	Page and figure numbers in the book	Source of Materials	Occurences	Others
Neochonetes (*Huangichonetes*) *substrophomenoides* (=*N.* (*Huangichonetes*) *archboldi* Zhang et al. 2013)	LZ2705143	Fig. 9.44h	Fig. 11J; Zhang et al. (2013)	Bed 27-5; *Fusichonetes pygmaea* Z	
Neochonetes (*Huangichonetes*) *substrophomenoides* (=*N.* (*Huangichonetes*) *archboldi* Zhang et al. 2013)	LZ2703148	Fig. 9.44i	Fig. 11K; Zhang et al. (2013)	Bed 27-3; *Fusichonetes pygmaea* Z	
Neochonetes (*Sommeriella*) *wufengensis* (*N.* (*Huangichonetes*?) *wufengensis* He and Shi in He et al. 2014	DCB-34-395	Fig. 9.45a	Fig. 9H; He et al. (2014)	Bed 34; *Pseudotirolites* Z	
Neochonetes (*Sommeriella*) *wufengensis* (*N.* (*Huangichonetes*?) *wufengensis* He and Shi in He et al. 2014	DCB-35-398	Fig. 9.45b	Fig. 9I; He et al. (2014)	Bed 35; *Pseudotirolites* Z	Holotype
Neochonetes (*Sommeriella*) *wufengensis* (*N.* (*Huangichonetes*?) *wufengensis* He and Shi in He et al. 2014	DCB-35-399	Fig. 9.45c	Fig. 9J; He et al. (2014)	Bed 35; *Pseudotirolites* Z	Paratype
Neochonetes (*Sommeriella*) *wufengensis* (*N.* (*Huangichonetes*?) *wufengensis* He and Shi in He et al. 2014	DCB-35-400	Fig. 9.45d	Fig. 9K; He et al. (2014)	Bed 35; *Pseudotirolites* Z	
Neochonetes (*Sommeriella*) *wufengensis* (*N.* (*Huangichonetes*?) *wufengensis* He and Shi in He et al. 2014	DCB-34-394	Fig. 9.45e	Fig. 9L; He et al. (2014)	Bed 34 *Pseudotirolites* Z	
Neochonetes (*Zhongyingia*) *zhongyingensis*	LZ1200082	Fig. 9.45f	Fig. 12Z; Zhang et al. (2013)	Bed 12; *Fusichonetes pygmaea* Z	
Neochonetes (*Zhongyingia*) *zhongyingensis*	LZ0400085	Fig. 9.45g	Fig. 12AA; Zhang et al. (2013)	Bed 4; *Fusichonetes pygmaea* Z	
Neochonetes (*Zhongyingia*) *zhongyingensis*	LZ0400127	Fig. 9.45h	Fig. 12Y; Zhang et al. (2013)	Bed 4; *Fusichonetes pygmaea* Z	
Neochonetes (*Neochonetes*) *liaoi* (=*N.* (*Zhongyingia*?) *liaoi* He and Shi in He et al. 2014)	CM-1-373	Fig. 9.45i	Fig. 9O; He et al. (2014)	Bed 1; *Konglingites* Z	

Neochonetes (*Neochonetes*) *liaoi* (=*N.* (*Zhongyingia*?) *liaoi* He and Shi in He et al. 2014)	CM-1-372	Fig. 9.45j	Fig. 11A; He et al. (2014)	Bed 1; *Konglingites* Z	
Neochonetes (*Neochonetes*) *liaoi* (=*N.* (*Zhongyingia*?) *liaoi* He and Shi in He et al. 2014)	CM-1-364	Fig. 9.45k	Fig. 11C; He et al. (2014)	Bed 1; *Konglingites* Z	Holotype
Neochonetes (*Neochonetes*) *liaoi* (=*N.* (*Zhongyingia*?) *liaoi* He and Shi in He et al. 2014)	CM-1-376	Fig. 9.45l	Fig. 11D; He et al. (2014)	Bed 1; *Konglingites* Z	Paratype
Neochonetes (*Neochonetes*) *convex* (=*N.* (*Huangichonetes*) *substrophomenoides* of Zhang et al. 2013)	LZ0400128	Fig. 9.46a	Fig. 9T; Zhang et al. (2013)	Bed 4; *Fusichonetes pygmaea* Z	
Neochonetes (*Neochonetes*) *convex* (=*N.* (*Sommeriella*) *waterhousei* Zhang et al. 2013	LZ1200074	Fig. 9.46b	Fig. 12D; Zhang et al. (2013)	Bed 12; *Fusichonetes pygmaea* Z	
Neochonetes (*Neochonetes*) *convex* (=*N.* (*Zhongyingia*) *zhongyingensis* of Zhang et al. 2013)	LZ0400124	Fig. 9.46c	Fig. 12W; Zhang et al. (2013)	Bed 4; *Fusichonetes pygmaea* Z	
Neochonetes (*Neochonetes*) *convex* (=*Neochonetes semicircularis* Zhang et al. 2013)	LZ2704210	Fig. 9.46d	Fig. 14C; Zhang et al. (2013)	Bed 27-4; *Fusichonetes pygmaea* Z	
Neochonetes (*Neochonetes*) *convex* (=*N.* (*Sommeriella*) *waterhousei* Zhang et al. 2013	LZ0400100	Fig. 9.46e	Fig. 12I; Zhang et al. (2013)	Bed 4; *Fusichonetes pygmaea* Z	
Neochonetes (*Neochonetes*) *convex* (=*N.* (*Sommeriella*) *waterhousei* Zhang et al. 2013	LZ1200132	Fig. 9.46f	Fig. 12J; Zhang et al. (2013)	Bed 12; *Fusichonetes pygmaea* Z	
Neochonetes (*Neochonetes*) *convex* (=*N.* (*Huangichonetes*) *substrophomenoides* of Zhang et al. 2013)	LZ1200102	Fig. 9.46g	Fig. 9Q; Zhang et al. (2013)	Bed 12; *Fusichonetes pygmaea* Z	
Neochonetes (*Neochonetes*) *convex* (=*N.* (*Sommeriella*) *rectangularis* Zhang et al. 2013)	LZ1400033	Fig. 9.46h	Fig. 12N; Zhang et al. (2013)	Bed 14; *Fusichonetes pygmaea* Z	
Neochonetes (*Neochonetes*) *convex* (=*N.* (*Sommeriella*) *rectangularis* Zhang et al. 2013)	LZ2705020	Fig. 9.46i	Fig. 12O; Zhang et al. (2013)	Bed 27-5; *Fusichonetes pygmaea* Z	

(continued)

Fossil name in the book	Registered number	Page and figure numbers in the book	Source of Materials	Occurences	Others
Neochonetes (*Neochonetes*) *convex* (=*Neochonetes semicircularis* Zhang et al. 2013)	LZ2702212	Fig. 9.46j	Fig. 14D; Zhang et al. (2013)	Bed 27-2; *Fusichonetes pygmaea* Z	
Neochonetes (*Neochonetes*) *convex* (=*N.* (*Sommeriella*) *rectangularis* Zhang et al. 2013)	LZ2702049	Fig. 9.46k	Fig. 12R; Zhang et al. (2013)	Bed 27-2; *Fusichonetes pygmaea* Z	
Neochonetes (*Neochonetes*) *convex* (*N.* (*Sommeriella*) *strophomenoides* of Zhang et al. 2013	LZ1200133	Fig. 9.46l	Fig. 11V; Zhang et al. (2013)	Bed 12; *Fusichonetes pygmaea* Z	
Neochonetes (*Neochonetes*) *convex* (*N.* (*Sommeriella*) *strophomenoides* of Zhang et al. 2013	LZ0400105	Fig. 9.46m	Fig. 11T; Zhang et al. (2013)	Bed 4; *Fusichonetes pygmaea* Z	
Neochonetes (*Neochonetes*) *convex* (=*N.* (*Huangichonetes*) *archboldi* Zhang et al. 2013)	LZ2702289	Fig. 9.46n	Fig. 11M; Zhang et al. (2013)	Bed 27-2; *Fusichonetes pygmaea* Z	
Neochonetes (*Neochonetes*) *convex* (*N.* (*Sommeriella*) *regularis* of Zhang et al. 2013	LZ0400096	Fig. 9.46o	Fig. 11X; Zhang et al. (2013)	Bed 4; *Fusichonetes pygmaea* Z	
Chaohochonetes triangusinuata	CM-15-8	Fig. 9.48a	In this book	Bed 15; *Pseudotirolites*–*Rotodiscoceras* Z	
Chaohochonetes triangusinuata	CM-15-8	Fig. 9.48b (enlarged portion of Fig. 9.48a in the book)	In this book	Bed 15; *Pseudotirolites*–*Rotodiscoceras* Z	
Chaohochonetes triangusinuata	CM-15-7	Fig. 9.48c	Fig. 8E; He et al. (2014)	Bed 15; *Pseudotirolites*–*Rotodiscoceras* Z	
Chaohochonetes triangusinuata	CM-15-7	Fig. 9.48d (enlarged portion of Fig. 9.48c in the book)	In this book	Bed 15; *Pseudotirolites*–*Rotodiscoceras* Z	
Chaohochonetes triangusinuata	CM-15-1	Fig. 9.48e	Fig. 8A; He et al. (2014)	Bed 15; *Pseudotirolites*–*Rotodiscoceras* Z	Holotype
Chaohochonetes triangusinuata	CM-15-2	Fig. 9.48f	Fig. 8B; He et al. (2014)	Bed 15; *Pseudotirolites*–*Rotodiscoceras* Z	
Chaohochonetes triangusinuata	CM-15-3	Fig. 9.48g	Fig. 8C; He et al. (2014)	Bed 15; *Pseudotirolites*–*Rotodiscoceras* Z	
Chaohochonetes triangusinuata	CM-14-9	Fig. 9.48h	Fig. 8F; He et al. (2014)	Bed 14; *Pseudotirolites*–*Rotodiscoceras* Z	
Chaohochonetes triangusinuata	CM-15-5	Fig. 9.49a	Fig. 8H; He et al. (2014)	Bed 15; *Pseudotirolites*–*Rotodiscoceras* Z	
Chaohochonetes triangusinuata	CM-18-20	Fig. 9.49b	Fig. 8I; He et al. (2014)	Bed 18; uppermost Permian	
Chaohochonetes triangusinuata	CM-16-23	Fig. 9.49c	Fig. 8J; He et al. (2014)	Bed 16; *Pseudotirolites*–*Rotodiscoceras* Z	
Chaohochonetes triangusinuata	CM-18-24	Fig. 9.49d	Fig. 8K; He et al. (2014)	Bed 18; uppermost Permian	
Chaohochonetes triangusinuata	CM-16-14	Fig. 9.49e	Fig. 8M; He et al. (2014)	Bed 16; *Pseudotirolites*–*Rotodiscoceras* Z	

Chaohochonetes triangusinuata	CM-13-26	Fig. 9.49f	Fig. 8N; He et al. 2014	Bed 13; *Pseudotirolites–Rotodiscoceras* Z	
Chaohochonetes triangusinuata	CM-15-17	Fig. 9.49g	Fig. 9A; He et al. (2014)	Bed 15; *Pseudotirolites–Rotodiscoceras* Z	Paratype
Chaohochonetes triangusinuata	CM-14-18	Fig. 9.49h	Fig. 9B; He et al. (2014)	Bed 14; *Pseudotirolites–Rotodiscoceras* Z	
Chaohochonetes triangusinuata	CM-15-13	Fig. 9.49i	Fig. 9D; He et al. (2014)	Bed 15; *Pseudotirolites–Rotodiscoceras* Z	
Chaohochonetes sp.	CM-15-87	Fig. 9.49j	Fig. 9G; He et al. (2014)	Bed 15; *Pseudotirolites–Rotodiscoceras* Z	
Chaohochonetes sp.	CM-12-378	Fig. 9.49k	Fig. 9E; He et al. (2014)	Bed 12; *Pseudotirolites–Rotodiscoceras* Z	
Chaohochonetes sp.	XM-2-410	Fig. 9.49l	Fig. 9F; He et al. (2014)	Bed 2; *Clarkina changxingensis* Z	
Chaohochonetes triangusinuata	CM14-0599	Fig. 9.49m	In this book	Bed 14; *Pseudotirolites–Rotodiscoceras* Z	
Chaohochonetes triangusinuata	CM-15-6	Fig. 9.49n	Fig. 8D; He et al. (2014)	Bed 15; *Pseudotirolites–Rotodiscoceras* Z	
Leptodus richthofeni (=*Leptodus*? sp. of He et al. 2014)	CM-4-62	Fig. 9.50a	Fig. 19C; He et al. (2014)	Bed 4; *Tapashanites* Z	
Leptodus richthofeni (=*Leptodus*? sp. of He et al. 2014)	CM-4-60	Fig. 9.50b	Fig. 19D; He et al. (2014)	Bed 4; *Tapashanites* Z	
Leptodus richthofeni (=*Leptodus*? sp. of He et al. 2014)	XM-4-615	Fig. 9.50c	Fig. 19E; He et al. (2014)	Bed 4; *Clarkina yini* Z	
Leptodus richthofeni	HZS19-0620	Fig. 9.50d	In this book	Bed 19; *Clarkina meishanensis* Z	
Leptodus richthofeni	HZS19-0621	Fig. 9.50e	In this book	Bed 19; *Clarkina meishanensis* Z	
Leptodus richthofeni	XM18525-1	Fig. 9.50f	Fig. 8Z; Wu et al. (submitted)	Bed 2; *Clarkina changxingensis* Z	
Leptodus richthofeni	XM18525	Fig. 9.50g	Fig. 8Y; Wu et al. (submitted)	Bed 2; *Clarkina changxingensis* Z	
Oldhamina interrupta	LZ1200363	Fig. 9.50h	Fig. 8H; Zhang et al. (2015)	Bed 12; *Fusichonetes pygmaea* Z	
Matanoleptodus sp.	HZS18-0622	Fig. 9.50i	In this book	Bed 18; *Clarkina meishanensis* Z	
Leptodus richthofeni	XM18024	Fig. 9.50j	Fig. 8AA; Wu et al. (submitted)	Bed 2; *Clarkina changxingensis* Z	
Matanoleptodus sp.	HZS18-0623	Fig. 9.50k	In this book	Bed 18; *Clarkina meishanensis* Z	
Martinia liuqiaoiensis (=?*Martinia* sp. of He et al. 2014)	DP-1-55	Fig. 9.51a	Fig. 22A; He et al. (2014)	Bed 1; *Pseudotirolites–Rotodiscoceras* Z	
Martinia liuqiaoiensis (=?*Martinia* sp. of He et al. 2014)	DP-1-56	Fig. 9.51b	Fig. 22B; He et al. (2014)	Bed 1; *Pseudotirolites–Rotodiscoceras* Z	Holotype
Martinia liuqiaoiensis (=?*Martinia* sp. of He et al. 2014)	DP-2-57-2	Fig. 9.51c	Fig. 22C; He et al. (2014)	Bed 2; *Pseudotirolites–Rotodiscoceras* Z	
Martinia liuqiaoiensis (=?*Martinia* sp. of He et al. 2014)	DP-2-57-1	Fig. 9.51d	Fig. 22D; He et al. (2014)	Bed 2; *Pseudotirolites–Rotodiscoceras* Z	

(continued)

Fossil name in the book	Registered number	Page and figure numbers in the book	Source of Materials	Occurences	Others
Martinia liuqiaoiensis (=?*Martinia* sp. of He et al. 2014)	DS-1-51	Fig. 9.51e	Fig. 22G; He et al. (2014)	Bed 1; *Pseudotirolites–Rotodiscoceras* Z	
Martinia liuqiaoiensis (=?*Martinia* sp. of He et al. 2014)	SNM-47	Fig. 9.51f	Fig. 22H; He et al. (2014)	Bed 2; *Pseudotirolites* Z	
Martinia liuqiaoiensis (=?*Martinia* sp. of He et al. 2014)	SNM-49	Fig. 9.51g	Fig. 22I; He et al. (2014)	Bed 2; *Pseudotirolites* Z	
Martinia liuqiaoiensis (=?*Martinia* sp. of He et al. 2014)	SNM-54	Fig. 9.51h	Fig. 22J; He et al. (2014)	Bed 2; *Pseudotirolites* Z	
Martinia liuqiaoiensis (=?*Martinia* sp. of He et al. 2014)	DP-9-321	Fig. 9.51i	Fig. 22M; He et al. (2014)	Bed 9; *Pseudotirolites–Rotodiscoceras* Z	
Martinia liuqiaoiensis (=?*Martinia* sp. of He et al. 2014)	DS-1-53	Fig. 9.51j	Fig. 22N; He et al. (2014)	Bed 1; *Pseudotirolites–Rotodiscoceras* Z	
Martinia liuqiaoiensis (=?*Martinia* sp. of He et al. 2014)	DS-1-52	Fig. 9.51k	Fig. 22F; He et al. (2014)	Bed 1; *Pseudotirolites–Rotodiscoceras* Z	
Martinia liuqiaoiensis (=?*Martinia* sp. of He et al. 2014)	SW-5-46-1	Fig. 9.51l	Fig. 22K; He et al. (2014)	Bed 5; *Hunanopecten exilis–Claraia primitiva* Z	
Martinia liuqiaoiensis (=?*Martinia* sp. of He et al. 2014)	DP-2-59	Fig. 9.51m	Fig. 22E; He et al. (2014)	Bed 2; *Pseudotirolites–Rotodiscoceras* Z	
Martinia liuqiaoiensis (=?*Martinia* sp. of He et al. 2014)	SNM-48	Fig. 9.51n	Fig. 22L; He et al. (2014)	Bed 2; *Pseudotirolites* Z	
Martinia liuqiaoiensis	DP2-0108	Fig. 9.51o	In this book	Bed 2; *Pseudotirolites–Rotodiscoceras* Z	
Martinia liuqiaoiensis	DP2-0117	Fig. 9.51p	In this book	Bed 2; *Pseudotirolites–Rotodiscoceras* Z	
Martinia liuqiaoiensis	DP10-0107	Fig. 9.52a	In this book	Bed 10; *Pseudotirolites–Rotodiscoceras* Z	
Martinia liuqiaoiensis	DP3-0111	Fig. 9.52b	In this book	Bed 3; *Pseudotirolites–Rotodiscoceras* Z	
Martinia liuqiaoiensis	DP2-0114	Fig. 9.52c	In this book	Bed 2; *Pseudotirolites–Rotodiscoceras* Z	
Martinia liuqiaoiensis	DP2-0114	Fig. 9.52d	In this book	Bed 2; *Pseudotirolites–Rotodiscoceras* Z	
Martinia liuqiaoiensis	DP5-0118	Fig. 9.52e	In this book	Bed 5; *Pseudotirolites–Rotodiscoceras* Z	
Martinia liuqiaoiensis	DP5-0118	Fig. 9.52f	In this book	Bed 5; *Pseudotirolites–Rotodiscoceras* Z	
Martinia liuqiaoiensis	DP5-0118	Fig. 9.52g	In this book	Bed 5; *Pseudotirolites–Rotodiscoceras* Z	
Martinia liuqiaoiensis	DP7-0121-2	Fig. 9.52h	In this book	Bed 7; *Pseudotirolites–Rotodiscoceras* Z	
Martinia liuqiaoiensis	DP2-0121	Fig. 9.52i	In this book	Bed 2; *Pseudotirolites–Rotodiscoceras* Z	
Martinia liuqiaoiensis	DP7-0122	Fig. 9.52j	In this book	Bed 7; *Pseudotirolites–Rotodiscoceras* Z	
Martinia liuqiaoiensis	DP10-0126	Fig. 9.52k	In this book	Bed 10; *Pseudotirolites–Rotodiscoceras* Z	
Martinia liuqiaoiensis	DP2-0124	Fig. 9.53a	In this book	Bed 2; *Pseudotirolites–Rotodiscoceras* Z	

Martinia liuqiaoiensis	DP7-0145	Fig. 9.53b	In this book	Bed 7; *Pseudotirolites–Rotodiscoceras* Z	
Martinia liuqiaoiensis	DP10-0125	Fig. 9.53c	In this book	Bed 10; *Pseudotirolites–Rotodiscoceras* Z	
Martinia liuqiaoiensis	DP3-0129	Fig. 9.53d	In this book	Bed 3; *Pseudotirolites–Rotodiscoceras* Z	
Martinia liuqiaoiensis	DP10-0131	Fig. 9.53e	In this book	Bed 10; *Pseudotirolites–Rotodiscoceras* Z	
Martinia liuqiaoiensis	DP10-0127	Fig. 9.53f	In this book	Bed 10; *Pseudotirolites–Rotodiscoceras* Z	
Martinia liuqiaoiensis	DP3-0146	Fig. 9.53g	In this book	Bed 3; *Pseudotirolites–Rotodiscoceras* Z	
Martinia liuqiaoiensis	PB-0144	Fig. 9.53h	In this book	*Neoalbaillella optima* Z	
Martinia liuqiaoiensis	DP7-0139	Fig. 9.53i	In this book	Bed 7; *Pseudotirolites–Rotodiscoceras* Z	
Martinia liuqiaoiensis	DP3-0140	Fig. 9.53j	In this book	Bed 3; *Pseudotirolites–Rotodiscoceras* Z	Paratype
Martinia liuqiaoiensis	DP7-0310	Fig. 9.53k	In this book	Bed 7; *Pseudotirolites–Rotodiscoceras* Z	Paratype
Phricodothyris sp.	PB5-0262	Fig. 9.55a	In this book	Bed 5; *Neoalbaillella optima* Z	
Phricodothyris sp.	PB5-0268	Fig. 9.55b	In this book	Bed 5; *Neoalbaillella optima* Z	
Phricodothyris sp.	PB7-0257	Fig. 9.55c	In this book	Bed 7; *Neoalbaillella optima* Z	
Phricodothyris sp.	PB8-0265	Fig. 9.55d	In this book	Bed 8; *Neoalbaillella optima* Z	
Phricodothyris sp.	PB7-0267	Fig. 9.55e	In this book	Bed 7; *Neoalbaillella optima* Z	
Phricodothyris sp.	PB7-0260	Fig. 9.55f	In this book	Bed 7; *Neoalbaillella optima* Z	
Phricodothyris sp.	PB9-001	Fig. 9.55g	In this book	Bed 9; *Neoalbaillella optima* Z	
Phricodothyris sp.	PB9-001	Fig. 9.55h (enlarged portion of Fig. 9.55g in the book)	In this book	Bed 9; *Neoalbaillella optima* Z	
Phricodothyris sp.	PB9-001	Fig. 9.55i (enlarged portion of Fig. 9.55h in the book)	In this book	Bed 9; *Neoalbaillella optima* Z	
Phricodothyris sp.	PB5-0266	Fig. 9.55j	In this book	Bed 5; *Neoalbaillella optima* Z	
Attenuatella mengi	DP-7-1063	Fig. 9.58a	Fig. 4A; He et al. (2012)	Bed 7; *Pseudotirolites–Rotodiscoceras* Z	
Attenuatella mengi	DP-7-1063	Fig. 9.58b (enlarged portion of Fig. 9.58a in the book)	Fig. 4B; He et al. (2012)	Bed 7; *Pseudotirolites–Rotodiscoceras* Z	
Attenuatella mengi	DP-10-1062	Fig. 9.58c	Fig. 3F; He et al. (2012)	Bed 10; *Pseudotirolites–Rotodiscoceras* Z	
Attenuatella mengi	DP-10-1062	Fig. 9.58d (enlarged portion of Fig. 9.58c in the book)	Fig. 3G; He et al. (2012)	Bed 10; *Pseudotirolites–Rotodiscoceras* Z	
Attenuatella mengi	DP-9-2-351	Fig. 9.58e	Fig. 4M; He et al. (2012)	Bed 9; *Pseudotirolites–Rotodiscoceras* Z	
Attenuatella mengi	DP-5-1070	Fig. 9.58f	Fig. 4J; He et al. (2012)	Bed 5; *Pseudotirolites–Rotodiscoceras* Z	

(continued)

Fossil name in the book	Registered number	Page and figure numbers in the book	Source of Materials	Occurences	Others
Attenuatella mengi	DP-2-350	Fig. 9.58g	Fig. 4K; He et al. (2012)	Bed 2; *Pseudotirolites–Rotodiscoceras* Z	
Attenuatella mengi	DP-9-8-354	Fig. 9.58h	Fig. 4P; He et al. (2012)	Bed 9; *Pseudotirolites–Rotodiscoceras* Z	
Attenuatella mengi	DP-9-353	Fig. 9.58i	Fig. 4L; He et al. (2012)	Bed 9; *Pseudotirolites–Rotodiscoceras* Z	
Attenuatella mengi	DP-5-349	Fig. 9.58j	Fig. 4O; He et al. (2012)	Bed 5; *Pseudotirolites–Rotodiscoceras* Z	
Attenuatella mengi	SW-4–1003	Fig. 9.59a	In this book	Bed 4; *Hunanopecten exilis–Claraia primitiva* Z	
Attenuatella mengi	SW-4–1003	Fig. 9.59b (enlarged portion of Fig. 9.59a in the book)	In this book	Bed 4; *Hunanopecten exilis–Claraia primitiva* Z	
Attenuatella mengi	DP-7-1069	Fig. 9.59c	Fig. 3E; He et al. (2012)	Bed 7; *Pseudotirolites–Rotodiscoceras* Z	
Attenuatella mengi	DP-8-1061	Fig. 9.59d	Fig. 4I; He et al. (2012)	Bed 8; *Pseudotirolites–Rotodiscoceras* Z	
Attenuatella mengi	DP-8-1068	Fig. 9.59e	Fig. 4D; He et al. (2012)	Bed 8; *Pseudotirolites–Rotodiscoceras* Z	
Attenuatella mengi	DP-10-1	Fig. 9.59f	Fig. 6D; He et al. (2007a)	Bed 10; *Pseudotirolites–Rotodiscoceras* Z	
Attenuatella mengi	DP-5-356	Fig. 9.60a	Fig. 4C; He et al. (2012)	Bed 5; *Pseudotirolites–Rotodiscoceras* Z	
Attenuatella mengi	DP-5-1071	Fig. 9.60b	Fig. 4F; He et al. (2012)	Bed 5; *Pseudotirolites–Rotodiscoceras* Z	
Attenuatella mengi	DP-7-1066	Fig. 9.60c	Fig. 3D; He et al. (2012)	Bed 7; *Pseudotirolites–Rotodiscoceras* Z	
Attenuatella mengi	DP-5-1071	Fig. 9.60d	Fig. 4G; He et al. (2012)	Bed 5; *Pseudotirolites–Rotodiscoceras* Z	
Attenuatella mengi	DP-5-1071	Fig. 9.60e (enlarged portion of Fig. 9.60d in the book)	Fig. 4H; He et al. (2012)	Bed 5; *Pseudotirolites–Rotodiscoceras* Z	
Attenuatella sp.	DP-9-12	Fig. 9.60f	Fig. 5Q; He et al. 2007a	Bed 9; *Pseudotirolites–Rotodiscoceras* Z	
Speciothyris speciosa (=*Orbicoelia speciosa* of Zhang et al. 2014)	LZ2704642	Fig. 9.64a	Fig. 10D; Zhang et al. (2014)	Bed 27-4; *Fusichonetes pygmaea* Z	
Speciothyris speciosa (=*Orbicoelia speciosa* of Zhang et al. 2014)	LZ2704642	Fig. 9.64b	Fig. 10C; Zhang et al. (2014)	Bed 27-4; *Fusichonetes pygmaea* Z	
Speciothyris speciosa (=*Orbicoelia speciosa* of Zhang et al. 2014)	LZ1400444	Fig. 9.64c	Fig. 10A; Zhang et al. (2014)	Bed 14; *Fusichonetes pygmaea* Z	
Speciothyris speciosa (=*Orbicoelia* cf. *speciosa* of Zhang et al. 2014)	LZ1400482	Fig. 9.64d	Fig. 10M; Zhang et al. (2014)	Bed 14; *Fusichonetes pygmaea* Z	
Speciothyris speciosa (=*Orbicoelia speciosa* of Zhang et al. 2014)	LZ0400463	Fig. 9.64e	Fig. 10H; Zhang et al. (2014)	Bed 4; *Fusichonetes pygmaea* Z	
Speciothyris speciosa (=*Orbicoelia speciosa* of Zhang et al. 2014)	LZ1400452	Fig. 9.64f	Fig. 10G; Zhang et al. (2014)	Bed 14; *Fusichonetes pygmaea* Z	

Speciothyris speciosa (=*Orbicoelia speciosa* of Zhang et al. 2014)	LZ0400641	Fig. 9.64g	Fig. 10I; Zhang et al. (2014)	Bed 4; *Fusichonetes pygmaea* Z	
Speciothyris speciosa (=*Orbicoelia* cf. *speciosa* of Zhang et al. 2014)	LZ0400454	Fig. 9.64h	Fig. 10P; Zhang et al. (2014)	Bed 4; *Fusichonetes pygmaea* Z	
Speciothyris speciosa (=*Orbicoelia* cf. *speciosa* of Zhang et al. 2014)	LZ0400486	Fig. 9.64i	Fig. 10S; Zhang et al. (2014)	Bed 4; *Fusichonetes pygmaea* Z	
Speciothyris speciosa	HZS20-0683	Fig. 9.64j	In this book	Bed 20; *Clarkina meishanensis* Z	
Speciothyris speciosa	HZS20-0683	Fig. 9.64k	In this book	Bed 20; *Clarkina meishanensis* Z	
Speciothyris speciosa	HZS20-0683	Fig. 9.64l	In this book	Bed 20; *Clarkina meishanensis* Z	
Speciothyris speciosa	HZS23-0679	Fig. 9.64m	In this book	Bed 23; *Clarkina meishanensis* Z	
Speciothyris speciosa	HZS20-0682	Fig. 9.64n	In this book	Bed 20; *Clarkina meishanensis* Z	
Speciothyris speciosa	HZS20-0682	Fig. 9.64o	In this book	Bed 20; *Clarkina meishanensis* Z	
Paracrurithyris pygmaea (=*Crurithyris tazawai* He et al. 2012)	CM-1-1005	Fig. 9.61a	Fig. 5C; He et al. (2012)	Bed 1; *Konglingites* Z	
Paracrurithyris pygmaea (=*Crurithyris tazawai* He et al. 2012)	CM-1-1005	Fig. 9.61b (enlarged portion of Fig. 9.61a in the book)	Fig. 5D; He et al. (2012)	Bed 1; *Konglingites* Z	
Paracrurithyris pygmaea (=*Crurithyris tazawai* He et al. 2012)	CM-13-1007	Fig. 9.61c	Fig. 5G; He et al. (2012)	Bed 13; *Pseudotirolites–Rotodiscoceras* Z	
Paracrurithyris pygmaea (=*Crurithyris tazawai* He et al. 2012)	CM-13-1007	Fig. 9.61d (enlarged portion of Fig. 9.61c in the book)	Fig. 5H; He et al. (2012)	Bed 13; *Pseudotirolites–Rotodiscoceras* Z	
Paracrurithyris pygmaea (=*Crurithyris tazawai* He et al. 2012)	CM-13-1018	Fig. 9.61e	Fig. 5R; He et al. (2012)	Bed 13; *Pseudotirolites–Rotodiscoceras* Z	
Paracrurithyris pygmaea (=*Crurithyris tazawai* He et al. 2012)	CM-13-1018	Fig. 9.61f (enlarged portion of Fig. 9.61e in the book)	Fig. 5S; He et al. (2012)	Bed 13; *Pseudotirolites–Rotodiscoceras* Z	
Paracrurithyris pygmaea (=*Crurithyris tazawai* He et al. 2012)	SR-23b-1014	Fig. 9.61g	Fig. 5P; He et al. (2012)	Bed 23; *Clarkina yini* Z	
Paracrurithyris pygmaea (=*Crurithyris tazawai* He et al. 2012)	SR-23b-1014	Fig. 9.61h (enlarged portion of Fig. 9.61g in the book)	Fig. 5Q; He et al. (2012)	Bed 23; *Clarkina yini* Z	

(continued)

Fossil name in the book	Registered number	Page and figure numbers in the book	Source of Materials	Occurences	Others
Paracrurithyris pygmaea (=*Crurithyris tazawai* He et al. 2012)	SR-23b-1011	Fig. 9.61i	Fig. 5M; He et al. (2012)	Bed 23; *Clarkina yini* Z	
Paracrurithyris pygmaea (=*Crurithyris tazawai* He et al. 2012)	CM-14-1016	Fig. 9.61j	Fig. 5N; He et al. (2012)	Bed 14; *Pseudotirolites*–*Rotodiscoceras* Z	
Paracrurithyris pygmaea (=*Crurithyris tazawai* He et al. 2012)	SR-23b-1023	Fig. 9.61k	Fig. 5O; He et al. (2012)	Bed 23; *Clarkina yini* Z	
Paracrurithyris pygmaea (=*Crurithyris tazawai* He et al. 2012)	CM-14-1021	Fig. 9.62a	Fig. 6C; He et al. (2012)	Bed 14; *Pseudotirolites*–*Rotodiscoceras* Z	
Paracrurithyris pygmaea (=*Crurithyris tazawai* He et al. 2012)	CM-14-1021	Fig. 9.62b (enlarged portion of Fig. 9.62a in the book)	Fig. 6D; He et al. (2012)	Bed 14; *Pseudotirolites*–*Rotodiscoceras* Z	
Paracrurithyris pygmaea (=*Crurithyris tazawai* He et al. 2012)	SR-23b-1028	Fig. 9.62c	Fig. 6F; He et al. (2012)	Bed 23; *Clarkina yini* Z	
Paracrurithyris pygmaea (=*Crurithyris tazawai* He et al. 2012)	SR-23c-1027	Fig. 9.62d	Fig. 6E; He et al. (2012)	Bed 23; *Clarkina yini* Z	
Paracrurithyris pygmaea (=*Crurithyris tazawai* He et al. 2012)	CM-14-1016-2	Fig. 9.62e	Fig. 6H; He et al. (2012)	Bed 14; *Pseudotirolites*–*Rotodiscoceras* Z	
Paracrurithyris pygmaea (=*Crurithyris tazawai* He et al. 2012)	CM-14-1016-2	Fig. 9.62f (enlarged portion of Fig. 9.62e in the book)	In this book	Bed 14; *Pseudotirolites*–*Rotodiscoceras* Z	
Paracrurithyris pygmaea (=*Crurithyris tazawai* He et al. 2012)	CM-12-508	Fig. 9.62g	Fig. 6J; He et al. (2012)	Bed 12; *Pseudotirolites*–*Rotodiscoceras* Z	
Paracrurithyris pygmaea (=*Crurithyris tazawai* He et al. 2012)	CM-15-1022	Fig. 9.62h	In this book	Bed 15; *Pseudotirolites*–*Rotodiscoceras* Z	
Paracrurithyris sp.; (=*Crurithyris* sp. of He et al. 2012)	CM-15-542	Fig. 9.62i	Fig. 6K; He et al. (2012)	Bed 15; *Pseudotirolites*–*Rotodiscoceras* Z	
Paracrurithyris pygmaea	CM-16-1052	Fig. 9.63a	Fig. 7A; He et al. (2012)	Bed 16; *Pseudotirolites*–*Rotodiscoceras* Z	

Paracrurithyris pygmaea	CM-15-1056	Fig. 9.63b	Fig. 7B; He et al. (2012)	Bed 15; *Pseudotirolites–Rotodiscoceras* Z	
Paracrurithyris pygmaea	XM-1-1037	Fig. 9.63c	Fig. 7E; He et al. (2012)	Bed 1; *Clarkina changxingensis* Z.	
Paracrurithyris pygmaea	CM-16-1045	Fig. 9.63d	Fig. 7J; He et al. (2012)	Bed 16; *Pseudotirolites–Rotodiscoceras* Z	
Paracrurithyris pygmaea	CM-13-1040	Fig. 9.63e	Fig. 7F; He et al. (2012)	Bed 13; *Pseudotirolites–Rotodiscoceras* Z	
Paracrurithyris pygmaea	CM-12-1039	Fig. 9.63f	Fig. 7H; He et al. (2012)	Bed 12; *Pseudotirolites–Rotodiscoceras* Z	
Paracrurithyris pygmaea	CM-14-1036	Fig. 9.63g	Fig. 7D; He et al. (2012)	Bed 14; *Pseudotirolites–Rotodiscoceras* Z	
Paracrurithyris pygmaea	CM-14-1041	Fig. 9.63h	Fig. 7G; He et al. (2012)	Bed 14; *Pseudotirolites–Rotodiscoceras* Z	
Paracrurithyris pygmaea	CM-16-1047	Fig. 9.63i	Fig. 7L; He et al. (2012)	Bed 16; *Pseudotirolites–Rotodiscoceras* Z	
Paracrurithyris pygmaea	CM-16-1047	Fig. 9.63j (enlarged portion of Fig. 9.63i in the book)	Fig. 7M; He et al. (2012)	Bed 16; *Pseudotirolites–Rotodiscoceras* Z	
Paracrurithyris pygmaea	CM-16-1044	Fig. 9.63k	Fig. 7I; He et al. (2012)	Bed 16; *Pseudotirolites–Rotodiscoceras* Z	
Paracrurithyris pygmaea	XM-4-1059	Fig. 9.63l	Fig. 7K; He et al. (2012)	Bed 4; *Clarkina yini* Z	
Rhipidomella parvula	DP10-0240	Fig. 9.65a	In this book	Bed 10; *Pseudotirolites–Rotodiscoceras* Z	Holotype
Rhipidomella parvula	DP9-0243	Fig. 9.65b	In this book	Bed 9; *Pseudotirolites–Rotodiscoceras* Z	
Rhipidomella parvula	DP8-0242	Fig. 9.65c	In this book	Bed 8; *Pseudotirolites–Rotodiscoceras* Z	Paratype
Rhipidomella parvula	DP10-0249	Fig. 9.65d	In this book	Bed 10; *Pseudotirolites–Rotodiscoceras* Z	
Rhipidomella parvula	DP10-0247	Fig. 9.65e	In this book	Bed 10; *Pseudotirolites–Rotodiscoceras* Z	
Rhipidomella parvula	DP10-0246	Fig. 9.65f	In this book	Bed 10; *Pseudotirolites–Rotodiscoceras* Z	
Rhipidomella parvula	DP10-0245	Fig. 9.65g	In this book	Bed 10; *Pseudotirolites–Rotodiscoceras* Z	
Rhipidomella parvula	DP10-0250	Fig. 9.65h	In this book	Bed 10; *Pseudotirolites–Rotodiscoceras* Z	
Rhipidomella parvula	DP10-0241	Fig. 9.65i	In this book	Bed 10; *Pseudotirolites–Rotodiscoceras* Z	
Rhipidomella parvula	DP10-0244	Fig. 9.65j	In this book	Bed 10; *Pseudotirolites–Rotodiscoceras* Z	
Rhipidomella parvula	DP10-0252	Fig. 9.65k	In this book	Bed 10; *Pseudotirolites–Rotodiscoceras* Z	
Rhipidomella parvula	DP10-0248	Fig. 9.66a	In this book	Bed 10; *Pseudotirolites–Rotodiscoceras* Z	
Rhipidomella parvula	DP10-0248	Fig. 9.66b (enlarged portion of Fig. 9.66a in the book)	In this book	Bed 10; *Pseudotirolites–Rotodiscoceras* Z	Paratype
Rhipidomella parvula	DP10-0248	Fig. 9.66c (enlarged portion of Fig. 9.66b in the book)	In this book	Bed 10; *Pseudotirolites–Rotodiscoceras* Z	
Permorhipidomella ovatus	XC1-0283	Fig. 9.68a	In this book	*Pseudotirolites–Rotodiscoceras* Z	
Permorhipidomella ovatus	DP10-0284	Fig. 9.68b	In this book	Bed 10; *Pseudotirolites–Rotodiscoceras* Z	
Permorhipidomella ovatus	DP10-0286	Fig. 9.68c	In this book	Bed 10; *Pseudotirolites–Rotodiscoceras* Z	
Permorhipidomella ovatus	DP2-0292	Fig. 9.68d	In this book	Bed 2; *Pseudotirolites–Rotodiscoceras* Z	

(continued)

Fossil name in the book	Registered number	Page and figure numbers in the book	Source of Materials	Occurences	Others
Permorhipidomella ovatus	DP3-0278	Fig. 9.68e	In this book	Bed 3; *Pseudotirolites–Rotodiscoceras* Z	
Permorhipidomella ovatus	DP3-0290	Fig. 9.68f	In this book	Bed 3; *Pseudotirolites–Rotodiscoceras* Z	
Permorhipidomella ovatus	DP3-0289	Fig. 9.68g	In this book	Bed 3; *Pseudotirolites–Rotodiscoceras* Z	Paratype
Permorhipidomella ovatus	DP3-0285	Fig. 9.68h	In this book	Bed 3; *Pseudotirolites–Rotodiscoceras* Z	Paratype
Permorhipidomella ovatus	DP3-0285	Fig. 9.68i	In this book	Bed 3; *Pseudotirolites–Rotodiscoceras* Z	
Permorhipidomella ovatus	DP8-0280	Fig. 9.68j	In this book	Bed 8; *Pseudotirolites–Rotodiscoceras* Z	
Permorhipidomella ovatus	DP9-0279	Fig. 9.68k	In this book	Bed 9; *Pseudotirolites–Rotodiscoceras* Z	
Permorhipidomella ovatus	DP3-0277	Fig. 9.69a	In this book	Bed 3; *Pseudotirolites–Rotodiscoceras* Z	Holotype
Permorhipidomella ovatus	DP9-0282	Fig. 9.69b	In this book	Bed 9; *Pseudotirolites–Rotodiscoceras* Z	
Permorhipidomella ovatus	DP8-0281	Fig. 9.69c	In this book	Bed 8; *Pseudotirolites–Rotodiscoceras* Z	
Permorhipidomella ovatus	DP10-0291	Fig. 9.69d	In this book	Bed 10; *Pseudotirolites–Rotodiscoceras* Z	
Permorhipidomella ovatus	DP10-0288	Fig. 9.69e	In this book	Bed 10; *Pseudotirolites–Rotodiscoceras* Z	
Permorhipidomella ovatus	DP7-0276	Fig. 9.69f	In this book	Bed 7; *Pseudotirolites–Rotodiscoceras* Z	
Permorhipidomella ovatus	DP7-0276	Fig. 9.69g	In this book	Bed 7; *Pseudotirolites–Rotodiscoceras* Z	
Permorhipidomella ovatus	DP9-0287	Fig. 9.69h	In this book	Bed 9; *Pseudotirolites–Rotodiscoceras* Z	
Enteletes subaequivalis	DSH-0294	Fig. 9.71a	In this book	*Pseudotirolites–Rotodiscoceras* Z	
Enteletes subaequivalis	DP7-0295	Fig. 9.71b	In this book	Bed 7; *Pseudotirolites–Rotodiscoceras* Z	
Enteletes subaequivalis	DP8-0297	Fig. 9.71c	In this book	Bed 8; *Pseudotirolites–Rotodiscoceras* Z	
Enteletes subaequivalis	DP2-0300	Fig. 9.71d	In this book	Bed 2; *Pseudotirolites–Rotodiscoceras* Z	
Enteletes subaequivalis	DP2-0306	Fig. 9.71e	In this book	Bed 2; *Pseudotirolites–Rotodiscoceras* Z	
Enteletes subaequivalis	DP3-0307	Fig. 9.71f	In this book	Bed 3; *Pseudotirolites–Rotodiscoceras* Z	
Enteletes subaequivalis	DP3-0301	Fig. 9.71g	In this book	Bed 3; *Pseudotirolites–Rotodiscoceras* Z	
Enteletes subaequivalis	DP5-0302	Fig. 9.71h	In this book	Bed 5; *Pseudotirolites–Rotodiscoceras* Z	
Enteletes subaequivalis	PB5-0303	Fig. 9.71i	In this book	Bed 5; *Neoalbaillella optima* Z	
Enteletes subaequivalis	PB5-0298	Fig. 9.71j	In this book	Bed 5; *Neoalbaillella optima* Z	
Enteletes subaequivalis	DP10-0299	Fig. 9.71k	In this book	Bed 10; *Pseudotirolites–Rotodiscoceras* Z	
Enteletes subaequivalis	DP3-0304	Fig. 9.71l	In this book	Bed 3; *Pseudotirolites–Rotodiscoceras* Z	
Enteletes subaequivalis	DP3-0308	Fig. 9.72a	In this book	Bed 3; *Pseudotirolites–Rotodiscoceras* Z	
Enteletes subaequivalis	DP5-0309	Fig. 9.72b	In this book	Bed 5; *Pseudotirolites–Rotodiscoceras* Z	
Enteletes subaequivalis	DP5-0309	Fig. 9.72c	In this book	Bed 5; *Pseudotirolites–Rotodiscoceras* Z	
Orthotichia sp.1	PB2-0317	Fig. 9.72d	In this book	Bed 2; *Neoalbaillella optima* Z	
Orthotichia sp.1	DP5-0313	Fig. 9.72e	In this book	Bed 5; *Pseudotirolites–Rotodiscoceras* Z	

Orthotichia sp.1	DP3-0314	Fig. 9.72f	In this book	Bed 3; *Pseudotirolites–Rotodiscoceras* Z	
Orthotichia sp.1	DP3-0315	Fig. 9.72g	In this book	Bed 3; *Pseudotirolites–Rotodiscoceras* Z	
Orthotichia sp.1	DP2-0320	Fig. 9.72h	In this book	Bed 2; *Pseudotirolites–Rotodiscoceras* Z	
Orthotichia sp.1	DP3-0319	Fig. 9.72i	In this book	Bed 3; *Pseudotirolites–Rotodiscoceras* Z	
Orthotichia sp.2	DP7-0318	Fig. 9.72j	In this book	Bed 7; *Pseudotirolites–Rotodiscoceras* Z	
Orthotichia sp.3	DP5-0311	Fig. 9.72k	In this book	Bed 5; *Pseudotirolites–Rotodiscoceras* Z	
Orthotichia sp.4	DP5-0316	Fig. 9.72l	In this book	Bed 5; *Pseudotirolites–Rotodiscoceras* Z	
Acosarina minuta	LZ1200379	Fig. 9.73a	Fig. 9D; Zhang et al. (2014)	Bed 12; *Fusichonetes pygmaea* Z	
Acosarina minuta	LZ1400371	Fig. 9.73b	Fig. 7X; Zhang et al. (2014)	Bed 14; *Fusichonetes pygmaea* Z	
Acosarina minuta	LZ1400377	Fig. 9.73c	Fig. 7Z; Zhang et al. (2014)	Bed 14; *Fusichonetes pygmaea* Z	
Acosarina minuta	LZ1400378	Fig. 9.73d	Fig. 9A; Zhang et al. (2014)	Bed 14; *Fusichonetes pygmaea* Z	
Acosarina minuta	LZ1400376	Fig. 9.73e	Fig. 9C; Zhang et al. (2014)	Bed 14; *Fusichonetes pygmaea* Z	
Acosarina minuta	LZ1400375	Fig. 9.73f	Fig. 7AA; Zhang et al. (2014)	Bed 14; *Fusichonetes pygmaea* Z	
Acosarina minuta	XM140C01	Fig. 9.73g	Fig. 8F; Wu et al. (submitted)	Basal Changhsing Formation; Lower Changhsingian	
Acosarina minuta	XM15115	Fig. 9.73h	Fig. 8G; Wu et al. (submittted)	Bed 2; *Clarkina changxingensis* Z	
Acosarina minuta	LZ1400372	Fig. 9.73i	Fig. 7AB; Zhang et al. 2014	Bed 14; *Fusichonetes pygmaea* Z	
Acosarina minuta	LZ1400372	Fig. 9.73j	Fig. 7AC; Zhang et al. (2014)	Bed 14; *Fusichonetes pygmaea* Z	
Prelissorhynchia pseudoutah	LZ1400334	Fig. 9.74a	In this book	Bed 14; *Fusichonetes pygmaea* Z	
Prelissorhynchia pseudoutah	LZ2702680	Fig. 9.74b	Fig. 9P; Zhang et al. (2014)	Bed 27-2; *Fusichonetes pygmaea* Z	
Prelissorhynchia pseudoutah	LZ2700385	Fig. 9.74c	Fig. 9M; Zhang et al. (2014)	Bed 27; *Fusichonetes pygmaea* Z	
Prelissorhynchia pseudoutah	LZ2702679	Fig. 9.74d	In this book	Bed 27-2; *Fusichonetes pygmaea* Z	
Prelissorhynchia pseudoutah	LZ2702679	Fig. 9.74e (enlarged portion of Fig. 9.74d in the book)	In this book	Bed 27-2; *Fusichonetes pygmaea* Z	
Prelissorhynchia pseudoutah	LZ2702681	Fig. 9.74f	Fig. 9R; Zhang et al. (2014)	Bed 27-2; *Fusichonetes pygmaea* Z	
Prelissorhynchia pseudoutah	LZ2702681	Fig. 9.74g	Fig. 9Q; Zhang et al. (2014)	Bed 27-2; *Fusichonetes pygmaea* Z	

(continued)

Fossil name in the book	Registered number	Page and figure numbers in the book	Source of Materials	Occurences	Others
Prelissorhynchia pseudoutah	LZ2702681	Fig. 9.74h (enlarged portion of Fig. 9.74g in the book)	In this book	Bed 27-2; *Fusichonetes pygmaea* Z	
Prelissorhynchia pseudoutah	LZ1600336	Fig. 9.74i	Fig. 9K; Zhang et al. (2014)	Bed 16; *Fusichonetes pygmaea* Z	
Prelissorhynchia pseudoutah	XM16709	Fig. 9.74j	Fig. 8J; Wu et al. (submitted)	Bed 2; *Clarkina changxingensis* Z	
Prelissorhynchia pseudoutah	XM283C08	Fig. 9.74k	Fig. 8R; Wu et al. (submitted)	Bed 4; *Clarkina yini* Z	
Prelissorhynchia pseudoutah	XM283C08	Fig. 9.74l	Fig. 8S; Wu et al. (submitted)	Bed 4; *Clarkina yini* Z	
Prelissorhynchia pseudoutah	XM283C08	Fig. 9.74m	Fig. 8T; Wu et al. (submitted)	Bed 4; *Clarkina yini* Z	
Orthothetina frechi	LZ1200356	Fig. 9.75a	Fig. 7H; Zhang et al. (2014)	Bed 12; *Fusichonetes pygmaea* Z	
Orthothetina frechi	LZ0400122	Fig. 9.75b	Fig. 7C; Zhang et al. (2014)	Bed 4; *Fusichonetes pygmaea* Z	
Orthothetina frechi	LZ1200353	Fig. 9.75c	Fig. 7E; Zhang et al. (2014)	Bed 12; *Fusichonetes pygmaea* Z	
Orthothetina frechi	LZ1200354	Fig. 9.75d	Fig. 7F; Zhang et al. (2014)	Bed 12; *Fusichonetes pygmaea* Z	
Orthothetina frechi	LZ1200354	Fig. 9.75e (enlarged portion of Fig. 9.75d in the book)	In this book	Bed 12; *Fusichonetes pygmaea* Z	
Orthothetina frechi	LZ1200351	Fig. 9.75f	Fig. 7D; Zhang et al. (2014)	Bed 12; *Fusichonetes pygmaea* Z	
Orthothetina frechi	LZ1600352	Fig. 9.75g	Fig. 7B; Zhang et al. (2014)	Bed 16; *Fusichonetes pygmaea* Z	
Orthothetina frechi	LZ1600350	Fig. 9.75h	Fig. 7A; Zhang et al. (2014)	Bed 16; *Fusichonetes pygmaea* Z	
Orthothetina regularis	XM14907	Fig. 9.75i	Fig. 8E; Wu et al. (in press)	Bed 2; *Clarkina changxingensis* Z	
Orthothetina regularis	XM14907	Fig. 9.75j (enlarged portion of Fig. 9.75i in the book)	In this book	Bed 2; *Clarkina changxingensis* Z	
Orthothetina ruber	SR-21-143	Fig. 9.75k	Fig. 21F; He et al. (2014)	Bed 21; *Clarkina changxingensis–C. deflecta* Z	
Orthothetina ruber	SR-20-133	Fig. 9.75l	Fig. 21E; He et al. (2014)	Bed 20; *Clarkina changxingensis–C. deflecta* Z	
Goniarina sp.	DP-2-342	Fig. 9.75m	Fig. 21L; He et al. (2014)	Bed 2; *Pseudotirolites–Rotodiscoceras* Z	
Goniarina sp.	LQ-3-343	Fig. 9.75n	Fig. 21M; He et al. (2014)	Bed 3; *Neoalbaillella optima* Z	

Orthothetina regularis (=*Goniarina* sp. of He et al. 2014)	XM-2-75	Fig. 9.75o	Fig. 21K; He et al. (2014)	Bed 2; *Clarkina changxingensis* Z	
Streptorhynchus sp.	XM-2-74	Fig. 9.75p	Fig. 21O; He et al. (2014)	Bed 2; *Clarkina changxingensis* Z	
Streptorhynchus sp.	SR-23-145	Fig. 9.75q	Fig. 21N; He et al. (2014)	23; *Clarkina yini* Z	
Orthothetina regularis	LZ1400355	Fig. 9.76a	Fig. 7V; Zhang et al. (2014)	Bed 14; *Fusichonetes pygmaea* Z	
Orthothetina regularis	LZ1400327	Fig. 9.76b	Fig. 7O; Zhang et al. (2014)	Bed 14; *Fusichonetes pygmaea* Z	
Orthothetina regularis	LZ1400328	Fig. 9.76c	In this book	Bed 14; *Fusichonetes pygmaea* Z	
Orthothetina regularis	LZ1400324	Fig. 9.76d	Fig. 7K; Zhang et al. (2014)	Bed 14; *Fusichonetes pygmaea* Z	
Orthothetina regularis	LZ0400329	Fig. 9.76e	Fig. 7Q; Zhang et al. (2014)	Bed 4; *Fusichonetes pygmaea* Z	
Orthothetina regularis	LZ1200322	Fig. 9.76f	Fig. 7J; Zhang et al. (2014)	Bed 12; *Fusichonetes pygmaea* Z	
Orthothetina regularis	LZ1400321	Fig. 9.76g	Fig. 7I; Zhang et al. (2014)	Bed 14; *Fusichonetes pygmaea* Z	
Orthothetina regularis	LZ0400326	Fig. 9.76h	Fig. 7M; Zhang et al. (2014)	Bed 4; *Fusichonetes pygmaea* Z	
Orthothetina regularis	LZ0400326	Fig. 9.76i (enlarged portion of Fig. 9.76h in the book)	In this book	Bed 4; *Fusichonetes pygmaea* Z	
Orthothetina regularis	LZ0400330	Fig. 9.76j	Fig. 7R; Zhang et al. (2014)	Bed 4; *Fusichonetes pygmaea* Z	
Orthothetina regularis	LZ0400330	Fig. 9.76k	Fig. 7S; Zhang et al. (2014)	Bed 4; *Fusichonetes pygmaea* Z	
Orthothetina regularis	LZ1600331	Fig. 9.76l	Fig. 7T; Zhang et al. (2014)	Bed 16; *Fusichonetes pygmaea* Z	
Orthothetina regularis	LZ1400325	Fig. 9.76m	Fig. 7L; Zhang et al. (2014)	Bed 14; *Fusichonetes pygmaea* Z	
Orbiculoidea nucleoli (=*Orbiculoidea elegans* Liao 1980a)	LZ1200182	Fig. 9.77a	Fig. 4B; Zhang et al. (2014)	Bed 12; *Fusichonetes pygmaea* Z	
Orbiculoidea nucleoli (=*Orbiculoidea elegans* Liao 1980a)	LZ1200203	Fig. 9.77b	Fig. 4D; Zhang et al. (2014)	Bed 12; *Fusichonetes pygmaea* Z	
Orbiculoidea nucleoli (=*Orbiculoidea elegans* Liao 1980a)	LZ1200625	Fig. 9.77c	Fig. 4E; Zhang et al. (2014)	Bed 12; *Fusichonetes pygmaea* Z	
Orbiculoidea nucleoli (=*Orbiculoidea elegans* Liao 1980a)	LZ1200625	Fig. 9.77d	Fig. 4F; Zhang et al. (2014)	Bed 12; *Fusichonetes pygmaea* Z	
Orbiculoidea nucleoli (=*Orbiculoidea elegans* Liao 1980a)	LZ1200623	Fig. 9.77e	Fig. 4K; Zhang et al. (2014)	Bed 12; *Fusichonetes pygmaea* Z	
Orbiculoidea nucleoli (=*Orbiculoidea elegans* Liao 1980a)	LZ1200622	Fig. 9.77f	Fig. 4G; Zhang et al. (2014)	Bed 12; *Fusichonetes pygmaea* Z	

(continued)

Fossil name in the book	Registered number	Page and figure numbers in the book	Source of Materials	Occurences	Others
Orbiculoidea nucleoli (=*Orbiculoidea elegans* Liao 1980a)	LZ1200622	Fig. 9.77g	Fig. 4H; Zhang et al. (2014)	Bed 12; *Fusichonetes pygmaea* Z	
Orbiculoidea nucleoli (=*Orbiculoidea elegans* Liao 1980a)	LZ1200606	Fig. 9.77h	Fig. 4I; Zhang et al. (2014)	Bed 12; *Fusichonetes pygmaea* Z	
Orbiculoidea liaoi	LZ2702628	Fig. 9.77i	Fig. 5T; Zhang et al. (2014)	Bed 27-2; *Fusichonetes pygmaea* Z	
Orbiculoidea liaoi	LZ2702614	Fig. 9.77j	Fig. 5U; Zhang et al. (2014)	Bed 27-2; *Fusichonetes pygmaea* Z	
Orbiculoidea liaoi	LZ2701198	Fig. 9.77k	Fig. 5P; Zhang et al. (2014)	Bed 27-1; *Fusichonetes pygmaea* Z	Holotype
Orbiculoidea nucleola	LZ1600208	Fig. 9.77l	Fig. 5B; Zhang et al. (2014)	Bed 16; *Fusichonetes pygmaea* Z	
Orbiculoidea nucleola	LZ1200611	Fig. 9.77m	Fig. 5D; Zhang et al. (2014)	Bed 12; *Fusichonetes pygmaea* Z	
Orbiculoidea nucleola	LZ1200611	Fig. 9.77n	Fig. 5E; Zhang et al. (2014)	Bed 12; *Fusichonetes pygmaea* Z	
Orbiculoidea nucleola	LZ0200199	Fig. 9.77o	Fig. 5C; Zhang et al. (2014)	Bed 2; *Fusichonetes pygmaea* Z	
Orbiculoidea liaoi (=*Orbiculoidea qinglongensis* of Zhang et al. 2014)	LZ0700187	Fig. 9.77p	Fig. 5R; Zhang et al. (2014)	Bed 7; *Fusichonetes pygmaea* Z	
?*Lingularia borealis* (=*Sinoglottidia* sp. of He et al. 2014)	SR-17-88	Fig. 9.78a	Fig. 21Q; He et al. (2014)	Bed 17; Upper Permian	
?*Lingularia borealis* (=*Sinoglottidia* sp. of He et al. 2014)	SR-15-89	Fig. 9.78b	Fig. 21U; He et al. (2014)	Bed 15; *Konglingites* Z	
?*Lingularia borealis* (=*Sinoglottidia* sp. of He et al. 2014)	SR-17-90	Fig. 9.78c	Fig. 21S; He et al. (2014)	Bed 17; Upper Permian	
?*Lingularia borealis* (=*Sinoglottidia* sp. of He et al. 2014)	CM-13-97	Fig. 9.78d	Fig. 21R; He et al. (2014)	Bed 13; *Pseudotirolites–Rotodiscoceras* Z	
?*Lingularia borealis* (=*Sinoglottidia* sp. of He et al. 2014)	CM-10-98	Fig. 9.78e	Fig. 21T; He et al. (2014)	Bed 10; *Pseudotirolites–Rotodiscoceras* Z	
?*Lingularia borealis*	CM-10-98	Fig. 9.78f	In this book	Bed 10; *Pseudotirolites–Rotodiscoceras* Z	
?*Lingularia borealis* (=*Sinoglottidia* sp. of He et al. 2014)	XJP-11-93	Fig. 9.78g	Fig. 21P; He et al. (2014)	Bed 11; Upper Permian	
?*Lingularia borealis*	XJP-2f-87	Fig. 9.78h	In this book	Upper Permian	
Lingularia sp. 1	HZS44-0699	Fig. 9.78i	In this book	Bed 44; *Ophiceras* Z	
Lingularia sp. 2	HZS37-0701	Fig. 9.78j	In this book	Bed 37; *Hindeodus parvus* Z	
?*Semilingula* sp.	HZS37-0698	Fig. 9.78k	In this book	Bed 37; *Hindeodus parvus* Z	
?*Semilingula* sp.	HZS37-0702	Fig. 9.78l	In this book	Bed 37; *Hindeodus parvus* Z	

Appendix 2: Index for Abbreviations of Brachiopod Morphological Terms in This Book

ads adductor scars
br brachial ridges
bs scars of brachial ridges
cp cardinal process
crp crural plates
dds diductor scars
del delthyrium
dp dental plates
ebaf ear baffles
ens endospines
es spines on ears
geni geniculation
gr a pair of grooves separated ears and disk (for *Paryphella corculum*)
gs groove (for the groove at the base of each spine for *Attenuatella mengi*)
hs hinge spines
iar interarea
is inner socket ridges
ls lateral septa
lam finely concentric lamellae (for *Rhipidomella parvula*)
mar marginal ridge
mg median groove
mr median ridge
ms median septum
npm netlike pallial markings
pa papillae
psd pseudodeltidium
pvm pinnate vascular markings
pr micro-protuberances (for *Streptorhynchus*)
r radial ornaments on ears (for *Anidanthus parvimucronata*)
rs ridge (for ridges at the base of each spine for *Attenuatella mengi*)
sc spine canals
soc sockets
sp spines
t teeth-like structures
tu tubes (a kind of micro-ornamentation)
th tooth
vt vascular trunks (for *Neochonetes*)
vm vascular markings
br bladed brachiophores (for *Rhipidomella parvula*)